NUREG/CR-1469
EGG-2038

U.S. Department of Energy
Idaho Operations Office • Idaho National Engineering Laboratory

Experiment Data Report for Semiscale Mod-3 Small Break Test Series (Tests S-SB-2 and S-SB-2A)

Dean H. Miyasaki

June 1980

THIS DOCUMENT CONTAINS POOR QUALITY PAGES

Prepared for the
U.S. Nuclear Regulatory Commission
Under DOE Contract No.DE-AC07-76ID01570

EG&G Idaho

8007140092

Available from

GPO Sales Program
Division of Technical Information and Document Control
U.S. Nuclear Regulatory Commission
Washington, D.C. 20555

and

National Technical Information Service
Springfield, Virginia 22161

NUREG/CR 1459
EGG-2038
Distribution Category: R2

EXPERIMENT DATA REPORT FOR SEMISCALE MOD-3 SMALL BREAK TEST SERIES (TESTS S-SB-2 AND S-SB-2A)

Dean H. Miyasaki

Published June 1980

EG&G Idaho, Inc.
Idaho Falls, Idaho 83415

Prepared for the
U.S. Nuclear Regulatory Commission
Washington, D.C. 20555
Under DOE Contract No.DE-AC07-76IDO1570
FIN No. A6038

ABSTRACT

Test data from the Semiscale Mod-3 system at Idaho National Engineering Laboratories are presented for Tests S-SB-2 and S-SB-2A. These tests are two of the Semiscale Mod-3 Small Break Test Series, which is conducted to investigate the thermal-hydraulic phenomena resulting from a small break loss-of-coolant accident (LOCA) in a pressurized water reactor (PWR) system, and to provide experimental data for assessing the analytical capability of computer codes used in LOCA analysis. The primary objective of Test S-SB-2 is to provide data for a small break LOCA in which the break flow rate is greater than the high pressure safety injection rate. Test S-SB-2A, a comparative test of Test S-SB-2, was conducted to determine the sensitivity of the Mod-3 system behavior when the core power is augmented to offset system heat losses, and to assess the analytical capability of the computer codes to model the effects of the atypical heat losses in the Semiscale Mod-3 system. Tests S-SB-2 and S-SB-2A were conducted with approximate initial conditions of 15.5 MPa pressurizer pressure; 550 K cold leg temperature; and 2.1 MW core power level. The purpose of this report is to make available and provide comparison of uninterpreted data from Tests S-SB-2 and S-SB-2A for future data analysis. The data, presented in the form of graphs in engineering units, have been analyzed for reasonableness and consistency.

SUMMARY

Tests S-SB-2 and S-SB-2A were performed as part of the Semiscale Mod-3 portion of the Semiscale Program conducted by EG&G Idaho, Inc., for the United States Government. These tests were part of the Mod-3 Small Break Test Series performed to investigate the thermal-hydraulic phenomena resulting from a small break loss-of-coolant accident (LOCA) in a pressurized water reactor (PWR) system, and to provide experimental data for assessing the analytical capability of computer codes used in LOCA analysis. The primary objective of Test S-SB-2 is to provide data for a small break LOCA in which the break flow rate is greater than the high pressure safety injection rate. The primary objective of Test S-SB-2A is to determine the sensitivity of the Mod-3 system behavior when the core power is augmented to offset system heat losses, and to assess the analytical capability of the computer codes to model the effects of the atypical heat losses in the Semiscale Mod-3 system.

The Mod-3 system was equipped with a pressure vessel which contained an electrically heated core and other simulated reactor internals and an external downcomer assembly; an intact loop with steam generator, pump, and pressurizer; a broken loop with steam generator, pump, and rupture assembly; and a pressure suppression system with header, suppression tank, and steam supply system. High pressure coolant injection pumps, for high and low pressure injection systems and coolant injection accumulators were provided for the intact loop and broken loop.

The specified initial conditions for Tests S-SB-2 and S-SB-2A were a system pressure of 15.5 MPa, a core inlet temperature of 550 K with a core differential temperature of 33 K, and a core power of 2.1 MW. The simulated (2.5%) small break was located on the centerline of the broken loop cold leg and was volume scaled to represent an 11-cm break in a PWR. After initiation of blowdown, power to the electrically heated core was reduced to simulate the predicted heat flux response of nuclear fuel rods during a LOCA.

Tests S-SB-2 and S-SB-2A were generally conducted as specified. Conditions which did not conform to the specified test conditions were considered acceptable for the test objectives. Of 224 measurements taken for Test S-SB-2, 213 produced usable data. Of 264 measurements taken for Test S-SB-2A, 250 produced usable data.

CONTENTS

FIGURES

TABLES

EXPERIMENT DATA REPORT FOR SEMISCALE MOD-3 SMALL BREAK TEST SERIES (TESTS S-SB-2 AND S-SB-2A)

I. INTRODUCTION

The Semiscale Mod-3 experiments represent the current phase of the Semiscale Program conducted by EG&G Idaho, Inc., for the United States Government. The program, which is sponsored by the Nuclear Regulatory Commission (NRC) through the Department of Energy, is part of the overall NRC program designed to investigate the response of a pressurized water reactor (PWR) system to a hypothesized loss-of-coolant accident (LOCA). The underlying objectives of the Semiscale Program are to quantify the physical processes controlling system behavior during a LOCA, and to provide an experimental data base for assessing reactor safety evaluation models. The Semiscale Mod-3 Program has the further objective of providing support to other experimental programs in the form of instrumentation assessment, optimization of test series, selection of test parameters, and evaluation of test results.

Test S-SB-2 was conducted December 5, 1979, in the Semiscale Mod-3 System as part of the Small Break Test Series (Test Series SB). This series was designed to investigate the thermal-hydraulic phenomena resulting from a small-break LOCA in a PWR system, and to provide experimental data with which to assess the analytical capability of computer codes to predict PWR system behavior during a small-break LOCA. Test S-SB-2 was designed primarily to provide data for a small break LOCA in which the break flow rate is greater than the high pressure safety injection rate.

Test S-SB-2A was conducted January 11, 1980, in the Semiscale Mod-3 System as an additional test to the Small Break Test Series (Small Break Test S-SB-2A). Test S-SB-2A was designed primarily to determine the sensitivity of Mod-3 system behavior when the core power is augmented to offset system heat losses, and to assess the analytical capability of the computer codes which model the effects of the Semiscale Mod-3 System's atypical heat losses. These losses are caused by the structural surface area to fluid volume ratios being larger than volume scaling laws required.

The purpose of this report is to present the test data in an uninterpreted but readily usable form for use by the nuclear community in advance of detailed analysis and interpretation. Section II briefly describes the system configuration, procedures, and initial test conditions and events that are applicable to Tests S-SB-2 and S-SB-2A; Section III consists of data graphs and provides comments and supporting information necessary for interpretation of the data. A description of the overall Semiscale Program and test series and a more detailed description of the Semiscale Mod-3 system are given in References 1 and 2. Additional information describing the data acquisition system capabilities, posttest adjustments made to the data, and the methodology used to establish uncertainty limits for the data are given in three appendixes.

II. SYSTEM, PROCEDURES, CONDITIONS, AND EVENTS FOR TESTS S-SB-2 AND S-SB-2A

The following system configuration, procedures, initial test conditions and events are specific to Tests S-SB-2 and S-SB-2A as indicated.

1. System Configuration and Test Procedures

The Semiscale Mod-3 system used for these tests consisted of a pressure vessel with simulated reactor internals, including a 25-rod core with 22 electrically heated rods and an external downcomer assembly; an intact loop with pressurizer, steam generator, and pump; and a broken loop with a steam generator, pump, and rupture assembly. It also had emergency core coolant (ECC) from a high pressure coolant injection pump and a coolant injection accumulator for each loop and a pressure suppression system with header, suppression tank, and steam supply system. Reference 1 further describes the Semiscale Mod-3 system. The system configuration for these tests is shown in Figures 1 and 2. The communicative break simulator configuration with break nozzle near the loop piping is detailed further in Reference 2.

Twenty-two rods of the 25-rod core were operated at a rod peak axial power density of 40.45 kW/m for a total core power of 2.1 MW. Two rods were unpowered and another rod was replaced by a liquid level probe.

In preparation for the tests, the system was filled with treated demineralized water and vented at strategic points to ensure a liquid-full system. The system was pressurized to 15.60 MPa and was checked for leakage. Treated demineralized water in the steam generator feedwater tank was heated to 497 K. and the required liquid levels were established in the steam generator secondary sides. System instrumentation checkout was performed. Heatup to initial test conditions was accomplished with the heaters in the core. During heatup, the purification and sampling systems were valved into the primary system to maintain water chemistry requirements and to provide a water sample at system conditions for subsequent analysis. At 50-K temperature intervals from 300 K to 550 K, detector readings were sampled to check the integrity of the measurement instrumentation and the performance of the data acquisition system.

Prior to the establishment of the initial core power level, the accumulator for the intact loop and the accumulator for the broken loop were filled with treated demineralized water, drained to specified levels, and pressurized to 4.22 MPa with nitrogen. The pressure suppression system was pressurized to 0.65 MPa with saturated steam from the steam supply system. After the core power was increased to 2.1 MW, initial test conditions were held for approximately 600 s to establish system equilibrium. At the end of this period, all auxiliary systems were isolated to prevent blowdown through those systems.

A successful simulated small cold leg break, through a rupture assembly and blowdown nozzle having a total break area of 0.0613 cm^2, was accomplished. Pressure to operate the rupture assembly and initiate blowdown was taken from an accumulator system filled with water and pressurized with gaseous nitrogen to 15.6 MPa. Immediately (within 0.02 s) after initiation of pressure to operate the rupture assembly, the lines to the accumulator were again isolated. During blowdown the effluent was ejected from the primary system to the pressure suppression system which was vented to maintain a predetermined pressure curve.

When the pressurizer pressure had reached 12.48 MPa, the steam valve for each loop steam generator was closed. At 3.4 s after the pressurizer pressure had reached 12.48 MPa, the intact and broken loop pump speeds were reduced to simulate the pump coastdown of a PWR primary coolant pump; the power to the electrically heated core was automatically controlled to simulate the thermal response of nuclear fuel rods for Test S-SB-2 and to simulate the thermal response of nuclear fuel rods and to offset the Mod-3 System heat losses for Test S-SB-2A. For Test S-SB-2A, at the indication of core uncovering, the additional power for the system heat losses was removed and the test continued on a power decay curve similar to Test S-SB-2. At 8.8 s (8.1 s for Test S-SB-2A) after the pressurizer pressure had reached 12.48 MPa, the feedwater valve for the broken loop steam generator was closed. At 28.4 s (28.0 s for Test S-SB-2A) after the pressurizer reached 12.48 MPa, the high pressure injection pumps were activated to begin emergency core coolant at a rate varying according to the system pressure. At 63.4 s after the pressurizer reached 12.48 MPa, the broken loop pump was tripped and allowed to coast down naturally, and the auxiliary feedwater was started into the steam generator secondary sides at rates of 0.030 L/s

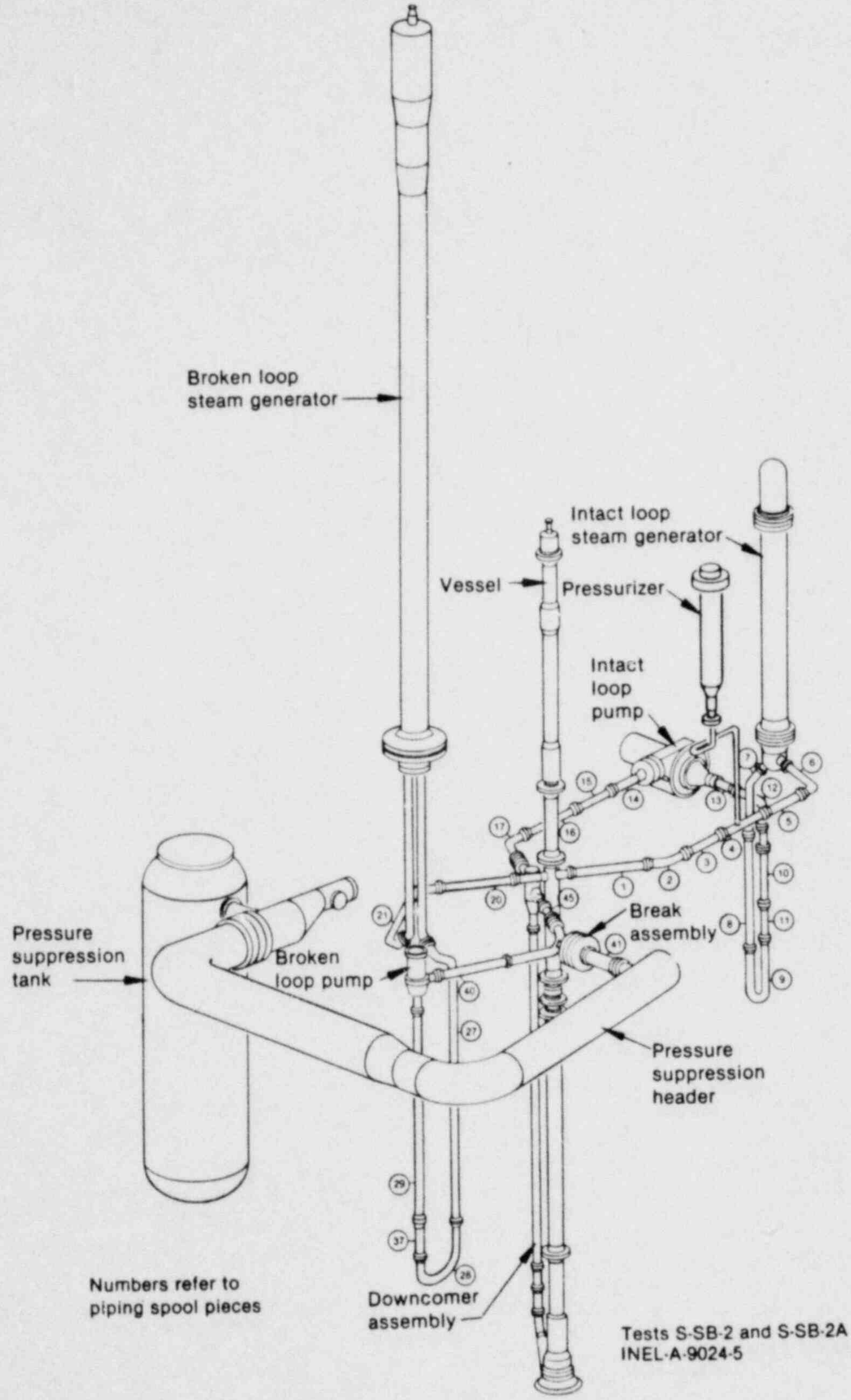

Figure 1. Semiscale Mod-3 system for cold leg break configuration - isometric.

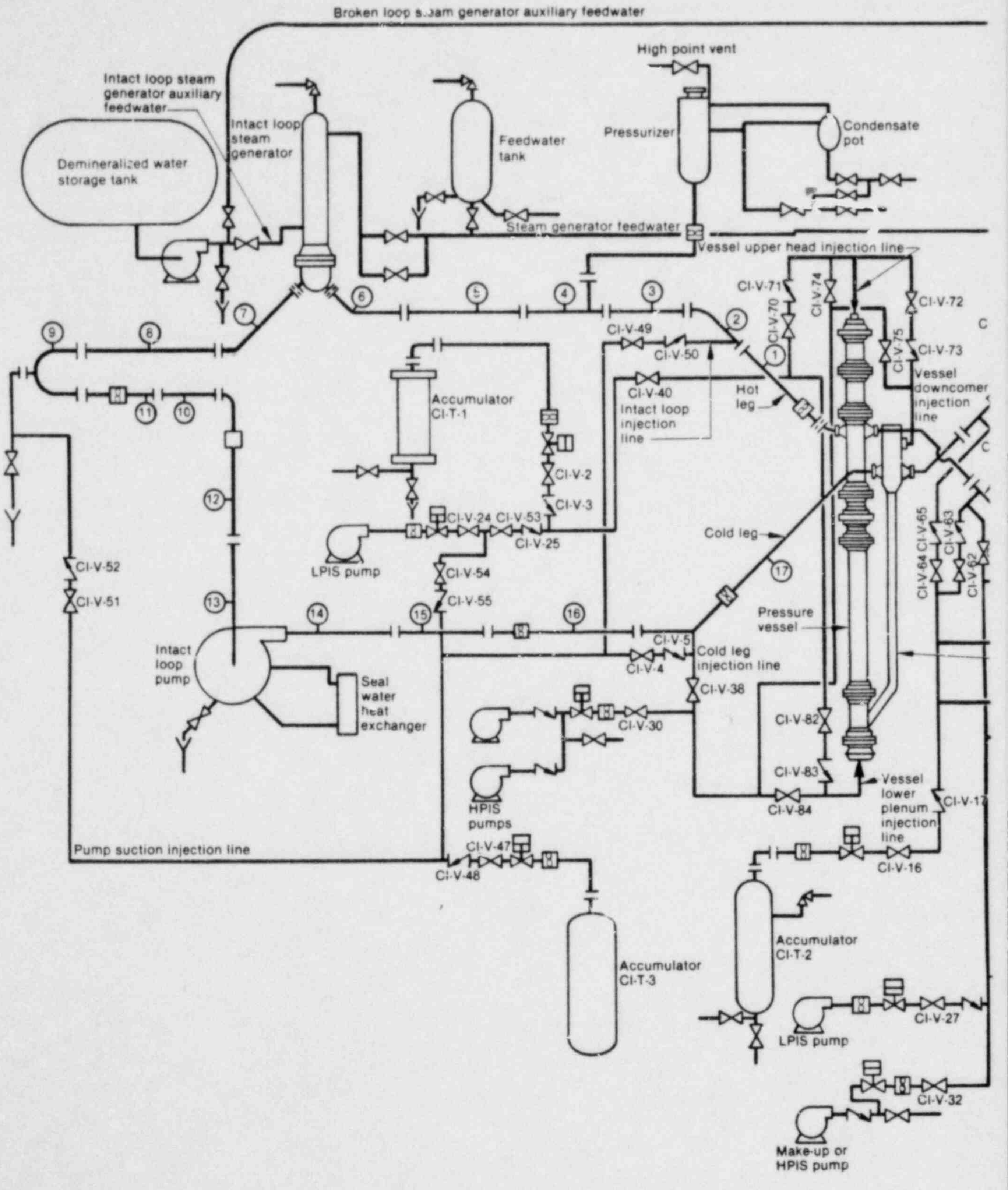

Figure 2. Se:niscale Mod-3 system for

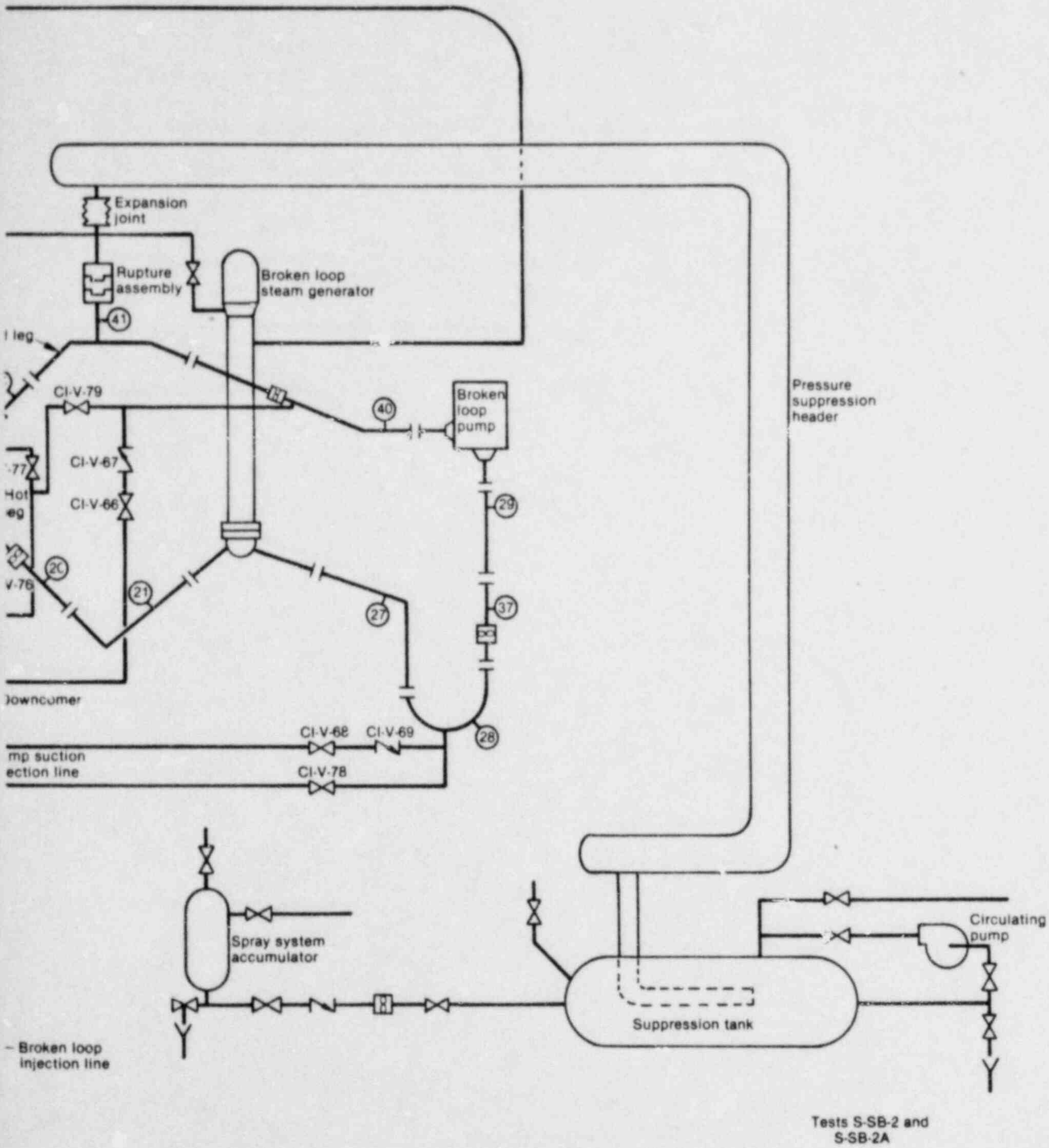

ld leg break configuration - schematic.

into the intact loop generator and of 0.010 L/s into the broken loop generator. At 752.8 s (123.3 s for Test S-SB-2A) after the pressurizer pressure had reached 12.48 MPa, the intact loop pump was tripped and allowed to coast down naturally. When the system pressure reached 4.22 MPa, the accumulators began to discharge water into the broken and intact loops. After the preset water volumes were injected, nitrogen was injected until the test was terminated. When the system stabilized (i.e., pressure stopped declining) at a pressure greater than 0.91 MPa, the steam generator steam valves were opened to enhance system depressurization. When system pressure reached 0.91 MPa, the high pressure injection pump rates were increased substantially to simulate the sum of the low pressure injection system and the high pressure system ECC flows. The tests were terminated after the system pressure was below 0.91 MPa which was the initiation pressure for the low pressure injection system.

2. Initial Test Conditions and Sequence of Events

Initial conditions in the Semiscale Mod-3 System just before blowdown are given in Tables 1 and 2.

The following deviations from specified test conditions occurred, but were considered acceptable:

1. In both tests, the pressure in the accumulators was readjusted to 4.22 MPa prior to reaching the system pressure when injection was to start

2. In both tests, the water volume from the broken loop accumulator was 8.4 liters which was less than the specified volume of 1[illegible] liters

3. In Test S-SB-2, the intact loop pump continued to run 629 s more than was specified

4. In Test S-SB-2A the pressure in the pressure suppression system was not controlled as specified because sufficient steam flow could not be obtained from the steam supply system.

The sequence of events relative to rupture is given in Table 3.

TABLE 1. CONDITIONS AT BLOWDOWN INITIATION

	Measured[a]		Specified
	Test S-SB-2	Test S-SB-2A	Tests S-SB-2 and S-SB-2A
Core power (MW)	2.11	2.11	2.10 ± 0.05
System pressure (MPa)	15.69	15.56	15.51 ± 0.04
Intact loop cold leg fluid temperature (K)	551.0	550.0	550 ± 1
Broken loop cold leg fluid temperature (K)	551.0	550.0	550 ± 1
Intact loop hot leg to cold leg temperature differential (K)	34.0	37.0	33 ± 1
Broken loop hot leg to cold leg temperature differential (K)	34.0	34.0	33. ± 1
Intact loop cold leg flow (L/s)	11.27	11.33	b
Broken loop cold leg flow (L/s)	3.68	3.71	b
Steam generator feedwater temperature[c] (K)	487.0	488.0	495. ± 6
Intact loop steam generator liquid level (cm) (above top of tube sheet)	329	315	295 ± 5
Broken loop steam generator liquid level (cm) (above top of tube sheet)	949	1005	998 ± 5
Pressure suppression tank pressure (MPa)	0.65	0.22	0.65
Pressure suppression tank water level (cm)	empty	empty	empty

a. Measured initial conditions are taken from digital acquisition system read just prior to blowdown initiation.

b. Flow is not specified since it must be adjusted to achieve the required differential temperature across the core.

c. One source of feedwater was used for both intact and broken loops.

TABLE 2. PRIMARY COOLANT TEMPERATURE DISTRIBUTION PRIOR TO RUPTURE[a]

	Detector	Temperature (K)	
		Test S-SB-2	Test S-SB-2A
Intact loop hot leg (near vessel)	RFI-2	585	586
Intact loop pump suction	RFI-7	546	546
Intact loop cold leg (near downcomer)	RFI-17	551	550
Broken loop hot leg (near vessel)	RFB-20	585	585
Broken loop pump suction	TFB-SGOL	553	553
Broken loop cold leg (near downcomer)	RFB-45	551	550
Downcomer (near top)	TFD-83 or TFD-170	551	551
Downcomer (middle)	TFD-269	552	552
Downcomer (near bottom)	TFD-347	551	551
Core (top of heated length)	TFG-10DE-12	599	599
Core (middle of heated length)	TFG-5AB-45	568	568
Core (bottom of heated length)	TFG-1AB-12	552	553

a. Average of data taken from 5 s to 0.5 s prior to blowdown initiation.

TABLE 3. SEQUENCE OF EVENTS DURING TESTS S-SB-2 AND S-SB-2A

Event	Time Relative to Rupture (s) Test S-SB-2	Test S-SB-2A
Core power level established	-257	-239
Makeup pump and pressurizer heaters off	-2.5	-2.5
Pressurizer pressure equal to 12.48 MPa	17.2	16.9
Steam valves on steam generators close	18.0	17.0
Core power decay starts	20.6	20.3
Intact and broken loop pump coastdowns start	20.6	20.3
Feedwater valves on steam generators close (BL)	26.0	25.0
Feedwater valves on steam generators close (IL)	--	28.0
HPIS injection starts	45.6	45.0
Broken loop pump tripped off	80.6	80.5
Auxiliary feedwater started	80.6	78.0
Intact loop pump tripped off	770.0	140.2
Core uncovery and start core power ramp	--	502.0
ECC accumulator intact loop cold leg flow started	647.7	724.2
ECC accumulator broken loop cold leg flow started	683.4	759.9
Auxiliary feedwater shut off	4533.9	1830.0
Core power terminated	4533.9	4395.6
DAS off	4686.9	4962.6

III. DATA PRESENTATION

The data from Semiscale Mod-3 Tests S-SB-2 and S-SB-2A are presented with brief comment. Processing analysis has been performed only to the extent necessary to obtain appropriate engineering units and to ensure that data are reasonable and consistent. In all cases, in converting transducer output to engineering units a homogeneous fluid was assumed. Further interpretation and analysis should consider that sudden decompression processes such as those occurring during blowdown may have subjected the measurement device to nonhomogeneous fluid conditions.

The performance of the system during Tests S-SB-2 and S-SB-2A was monitored by detectors. The data obtained were recorded on a digital data acquisition system. The long term data (-0 to 4500 s) for Tests S-SB-2 and S-SB-2A presented in this report were recorded at an effective sample rate of 0.20 and 0.19 points per second, respectively. Short term data (-20 to 256 s) were recorded at a sample rate of 3.33 points per second.

The data are presented in some instances in the form of composite graphs to facilitate comparison of the values of given variables. The scales selected for the graphs do not reflect the obtainable resolution of the data. (The data processing techniques are described further in Reference 1 and Appendix A.)

Figures 3 through 10 provide supporting information for interpretation of the data graphs. Table 4 groups the measurements according to type; identifies the location and range of the detector and actual recording range of the data acquisition system; provides brief comments regarding the data; and references the detector and comments to the corresponding figure. Figures 11 through 398 (data graphs) present all the blowdown data obtained. Time zero on the graphs is the time of rupture initiation. Appendix A provides information explaining the data acquisition system capabilities. Appendix B explains posttest data adjustments. Appendix C presents an analysis of selected data which provide a guide to the uncertainty associated with data measurements in the Semiscale Mod-3 system.

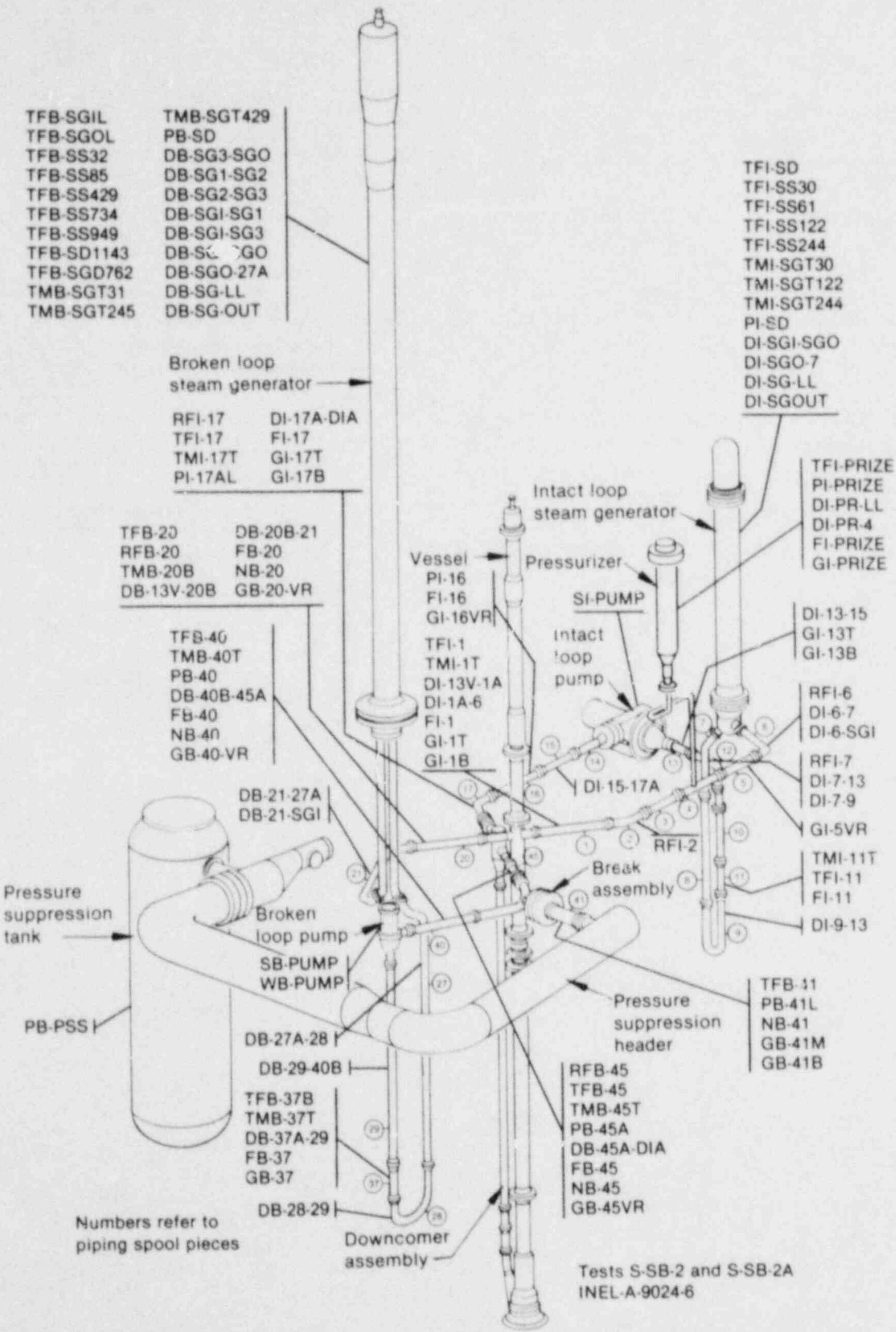

Figure 3. Semiscale Mod-3 system and instrumentation for cold leg break configuration—isometric.

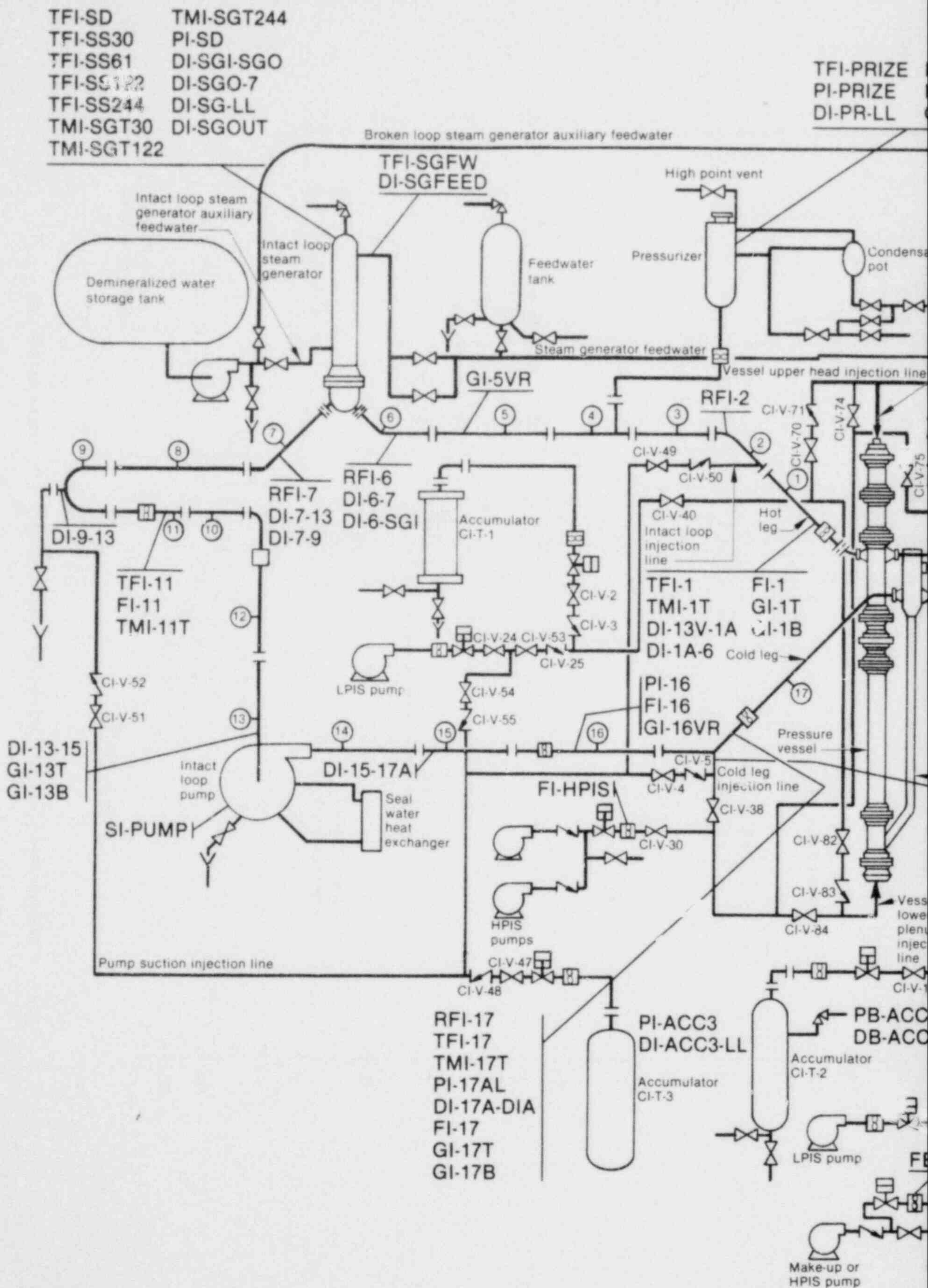

Figure 4. Semiscale Mod-3 system and in

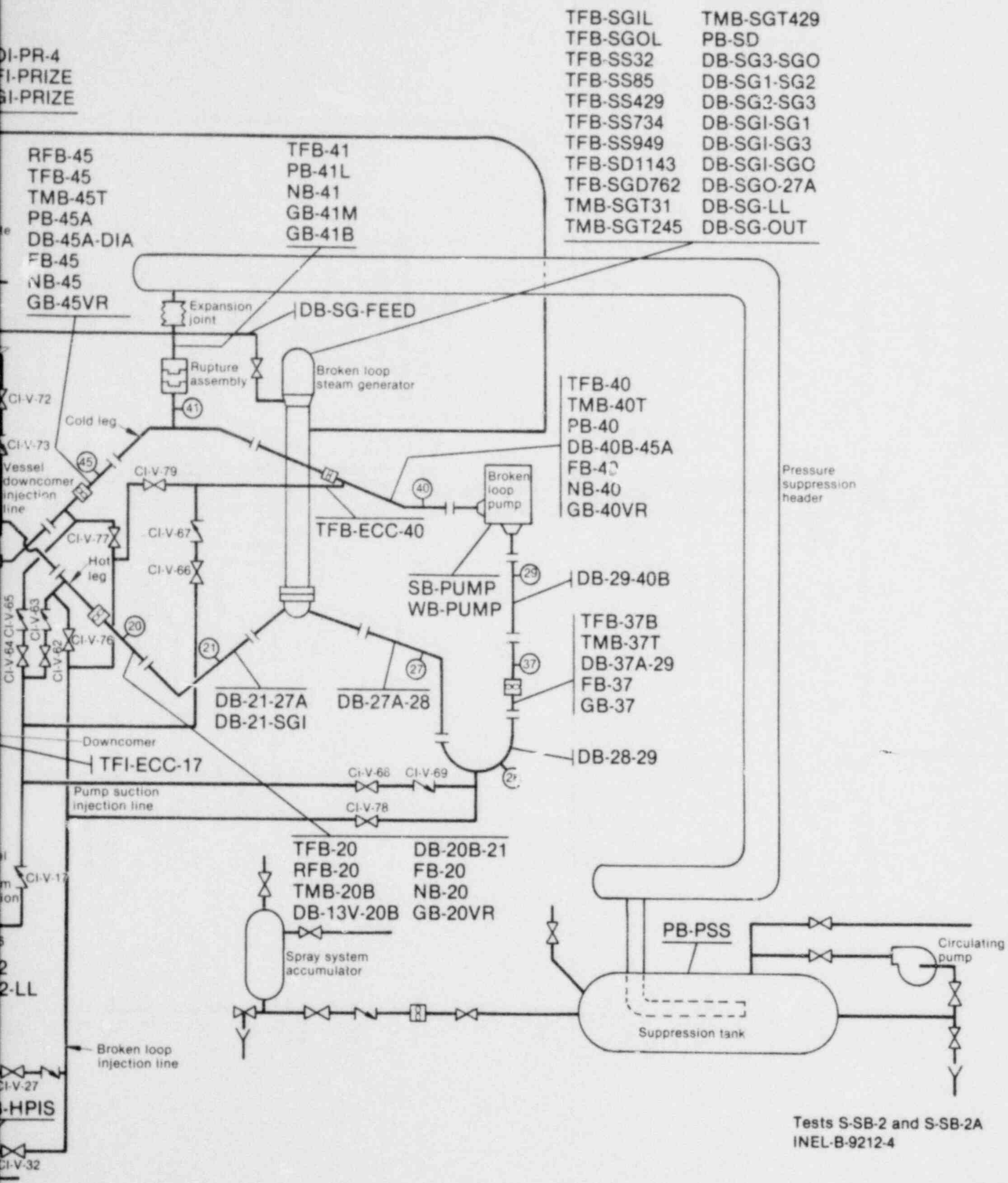

trumentation for cold leg break configur··ion—sc···tic.

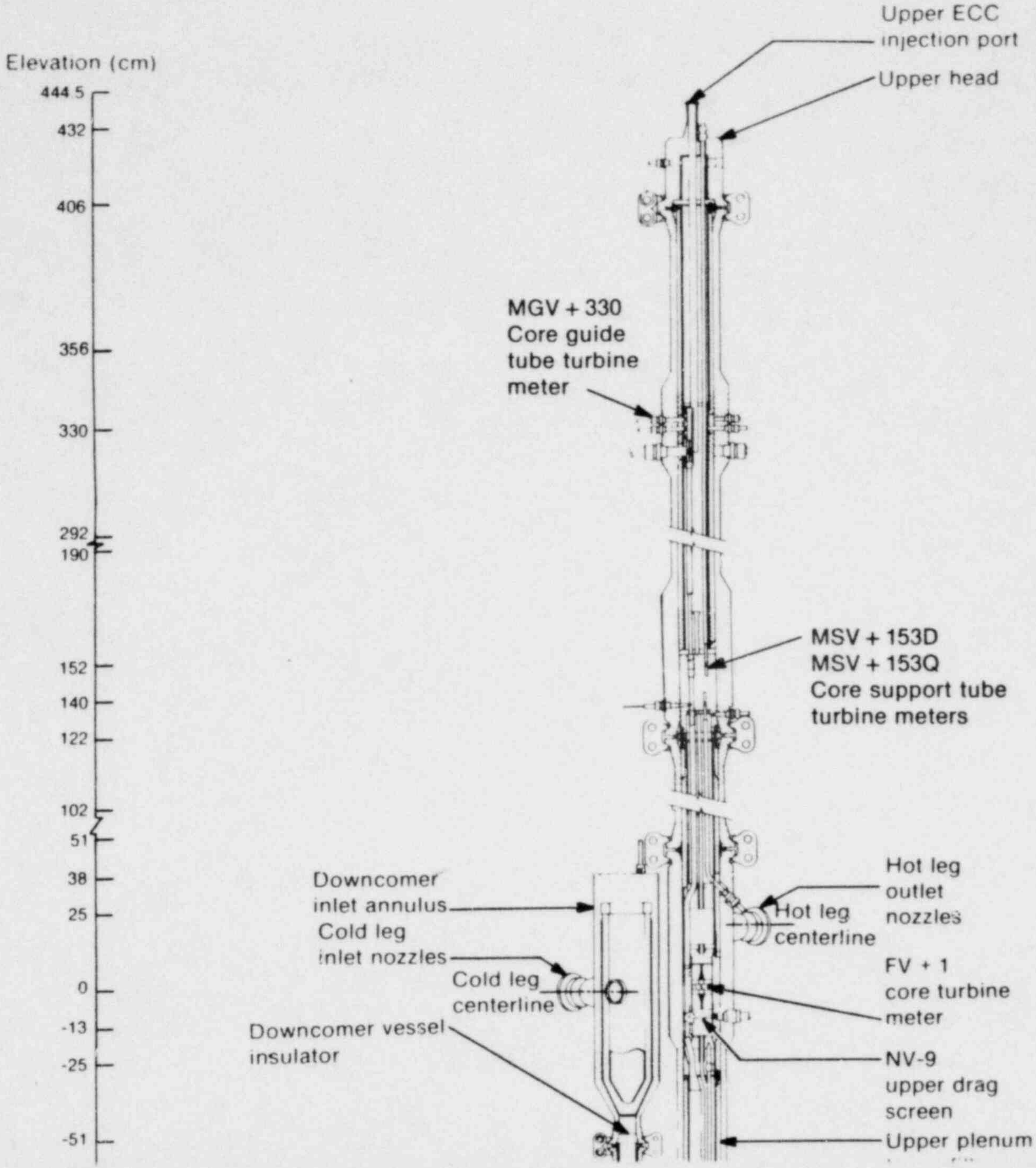

Elevation (cm)
444.5
432
406
356
330
292
190
152
140
122
102
51
38
25
0
-13
-25
-51
Upper ECC injection port
Upper head
MGV + 330
Core guide tube turbine meter
MSV + 153D
MSV + 153Q
Core support tube turbine meters
Hot leg outlet nozzles
Hot leg centerline
Downcomer inlet annulus
Cold leg inlet nozzles
Cold leg centerline
FV + 1 core turbine meter
Downcomer vessel insulator
NV-9 upper drag screen
Upper plenum

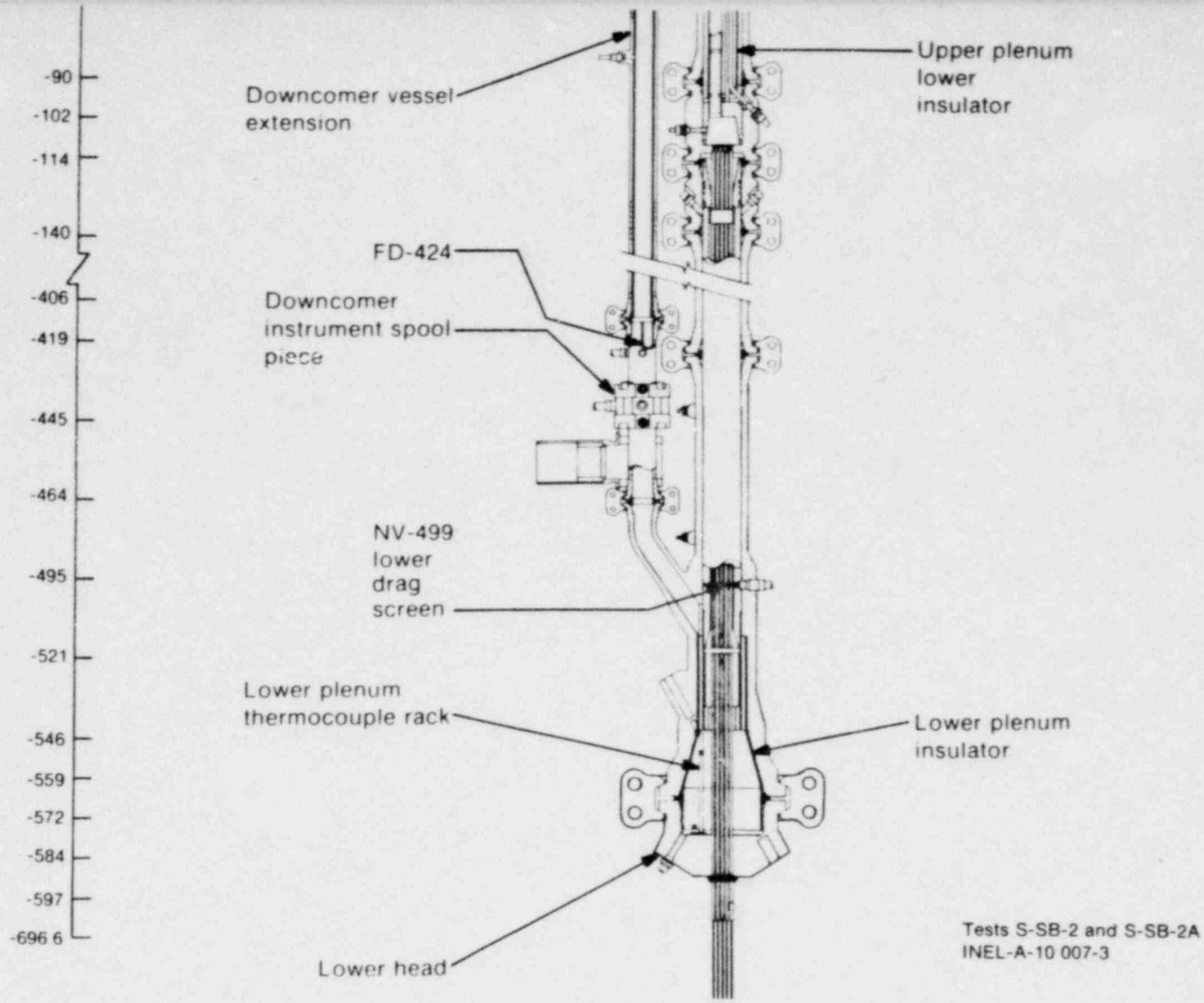

Figure 5. Semiscale Mod-3 pressure vessel and downcomer cross-section showing instrumentation.

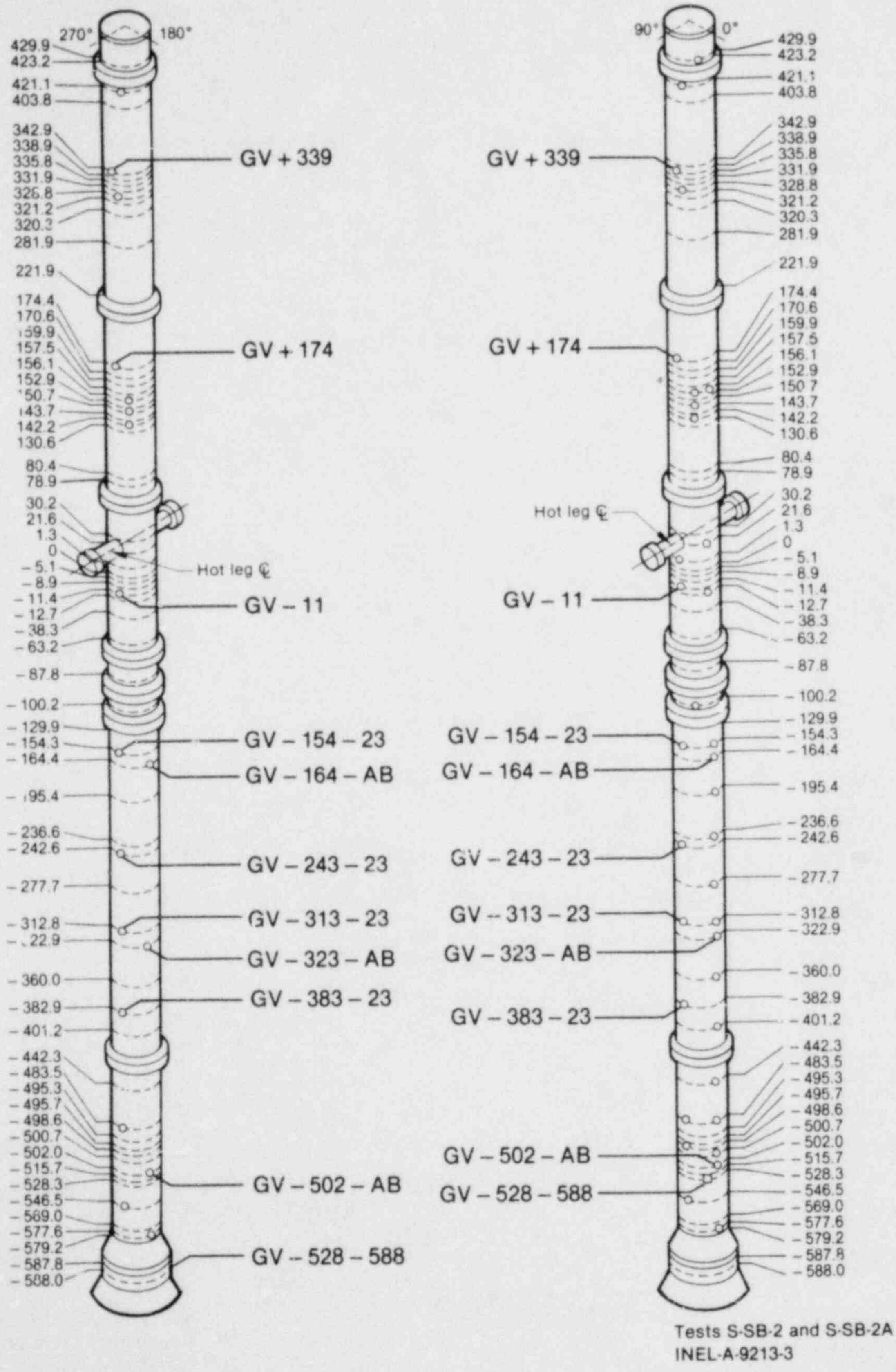

Figure 6. Semiscale Mod-3 pressure vessel—isometric showing instrumentation.

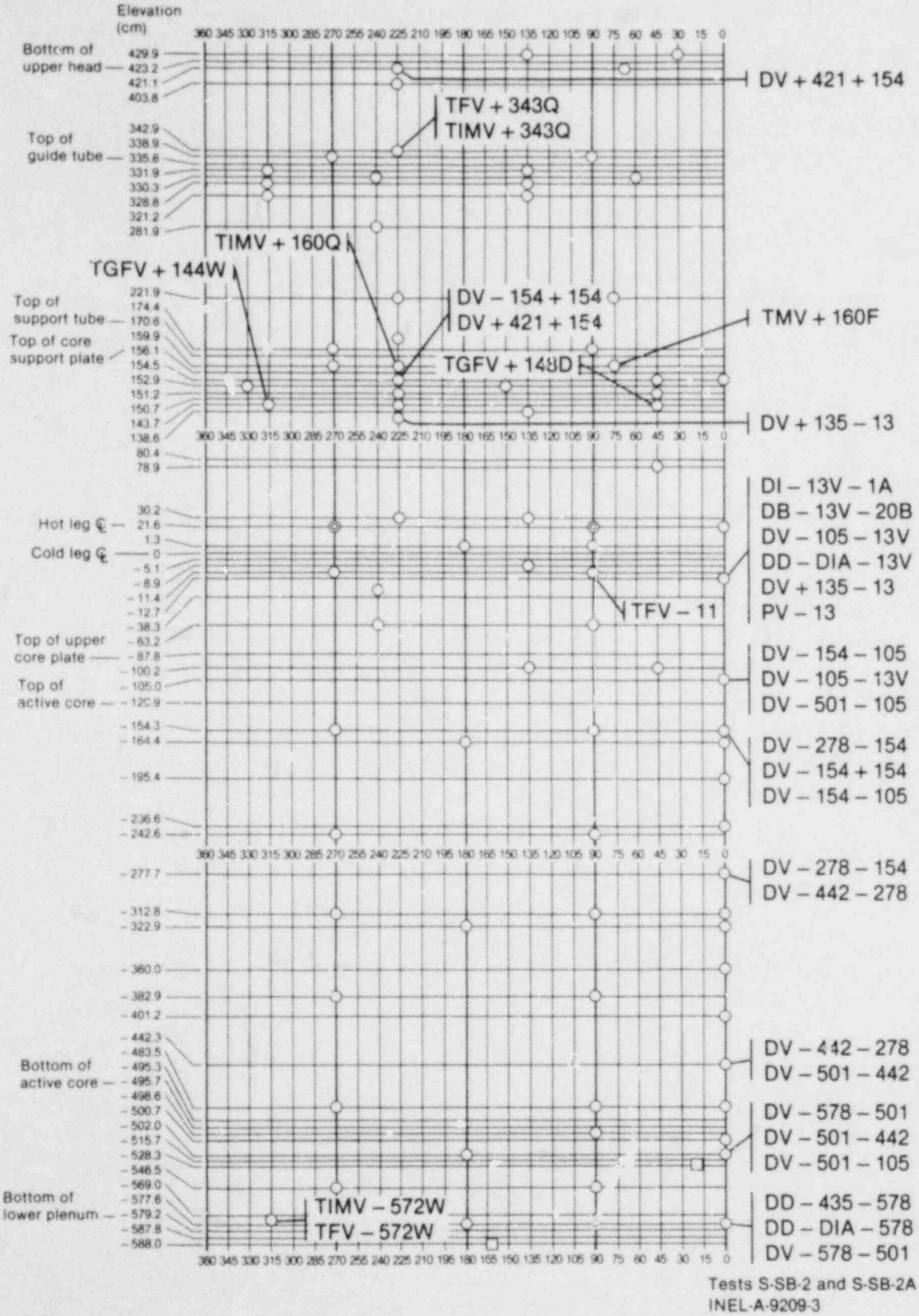

Figure 7. Semiscale Mod-3 pressure vessel—penetrations and instrumentation.

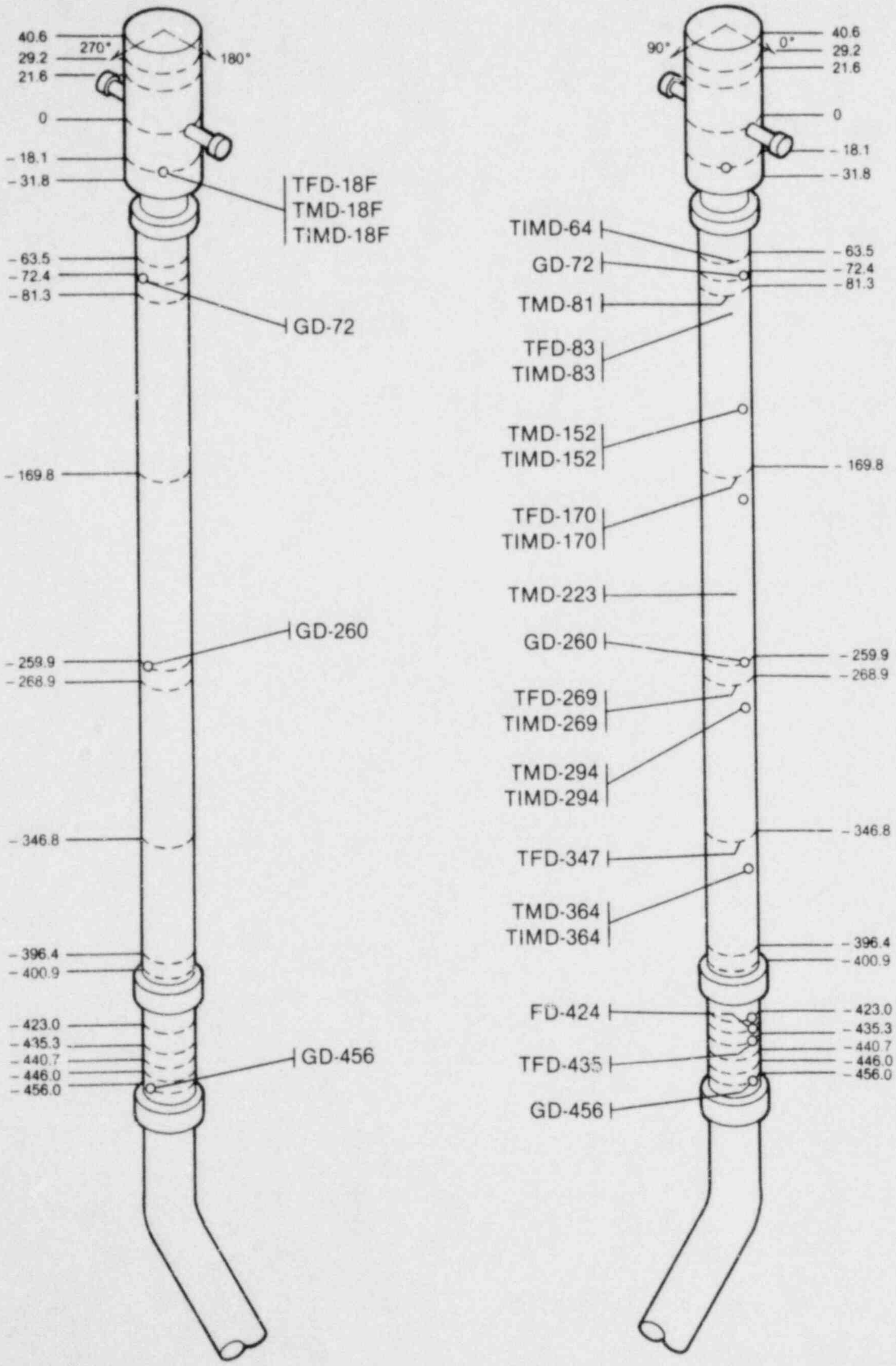

Figure 8. Semiscale Mod-3 downcomer—isometric showing instrumentation.

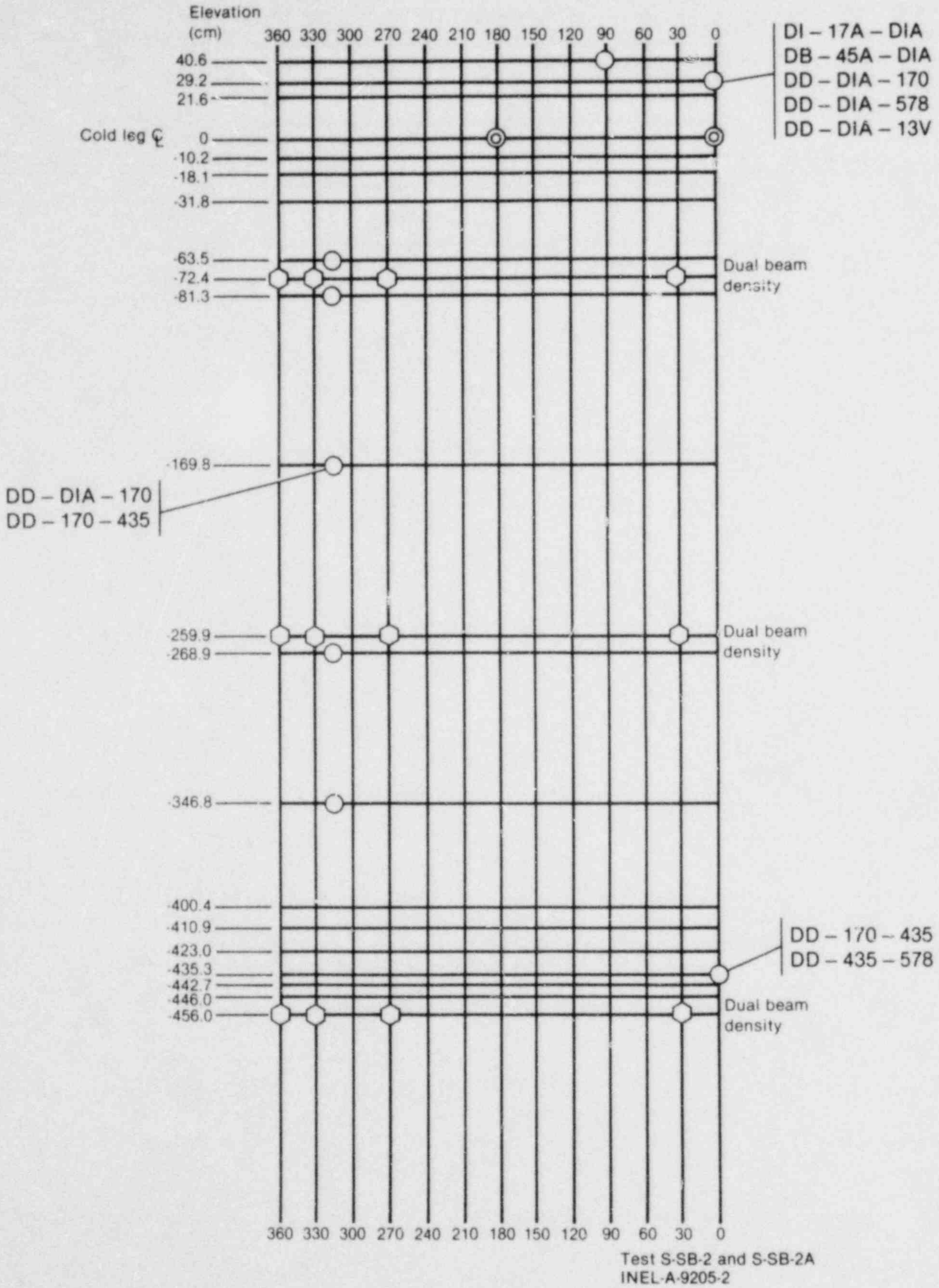

Figure 9. Semiscale Mod-3 downcomer—penetrations and instrumentation.

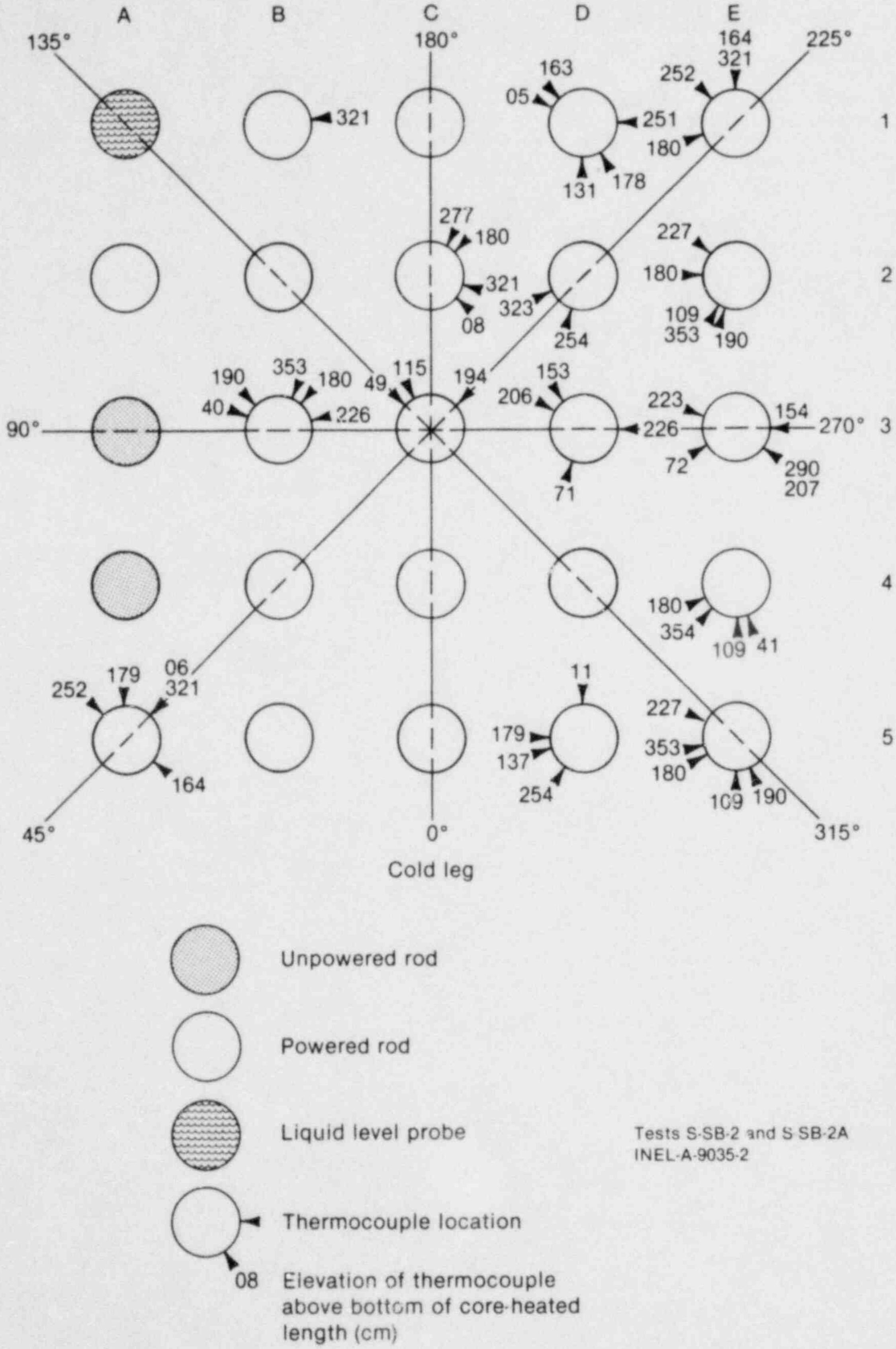

Figure 10. Semiscale Mod-3 heated core—plan view.

TABLE 4. DATA PRESENTATION FOR SEMISCALE MOD-3 TESTS MOD3- S-SB-2 AND S-SB-2A

Measurement	Location and Comments[a]	Data Acquisition Range[a]		Figure[a]	Measurement Comments[b]
		Detector	System		
FLUID TEMPERATURE	Chromel-Alumel thermocouples unless specified otherwise.				
Intact Loop		0 to 1533 K	0 to 820 K		
TFI-1	Hot leg, Spool 1, 50 cm from vessel center.			11	
RFI-2	Hot leg, Spool 2, 99 cm from vessel center, 10 cm upstream of hot leg injection port (platinum resistance bulb).	0 to 811 K	0 to 811 K	12	
RFI-6	Hot leg, Spool 6, 200 cm from vessel center (platinum resistance bulb).	0 to 811 K	0 to 811 K	13	
RFI-7	Cold leg, Spool 7, 964 cm from downcomer center (platinum resistance bulb).	0 to 811 K	0 to 811 K	14	
TFI-11	Cold leg, Spool 11, 438 cm from downcomer center.			15	Test S-SB-2A only.
RFI-17	Cold leg, Spool 17, 92 cm from downcomer center, 7 cm upstream of cold leg injection port (platinum resistance bulb).	0 to 811 K	0 to 811 K	16	
TFI-17	Cold leg, Spool 17, 60 cm from downcomer center.			17	
Broken Loop		0 to 1533 K	0 to 820 K		
RFB-20	Hot leg, Spool 20, 73 cm from vessel center, 14 cm downstream of hot leg injection port (platinum resistance bulb).	0 to 811 K	0 to 811 K	18	
TFB-20	Hot leg, Spool 20, 84 cm from vessel center, 25 cm downstream of hot leg injection port.			19	
TFB-SGIL	Steam generator inlet leg, 382 cm from vessel center.			20	
TFB-SGOL	Steam generator outlet leg, 936 cm from downcomer center.			21	
TFB-37B	Cold leg, Spool 37, 330 cm from downcomer center.			22	Test S-SB-2A only.
TFB-40	Cold leg, Spool 40, 213 cm from downcomer center.			23,24	
TFB-41	Cold leg, Spool 41, 6 cm upstream of rupture disc assembly, 191 cm from downcomer center.			25	
RFB-45	Cold leg, Spool 45, 89 cm from downcomer center (platinum resistance bulb).	0 to 811 K	0 to 811 K	26	
TFB-45	Cold leg, Spool 45, 78 cm from downcomer center.			27	
Downcomer		0 to 1533 K	0 to 820 K		
TFD-18F	In downcomer inlet annulus, 18 cm below cold leg centerline at 75°.				Detector failed on Test S-SB-2A; Test S-SB-2A only.
TFD-83	In downcomer extension, 83 cm below cold leg centerline.			28	Detector failed on Test S-SB-2A.
TFD-170	In downcomer extension, 170 cm below cold leg centerline.			29	Test S-SB-2A only.
TFD-269	In downcomer extension, 269 cm below cold leg centerline.			30	
TFD-347	In downcomer extension, 347 cm below cold leg centerline.			31	
TFD-435	In downcomer instrument spool, 435 cm below cold leg centerline.			32	Test S-SB-2A only.

TABLE 4. (continued)

Measurement	Location and Comments[a]	Data Acquisition Range[a] Detector	System	Figure[a]	Measurement Comments[b]
Vessel		0 to 1533 K	0 to 820 K		
Vessel Upper Plenum					
TFV-572W	In vessel lower plenum, 572 cm below cold leg centerline at 315°.			33	
Vessel Lower Plenum					
TFV-11	In vessel, 11 cm below cold leg centerline.			34	
Vessel Upper Head					
TFV+343Q	In vessel upper head filler, 343 cm above cold leg centerline at 325°.			35	
Vessel Guide Tube					
TFGV+144W	In vessel guide tube, 144 cm above cold leg centerline at 315°.			36	Test S-SB-2A only.
Vessel Support Tube					
TFSV+148D	In vessel support tube, 148 cm above cold leg centerline at 45°.			37	Test S-SB-2A only.
Core Grid Spacers		0 to 1533 K	0 to 1580 K		
Grid Spacer 1	490 cm below cold leg centerline, 6 cm above bottom of heated length.				
TFG-1AB-12	Thermocouple in space defined by Columns A and B, Rows 1 and 2.			38	
Grid Spacer 2	450 cm below cold leg centerline, 46 cm above bottom of heated length.				
TFG-2AB-23	Thermocouple in space defined by Columns A and B, Rows 2 and 3.			39	
Grid Spacer 4	370 cm below cold leg centerline, 126 cm above bottom of heated length.				
TFG-4AB-23	Thermocouple in space defined by Columns A and B, Rows 2 and 3.			40	Detector failed on Test S-SB-2.
Grid Spacer 5	330 cm below cold leg centerline, 166 cm above bottom of heated length.				
TFG-5AB-45	Thermocouple in space defined by Columns A and B, Rows 4 and 5.			41	
Grid Spacer 6	290 cm below cold leg centerline, 206 cm above bottom of heated length.				
TFG-6DE-34	Thermocouple in space defined by Columns D and E, Rows 3 and 4.			42	
Grid Spacer 7	250 cm below cold leg centerline, 246 cm above bottom of heated length.				
TFG-7AB-34	Thermocouple in space defined by Columns A and B, Rows 3 and 4.			43	
Grid Spacer 8	210 cm below cold leg centerline, 286 cm above bottom of heated length.				
TFG-8DE-23	Thermocouple in space defined by Columns D and E, Rows 2 and 3.			44	
Grid Spacer 9	170 cm below cold leg centerline, 326 cm above bottom of heated length.				
TFG-9DE-12	Thermocouple in space defined by Columns D and E, Rows 1 and 2.			45	
TFG-9DE-45	Thermocouple in space defined by Columns D and E, Rows 4 and 5.			46	Test S-SB-2A only.
Grid Spacer 10	130 cm below cold leg centerline, 366 cm above bottom of heated length.				
TFG-10DE-12	Thermocouple in space defined by Columns D and E, Rows 1 and 2.			47	

TABLE 4. (continued)

Measurement	Location and Comments[a]	Data Acquisition Range[a] Detector	System	Figure[a]	Measurement Comments[b]
ECC System		0 to 1533 K	0 to 820 K		
TFI-EEC-17	On centerline of ECC line, 72 cm from junction with Spool 17.			48	
TFG-ECC-40	On centerline of ECC line at junction with Spool 40.			49	Detector failed on Test S-SB-2.
Steam Generator		0 to 1533 K	0 to 820 K		
Intact Loop					
TFI-SGFW	In feedwater line leading to steam generator.			50	
TFI-SD	In steam generator steam dome, 320 cm above top of tube sheet.			51	
TFI-SS30	Secondary side, 30 cm above top of tube sheet.			52	
TFI-SS61	Secondary side, 61 cm above top of tube sheet.			53	Test S-SB-2A only.
TFI-SS122	Secondary side, 122 cm above top of tube sheet.			54	
TFI-SS244	Secondary side, 244 cm above top of tube sheet.			55	
Broken Loop					
TFB-SS32	Secondary side, 32 cm above top of tube sheet.			56	
TFB-SS85	Secondary side, 85 cm above top of tube sheet.			57	Test S-SB-2A only.
TFB-SS429	Secondary side, 429 cm above top of tube sheet.			58	
TFB-SS734	Secondary side, 734 cm above top of tube sheet.			59	Test S-SB-2A only.
TFB-SS949	Secondary side, 949 cm above bottom of tube sheet.			60	
TFB-SD1143	Secondary side steam dome, 1143 cm above top of tube sheet.			61	
TFB-SGD762	Secondary side, downcomer, 762 cm above top of tube sheet.			62	
Pressurizer		0 to 1533 K	0 to 820 K		
TFI-PRIZE	In surge line near pressurizer exit, between turbine flowmeter and pressurizer.			63	
MATERIAL TEMPERATURE	Chromel-Alumel thermocouples unless specified otherwise.				
Intact Loop		0 to 1533 K	0 to 820 K		
TMI-[illegible]	Hot leg, Spool 1, top, 1.6 mm from pipe inside diameter (ID), 68 cm from vessel center.			64	
TMI-11T	Cold leg, Spool 11, top, 1.6 mm from pipe ID, 46[illegible] cm from downcomer center.			65	Test S-SB-2A only.
TMI-17T	Cold leg, Spool 17, top, 1.6 mm from pipe ID, 68 cm from downcomer center.			66	
Broken Loop		0 to 1533 K	0 to 820 K		
TMB-20B	Hot leg, Spool 20, bottom, 1.6 mm from pipe ID, 91 cm from vessel center.			67	
TMB-37T	Cold leg, Spool 37, top, 1.6 mm from pipe ID, 321 cm from downcomer center.			68	Test S-SB-2A only.
TMB-40T	Cold leg, Spool 40, top, 1.6 mm from pipe ID, 196 cm from downcomer center.			[illegible]9	Test S-SB-2A only.
TMB-45T	Cold leg, Spool 45, top, 1.6 mm from pipe ID, 98 cm from downcomer center.			70	

TABLE 4. (continued)

Measurement	Location and Comments[a]	Data Acquisition Range[a] Detector	System	Figure[a]	Measurement Comments[b]
Downcomer		0 to 1533 K	0 to 820 K		
TMD-18F	On downcomer inlet annulus, 18 cm below cold leg centerline at 75°.			71	Test S-SB-2A only
TMD-81	On downcomer extension, 81 cm below cold leg centerline.			72	
TMD-152	On downcomer extension, 152 cm below cold leg centerline.			73	Test S-SB-2A only.
TMD-223	On downcomer extension, 223 cm below cold leg centerline.			74	Test S-SB-2A only.
TMD-294	On downcomer extension, 294 cm below cold leg centerline.			75	
TMD-364	On downcomer extension, 364 cm below cold leg centerline.			76	
TMD-456	On downcomer instrumented spool piece, 456 cm below cold leg centerline.				Detector failed on Test S-SB-2A; Test S-SB-2A only.
Downcomer Insulator		0 to 1533 K	0 to 820 K		
TIMD-18F	On downcomer inlet annulus insulator, 18 cm below cold leg centerline at 75°.			77	Test S-SB-2A only.
TIMD-64	On downcomer extension insulator, 64 cm below cold leg centerline.			78	Test S-SB-2A only.
TIMD-83	On downcomer extension insulator, 83 cm below cold leg centerline.			79	
TIMD-152	On downcomer extension insulator, 152 cm below cold leg centerline.			80	Test S-SB-2A only.
TIMD-170	On downcomer extension insulator, 170 cm below cold leg centerline.			81	Test S-SB-2A only.
TIMD-269	On downcomer extension insulator, 269 cm below cold leg centerline.			82	Test S-SB-2A only.
TIMD-294	On downcomer extension insulator, 294 cm below cold leg centerline.			83	
TIMD-364	On downcomer extension insulator, 364 cm below cold leg centerline.			84	
Vessel		0 to 1533 K	0 to 820 K		
TMV+160F	In vessel on upper head filler, 160 cm above cold leg centerline at 75°.			85	Test S-SB-2A only.
Vessel Insulator		0 to 1533 K	0 to 820 K		
TIMV+343Q	In vessel on upper head insulator, 343 cm above cold leg centerline at 225°.				Detector failed on Test S-SB-2A; Test S-SB-2A only.
TIMV+160Q	In vessel on upper plenum insulator, 160 cm above cold leg centerline at 225°.			86	Test S-SB-2A only.
TIMV-572W	In vessel on lower head insulator, 572 cm below cold leg centerline at 315°.			87	
Steam Generator		0 to 1533 K	0 to 820 K		
Intact Loop					
TMI-SGT30	On a steam generator tube, 30 cm above top of tube sheet on outside diameter (OD) tube.			88	Detector failed on Test S-SB-2A.
TMI-SGT122	On a steam generator tube, 122 cm above top of tube sheet on OD of tube.			89	
TMI-SGT244	On a steam generator tube, 244 cm above top of tube sheet on OD of tube.			90	Test S-SB-2A only.

TABLE 4. (continued)

Measurement	Location and Comments[a]	Data Acquisition Range[a] Detector	System	Figure[a]	Measurement Comments[b]
Broken Loop		0 to 1533 K	0 to 820 K		
TMB-SGT31	On a steam generator tube, 31 cm above top of tube sheet on OD of tube.			91	
TMB-SGT245	On a steam generator tube, 245 cm above top of tube sheet on OD of tube.			92	Test S-SB-2A only.
TMB-SGT429	On a steam generator tube, 429 cm above top of tube sheet on OD of tube.			93	
TMB-SGT734	On a steam generator tube, 734 cm above top of tube sheet on OD of tube.			9?	Test S-SB-2A only.
CORE HEATER CLADDING TEMPERATURE	Chromel-Alumel thermocouples.				
High-Power Heaters		0 to 1533 K	0 to 1580 K		
TH-B3-40 TH-B3-180 TH-B3-190 TH-B -226 TH-B3-353	Heater at Column B, Row 3. Toermocouples 40 cm (120°), 180 cm (225°), 190 cm (135°), 226 cm (270°), and 353 cm (210°) above bottom of heated length.			95, 96 97, 98 99	Detectors TH-B3-40 and TH-B3-190 on Test S-SB-2A only.
TH-C2-08 TH-C2-180 TH-C2-277 TH-C2-321	Heater at Column C, Row 2. Thermocouples 8 cm (285°), 180 cm (225°), 277 cm (210°), and 321 cm (270°) above bottom of heated length.			100, 101 102, 103	Detectors TH-C2-180 and TH-C2-277 on Test S-SB-2A only.
TH-C3-49 TH-C3-115 TH-C3-194	Heater at Column C, Row 3. Thermocouples 49 cm (135°), 115 cm (165°), and 194 cm (225°) above bottom of heated length.			104, 105 106	
TH-D2-254 TH-D2-323	Heater at Column D, Row 2. Thermocouples 254 cm (15°) and 323 cm (60°) above bottom of heated length.			107, 108	Detector TH-D2-254 on Test S-SB-2A only.
TH-D3-71 TH-D3-153 TH-D3-206 TH-D3-226	Heater at Column D, Row 3. Thermocouples 71 cm (15°), 153 cm (135°), 206 cm (120°), and 226 cm (270°) above bottom of heated length.			109, 110 111, 112	
Low-Power Heaters		0 to 1533 K	0 to 1580 K		
TH-A5-06 TH-A5-164 TH-A5-179 TH-A5-252 TH-A5-321	Heater at Column A, Row 5. Thermocouples 6 cm (225°), 164 cm (300°), 179 cm (180°), 252 cm (165°), and 321 cm (225°) above bottom of heared length.			113, 114 115, 116 117	Detector TH-A5-06 on Test S-SB-2 only.
TH-B1-321	Heater at Column B, Row 1. Thermocouple 321 cm (270°) above bottom of heated length.			118	
TH-D1-05 TH-D1-131 TH-D1-163 TH-D1-178 TH-D1-251	Heater at Column D, Row 1. Thermocouples 5 cm (105°), 131 cm (0°), 16? cm (120°), 178 cm (330°), and 251 cm (270°) above bottom of heated length.			119, 120 121, 122 123	Detector TH-D1-178 on Test S-SB-2A only.
TH-D5-11 TH-D5-137 TH-D5-179 TH-D5-254	Heater at Column D, Row 5. Thermocouples 11 cm (80°), 137 cm (75°), 179 cm (90°), and 254 cm (45°) above bottom of heated length.			124, 125 126, 127	Detector TH-D5-11 on Test S-SB-2 only.
TH-E1-164 TH-E1-180 TH-E1-252 TH-E1-321	Heater at Column E, Row 1. Thermocouples 164 cm (180°), 180 cm (60°), 252 cm (120°), and 321 cm (180°) above bottom of heated length.			128, 129 130, 131	
TH-E2-109 TH-E2-180 TH-E2-190 TH-E2-227 TH-E2-353	Heater at Column E, Row 2. Thermocouples 109 cm (30°), 180 cm (90°), 190 cm (15°), 227 cm (120°), and 353 cm (30°) above bottom of heated length.			132, 133 134, 135 136	Detector TH-E2-109 failed on Test S-SB-2. Detector TH-E2-227 on test S-SB-2A is good for trend only, and from 49 to 103 seconds invalid data were removed and replaced by a straight horizontal line.

TABLE 4. (continued)

Measurement	Location and Comments[a]	Data Acquisition Range[a] Detector	System	Figure[a]	Measurement Comments[b]
Low Power Heaters (continued)		0 to 1533 K	0 to 1580 K		
TH-E3-72 TH-E3-154 TH-E3-207 TH-E3-223 TH-E3-290	Heater at Column E, Row 3. Thermocouples 72 cm (60°), 154 cm (270°), 207 cm (300°), 223 cm (90°), and 290 cm (300°) above bottom of heated length.			137, 138 139, 140 141	
TH-E4-41 TH-E4-109 TH-E4-180 TH-E4-354	Heater at Column E, Row 4. Thermocouples 41 cm (345°), 109 cm (0°), 180 cm (60°), and 354 cm (45°) above bottom of heated length.			142, 143 144, 145	Detector TH-E4-109 on Test S-SB-2 only. Detector TH-E4-180 failed on Test S-SB-2A.
TH-E5-109 TH-E5-180 TH-E5-190 TH-E5-227 TH-E5-353	Heater at Column E, Row 5. Thermocouples 109 cm (0°), 180 cm (60°), 190 cm (345°), 227 cm (120°), and 353 cm (75°) above bottom of heated length.			146, 147 148, 149 150	
PRESSURE					
Intact Loop					
PI-16	Cold leg, Spool 16, 144 cm from downcomer center.	0 to 17.237 MPa	0 to 20.29 MPa	151	
PI-17AL	Cold leg, Spool 17, 60 cm from downcomer center (low range).	0 to 3.477 MPa	0 to 3.45 MPa	152	
Broken Loop					
PB-40	Cold leg, Spool 40, 209 cm from downcomer center.	0 to 1[illegible].237 MPa	0 to 21.07 MPa	153	Test S-SB-2A only.
PB-41L	Cold leg, Spool 41, 163 cm from downcomer center (low range).	0 to 3.477 MPa	0 to 3.48 MPa	154	
PB-45A	Cold leg, Spool 45, 90 cm from downcomer center.	0 to 17.237 MPa	0 to 20.77 MPa	155	
Vessel					
PV-13	In vessel hot leg extension, 13 cm below cold leg centerline (tee off DP tap).	0 to 17.237 MPa	0 to 21.49 MPa	156	Detector failed on Test S-SB-2A.
ECC System		0 to 6.895 MPa			
PI-ACC3	In accumulator for intact loop.		0 to 8.305 MPa	157	
PB-ACC2	In accumulator for broken loop.		0 to 8.551 MPa	158	
Steam Generator		0 to 8.305 MPa			
Intact Loop					
PI-SD	Intact loop steam generator, secondary side steam dome.		0 to 10.50 MPa	159	
Broken Loop					
PB-SD	Broken loop steam generator, secondary side steam dome.		0 to 10.77 MPa	160	
Pressurizer					
PI-PRIZE	Pressurizer steam dome.	0 to 17.237 MPa	0 to 22.83 MPa	161	
Pressure Suppression System					
PB-PSS	Suppression tank top.	0 to 0.689 MPa	0 to 0.856 MPa	162	Test S-SB-2A only.
DIFFERENTIAL PRESSURE	Elevation difference between transducer taps is zero unless specified otherwise.				
Intact Loop					
DI-13V-1A	From vessel lower section of upper plenum, 13 cm below cold leg centerline to hot leg, Spool 1, Tap A, 60 cm from vessel center. Lower upper plenum tap is 35 cm below Spool 1 tap.	±127 cm water	±17.25 kPa	163, 164	
DI-1A-6	Hot leg, Spool 1, Tap A, 60 cm from vessel center to hot leg, Spool 6, 271 cm from vessel center.	±127 cm water	±17.44 kPa	165, 166	

TABLE 4. (continued)

Measurement	Location and Comments[a]	Data Acquisition Range[a] Detector	System	Figure[a]	Measurement Comme
Intact Loop (continued)					
DI-6-7	Hot leg, Spool 6, 271 cm from vessel center across steam generator to cold leg, Spool 7, 927 cm from downcomer center. Spool 6 tap is 47 cm above Spool 7 tap.	±345 kPa	±353 kPa	167, 168	
DI-6-SGI	Hot leg, Spool 6, 271 cm from vessel center to intact loop steam generator inlet, 349 cm from vessel center. Spool 6 tap is 41 cm below SGI tap.	±127 cm water	±16.8 kPa	169, 170	
DI-SGI-SGO	Intact loop steam generator, inlet plenum to outlet plenum, across primary side tubes.	±254 cm water	±33.54 kPa	171	Test S-SB-2A only.
DI-SGO-7	Intact loop steam generator outlet plenum, 1023 cm from downcomer center to cold leg, Spool 7, 927 cm from downcomer center. SGO tap is 79 cm above Spool 7 tap.	±254 cm water	±33.54 kPa	172, 173	
DI-7-9	Cold leg, Spool 7, 927 cm from downcomer center to cold leg, Spool 9, 663 cm from downcomer center. Spool 7 tap is 136 cm above Spool 9 tap.	±762 cm water	±102.3 kPa	174, 175	
DI-7-13	Cold leg, Spool 7, 927 cm from downcomer center to cold leg, Spool 13, 332 cm from downcomer center.	±254 cm water	±33.76 kPa	176	Test S-SB-2A only.
DI-9-13	Cold leg, Spool 9, 663 cm from downcomer center to cold leg, Spool 13, 332 cm from downcomer center. Spool 9 tap is 257 cm below Spool 13 tap.	±254 cm water	±33.65 kPa	177, 178	
DI-13-15	Cold leg, Spool 13, 332 cm from downcomer center, across primary pump to cold leg, Spool 15, 175 cm from downcomer center. Spool 13 tap is 25 cm below Spool 15 tap.	±690 kPa	±690 kPa	179, 180	
DI-15-17A	Cold leg, Spool 15, 175 cm from downcomer center, across cold leg injection port to cold leg, Spool 17, Tap A, 60 cm from downcomer center.	±254 cm water	±33.49 kPa	181, 182	
DI-17A-DIA	Cold leg, Spool 17, Tap A, 60 cm from downcomer center, to downcomer inlet annulus, 30 cm above cold leg centerline. Spool 17 tap is 30 cm below DIA tap.	±127 cm water	±16.52 kPa	183, 184	
Broken Loop					
DB-13V-20B	In vessel from lower section of upper plenum, 13 cm below cold leg centerline to hot leg, Spool 20, Tap B, 22 cm above cold leg centerline, 84 cm from vessel center. 13V tap is 35 cm below Spool 20 tap.	±254 cm water	±33.42 kPa	185, 186	
DB-20B-21	Hot leg, Spool 20, Tap B, 84 cm from vessel center to hot leg, Spool 21, 220 cm from vessel center.	±127 cm water	±16.24 kPa	187, 188	
DB-21-27A	Hot leg, Spool 21, 220 cm from vessel center to cold leg, Spool 27, Tap A, 87? cm from downcomer center. Spool 21 tap is 4 cm above Spool 27 tap.	±345 kPa	±345 kPa	189	Test S-SB-2A only.
DB-21-SGI	Hot leg, Spool 21, 220 cm from vessel center to steam generator inlet leg, 377 cm from vessel center. Spool 21 tap is 134 cm below SGI tap.	±254 cm water	±37.13 kPa	190, 191	
DB-SGI-SGO	Steam generator, inlet leg, 377 cm from vessel center across primary side tubes to steam generator outlet leg, 946 cm from downcomer center. SGI tap is 76 cm above SGO tap.	±345 kPa	±345 kPa	192, 193	
DB-SGI-SGI	Steam generator inlet leg, 377 cm from vessel center across primary side tube, 91 cm above top of tube sheet. SGI tap is 166 cm below SGI tap.	±1270 cm water	±170.0 kPa	194,195	

TABLE 4. (continued)

Measurement	Location and Comments[a]	Data Acquisition Range[a] Detector	System	Figure[a]	Measurement Comments[b]
Broken Loop (continued)					
DB-SGI-SG3	Steam generator inlet leg, 377 cm from vessel center across primary side tube, 838 cm above top of tube sheet. SGI tap is 913 cm below SG3 tap.	±1270 cm water	±174.9 kPa	196, 197	
DB-SGI-SG2	Across steam generator primary side tube, 91 cm to 465 cm above top of tube sheet. Elevation difference between taps is 374 cm.	±1270 cm water	±169.0 kPa	198, 199	
DB-SG2-SG3	Across steam generator primary side tube, 465 cm to 838 cm above top of tube sheet. Elevation difference between taps is 373 cm.	±1270 cm water	±169.6 kPa	200, 201	
DB-SG3-SGO	Across steam generator primary side tube, 838 cm above top of tube sheet to steam generator outlet leg, 946 cm from downcomer center. SG3 tap is 985 cm above SGO tap.	±345 kPa	±345 kPa	202, 203	
DB-SGO-27A	Steam generator outlet leg, 946 cm from downcomer center to cold leg, Spool 27, Tap A, 872 cm from downcomer center. SGO tap is 65 cm above Spool 27 tap.	±254 cm water	±33.58 kPa	204, 205	
DB-27A-28	Cold leg, Spool 27, 872 cm from downcomer center to cold leg, Spool 28, 565 cm from downcomer center. Spool 27, Tap A is 304 cm above Spool 28 tap.	±762 cm water	±102.0 kPa	206, 207	
DB-28-29	Cold leg, Spool 28, 565 cm from downcomer center to cold leg, Spool 29, 323 cm from downcomer center. Spool 28 tap is 231 cm below Spool 29 tap.	±762 cm water	±102.8 kPa	208, 209	
DB-37A-29	Cold leg, Spool 37, Tap A, 498 cm from downcomer center to cold leg, Spool 29, 323 cm from downcomer center. Spool 37, Tap A is 175 cm below Spool 29 tap.	±254 cm water	±33.68 kPa	210	Test S-SF-2A only.
DB-29-40B	Cold leg, Spool 29, 323 cm from downcomer center across broken loop pump to cold leg, Spool 40, Tap B, 202 cm from downcomer center. Spool 29 tap is 53 cm below Spool 40, Tap B.	+690 kPa	±686 kPa	211, 212	
DB-40B-45A	Cold leg, Spool 40, Tap B, 202 cm from downcomer center to cold leg, Spool 45, Tap A, 89 cm from downcomer center.	± 1270 cm water	±167.9 kPa	213, 214	
DB-45A-DIA	Cold leg, Spool 45, Tap A, 89 cm from downcomer center to downcomer inlet annulus, 30 cm above cold leg centerline. Spool 45 tap is 30 cm below DIA tap.	±127 cm water	±17.18 kPa	215, 216	
Downcomer					
DD-DIA-13V	Downcomer inlet annulus, 30 cm above cold leg centerline to vessel lower upper plenum, 13 cm below cold leg centerline. Elevation difference between taps is 43 cm.	±345 kPa	±347 kPa	217, 218	
DD-DIA-170	Downcomer inlet annulus, 30 cm above cold leg centerline to downcomer extension, 170 cm below cold leg centerline. Elevation difference between taps is 200 cm.	±762 cm water	±102.2 kPa	219, 220	
DD-DIA-578	Downcomer inlet annulus, 30 cm above cold leg centerline to vessel lower head, 578 cm below cold leg centerline. Elevation difference between taps is 608 cm.	±1270 cm water	±170 kPa	221, 222	

TABLE 4. (continued)

Measurement	Location and Comments[a]	Data Acquisition Range[a] Detector	Data Acquisition Range[a] System	Figure[a]	Measurement Comments[b]
Downcomer (continued)					
DD-170-435	Downcomer extension, 170 cm below cold leg centerline to downcomer instrumented spool piece, 435 cm below cold leg center... ...vation difference between taps is 265 cm.	±762 cm water	±109 kPa	223, 224	
DD-435-578	Downcomer instrumented spool piece, 435 cm below cold leg centerline to vessel lower head, 578 cm below cold leg centerline. Elevation difference between taps is 143 cm.	±254 cm water	±33.5 kPa	225, 226	
Vessel					
DV-578-501	Vessel lower head, 578 cm below cold leg centerline to lower core region, 501 cm below cold leg centerline. Elevation difference between taps is 77 cm.	±254 cm water	±33.8 kPa	227, 228	
DV-501-442	Vessel lower core region, 501 cm below cold leg centerline to lower core region, 442 cm below cold leg centerline. Elevation difference between taps is 59 cm.	±254 cm water	±34.0 kPa	229, 230	
DV-501-105	Vessel lower core region, 501 cm below cold leg centerline to heater rod ground hub, 105 cm below cold leg centerline. Elevation difference between taps is 396 cm.	±1270 cm water	±172 kPa	231, 232	
DV-442-278	Vessel lower core region, 442 cm below cold leg centerline to mid-core region, 278 cm below cold leg centerline. Elevation difference between taps is 164 cm.	±762 cm water	±100 kPa	233, 234	
DV-278-154	Vessel midcore region, 278 cm below cold leg centerline to upper core region, 154 cm below cold leg centerline. Elevation difference between taps is 124 cm.	±762 cm water	±99.9 kPa	235, 236	
DV-154-105	Vessel upper core region 154 cm below cold leg centerline to heater rod ground hub, 105 cm below cold leg centerline. Elevation difference between taps is 49 cm.	±762 cm water	±99.9 kPa	237, 238	
DV-154+154	Vessel upper core region, 154 cm below cold leg centerline to vessel lower head, 154 cm above cold leg centerline. Elevation difference between taps is 308 cm.	±1270 cm water	±170 kPa	239	Test S-SB-2A only.
DV-105-13V	Heater rod ground hub, 105 cm below cold leg centerline to lower section of upper plenum, 13 cm below cold leg centerline. Elevation difference between taps is 92 cm.	±254 cm water	±33.58 kPa	240, 241	
DV+421+154	Vessel top head, 421 cm above cold leg centerline to core support tube, 154 cm above cold leg centerline. Elevation difference between taps is 267 cm.	±1270 cm water	± 168 kPa	242, 243	
DV+135-13	Vessel upper head region, 135 cm above cold leg centerline to vessel upper plenum, 13 cm below cold leg centerline. Elevation difference between taps is 148 cm.	±762 cm water	±101 kPa	244, 245	
ECC System					
Intact Loop					
DI-ACC3-LL	Top to bottom of accumulator for intact loop. Elevation difference between taps is 279 cm.	±127 cm water	±34.46 kPa	246, 247	

TABLE 4. (continued)

Measurement	Location and Comments[a]	Data Acquisition Range[a] Detector	System	Figure[a]	Measurement Comments[b]
Broken Loop					
DB-ACC2-LL	Top to bottom of accumulator for broken loop. Elevation difference between taps is 213 cm.	±254 cm water	±34.49 kPa	248, 24[illegible]	
Steam Generator					
Intact Loop					
DI-SG-LL	Liquid level for intact loop steam generator. Elevation difference between taps is 206 cm.	±1270 cm water	±166 kPa	250, 251	
DI-SGFEED	Across orifice plate in feedwater line to steam generator for intact loop.	0 to 890 cm water	0 to 153 kPa	252	Detector failed on Test S-SB-2.
DI-SGOUT	Across venturi tube in discharge line from steam generator for intact loop.	0 to 2865 cm water	0 to 492 kPa	253, 254	
Broken Loop					
DB-SG-LL	Liquid level for broken loop steam generator. Elevation difference between taps is 1067 cm.	±345 kPa	±356 kPa	255, 256	
DB-SGFEED	Across orifice plate in feedwater line to steam generator for broken loop.	0 to 635 cm water	0 to 109 kPa	257, 258	
DB-SGOUT	Across venturi tube in discharge line from steam generator for broken loop.	0 to 208 cm water	0 to 35.8 kPa		Detector failed on Tests S-SB-2 and S-SB-2A.
Pressurizer					
DI-PR-LL	Liquid level for pressurizer. Elevation difference between taps is 127 cm.	±127 cm water	±18.47 kPa	259, 260	
DI-PR-4	Pressurizer bottom to Spool 4. Elevation difference between taps is 157 cm. Spool 4 tap is 140 cm below pressurizer exit.	±762 cm water	±100 kPa	261	Test S-SB-2A only.
VOLUMETRIC FLOW RATE	Turbine flowmeter, bidirectional.				Data acquisition system range may exceed rated detection range; however, turbine response is linear to flow rates well beyond the rated range.
Intact Loop	3-in. Schedule 160 pipe.				
FI-1	Hot leg, Spool 1, 38 cm from vessel center.	±1.2[illegible] to ±12.6 L/s	±19 L/s	262, 263	
F[illegible]	Cold leg, Spool 11, 429 cm from downcomer center.	±1.26 to ±12.6 L/s	±19 L/s	264, 265	
FI-16	Cold leg, Spool 16, 145 cm from downcomer center.	±5.05 to ±50.5 L/s	±19 L/s	266, 267	
FI-17	Cold leg, Spool 17, 38 cm from downcomer center.	±1.26 to ±12.6 L/s	±19 L/s	268, 269	
Broken Loop					
FB-20	Hot leg, Spool 20, 100 cm from vessel center.	±1.26 to ±12.6 L/s	±5.5 L/s	270, 271	
FB-37	Cold leg, Spool 37, 466 cm from downcomer center.	±1.26 to ±12.6 L/s	±5.5 L/s	272, 273	
FB-40	Cold leg, Spool 40, 193 cm from downcomer center.	±1.26 to ±12.6 L/s	±5.5 L/s	274	Detector failed on Test [illegible]-SB-2.
FB-45	Cold leg, Spool 45, 110 cm from downcomer center.	±0.63 to ±6.31 L/s	±5.5 L/s	275	Detector failed on [illegible] S-SB-2A.
Downcomer					
FD-424	In downcomer, [illegible]pstream of instrumented spool piece, 424 cm below cold leg centerline.	±2.52 to ±25.2 L/s	±2[illegible]	276, 277	

TABLE 4. (continued)

Measurement	Location and Comments[a]	Data Acquisition Range[a]		Figure[a]	Measurement Comments[b]
		Detector	System		
Vessel					
FV+1	Core exit, 1 cm above cold leg centerline.	±2.52 to ±25.2 L/s	±20 L/s	278, 279	
FV-UK-DC	In upper head heatup by-pass line.	±0.47 to ±4.72 L/s	±3.0 L/s	280, 281	Detector was set for unidirectional flow on Test S-SB-2A
ECC System					
Intact Loop					
FI-HPIS	In line immediately after HPIS pump for intact loop; 1/2-in. line.	±0.0316 to ±0.316 L/s	±0.15 L/s	282, 28?	
FI-ACC3 -DP	Calculated volumetric flow rate from measurement DI-ACC3-LL and ACC3 tank configuration.			284, 285	
Broken Loop					
FB-HPIS	In line immediately after HPIS pump for intact loop, 1/2-in. line.	±0.0316 to ±0.316 L/s	±0.15 L/s	286, 287	Data from -20 to 1100 s is invalid due to instrument noise.
FB-ACC2-DP	Calculated volumetric flow rate from measurement DB-ACC2-LL and ACC2 tank configuration.			288, 289	
Pressurizer					
FI-PRIZE	In pressurizer surge line.	±2.52 to ±25.2 L/s	± 20 L/s	290, 291	
MOMENTUM FLUX	Drag-screen, bidirectional.				
Broken Loop					
NB-20	Hot leg, Spool 20, 79 cm from vessel center.	±0.05 to ±10.7 N	±2.5 N	292, 293	
NB-40	Cold leg, Spool 40, 215 cm from downcomer center.	±0.05 to ±10.7 N	±2.5 N		Detector failed for Tests S-SB-2 and S-SB-2A.
NB-41	Cold leg, Spool 41, 198 cm from downcomer center.	±0.22 to ±44.5 N	±35.61 N	294, 295	
NB-45	Cold leg, Spool 45, 84 cm from downcomer center.	±0.05 to ±10.7 N	±2.5 N	296, 297	
Vessel					
NV-9	In vessel lower upper plenum region, 9 cm below cold leg centerline.	±0.11 to ±22.2 N	±9.0 N	298, 299	
NV-499	In vessel at entrance to heated core, 499 cm below cold leg centerline.	±0.08 to ±15.1 N	±15.0 N	300	Detector failed on Test S-SB 2.
MSV+153D	Vessel support tube, 153 cm above cold leg centerline, 45°.	N/A	±0.3 N	301, 302	
MSV+153Q	Vessel support tube, 153 cm above cold leg centerline, 225°.	N/A	±0.3 N	303, 304	
MGV+330	Vessel go.‑w tube, 330 cm above cold leg centerline.	N/A	±0.8 N	305, 306	
DENSITY					
Intact Loop		1.6 to 1600 kg/m³	0 to 160v kg/m³		
GI-1T GI-1B GI-1C	Hot leg, Spool 1, 77 cm from vessel center. T (tangential) ranges 270° to 360°. B (body) ranges 30° to 330°. C is a mathematical composite of T and B.			307, 308 309, 310 311, 312	Data questionable for GI-1T on Test S-SB-2 and GI-1B on Test S-SB-2A.[c]
GI-5VR	Hot leg, Spool 5, 228 cm from vessel center, vertical.			313, 314	
GI-13T GI-13B GI-13C	Cold leg, Spool 13, 342 cm from downcomer center. T (tangential) ranges 270° to 360°. B (body) ranges 30° to 330°. C is a mathematical composite of T and B.			15, 316 317, 318 319, 320	Data questionable for GI-13B on Test S-SB-2A.[c]
GI-16VR	Cold leg, Spool 16, 131 cm from downcomer center.			321, 322	

TABLE 4. (continued)

Measurement	Location and Comments[a]	Data Acquisition Range[a]		Figure[a]	Measurement Comments[b]
		Detector	System		
Intact Loop (continued)					
GI-17T GI-17B GI-17C	Cold leg, Spool 17, 73 cm from downcomer center. T (tangential) ranges 270° to 360°. B (body) ranges 30° to 330°. C is a mathematical composite of T and B.			323, 324 325, 326 327, 328	Data questionable for GI-17T on Test S-SB-2.[c]
Broken Loop		1.6 to 1600 kg/m^3	0 to 1600 kg/m^3		
GB-20VR	Hot leg, Spool 20, 64 cm from vessel center, vertical.			329, 330	
GB-37	Cold leg, Spool 37, 360 cm from downcomer center.				Detector failed on Tests S-SB-2 and S-SB-2A.
GB-40VR	Cold leg, Spool 40, 230 cm from downcomer, vertical.			331, 332	
GB-41M GB-41B GB-41C	Cold leg, Spool 41, 170 cm from downcomer center. C is a mathematical composite of M and B.			333, 334 335, 336	Detector GB-41M failed on Test S-SB-2A. Data questionable GB-41B and GB-41M on Test S-SB-2.[c]
GB-45VR	Cold leg, Spool 45, 66 cm from downcomer, vertical.			337, 338	Data questionable on Test S-SB-2A.[c]
Downcomer		1.6 to 1600 kg/m^3	0 to 1600 [illegible]		
GD-72B	Downcomer, 72 cm below cold leg centerline. B (body) ranges 30° to 330°.			339, 340	
GD-260B	Downcomer, 260 cm below cold leg centerline. B (body) ranges 30° to 330°.			341, 342	
GD-456B	Downcomer, 456 cm below cold leg centerline. B (body) ranges 30° to 330°.			343, 344	
Vessel		1.6 to 1600 kg/m^3	0 to 1600 kg/m^3		
GV-528-588	Vessel lower head, 528 cm below cold leg centerline, at 15° to 588 cm below cold leg centerline at 165°.			345, 346	
GV-502-AB	At bottom of core heated length, 502 cm below cold leg centerline between heater rod Columns A and B.			347, 348	
GV-383-23	Lower part of core heated length, 383 cm below cold leg centerline between heater rod Rows 2 and 3.				Detector failed on Tests S-SB-2 and S-SB-2A.
GV-323-AB	Near center of core heated length, 323 cm below cold leg centerline between heater rod Columns A and B.			349, 350	
GV-313-23	Near center of core heated length, 313 cm below cold leg centerline between heater rod Rows 2 and 3.			351, 352	
GV-243-23	Upper part of core heated length, 243 cm below cold leg centerline between heater rod Rows 2 and 3.			353, 354	
GV-164-AB	Near top of core heated length, 164 cm below cold leg centerline between heater rod Columns A and B.			355, 356	
GV-154-23	Near top of core heated length, 154 cm below cold leg centerline between heater rod Rows 2 and 3.			357, 358	
GV-11	Vessel at base of core flow instrument housing, 11 cm below cold leg centerline.				Detector failed on Tests S-SB-2 and S-SB-2A.
GV+339	Vessel at top of control rod guide tube, 339 cm above cold leg centerline.			359, 360	
GV+174	Vessel at top of core support tube, 174 cm above cold leg centerline.			361, 362	

TABLE 4. (continued)

Measurement	Location and Comments[a]	Data Acquisition Range[a]		Figure[a]	Measurement Comments[b]
		Detector	System		
Pressurizer		1.6 to 1600 kg/m^3			
GI-PRIZE	Pressurizer surge line.			363, 364	
MASS FLOW RATE	Mass flow rate obtained by combining density (gamma attenuation technique) with volumetric flow rate (turbine flowmeter), or momentum flux (drag screen).	Range for mass flow is determined from ranges of individual detectors used in calculation.			
Intact Loop					
FI-1, GI-1C	Hot leg, Spool 1.			365, 66	
FI-16, GI-16VR	Cold leg, Spool 16.			367, .8	
FI-17, GI-17C	Cold leg, Spool 17.			369, 370	
Broken Loop					
FB-20, GB-20VR NB-20, GB-20VR	Hot leg, Spool 20.			371, 372 373, 374	
FB-40, GB-40VR	Cold leg, Spool 40.			375	Test S-SB-2 only.
NB-41, GB-41C	Cold leg, Spool 41.			376	Test S-SB-2 only.
FB-45, GB-45VR NB-45, GB-45VR	Cold leg, Spool 45.			377, 378 379	
Downcomer					
FD-424, GD-456B	Downcomer instrumented spool piece.			380, 381	
Vessel					
FV-1, GV-154-23	Top of core heated length.			382, 383	
NV-499, GV-502-AB	Core inlet.			384	Test S-SB-2A only.
CORE CHARACTERISTICS					
High-Power Bus					
AH-HI	Core amperage.	0 to 10 000 A	0 to 10 030 A	385, 386	
VH-HI	Core voltage.	0 to 400 V	0 to 402 V	387, 388	
Low-Power Bus					
AH-LO	Core amperage.	0 to 10 000 A	0 to 9330 A	389, 390	
VH-LO	Core voltage.	0 to 400 V	0 to 402 V	391, 392	
PUMP CHARACTERISTICS					
Intact Loop					
SI-PUMP	Pump speed.	377 rad/s	377 rad/s	393, 394	
Broken Loop					
SB-PUMP	Pump speed.	3770 rad/s	3770 rad/s	395, 396	
WB-PUMP	Pump power.	82 kW	20 kW	397,398	

a. Statements at the beginning of a measurement category regarding location and comments, range and figure apply to all subsequent measurements within the given category unless specified otherwise.

b. Detectors which were subjected to overrange conditions during portions of the test were capable of withstanding these conditions without change in operating or measuring characteristics when the physical conditions were again within the detector range.

c. Drain condition used for calibration check point did not yield a superheated steam (i.e. known density) conditions, but rather a saturated one. Calibration accomplished by assumption that saturated steam was dry.

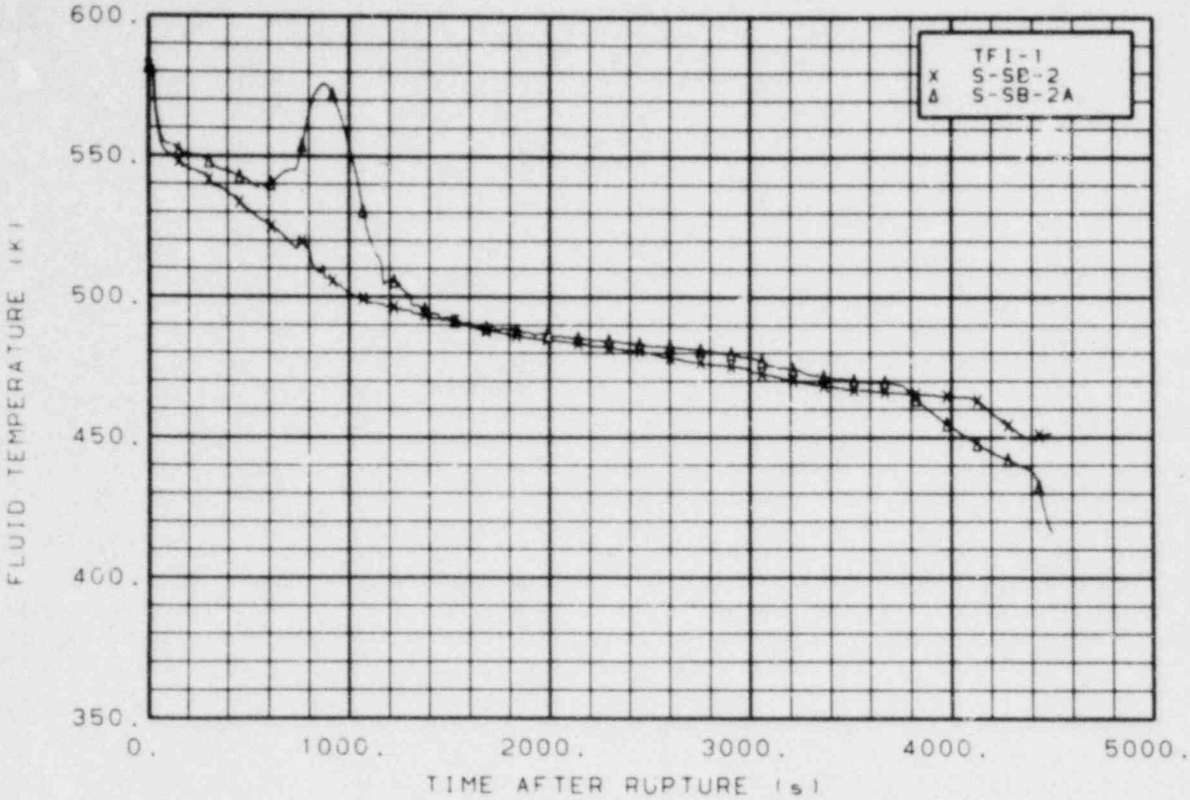

Figure 11. Fluid temperature in intact loop hot leg (TFI-1), from 0 to 4500 s.

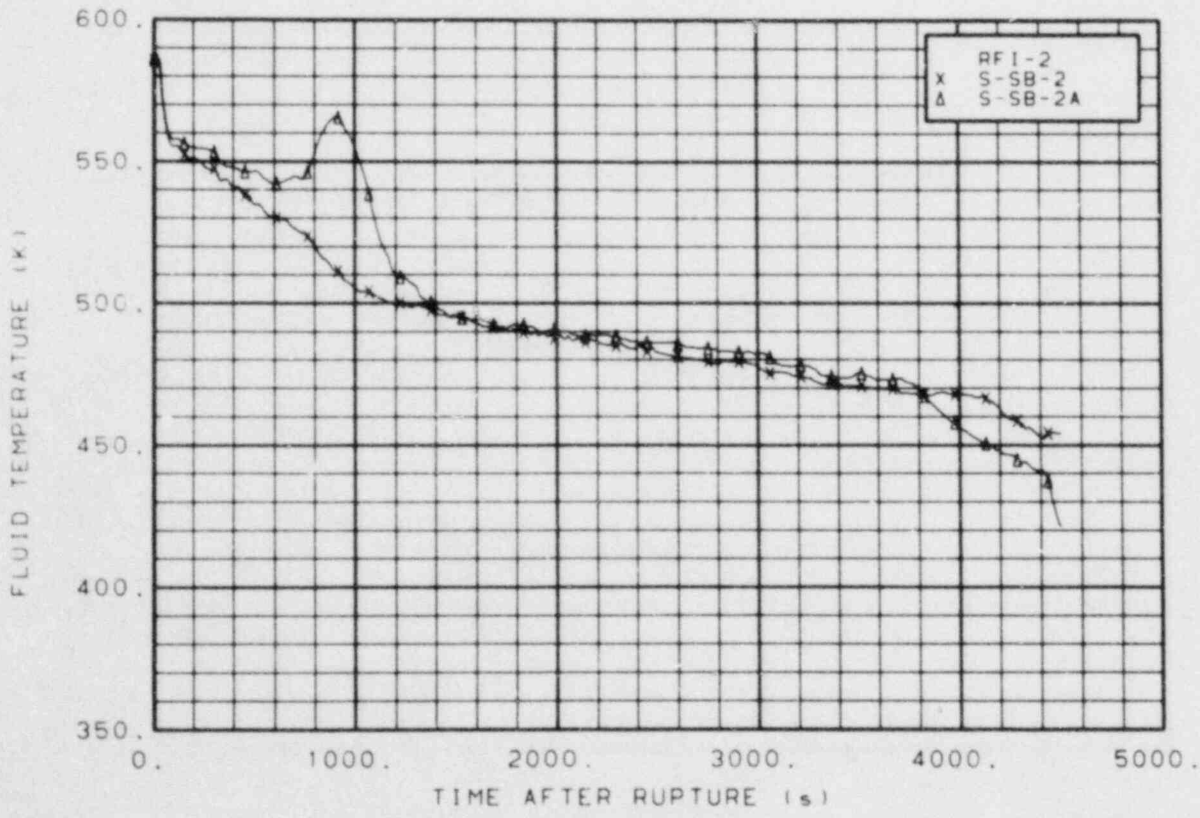

Figure 12. Fluid temperature in intact loop hot leg (RFI-2), from 0 to 4500 s.

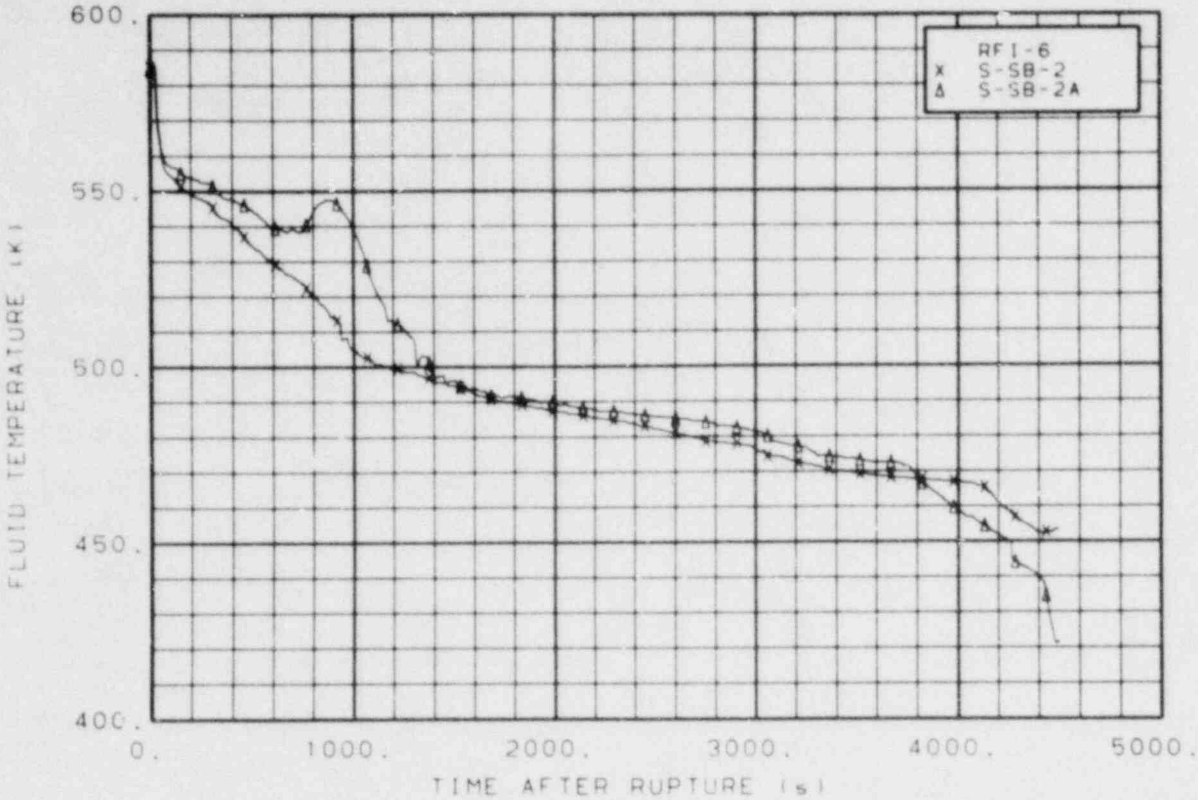

Figure 13. Fluid temperature in intact loop hot leg (RFI-6), from 0 to 4500 s.

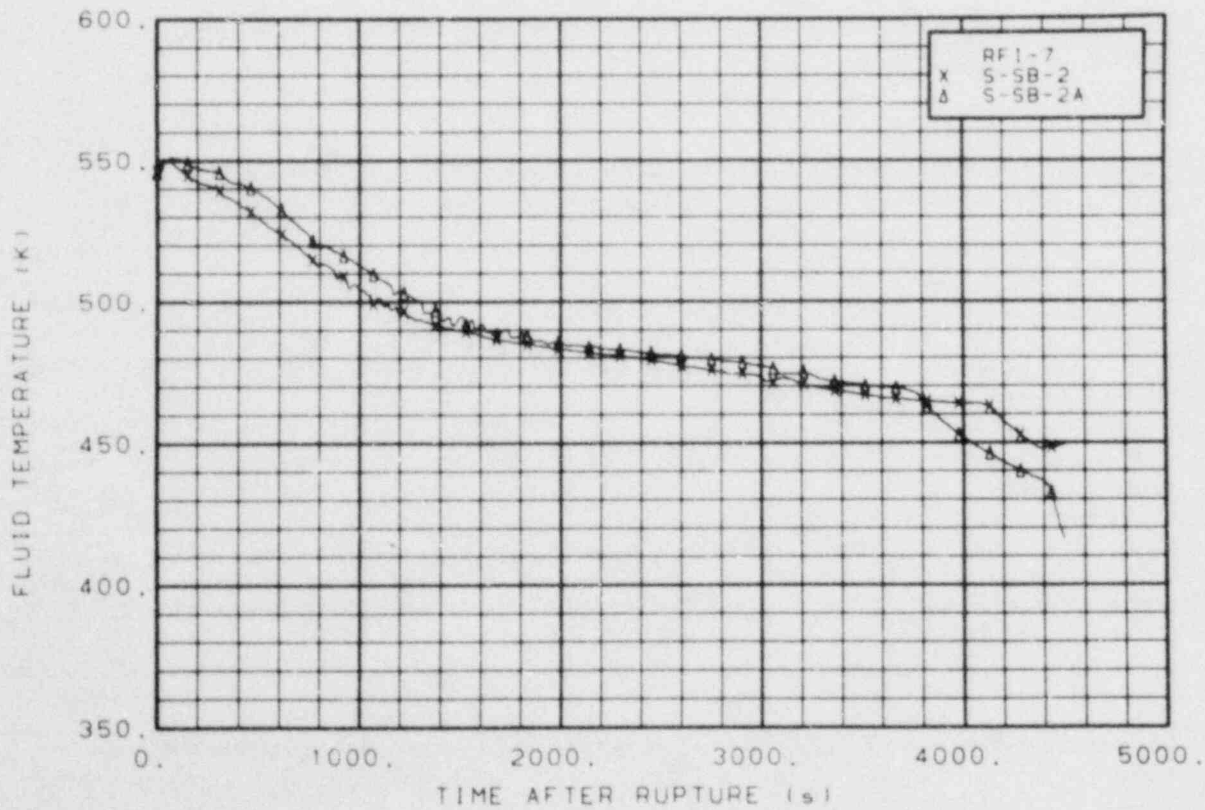

Figure 14. Fluid temperature in intact loop cold leg (RFI-7), from 0 to 4500 s.

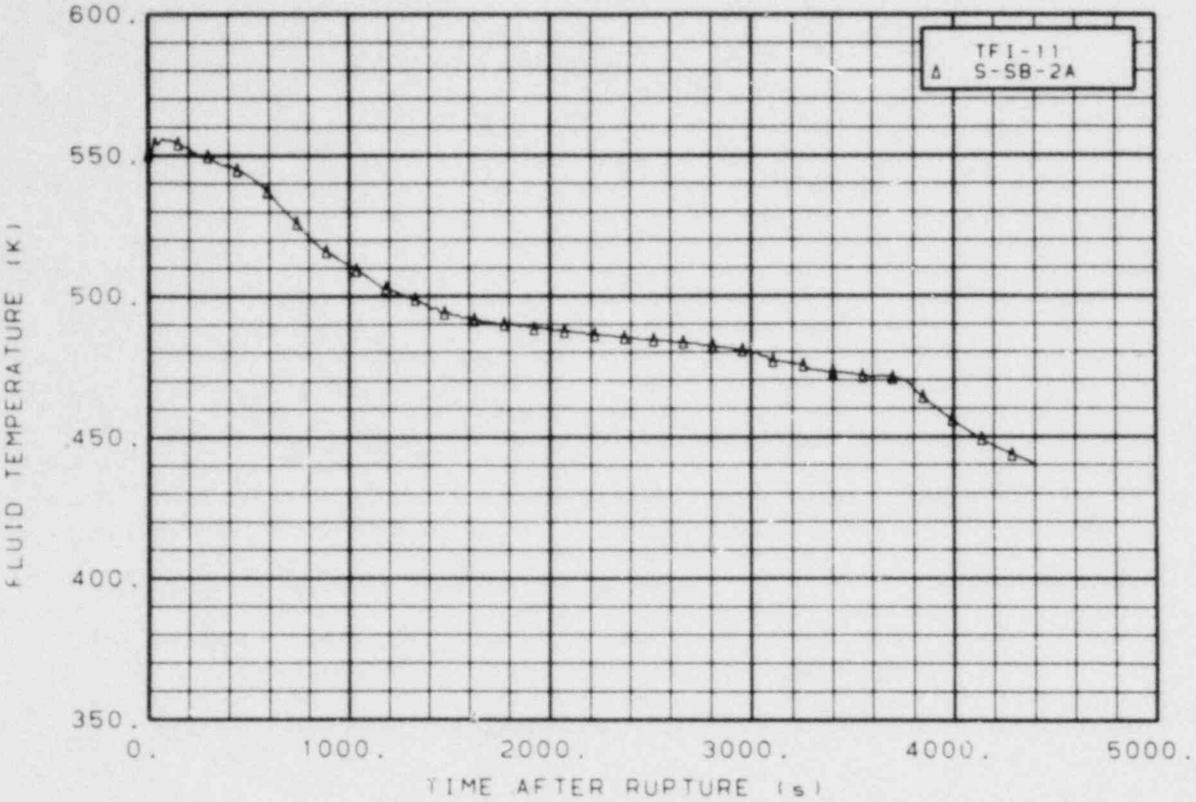

Figure 15. Fluid temperature in intact loop cold leg, Test S-SB-2A (TFI-11), from 0 to 4390 s.

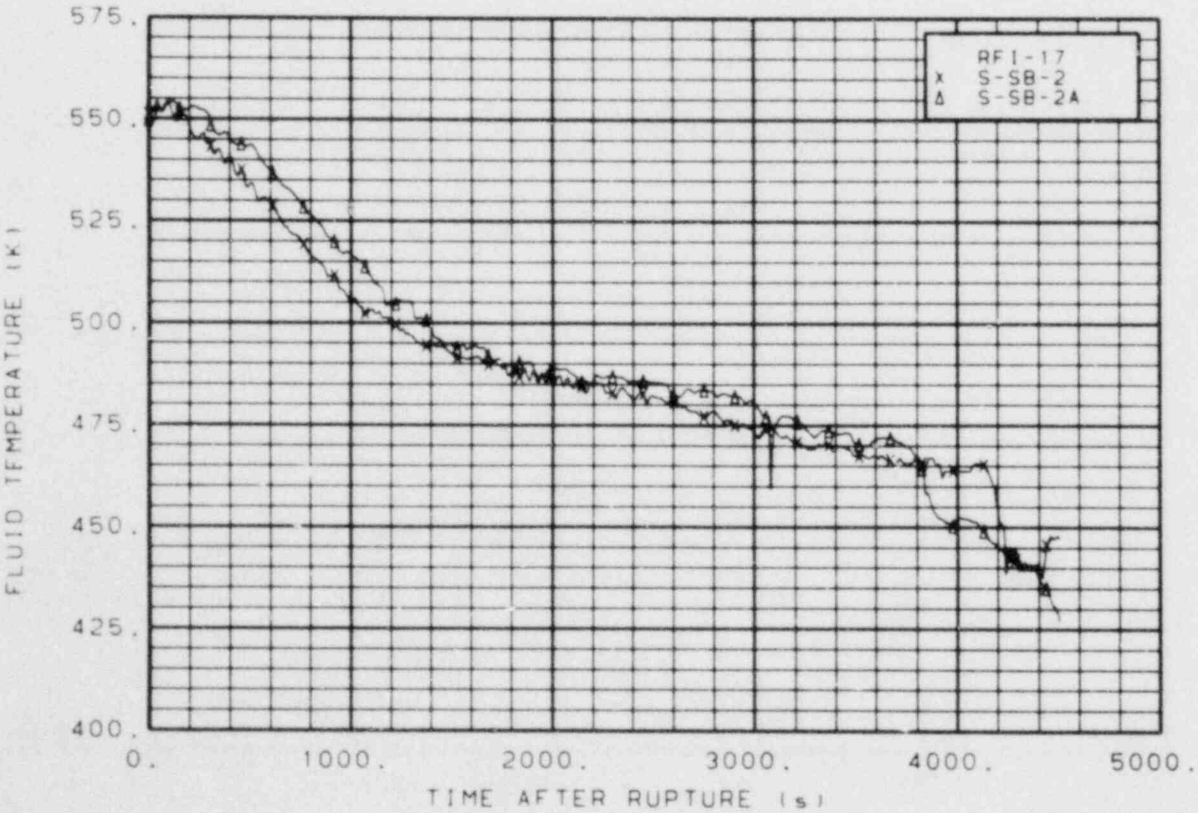

Figure 16. Fluid temperature in intact loop cold leg (RFI-17), from 0 to 4500 s.

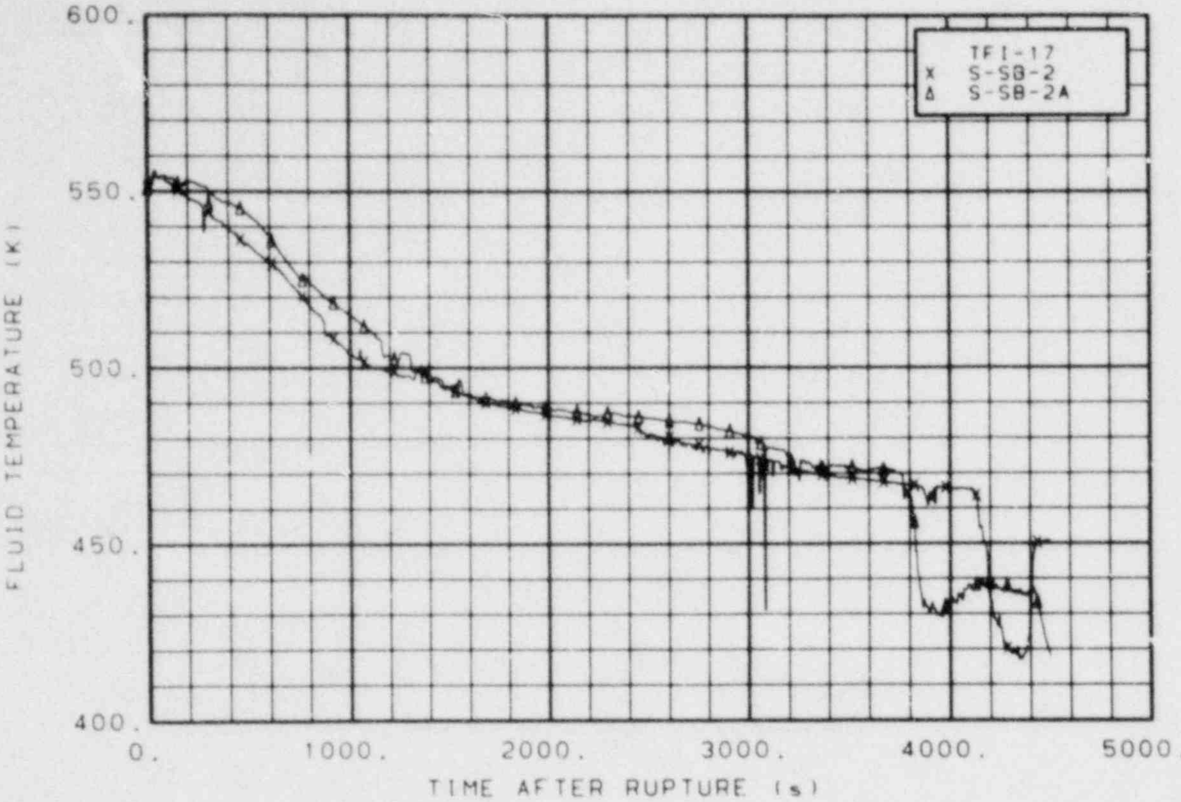

Figure 17. Fluid temperature in intact loop cold leg (TFI-17), from 0 to 4500 s.

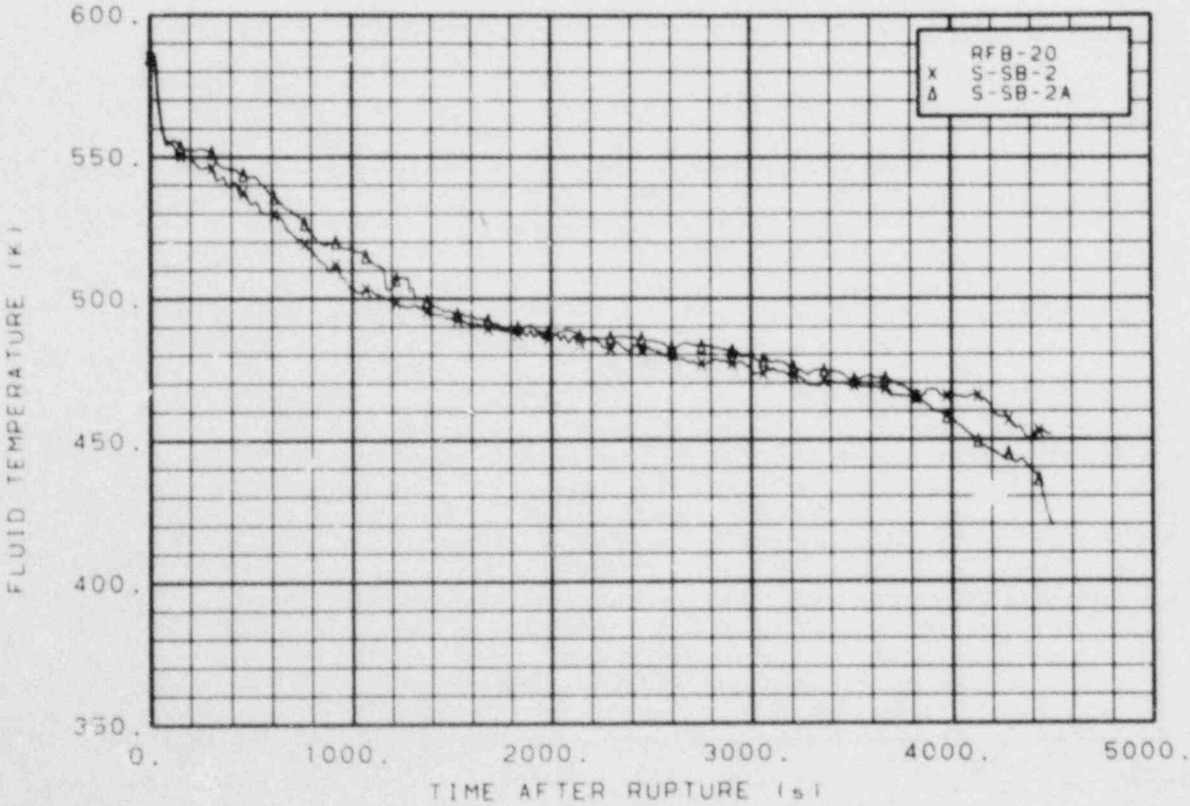

Figure 18. Fluid temperature in broken loop hot leg (RFB-20), from 0 to 4500 s.

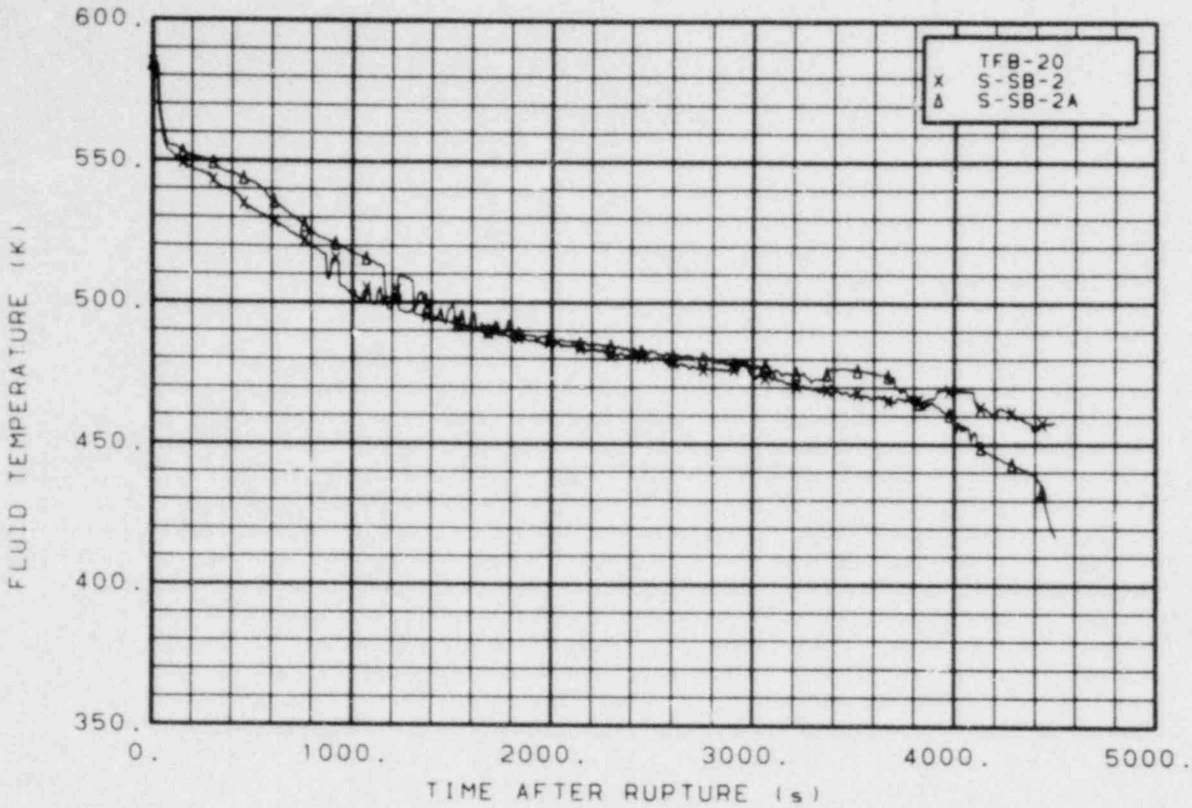

Figure 19. Fluid temperature in broken loop hot leg (TFB-20), from 0 to 4500 s.

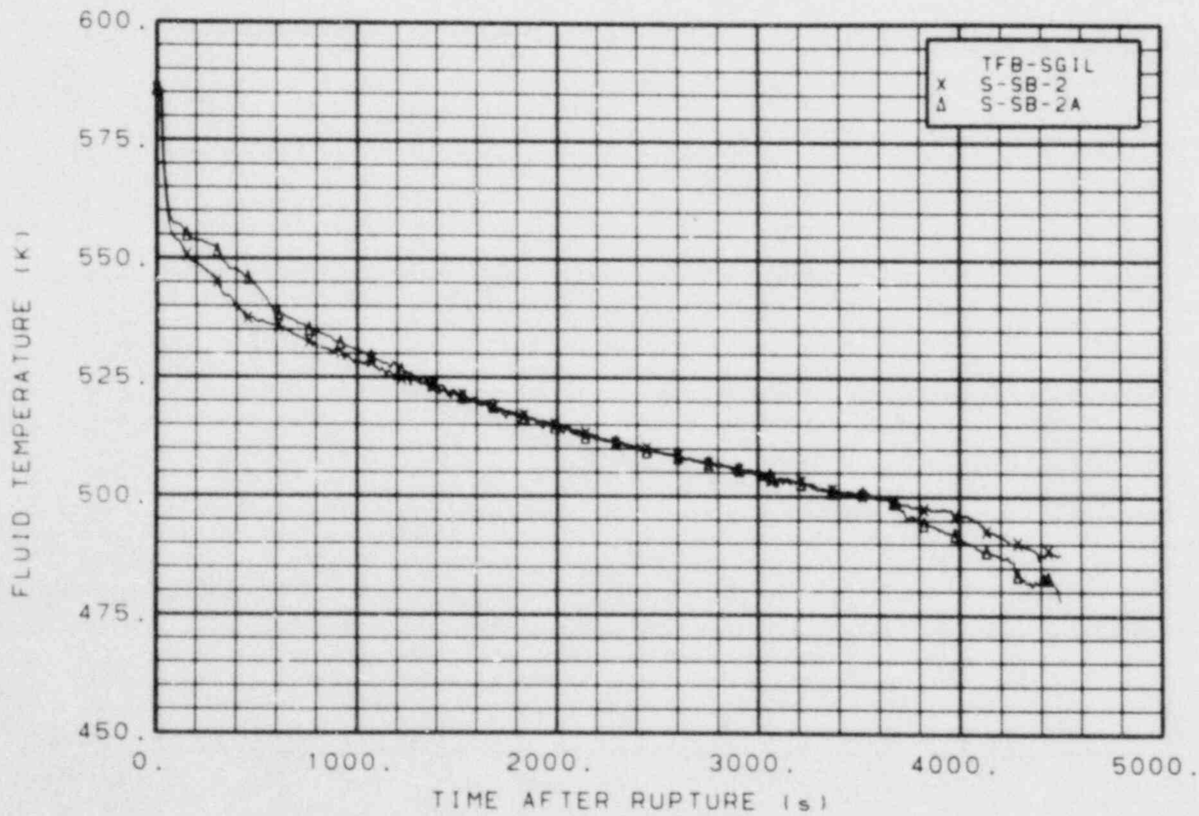

Figure 20. Fluid temperature in broken loop steam generator, inlet leg (TFB-SGIL), from 0 to 4500 s.

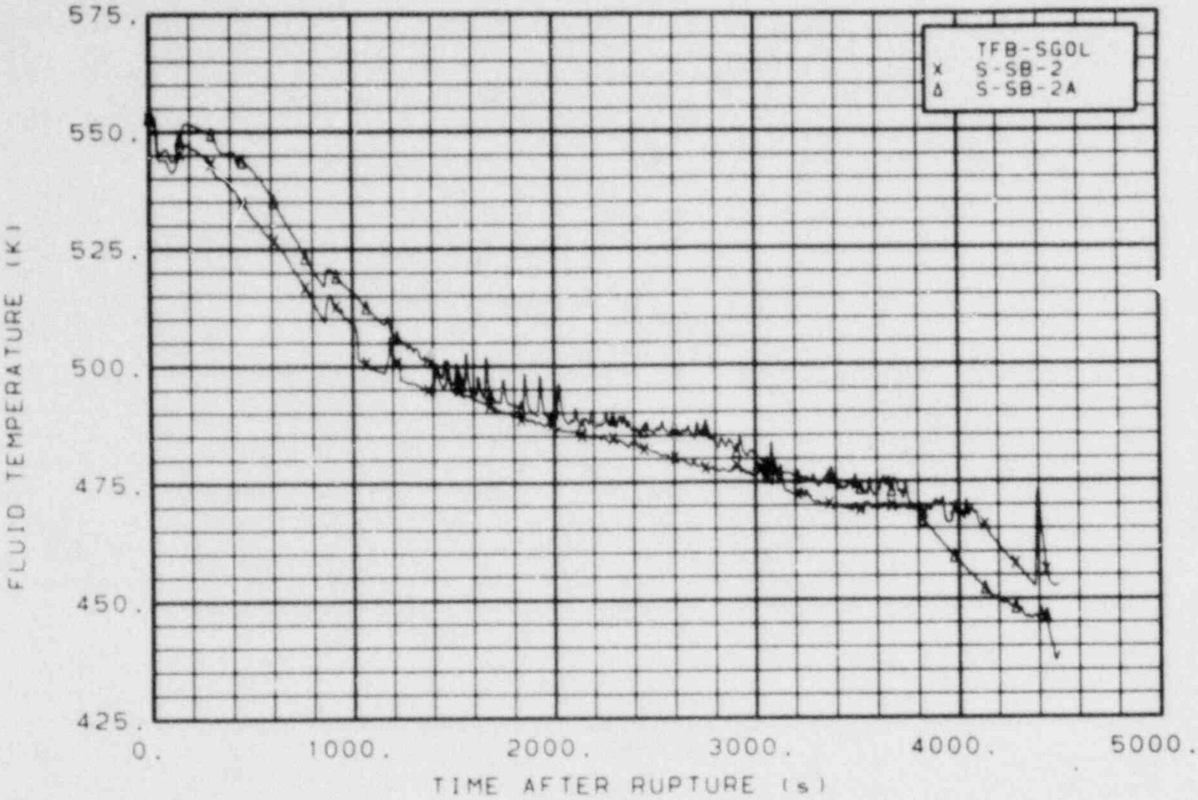

Figure 21. Fluid temperature in broken loop steam generator, outlet leg (TFB-SGOL), from 0 to 4500 s.

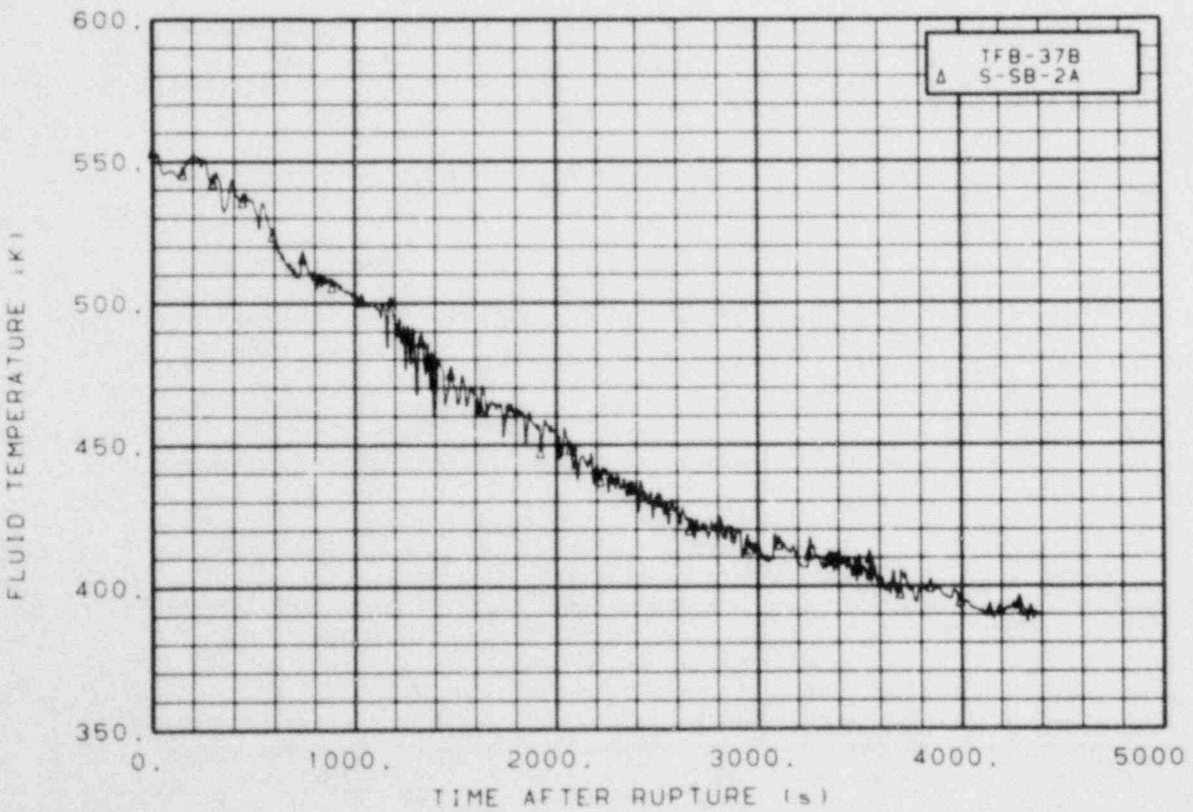

Figure 22. Fluid temperature in broken loop cold leg, Test S-SB-2A (TFB-37B), from 0 to 4390 s.

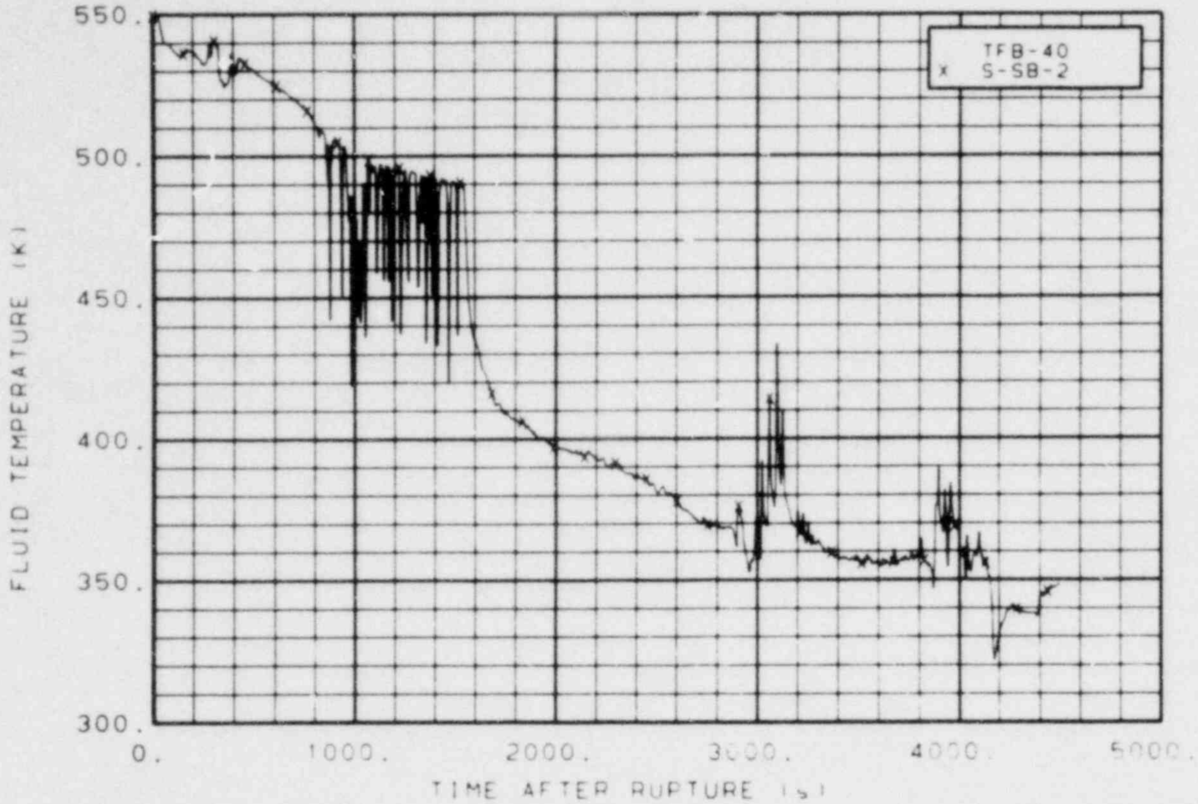

Figure 23. Fluid temperature in broken loop cold leg, Test S-SB-2 (TFB-40), from 0 to 4500 s.

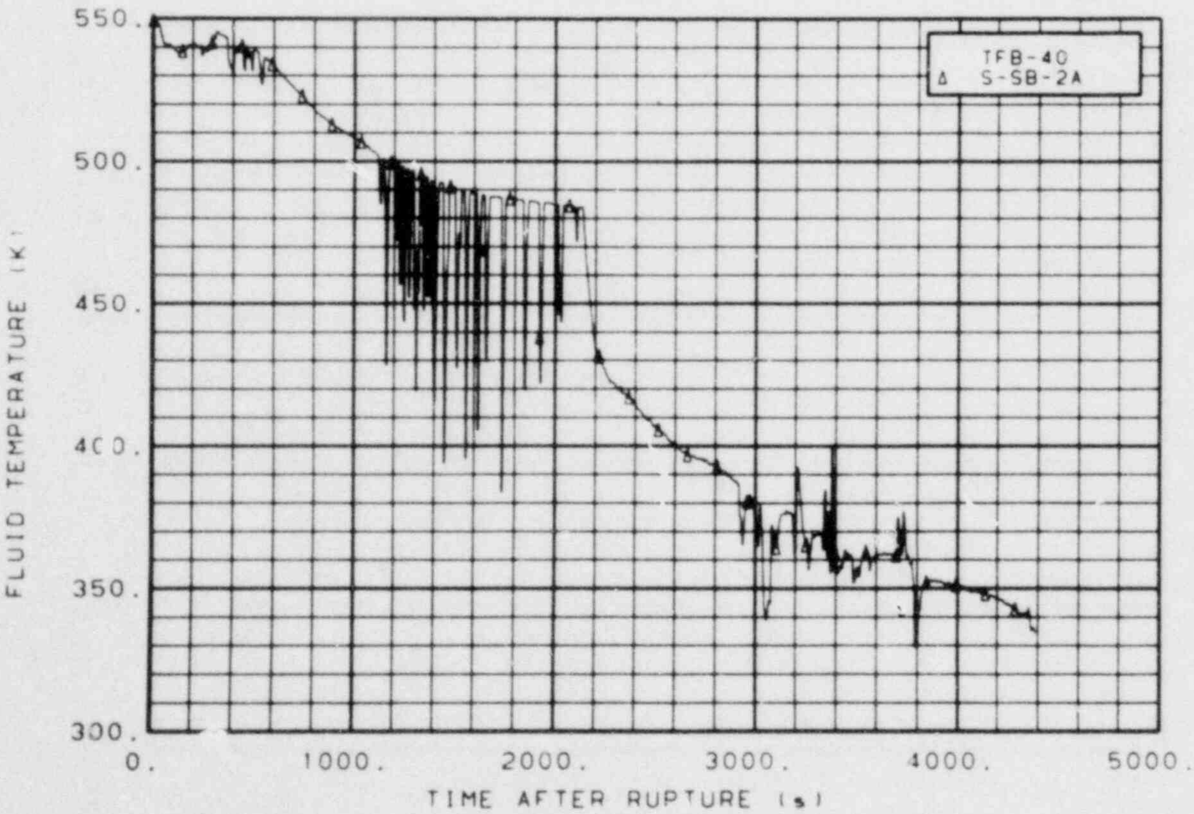

Figure 24. Fluid temperature in broken loop cold leg, Test S-SB-2A (TFB-40), from 0 to 4390 s.

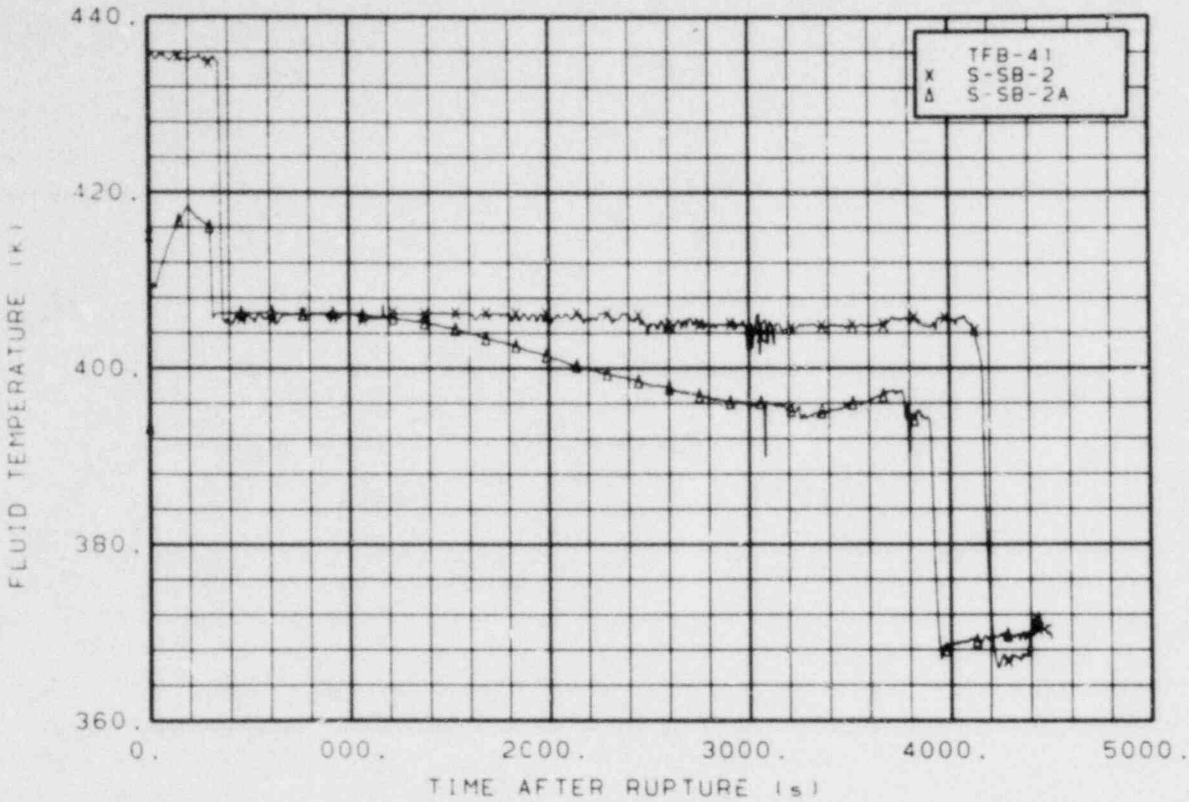

Figure 25. Fluid temperature in broken loop cold leg (TFB-41), from 0 to 4500 s.

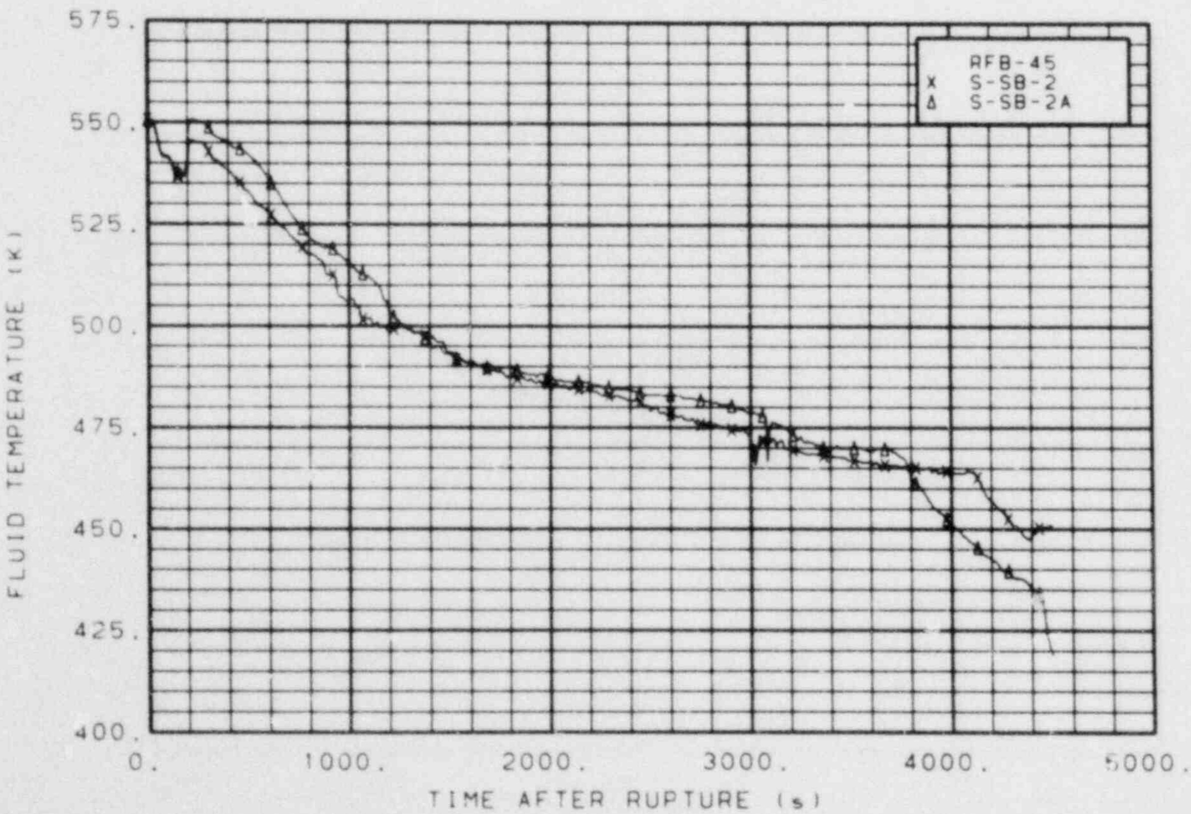

Figure 26. Fluid temperature in broken loop cold leg (RFB-45), from 0 to 4500 s.

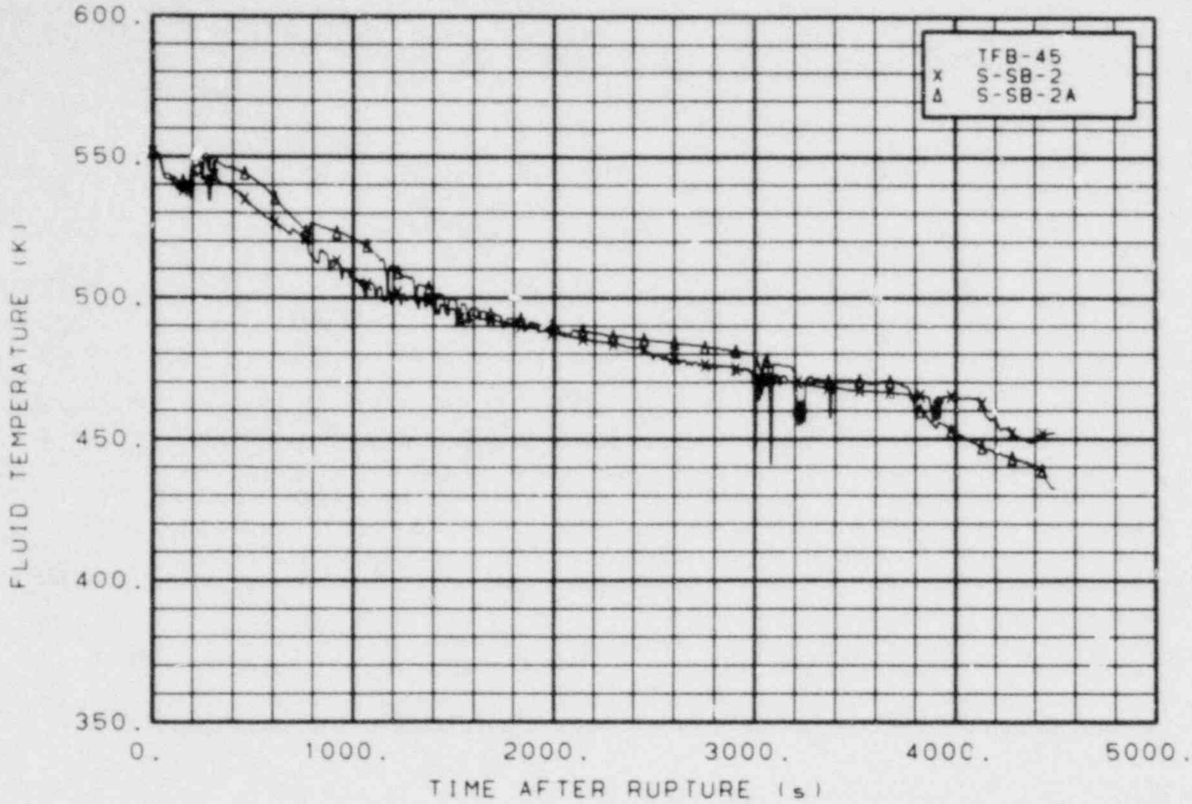

Figure 27. Fluid temperature in broken loop cold leg (TFB-45), from 0 to 4500 s.

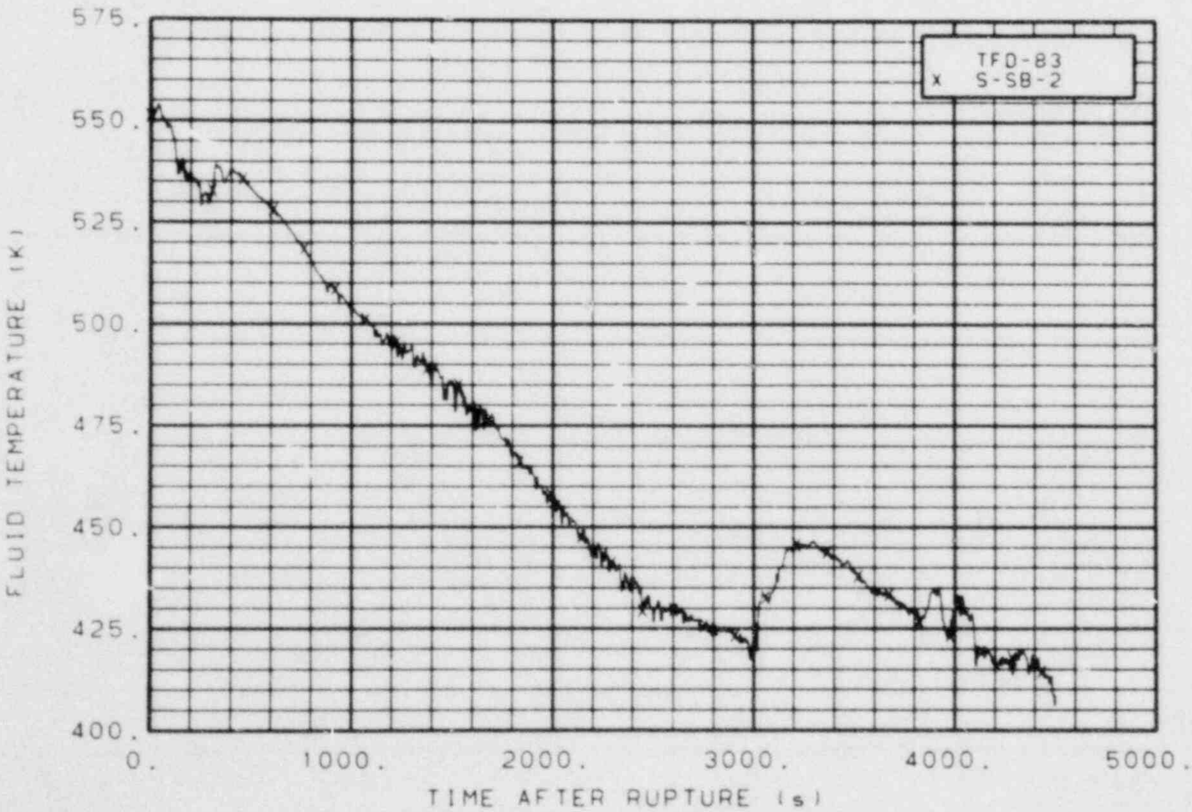

Figure 28. Fluid temperature in downcomer, Test S-SB-2 (TFD-83), from 0 to 4500 s.

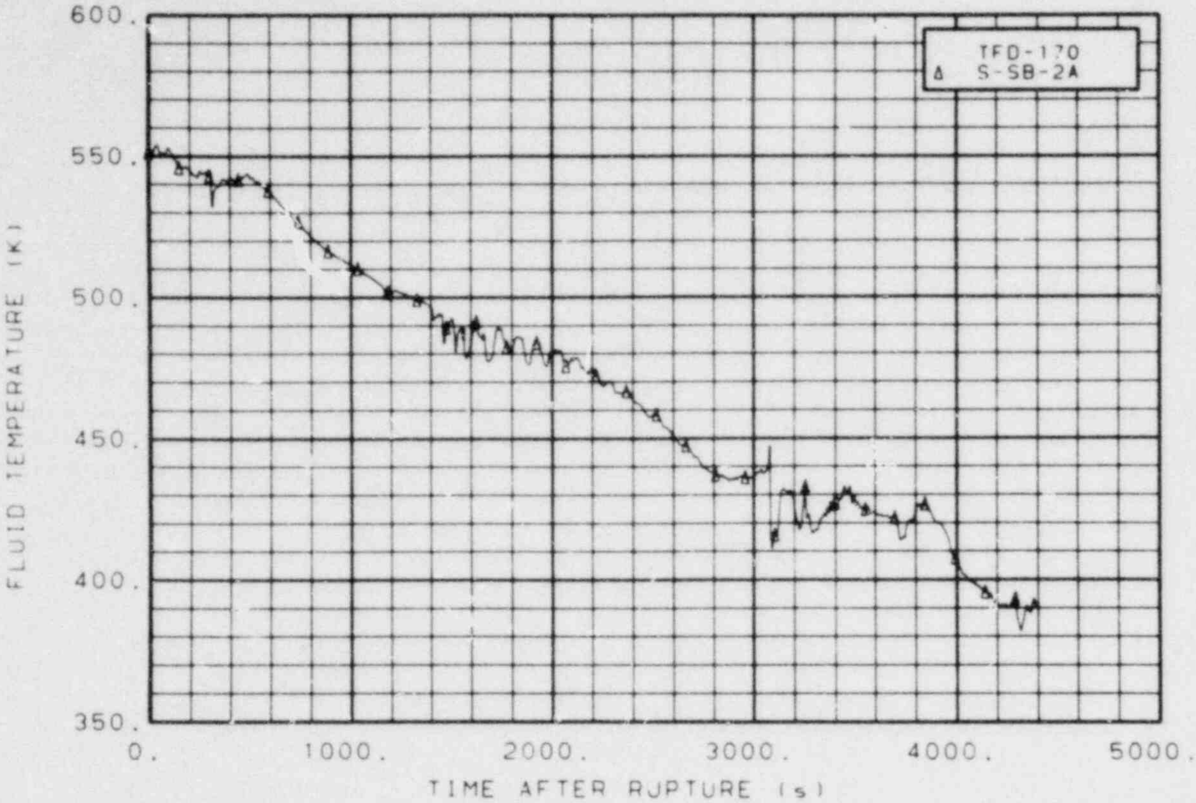

Figure 29. Fluid temperature in downcomer, Test S-SB-2A (TFD-170), from 0 to 4390 s.

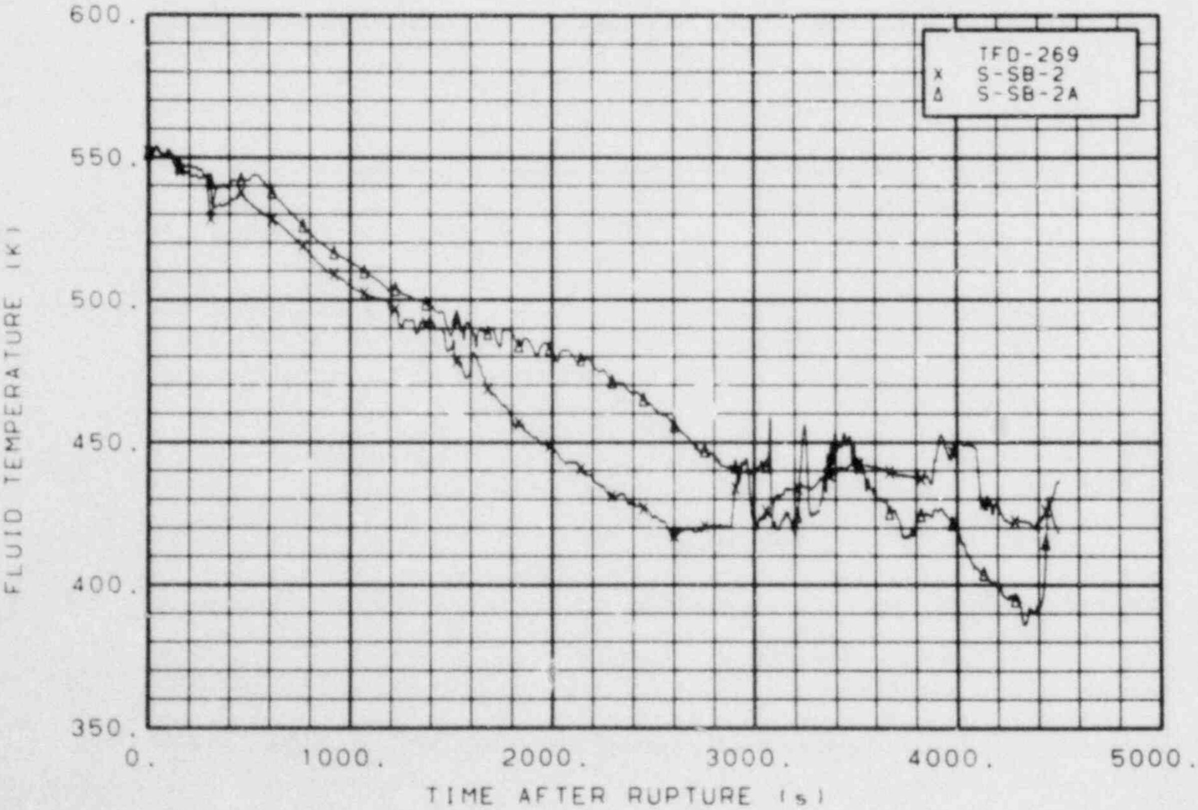

Figure 30. Fluid temperature in downcomer (TFD-269), from 0 to 4500 s.

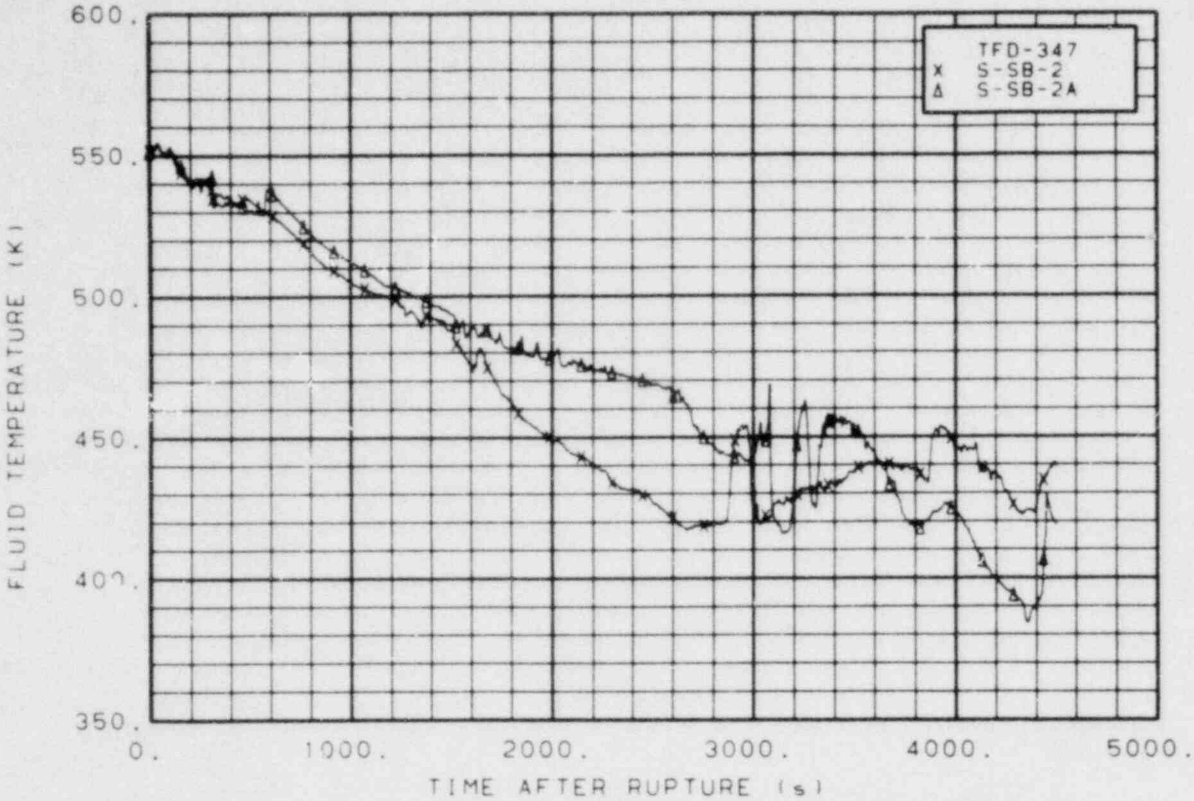

Figure 31. Fluid temperature in downcomer (TFD-347), from 0 to 4500 s.

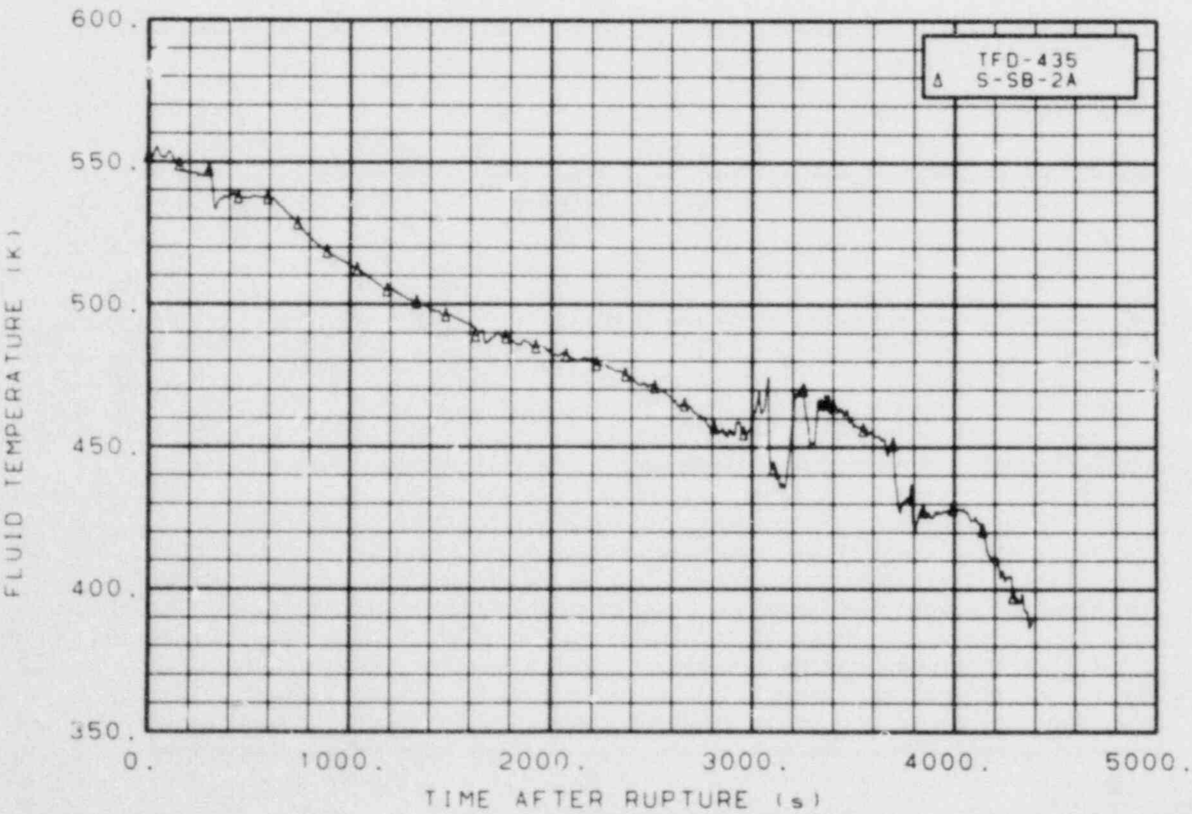

Figure 32. Fluid temperature in downcomer, Test S-SB-2A (TFD-435), from 0 to 4390 s.

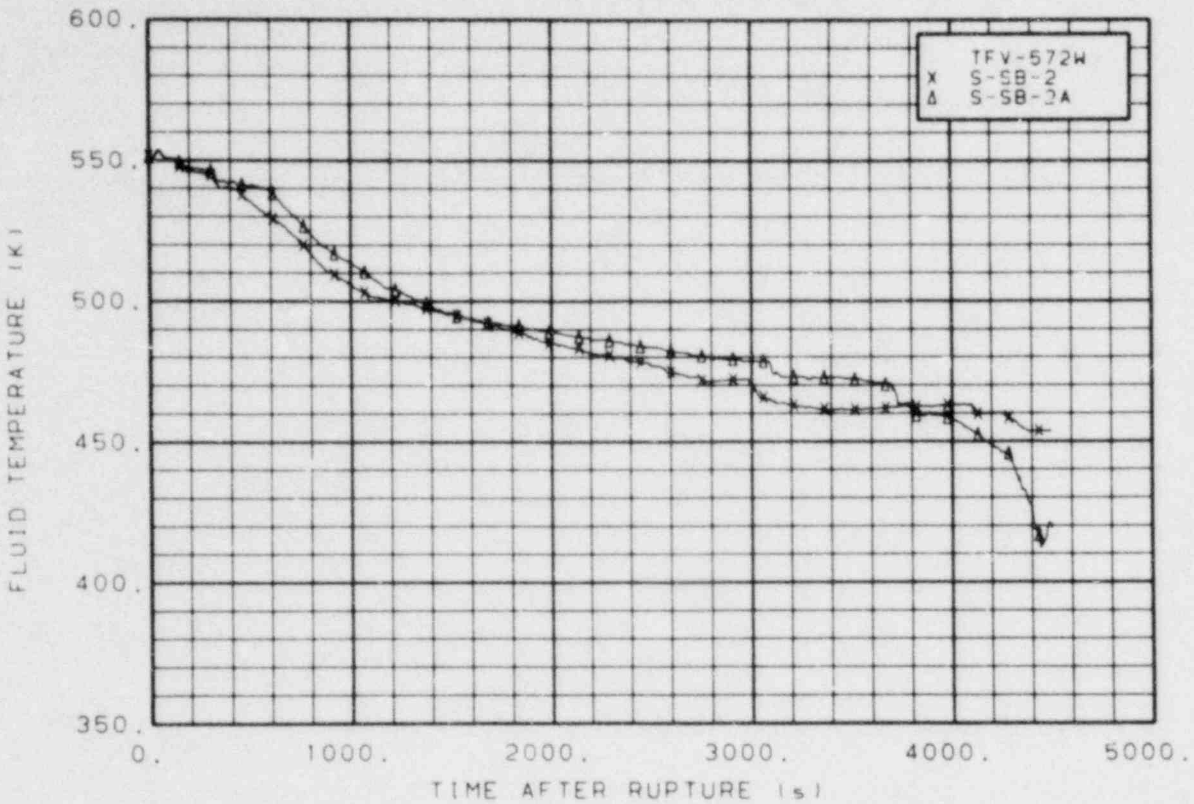

Figure 33. Fluid temperature in vessel (TFV-572W), from 0 to 4500 s.

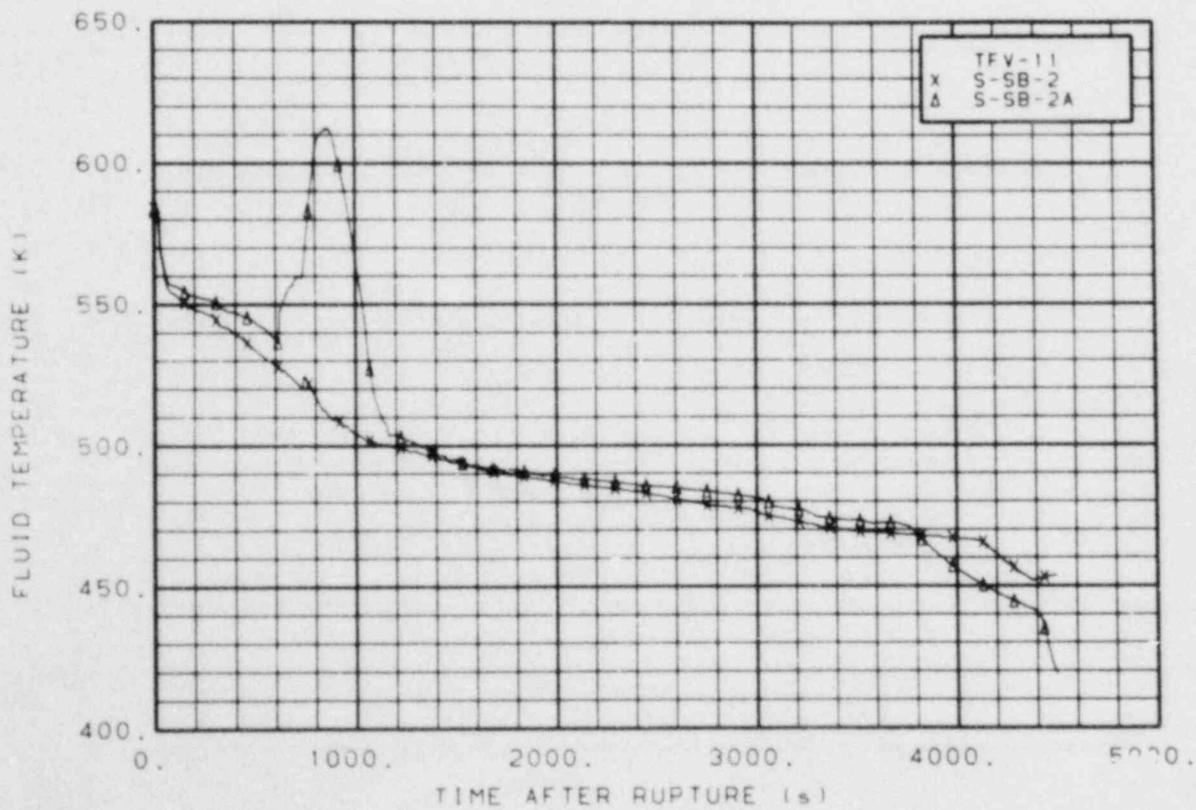

Figure 34. Fluid temperature in vessel (TFV-11), from 0 to 4500 s.

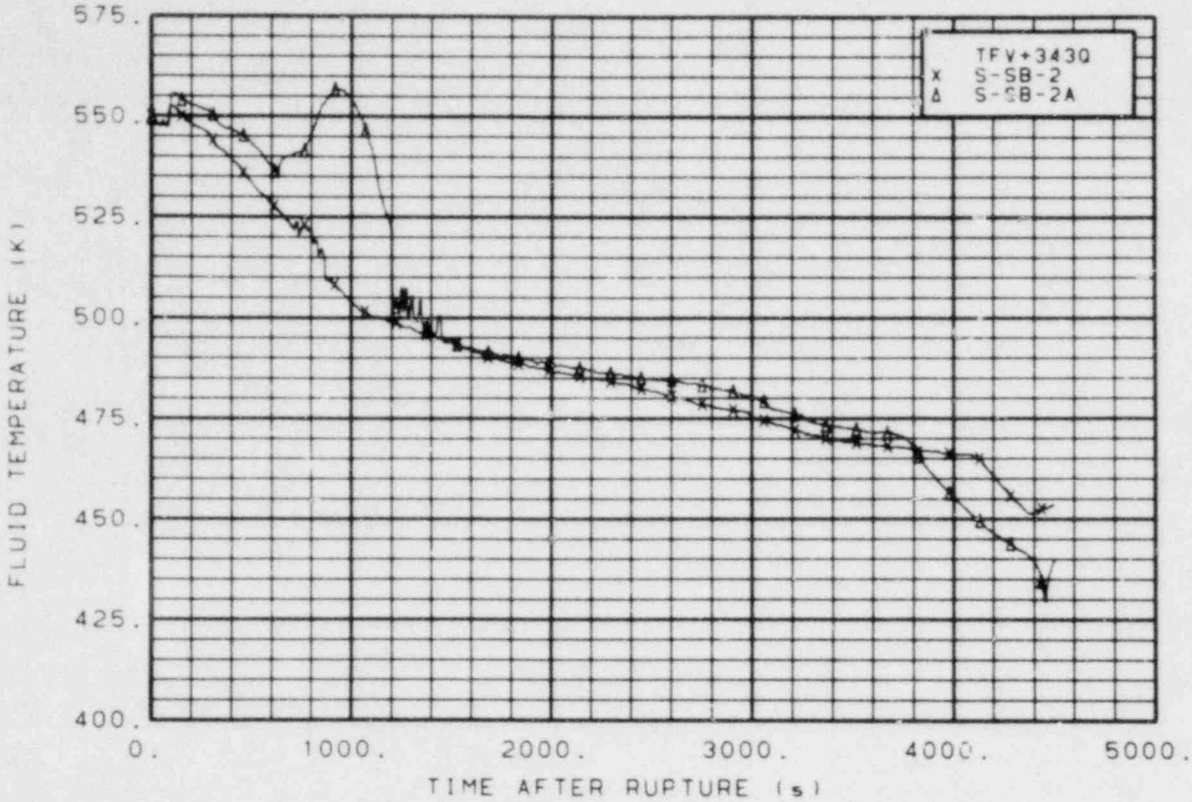

Figure 35. Fluid temperature in vessel (TFV + 343Q), from 0 to 4500 s.

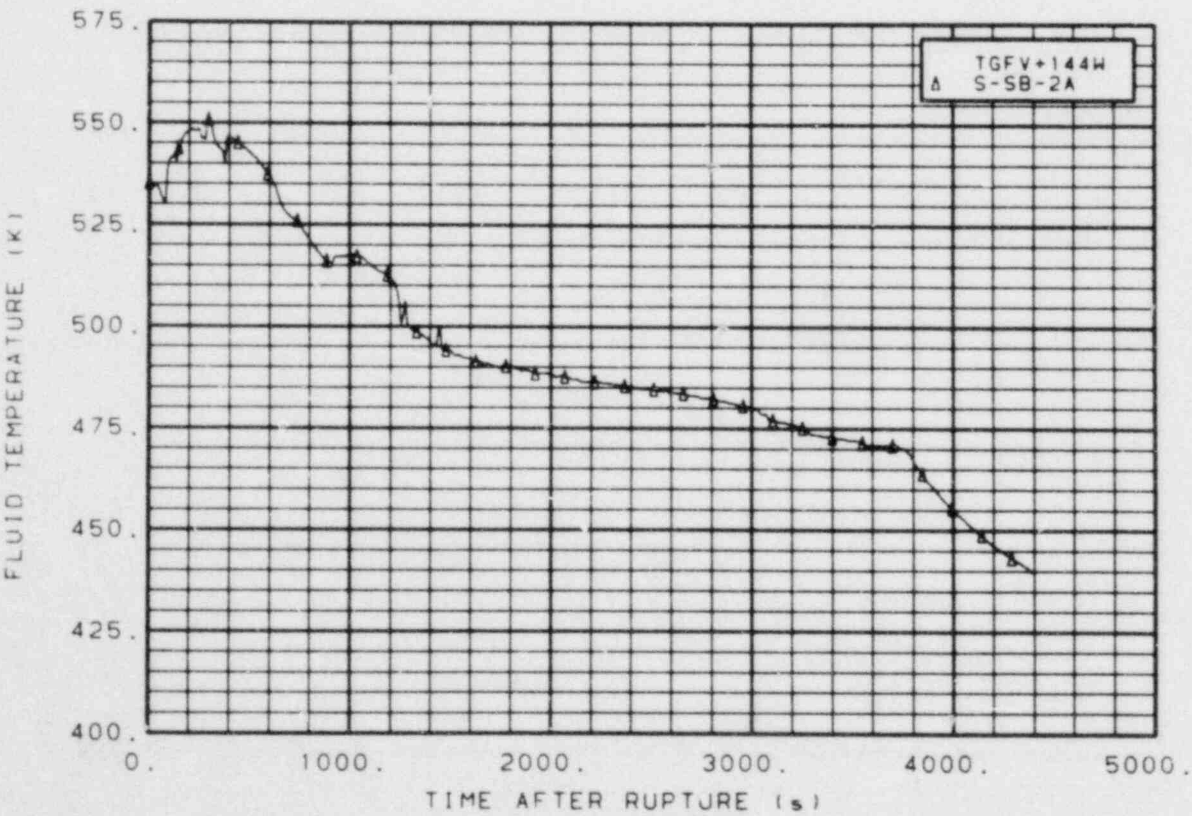

Figure 36. Fluid temperature in vessel core guide tube, Test S-SB-2A (TGFV + 144W), from 0 to 4390 s.

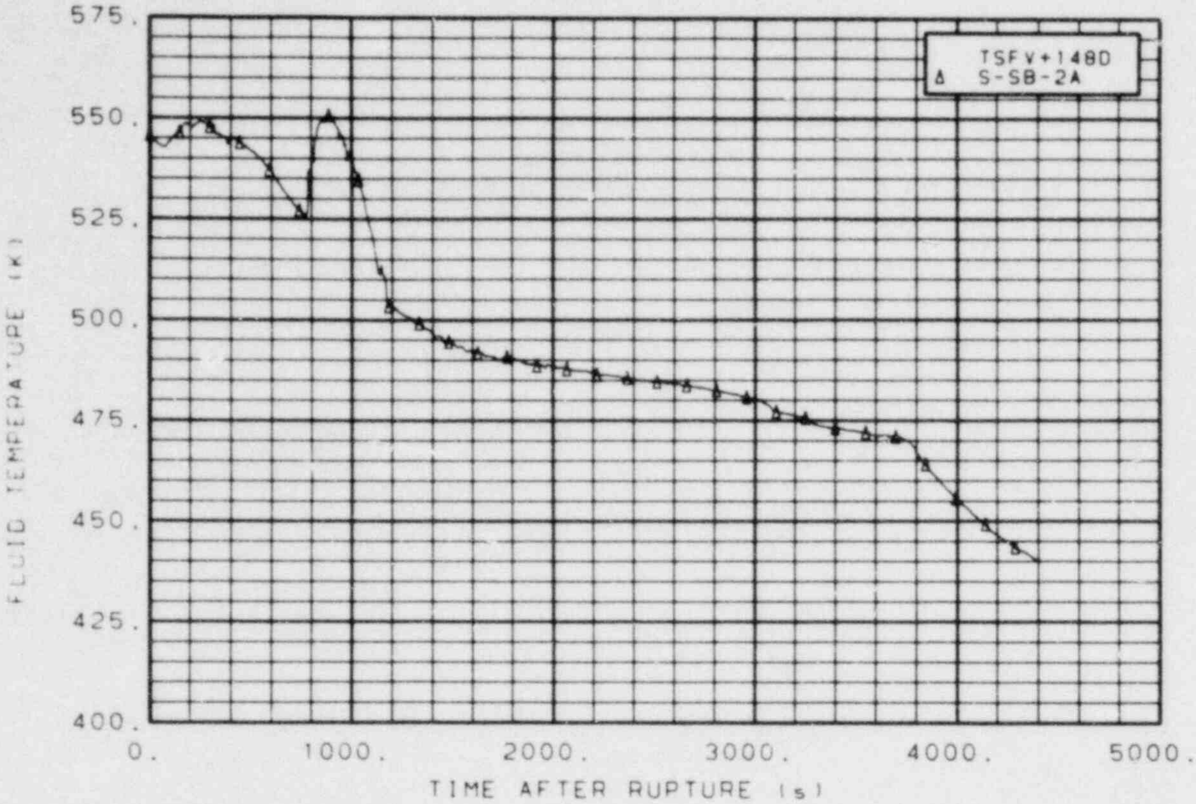

Figure 37. Fluid temperature in vessel support tube, Test S-SB-2A (TSFV + 148D), from 0 to 4390 s.

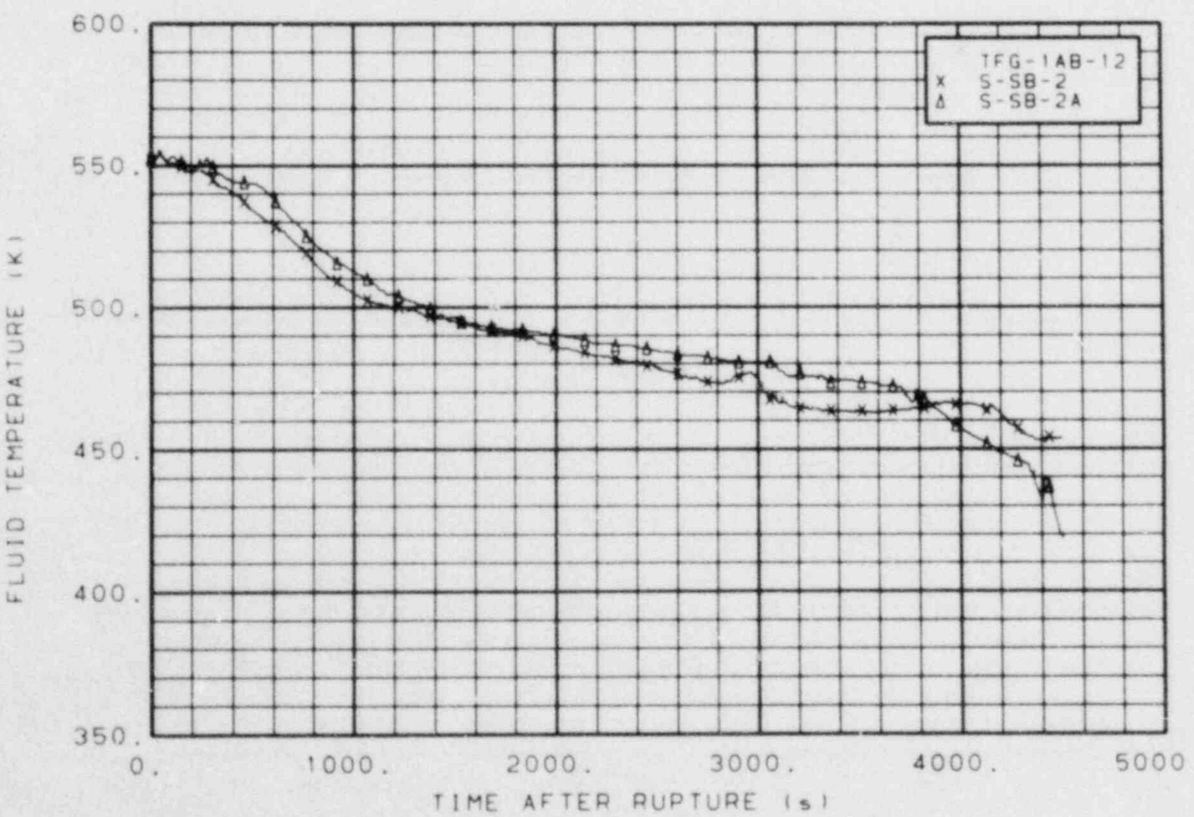

Figure 38. Fluid temperature in core, Grid Spacer 1 (TFG-1AB-12), from 0 to 4500 s.

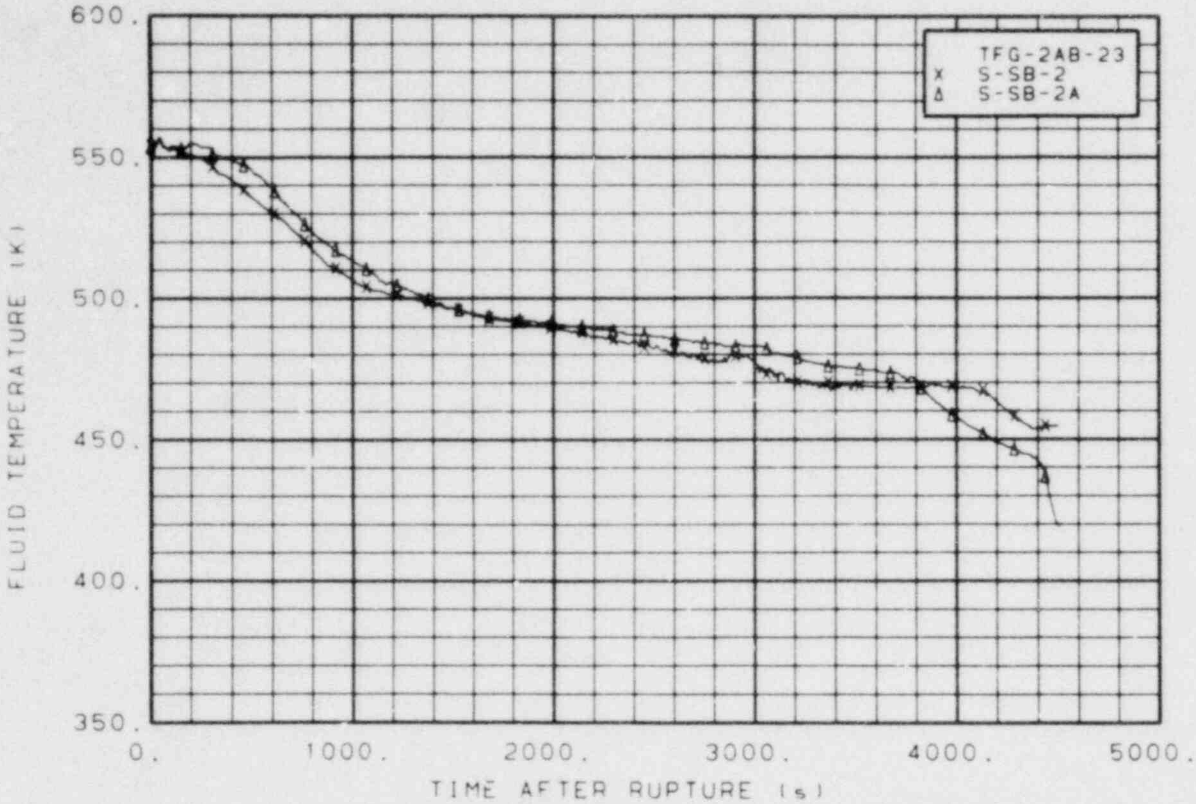

Figure 39. Fluid temperature in core, Grid Spacer 2 (TFG-2AB-23), from 0 to 4500 s.

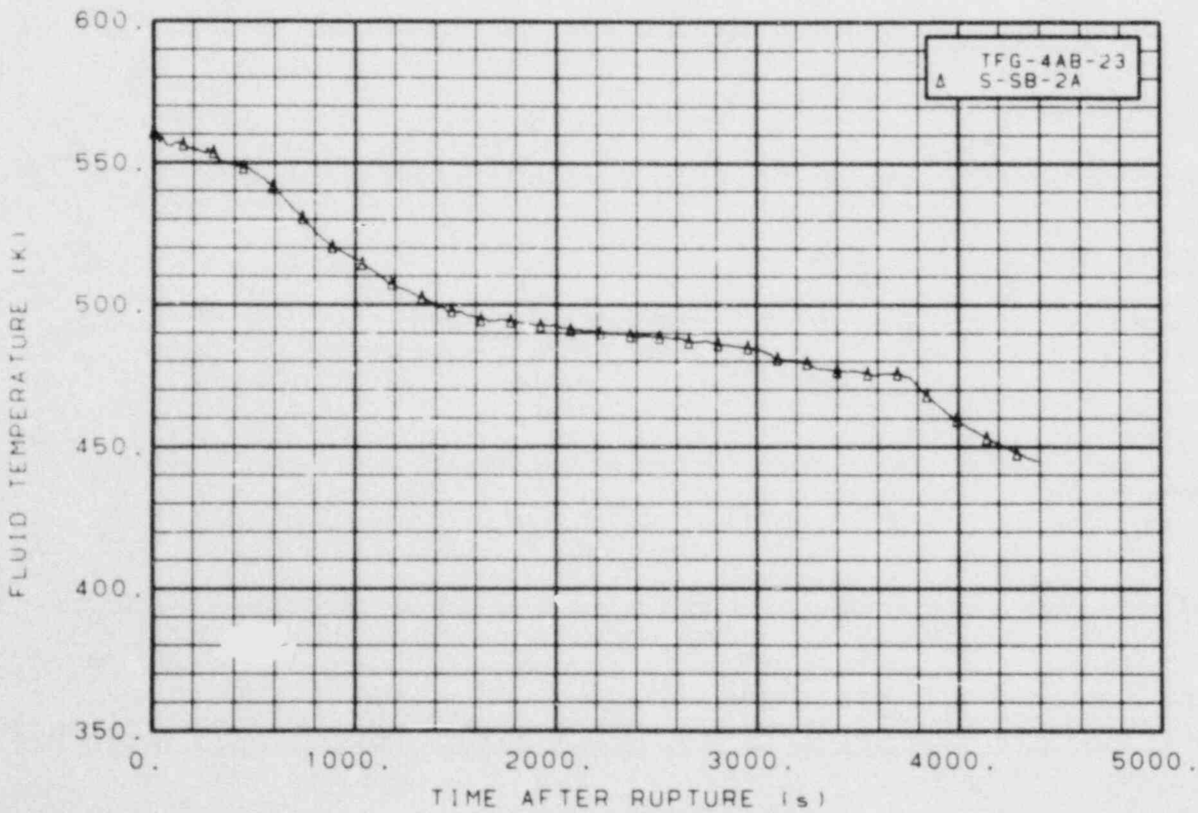

Figure 40. Fluid temperature in core, Grid Spacer 4, Test S-SB-2A (TFG-4AB-23), from 0 to 4390 s.

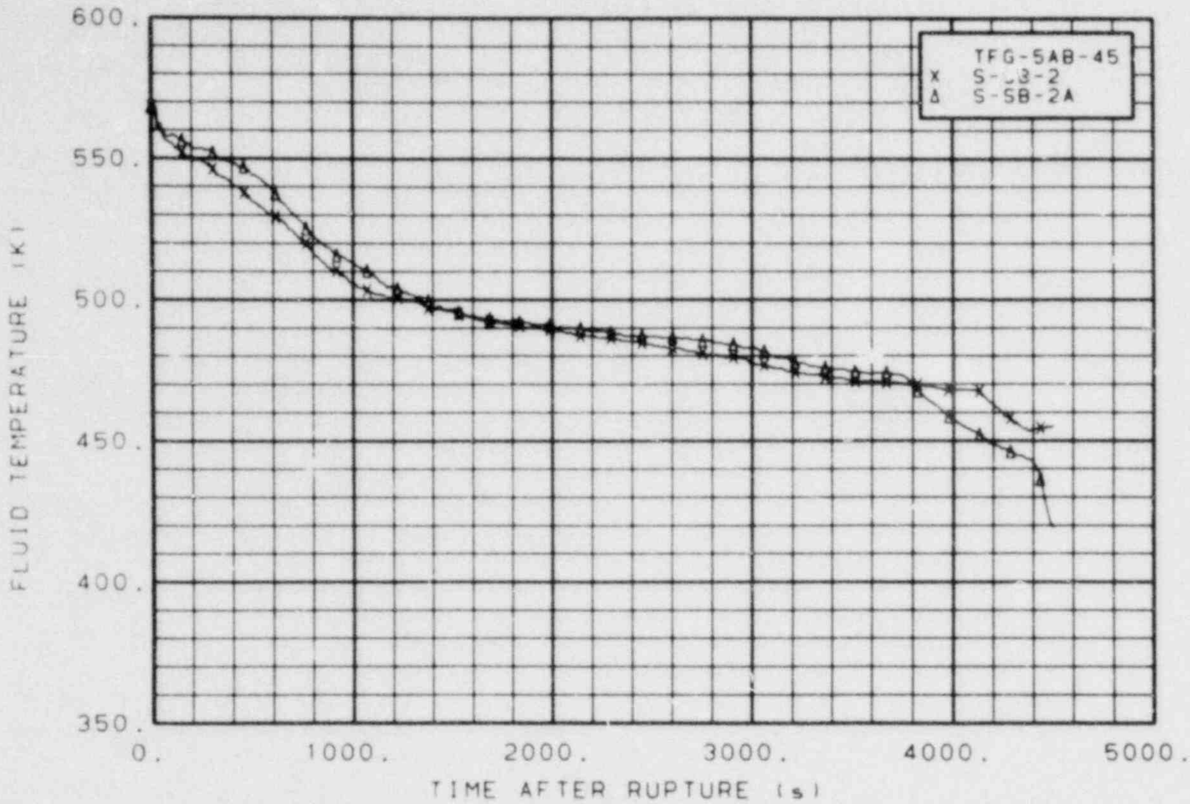

Figure 41. Fluid temperature in core, Grid Spacer 5 (TFG-5AB-45), from 0 to 4500 s.

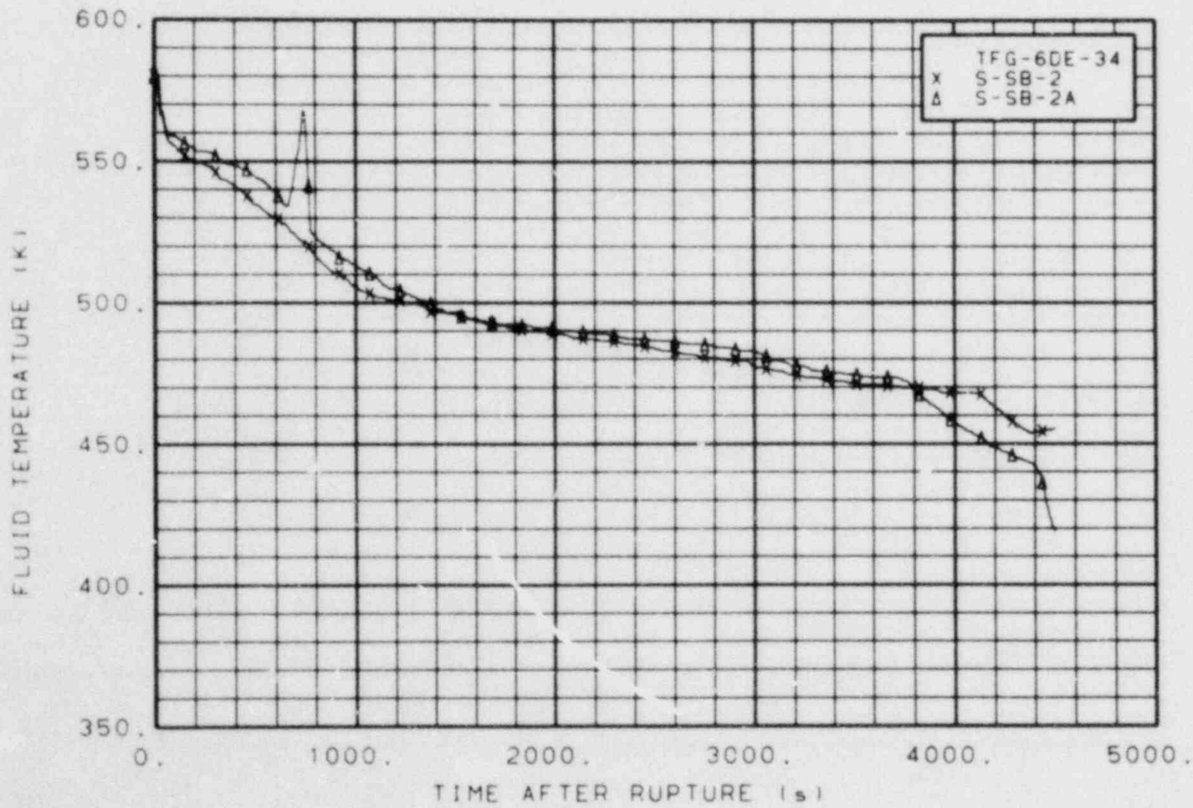

Figure 42. Fluid temperature in core, Grid Spacer 6 (TFG-6DE-34), from 0 to 4500 s.

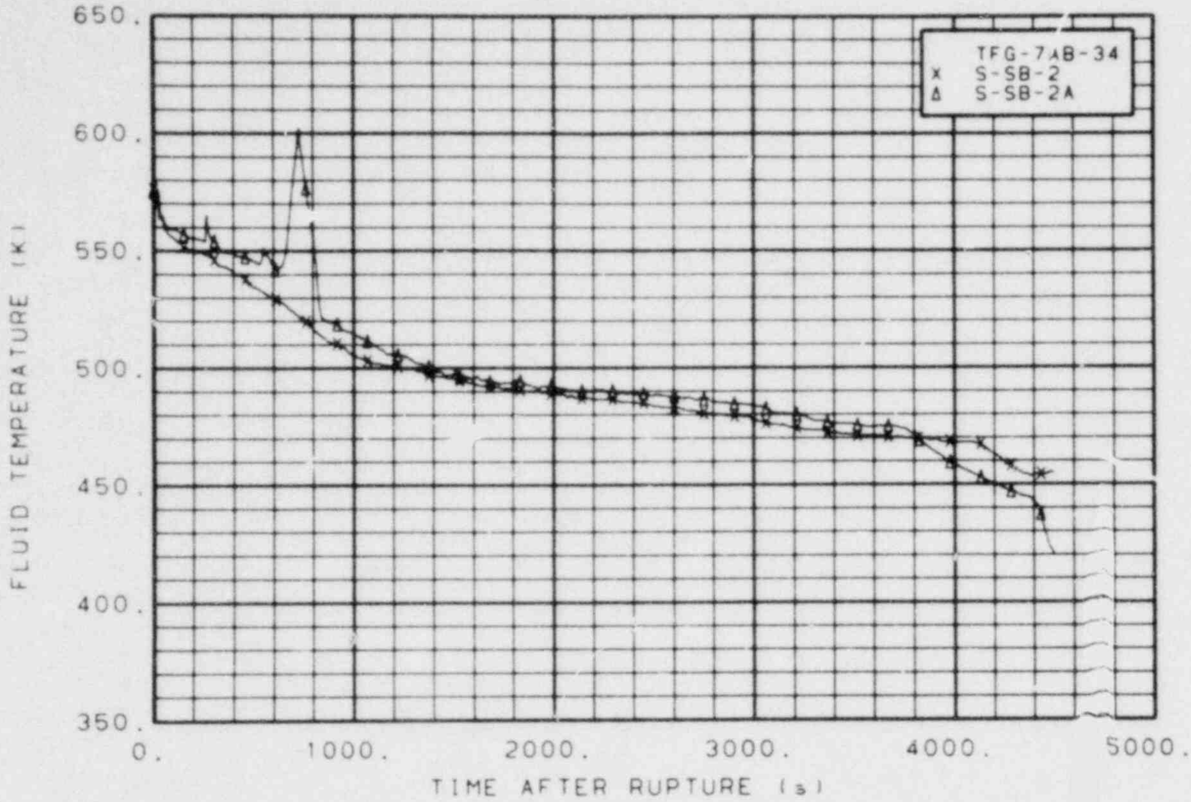

Figure 43. Fluid te..perature in core, Grid Spacer 7 (TFG-7AB-34), from 0 to 4500 .

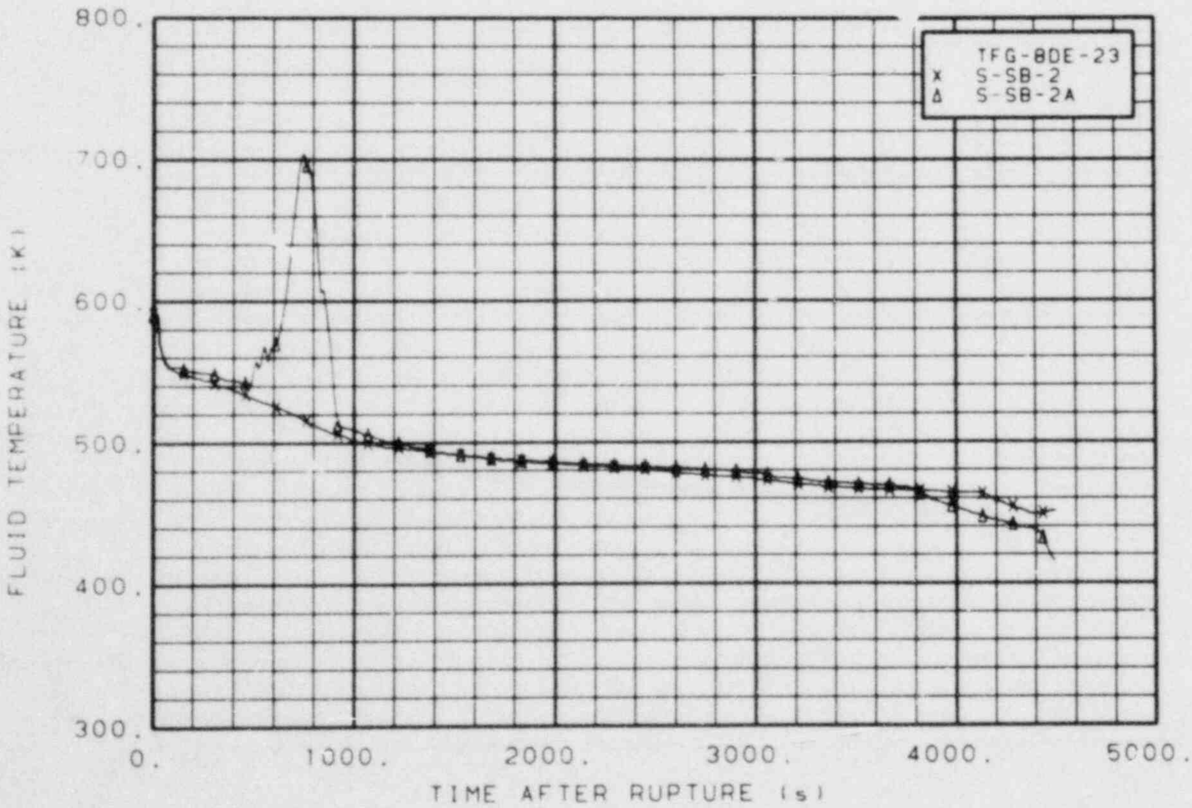

Figure 44. Fluid temperature in core, Grid Spacer 8 (TFG-8DE-23), from 0 to 4500 s.

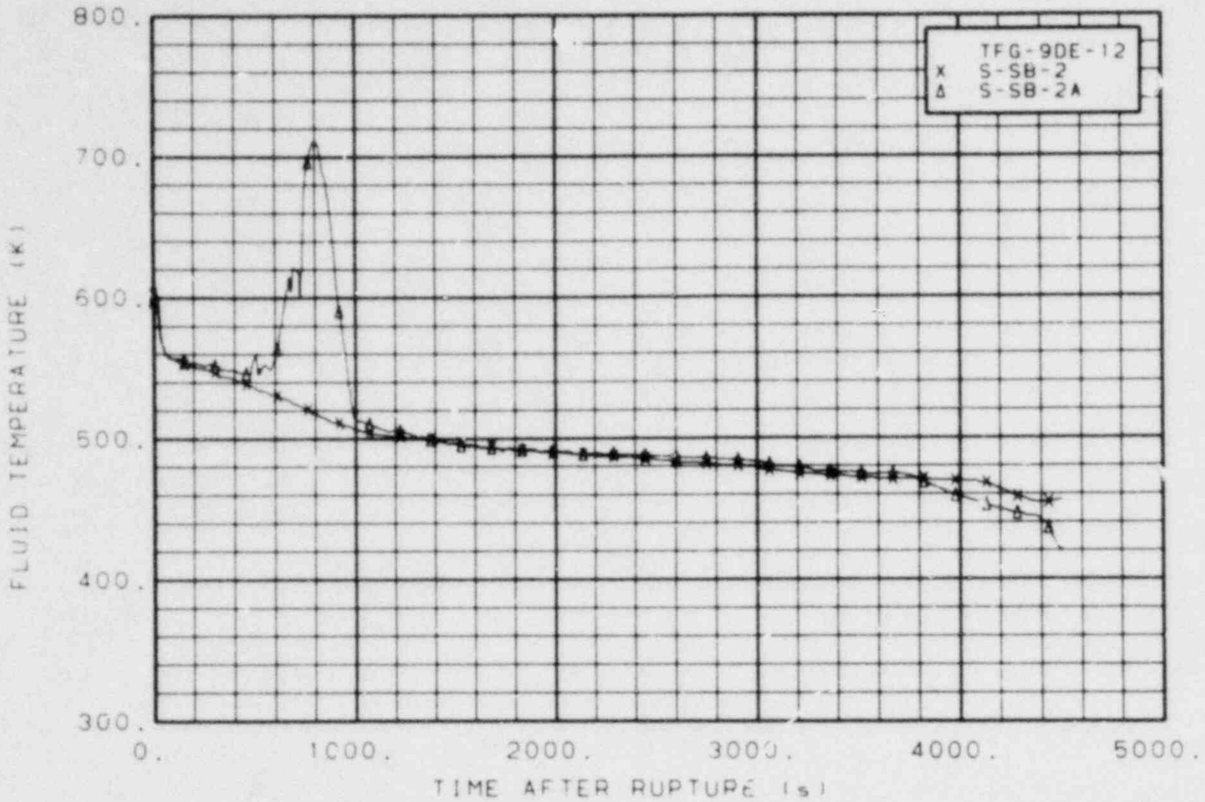

Figure 45. Fluid temperature in core, Grid Spacer 9 (TFG-9DE-12), from 0 to 4500 s.

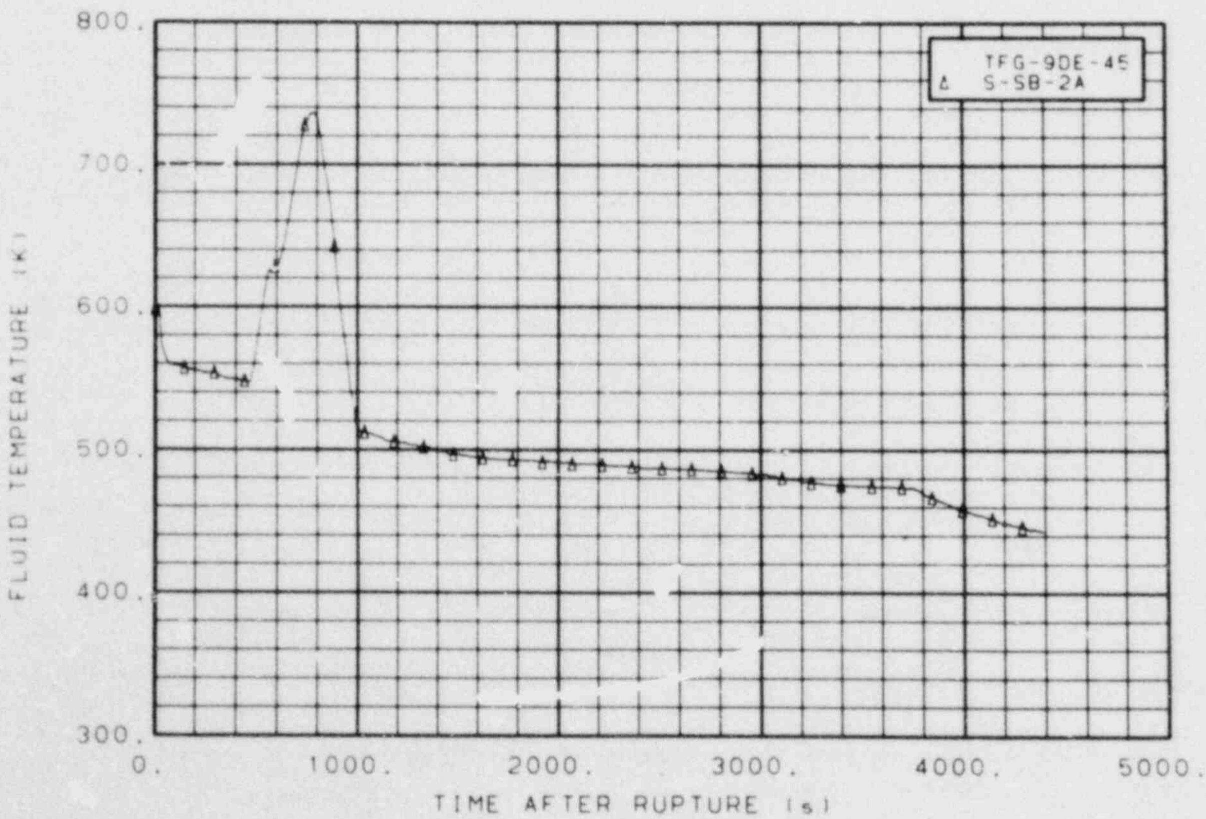

Figure 46. Fluid temperature in core, Grid Spacer 9, Test S-SB-2A (TFG-9DE-45), from 0 to 4390 s.

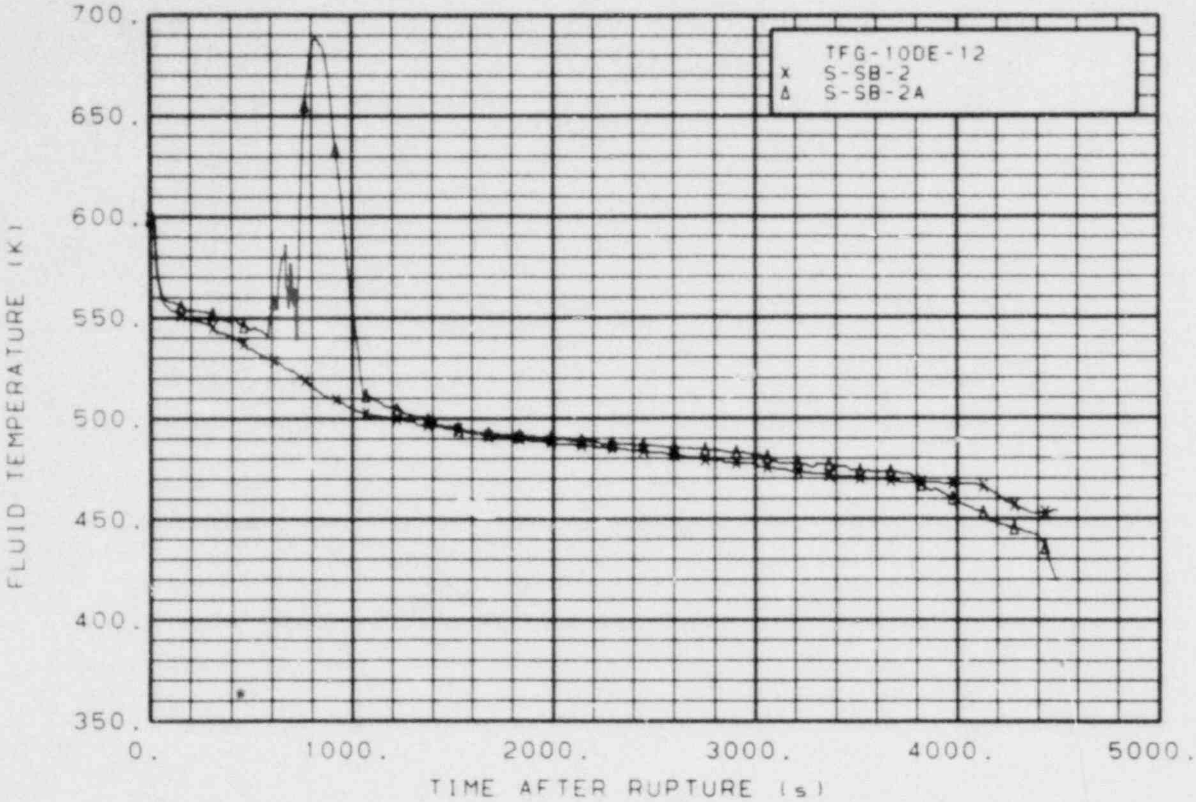

Figure 47. Fluid temperature in core, Grid Spacer 10 (TFG-10DE-12), from 0 to 4500 s.

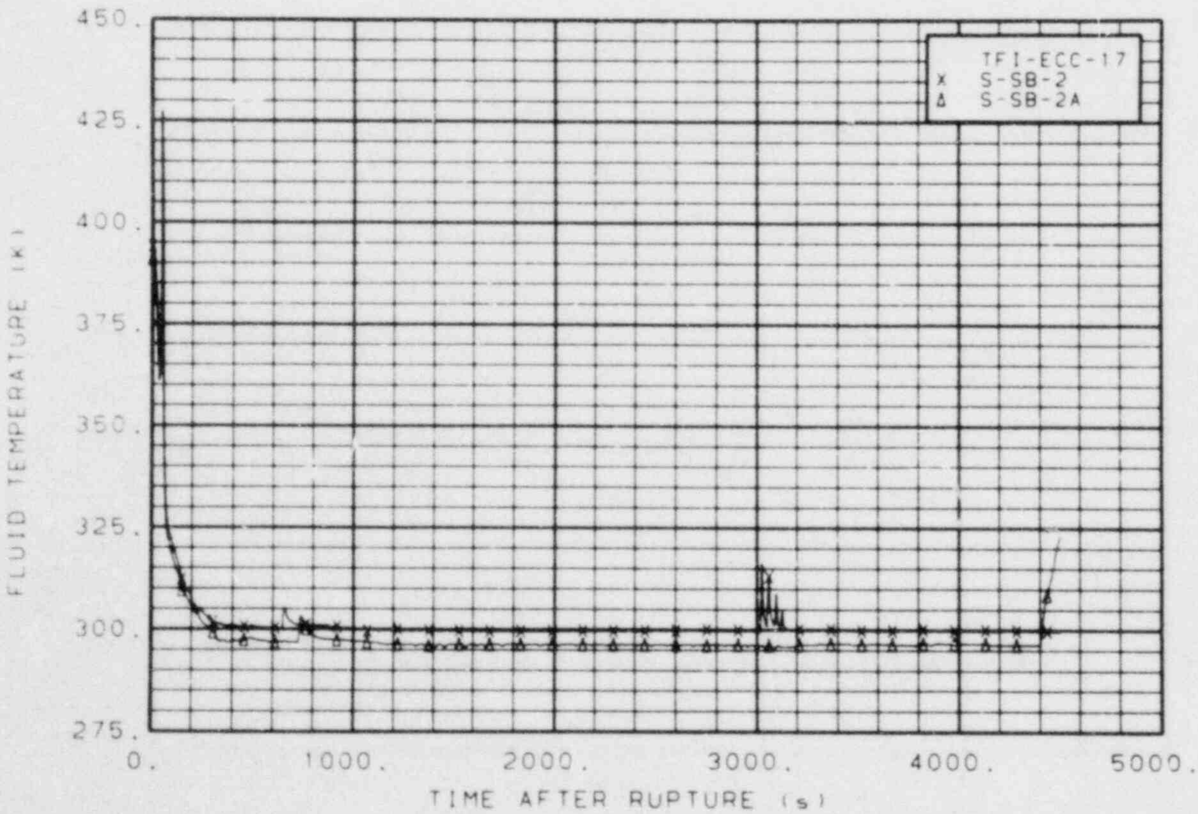

Figure 48. Fluid temperature in intact loop accumulator, coolant injection line (TFI-ECC-17), from 0 to 4500 s.

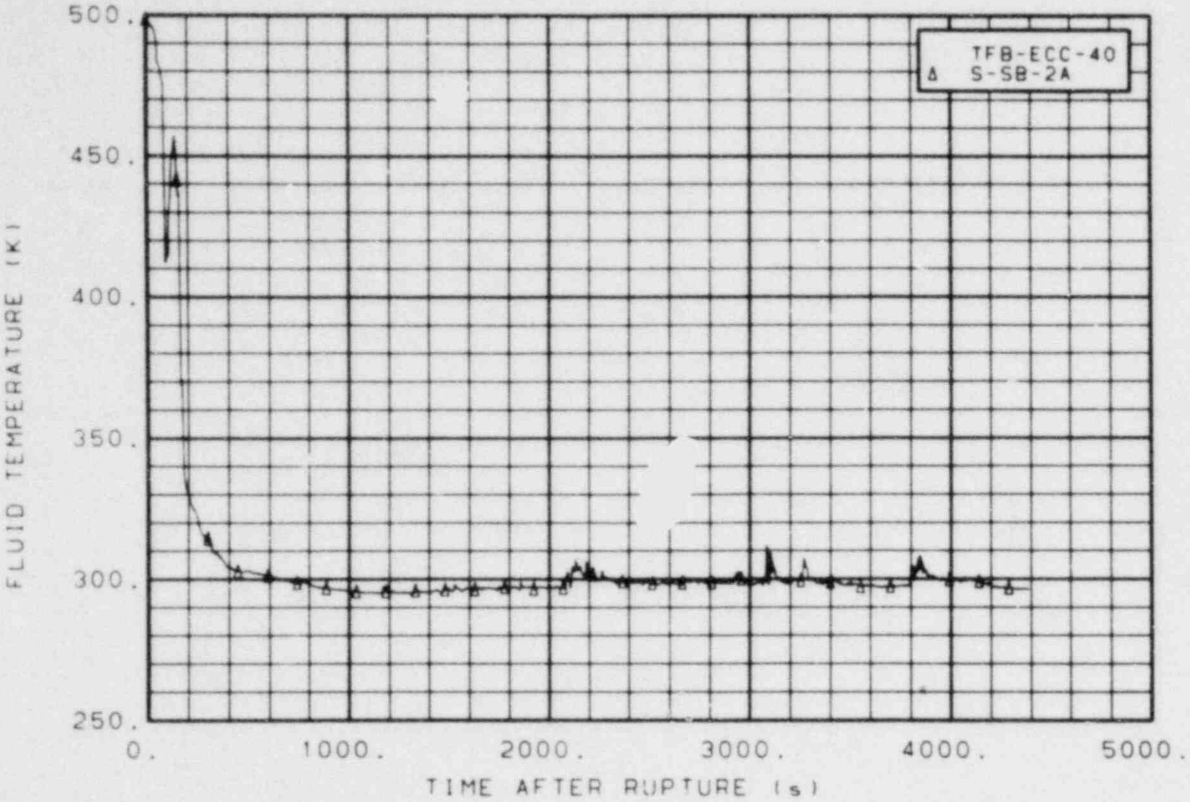

Figure 49. Fluid temperature in broken loop accumulator, coolant injection line, Test S-SB-2A (TFB-ECC-40), from 0 to 4390 s.

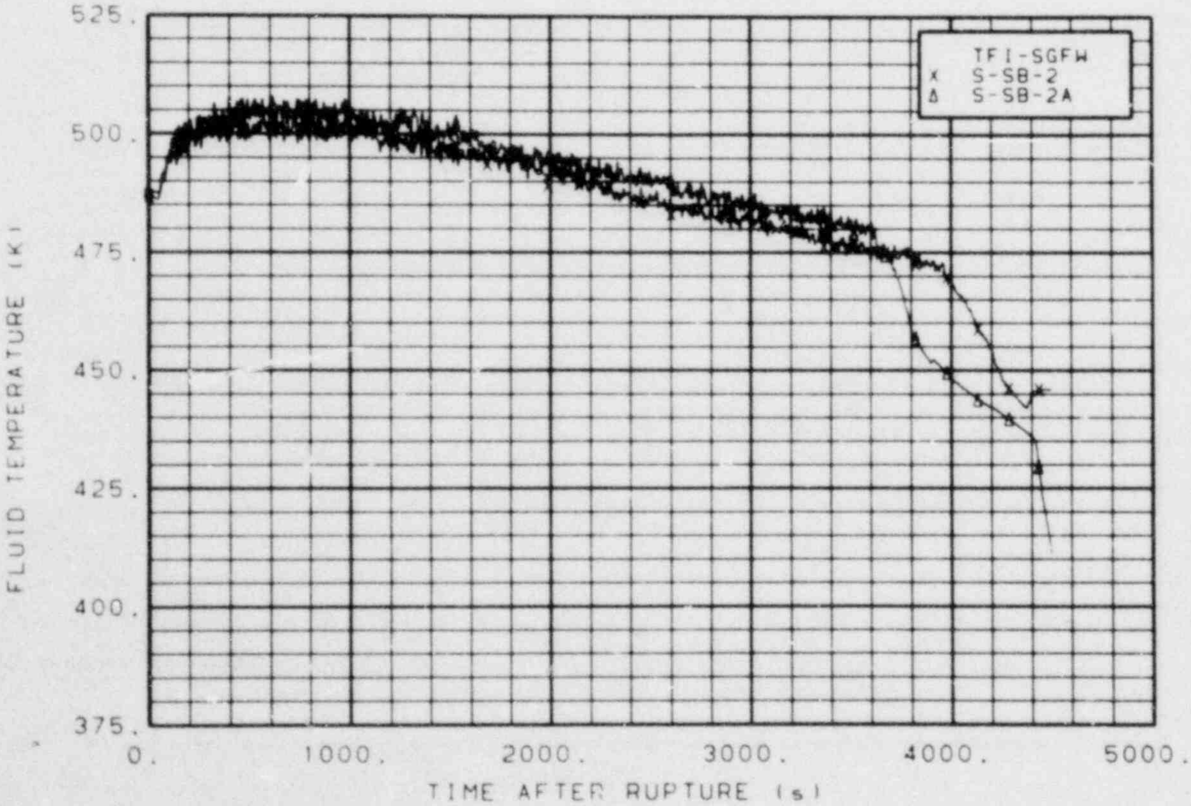

Figure 50. Fluid temperature in intact loop feedwater (TFI-SGFW), from 0 to 4500 s.

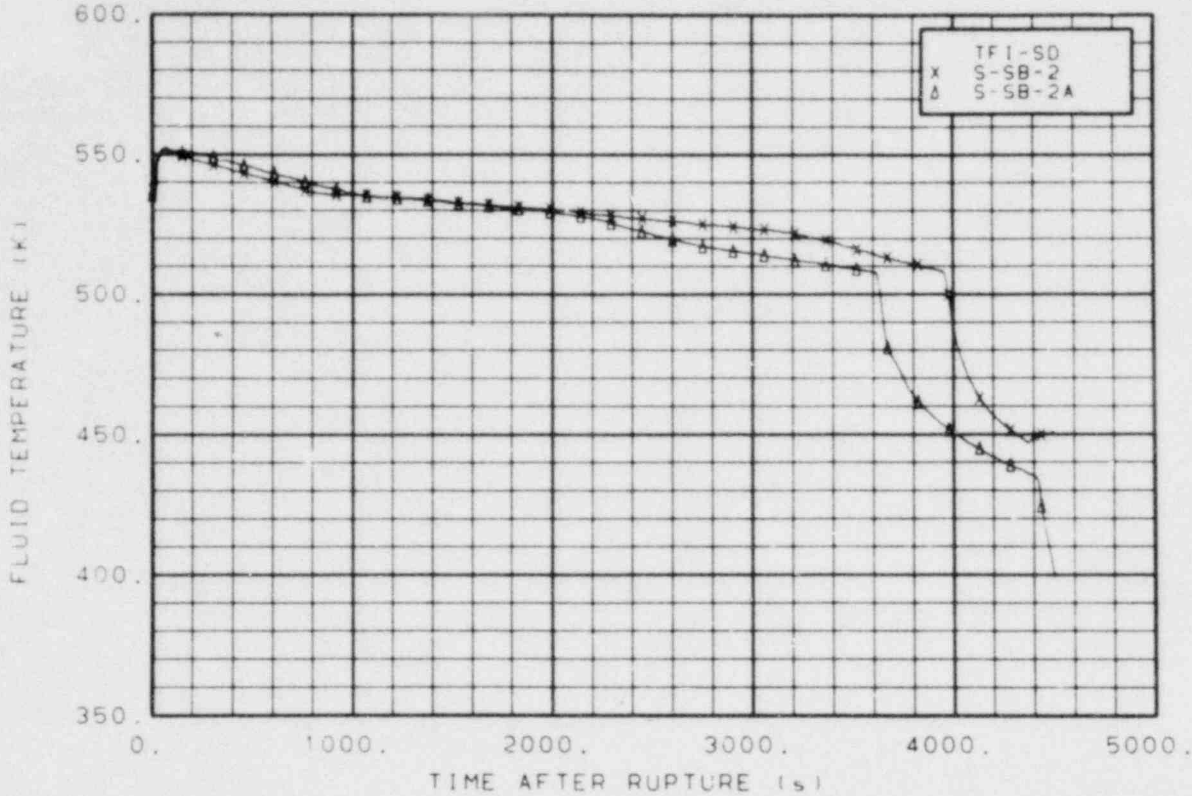

Figure 51. Fluid temperature in intact loop steam generator steam dome, secondary side (TFI-SD), from 0 to 4500 s.

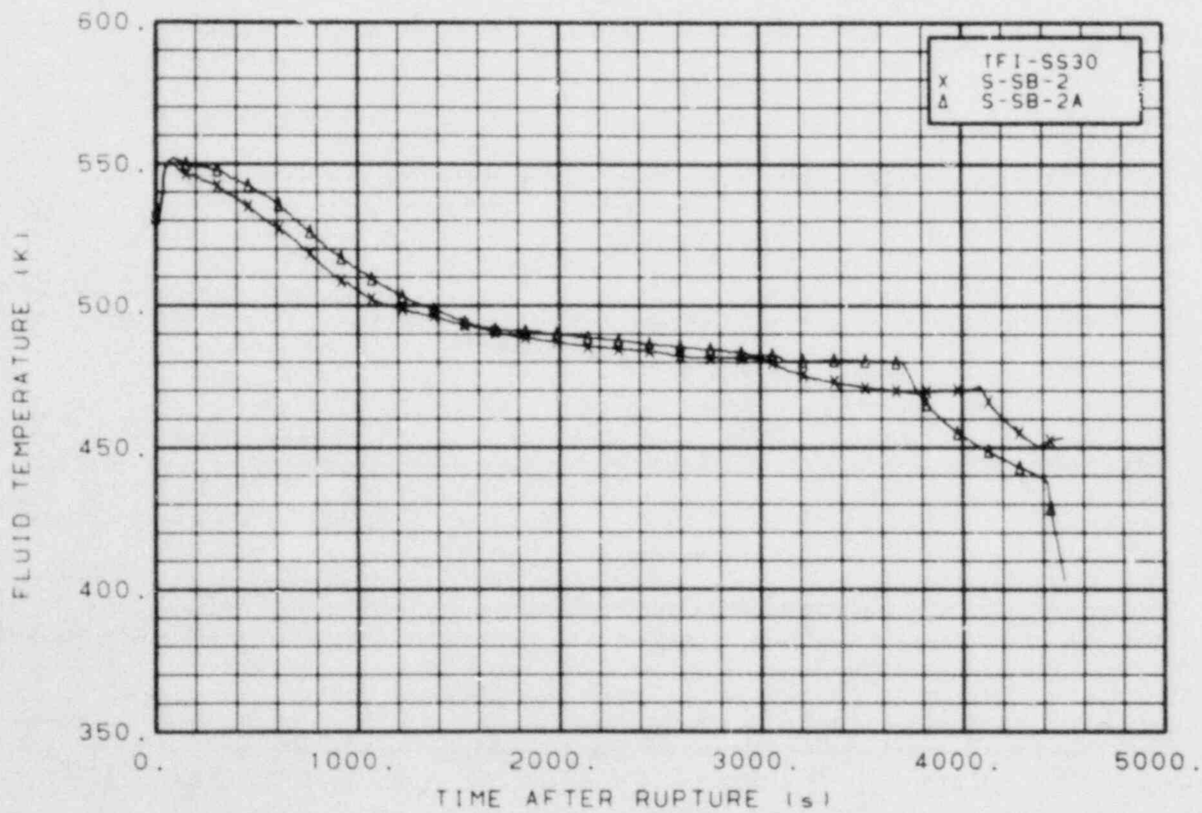

Figure 52. Fluid temperature in intact loop steam generator, secondary side (TFI-SS30), from 0 to 4500 s.

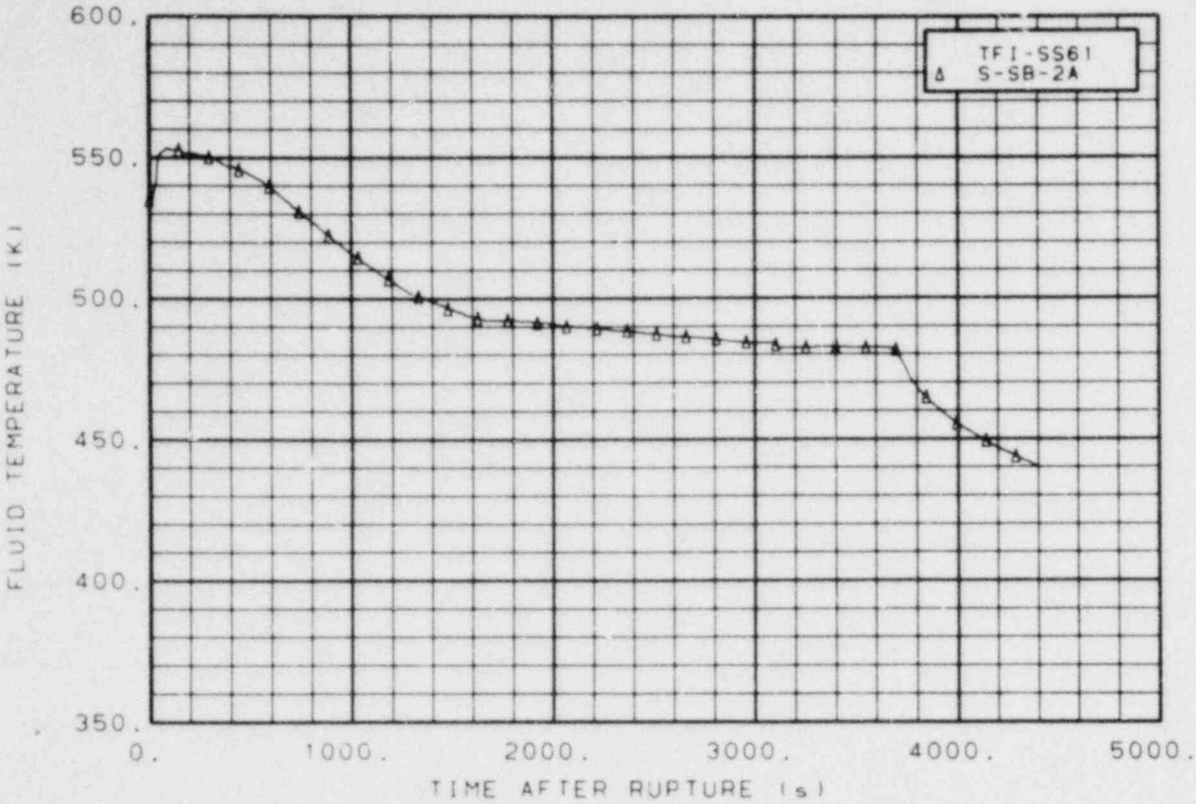

Figure 53. Fluid temperature in intact loop steam generator, secondary side, Test S-SB-2A (TFI-SS61), from 0 to 4390 s.

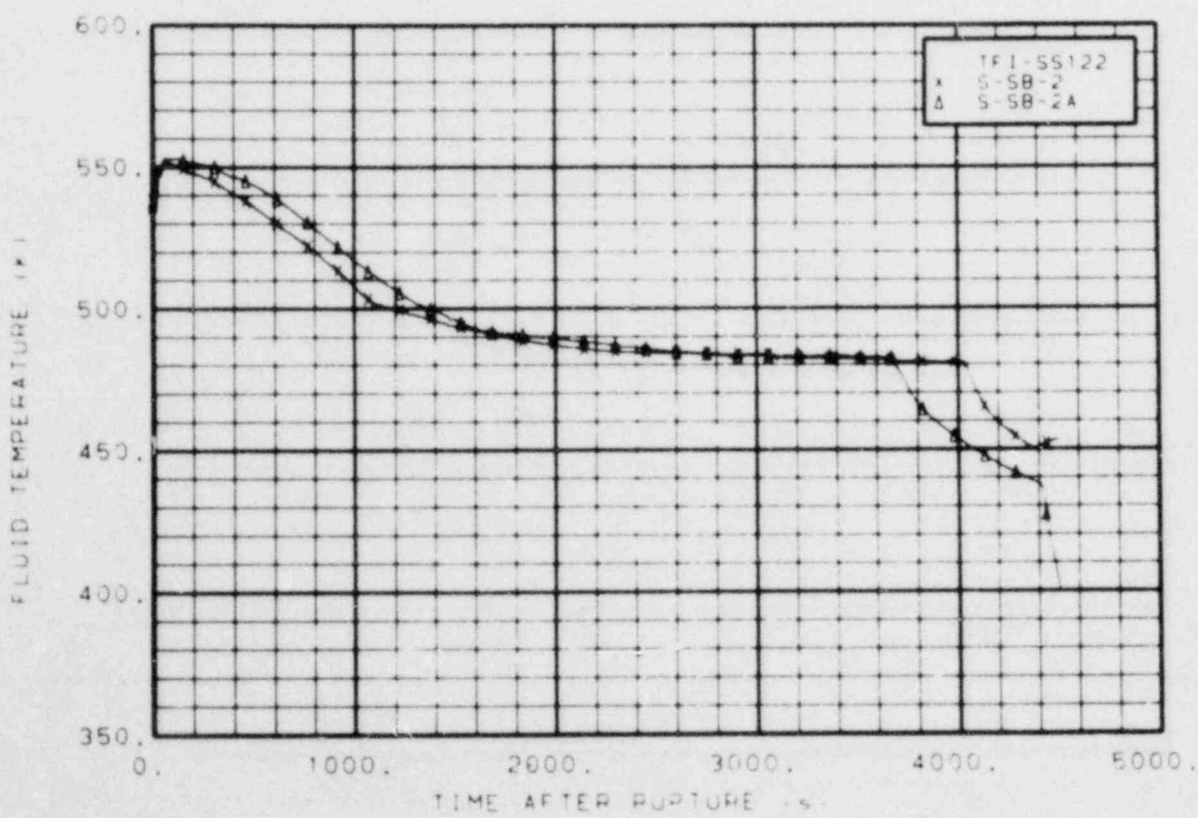

Figure 54. Fluid temperature in intact loop steam generator, secondary side (TFI-SS122), from 0 to 4500 s.

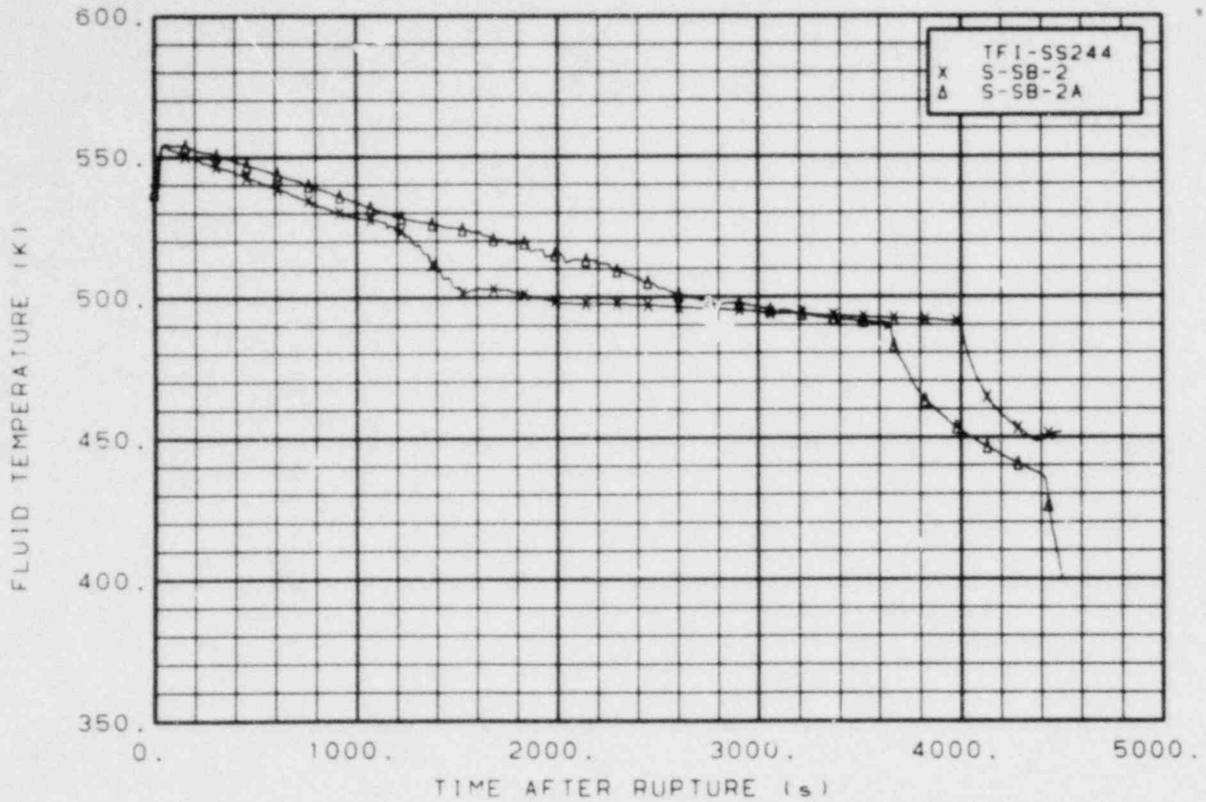

Figure 55. Fluid temperature in intact loop steam generator, secondary side (TFI-SS244), from 0 to 4500 s.

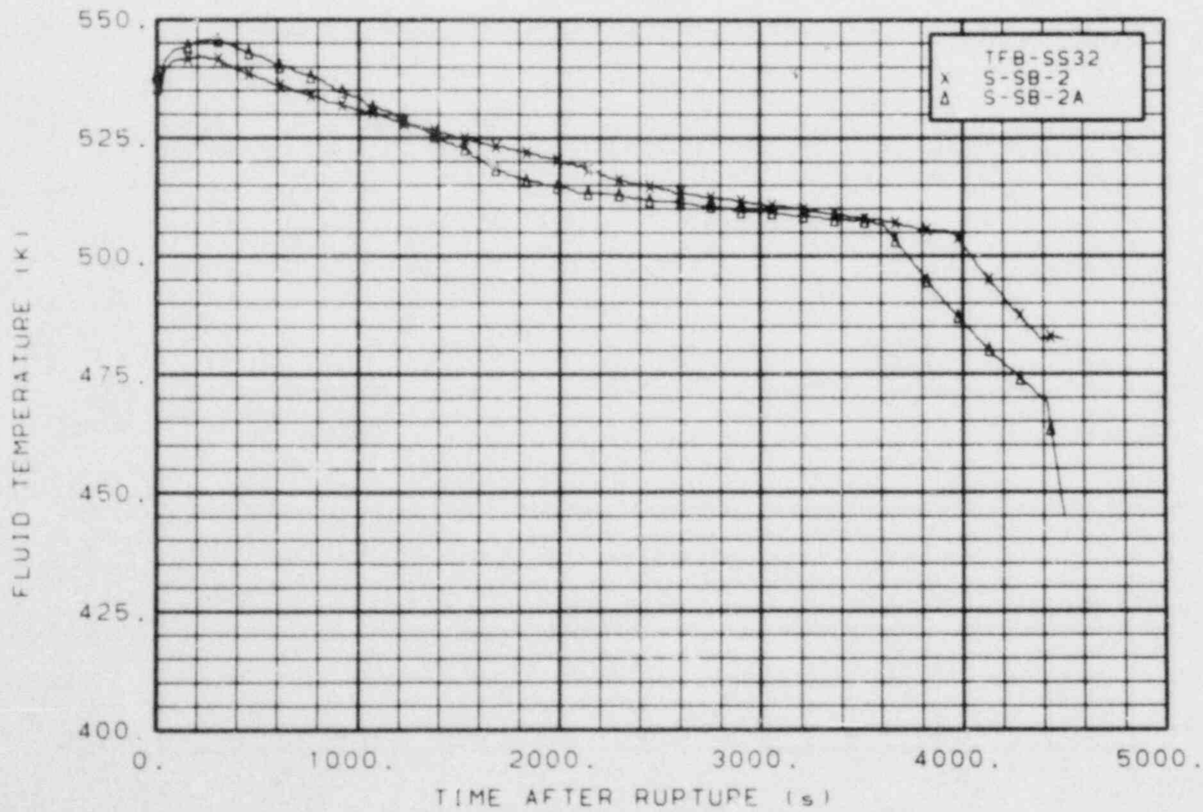

Figure 56. Fluid temperature in broken loop steam generator, secondary side (TFB-SS32), from 0 to 4500 s.

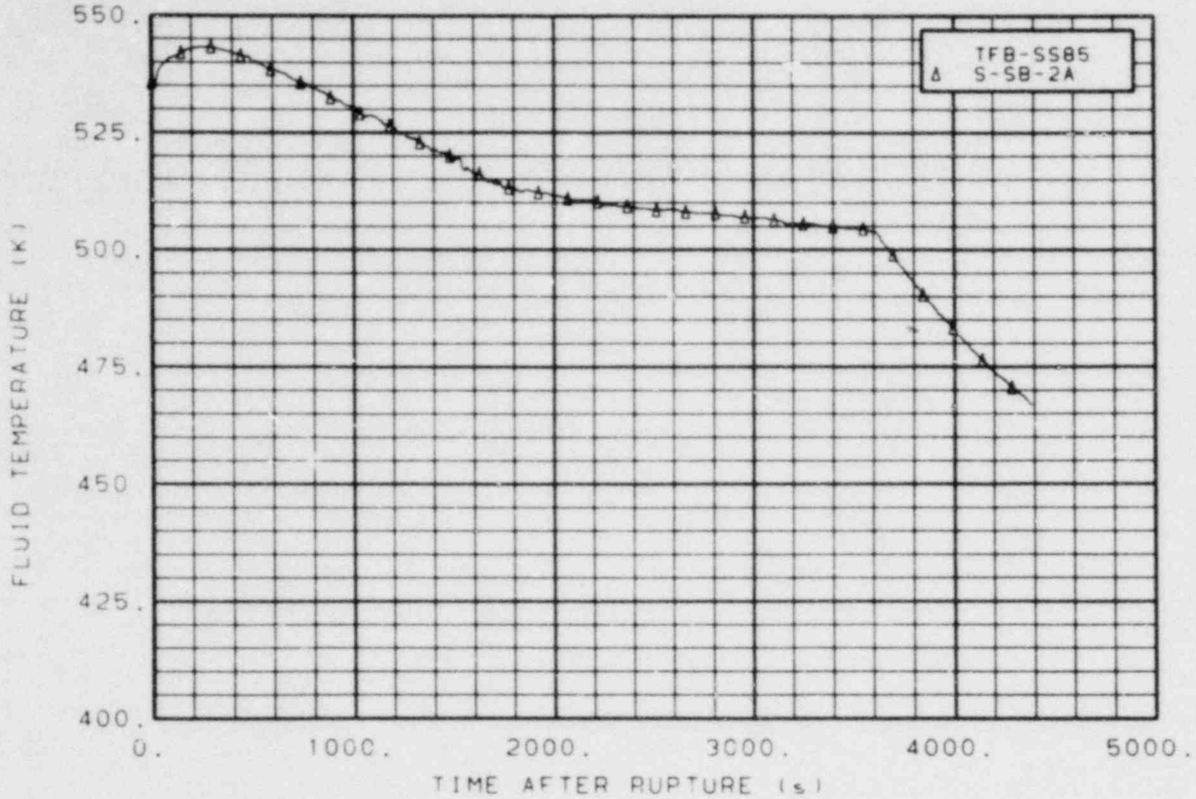

Figure 57. Fluid temperature in broken loop steam generator, secondary side, Test S-SB-2A (TFB-SS85), from 0 to 4390 s.

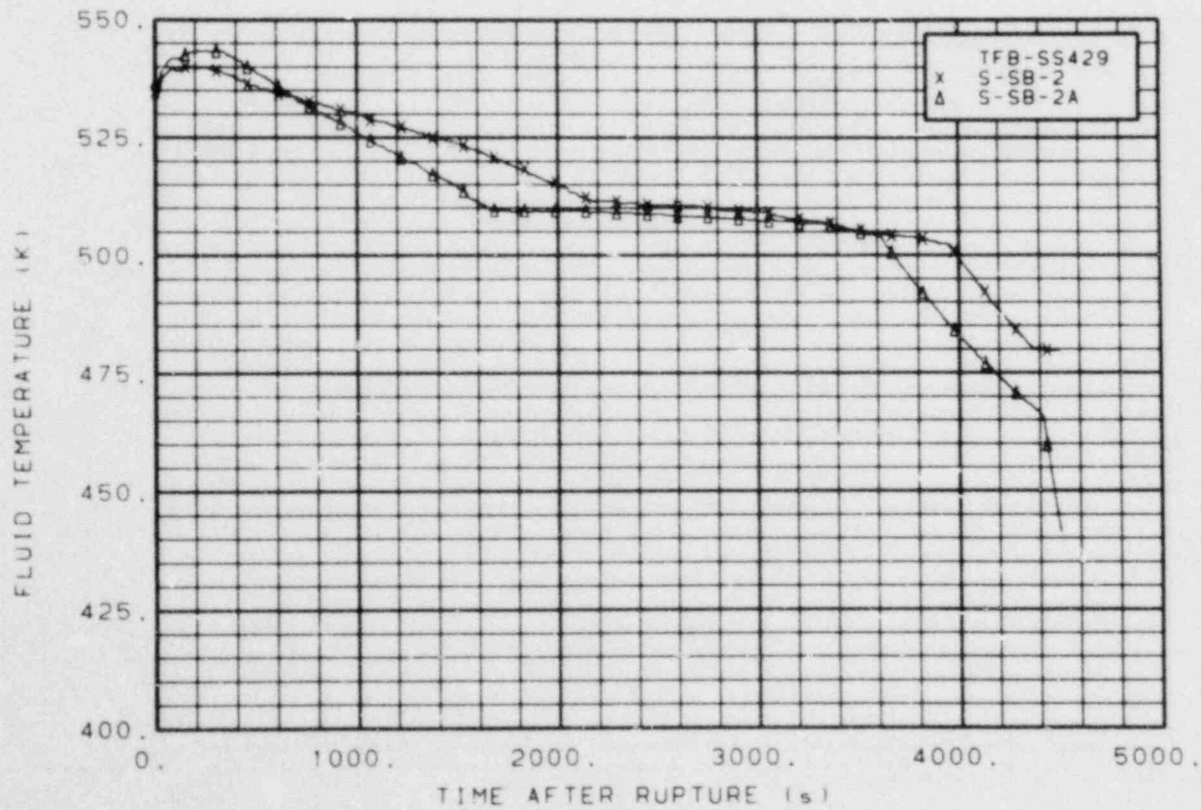

Figure 58. Fluid temperature in broken loop steam generator, secondary side (TFB-SS429), from 0 to 4500 s.

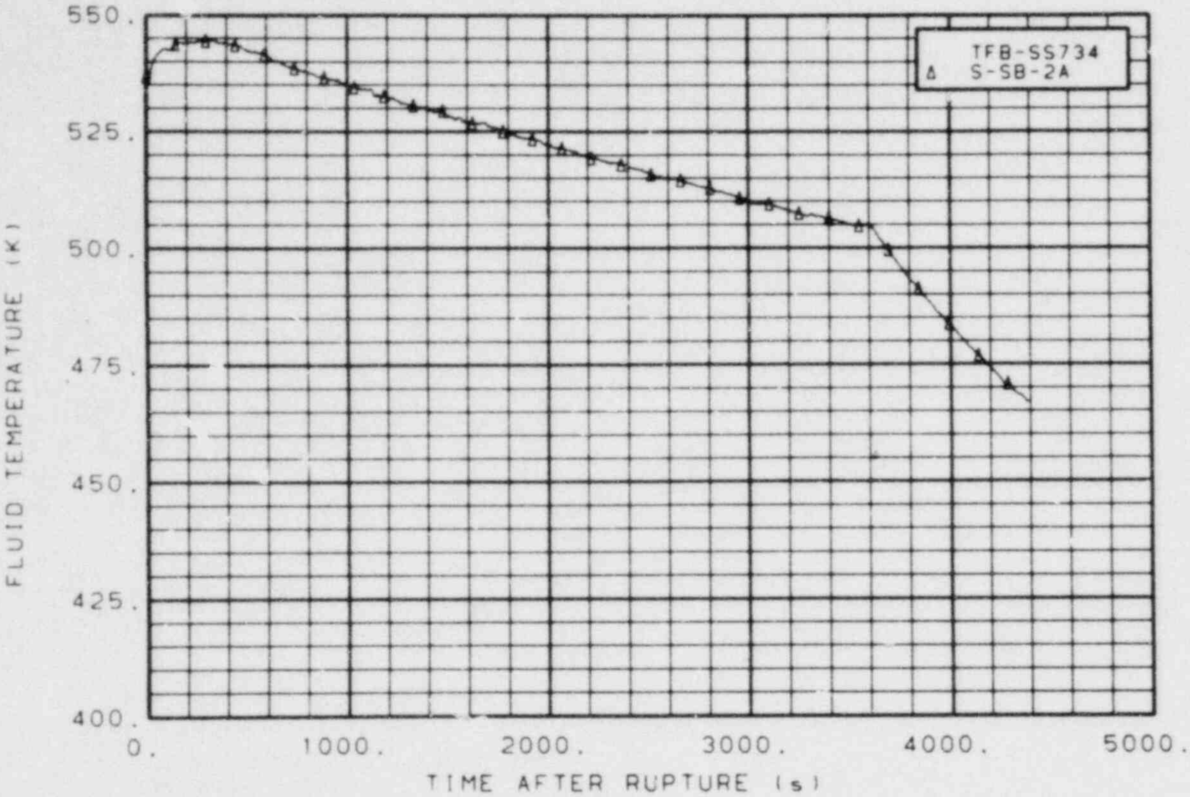

Figure 59. Fluid temperature in broken loop steam generator, secondary side, Test S-SB-2A (TFB-SS734), from 0 to 4390 s.

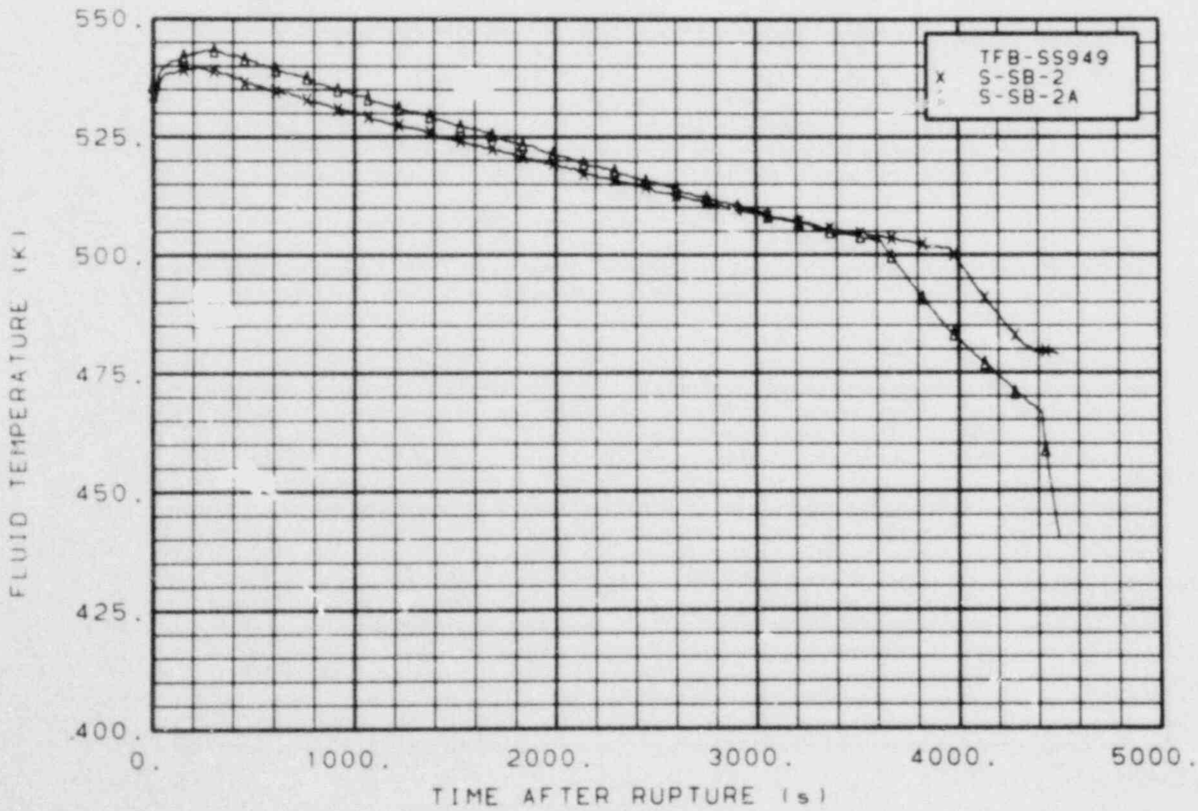

Figure 60. Fluid temperature in broken loop steam generator, secondary side (TFB-SS949), from 0 to 4500 s.

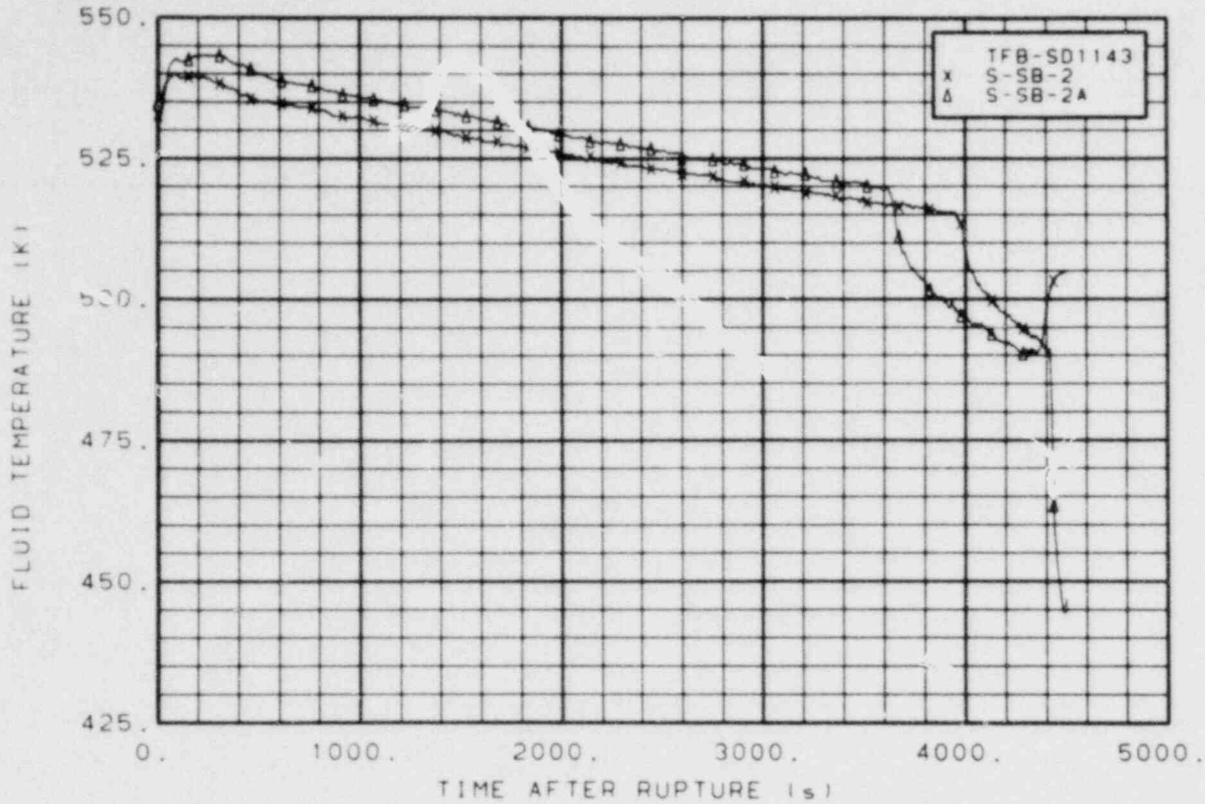

Figure 61. Fluid temperature in broken loop steam generator, steam dome (TFB-SD1143), from 0 to 4500 s.

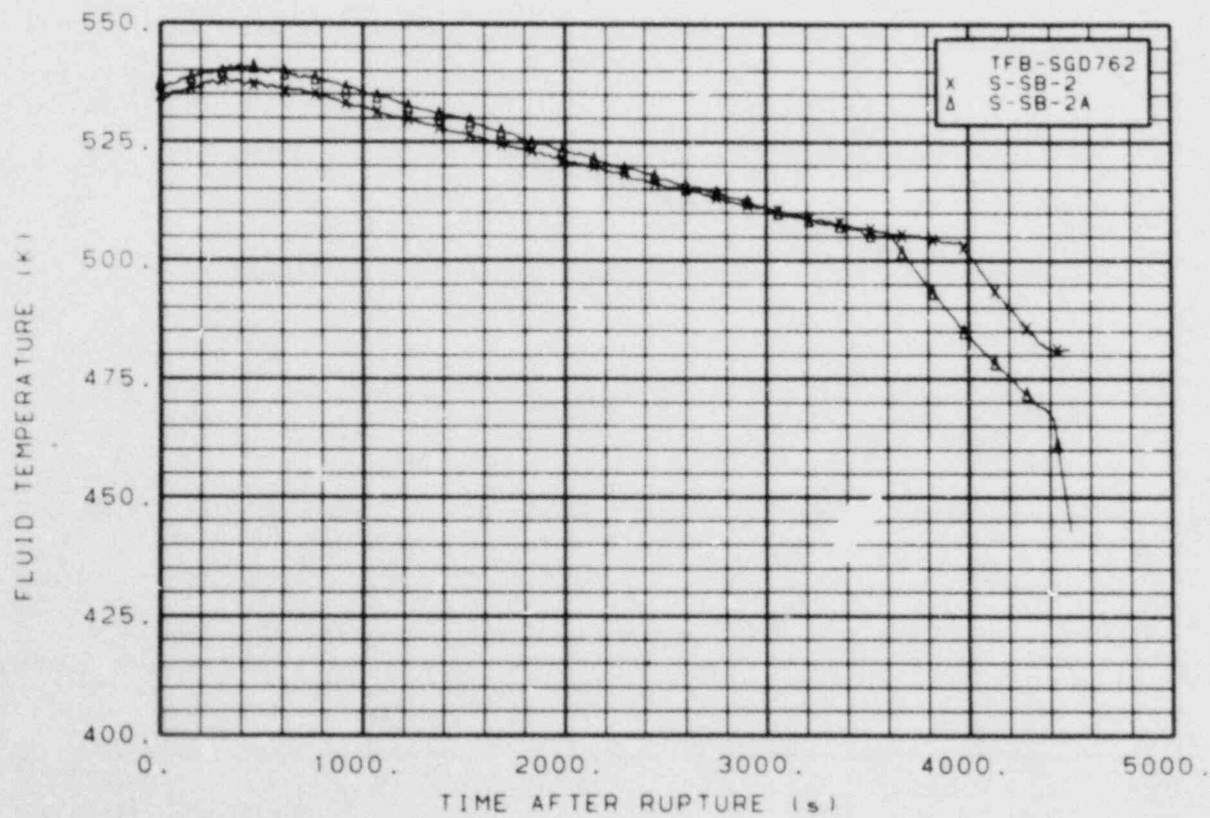

Figure 62. Fluid temperature in broken loop steam generator, secondary side downcomer (TFB-SGD762), from 0 to 4500 s.

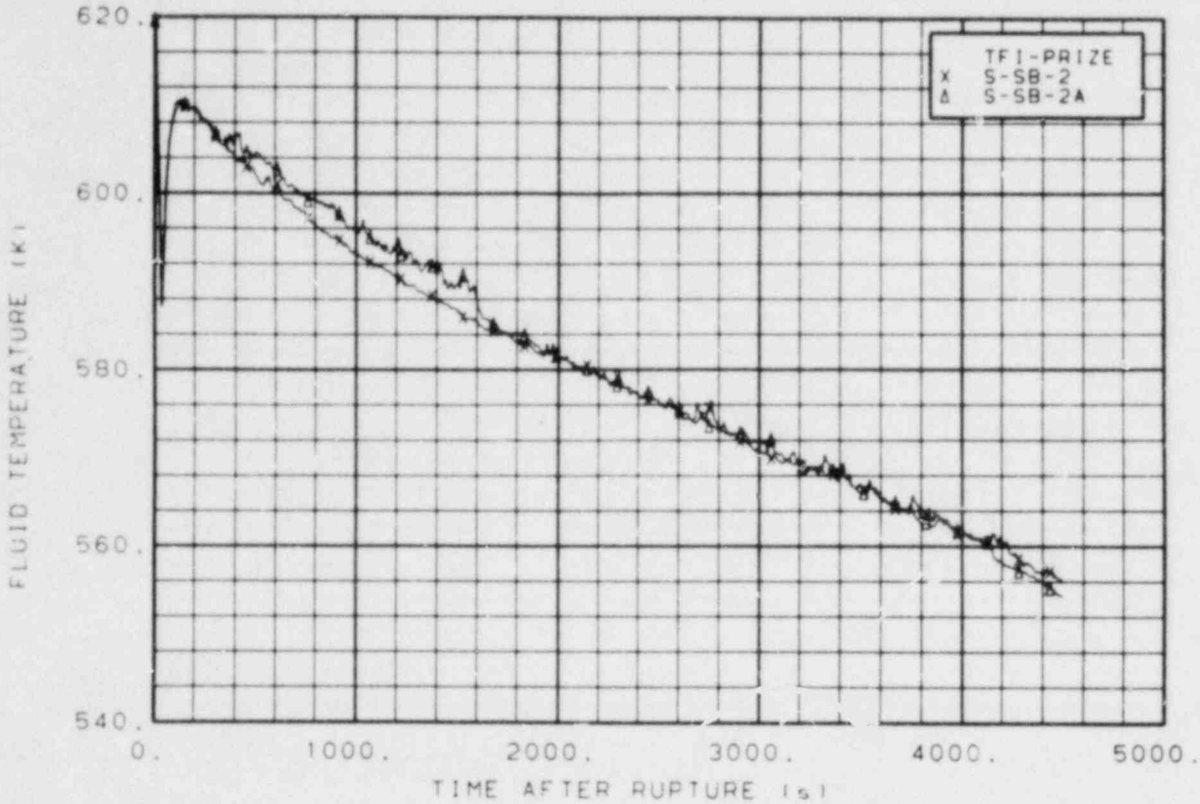

Figure 63. Fluid temperature in intact loop, pressurizer (TFI-PRIZE), from 0 to 4500 s.

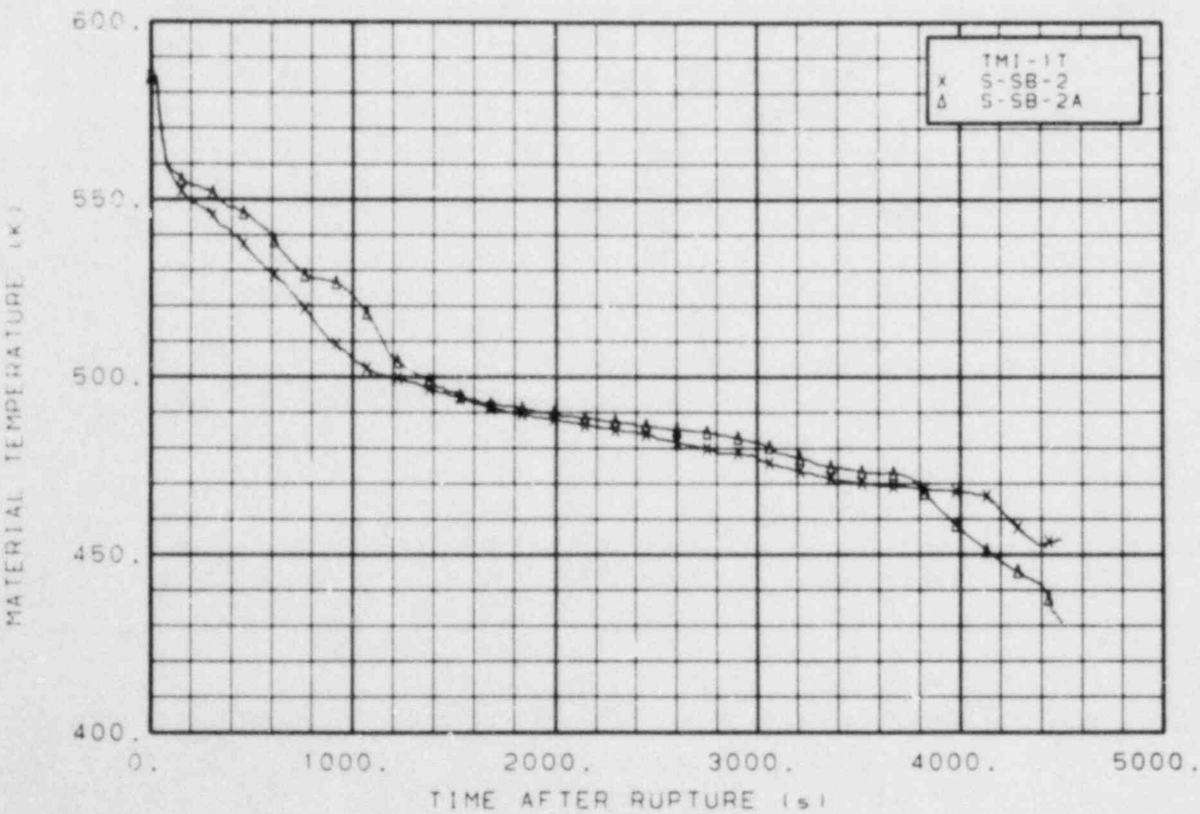

Figure 64. Material temperature in intact loop hot leg (TMI-1T), from 0 to 4500 s.

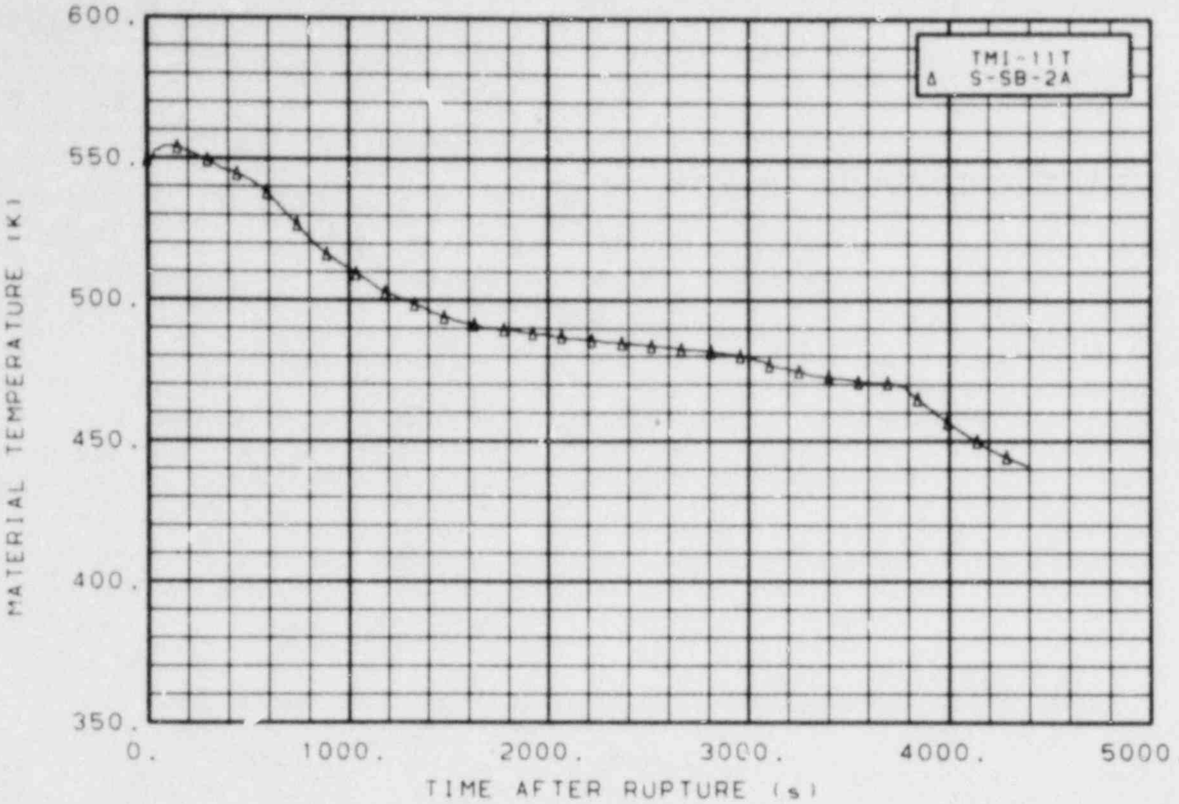

Figure 65. Material temperature in intact loop cold leg, Test S-SB-2A (TMI-11T), from 0 to 4390 s.

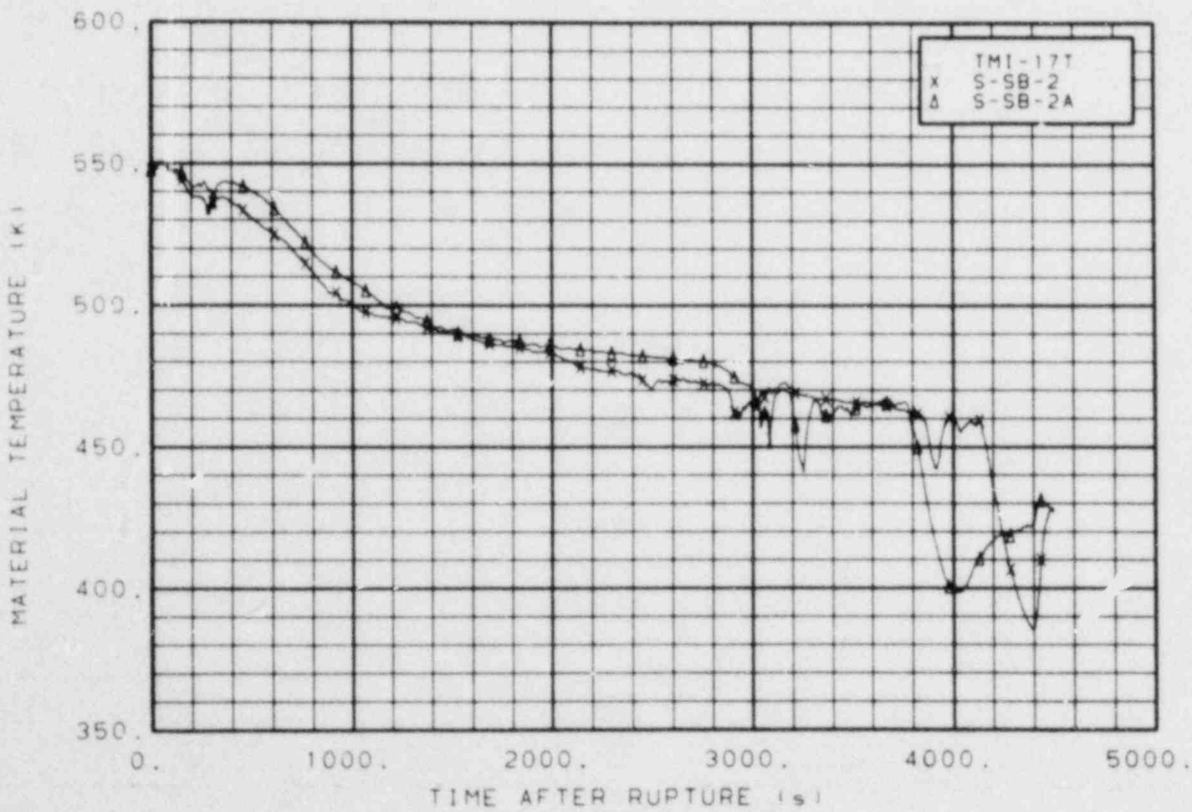

Figure 66. Material temperature in intact loop cold leg (TMI-17T), from 0 to 4500 s.

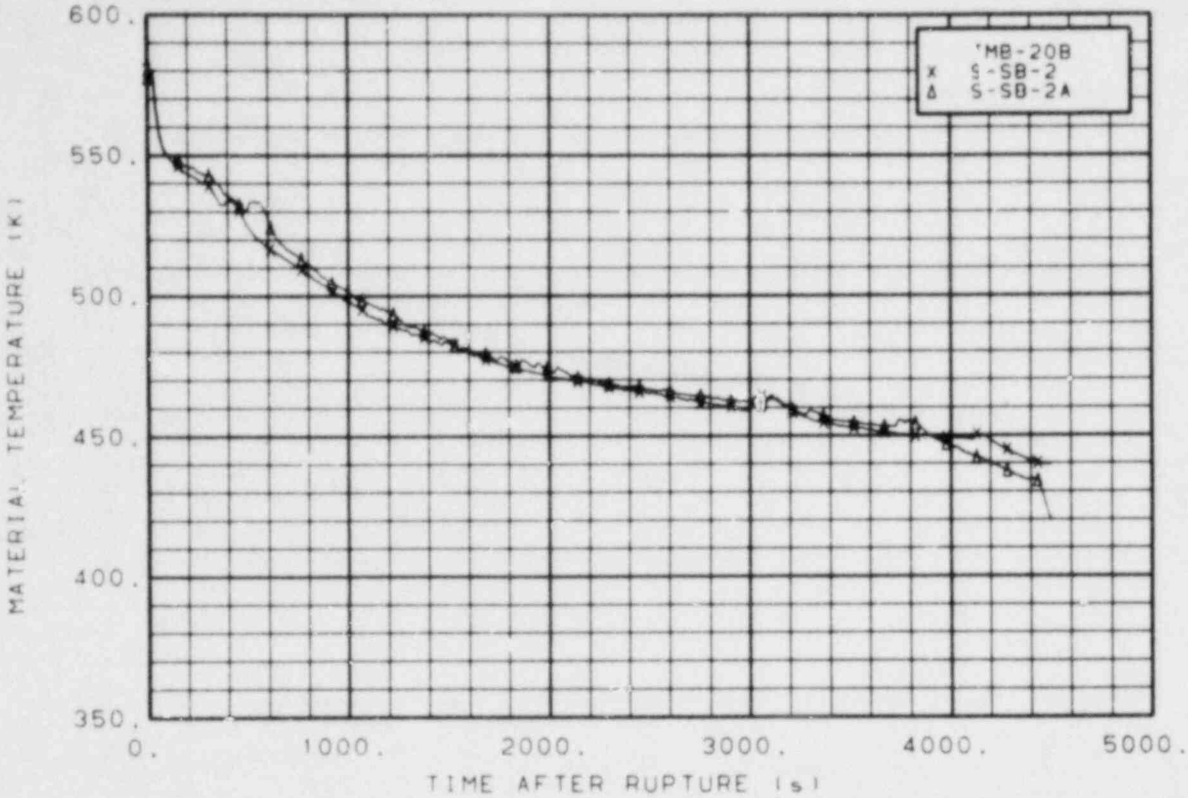

Figure 67. Material temperature in broken loop hot leg (TMB-20B), from 0 to 4500 s.

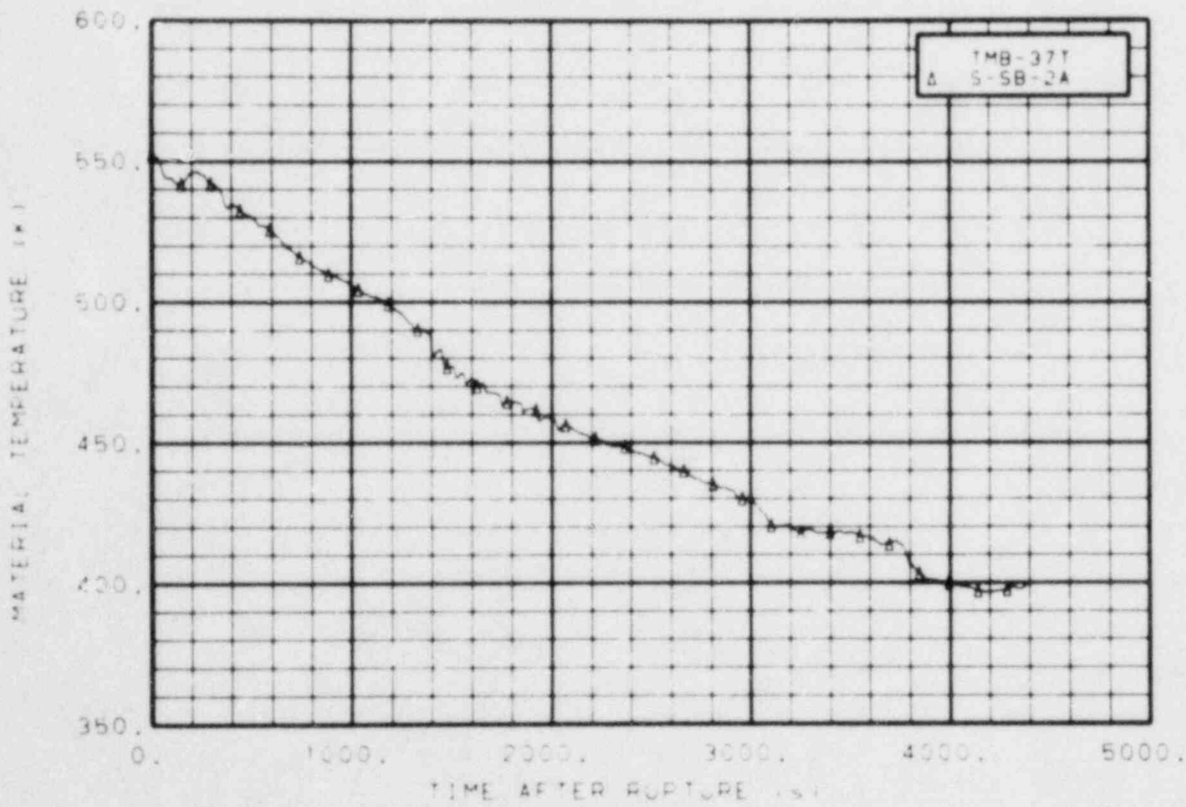

Figure 68. Material temperature in broken loop cold leg, Test S-SB-2 (TMB-37T), from 0 to 4390 s.

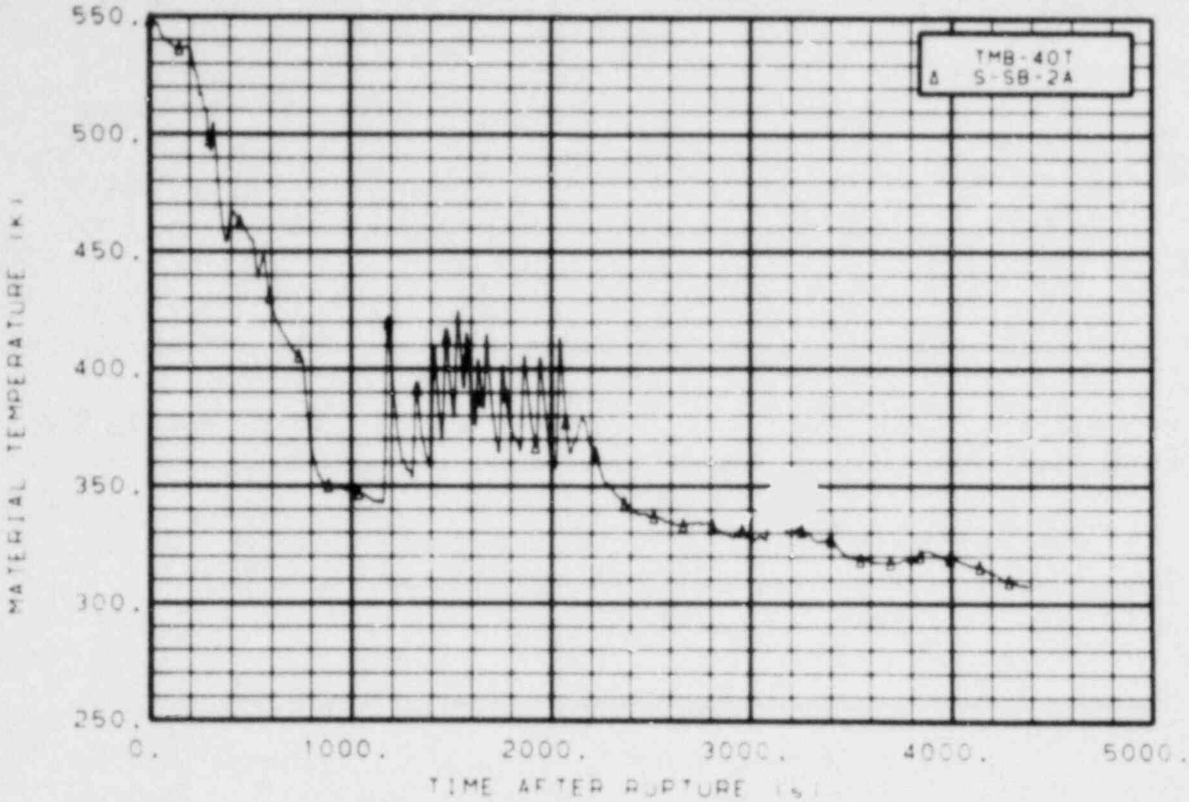

Figure 69. Material temperature in broken loop cold le... st S-SB-2A (TMB-40T), from 0 to 4390 s.

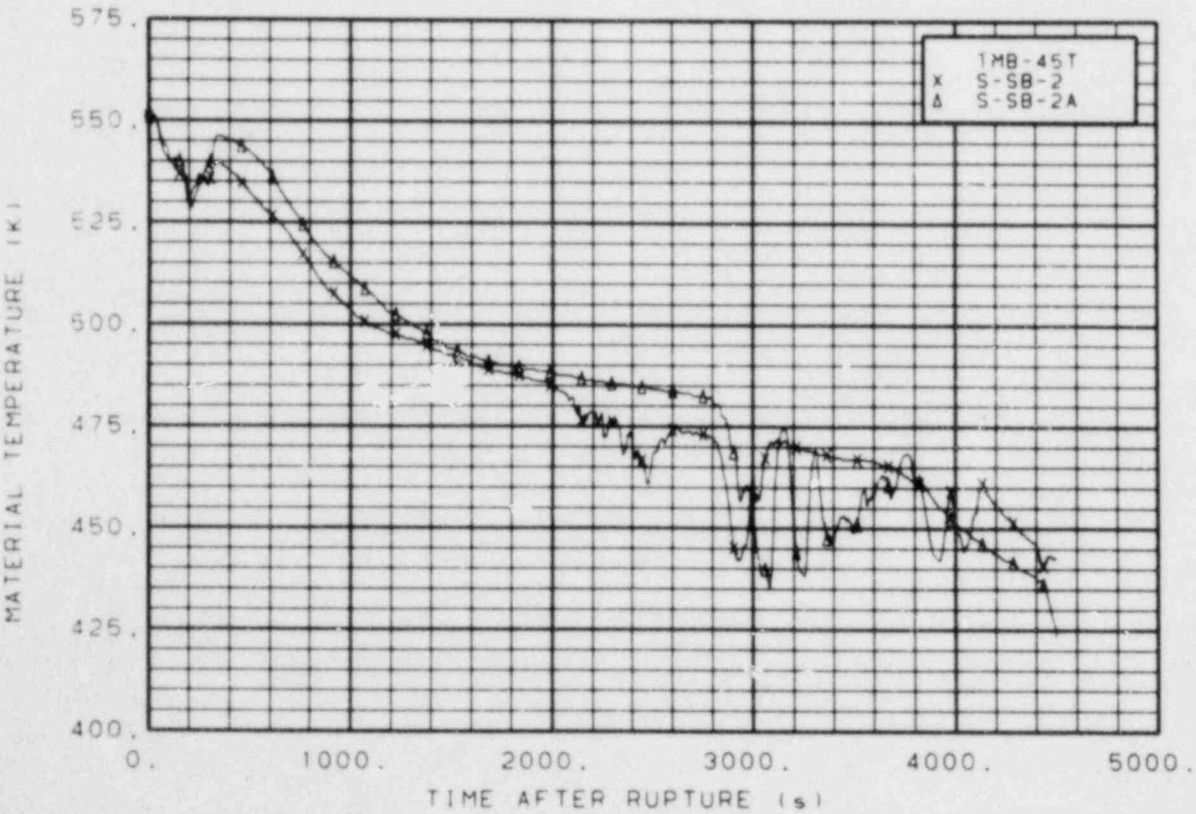

Figure 70. Material temperature in broken loop cold leg (TMB-45T), from 0 to 4500 s.

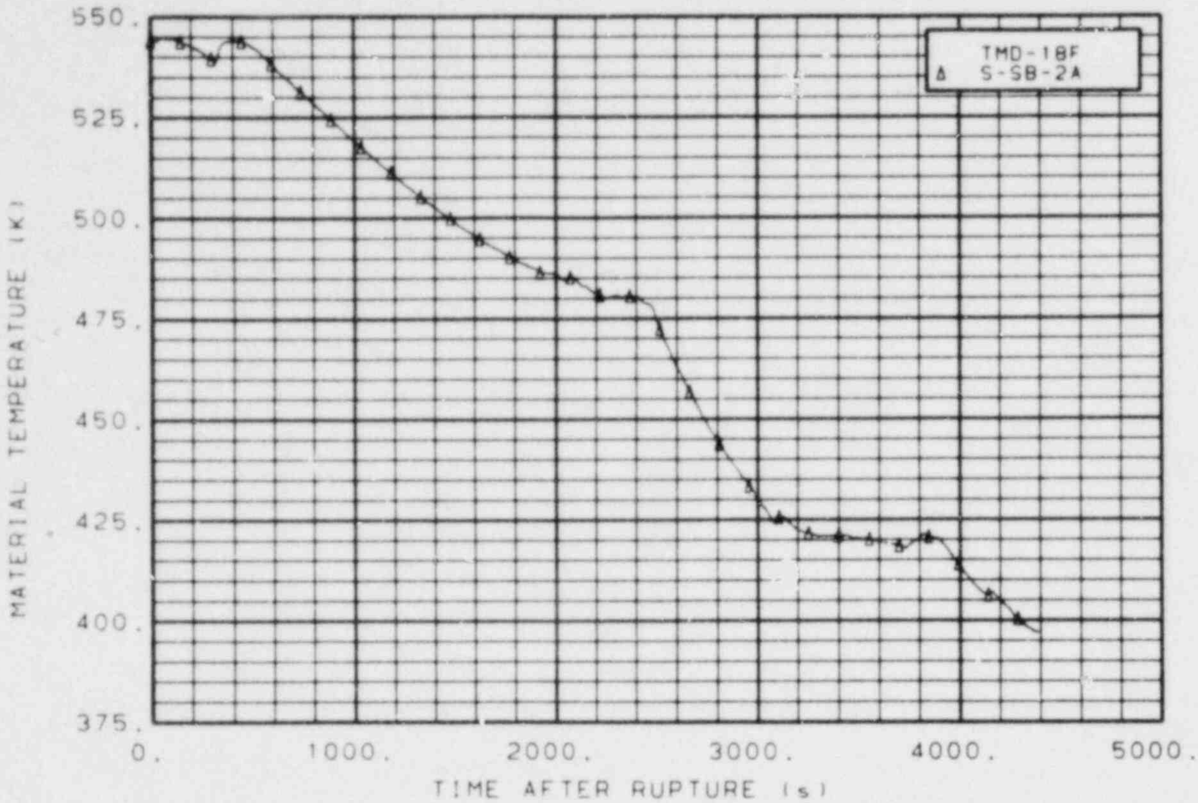

Figure 71. Material temperature in downcomer, Test S-SB-2A (TMD-18F), from 0 to 4390 s.

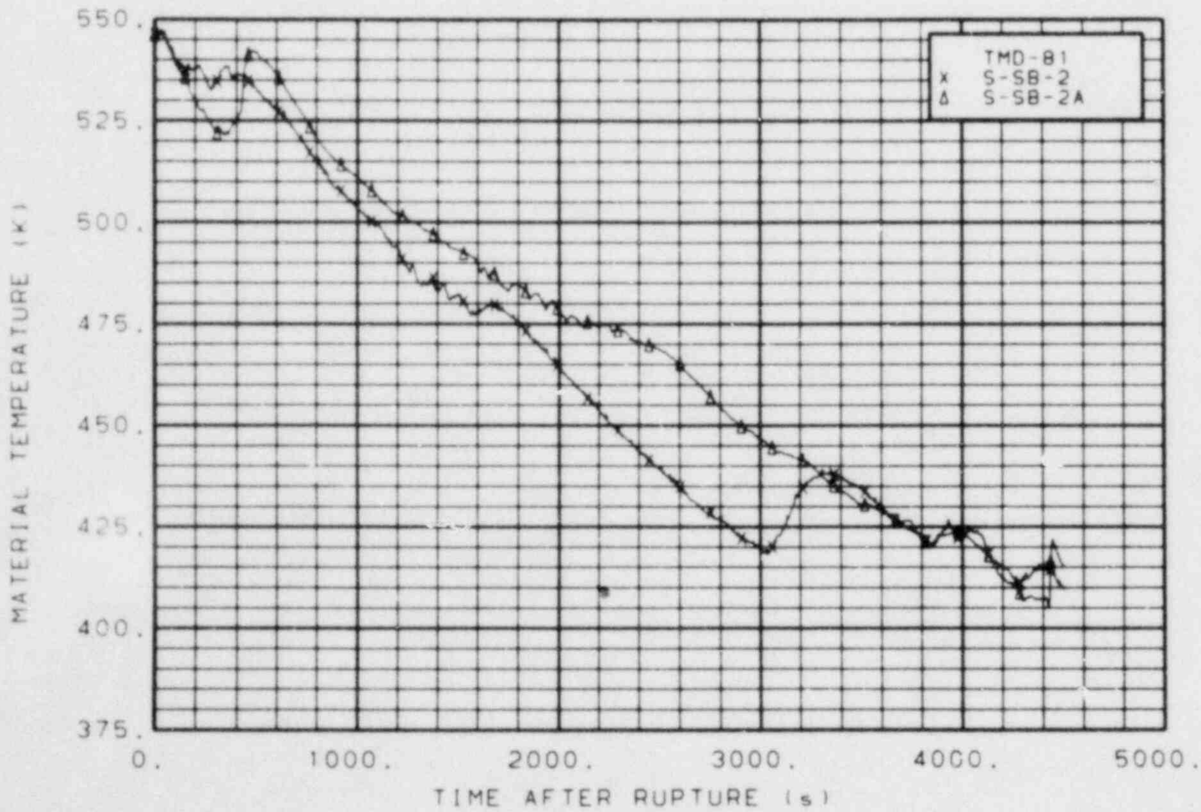

Figure 72. Material temperature in downcomer (TMD-81), from 0 to 4500 s.

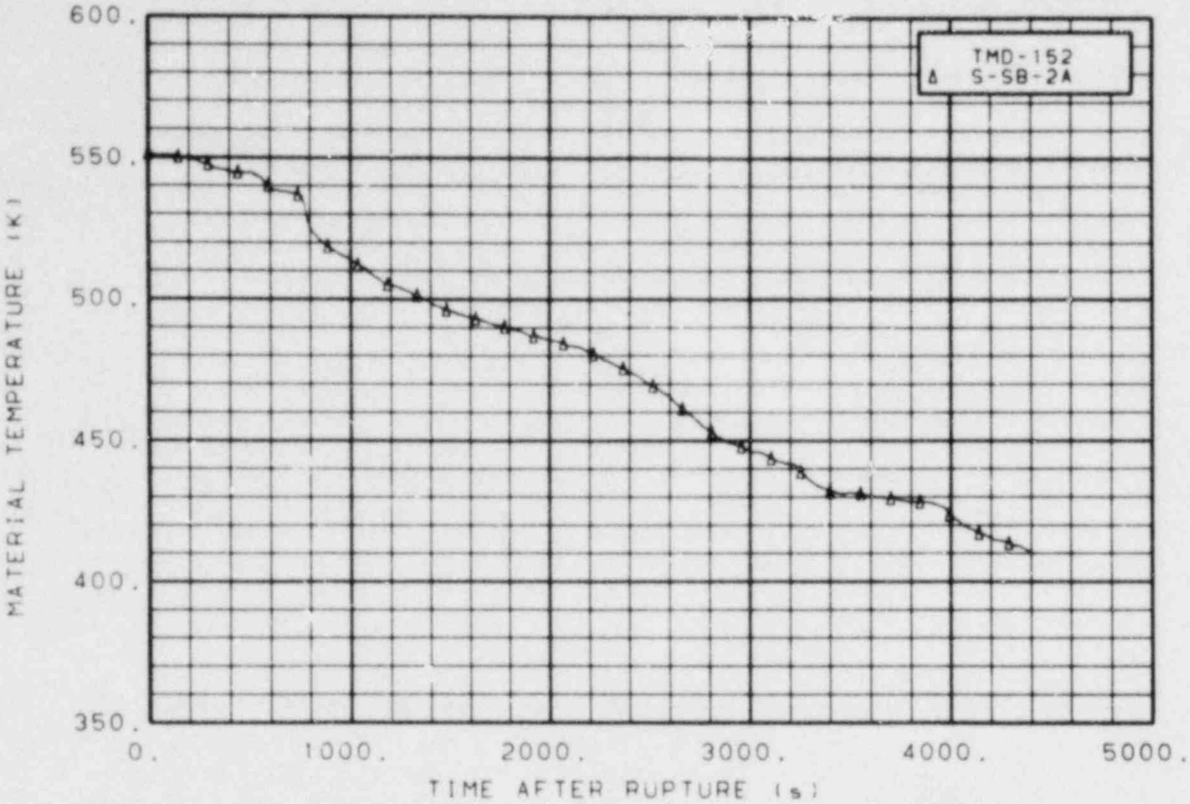

Figure 73. Material temperature in downcomer, Test S-SB-2A (TMD-152), from 0 to 4390 s.

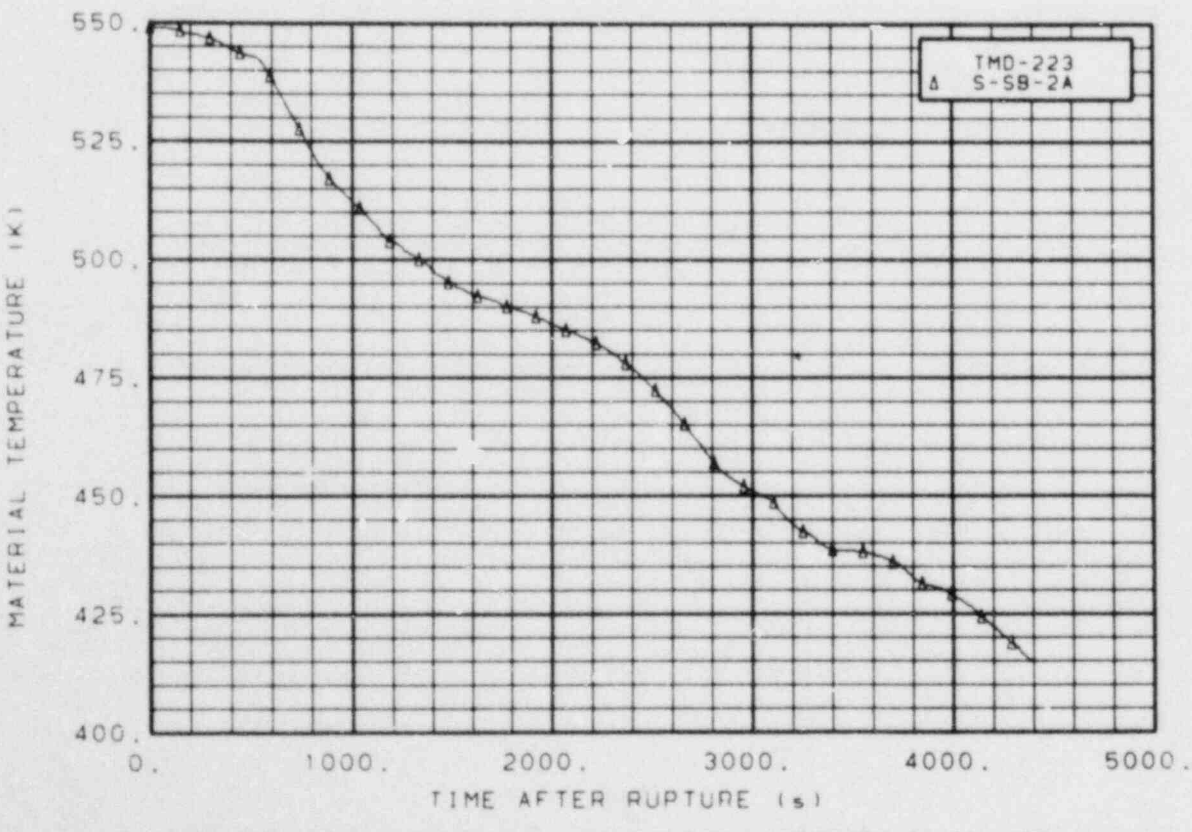

Figure 74. Material temperature in downcomer, Test S-SB-2A (TMD-223), from 0 to 4390 s.

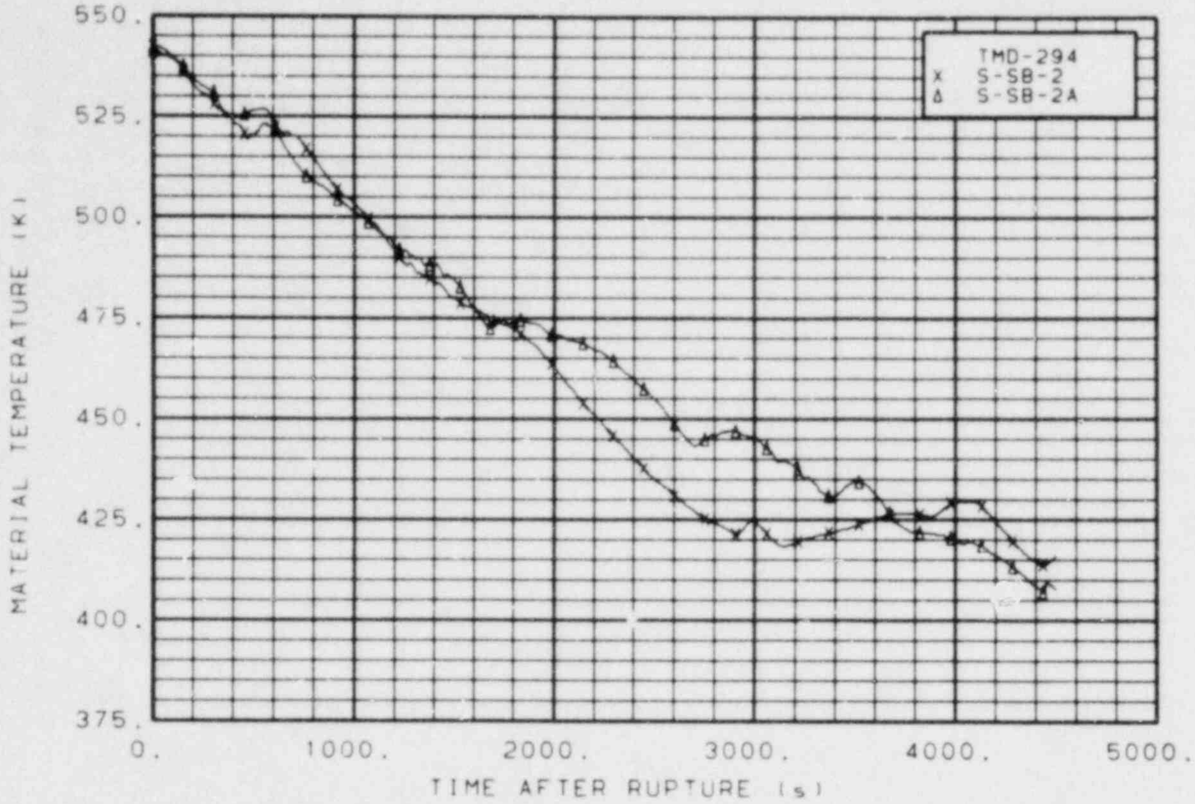

Figure 75. Material temperature in downcomer (TMD-294), from 0 to 4500 s.

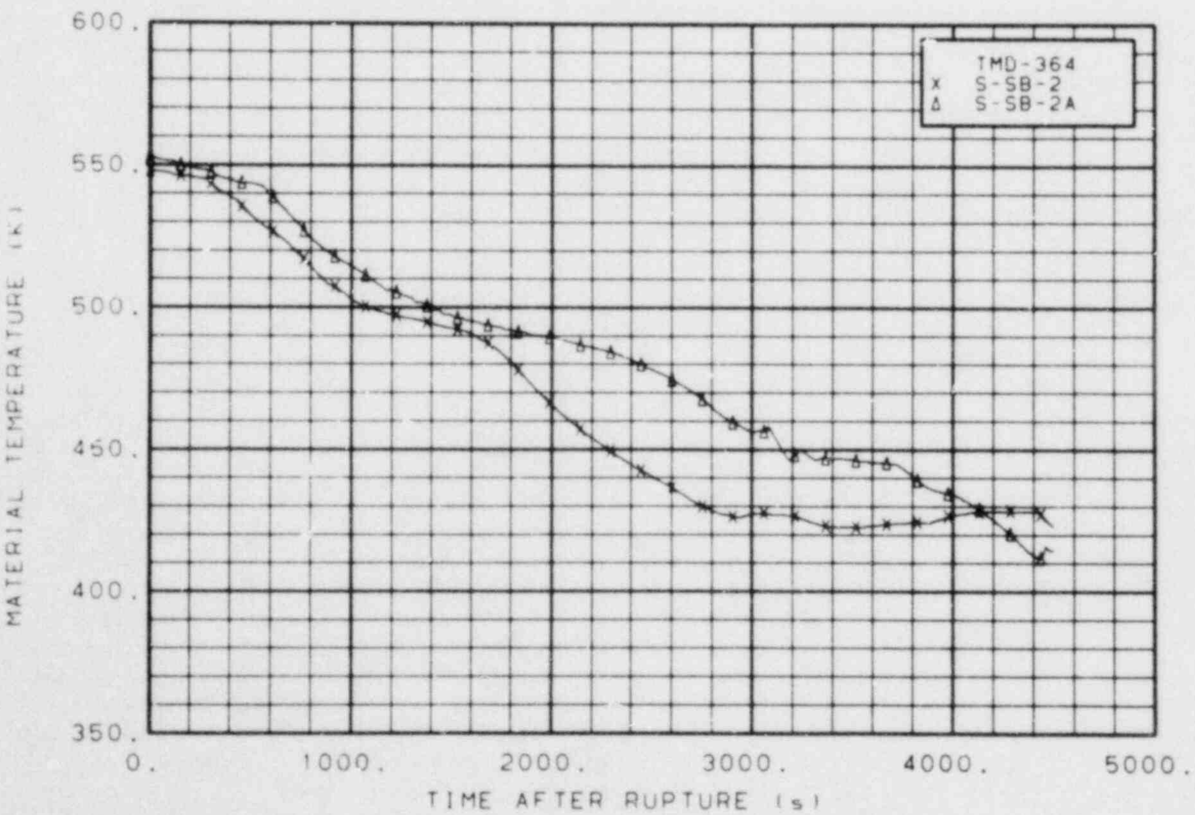

Figure 76. Material temperature in downcomer (TMD-364), from 0 to 4500 s.

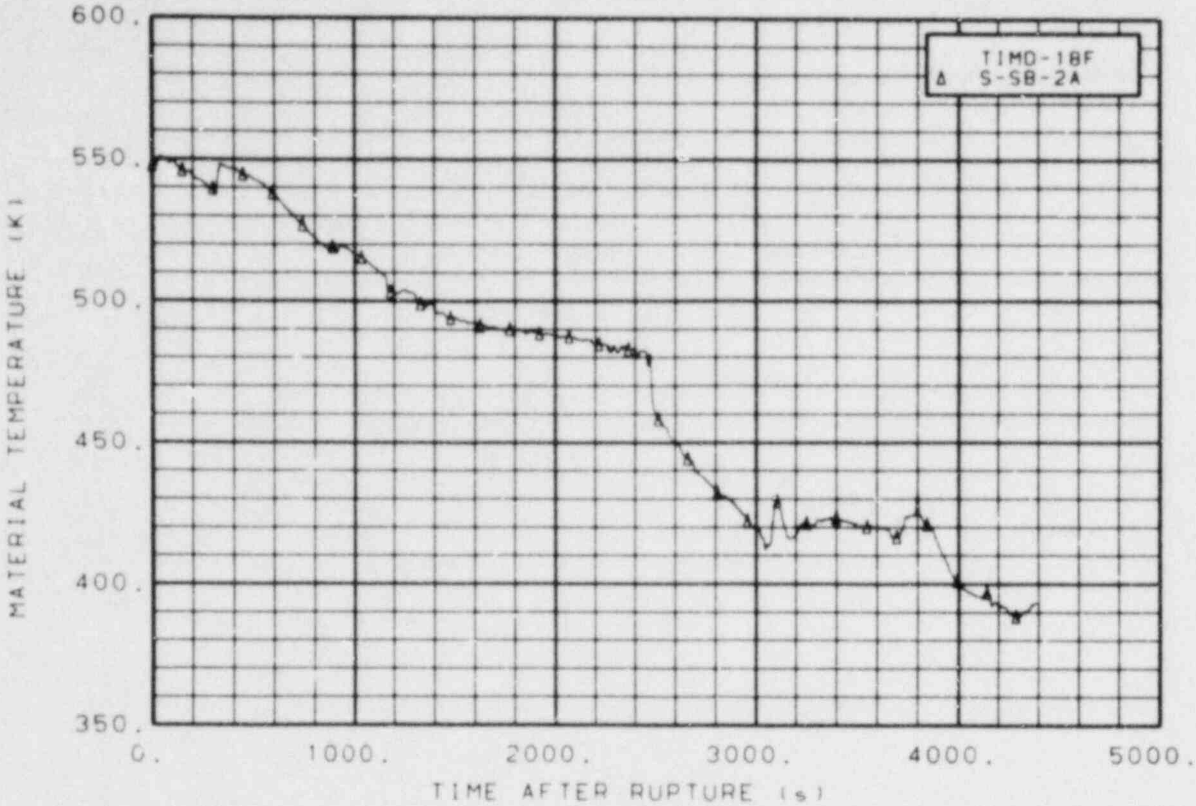

Figure 77. Material temperature in downcomer insulator, Test S-SB-2A (TIMD-18F), from 0 to 4390 s.

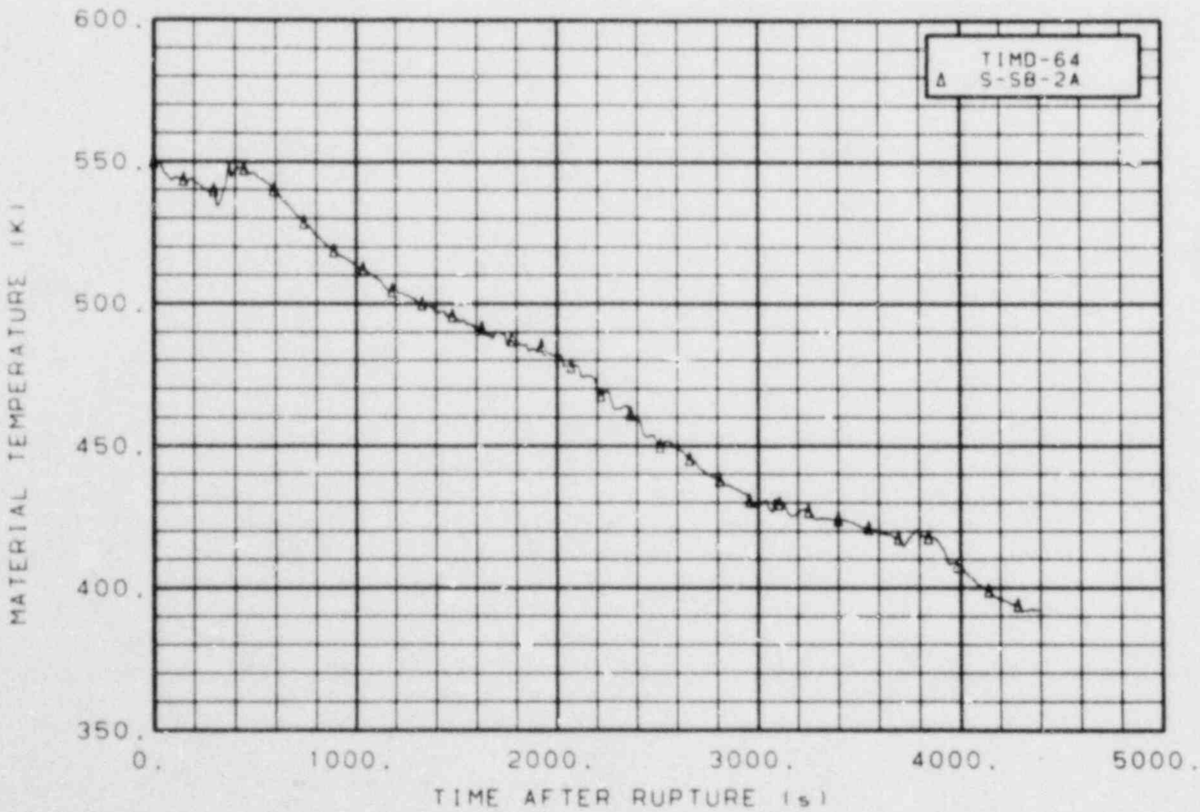

Figure 78. Material temperature in downcomer insulator, Test S-SB-2A (TIMD-64), from 0 to 4390 s.

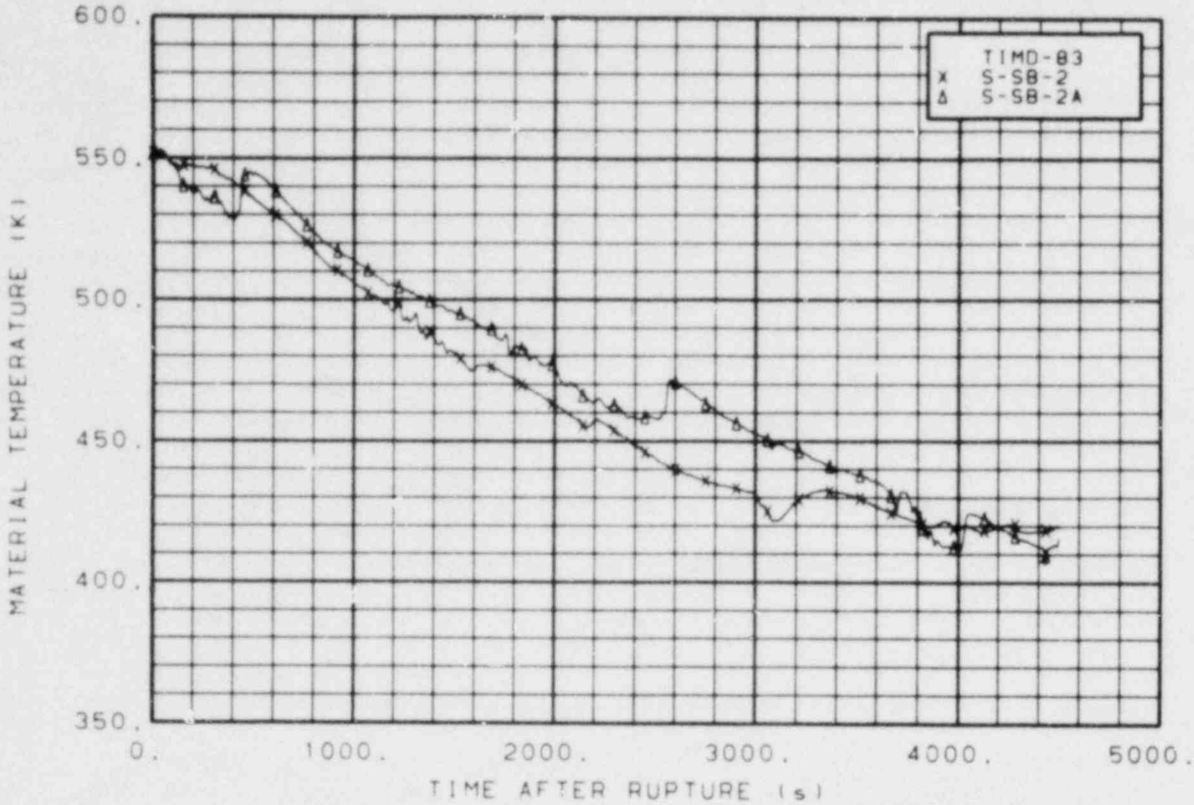

Figure 79. Material temperature in downcomer insulator (TIMD-83), from 0 to 4500 s.

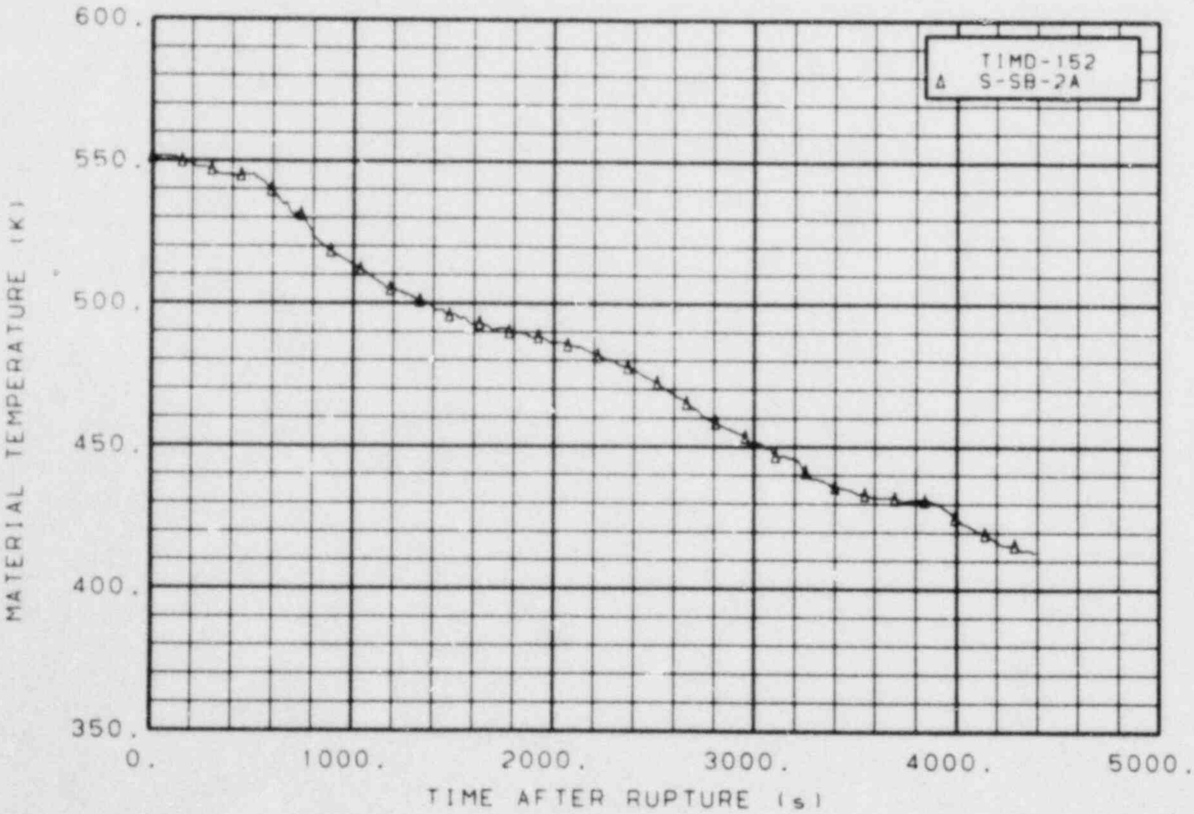

Figure 80. Material temperature in downcomer, Test S-SB-2A (TIMD-152), from 0 to 4390 s.

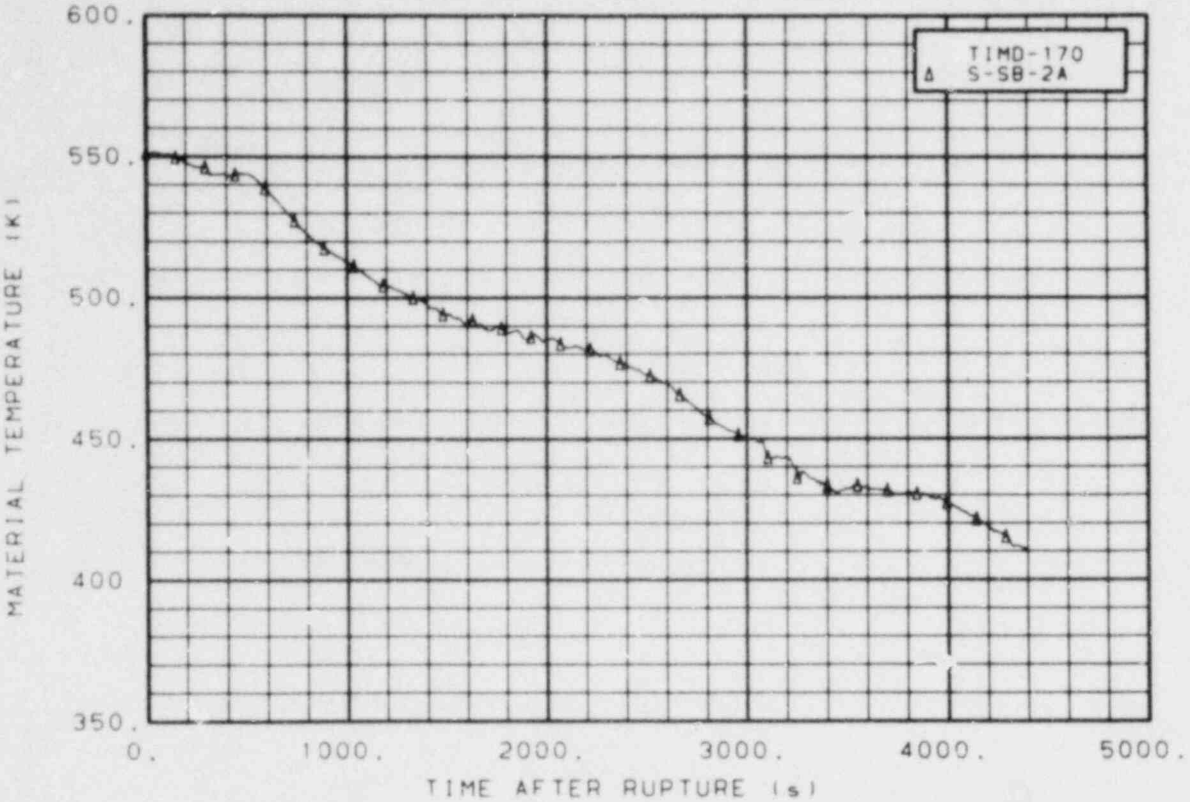

Figure 81. Material temperature in downcomer, Test S-SB-2A (TIMD-170), from 0 to 4390 s.

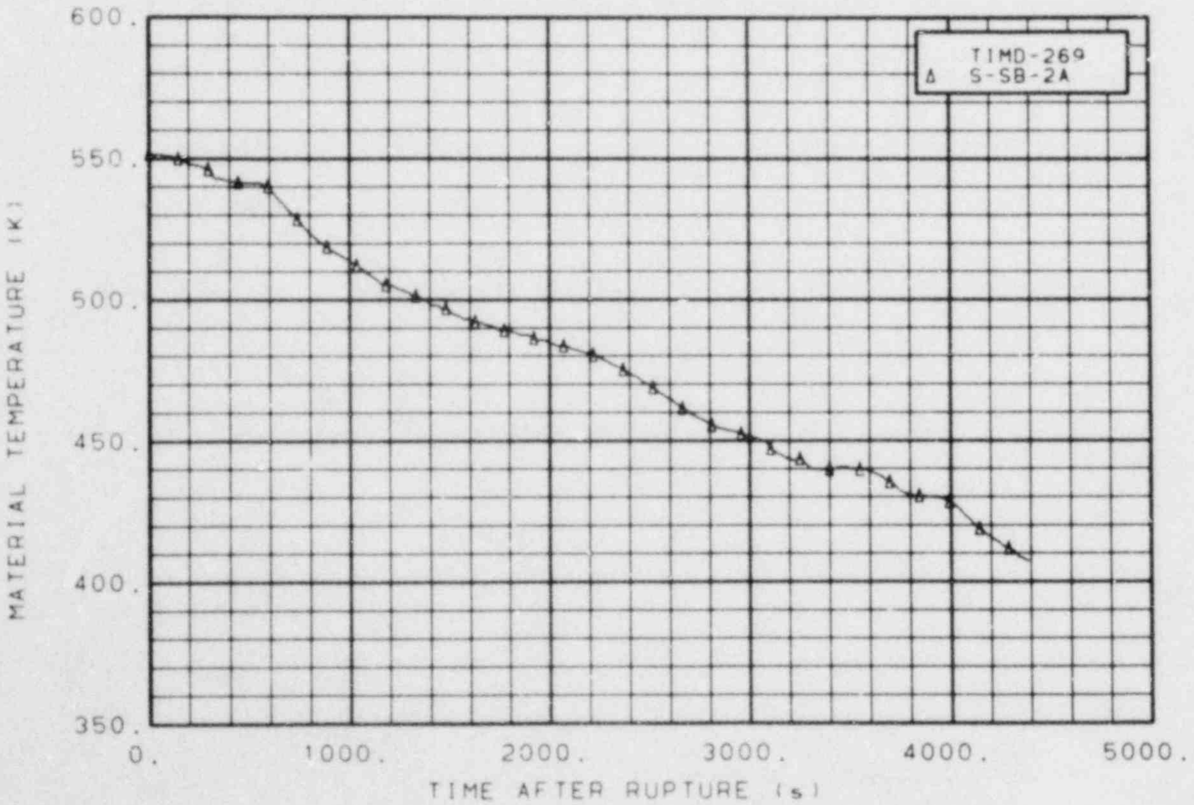

Figure 82. Material temperature in downcomer, Test S-SB-2A (TIMD-269), from 0 to 4390 s.

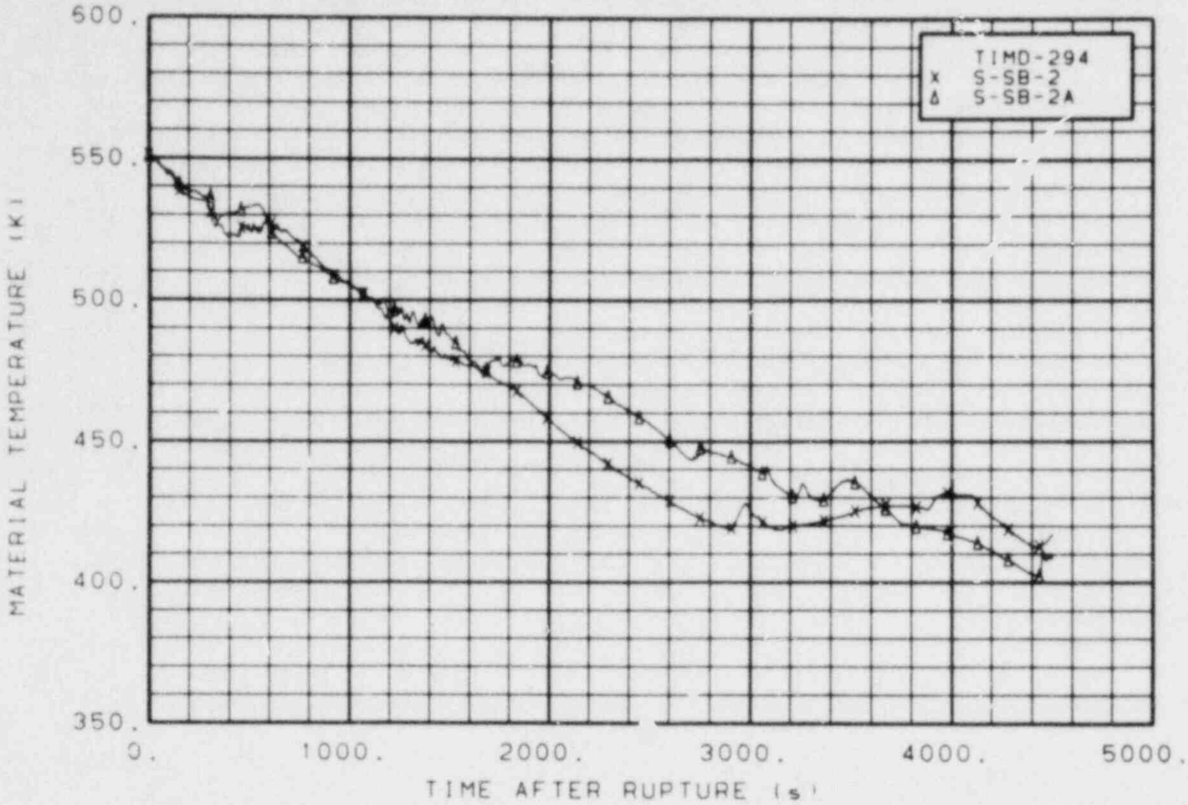

Figure 83. Material temperature in downcomer insulator (TIMD-294), from 0 to 4500 s.

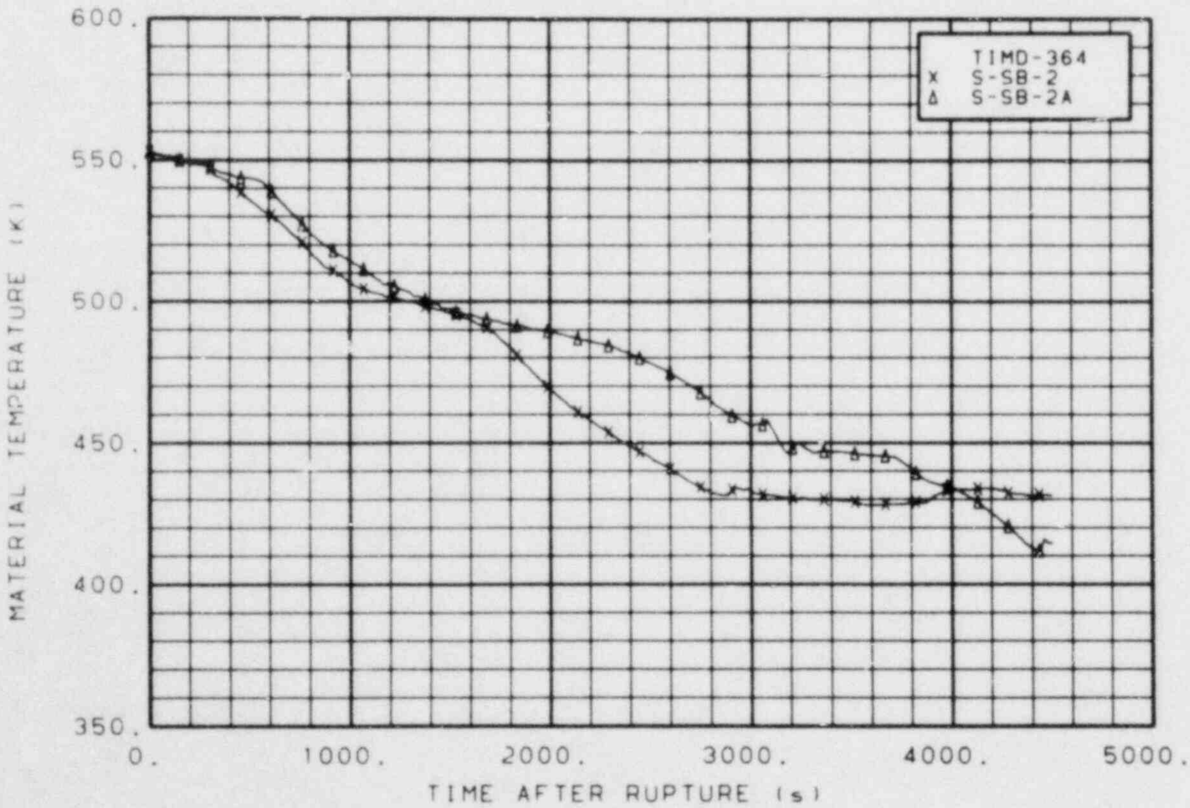

Figure 84. Material temperature in downcomer insulator (TIMD-364), from 0 to 4500 s.

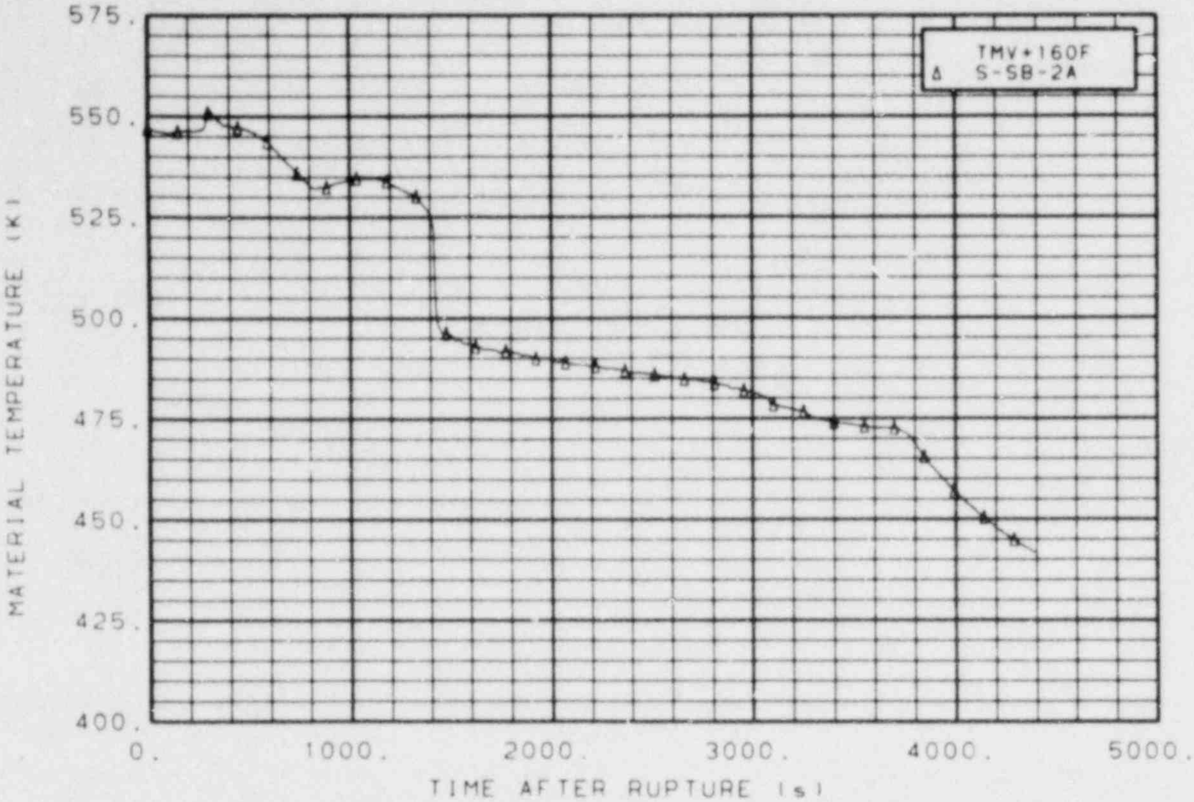

Figure 85. Material temperature on vessel upper head filler, Test S-SB-2A (TMV + 160F), from 0 to 4390 s.

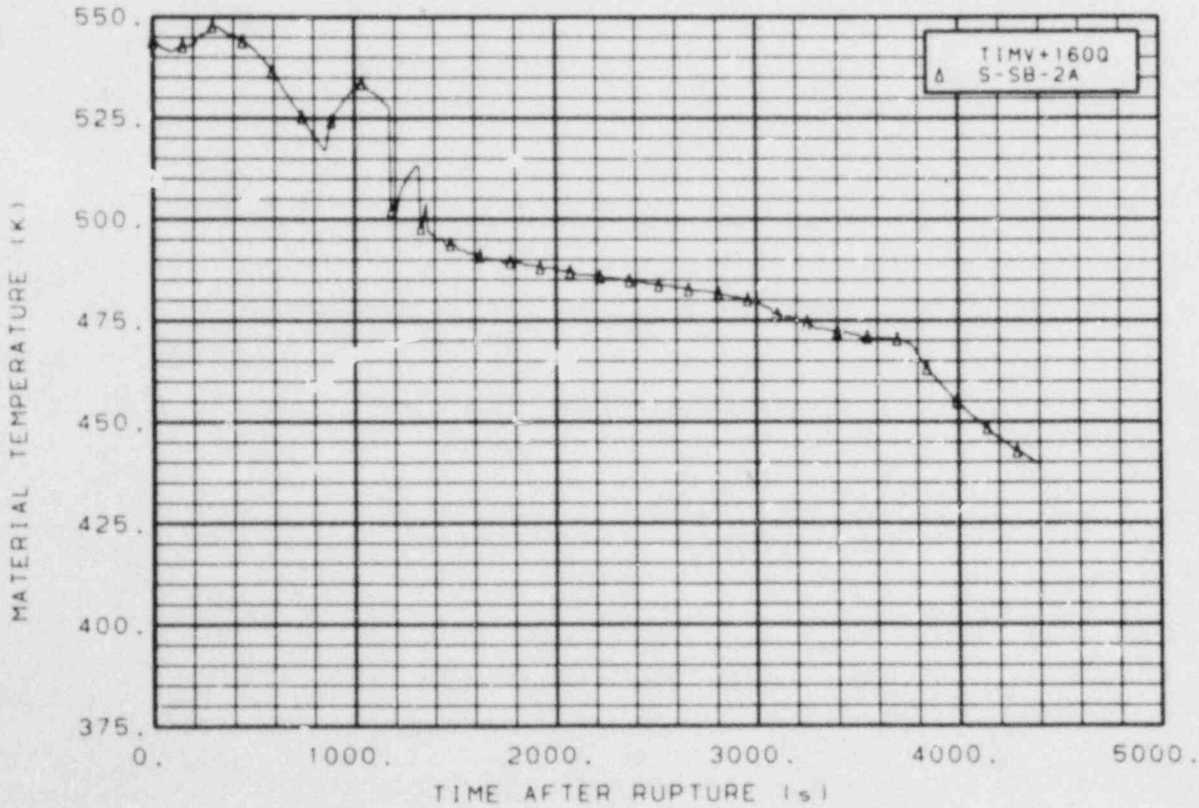

Figure 86. Material temperature on vessel insulator, Test S-SB-2A (TIMV + 160Q), from 0 to 4390 s.

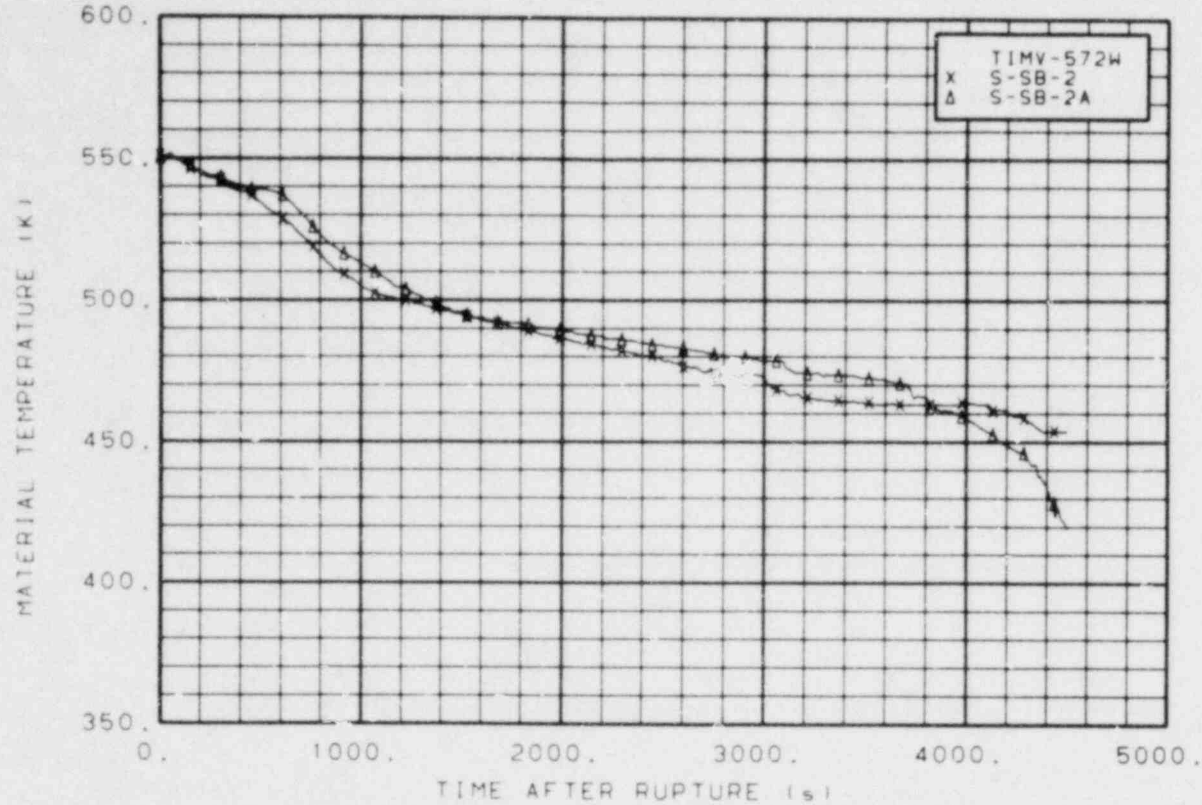

Figure 87. Material temperature on vessel insulator (TIMV + 572W), from 0 to 4500 s.

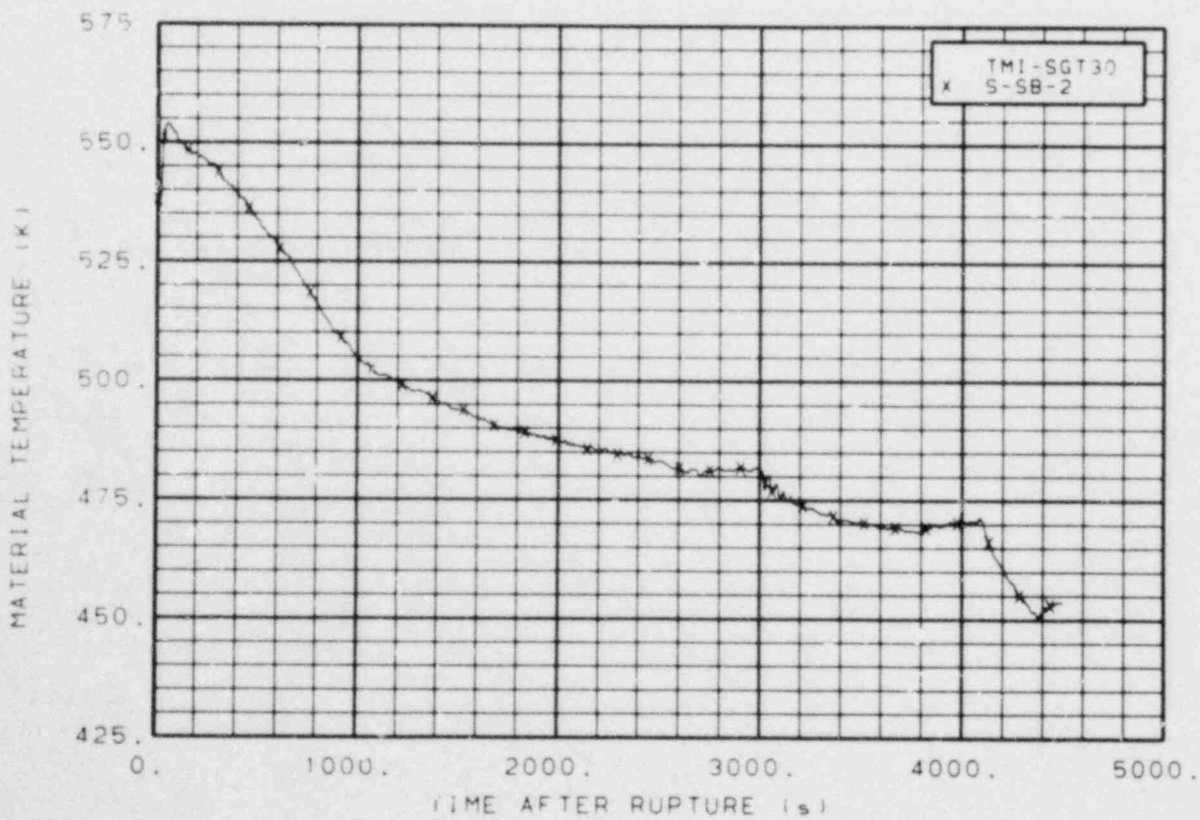

Figure 88. Material temperature in intact loop steam generator tube, Test S-SB-2 (TMI-SGT30), from 0 to 4500 s.

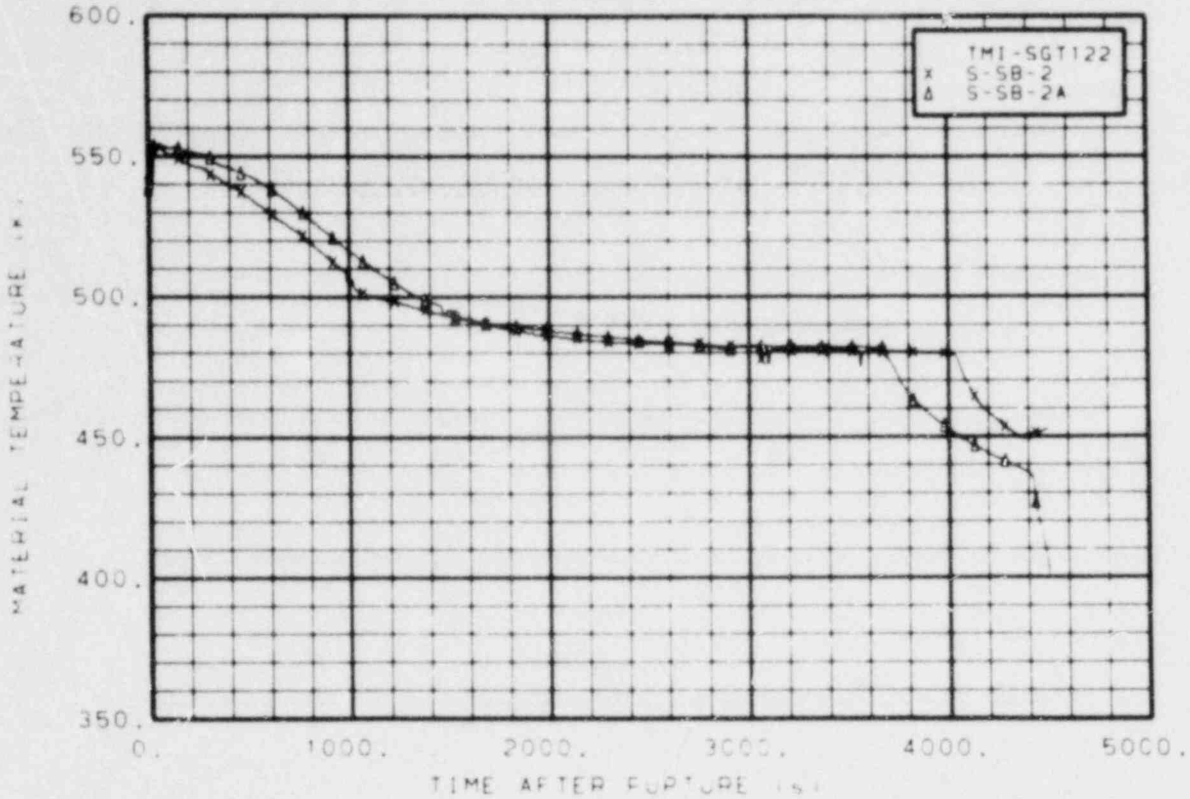

Figure 89. Material temperature in intact loop steam ɣ :nerator tube (TMI-SGT122), from 0 to 4500 s.

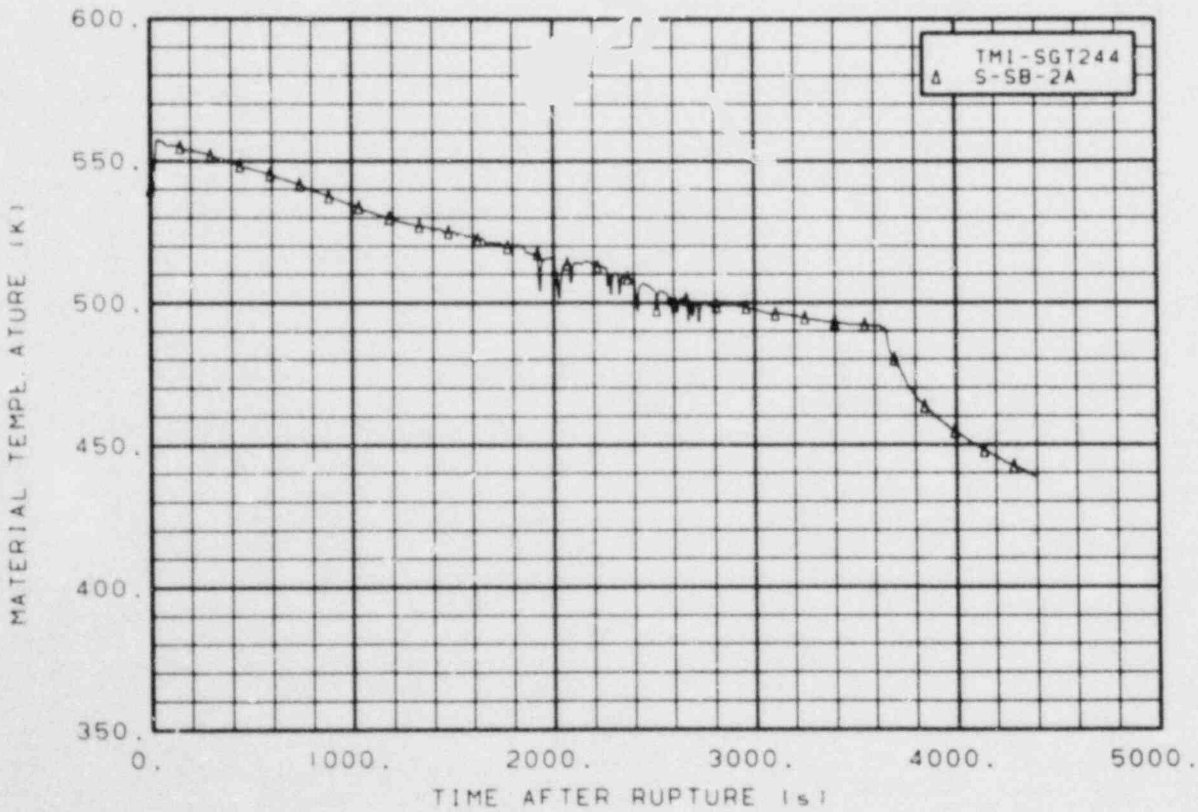

Figure 90. Material temperature in intact loop steam generator tube, Test S-SB-2A (TMI-SGT244), from 0 to 4390 s.

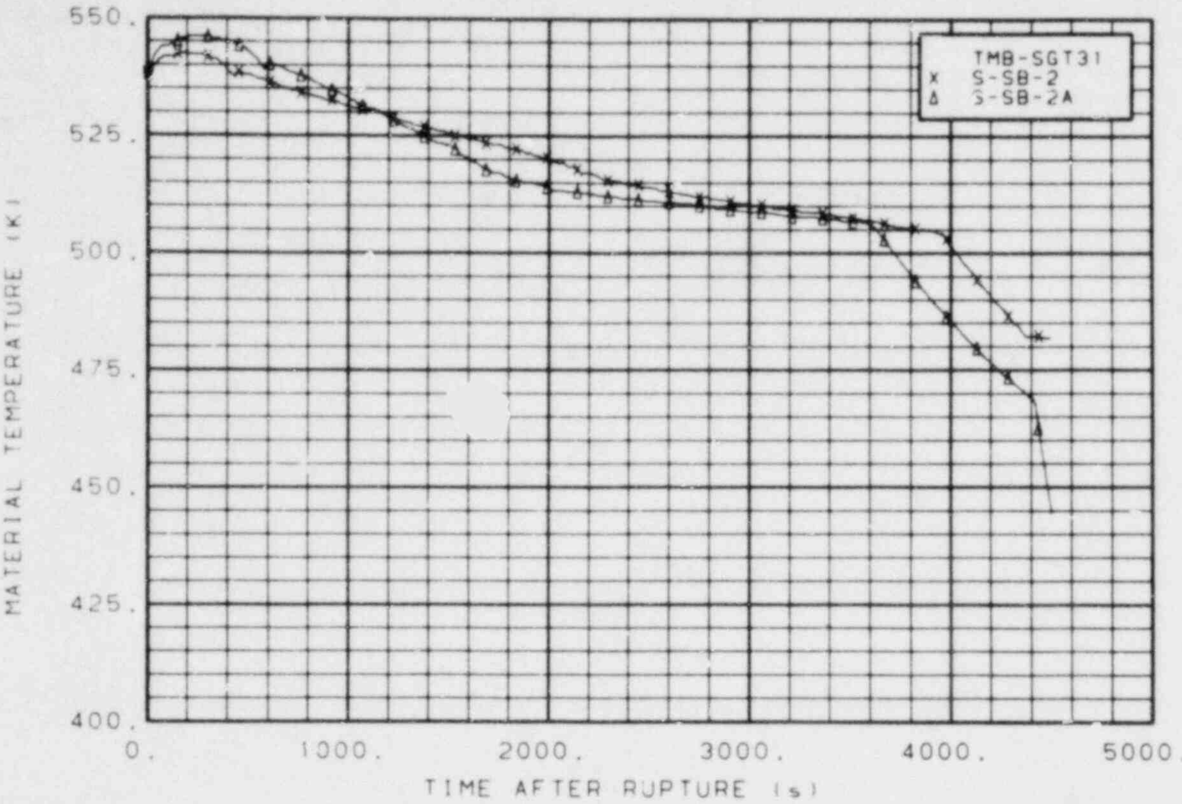

Figure 91. Material temperature in broken loop steam generator tube (TMB-SGT31), from 0 to 4500 s.

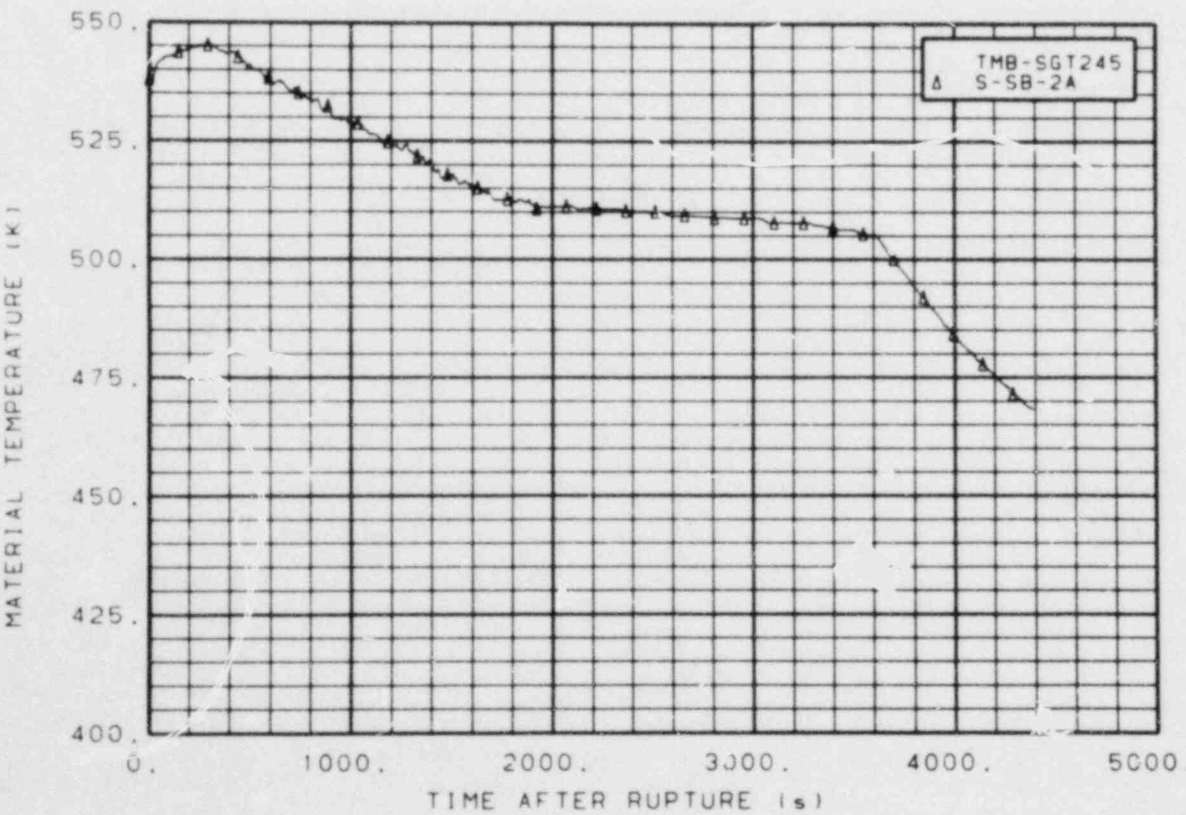

Figure 92. Material temperature in broken loop steam generator tube, Test S-SB-2A (TMB-SGT245), from 0 to 4390 s.

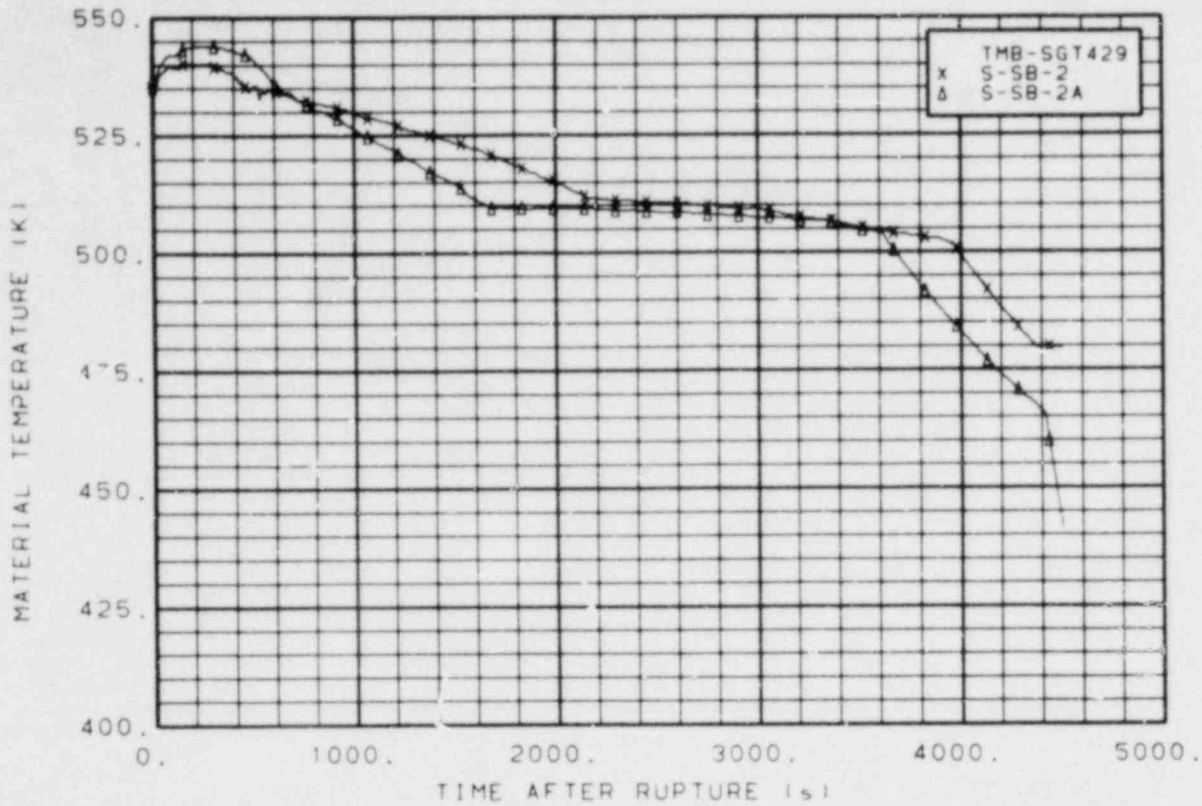

Figure 93. Material tempe.ature in broken loop steam generator tube (TMB-SGT429), from 0 to 4500 s.

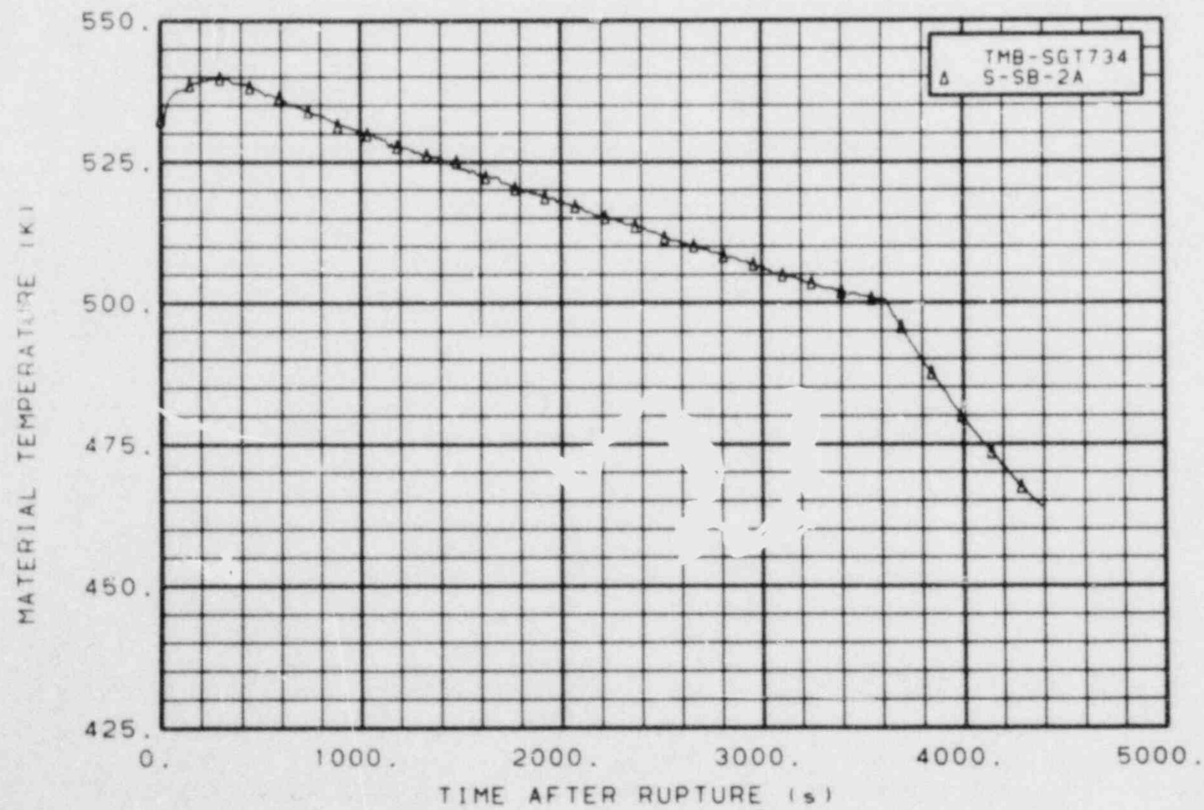

Figure 94. Material temperature in broken loop steam generator tube, Test S-SB-2A (TMB-SGT734), from 0 to 4390 s.

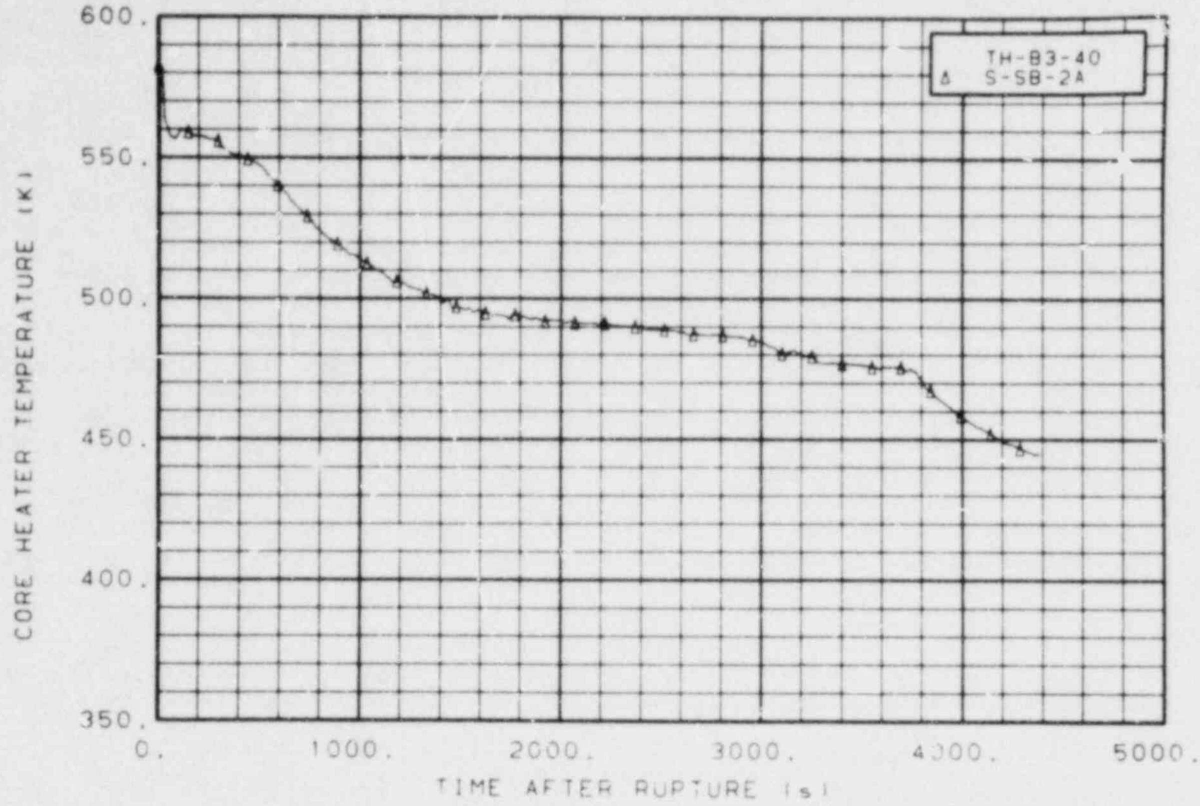

Figure 95. Core heater temperature, Test S-SB-2A, Rod B-3 (TH-B3-40), from 0 to 4390 s.

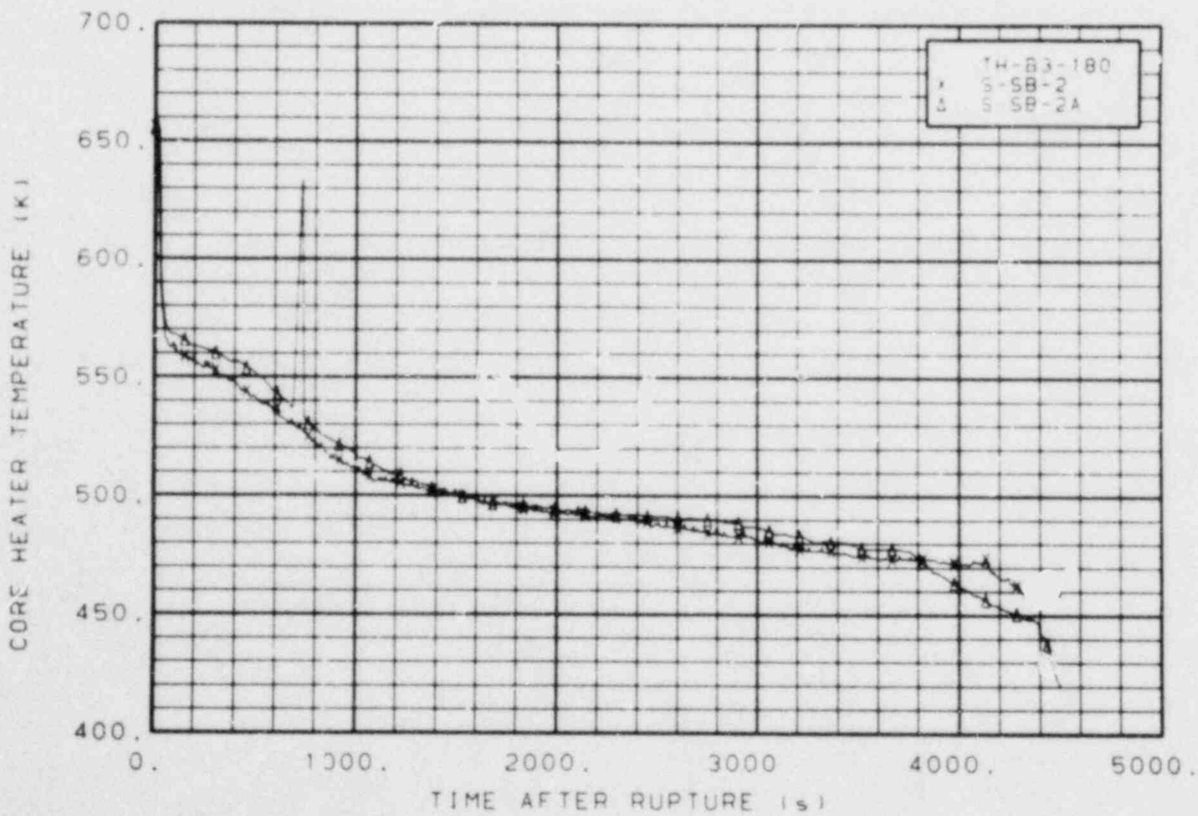

Figure 96. Core heater temperature, Rod B-3 (TH-B3-180), from 0 to 4500 s.

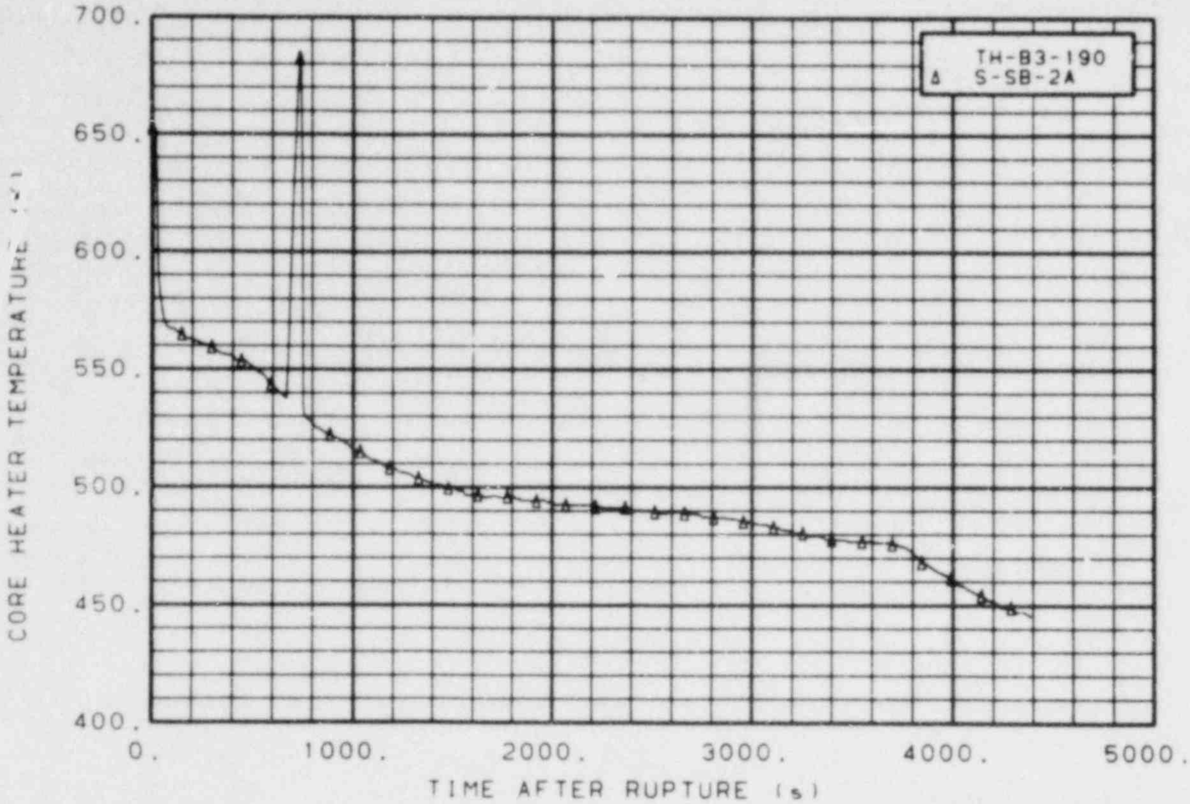

Figure 97. Core heater temperature, Test S-SB-2A, Rod B-3 (TH-B3-190), from 0 to 4390 s.

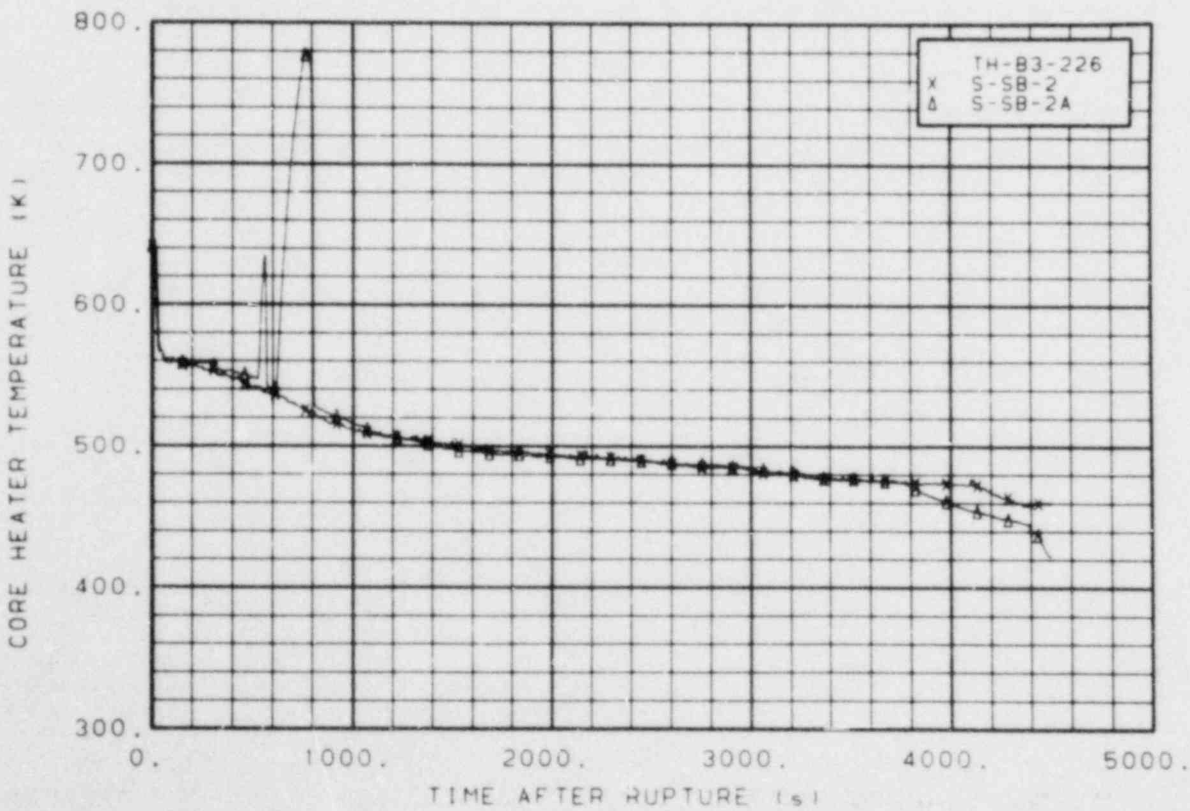

Figure 98. Core heater temperature, Rod B-3 (TH-B3-226), from 0 to 4500 s.

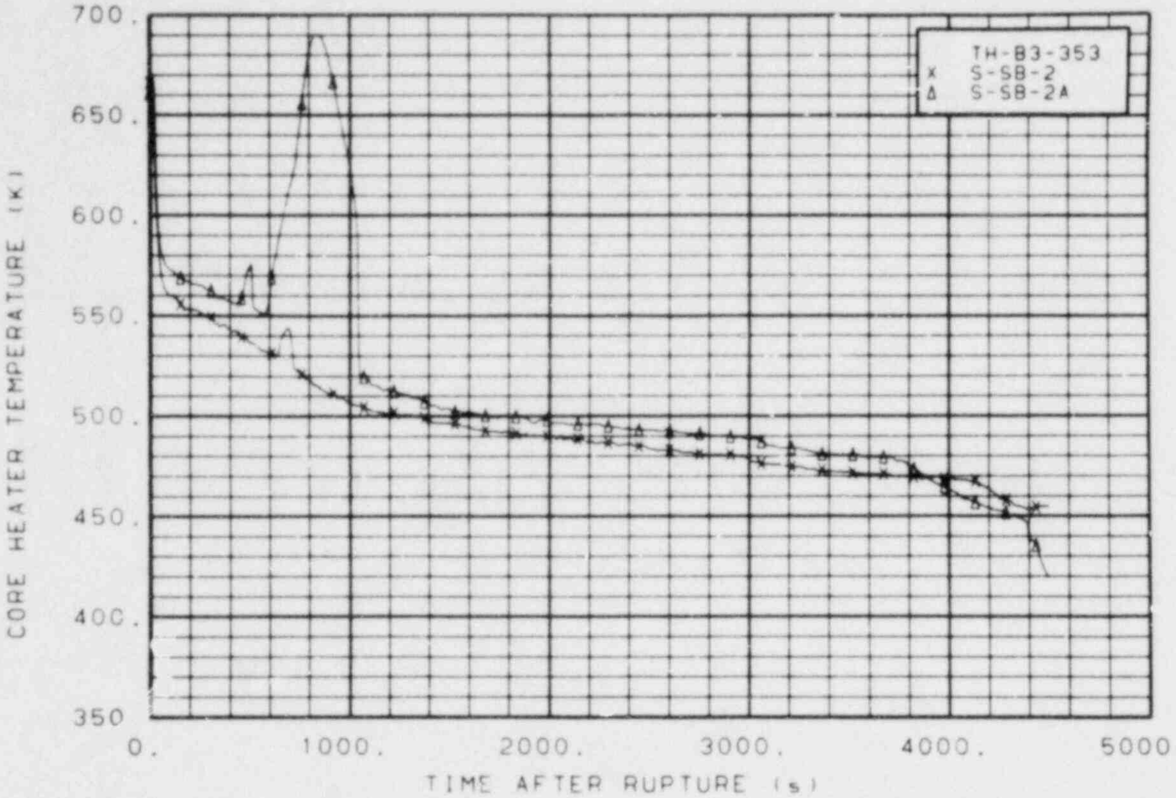

Figure 99. Core heater temperature, Rod B-3 (TH-B3-353), from 0 to 4500 s.

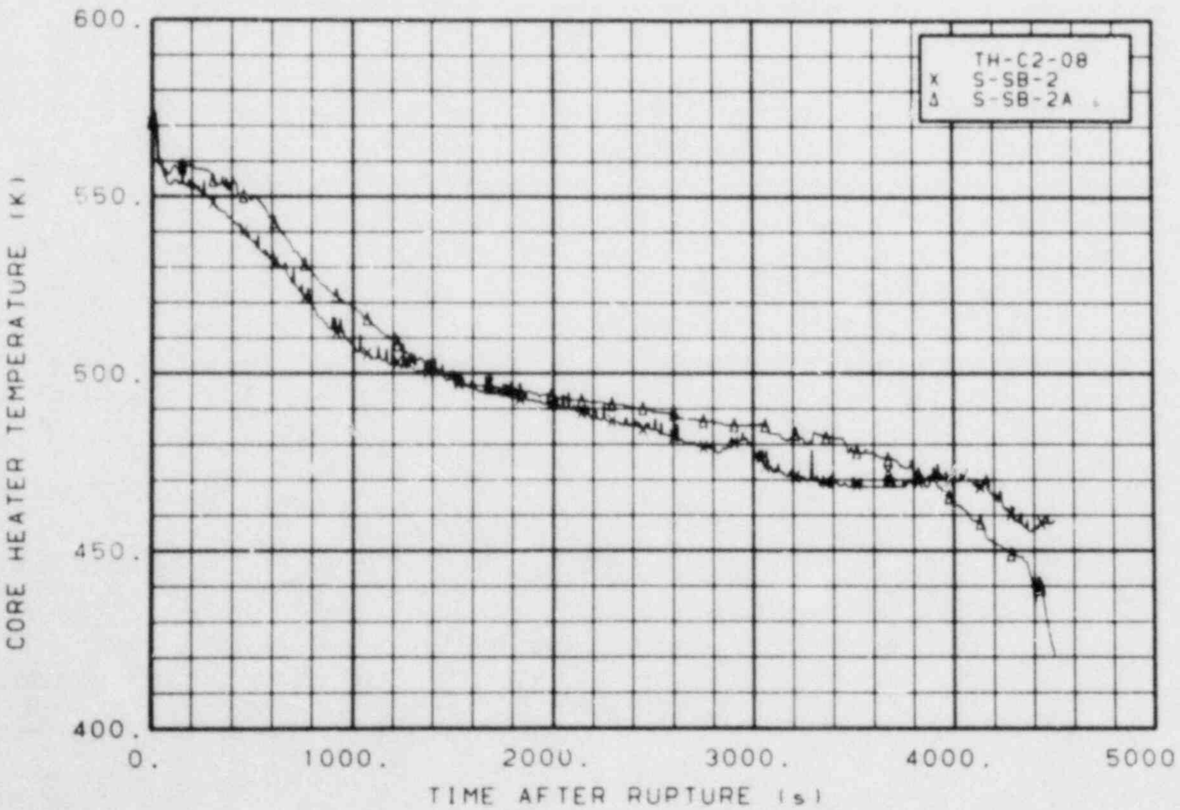

Figure 100. Core heater temperature, Rod C-2 (TH-C2-08), from 0 to 4500 s.

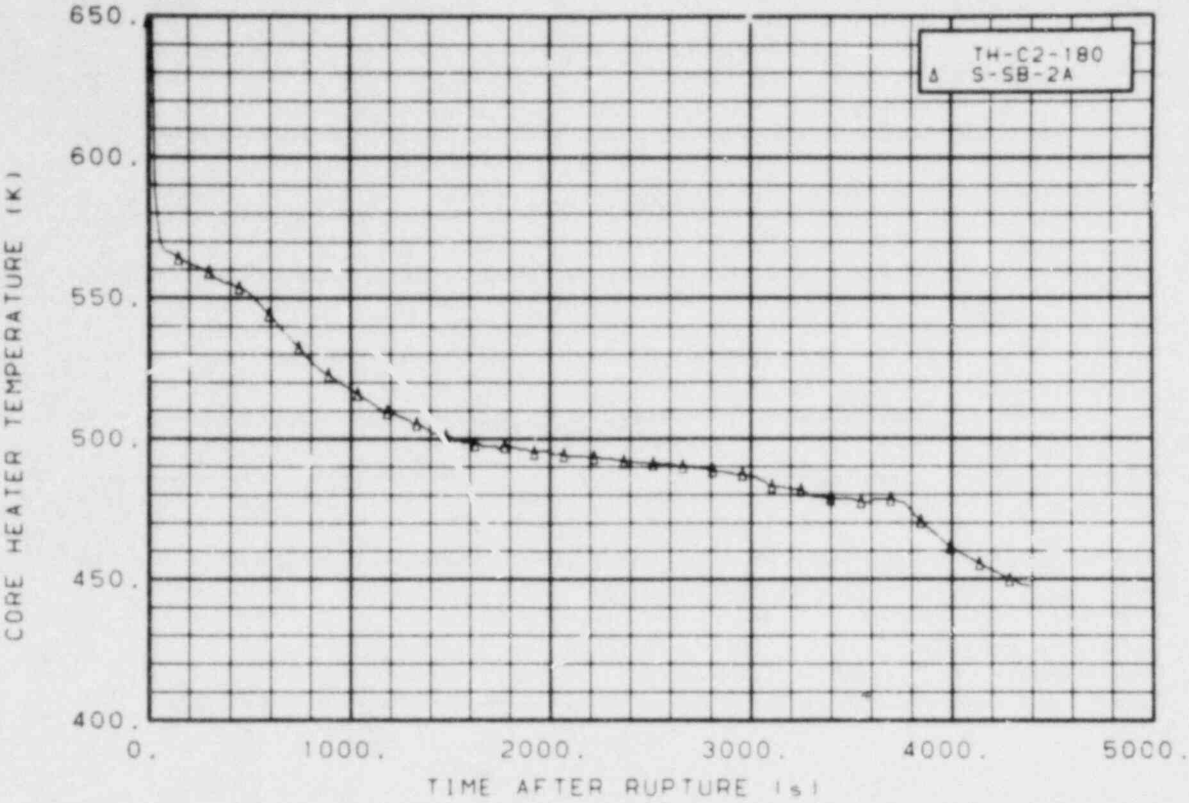

Figure 101. Core heater temperature, Test S-SB-2A, Rod C-2 (TH-C2-180), from 0 to 4390 s.

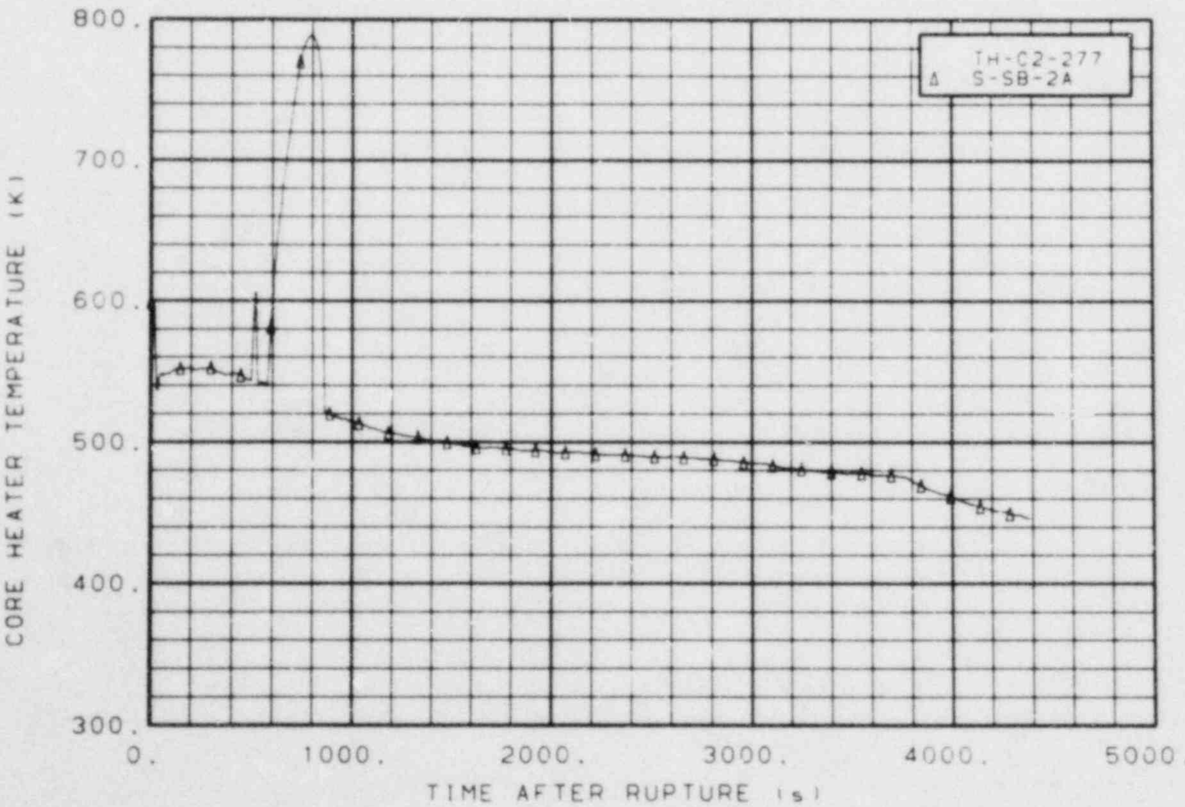

Figure 102. Core heater temperature, Test S-SB-2A, Rod C-2 (TH-C2-277), from 0 to 4390 s.

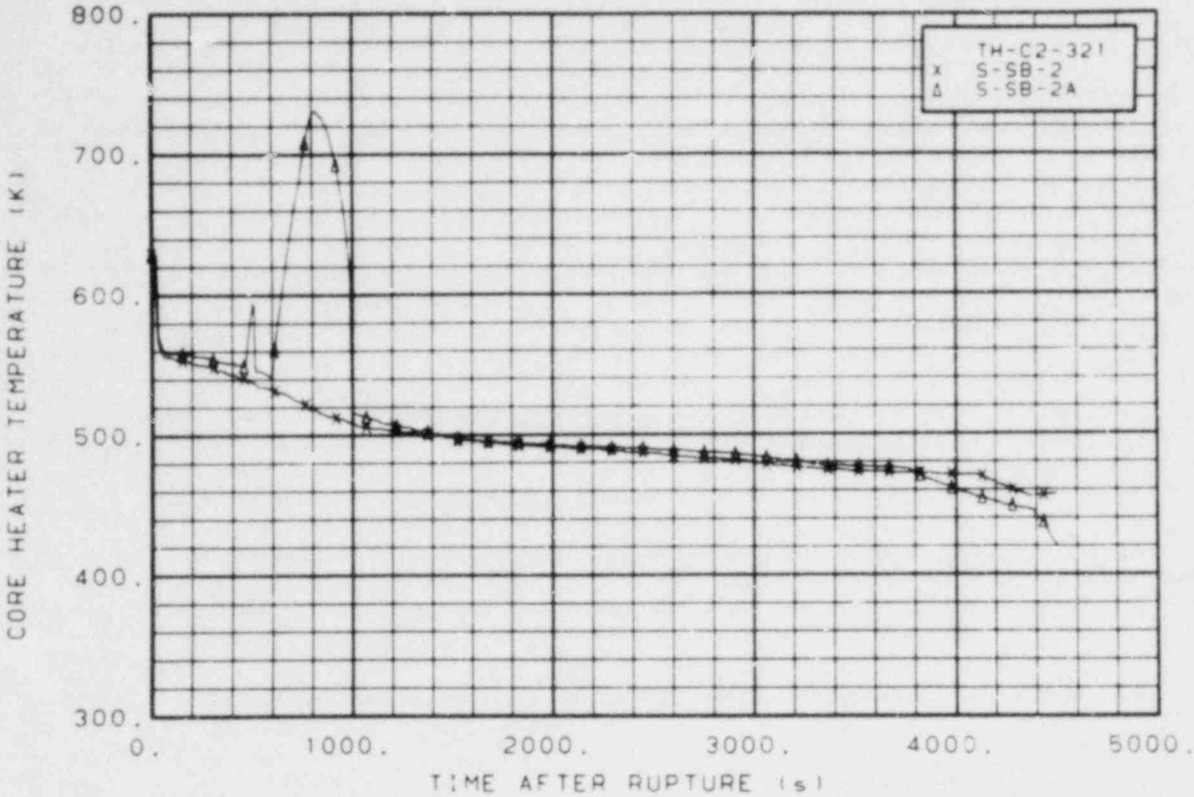

Figure 103. Core heater temperature, Rod C-2 (TH-C2-321), from 0 to 4500 s.

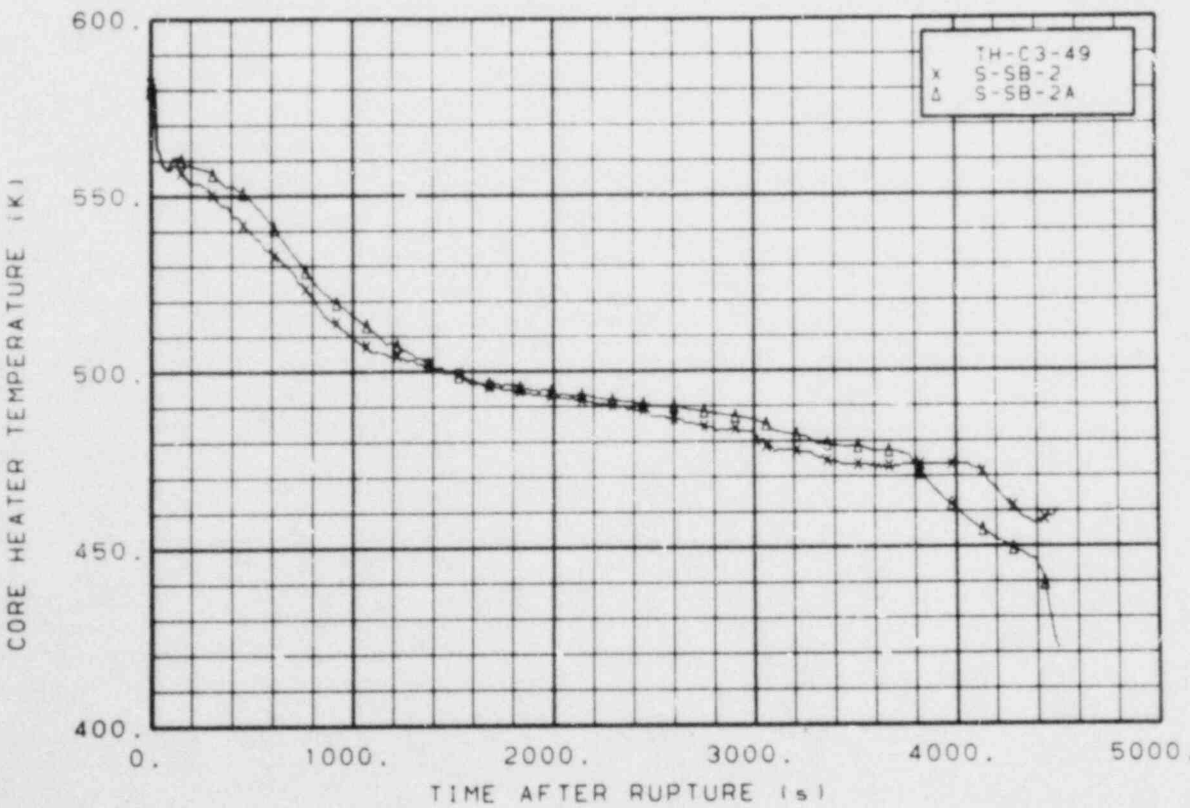

Figure 104. Core heater temperature, Rod C-3 (TH-C3-49), from 0 to 4500 s.

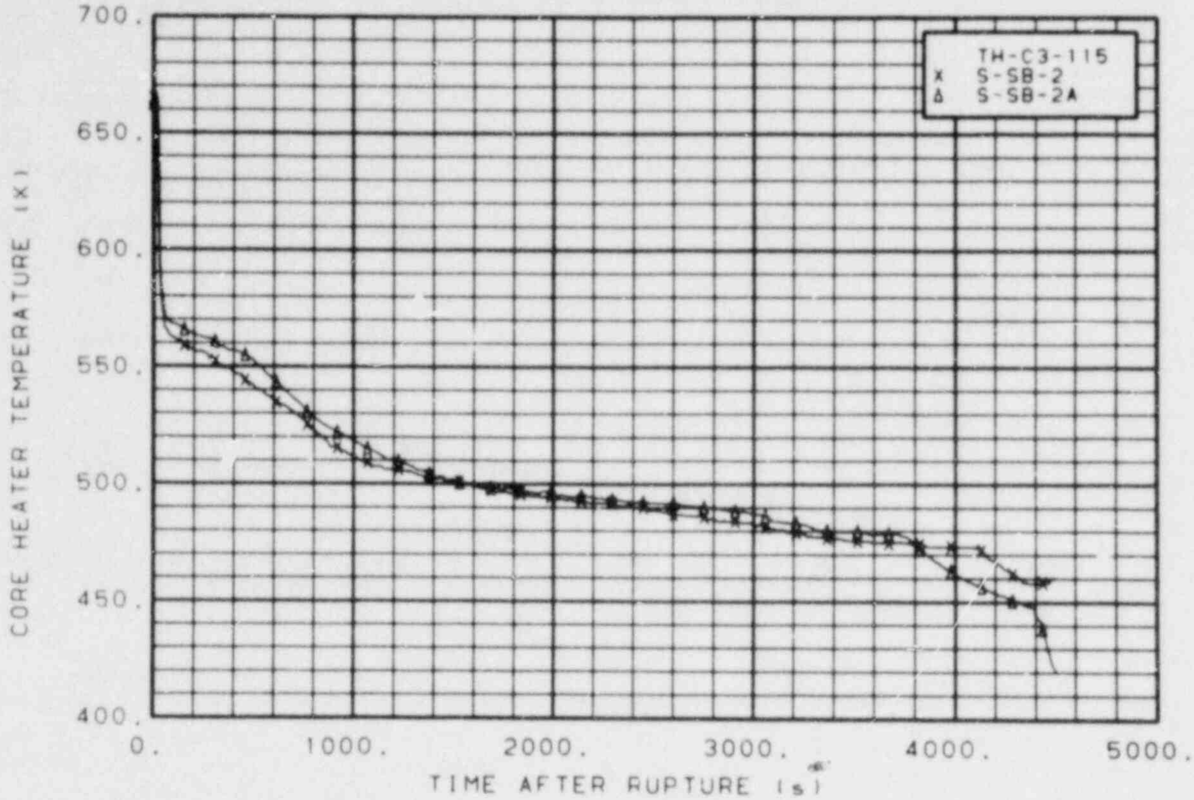

Figure 105. Core heater temperature, Rod C-3 (TH-C3-115), from 0 to 4500 s.

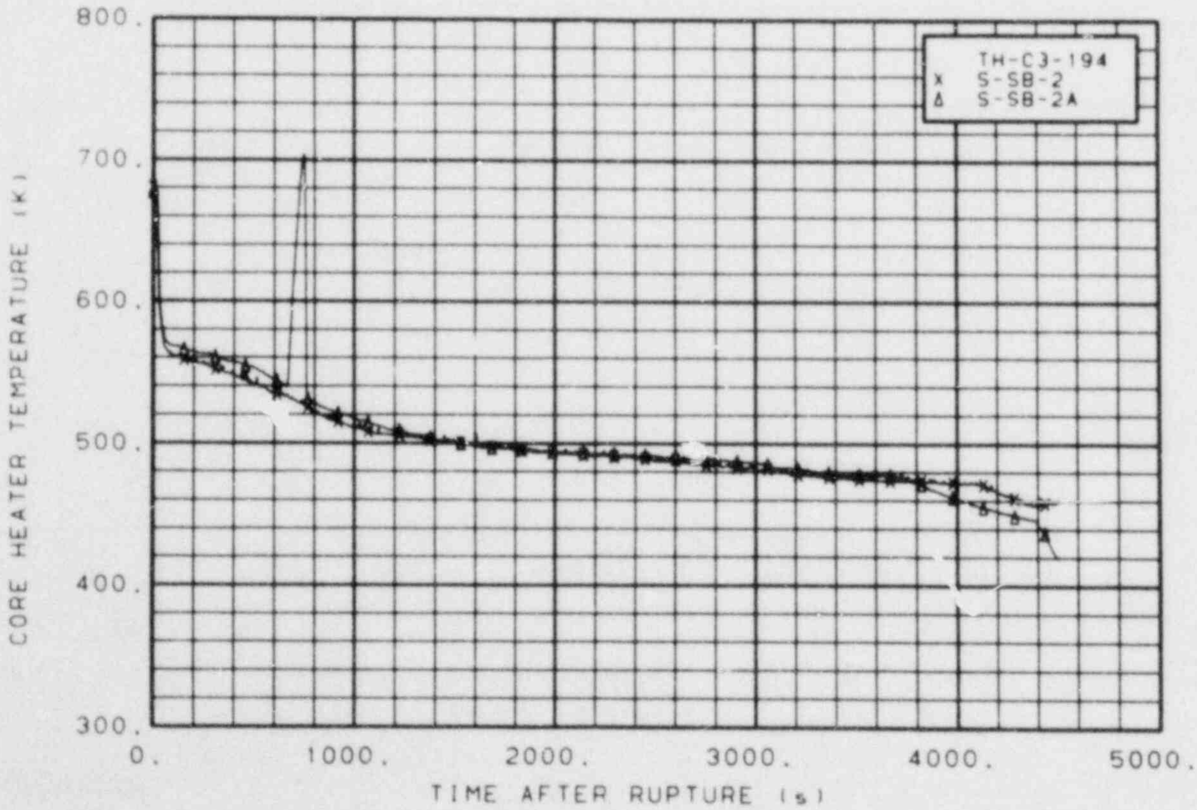

Figure 106. Core heater temperature, Rod C-3 (TH-C3-194), from 0 to 4500 s.

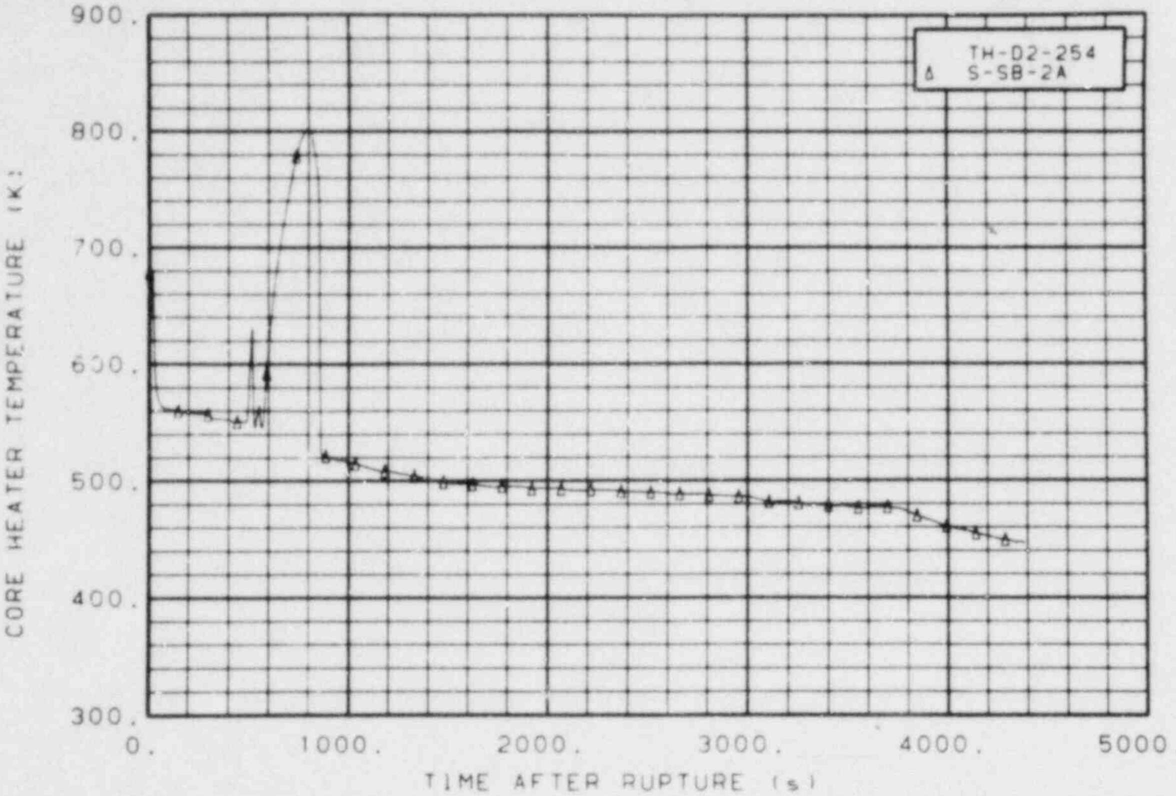

Figure 107. Core heater temperature, Test S-SB-2A, Rod D-2 (TH-D2-254), from 0 to 4390 s.

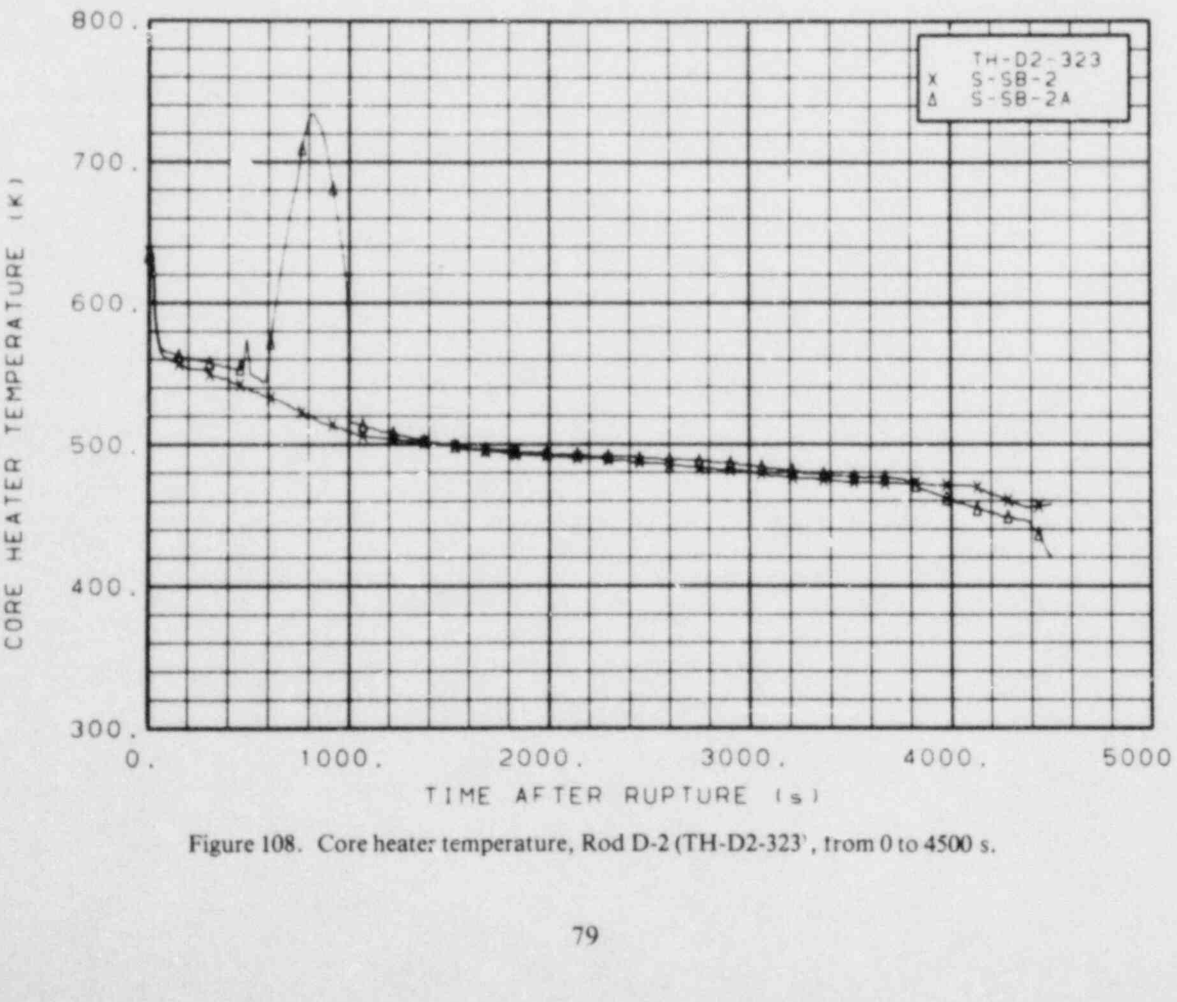

Figure 108. Core heater temperature, Rod D-2 (TH-D2-323', from 0 to 4500 s.

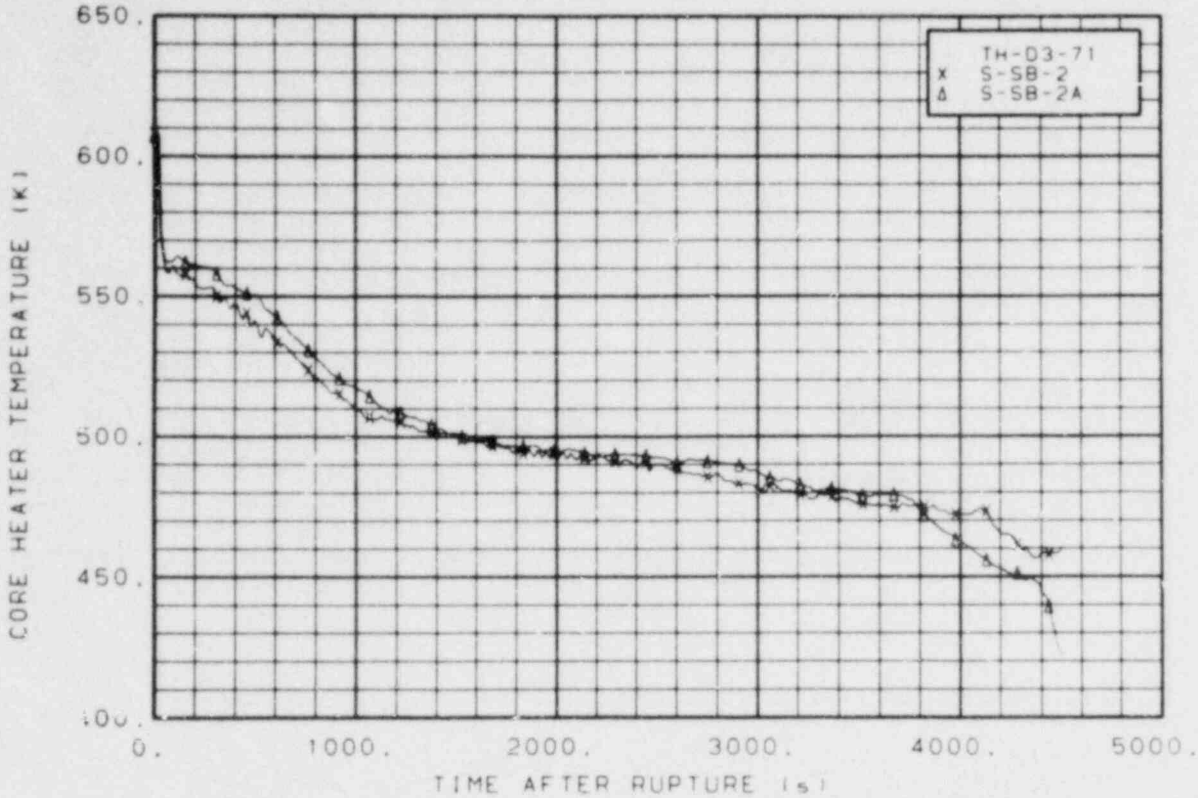

Figure 109. Core heater temperature, Rod D-3 (TH-D3-71), from 0 to 4500 s.

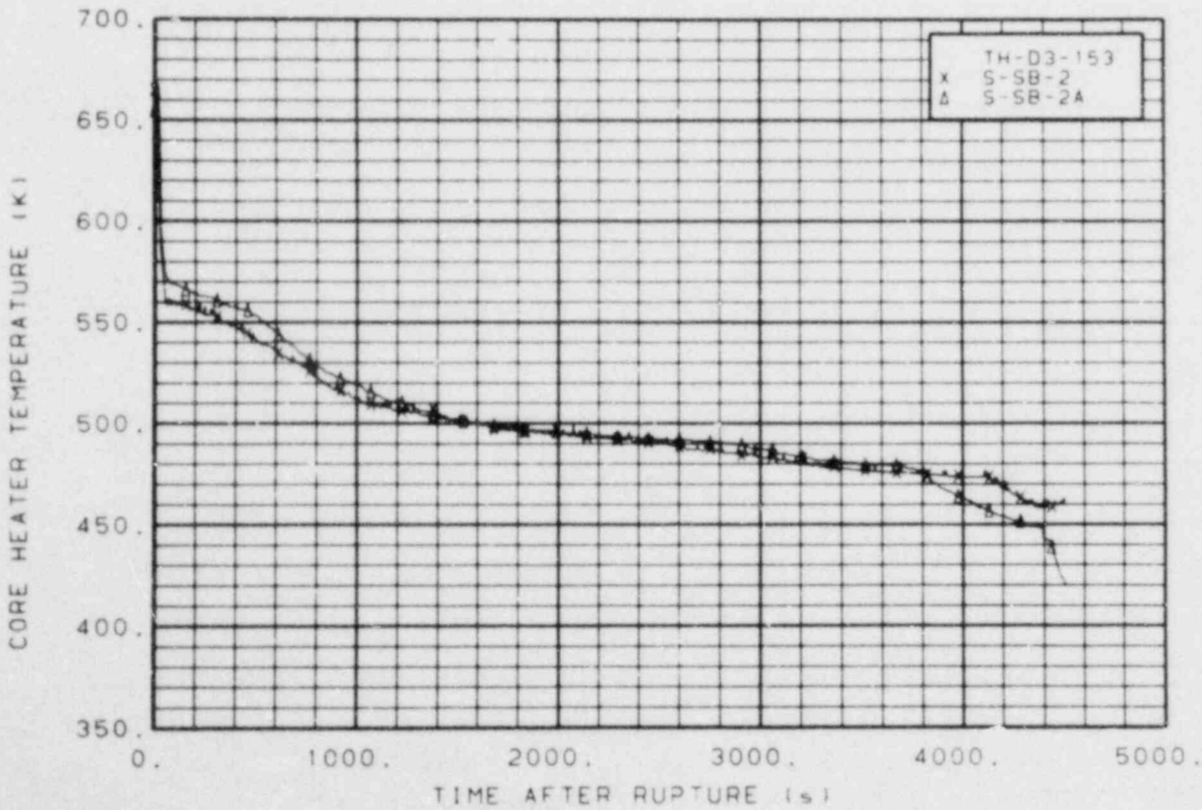

Figure 110. Core heater temperature, Rod D-3 (TH-D3-153), from 0 to 4500 s.

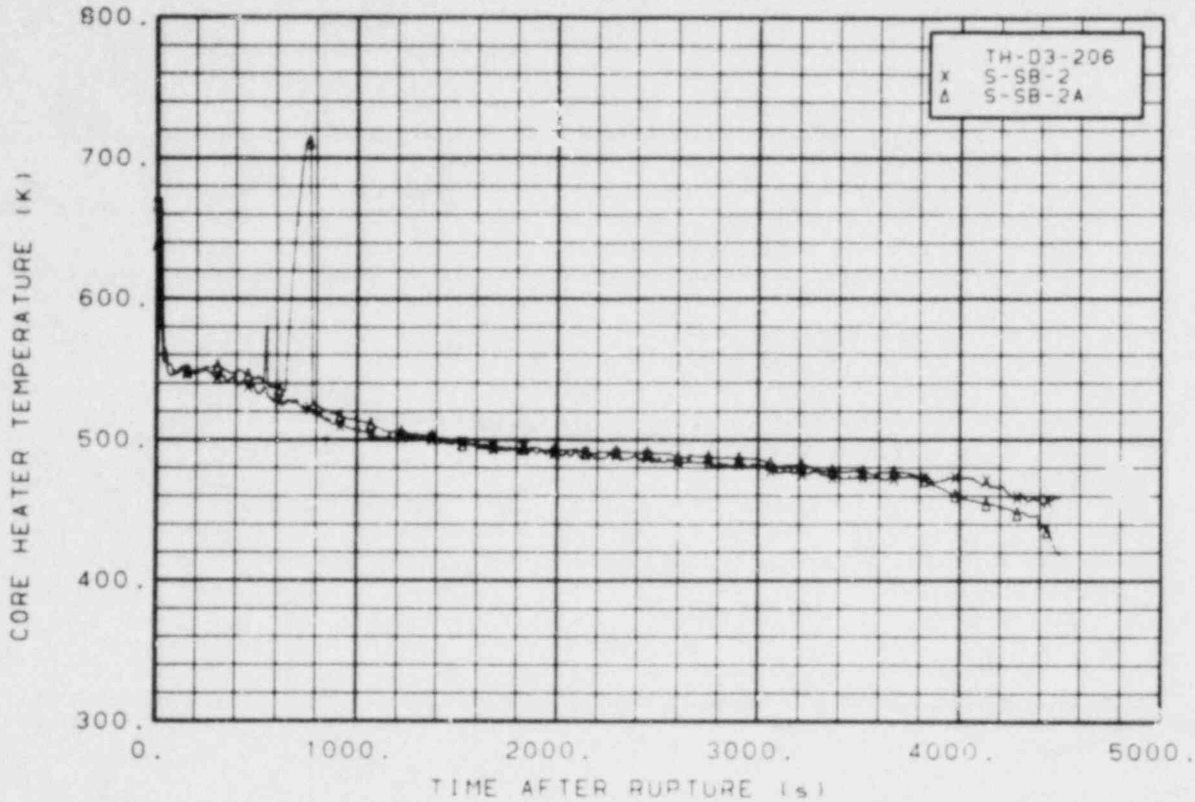

Figure 111. Core heater temperature, Rod D-3 (TH-D3-206), from 0 to 4500 s.

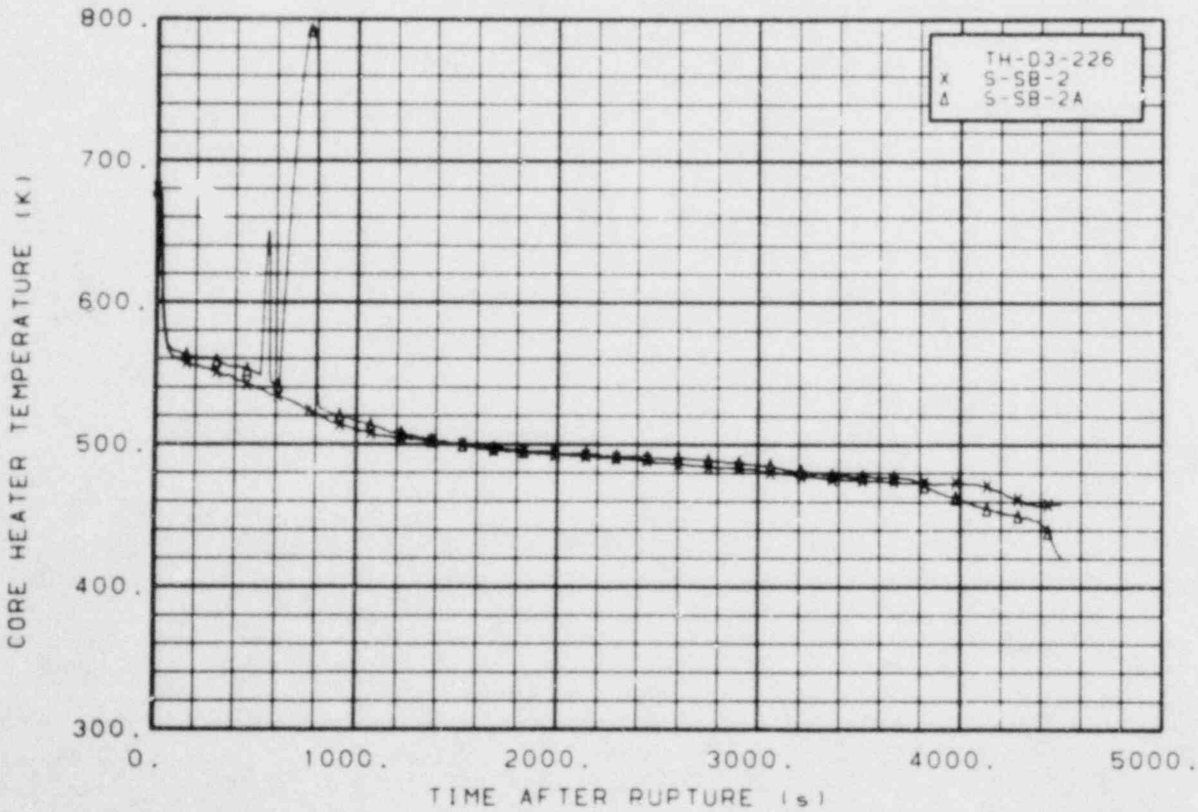

Figure 112. Core heater temperature, Rod D-3 (TH-D3-226), from 0 to 4500 s.

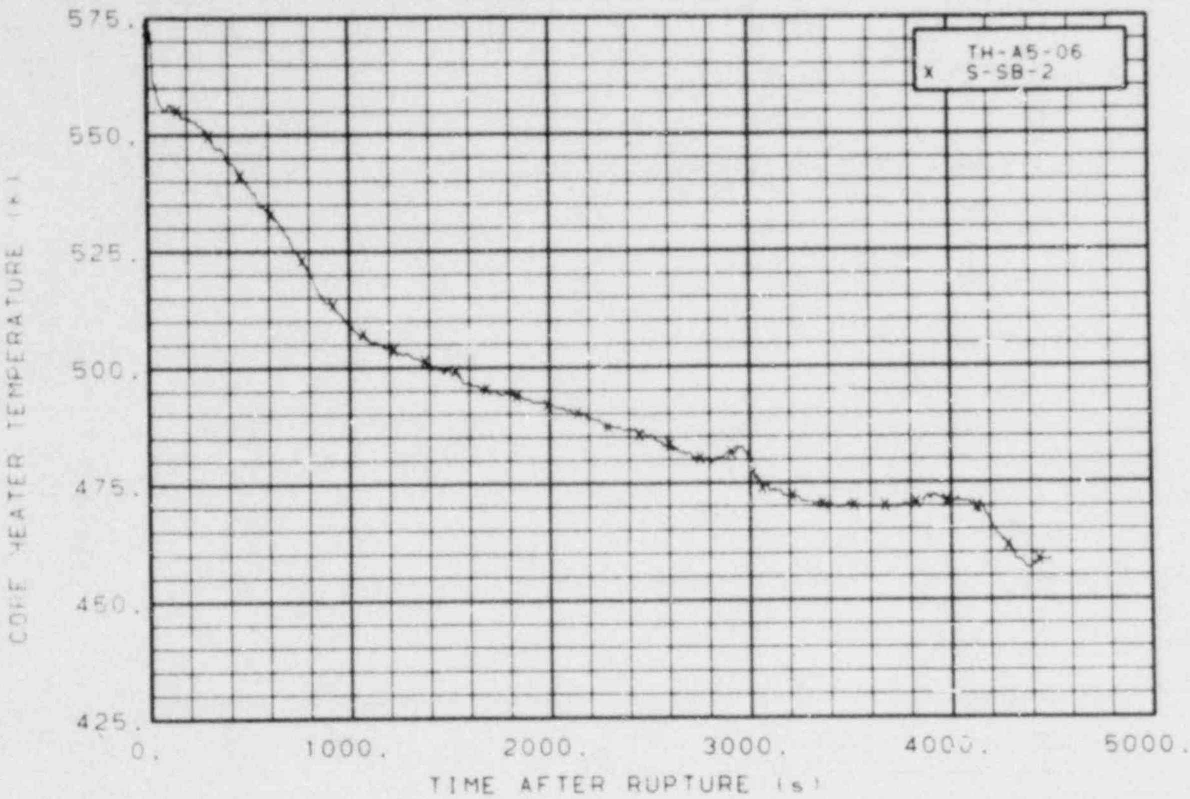

Figure 113. Core heater temperature, Test S-SB-2, Rod A-5 (TH-A5-06), from 0 to 4500 s.

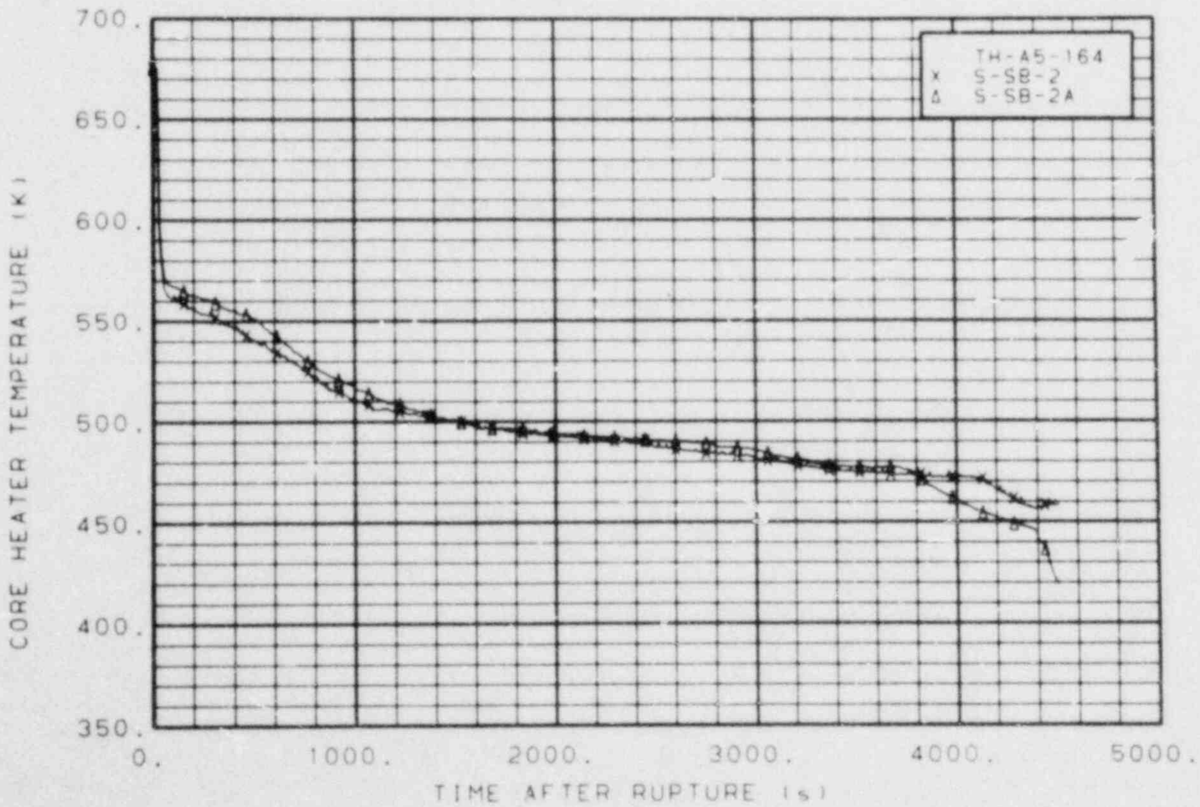

Figure 114. Core heater temperature, Rod A-5 (TH-A5-164), from 0 to 4500 s.

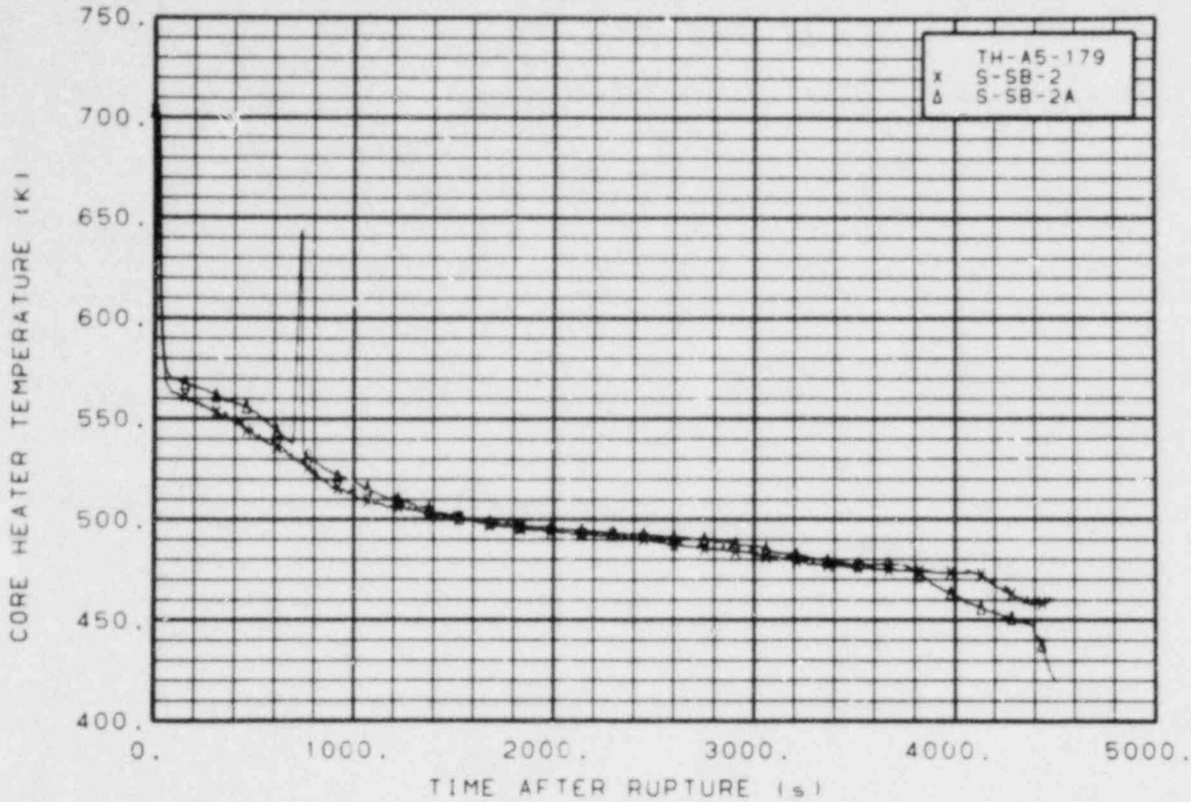

Figure 115. Core heater temperature, Rod A-5 (TH-A5-179), from 0 to 4500 s.

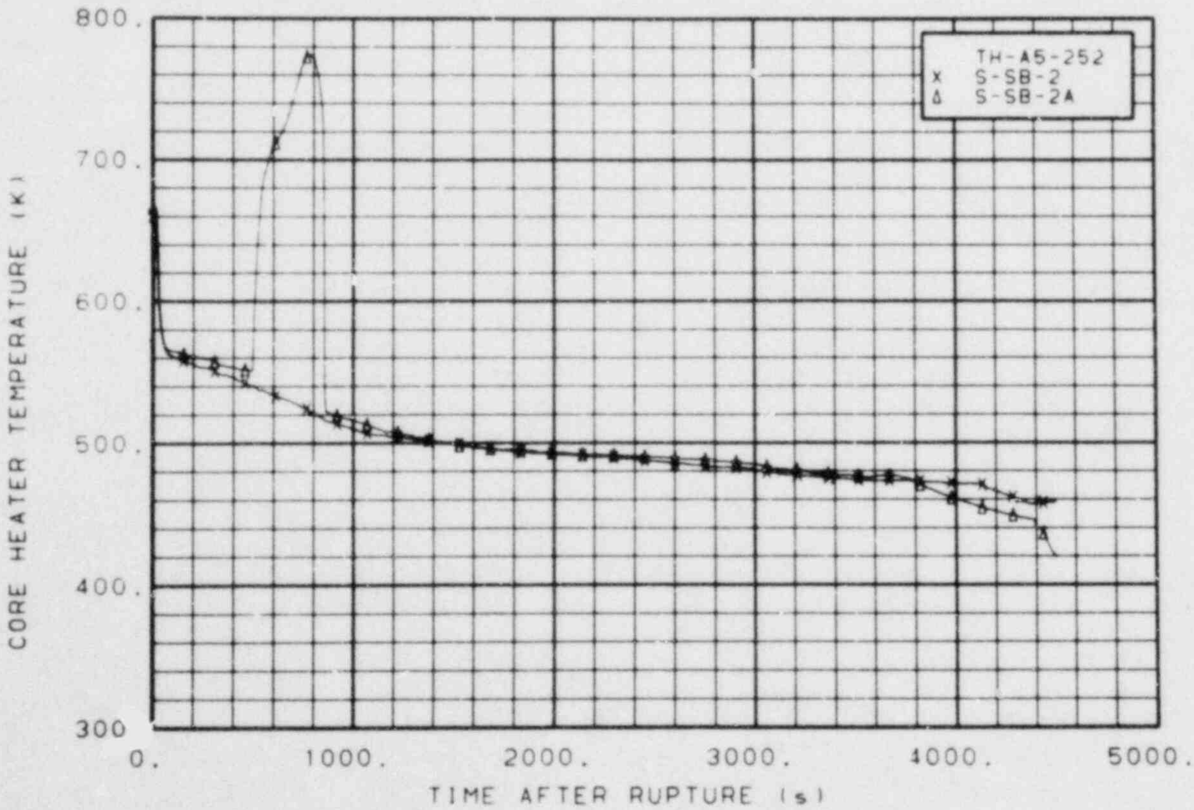

Figure 116. Core heater temperature, Rod A-5 (TH-A5-252), from 0 to 4500 s.

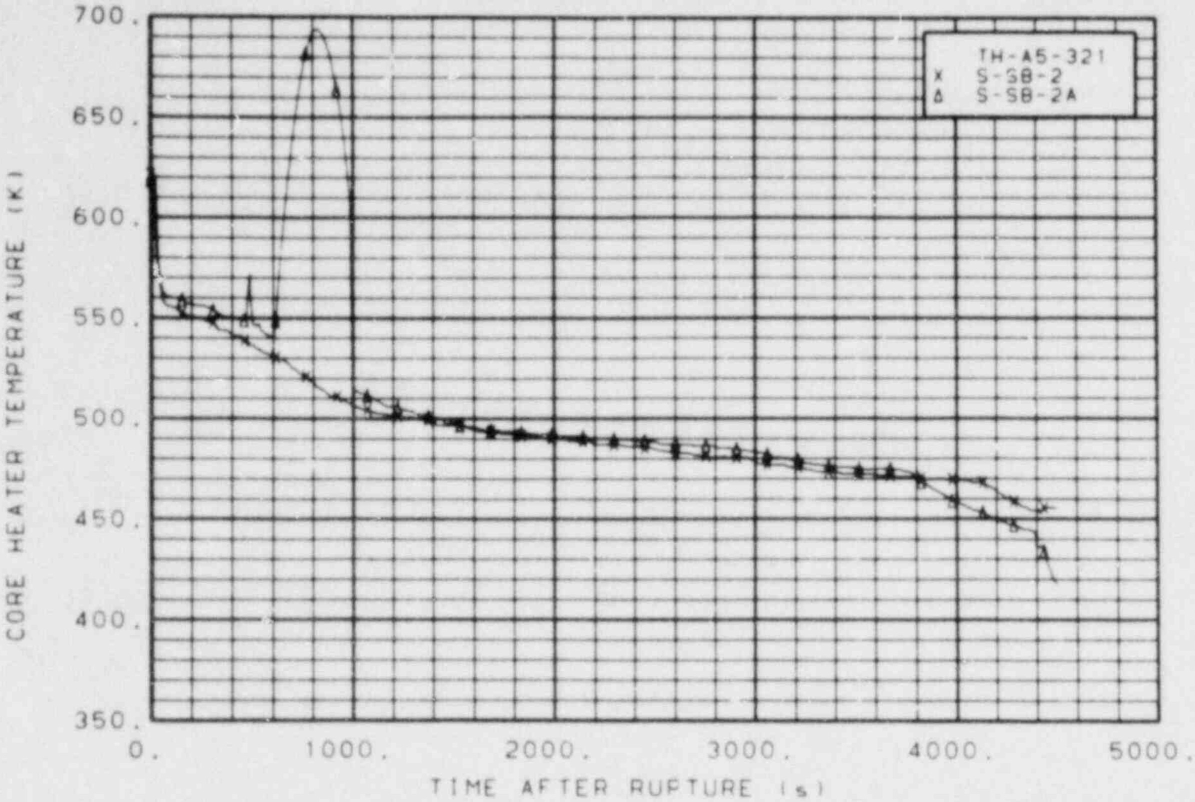

Figure 117. Core heater temperature, Rod A-5 (TH-A5-321), from 0 to 4500 s.

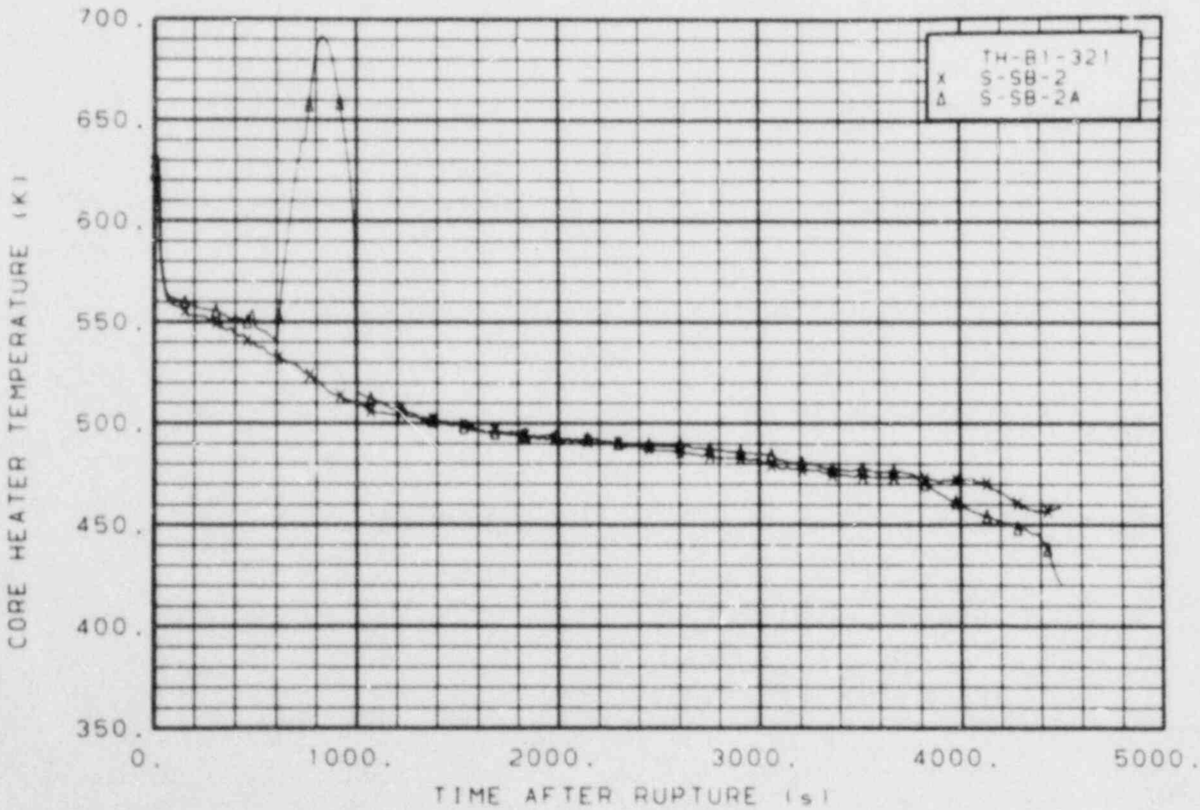

Figure 118. Core heater temperature, Rod B-1 (TH-B1-321), from 0 to 4500 s.

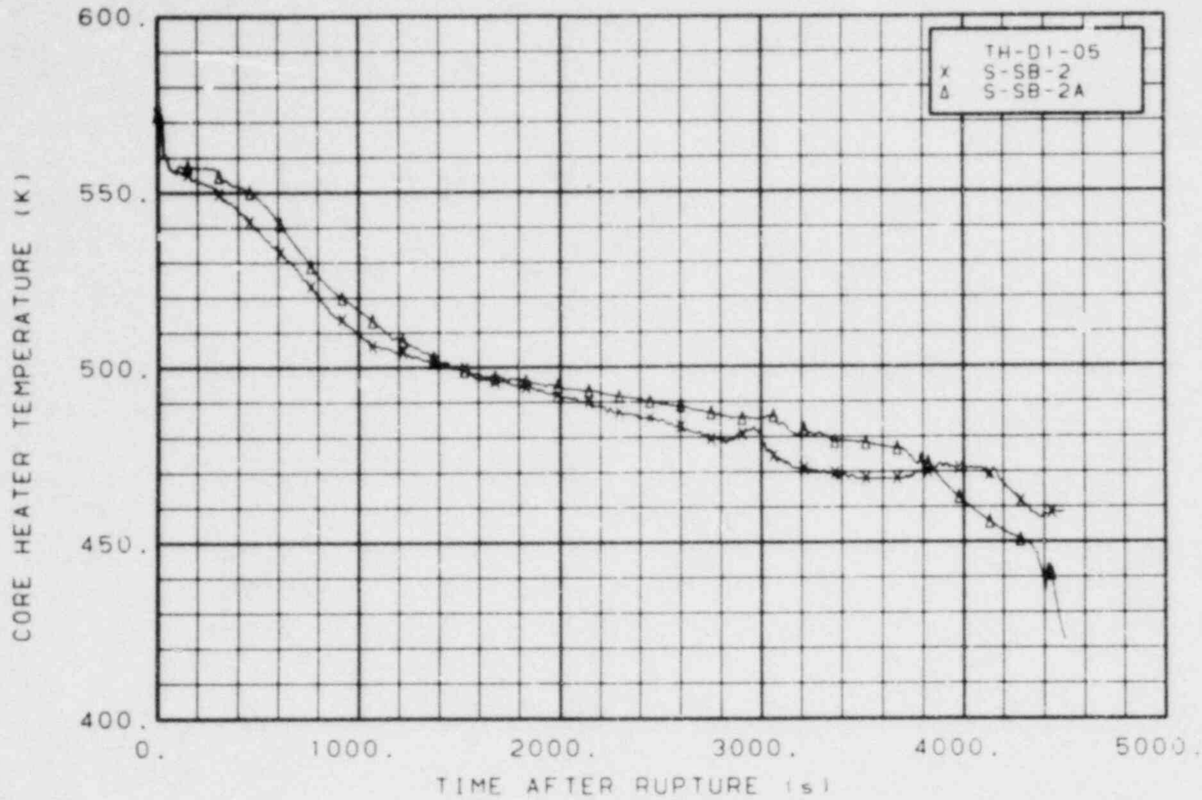

Figure 119. Core heater temperature, Rod D-1 (TH-D1-05), from 0 to 4500 s.

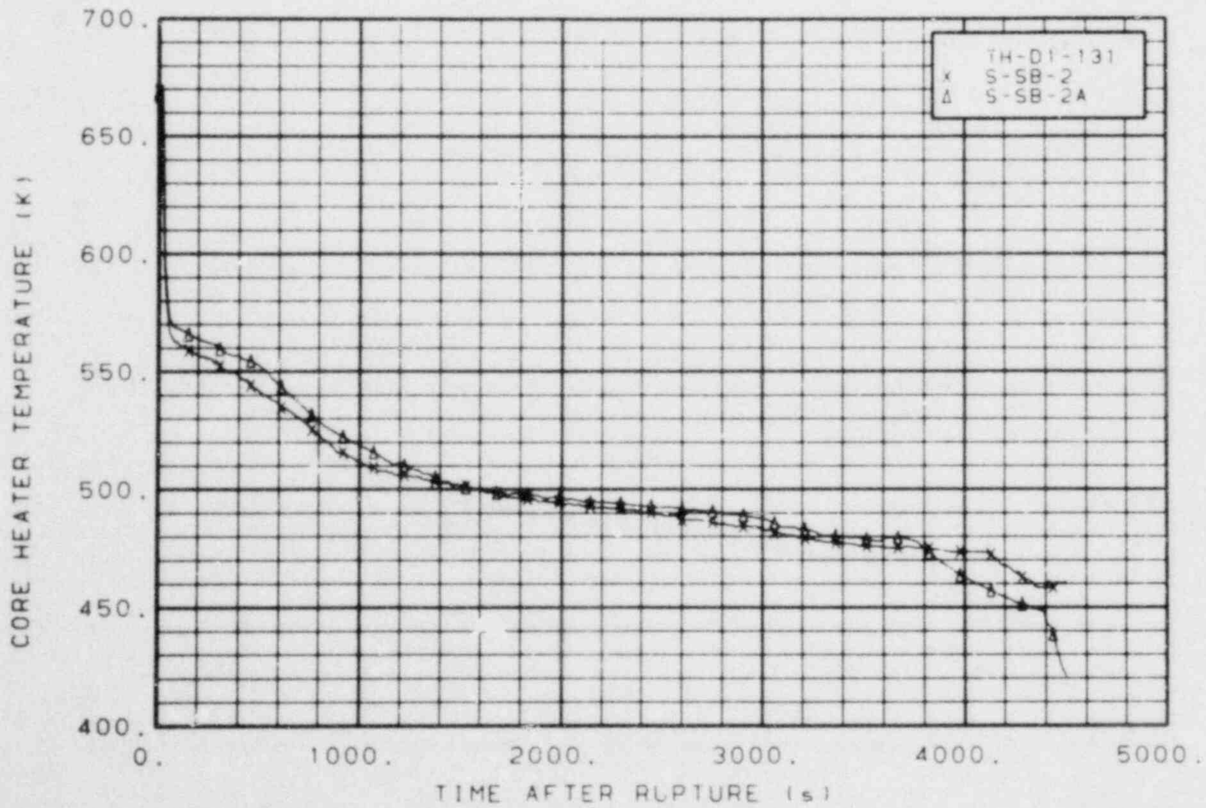

Figure 120. Core heater temperature, Rod D-1 (TH-D1-131), from 0 to 4500 s.

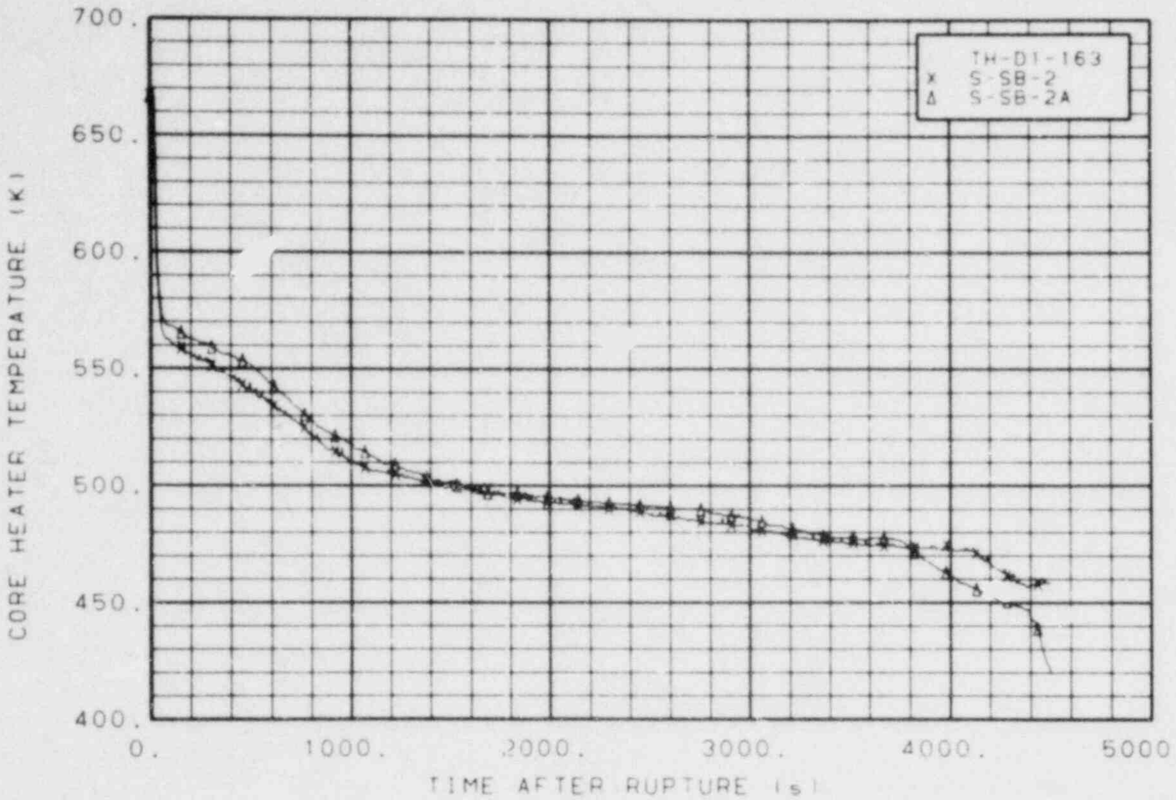

Figure 121. Core heater temperature, Rod D-1 (TH-D1-163), from 0 to 4500 s.

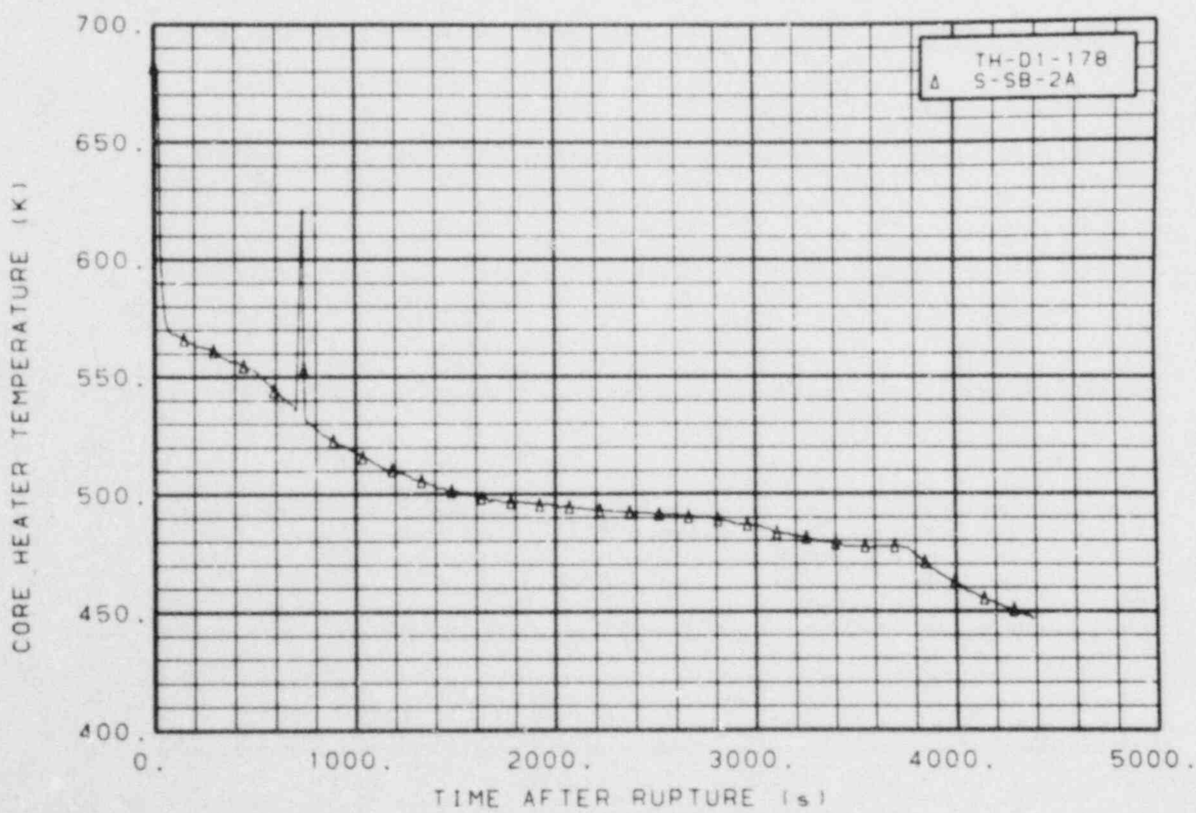

Figure 122. Core heater temperature, Test S-SB-2A, Rod D-1 (TH-D1-178), from 0 to 4390 s.

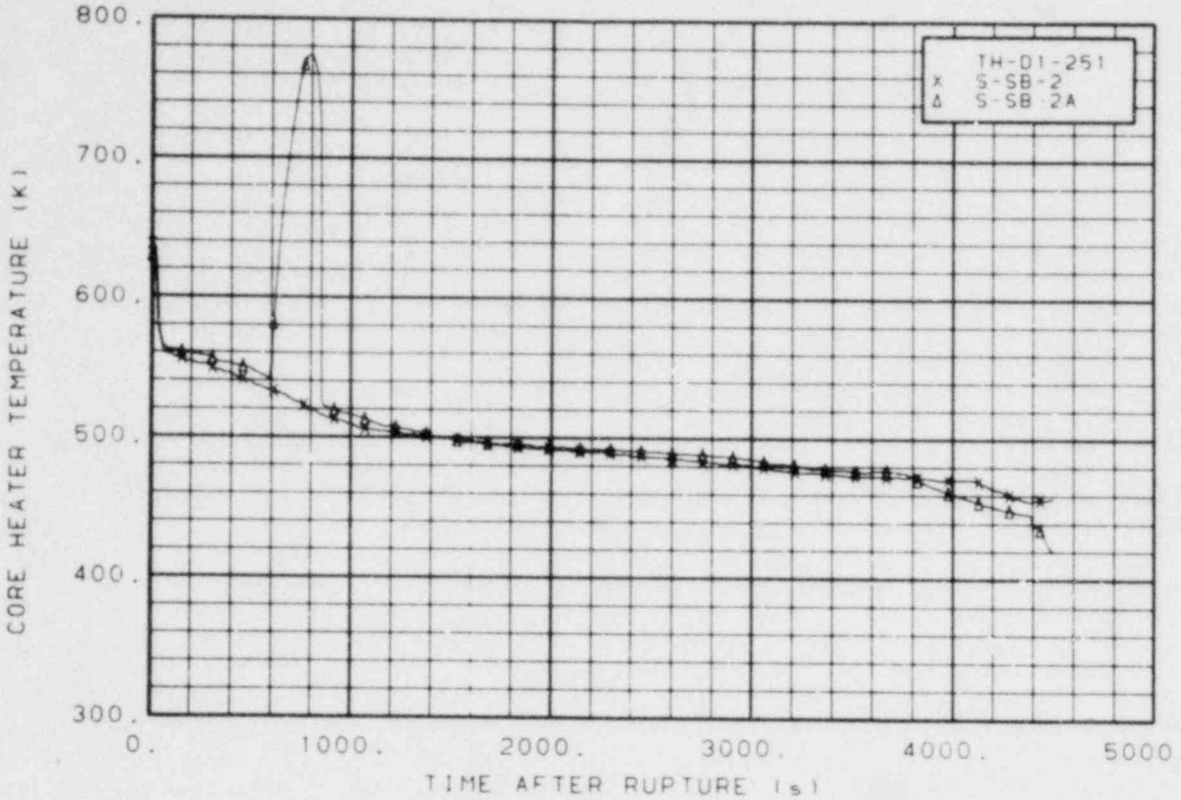

Figure 123. Core heater temperature, Rod D-1 (TH-D1 251), fro[illegible]) to 4500 s.

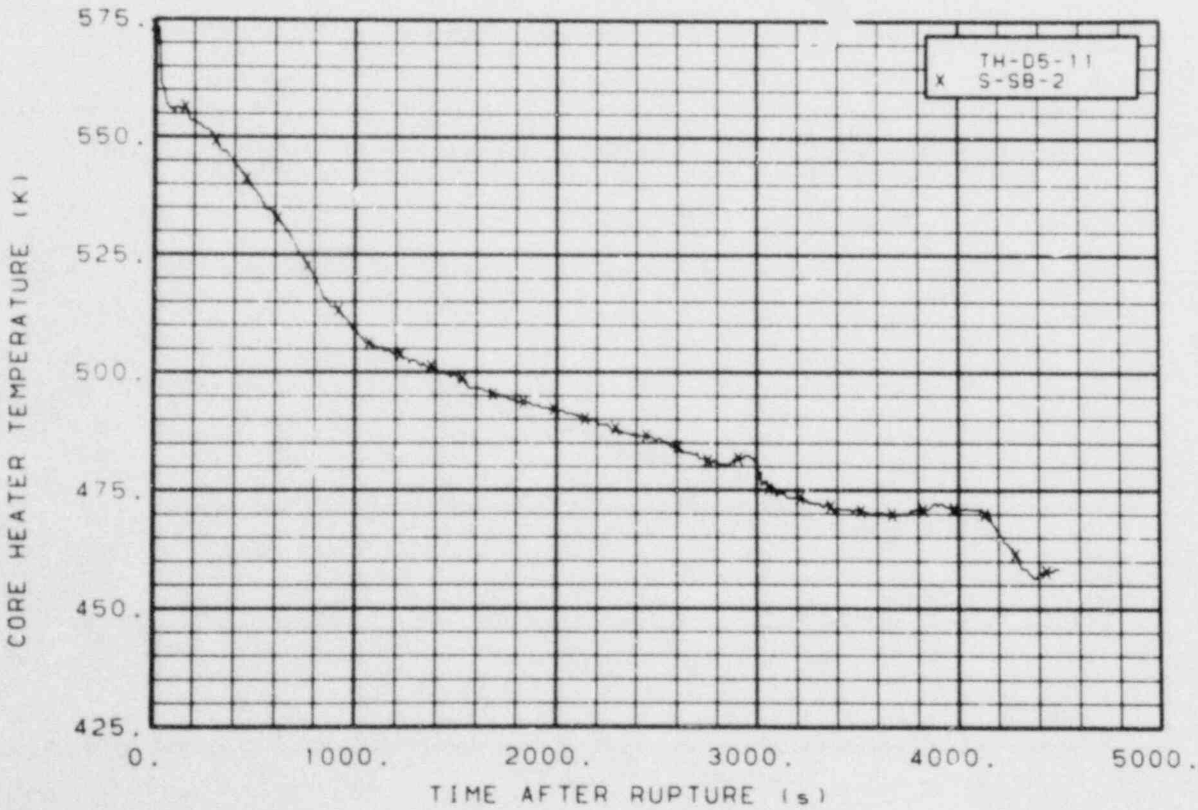

Figure 124. Core heater temperature, Test S-SB-2, Rod D-5 (TH-D5-11), from 0 to 4500 s.

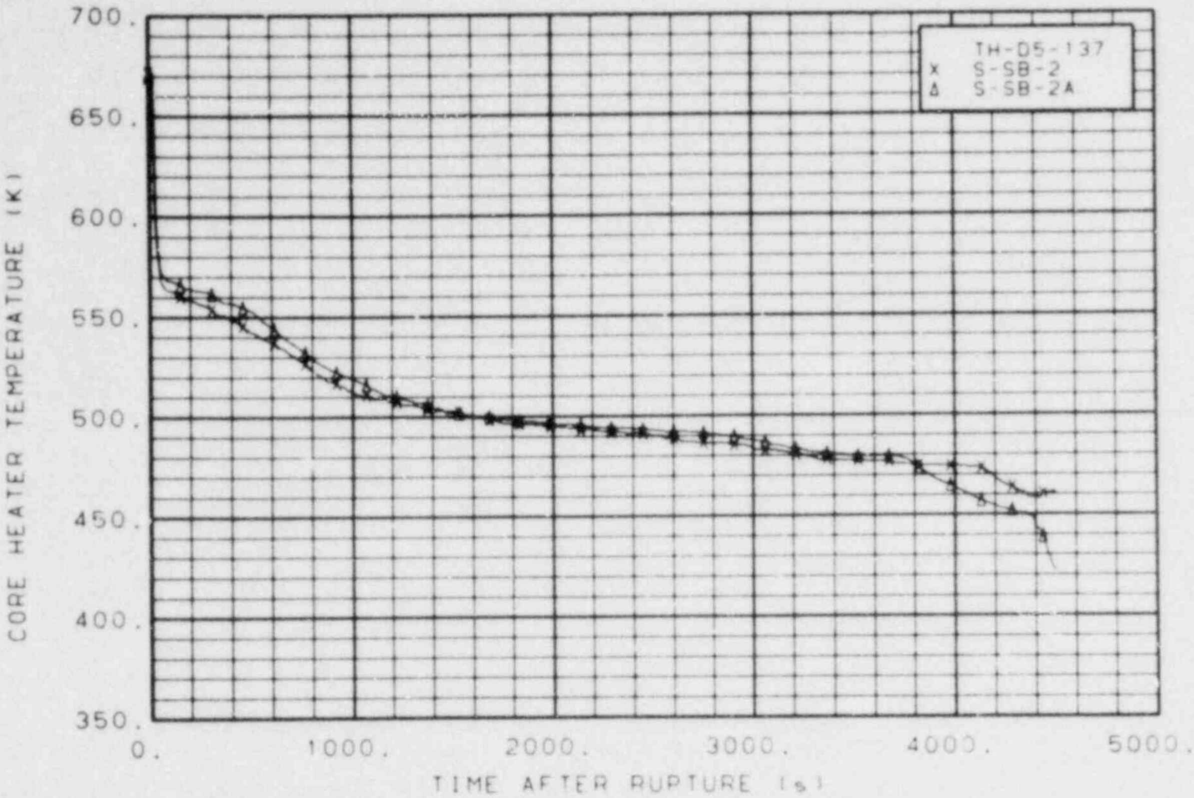

Figure 125. Core heater temperature, Rod D-5 (TH-D5-137), from 0 to 4500 s.

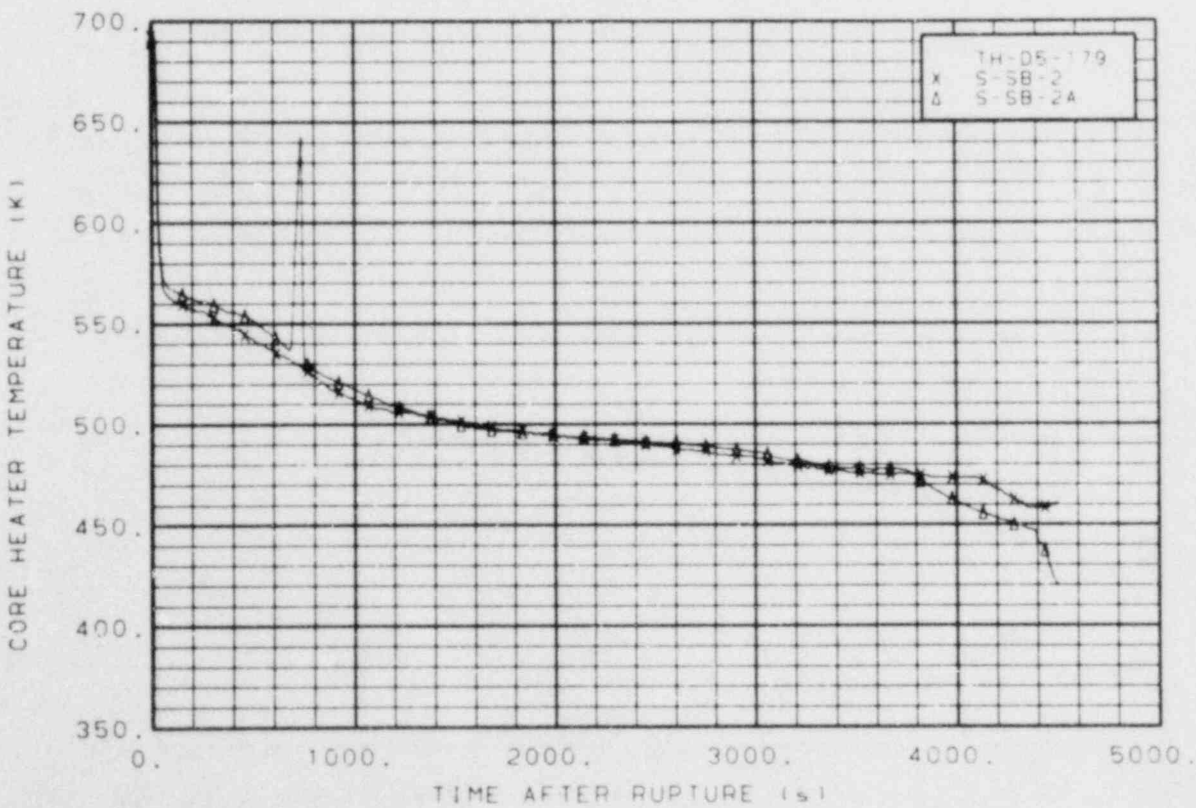

Figure 126. Core heater temperature, Rod D-5 (TH-D5-179), from 0 to 4500 s.

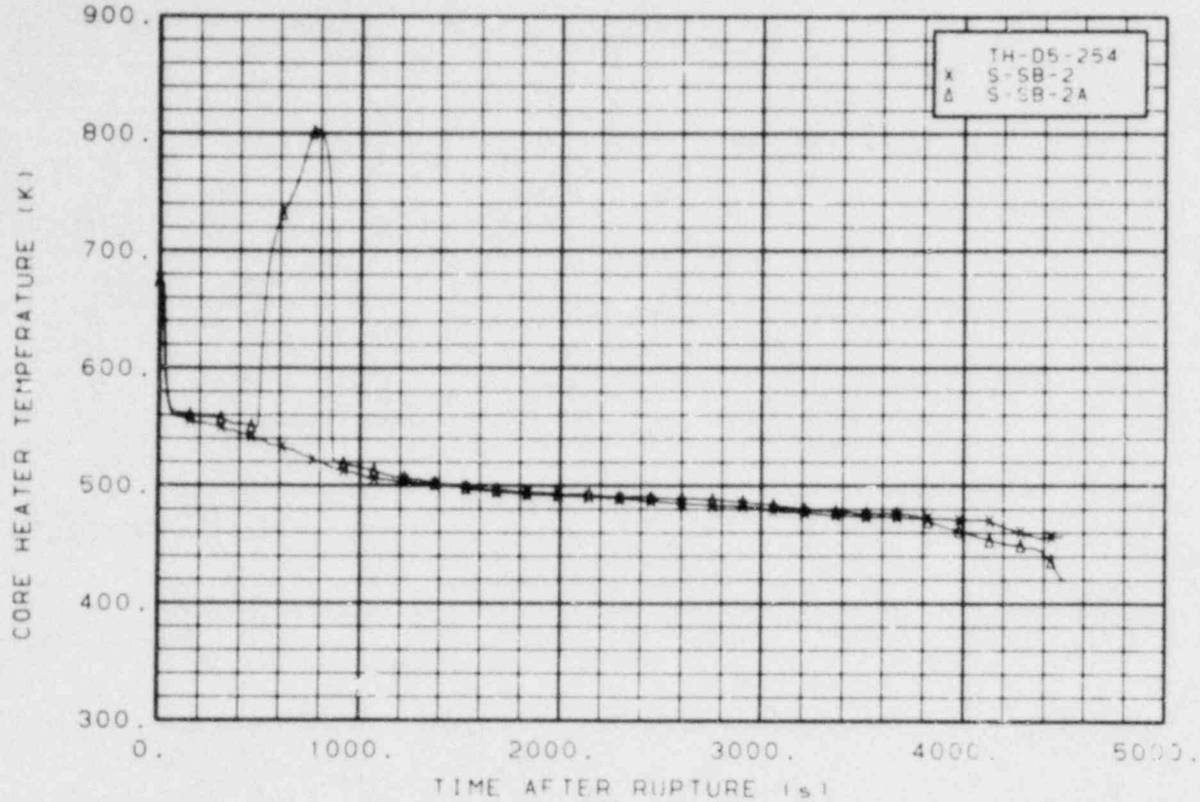

Figure 127. Core heater temperature, Rod D-5 (TH-D5-254), from 0 to 4500 s.

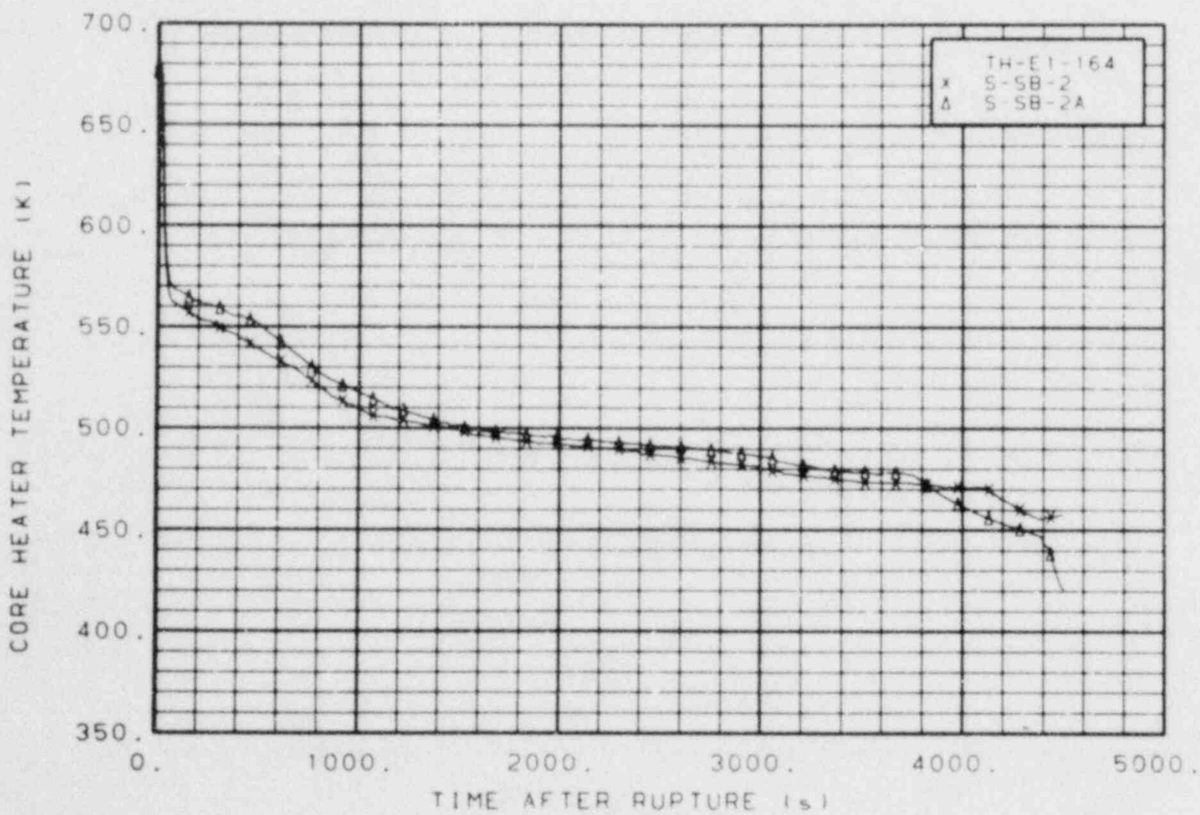

Figure 128. Core heater temperature, Rod E-1 (TH-E1-164), from 0 to 4500 s.

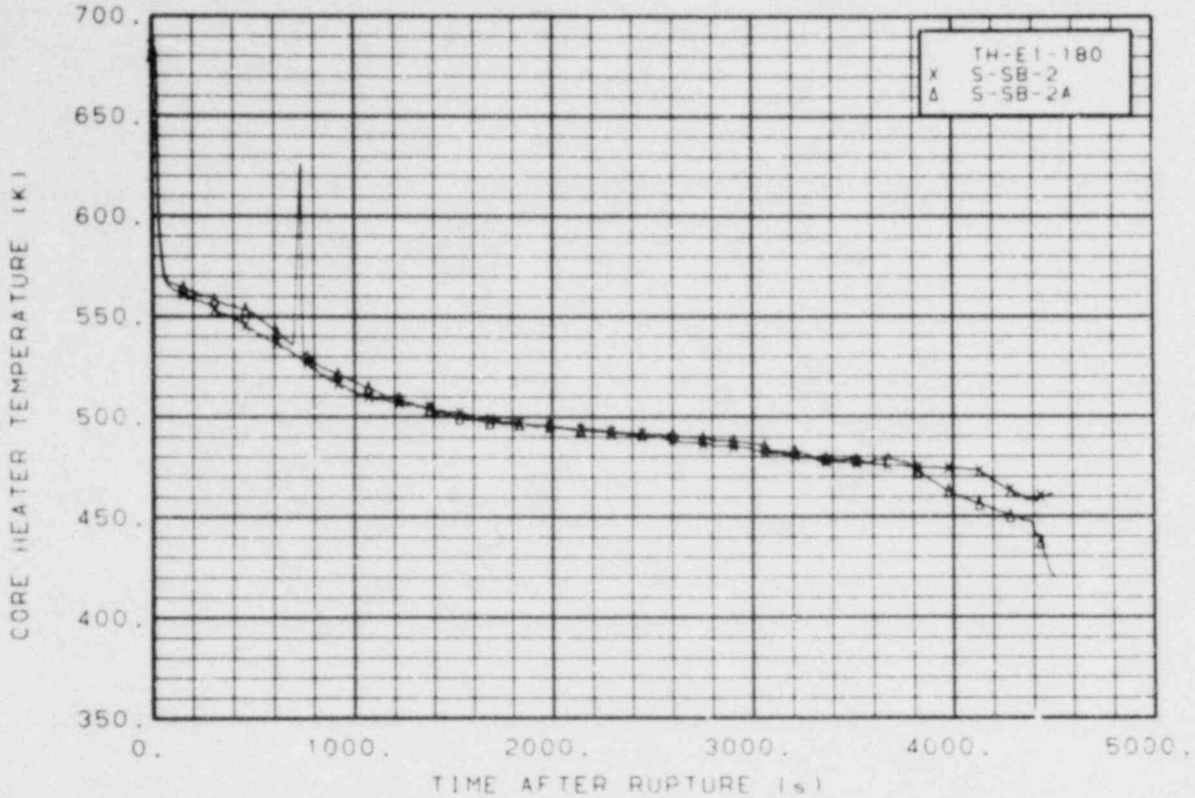

Figure 129. Core heater temperature, Rod E-1 (TH-E1-180), from 0 to 4500 s.

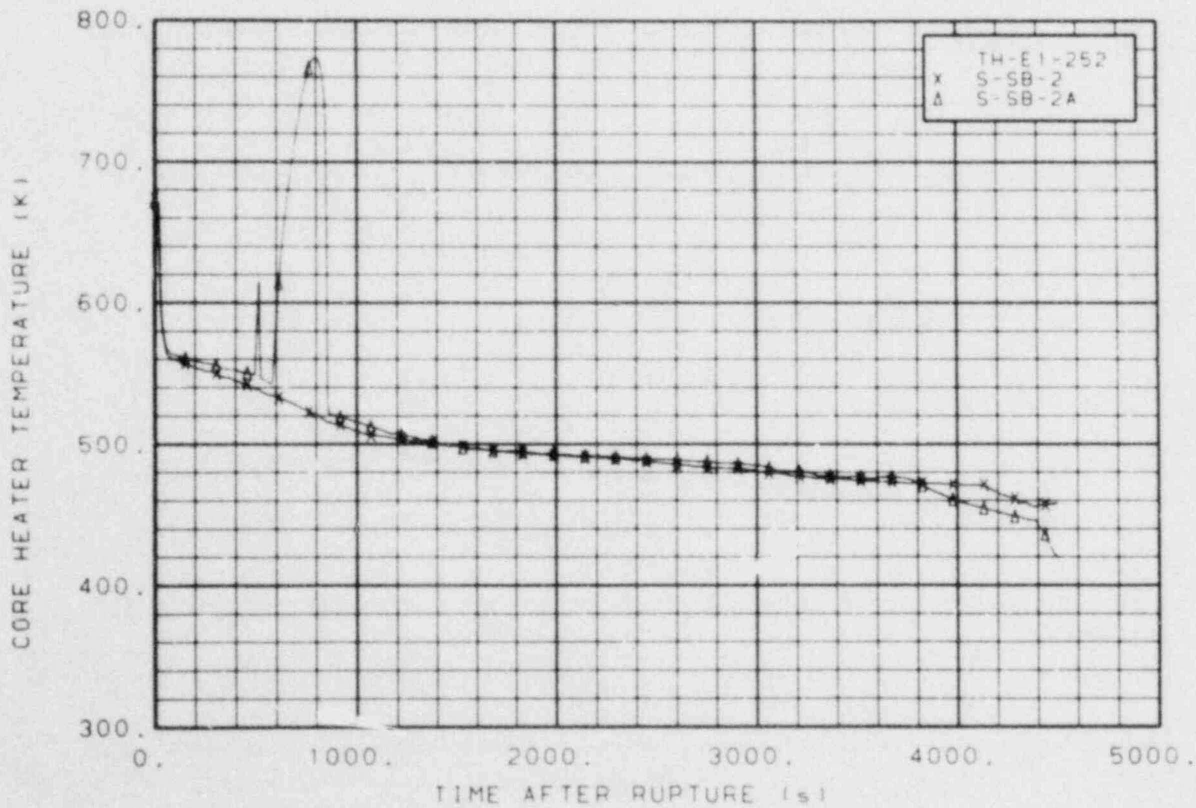

Figure 130. Core heater temperature, Rod E-1 (TH-E1-252), from 0 to 4500 s.

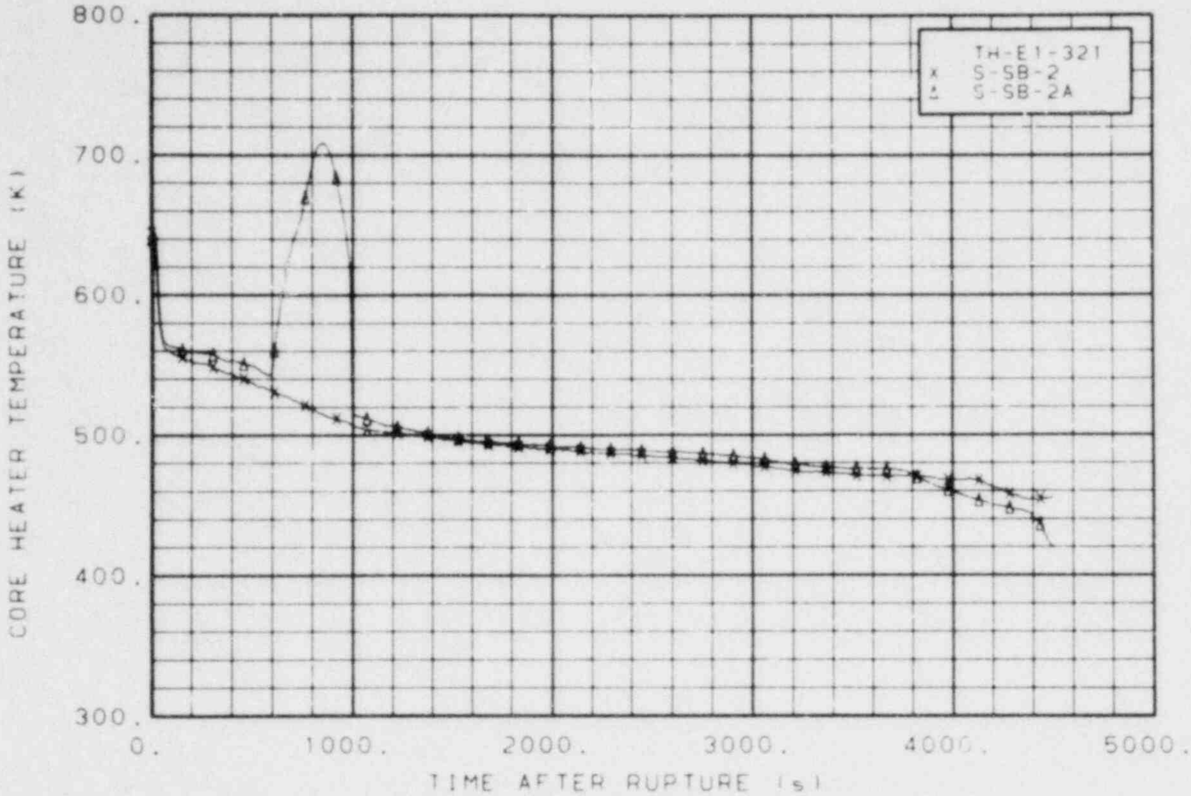

Figure 131. Core heater temperature, Rod E-1 (TH-E1-321), from 0 to 4500 s.

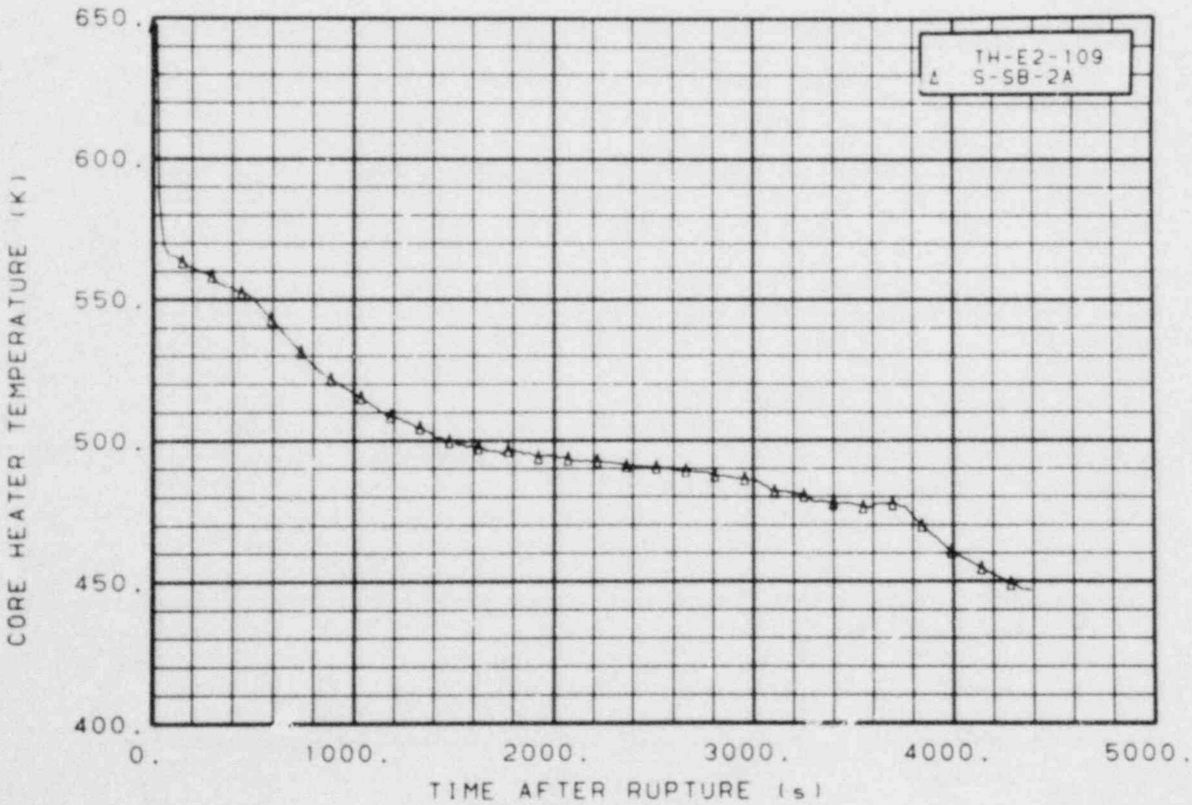

Figure 132. Co heater temperature, Test S-SB-2A, Rod E-2 (TH-E2-109), from 0 to 4390 s.

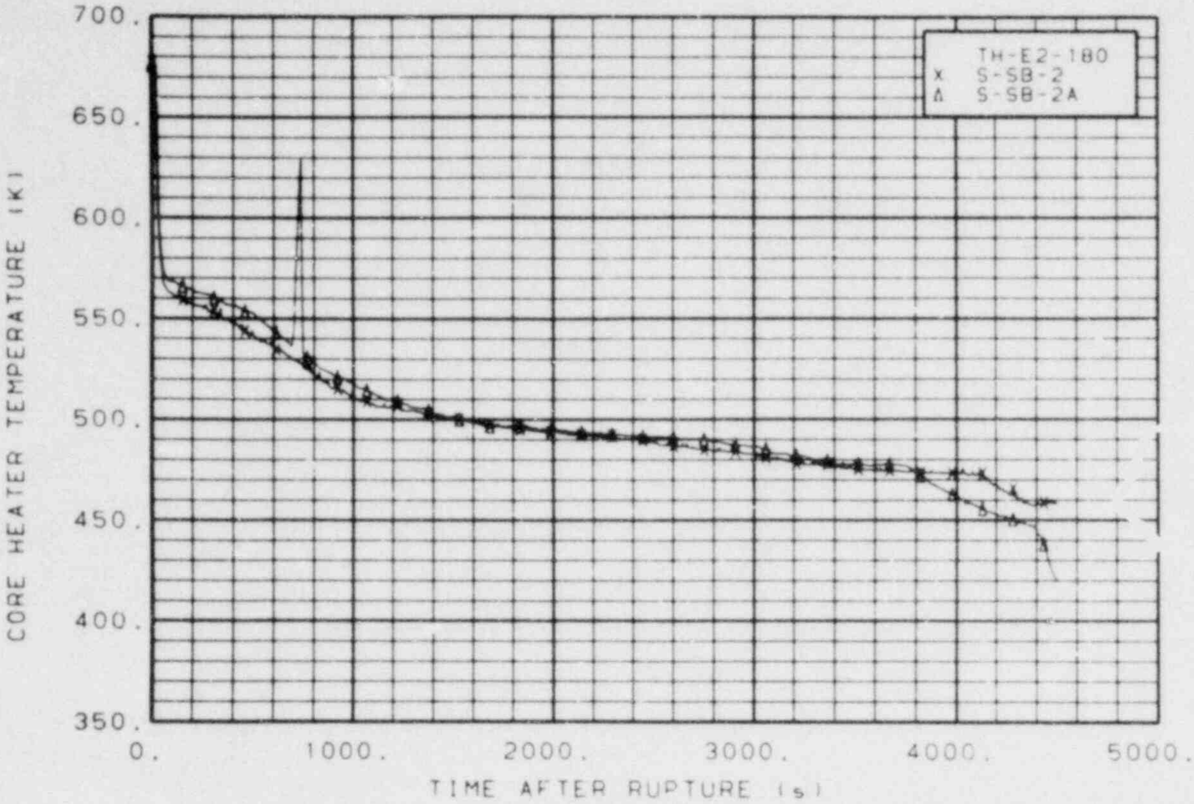

Figure 133. Core heater temperature, Rod E-2 (TH-E2-180), from 0 to 4500 s.

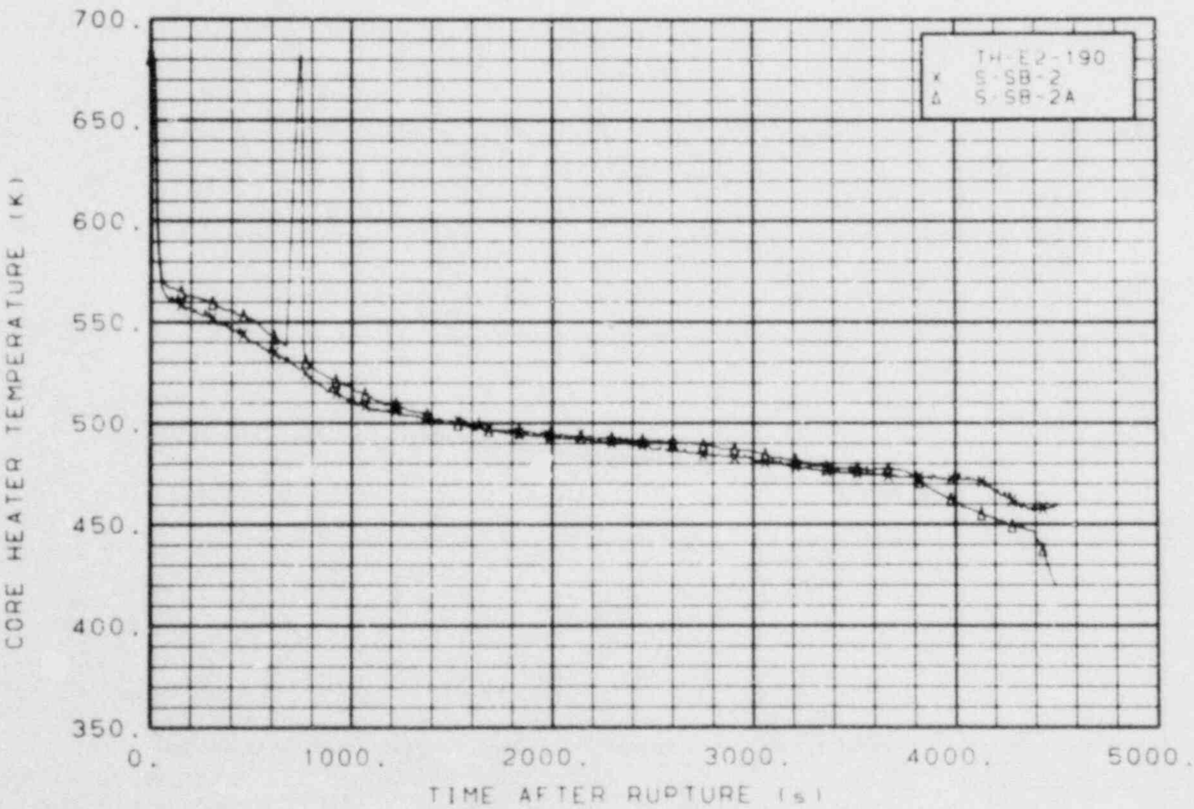

Figure 134. Core heater temperature, Rod E-2 (TH-E2-190), from 0 to 4500 s.

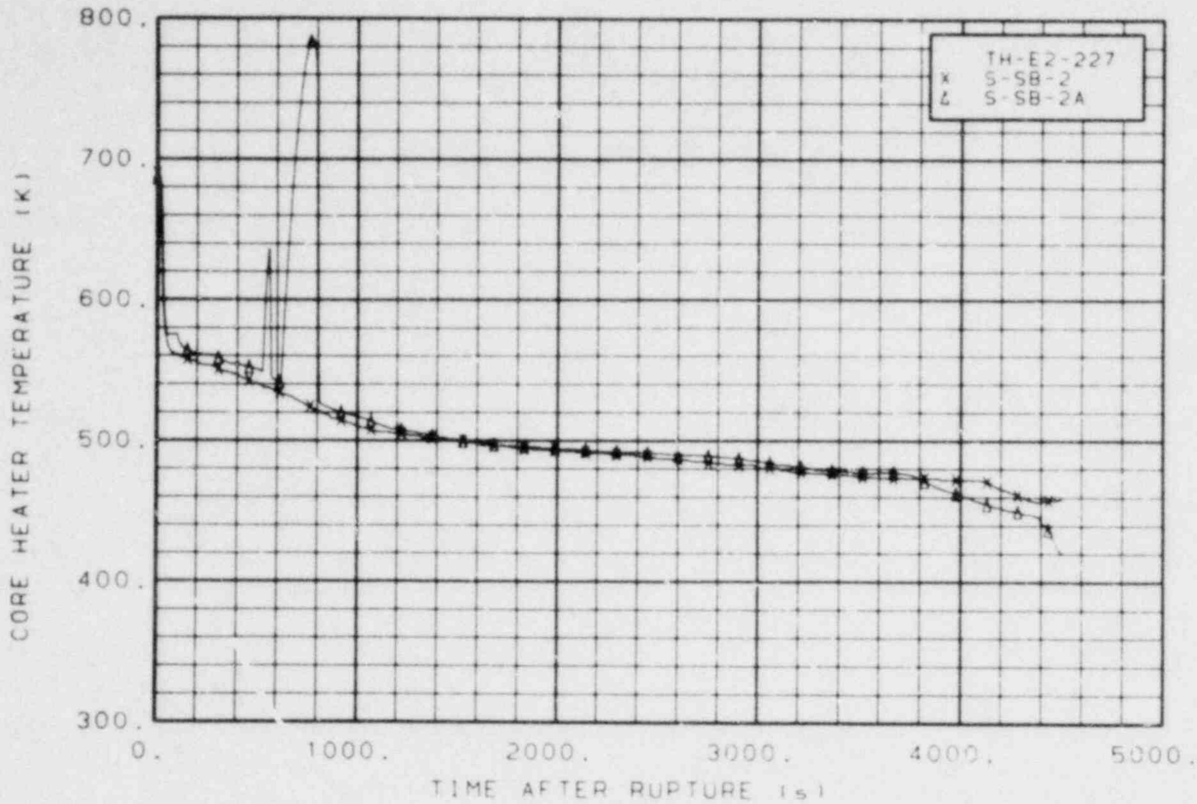

Figure 135. Core heater temperature, Rod E-2 (TH-E2-227), from 0 to 4500 s.

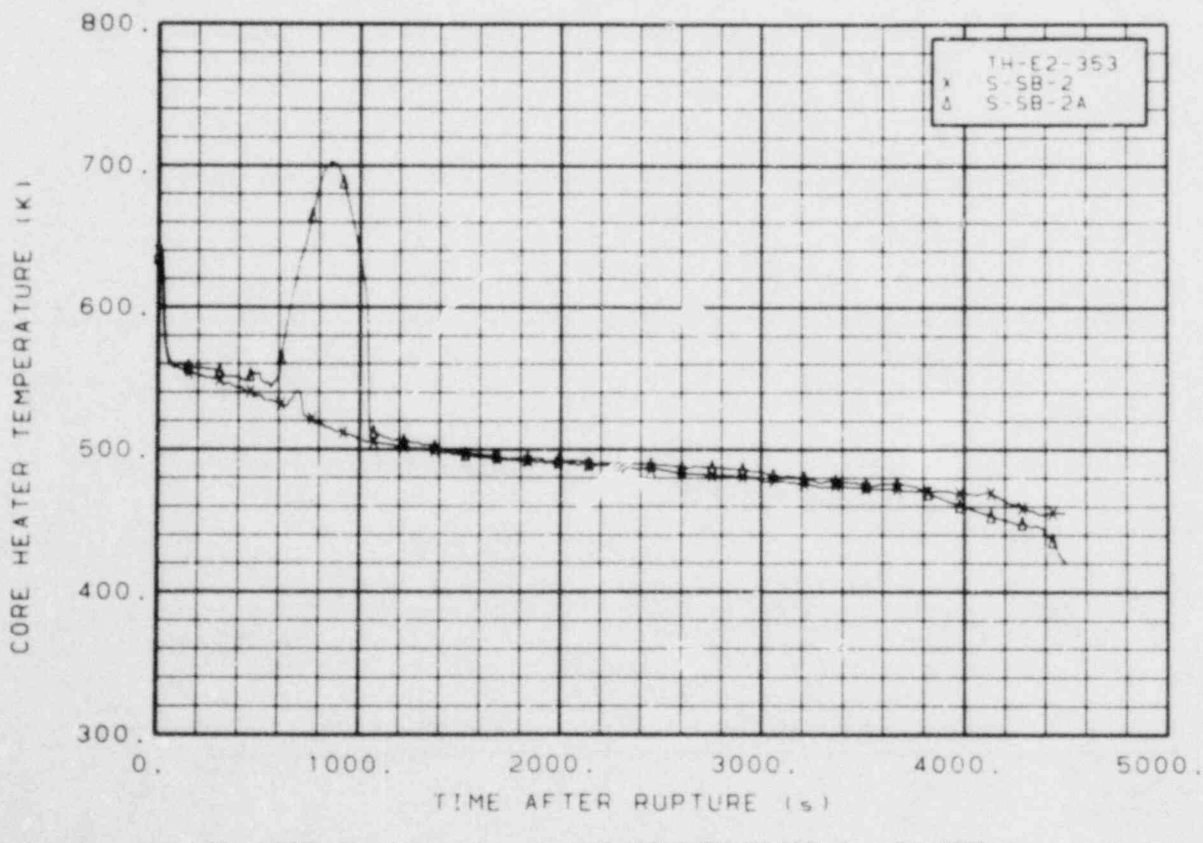

Figure 136. Core heater temperature, Rod E-2 (TH-E2-353), from 0 to 4500 s.

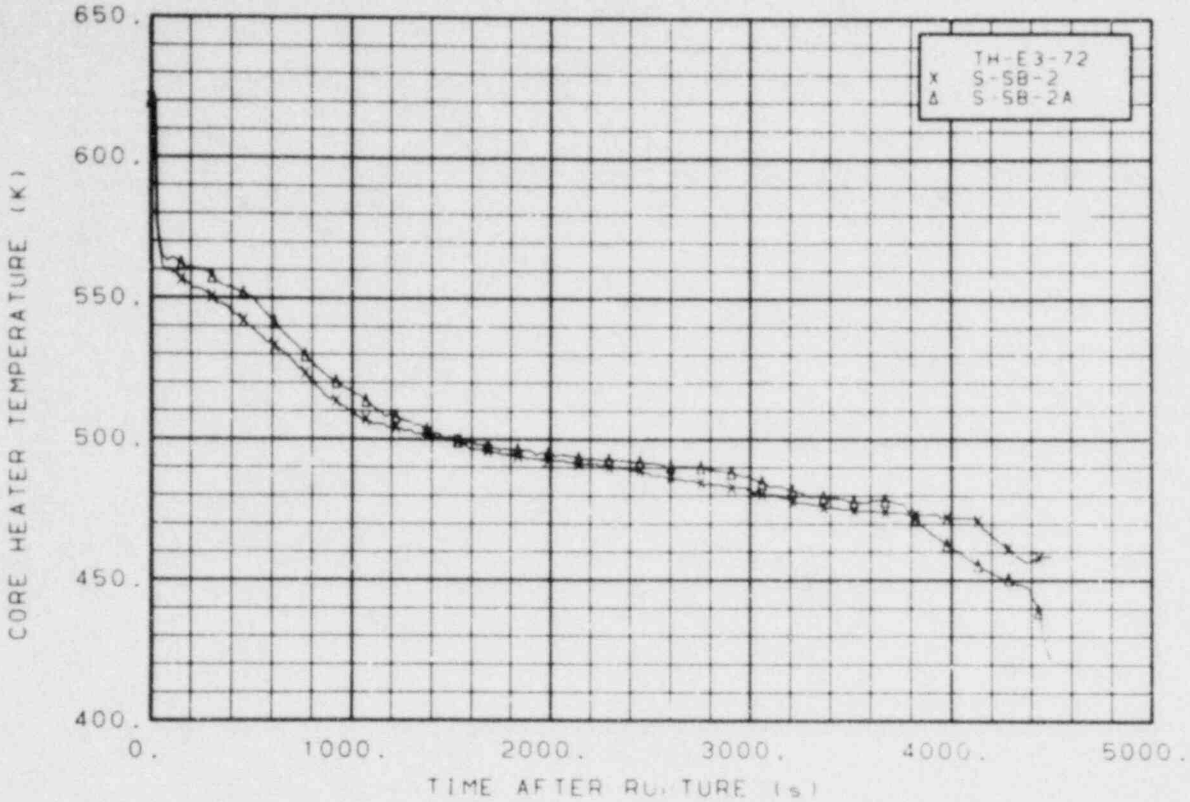

Figure 137. Core heater temperature, Rod E-3 (TH-E3-72), from 0 to 4500 s.

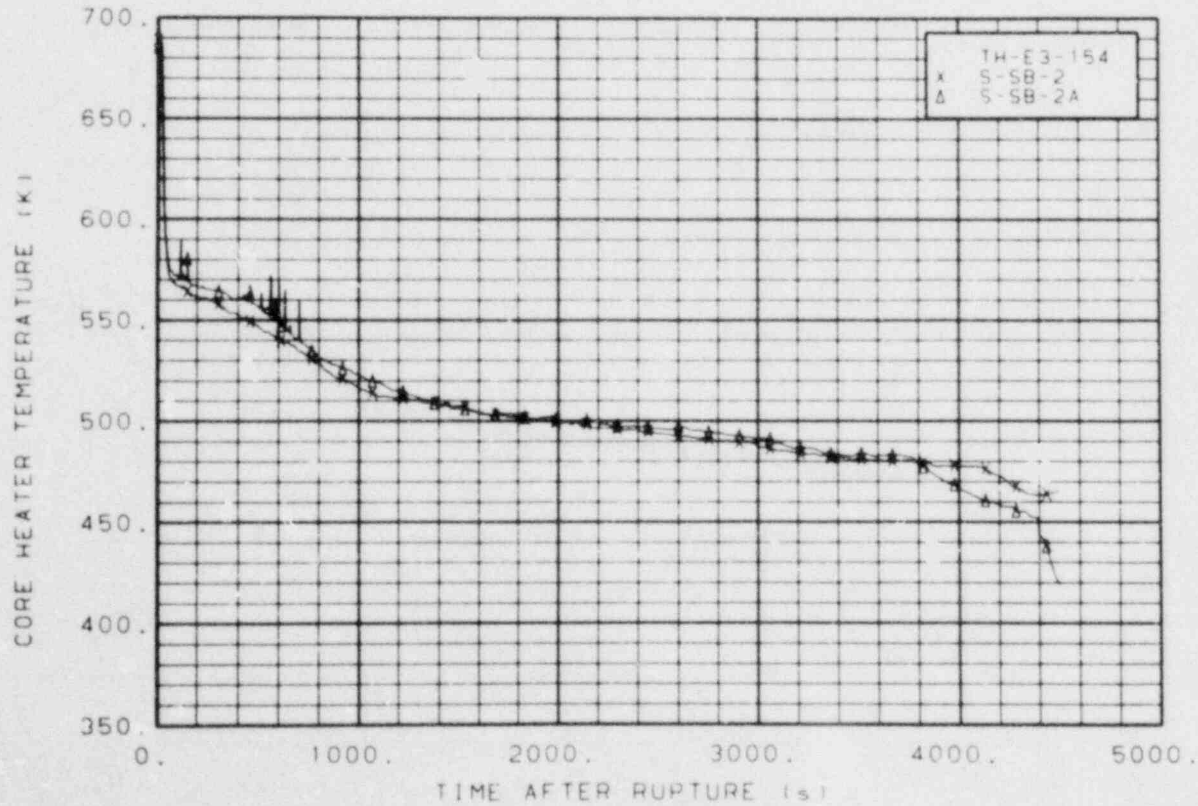

Figure 138. Core heater temperature, Rod E-3 (TH-E3-154), from 0 to 4500 s.

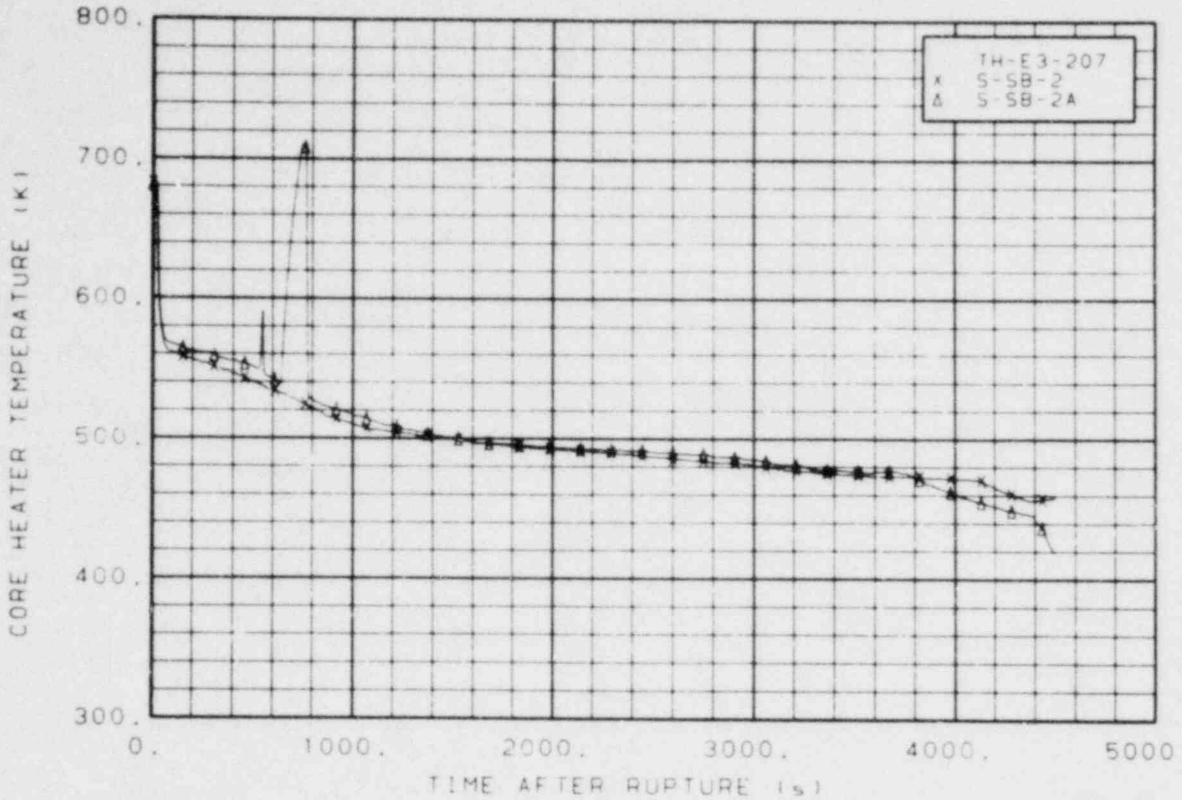

Figure 139. Core heater temperature, Rod E-3 (TH-E3-207), from 0 to 4500 s.

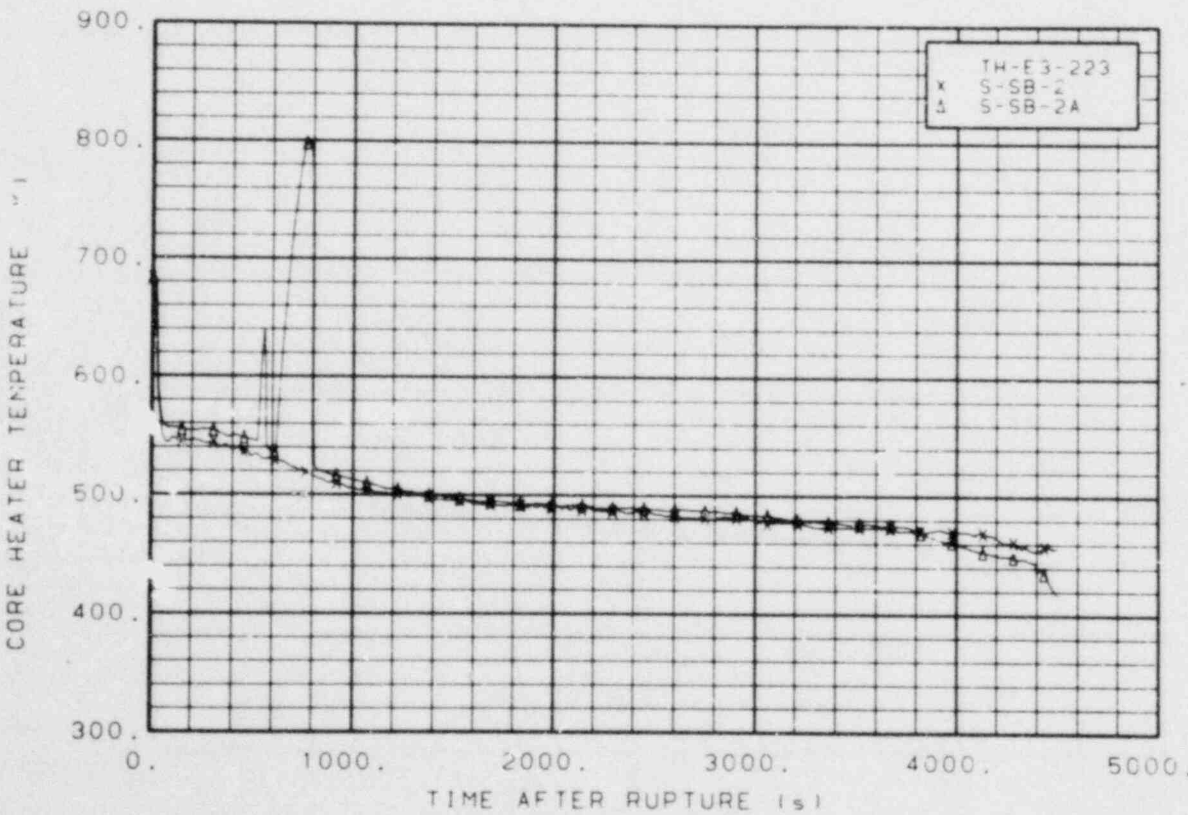

Figure 140. Core heater temperature, Rod E-3 (TH-E3-223), from 0 to 4500 s.

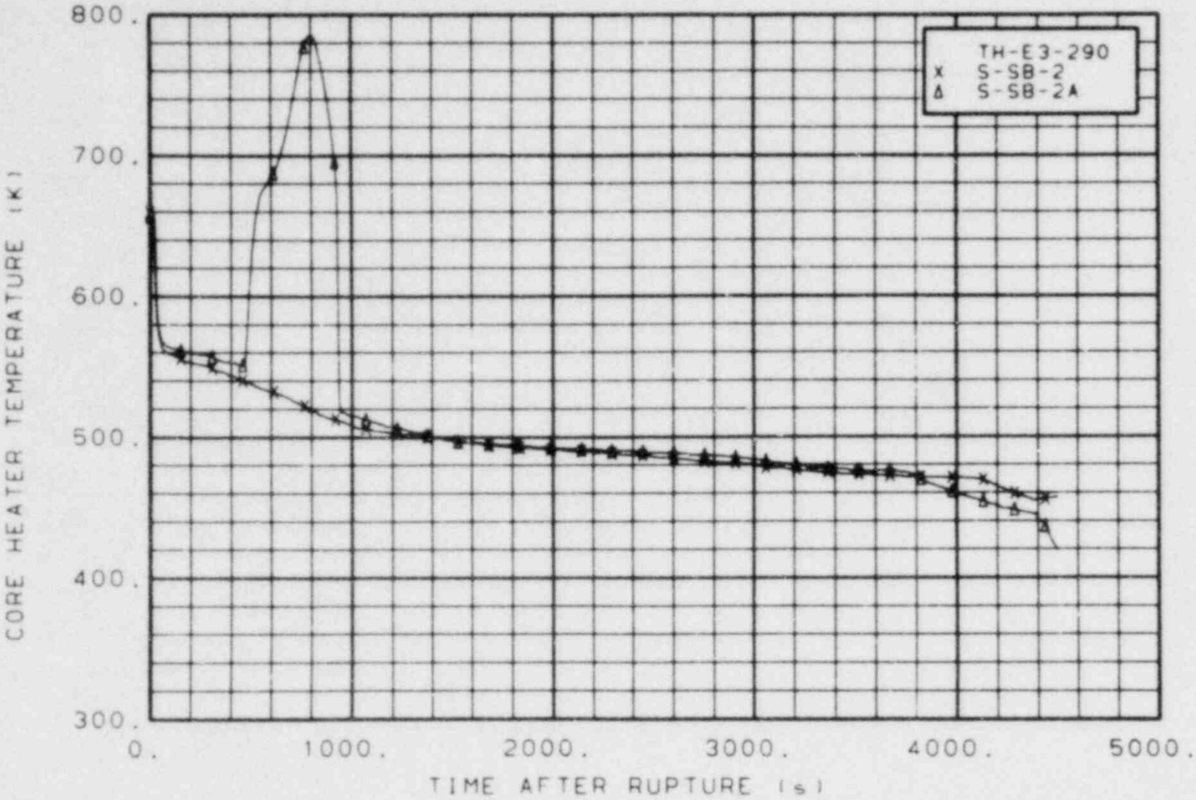

Figure 141. Core heater temperature, Rod E-3 (TH-E3-290), from 0 to 4500 s.

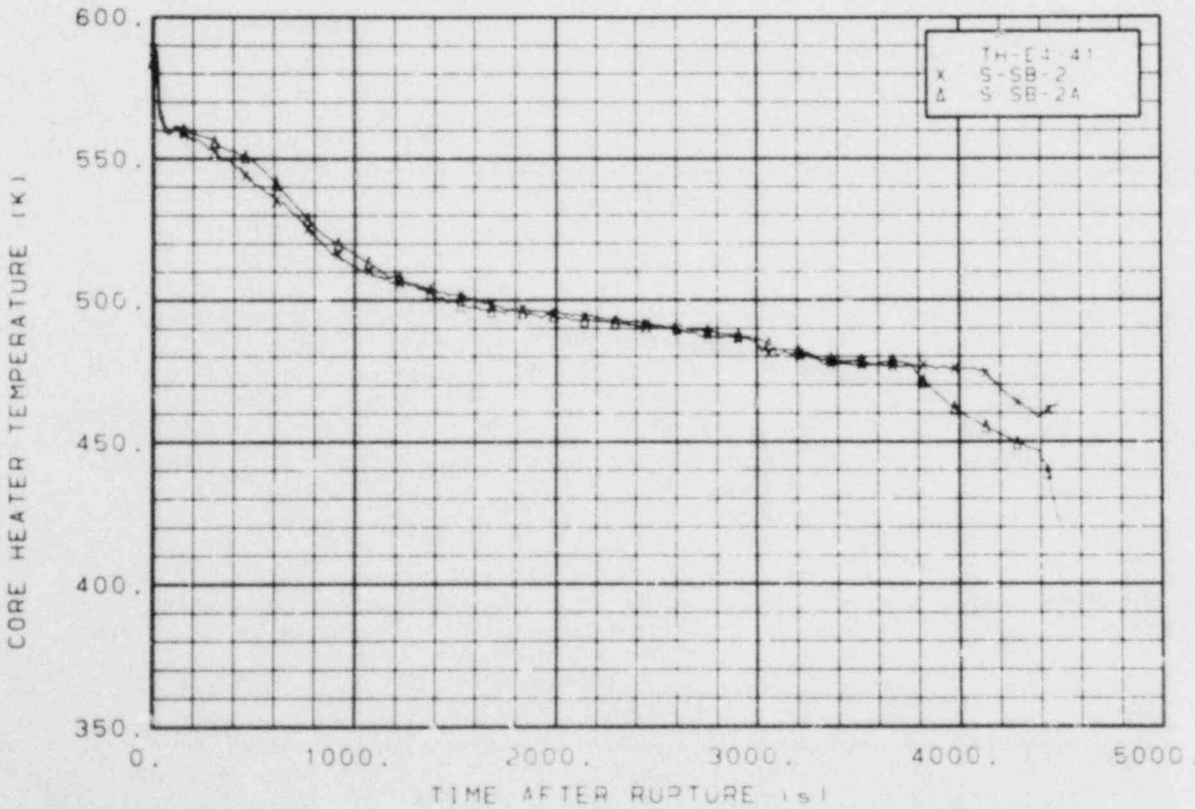

Figure 142. Core heater temperature, Rod E-4 (TH-E4-41), from 0 to 4500 s.

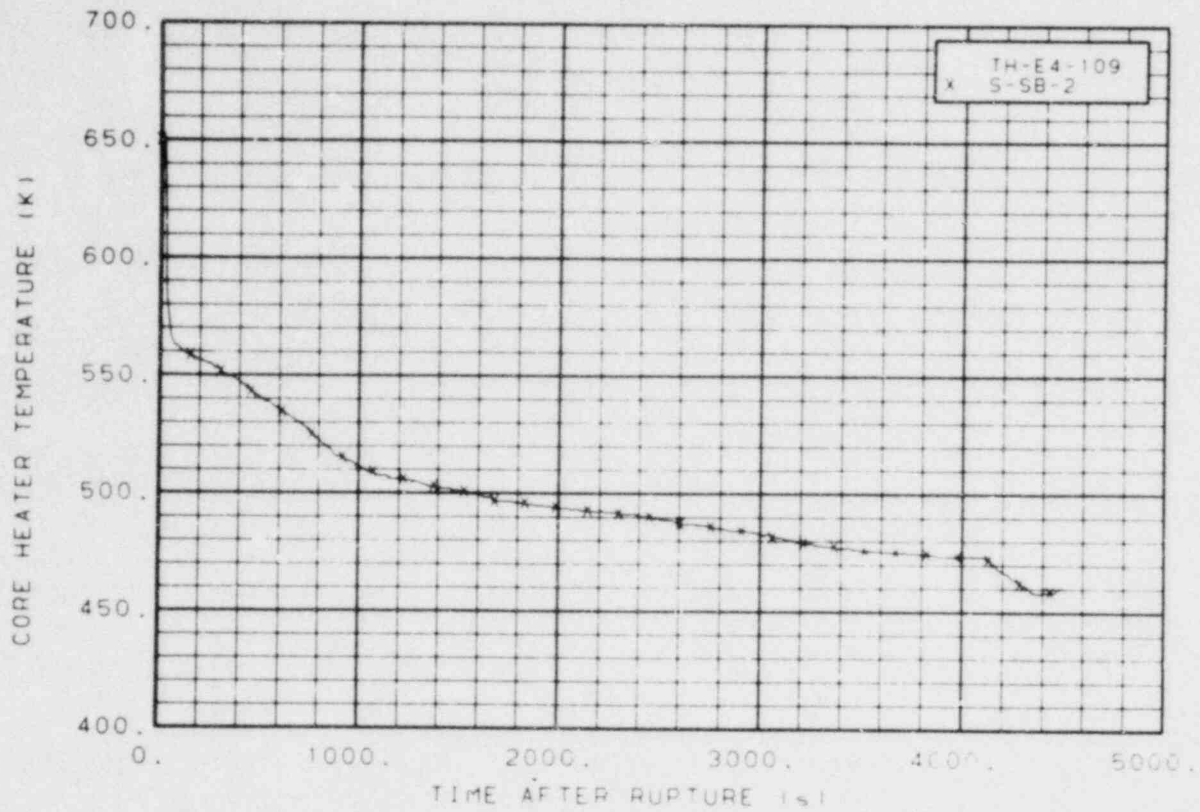

Figure 143. Core heater temperature, Test S-SB-2, Rod E-4 (TH-E4-109), from 0 to 4500 s.

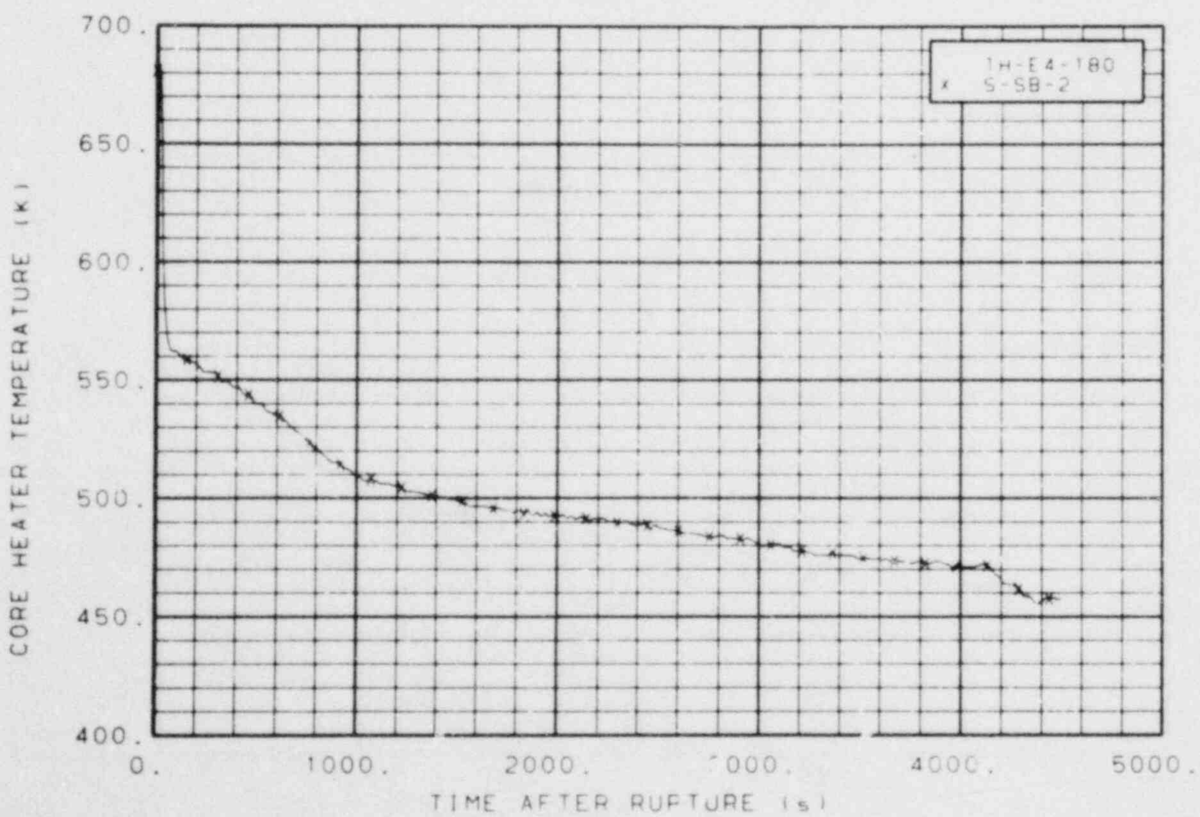

Figure 144. Core heater temperature, Test S-SB-2, Rod E-4 (TH-E4-180), from 0 to 4500 s.

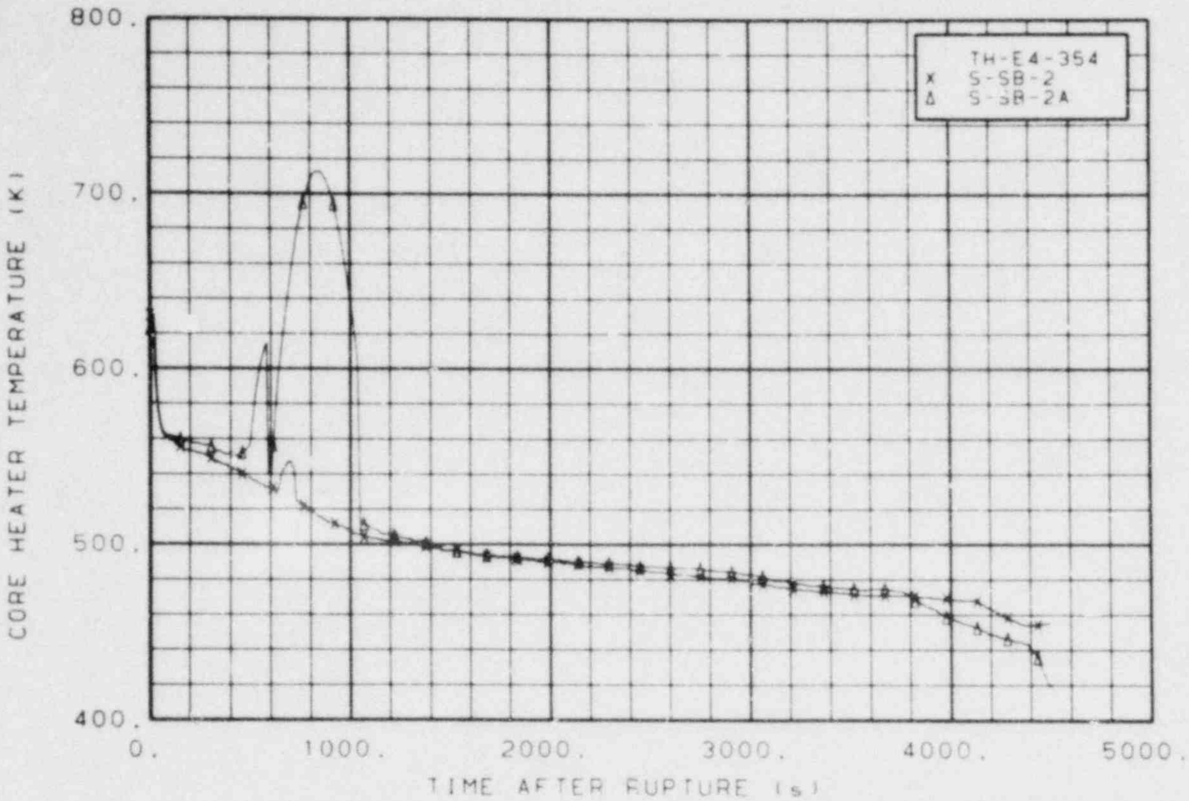

Figure 145. Core heater temperature, Rod E-4 (TH-E4-354), from 0 to 4500 s.

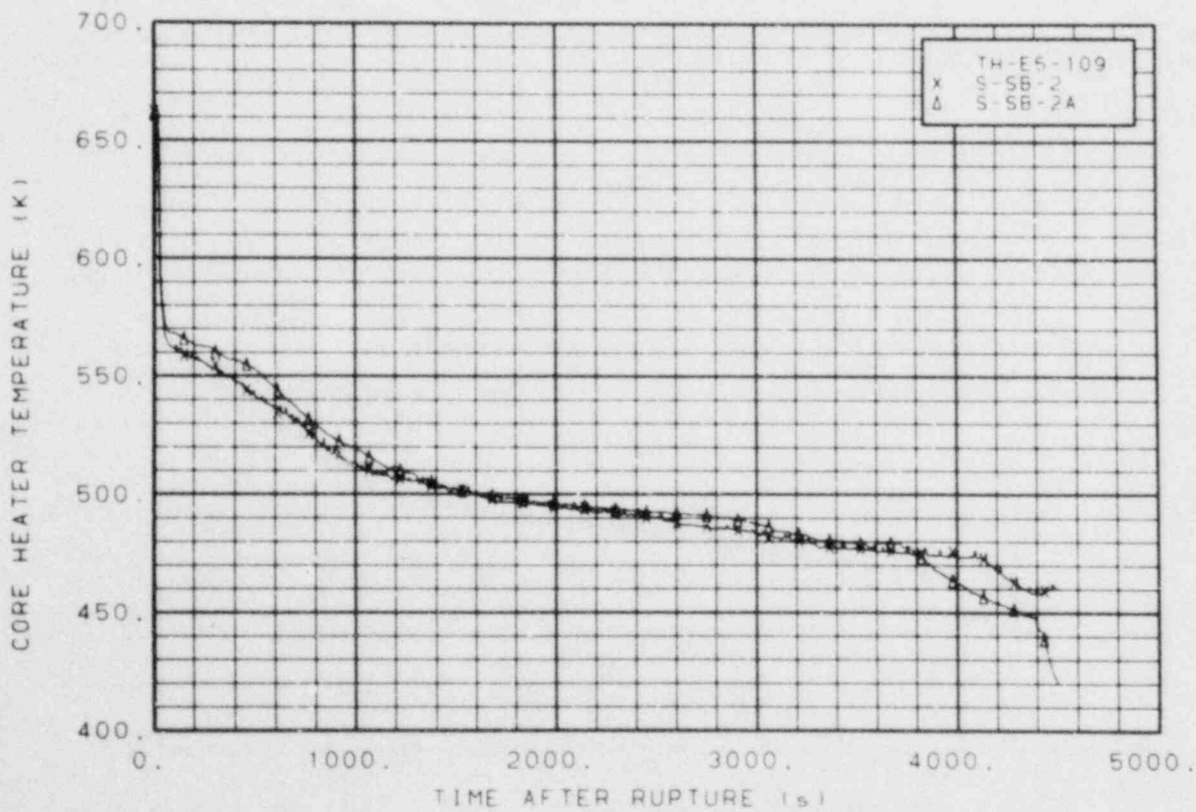

Figure 146. Core heater temperature, Rod E-5 (TH-E5-109), from 0 to 4500 s.

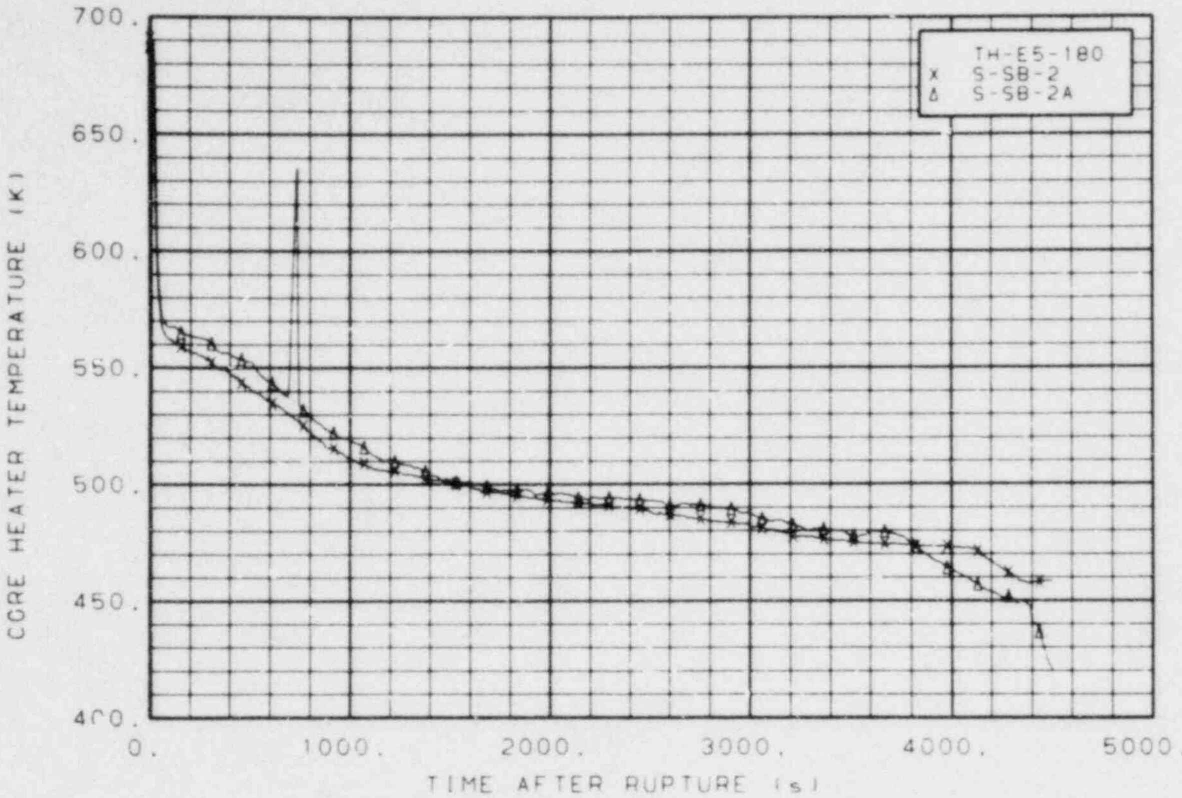

Figure 147. Core heater temperature, Rod E-5 (TH-E5-180), from 0 to 4500 s.

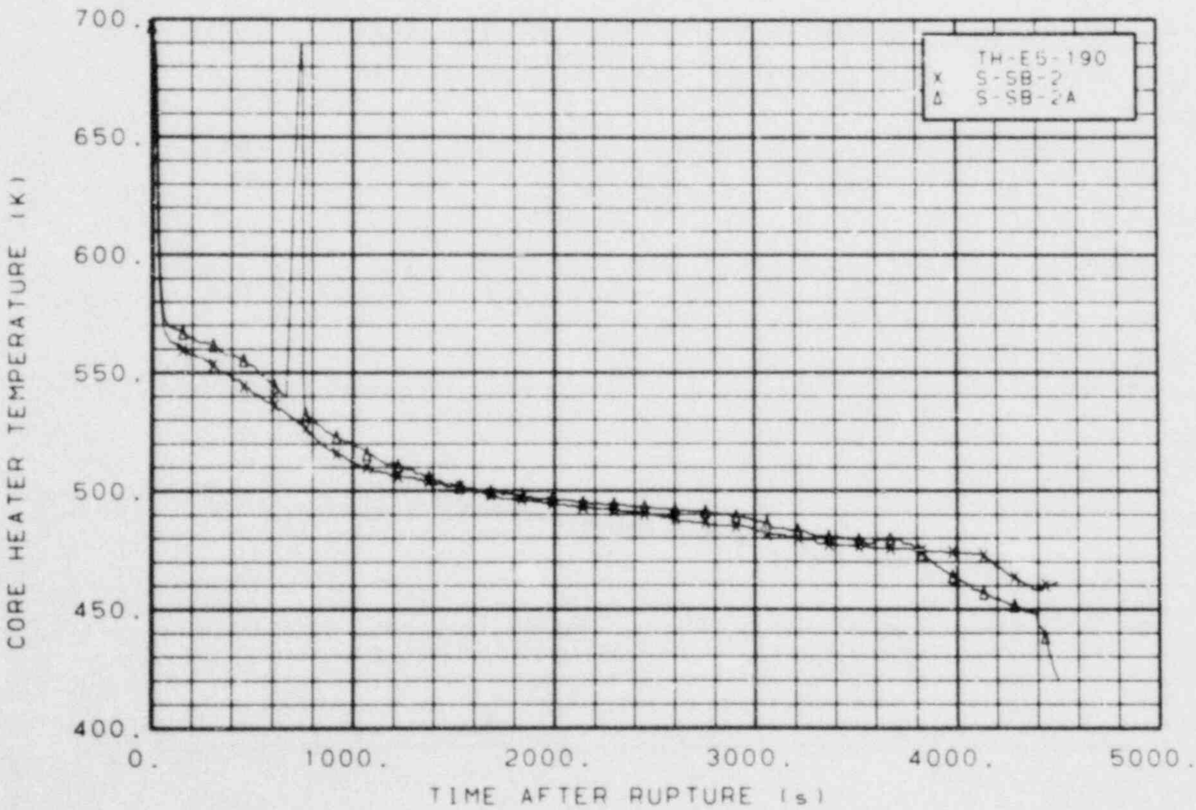

Figure 148. Core heater temperature, Rod E-5 (TH-E5-190), from 0 to 4500 s.

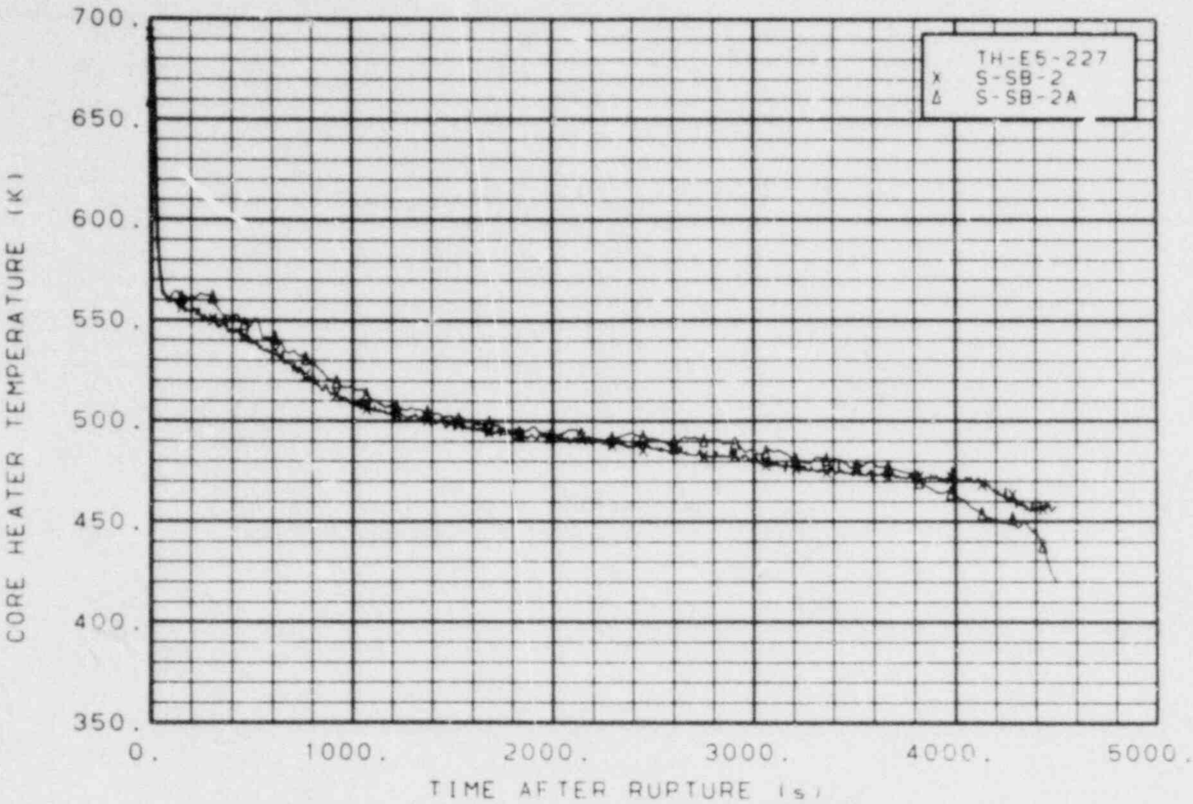

Figure 149. Core heater temperature, Rod E-5 (TH-E5-227), from 0 to 4500 s.

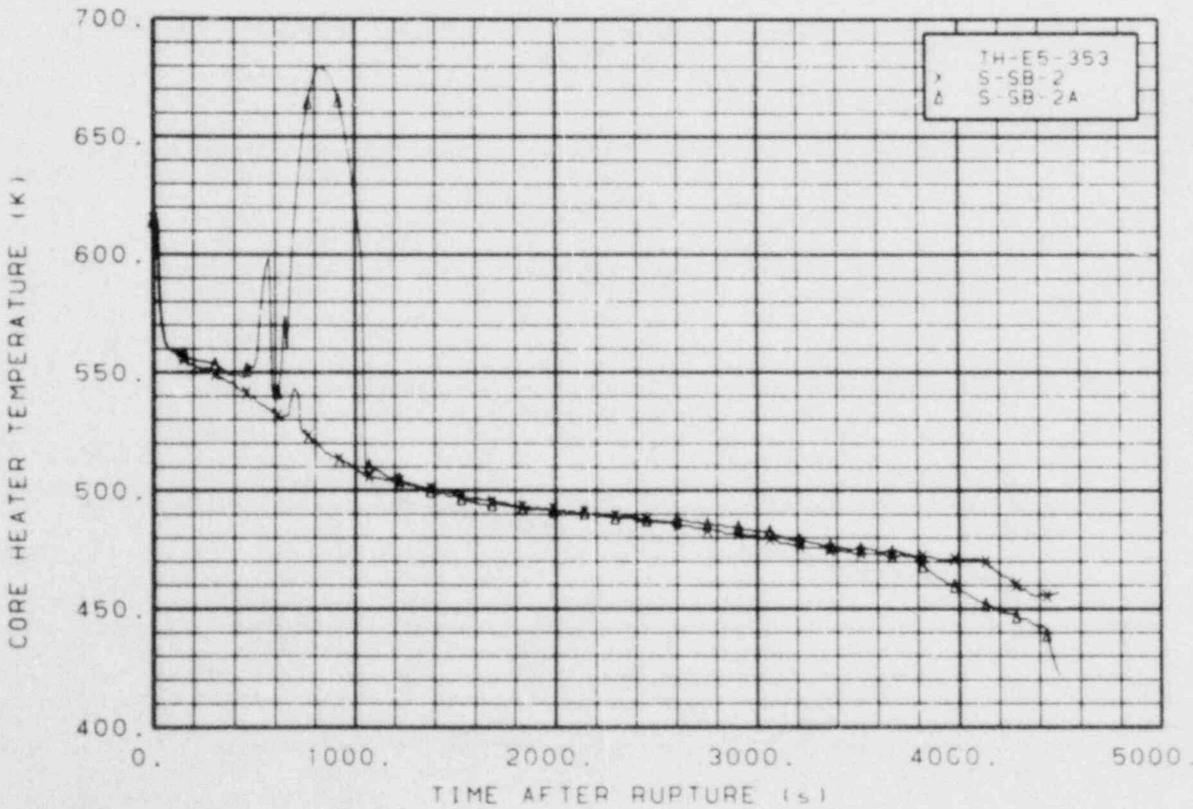

Figure 150. Core heater temperature, Rod E-5 (TH-E5-353), from 0 to 4500 s.

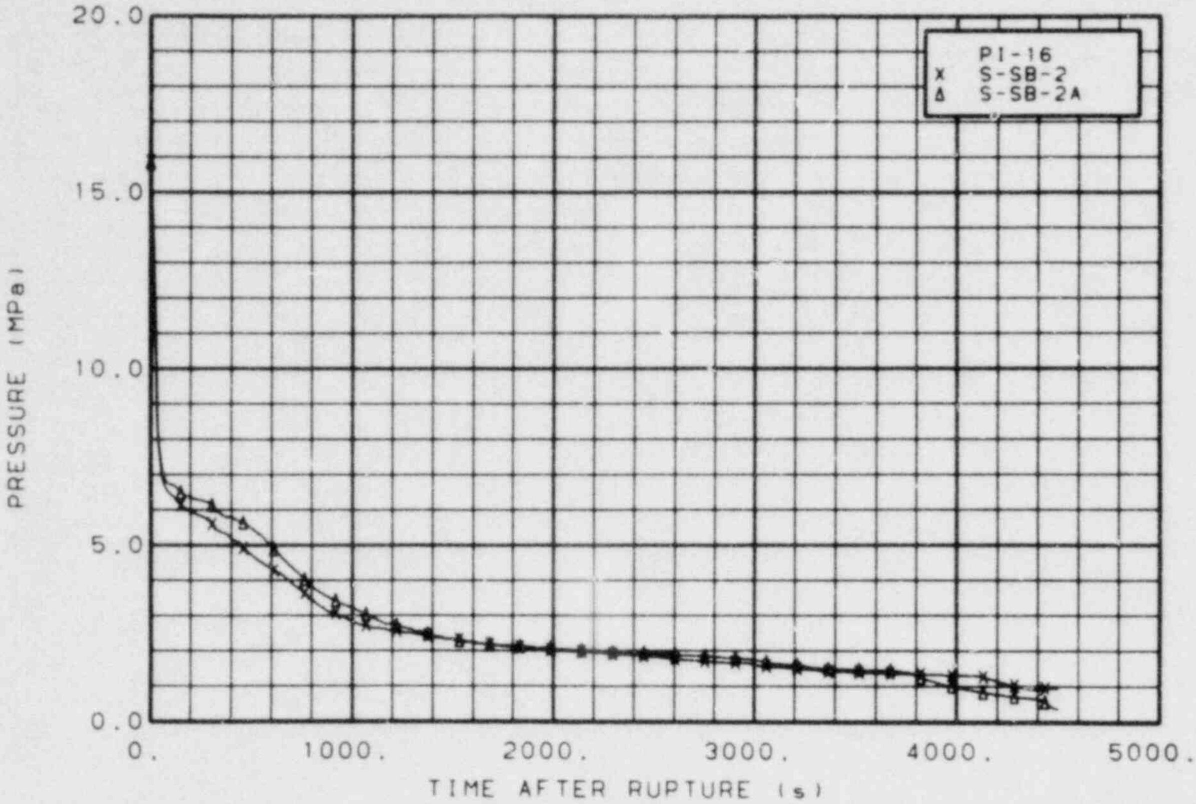

Figure 151. Pressure in intact loop cold leg (PI-16), from 0 to 4500 s.

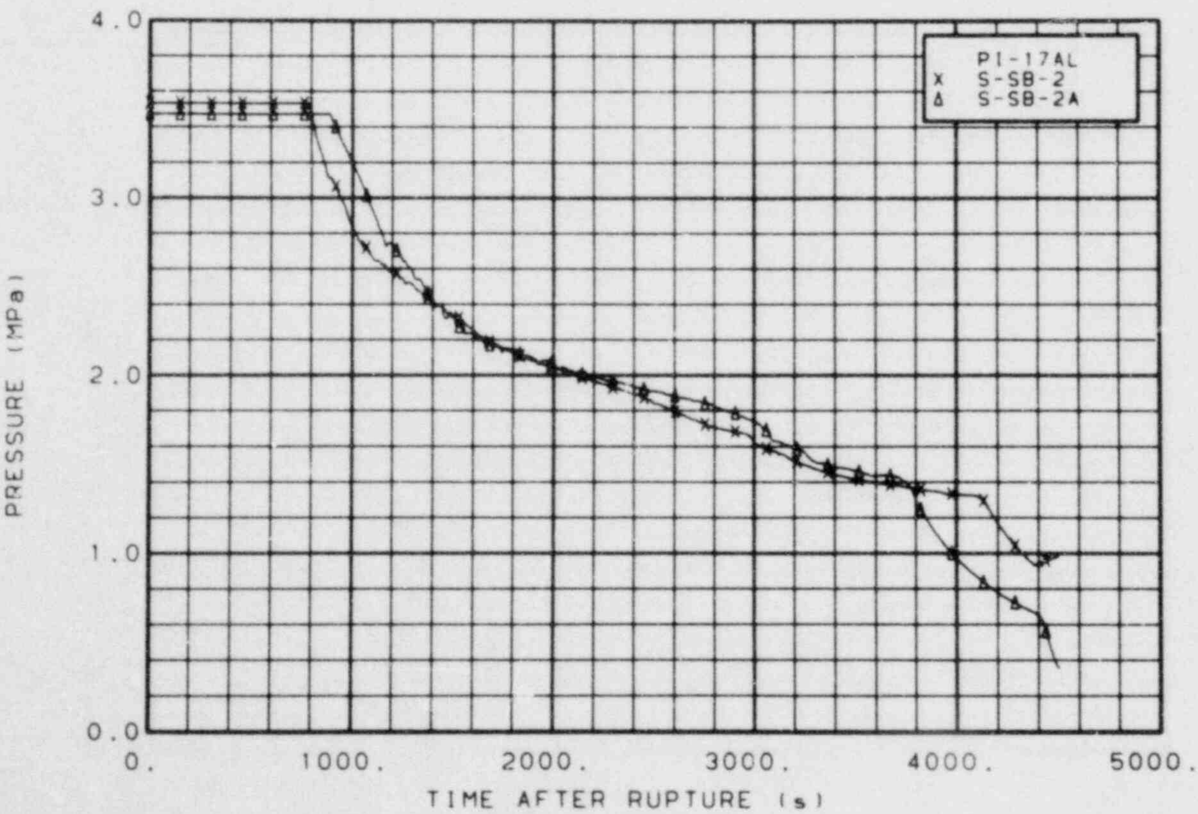

Figure 152. Pressure in intact loop cold leg (PI-17AL), from 0 to 4500 s.

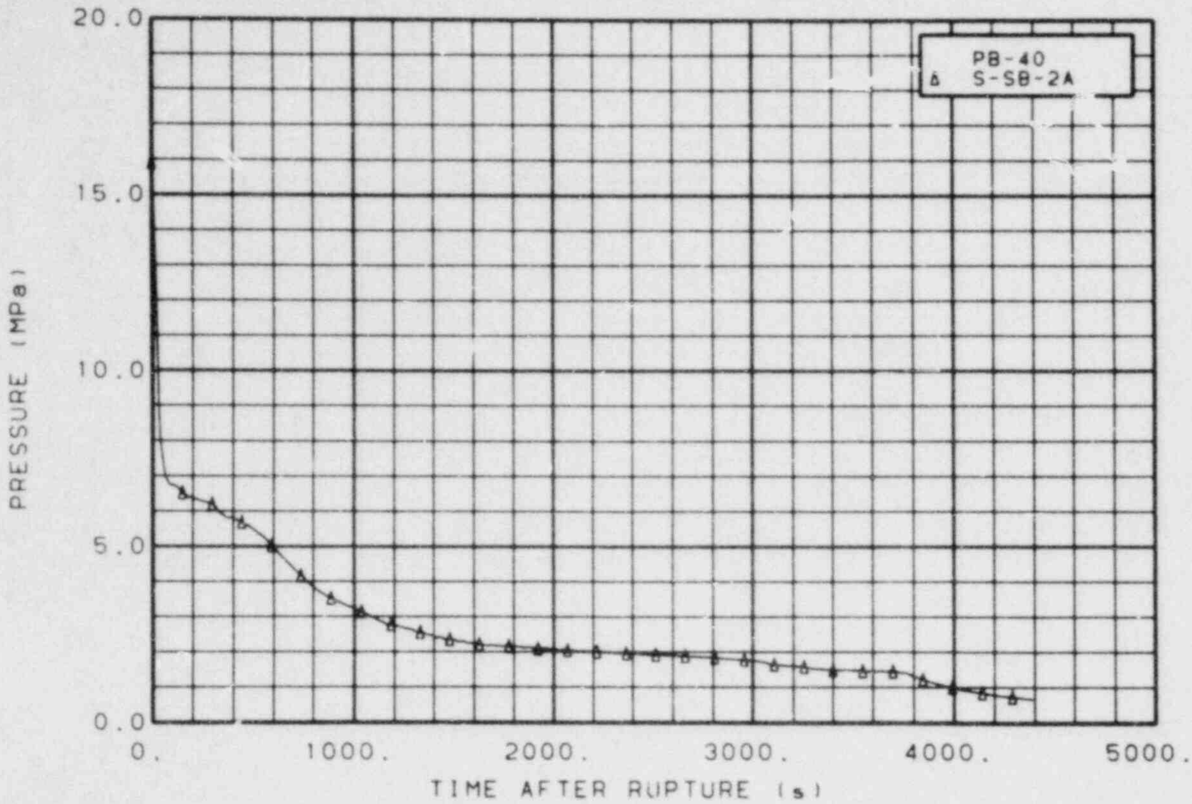

Figure 153. Pressure in broken loop cold leg, Test S-SB-2A (PB-40), from 0 to 4390 s.

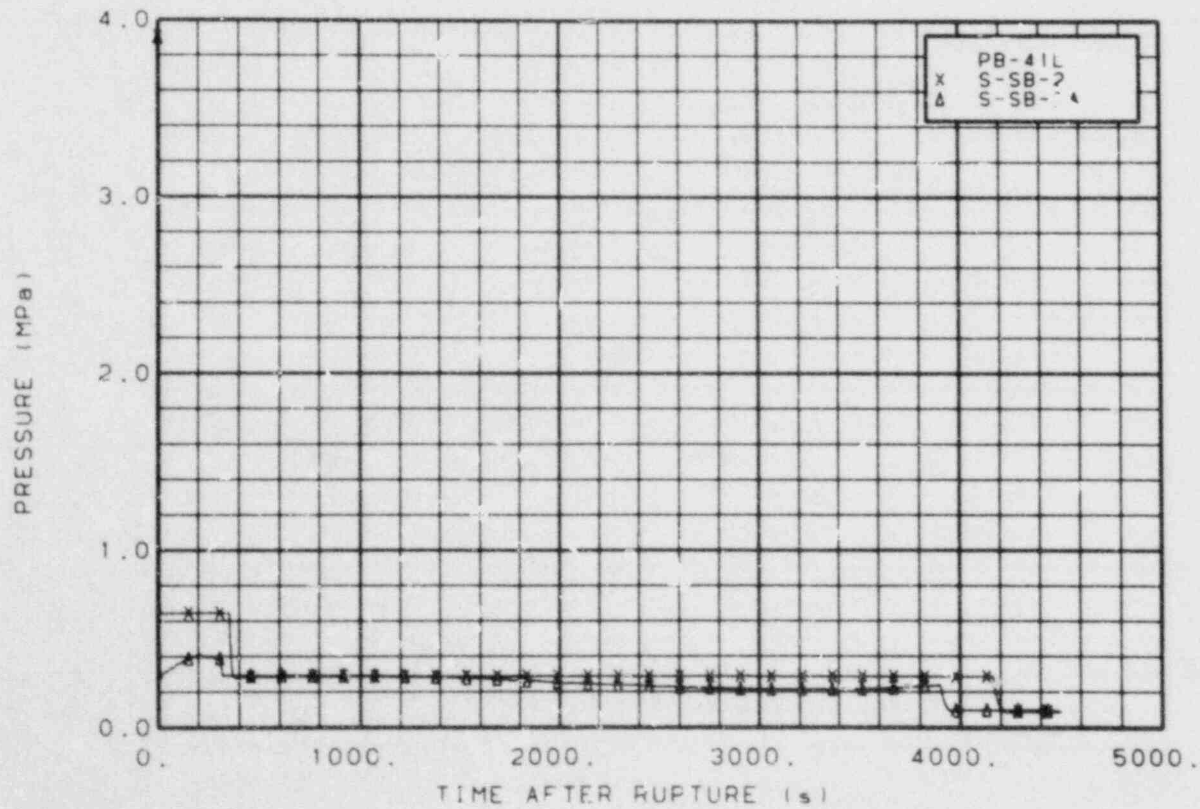

Figure 154. Pressure in broken loop cold leg (PB-41L), from 0 to 4500 s.

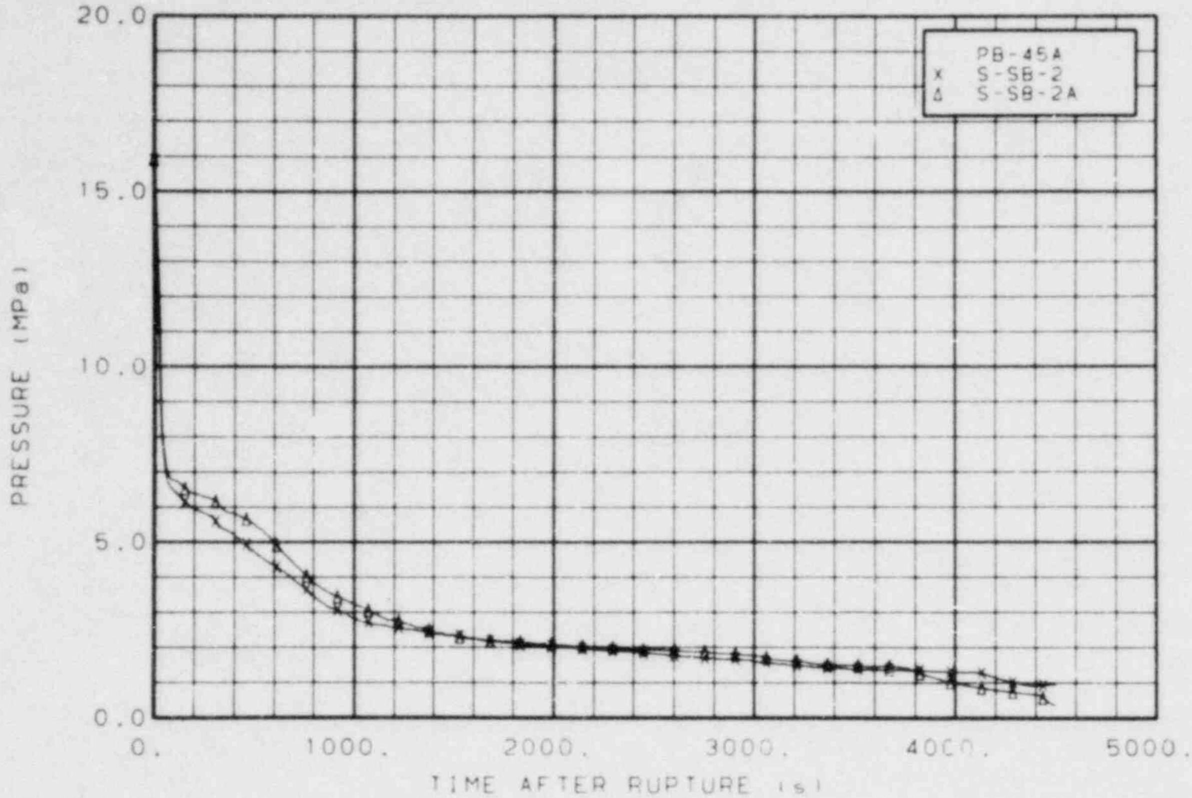

Figure 155. Pressure in broken loop cold leg (PB-45A), from 0 to 4500 s.

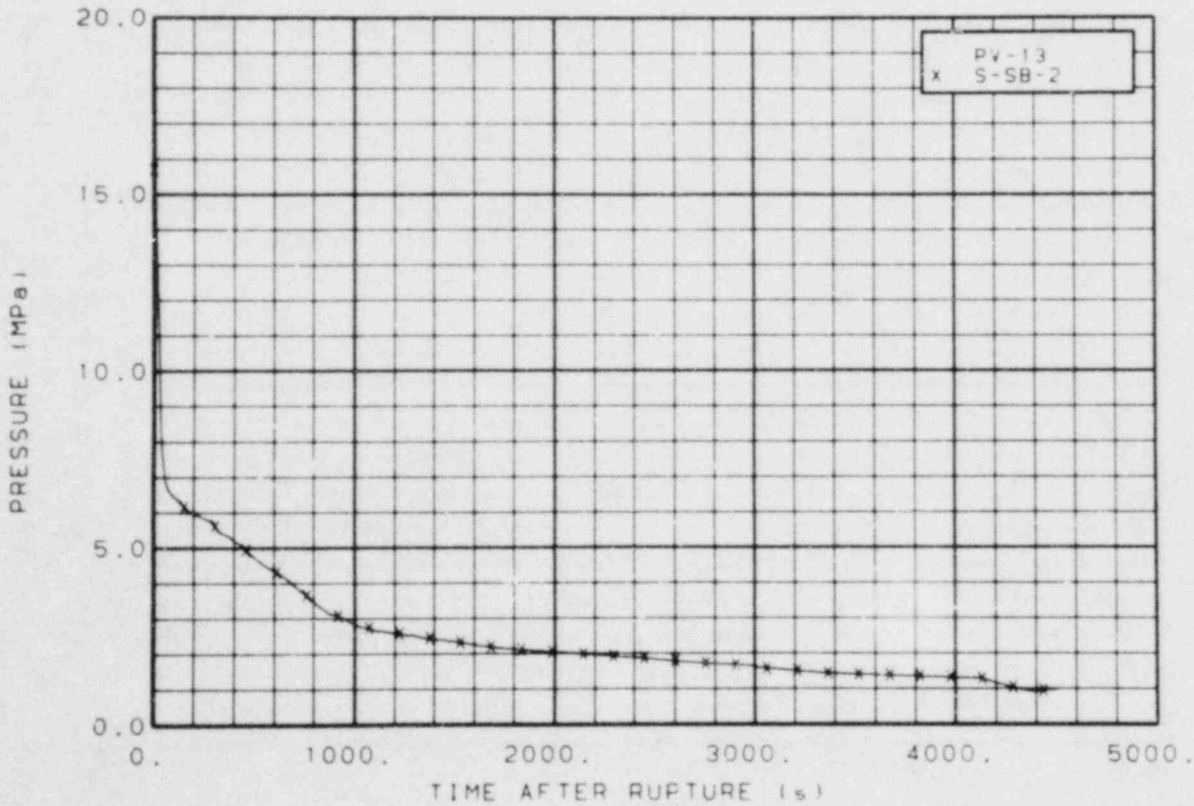

Fi;ure 156. Pressure in vessel upper plenum, Test S-SB-2 (PV-13), from 0 to 4500 s.

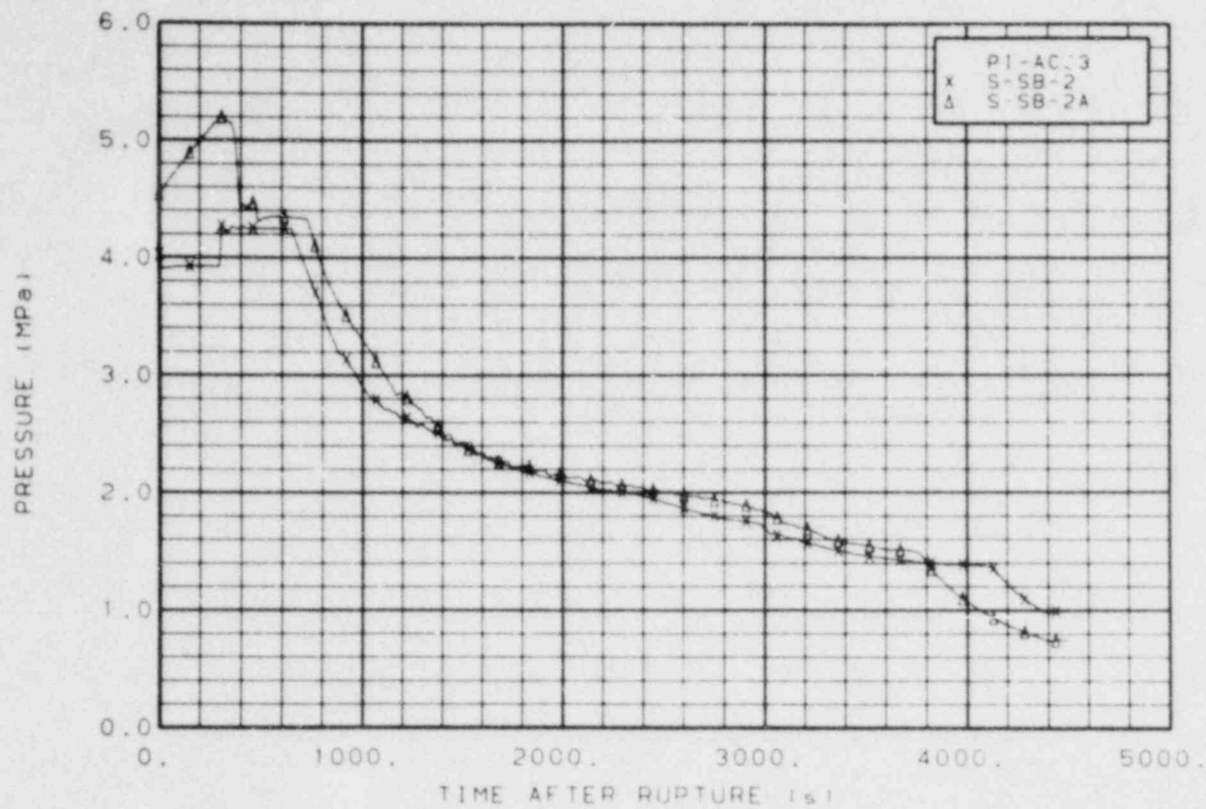

Figure 157. Pressure in intact loop ECC injection accumulator (PI-ACC3), from 0 to 4500 s.

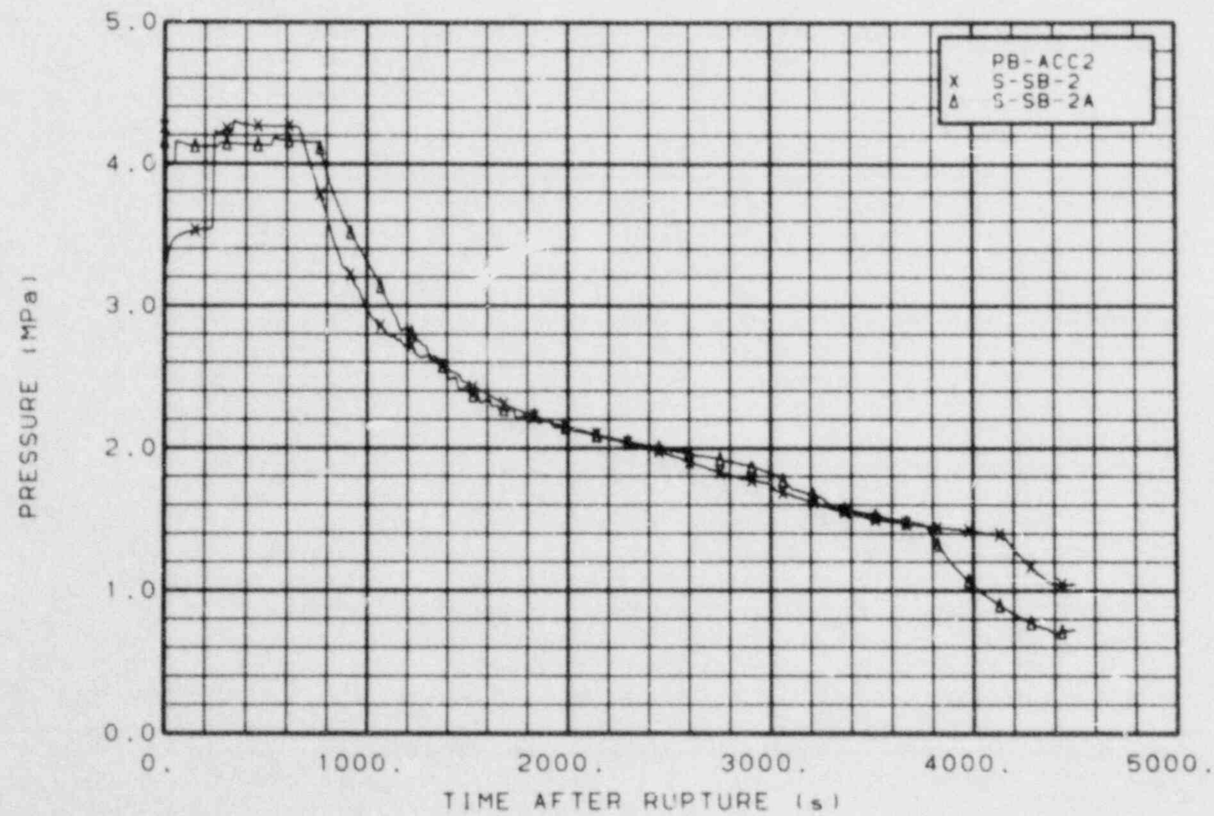

Figure 158. Pressure in broken loop ECC injection accumulator (PB-ACC2), from 0 to 4500 s.

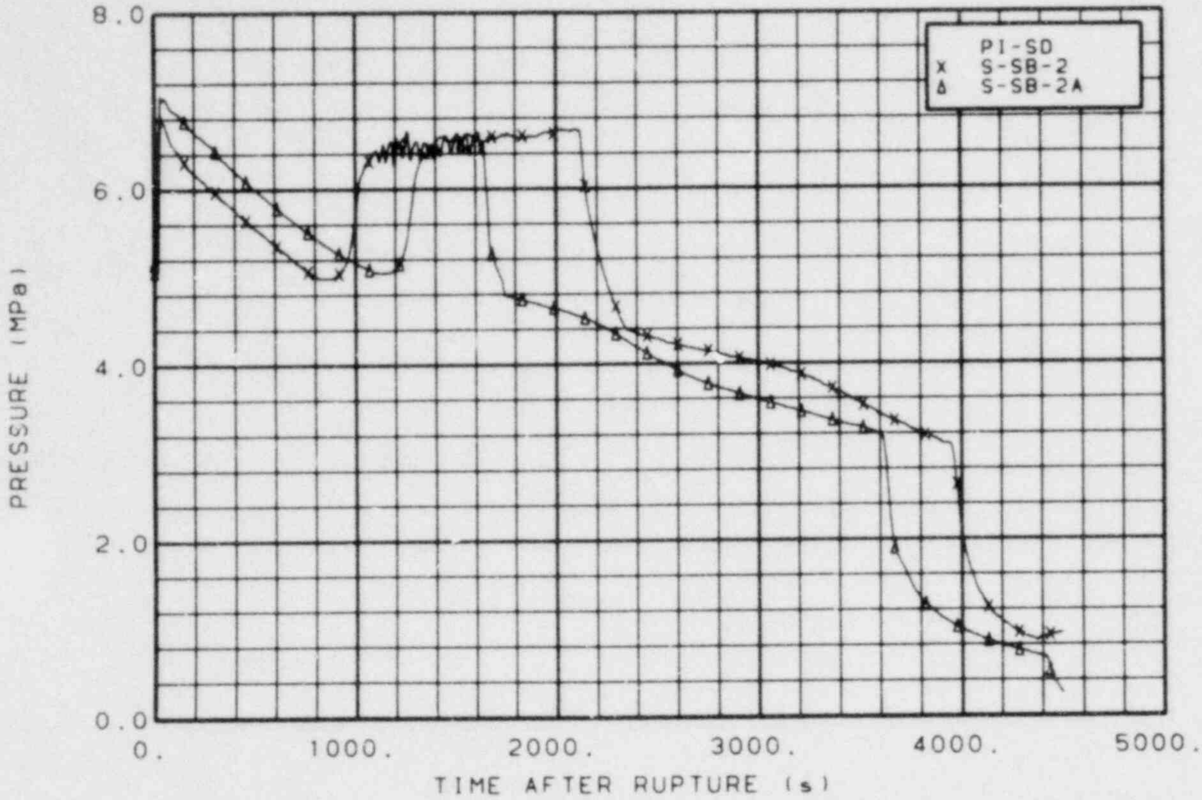

Figure 159. Pressure in intact loop steam generator, secondary side steam dome (PI-SD), from 0 to 4500 s.

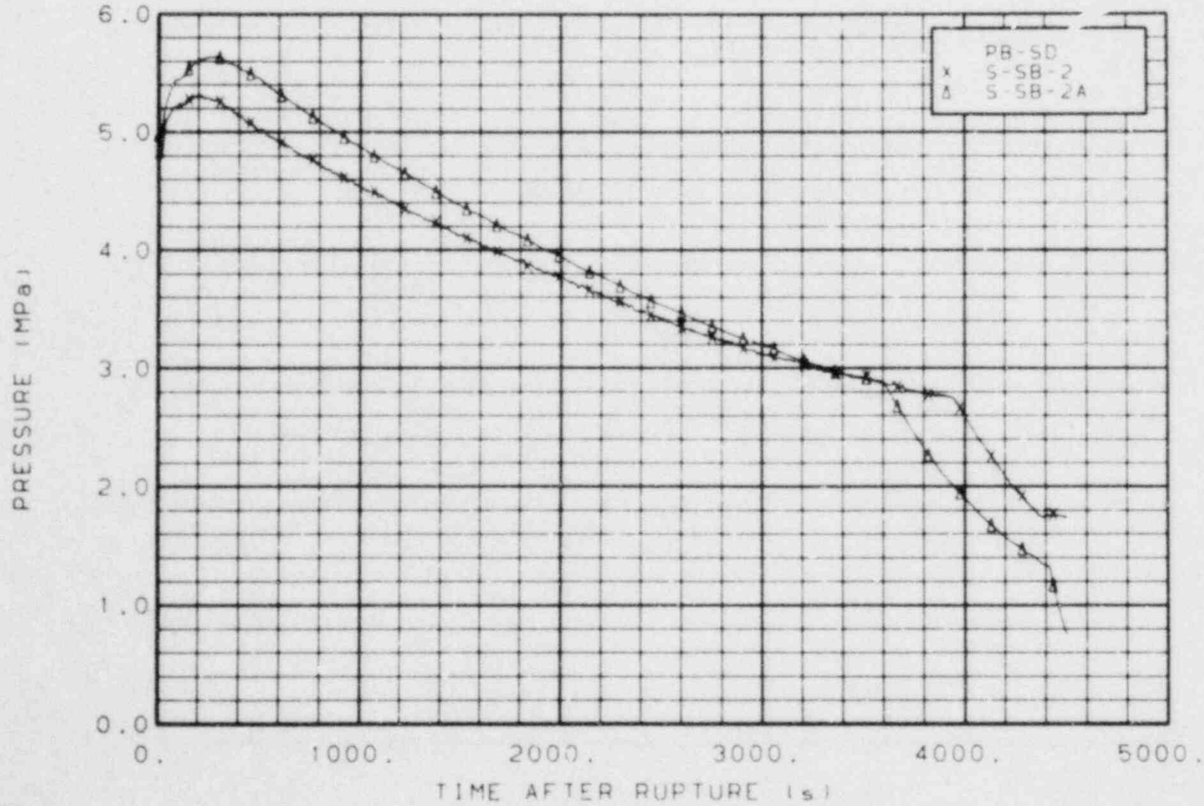

Figure 160. Pressure in broken loop steam generator, secondary side steam dome (PB-SD), from 0 to 4500 s.

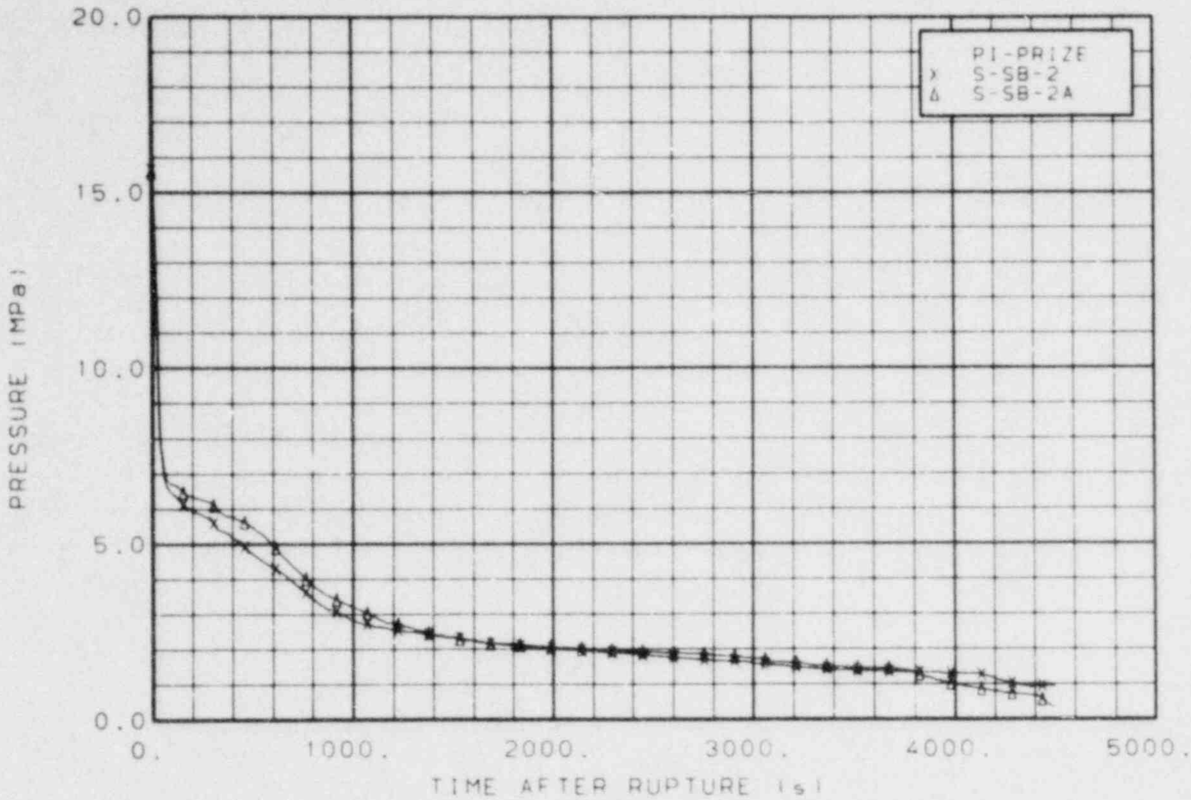

Figure 161. Pressure in pressurized steam dome (PI-PRIZE), from 0 to 4500 s.

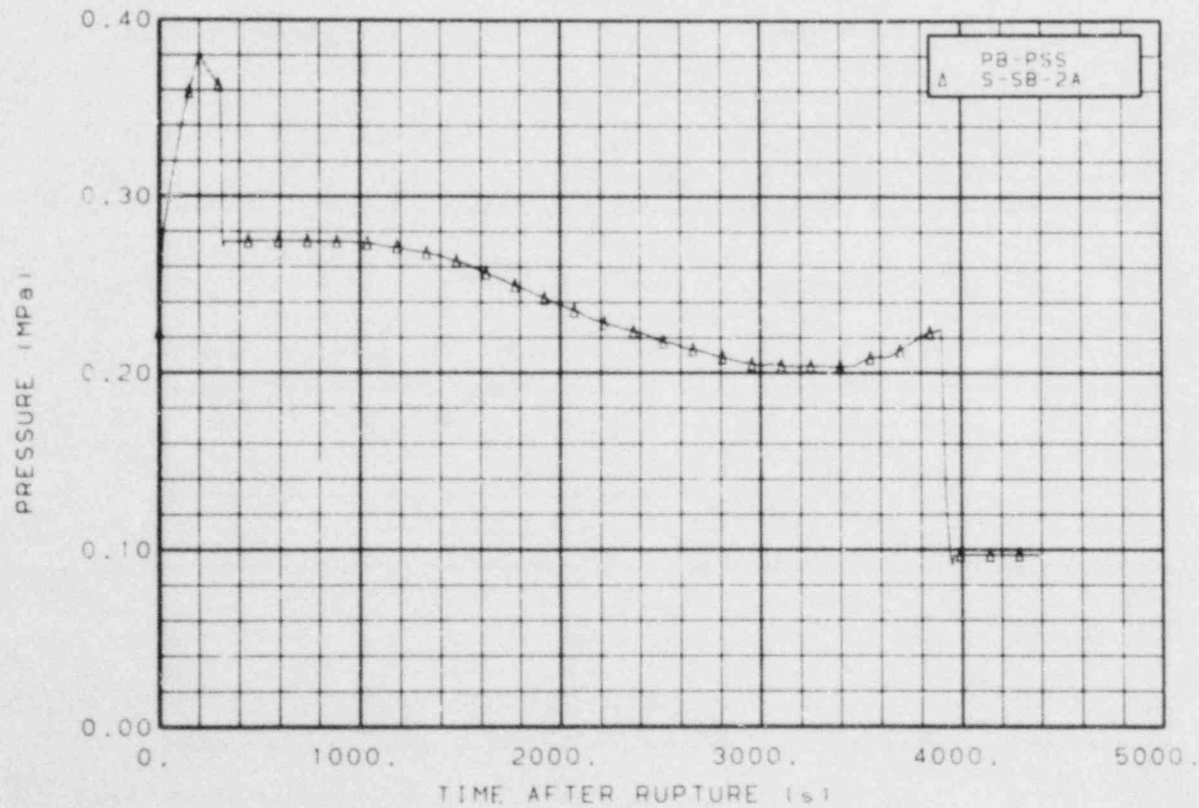

Figure 162. Pressure in broken loop pressure suppression tank, Test S-SB-2A (PB-PSS), from 0 to 4390 s.

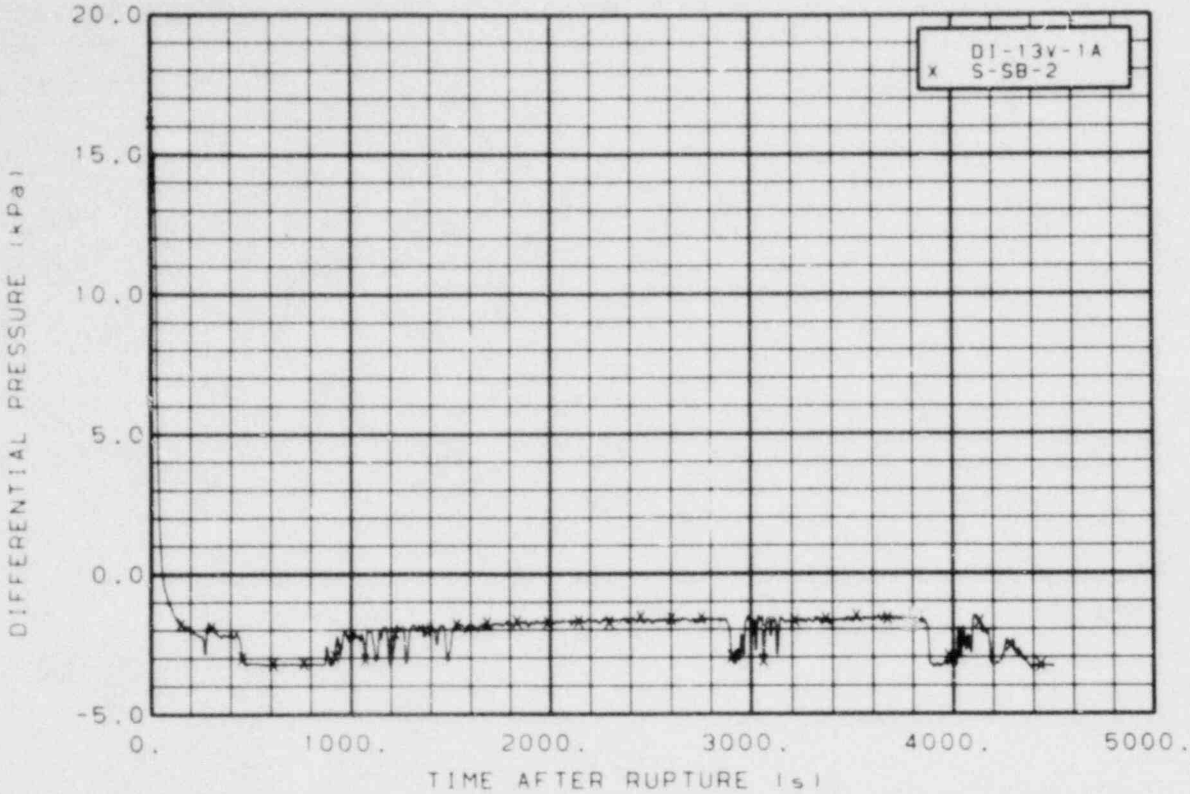

Figure 163. Differential pressure in intact loop, Test S-SB-2 (DI-13V-1A), from 0 to 4500 s.

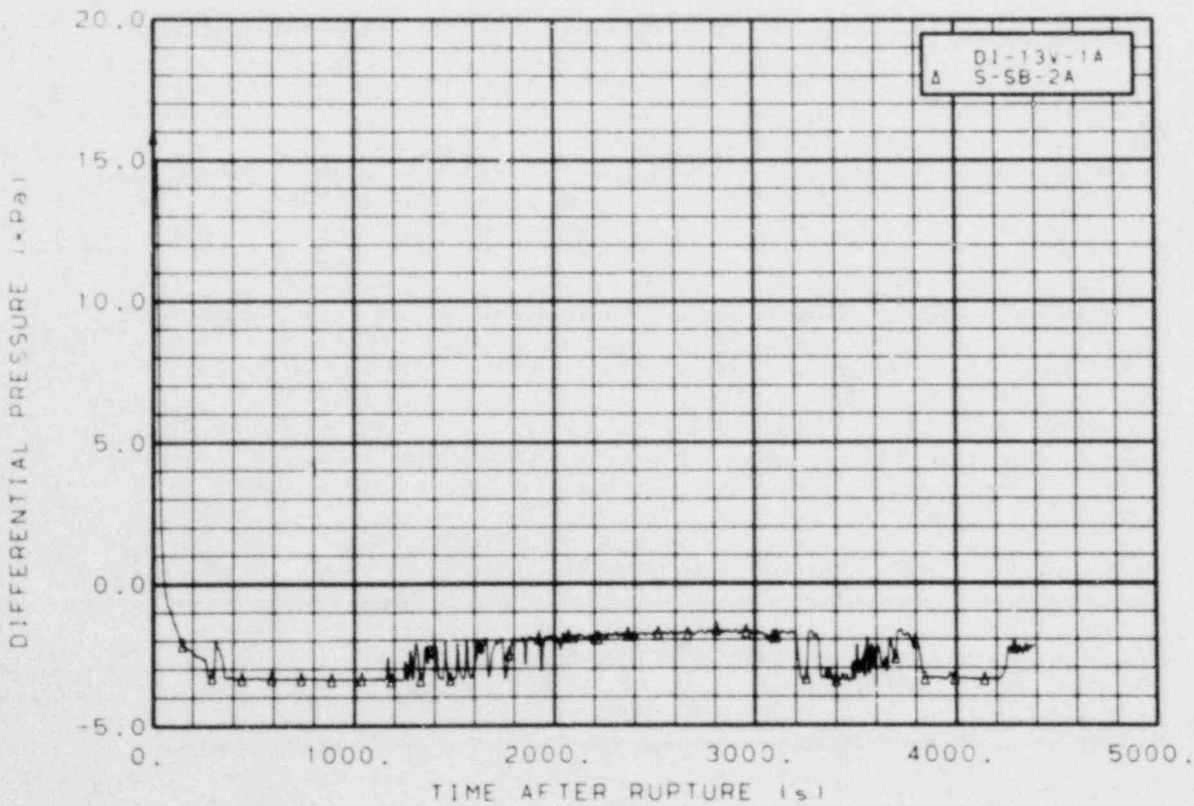

Figure 164. Differential pressure in intact loop, Test S-SB-2A (DI-13V-1A), from 0 to 4390 s.

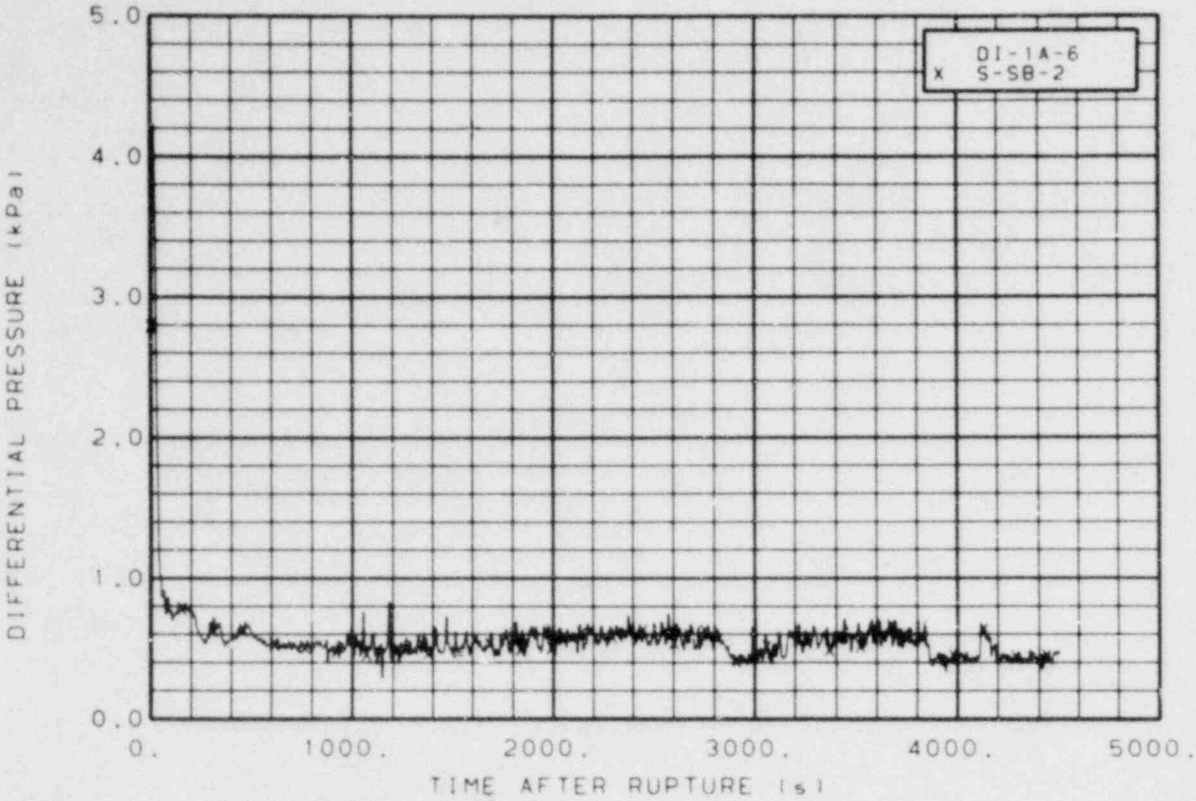

Figure 165. Differential pressure in intact loop, Test S-SB-2 (DI-1A-6), from 0 to 4500 s.

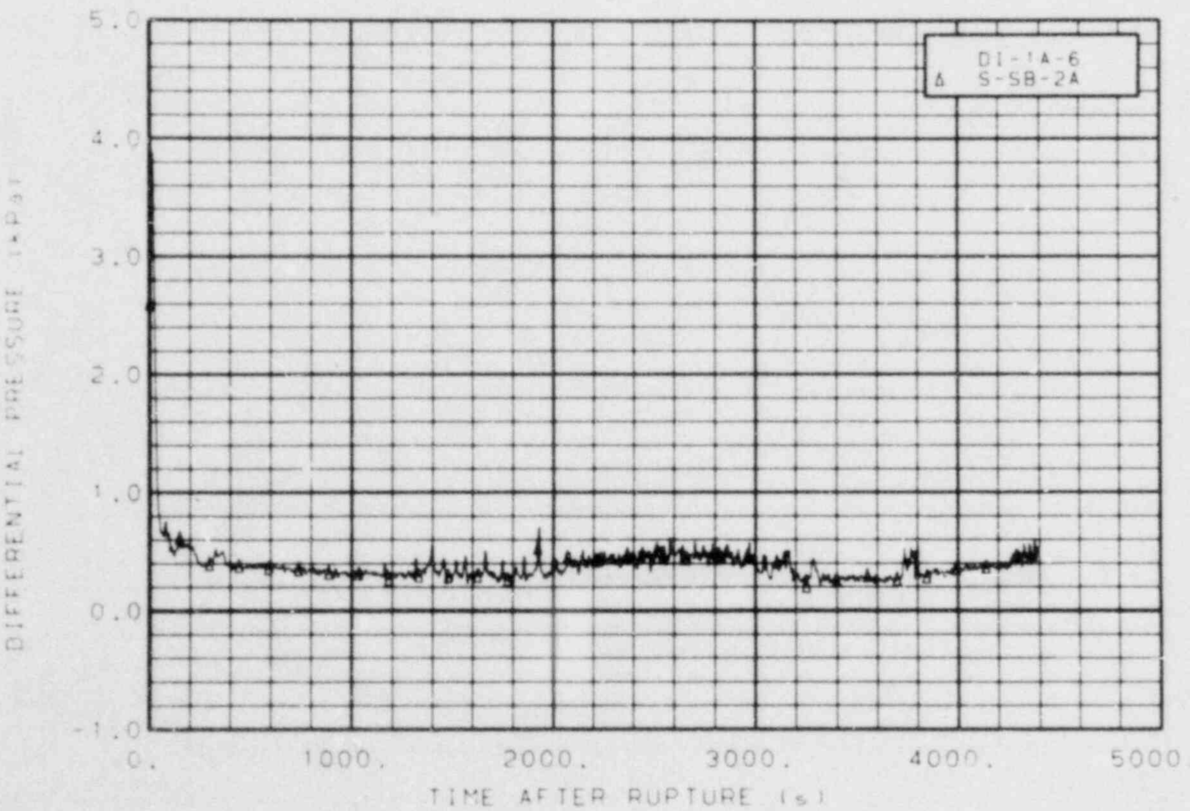

Figure 166. Differential pressure in intact loop, Test S-SB-2A (DI-1A-6), from 0 to 4390 s.

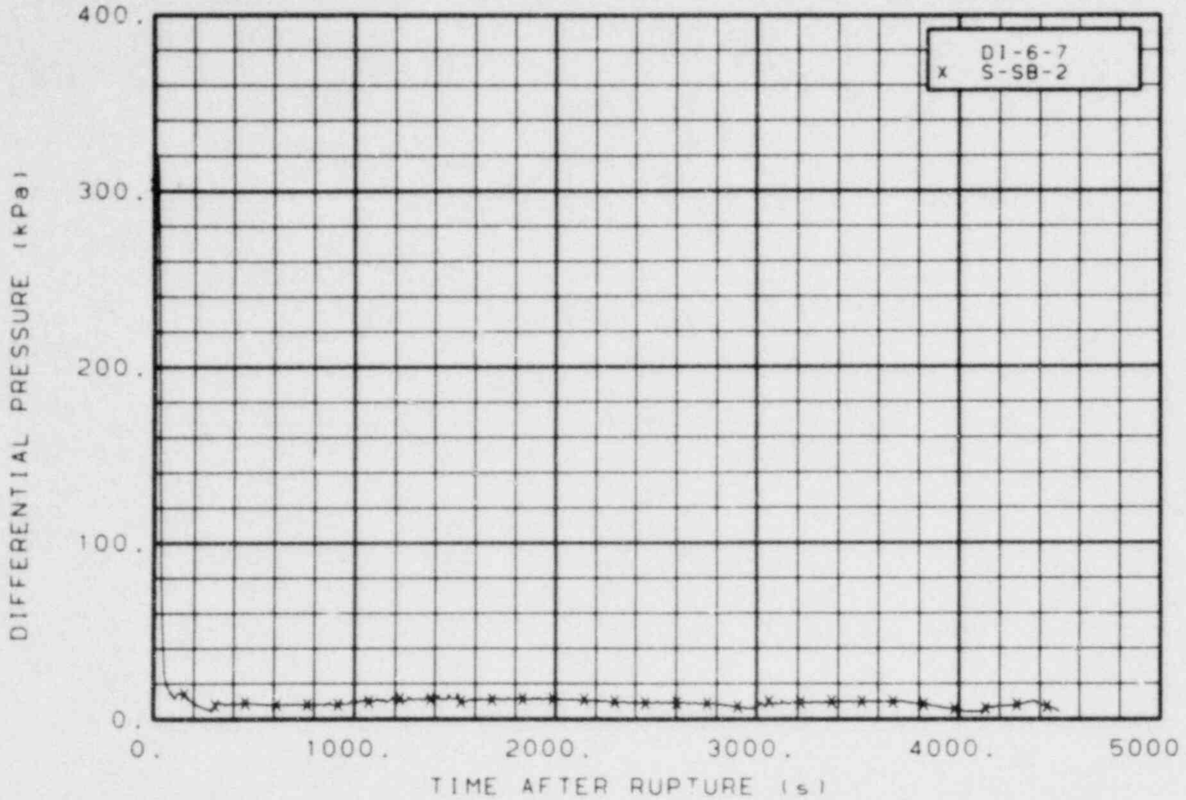

Figure 167. Differential pressure in intact loop, Test S-SB-2 (DI-6-7), from 0 to 4500 s.

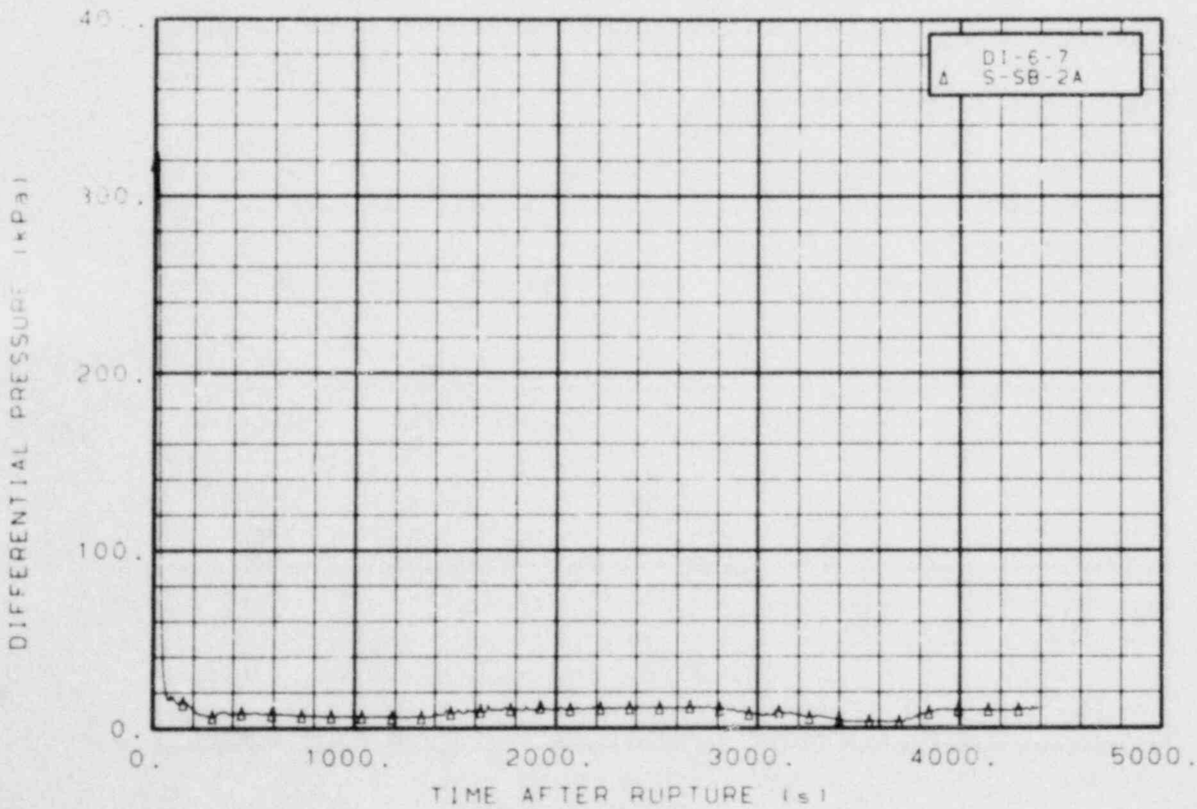

Figure 168. Differential pressure in intact loop, Test S-SB-2A (DI-6-7), from 0 to 4390 s.

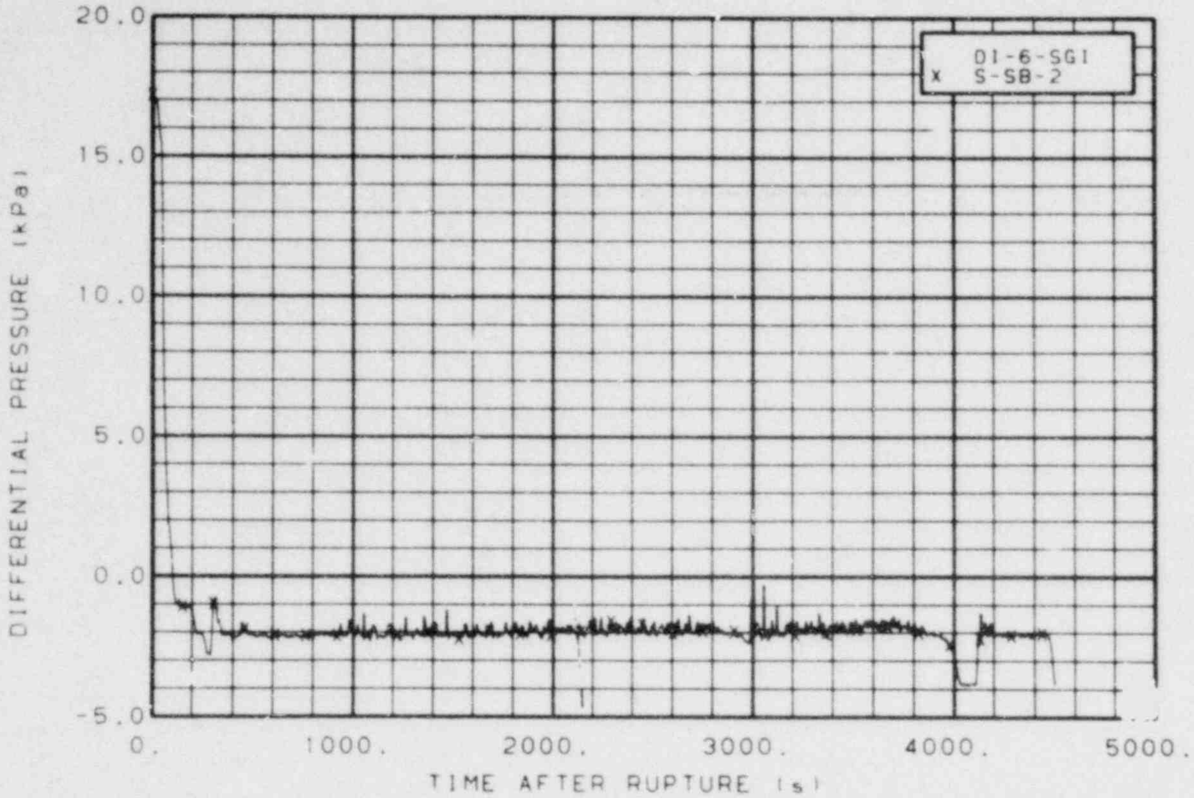

Figure 169. Differential pressure in intact loop, Test S-SB-2 (DI-6-SGI), from 0 to 4500 s.

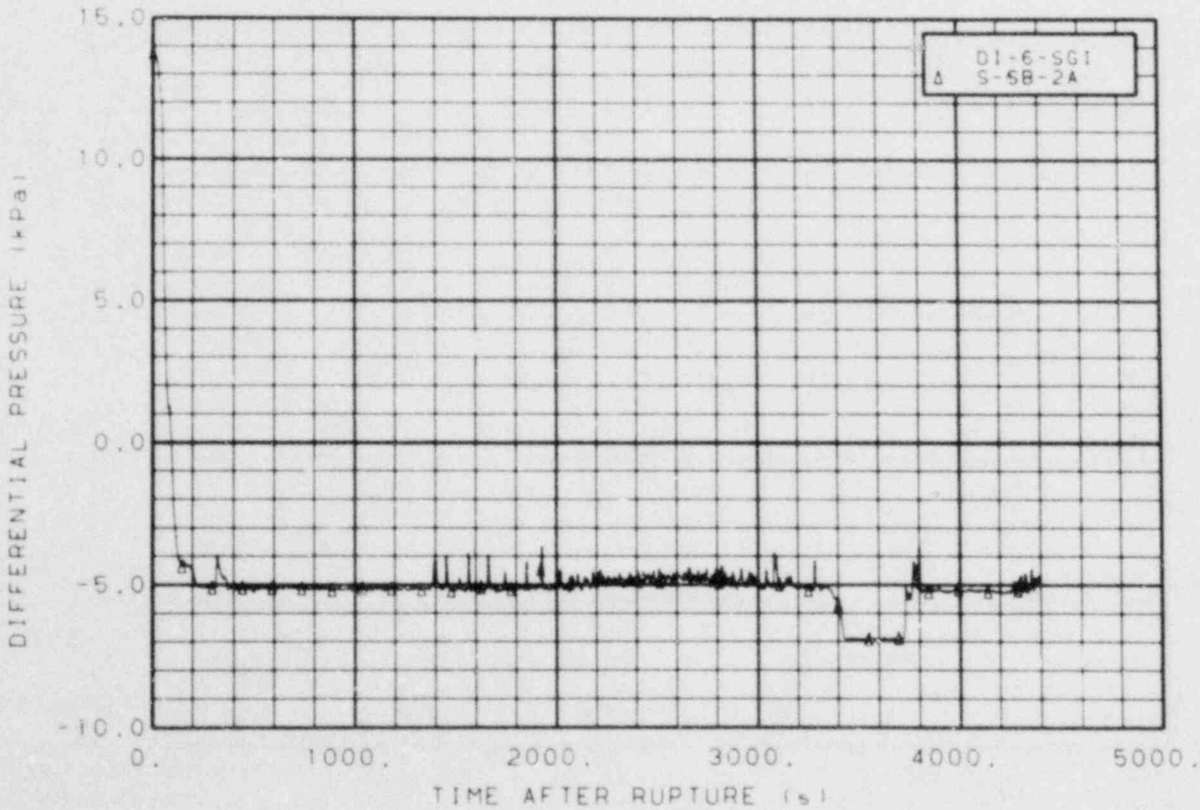

Figure 170. Differential pressure in intact loop, Test S-SB-2A (DI-6-SGI), from 0 to 4390 s.

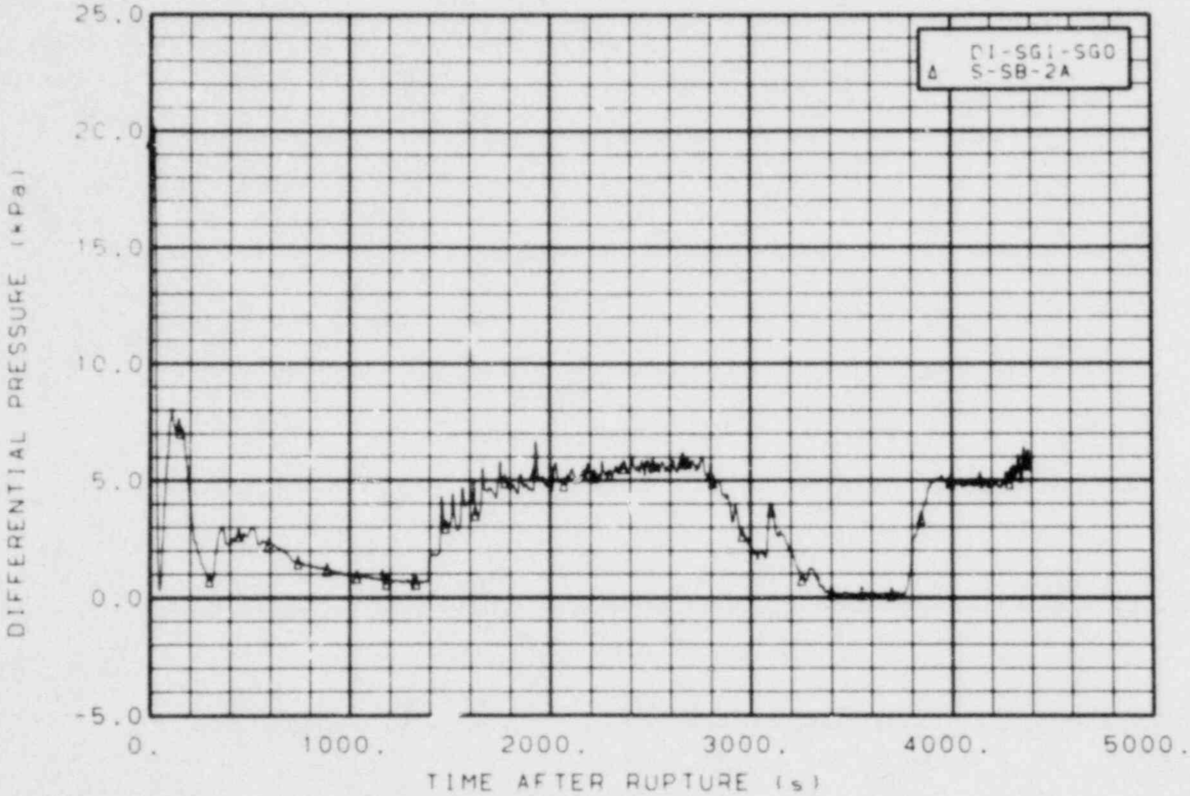

Figure 171. Differnetial pressure in intact loop, Test S-SB-2A (DI-SGI-SGO), from 0 to 4390 s.

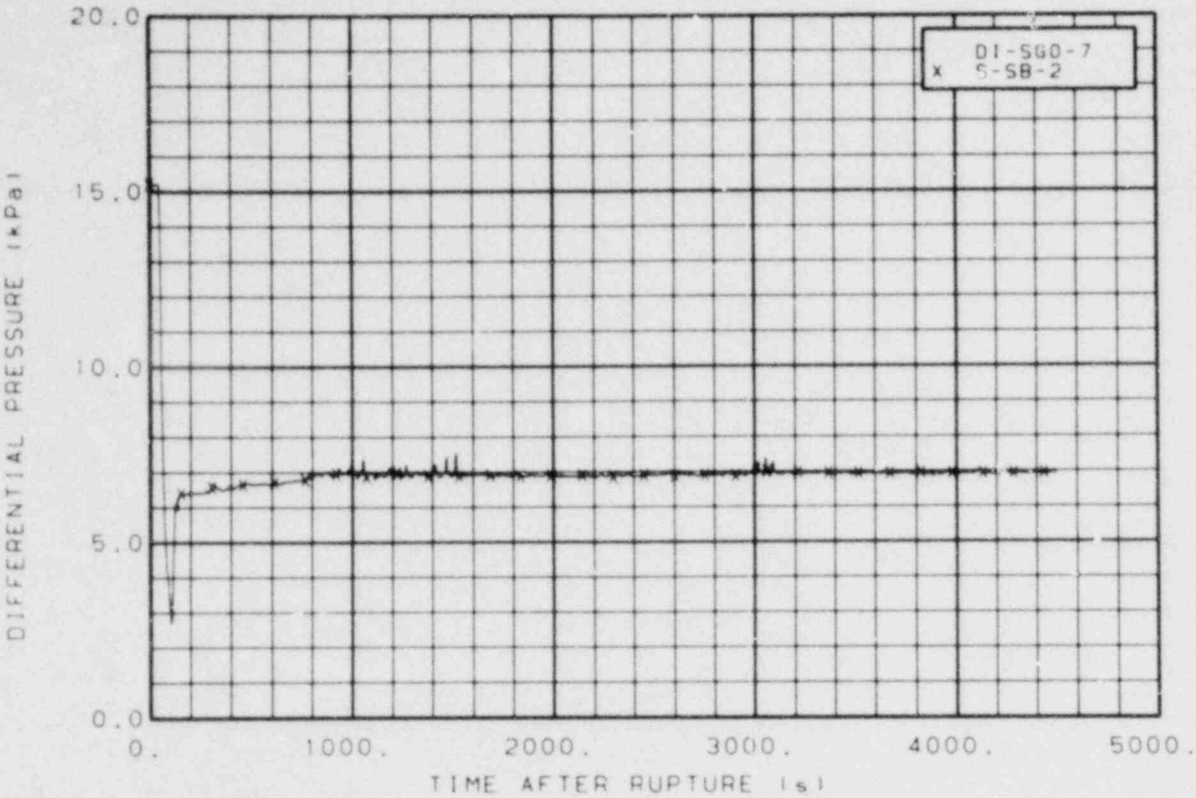

Figure 172. Differential pressure in intact loop, Test S-SB-2 (DI-SGO-7), from 0 to 4500 s.

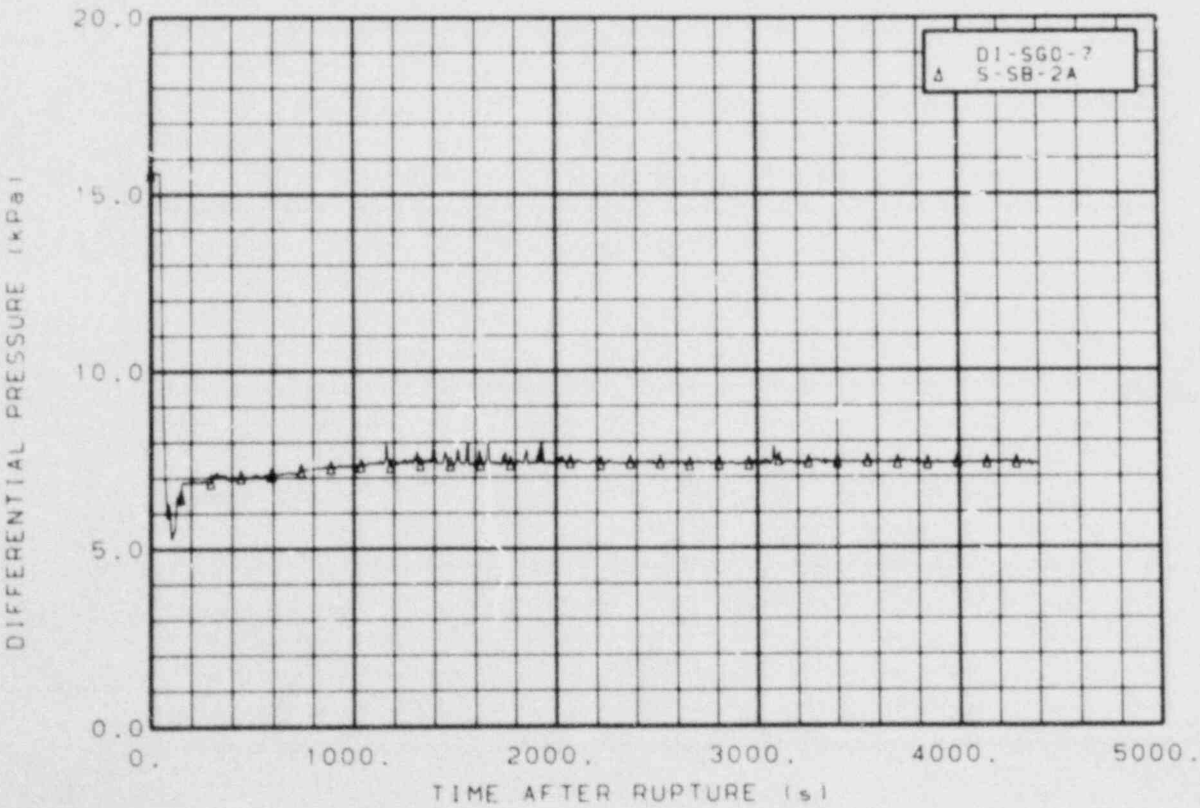

Figure 173. Differential pressure in intact loop, Test S-SB-2A (DI-SGO-7), from 0 to 4390 s.

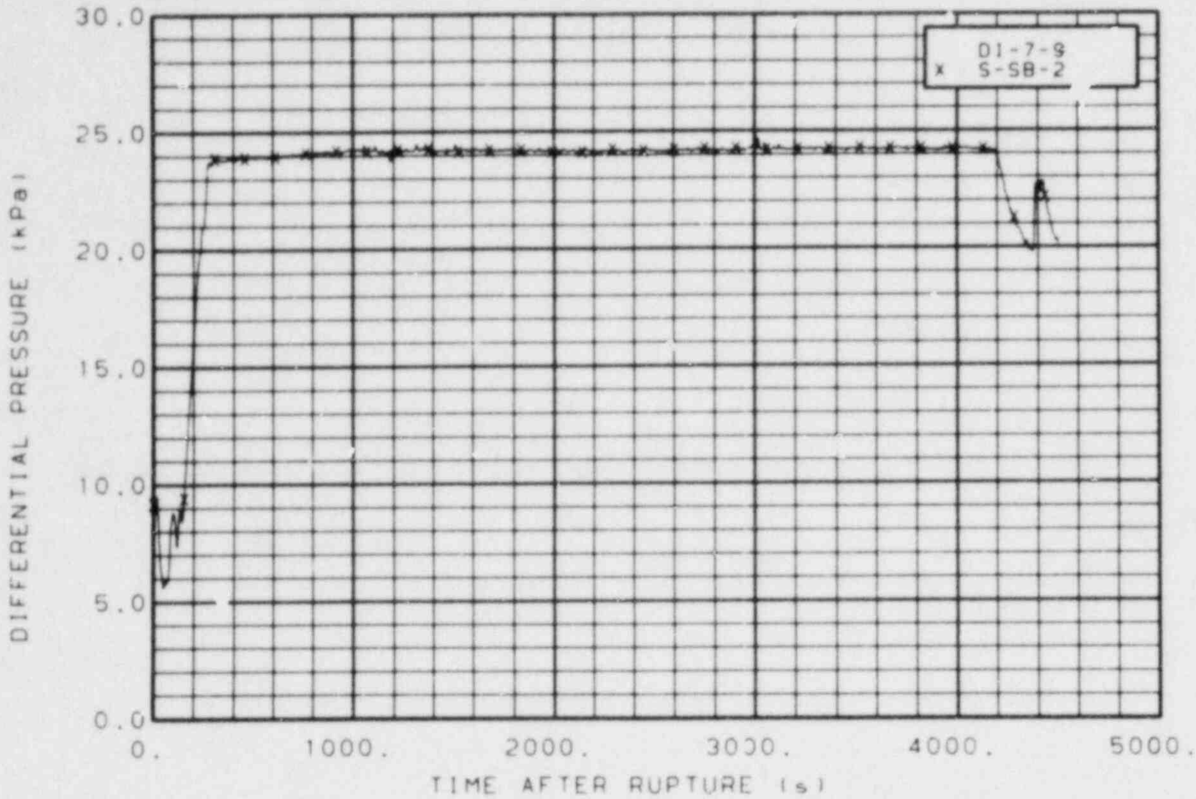

Figure 174. Differential pressure in intact loop, Test S-SB-2 (DI-7-9), from 0 to 4500 s.

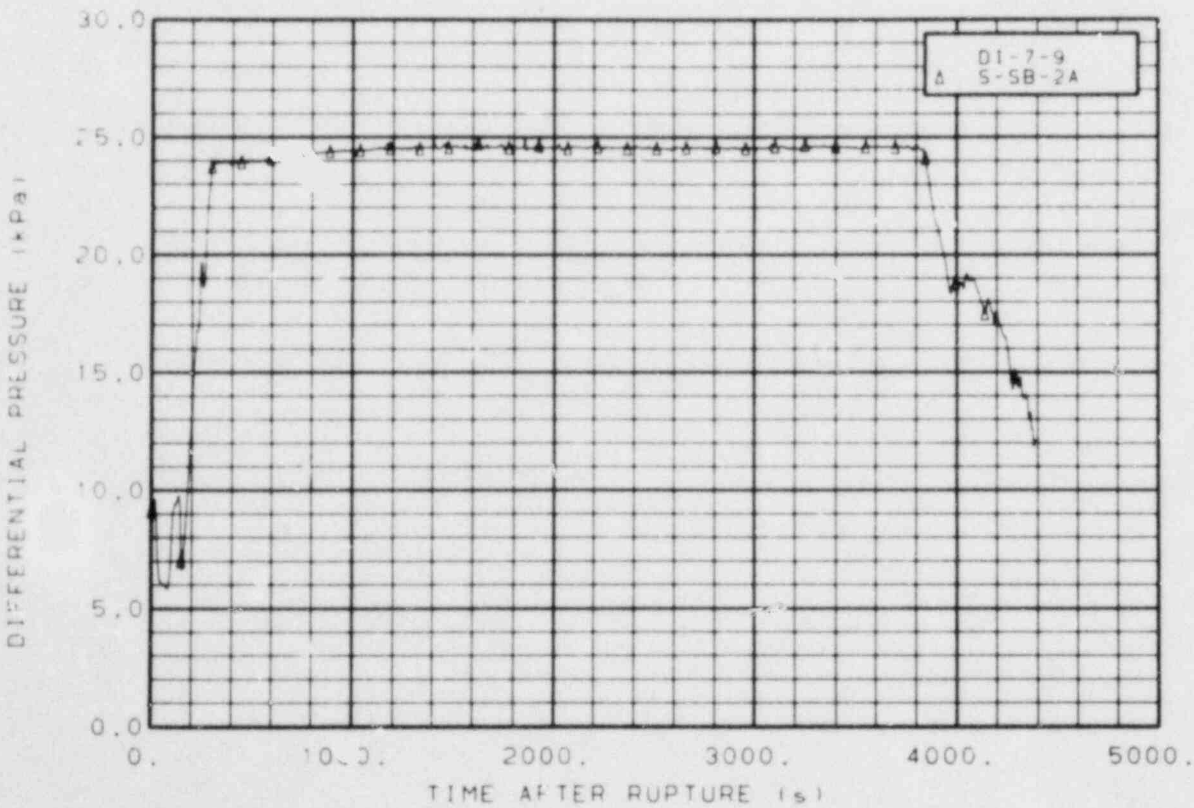

Figure 175. Differential pressure in intact loop, Test S-SB-2A (DI-7-9), from 0 to 4390 s.

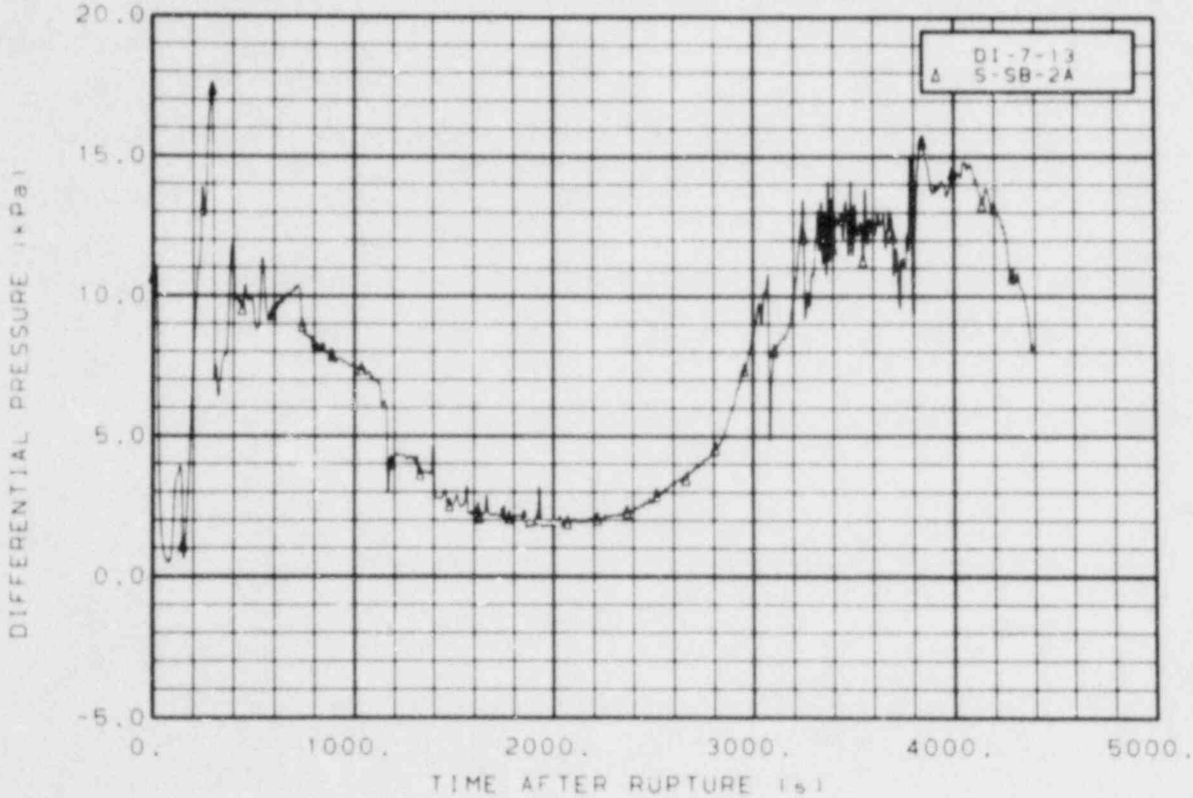

Figure 176. Differential pressure in intact loop, Test S-SB-2A (DI-7-13), from 0 to 4390 s.

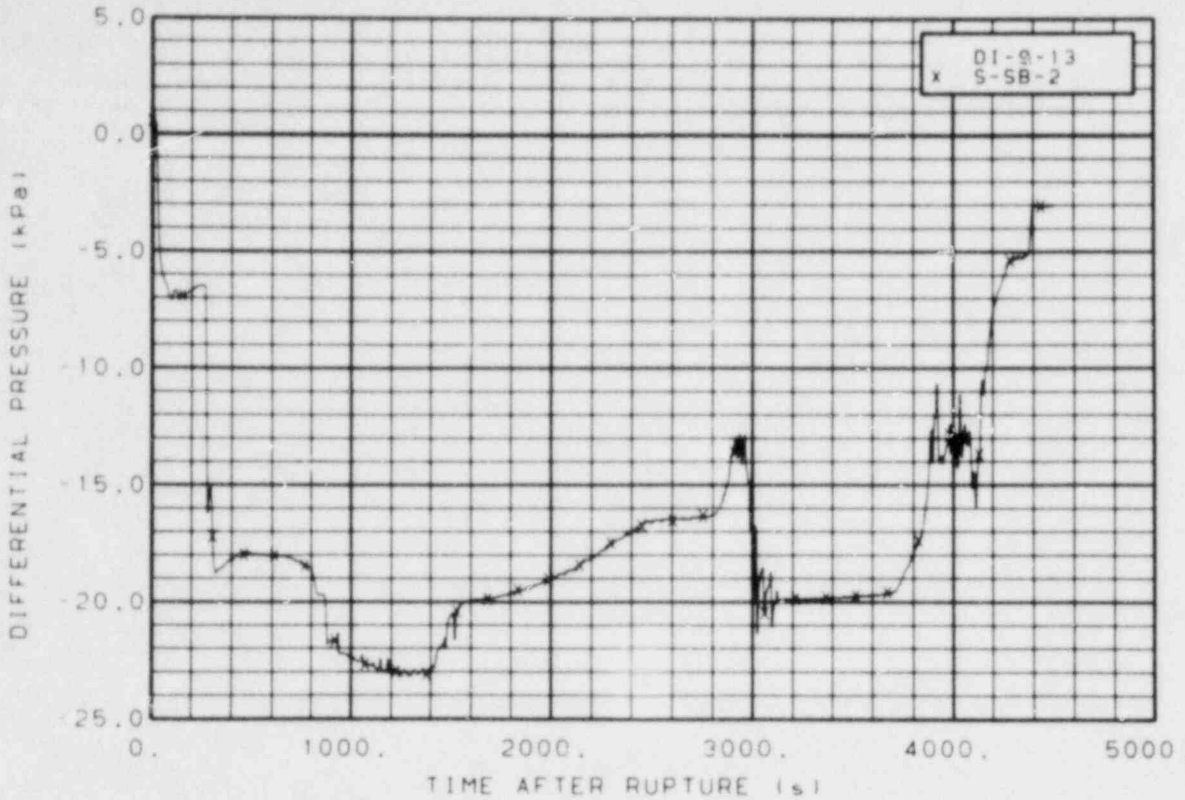

Figure 177. Differential pressure in intact loop, Test S-SB-2 (DI-9-13), from 0 to 4500 s.

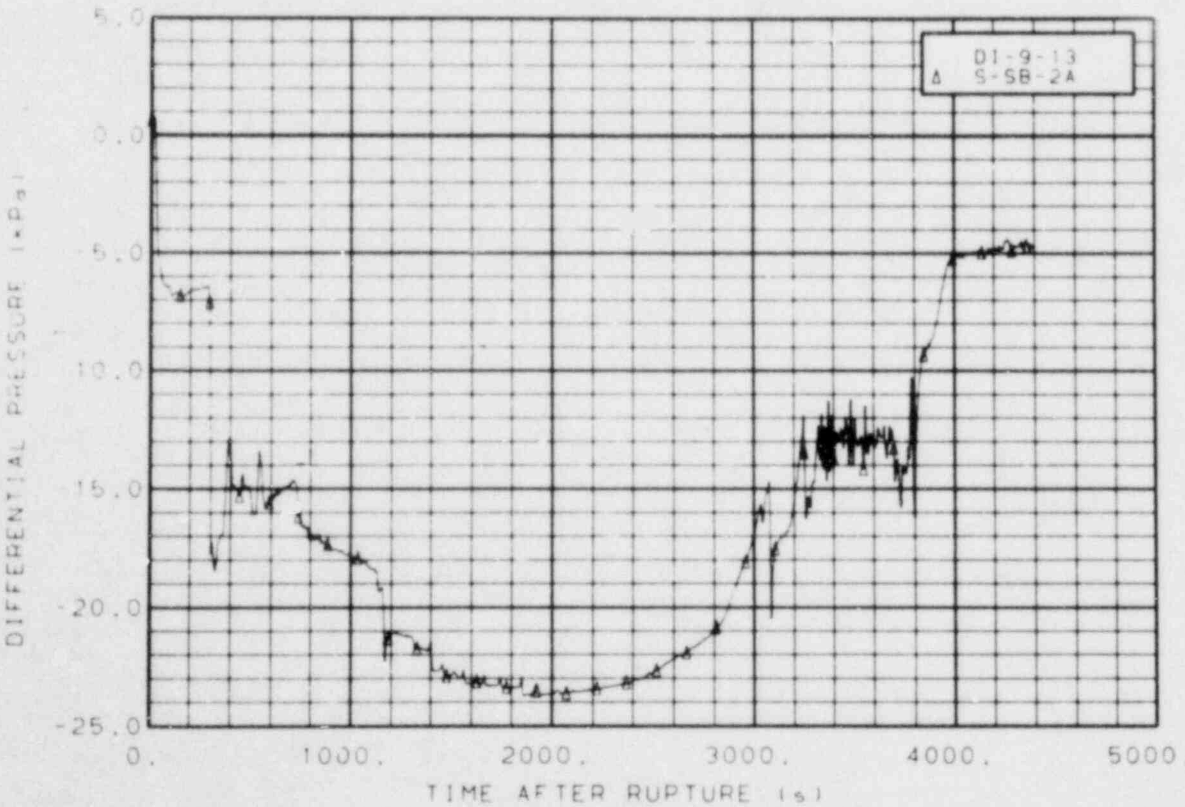

Figure 178. Differential pressure in intact loop, Test S-SB-2A (DI-9-13), from 0 to 4390 s.

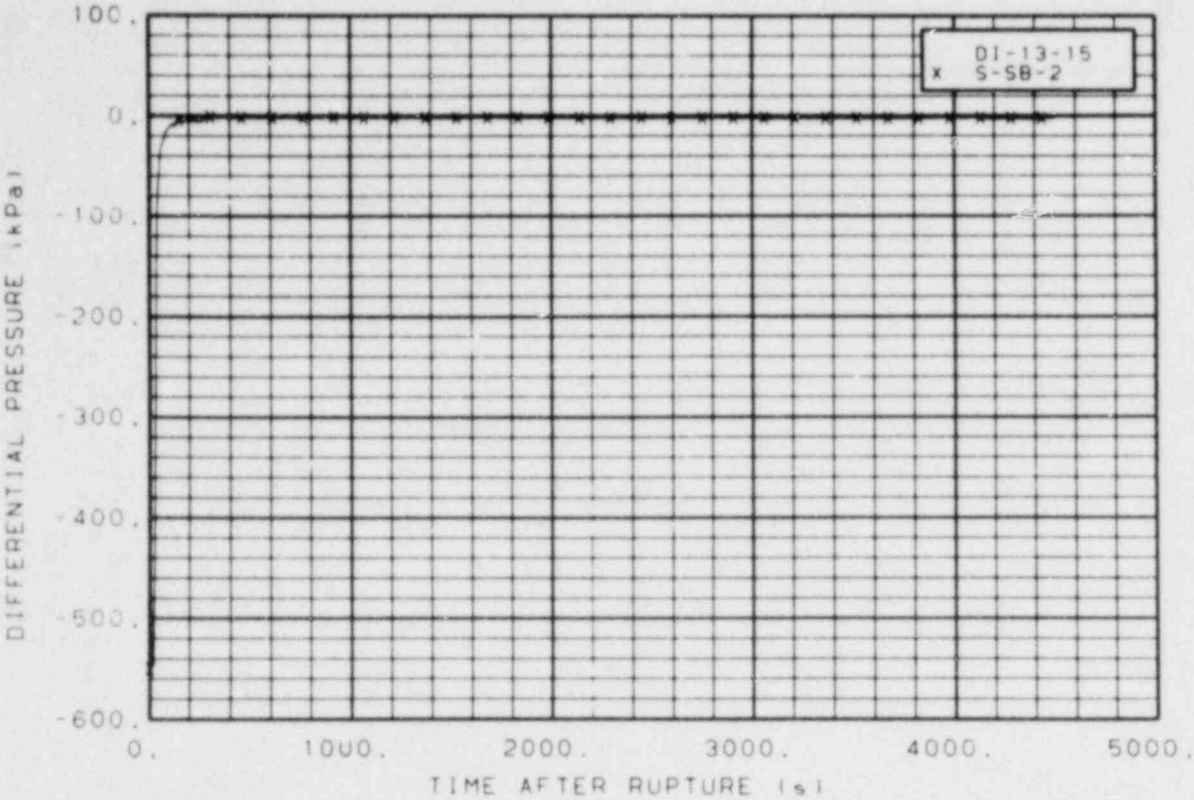

Figure 179. Differential pressure in intact loop, Test S-SB-2 (DI-13-15) from 0 to 4500 s.

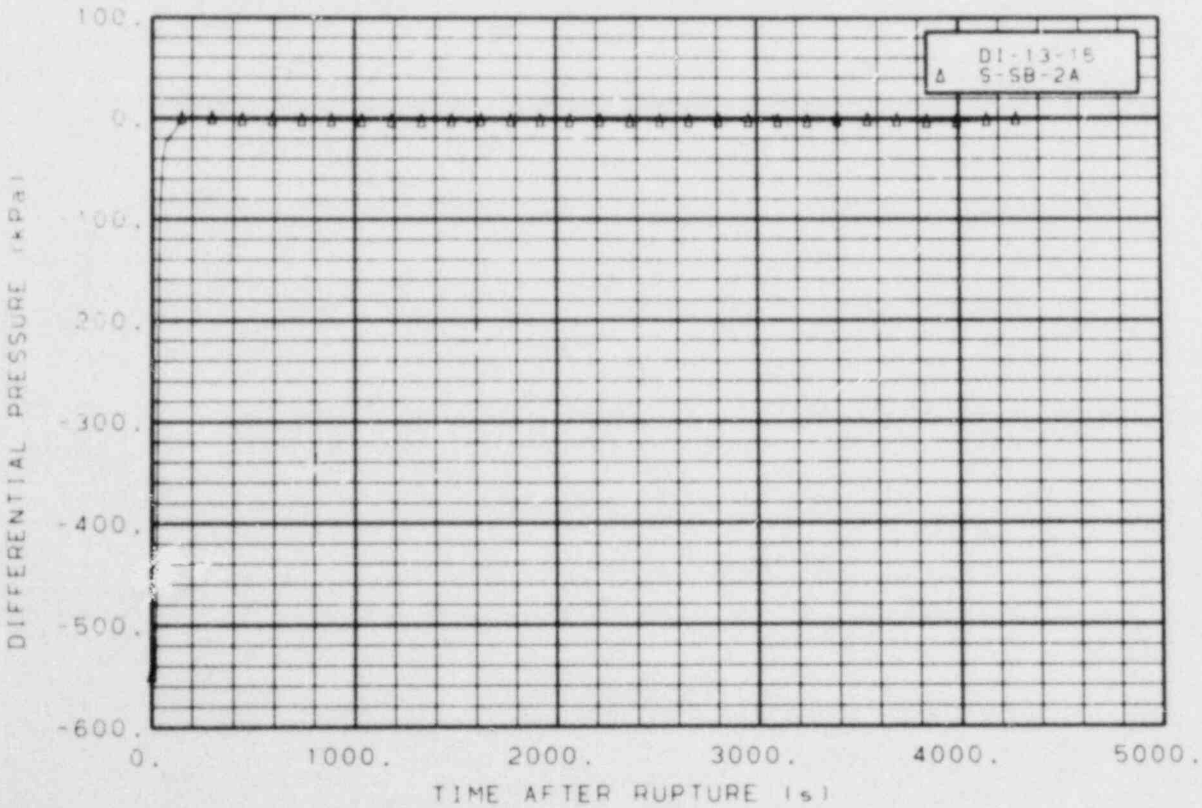

Figure 180. Differential pressure in intact loop, Test S-SB-2A (DI-13-15) from 0 to 4390 s.

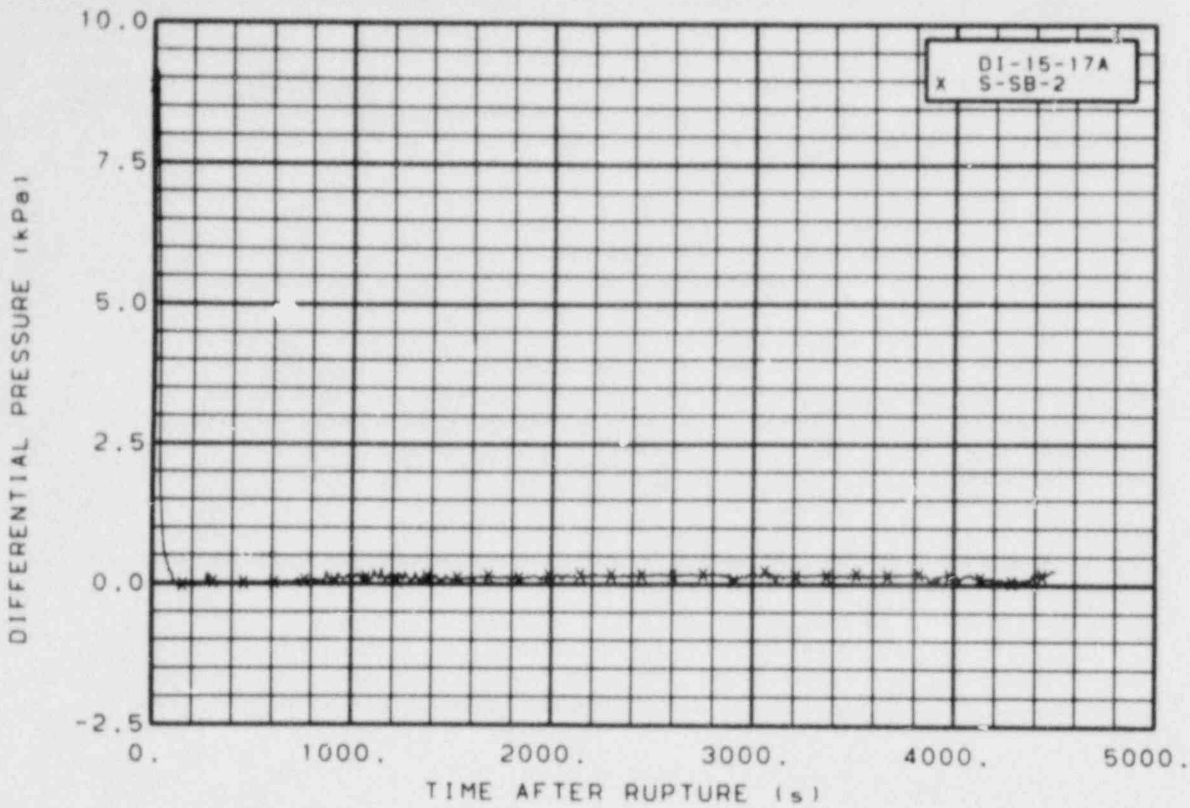

Figure 181. Differential pressure in intact loop, Test S-SB-2 (DI-15-17A) from 0 to 4500 s.

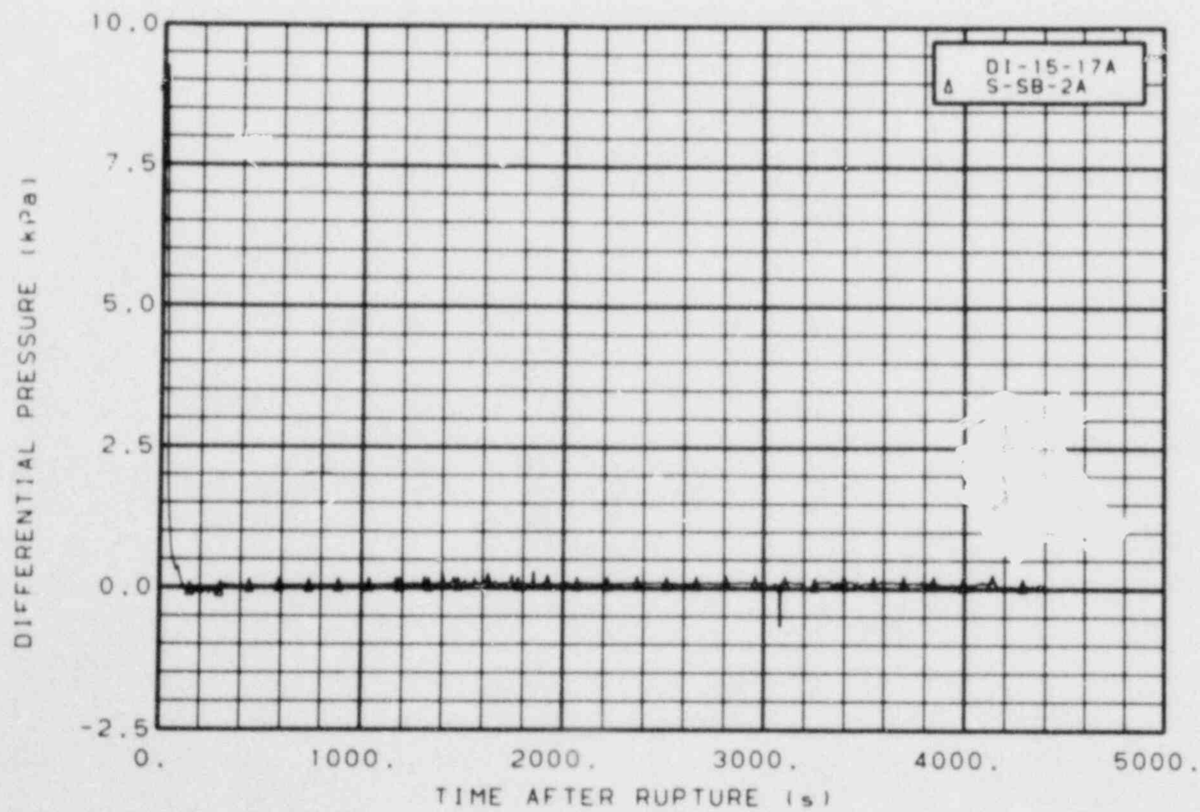

Figure 182. Differential pressure in intact loop, Test S-SB-2A (DI-15-17A), from 0 to 4390 s.

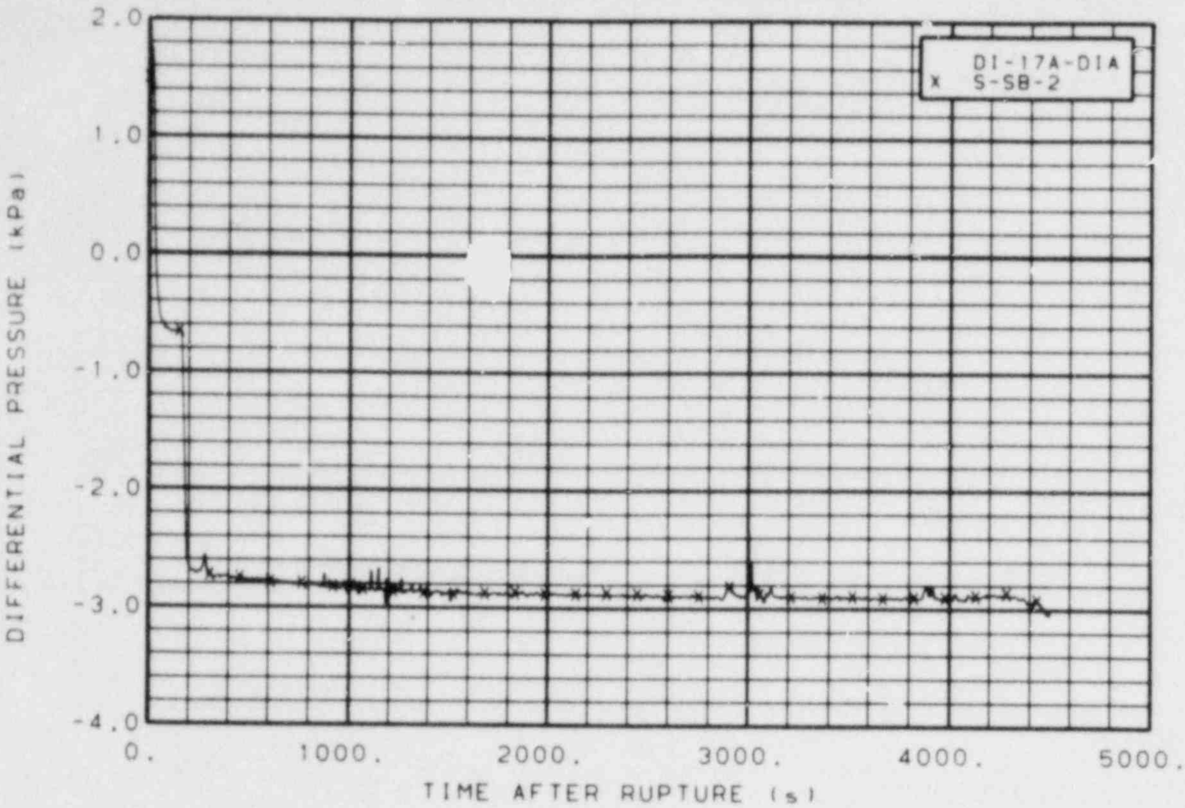

Figure 183. Differential pressure in intact loop, Test S-SB-2 (DI-17A-DIA), from 0 to 4500 s.

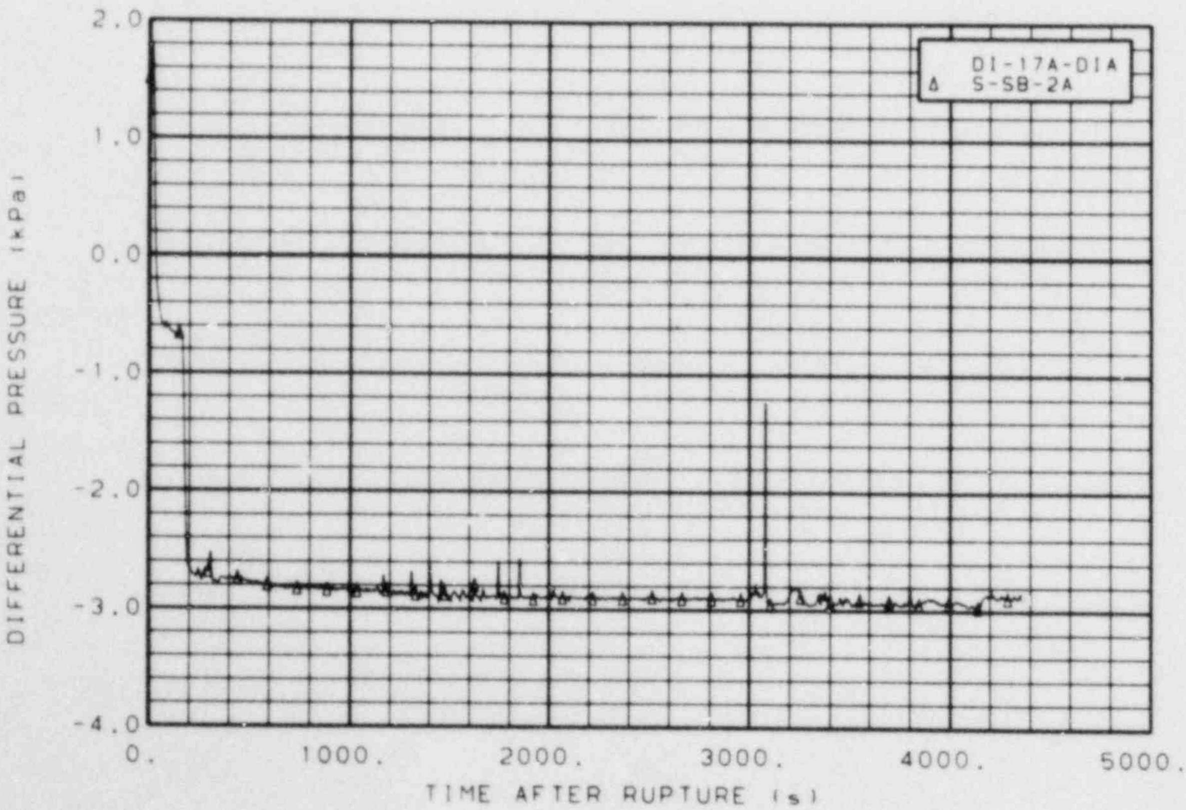

Figure 184. Differential pressure in intact loop, Test S-SB-2A (DI-17A-DIA), from 0 to 4390 s.

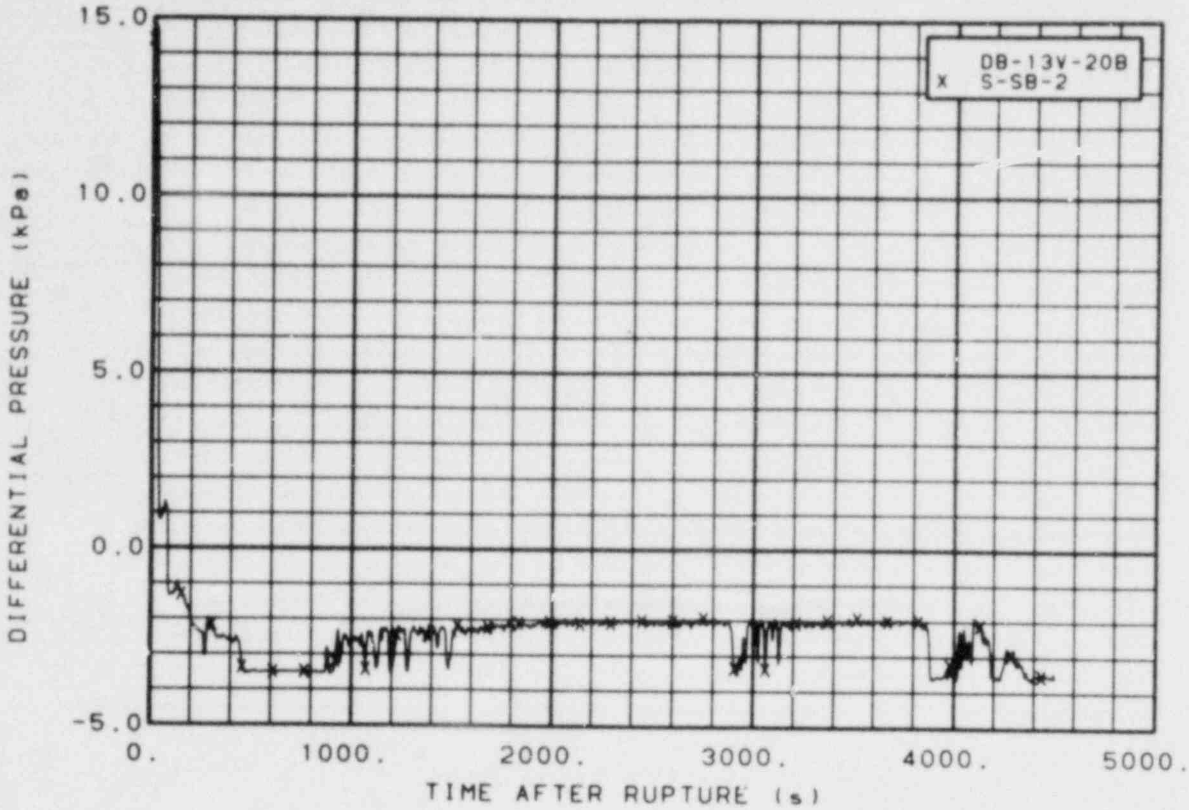

Figure 185. Differential pressure in broken loop, Test S-SB-2 (DB-13V-20B), from 0 to 4500 s.

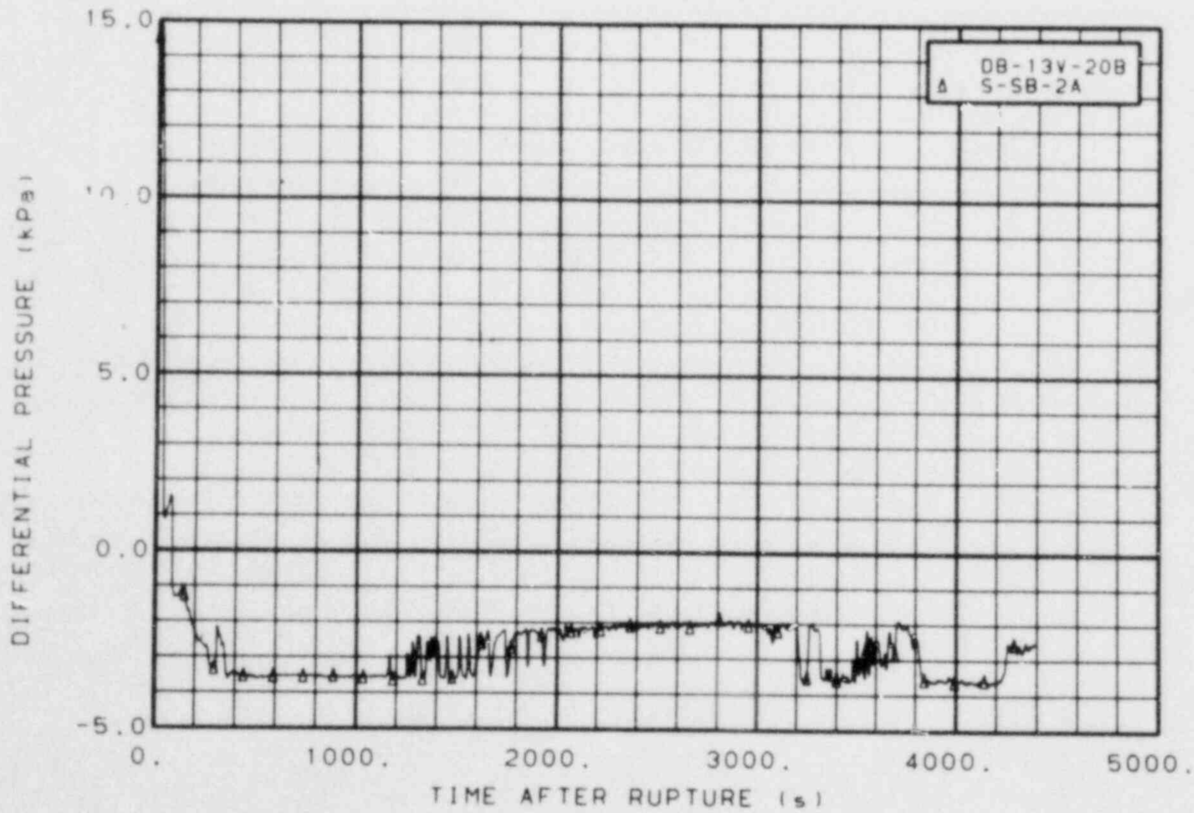

Figure 186. Differential pressure in broken loop, Test S-SB-2A (DB-13V-20B), from 0 to 4390 s.

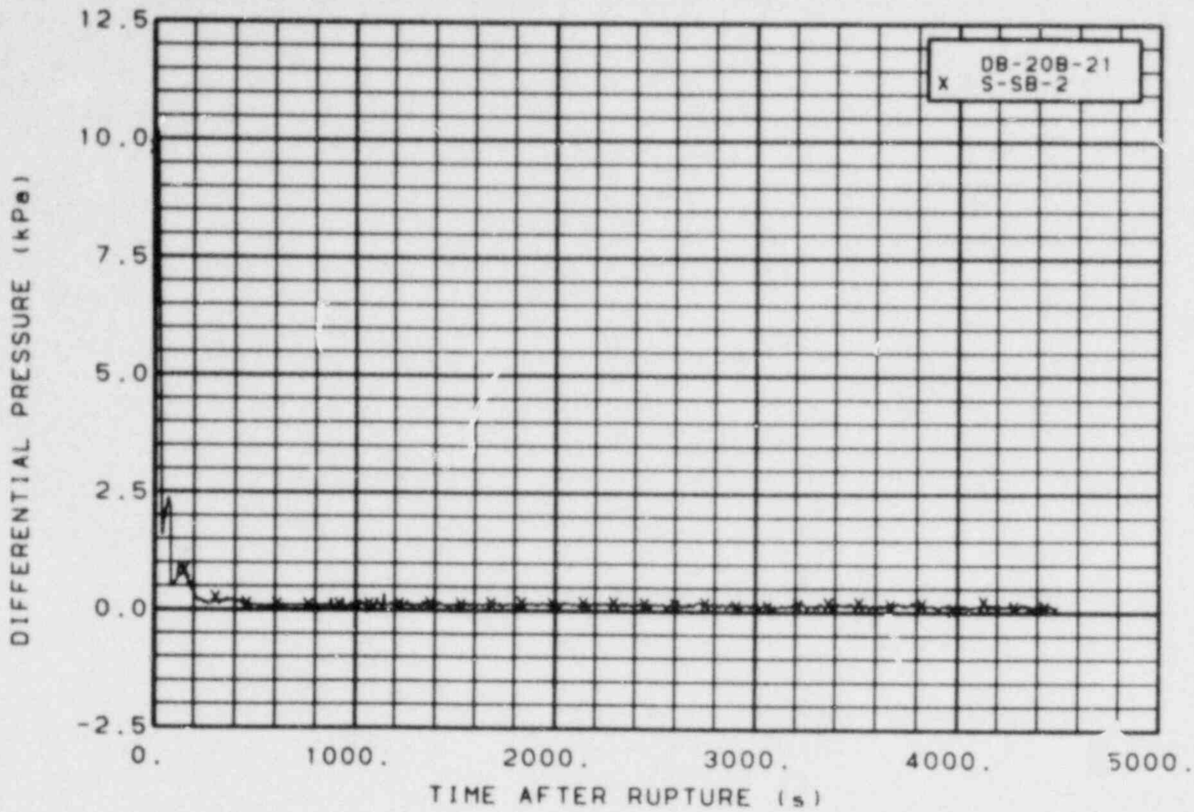

Figure 187. Differential pressure in broken loop, Test S-SB-2 (DB-20B-21), from 0 to 4500 s.

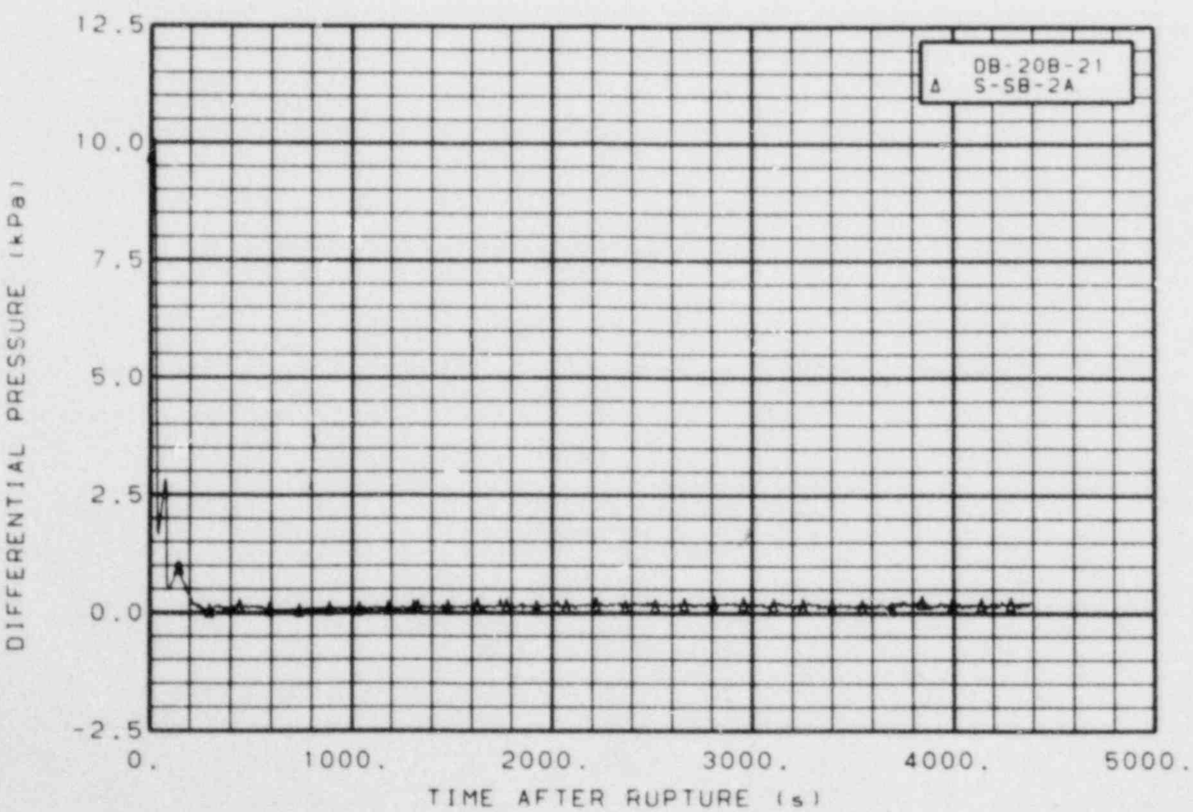

Figure 188. Differential pressure in broken loop, Test S-SB-2A (DB-20B-21), from 0 to 4390 s.

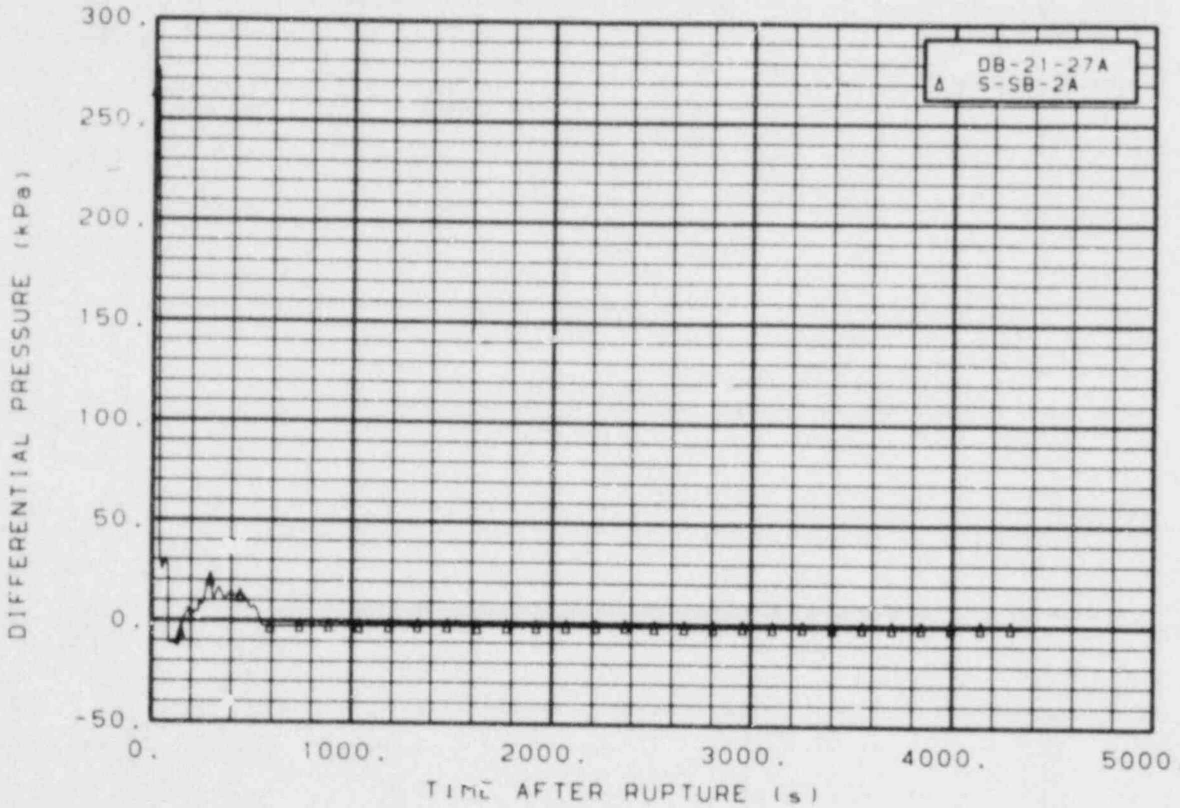

Figure 189. Differential pressure in broken loop, Test S-SB-2A (DB-21-27A), from 0 to 4390 s.

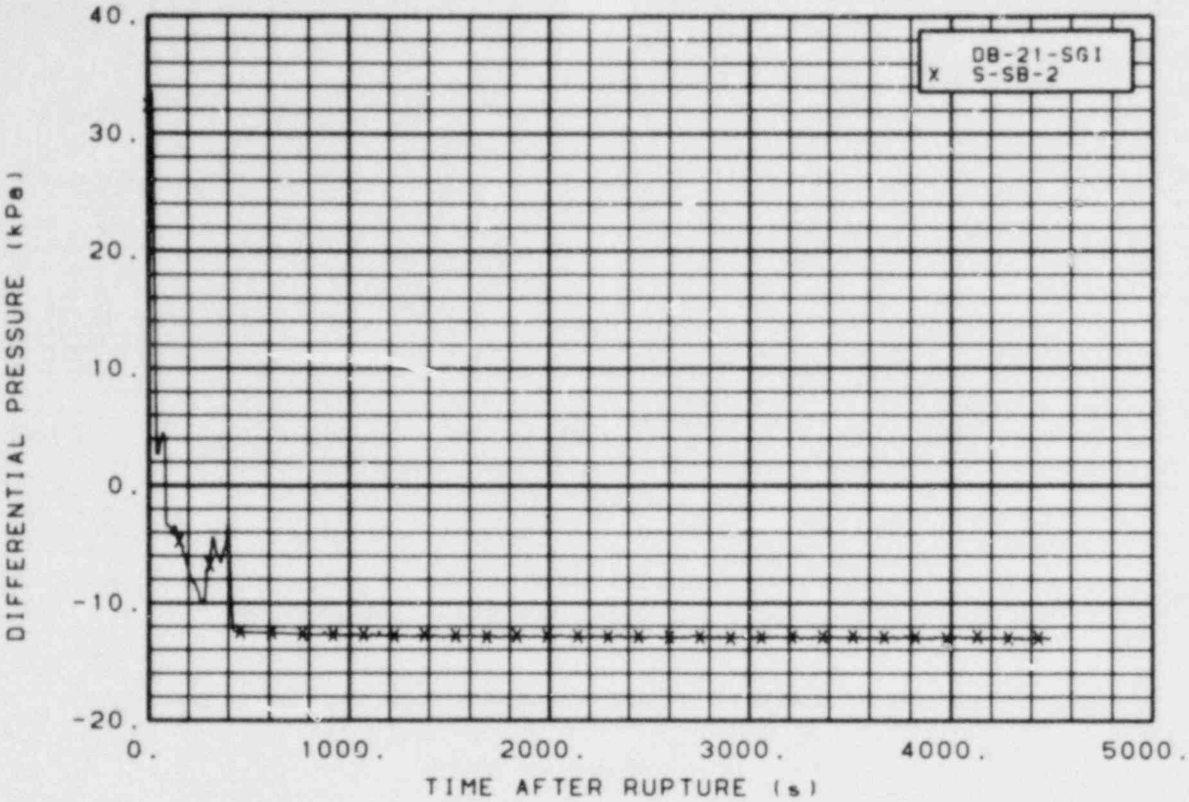

Figure 190. Differential pressure in broken loop, Test S-SB-2 (DB-21-SGI), from 0 to 4500 s.

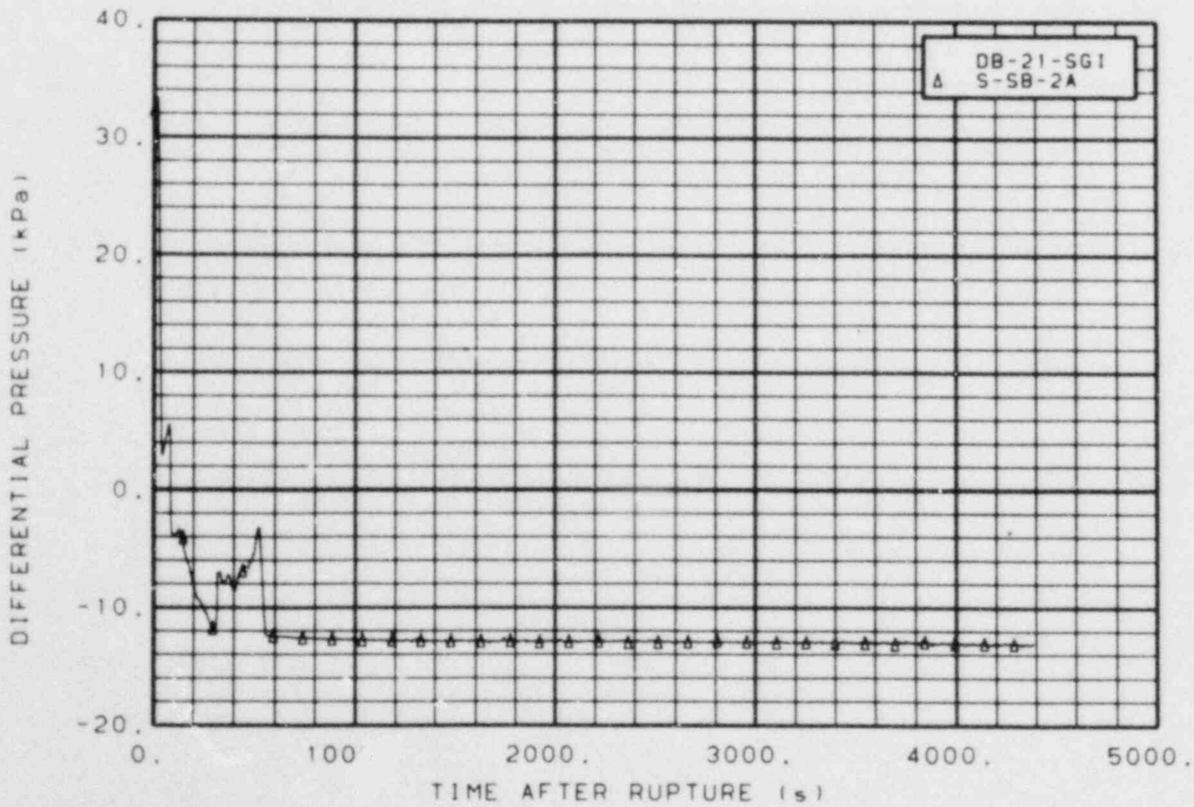

Figure 191. Differential pressure in broken loop, Test S-SB-2A (DB-21-SGI), from 0 to 4390 s.

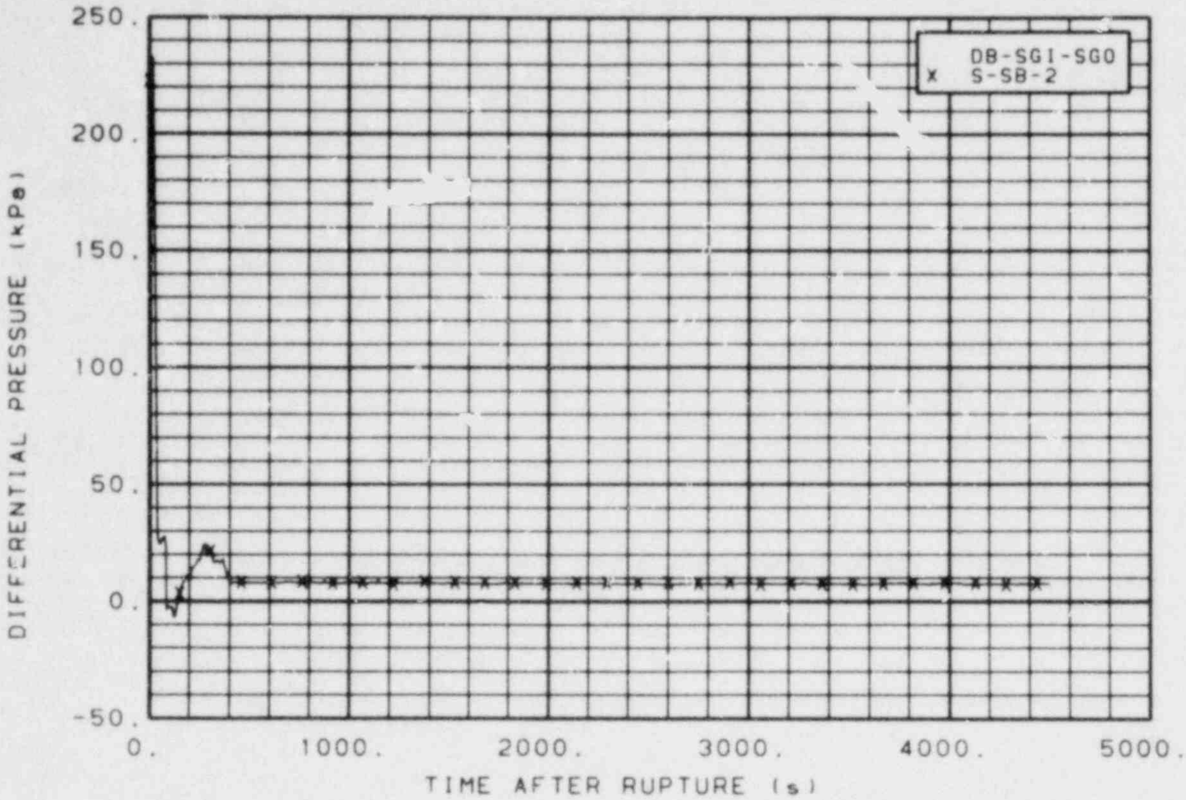

Figure 192. Differential pressure in broken loop, Test S-SB-2 (DB-SGI-SGO), from 0 to 4500 s.

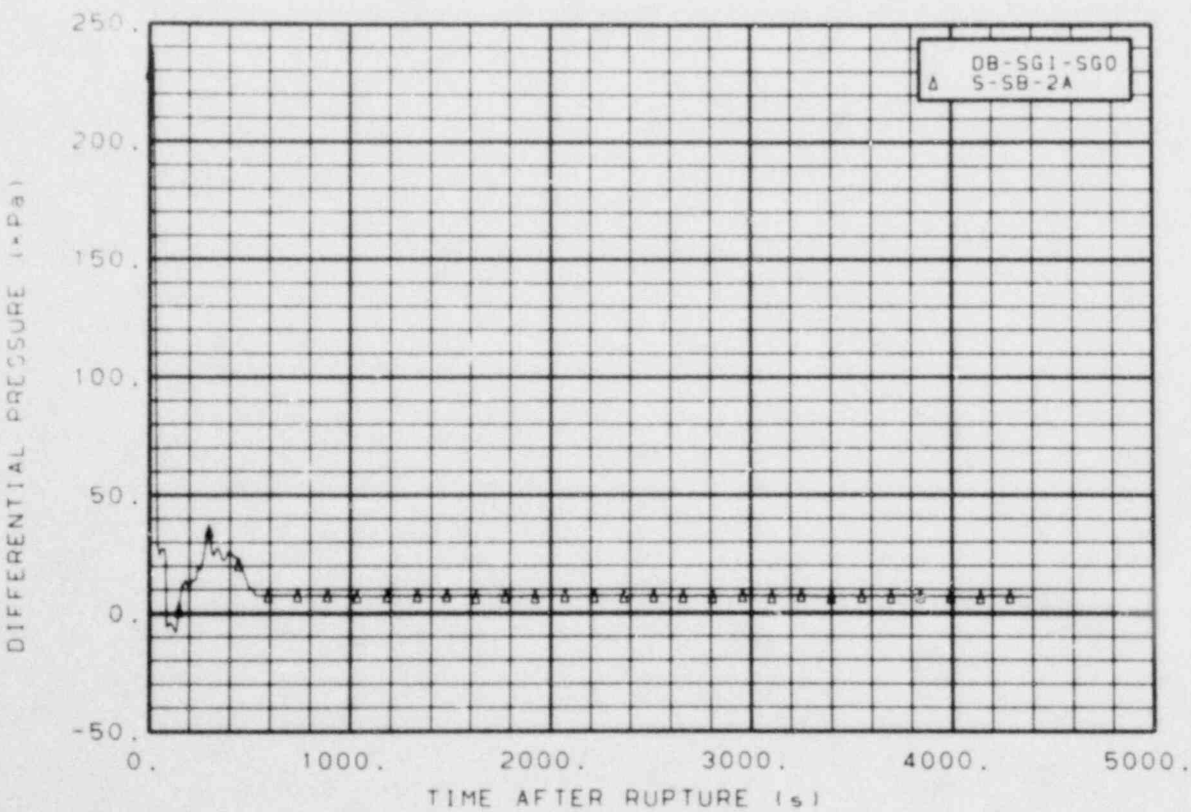

Figure 193. Differential pressure in broken loop, Test S-SB-2A (DB-SGI-SGO), from 0 to 4390 s.

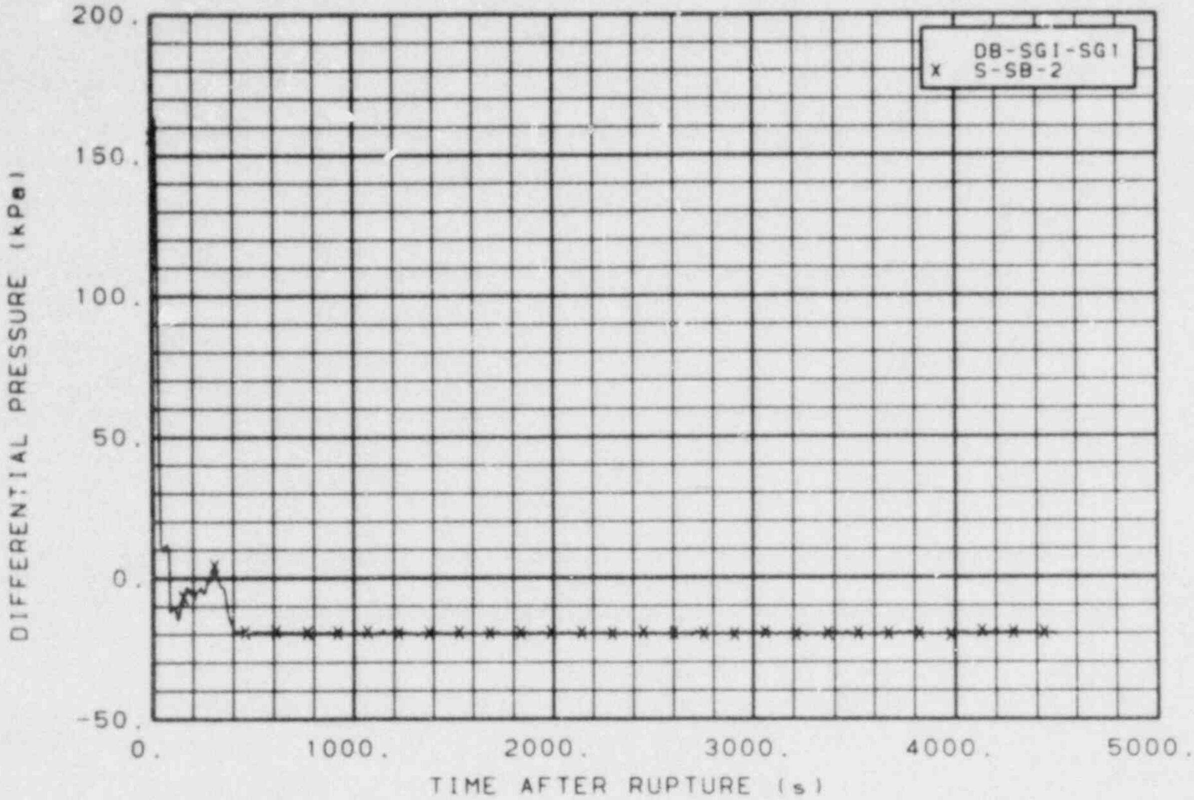

Figure 194. Differential pressure in broken loop, Test S-SB-2 (DB-SGI-SG1), from 0 to 4500 s.

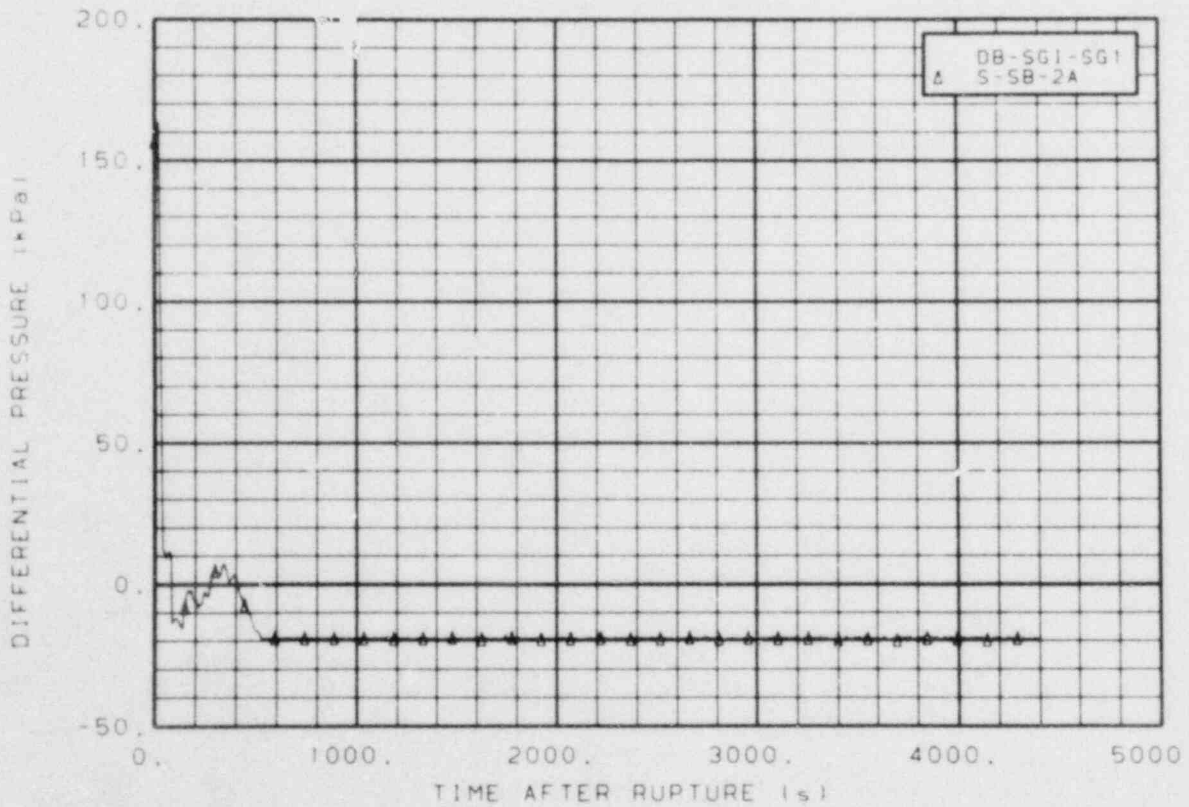

Figure 195. Differential pressure in broken loop, Test S-SB-2A (DB-SGI-SG1), from 0 to 4390 s.

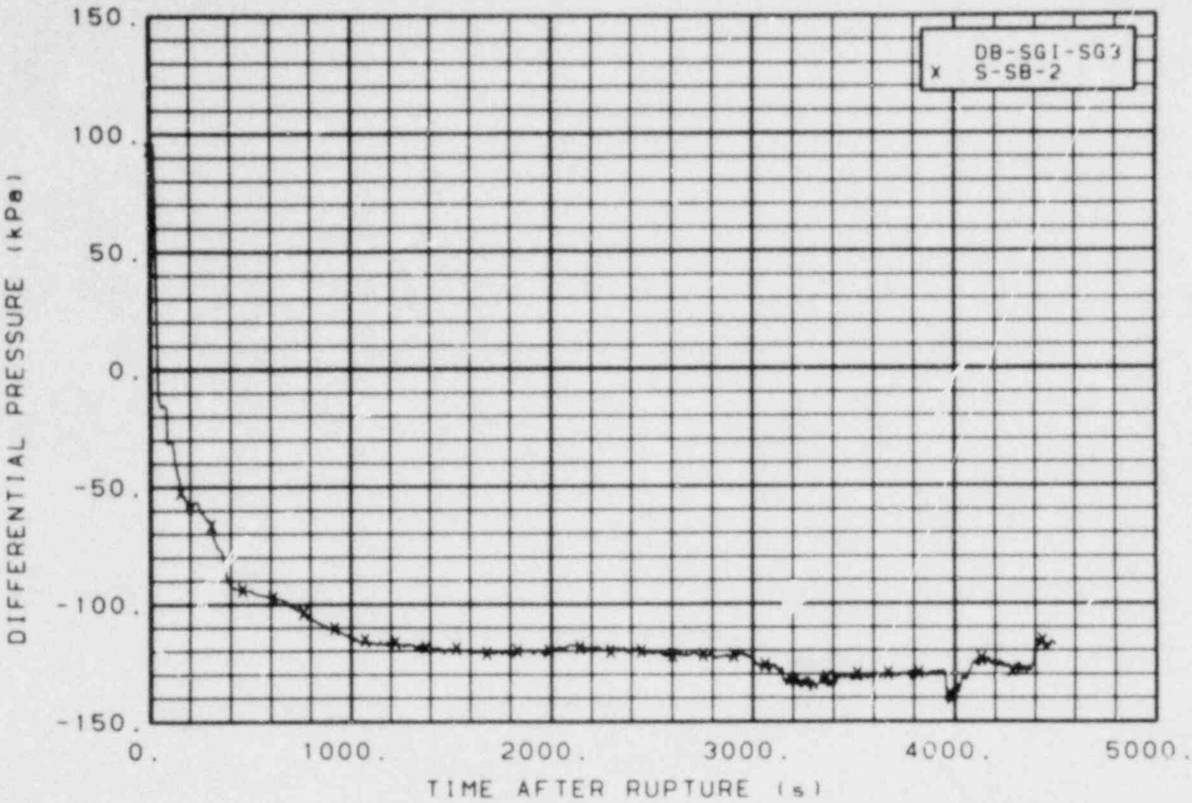

Figure 196. Differential pressure in broken loop, Test S-SB-2 (DB-SGI-SG3), from 0 to 4500 s.

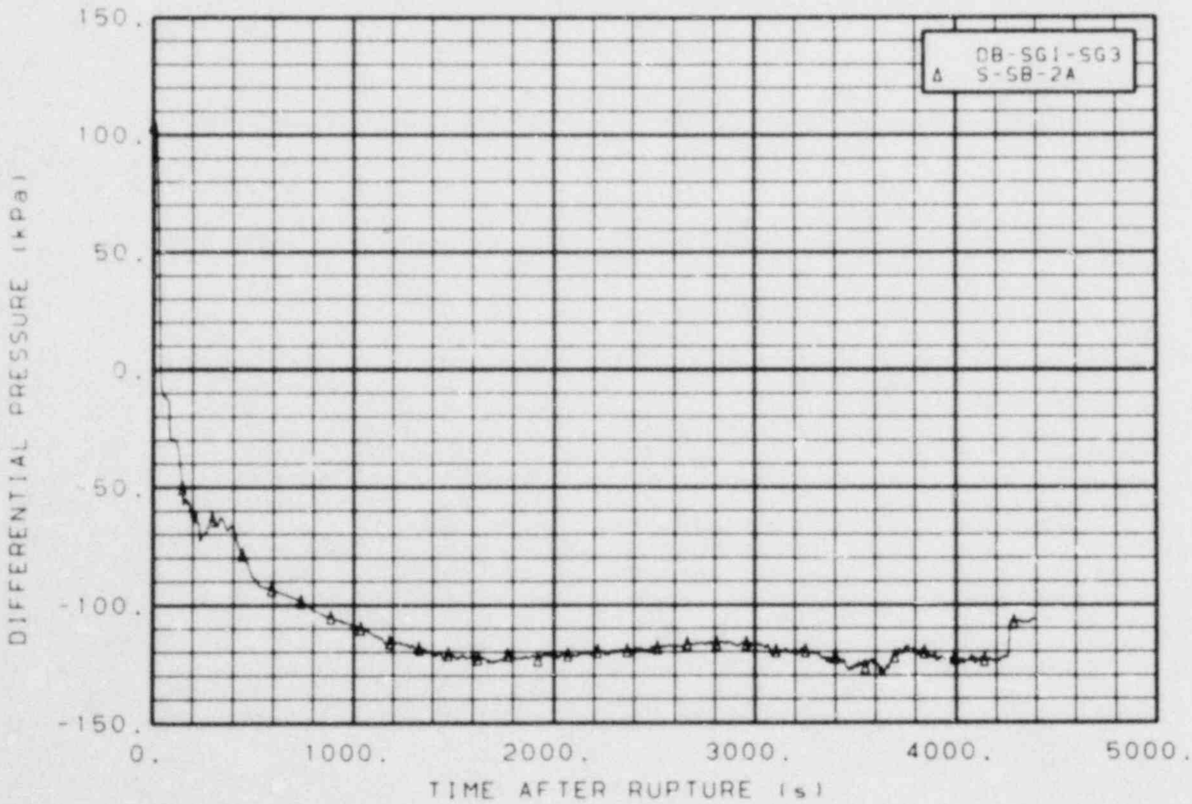

Figure 197. Differential pressure in broken loop, Test S-SB-2A (DB-SGI-SG3), from 0 to 4390 s.

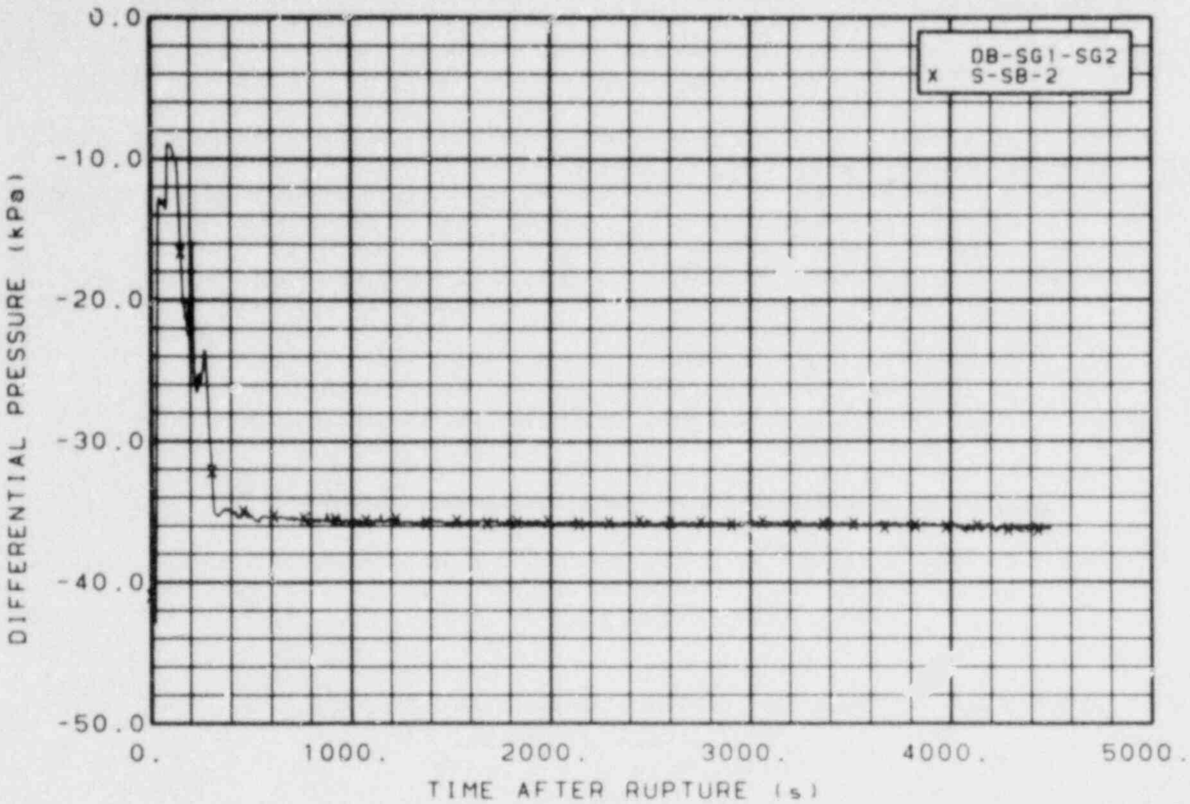

Figure 198. Differential pressure in broken loop, Test S-SB-2 (DB-SG1-SG2), from 0 to 4500 s.

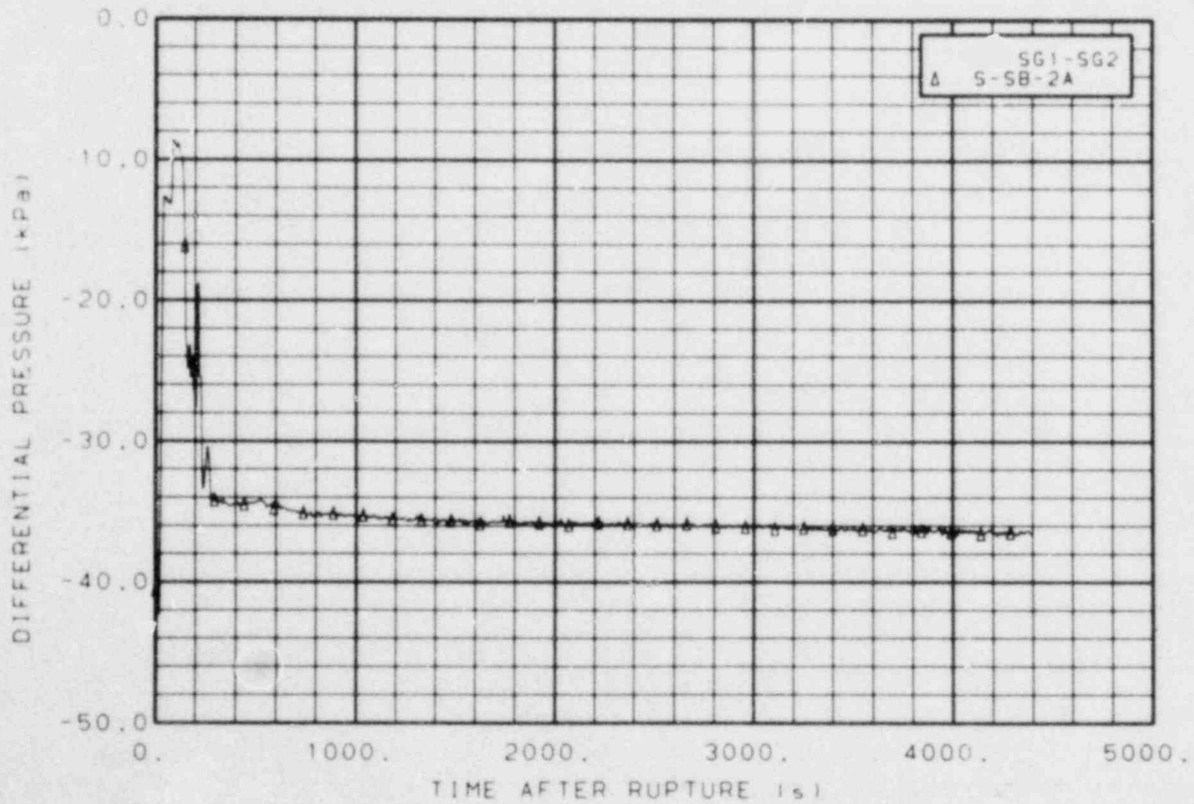

Figure 199. Differential pressure in broken loop, Test S-SB-2A (DB-SG1-SG2), from 0 to 4390 s.

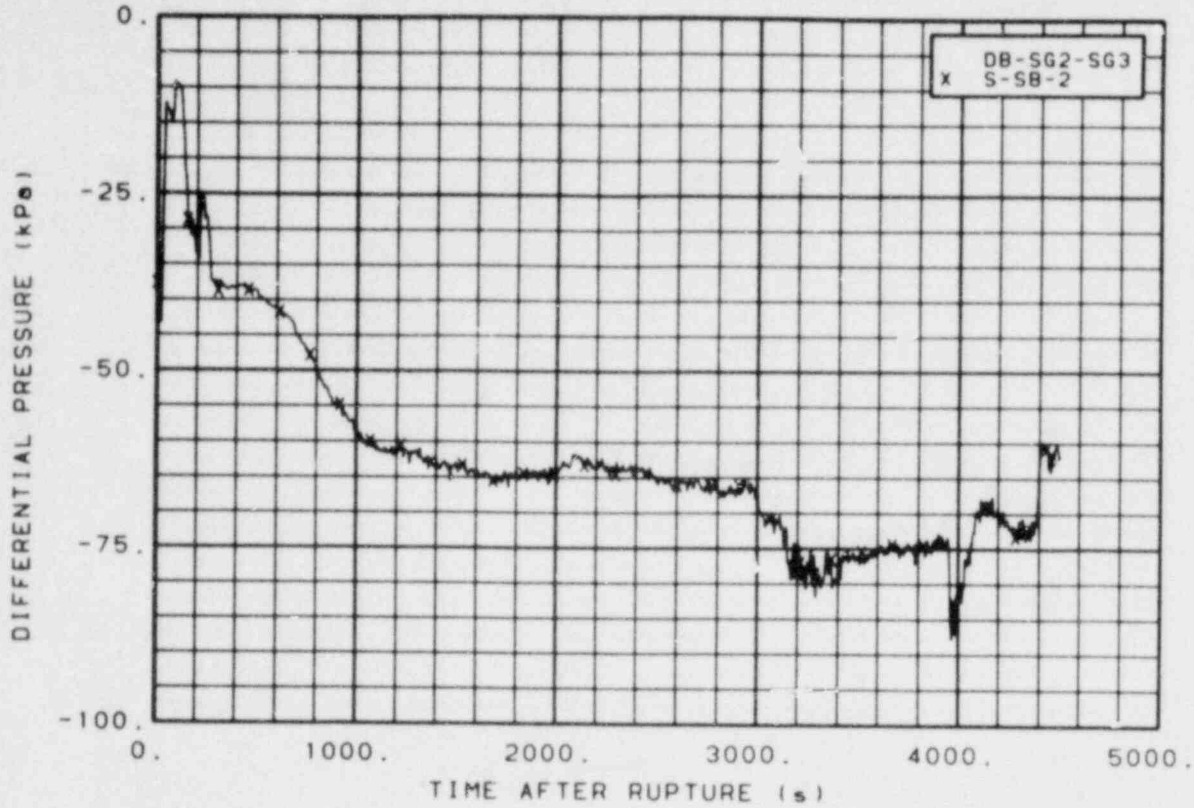

Figure 200. Differential pressure in broken loop, Test S-SB-2 (DB-SG2-SG3), from 0 to 4500 s.

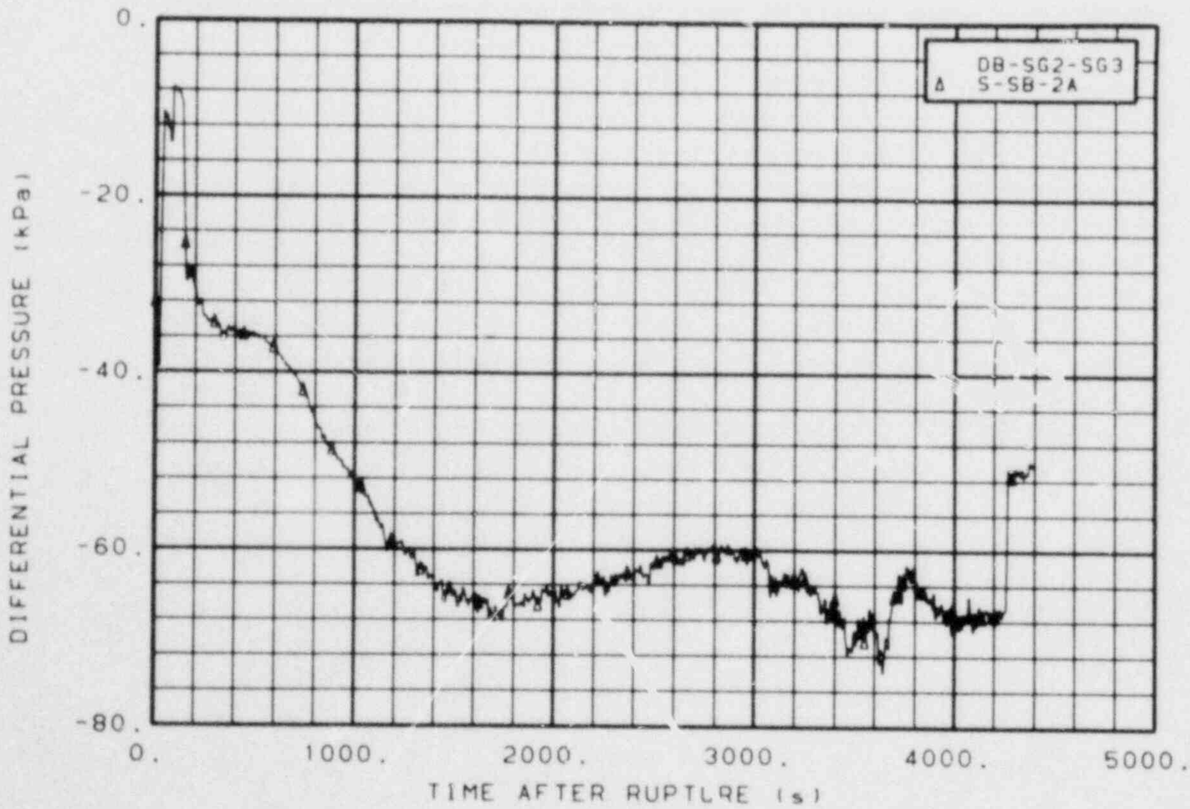

Figure 201. Differential pressure in broken loop, Test S-SB-2A (DB-SG2-SG3), from 0 to 4390s.

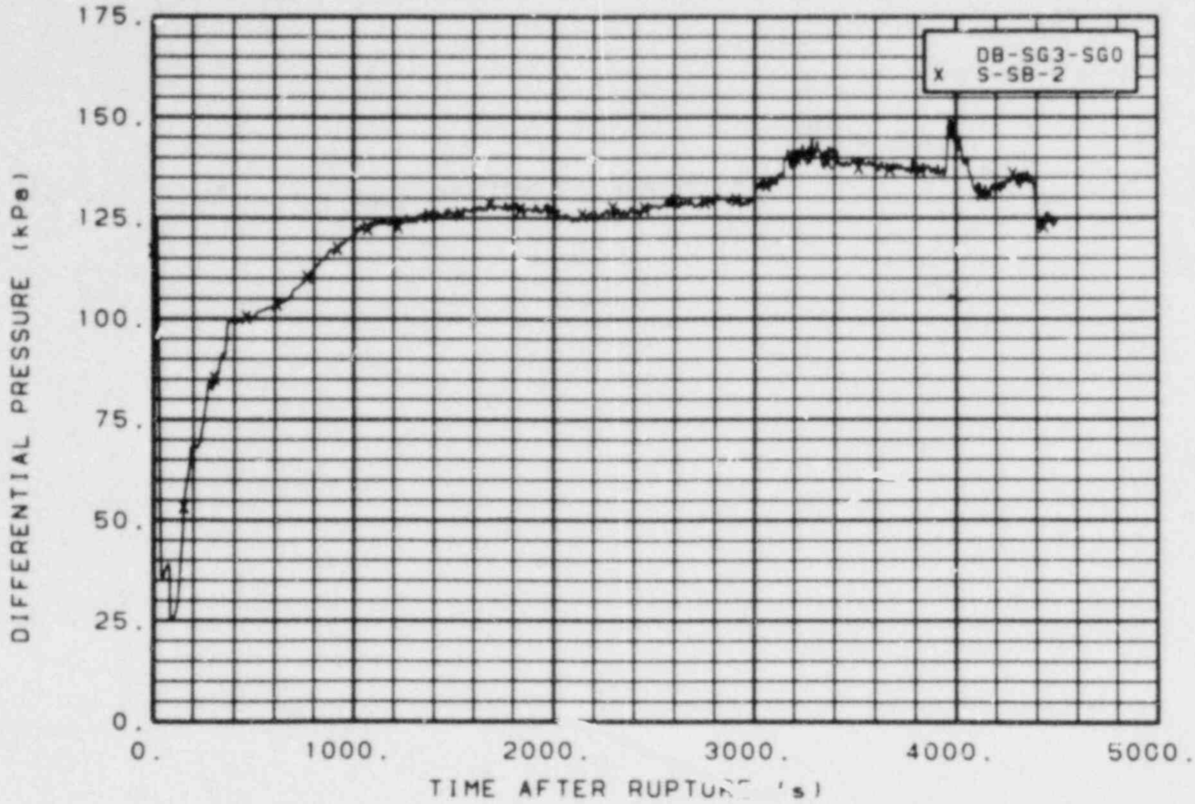

Figure 202. Differential pressure in broken loop, Test S-SB-2 (DB-SG3-SGO), from 0 to 4500 s.

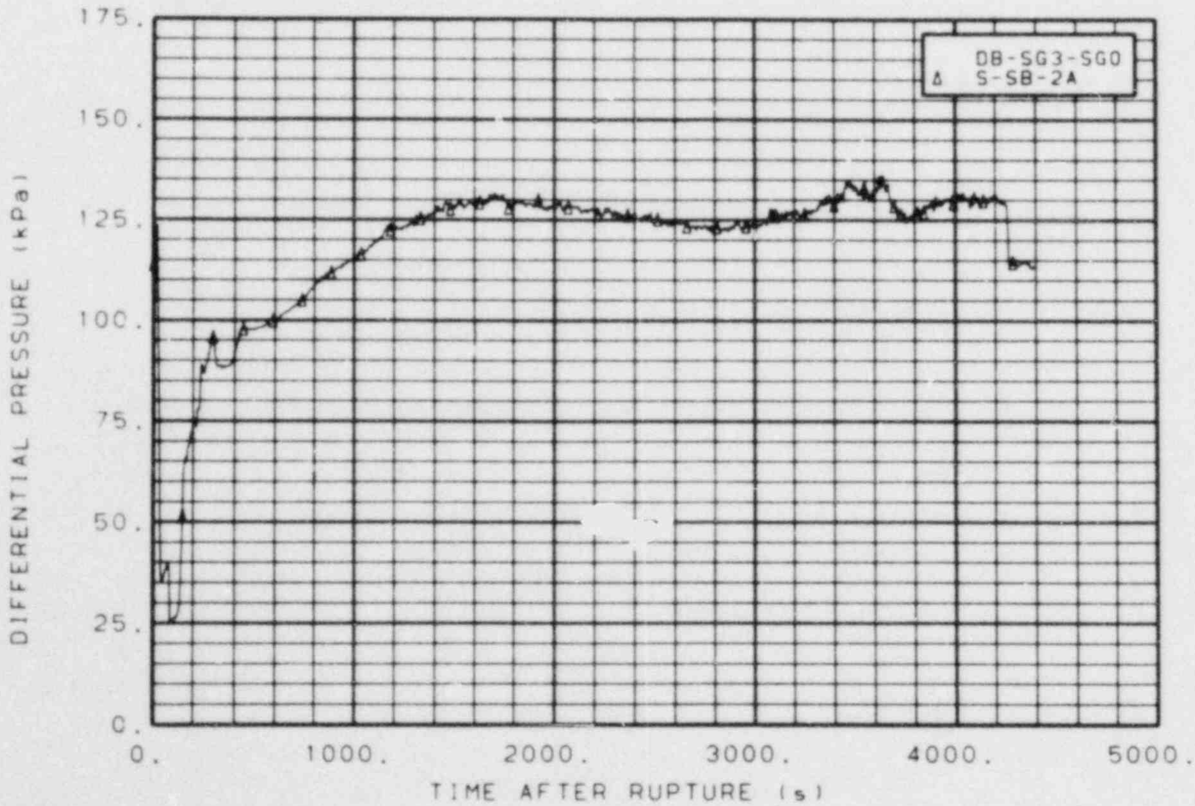

Figure 203. Differential pressure in broken loop, Test S-SB-2A (DB-SG3-SGO), from 0 to 4390 s.

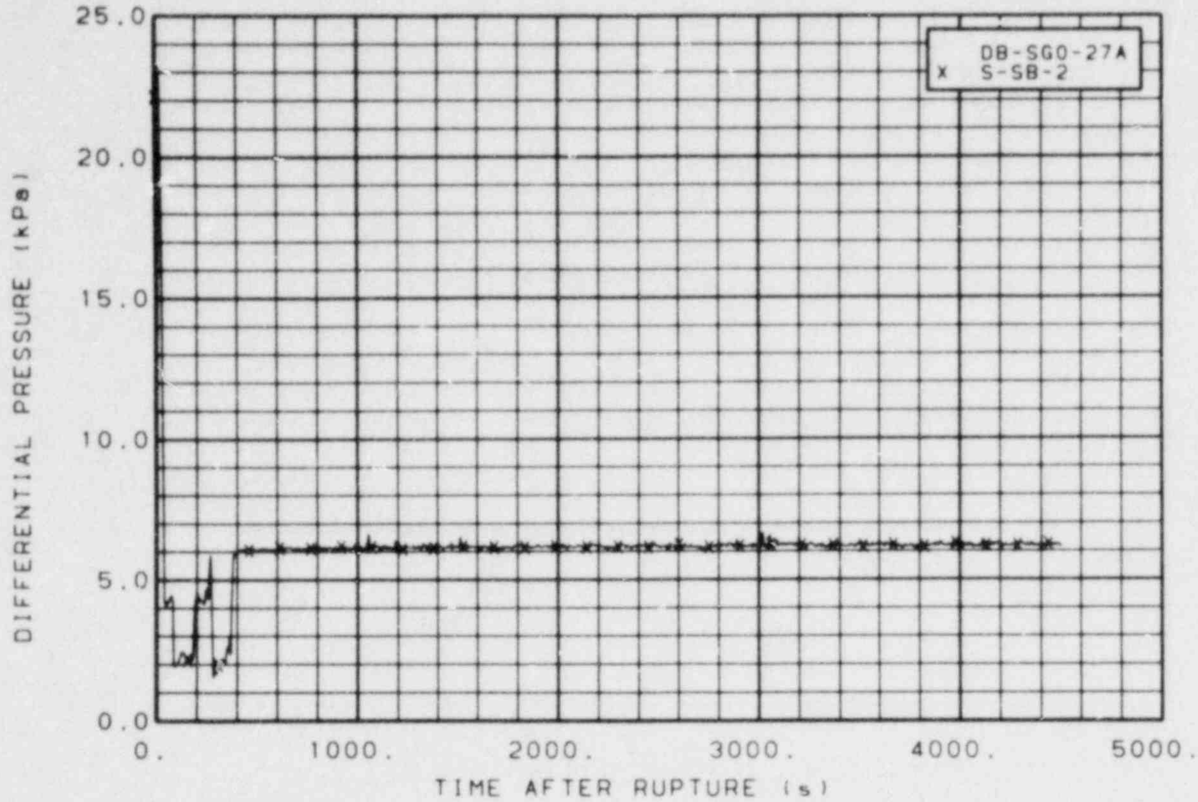

Figure 204. Differential pressure in broken loop, Test S-SB-2 (DB-SGO-27A), from 0 to 4500 s.

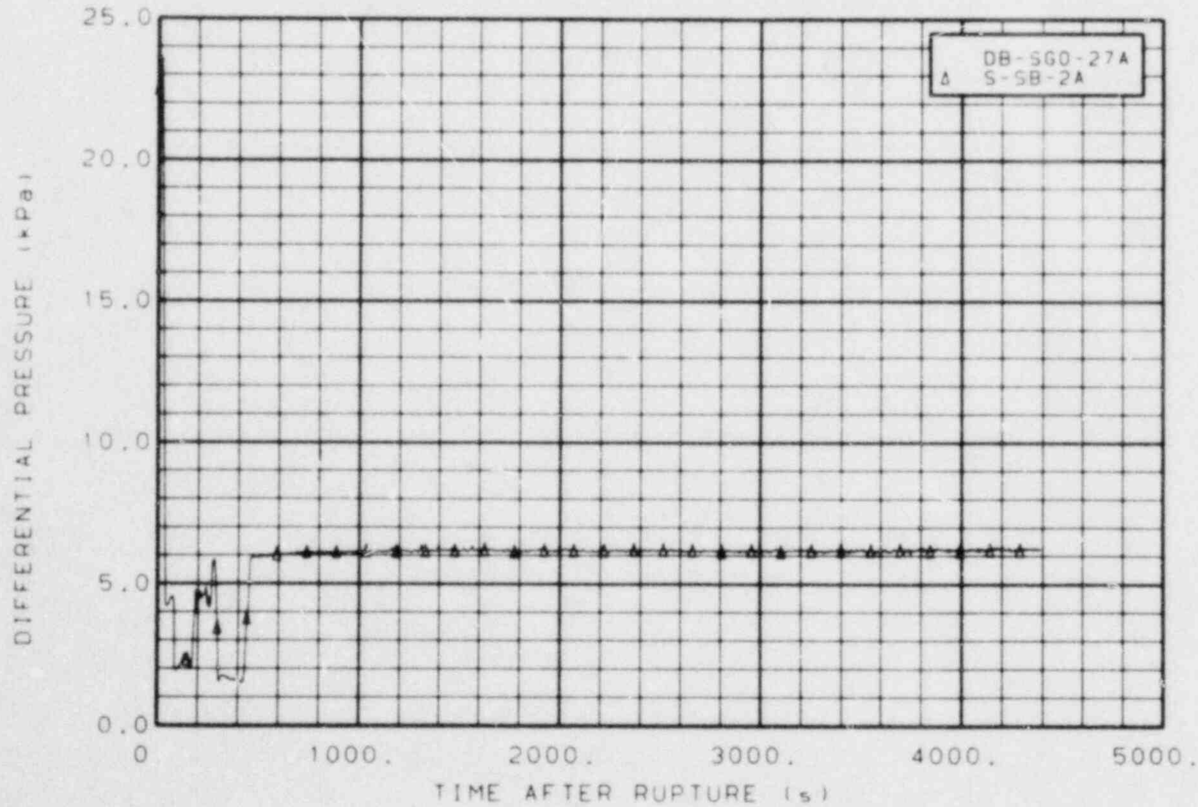

Figure 205. Differential pressure in broken loop, Test S-SB-2A (DB-SGO-27A), from 0 to 4390 s.

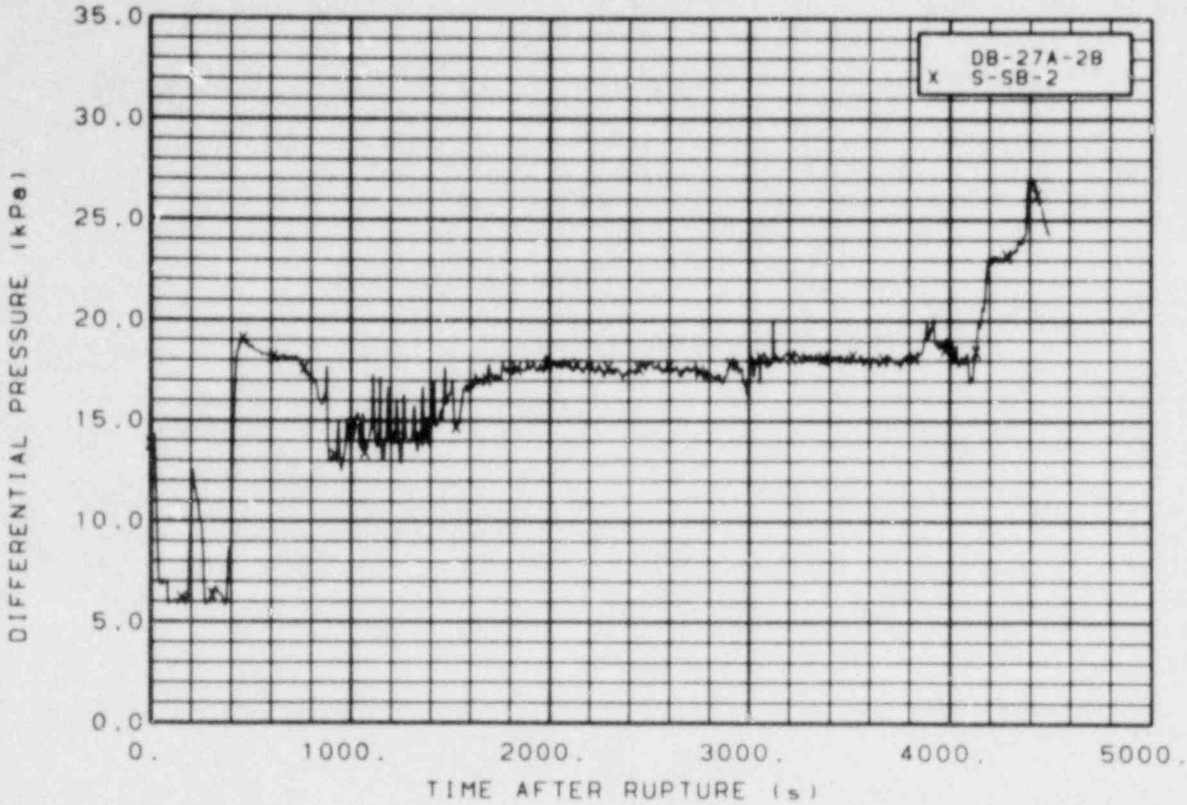

Figure 206. Differential pressure in broken loop, Test S-SB-2 (DB-27A-28), from 0 to 4500 s.

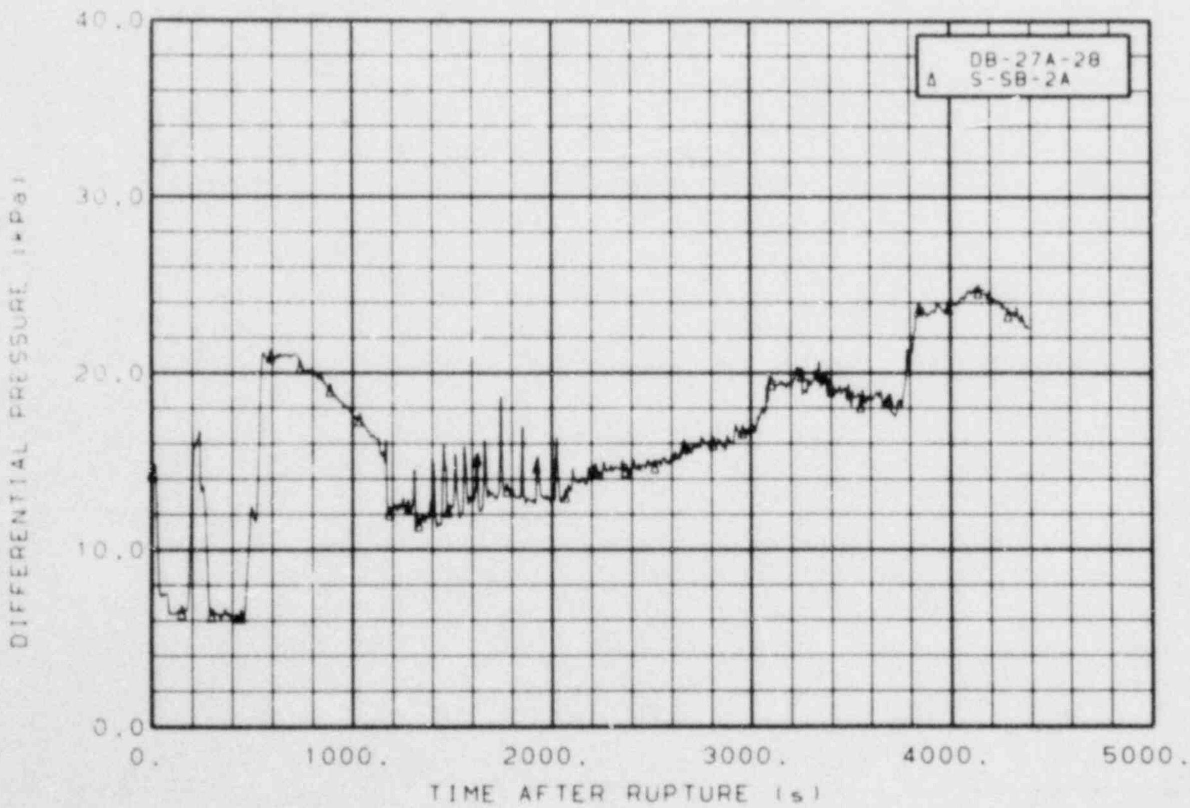

Figure 207. Differential pressure in broken loop, Test S-SB-2A (DB-27A-28), from 0 to 4390 s.

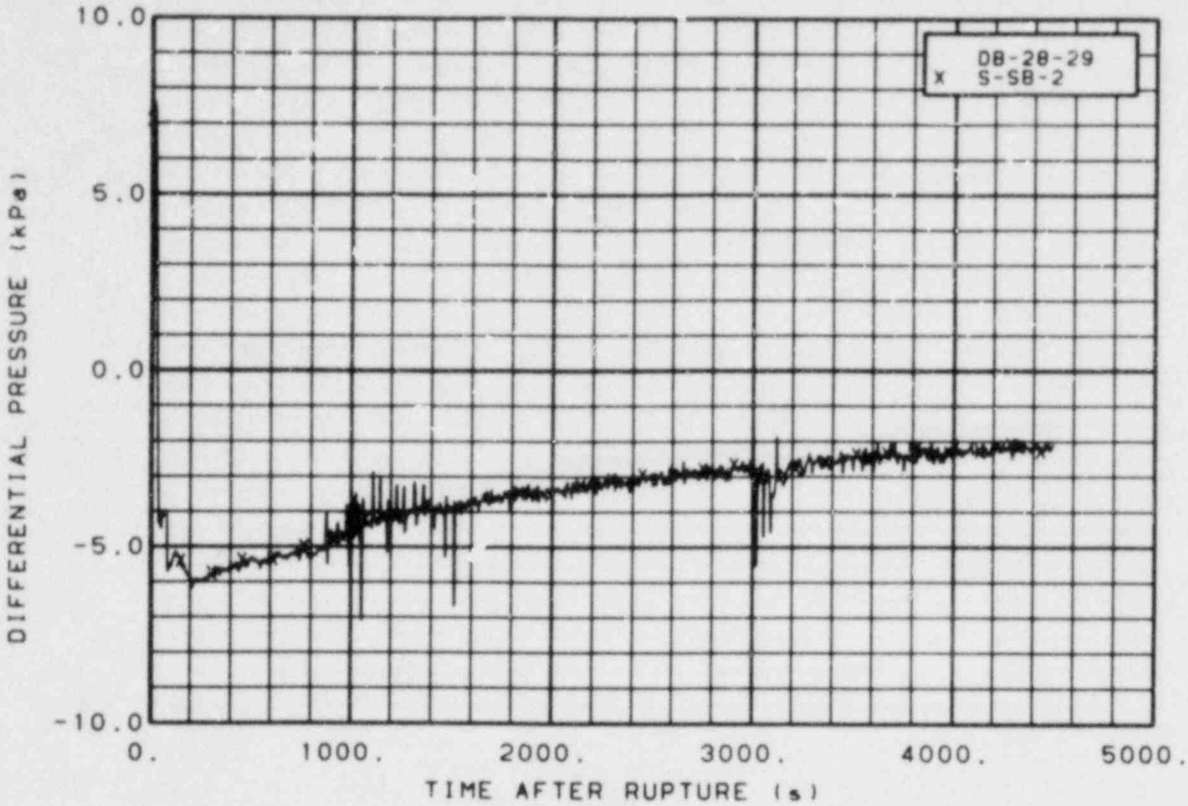

Figure 208. Differential pressure in broken loop, Test S-SB-2 (DB-28-29), from 0 to 4500 s.

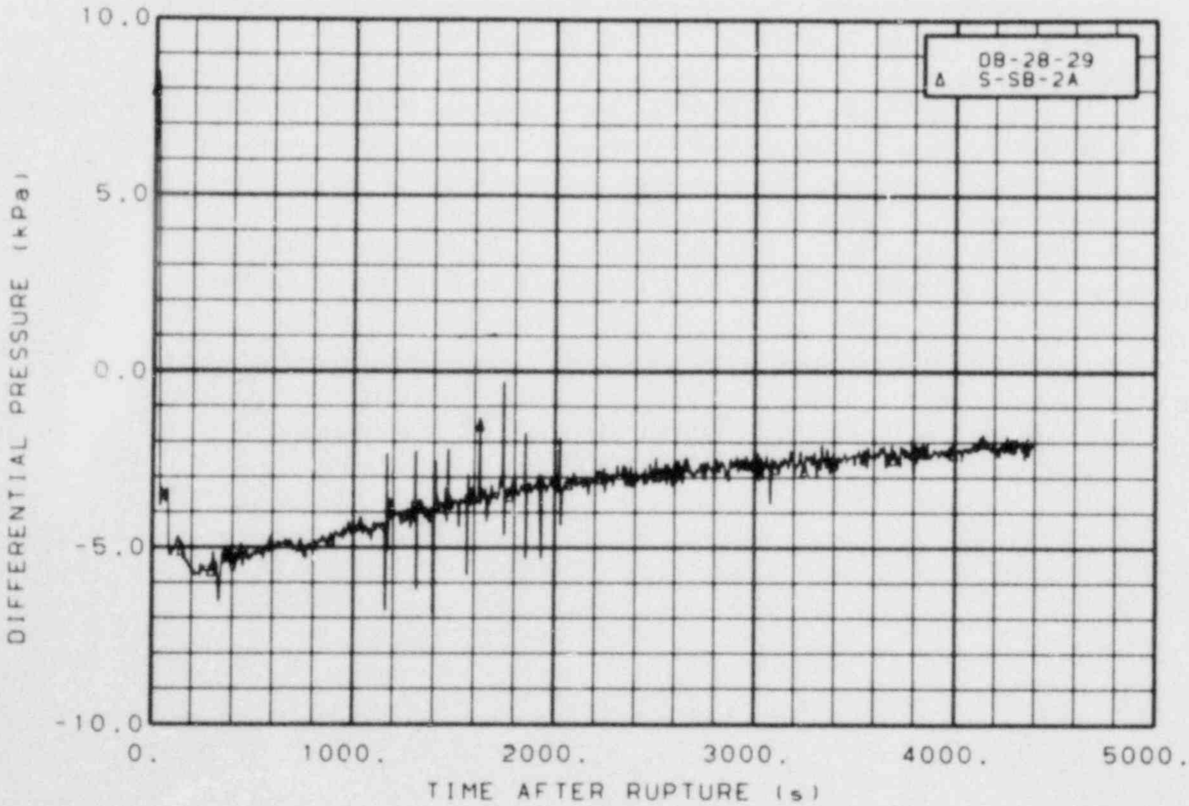

Figure 209. Differential pressure in broken loop, Test S-SB-2A (DB-28-29), from 0 to 4390 s.

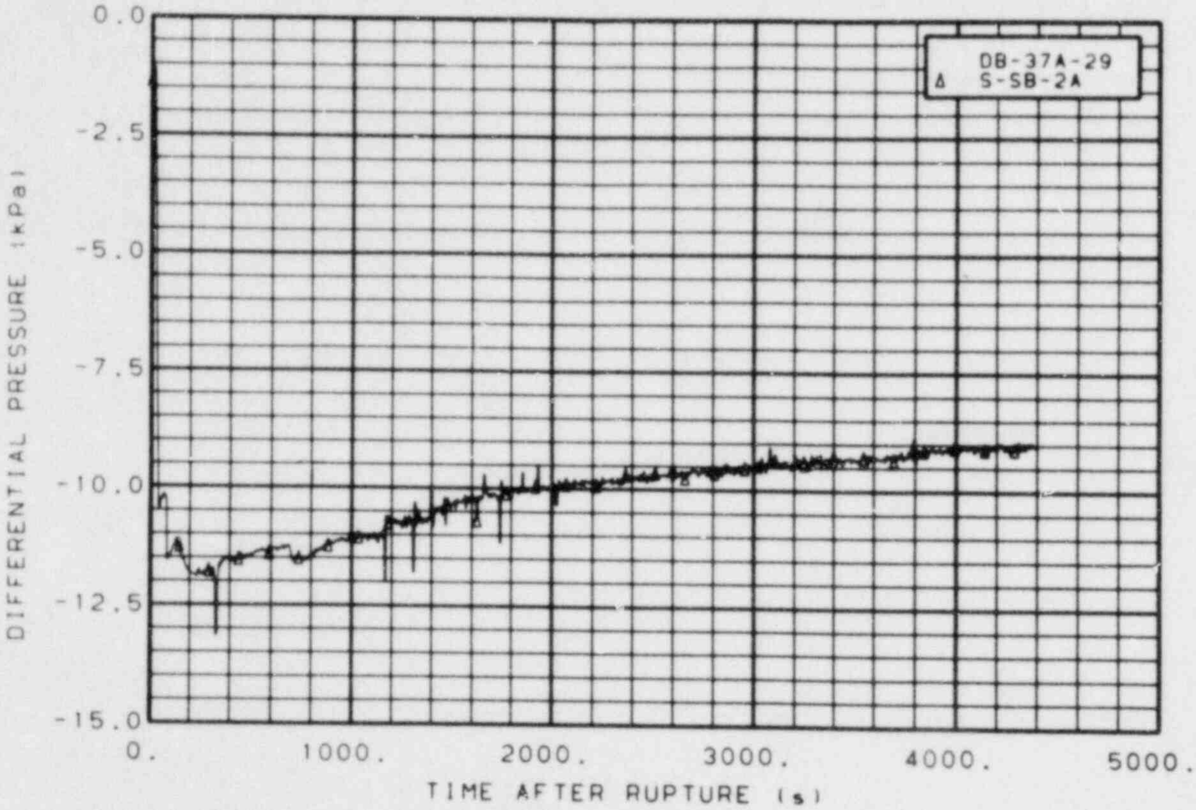

Figure 210. Differential pressure in broken loop, Test S-SB-2A (DB-37A-29), from 0 to 4390 s.

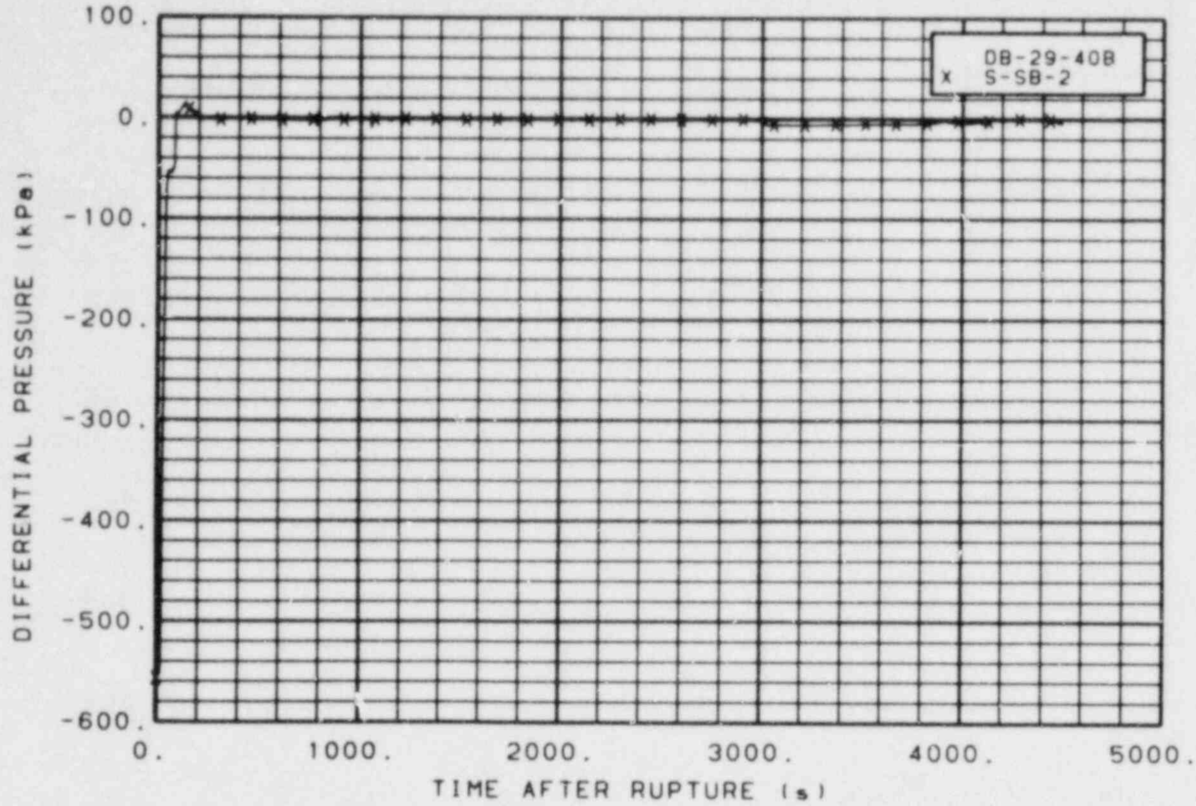

Figure 211. Differential pressure in broken loop, Test S-SB-2 (DB-29-40B), from 0 to 4500 s.

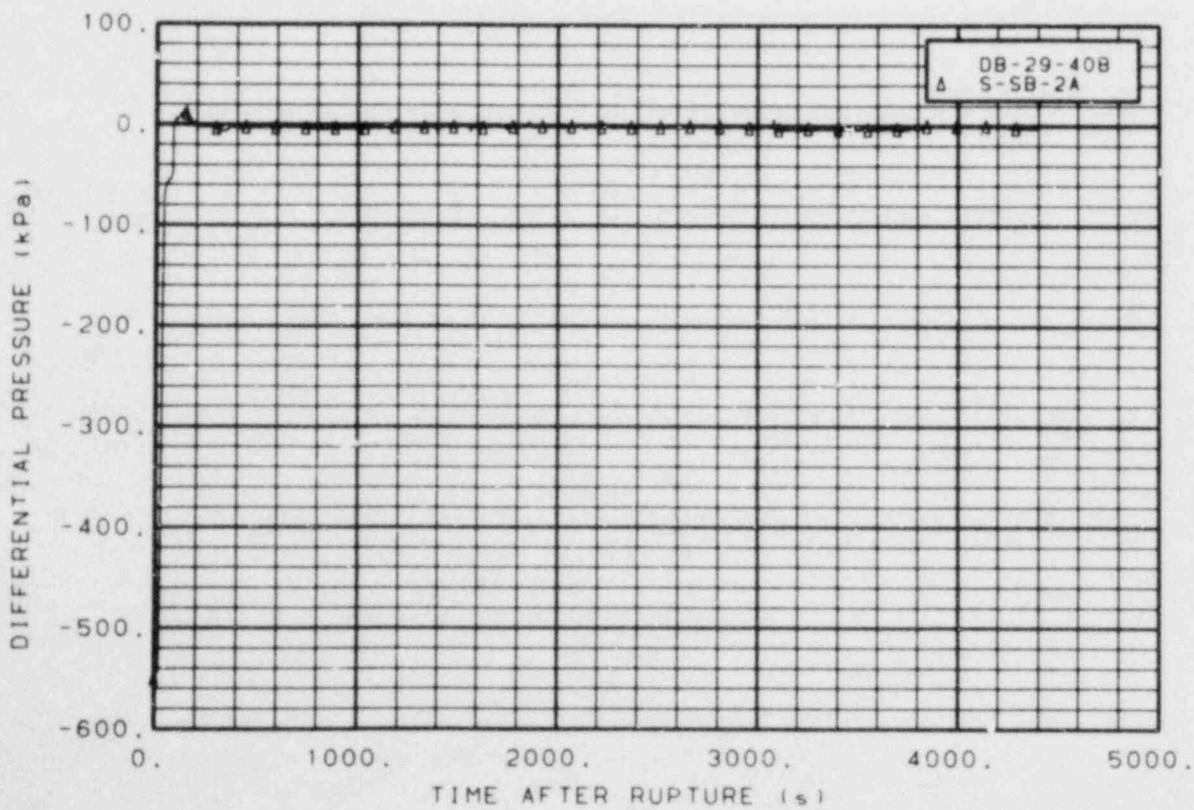

Figure 212. Differential pressure in broken loop, Test S-SB-2A (DB-29-40B), from 0 to 4390 s.

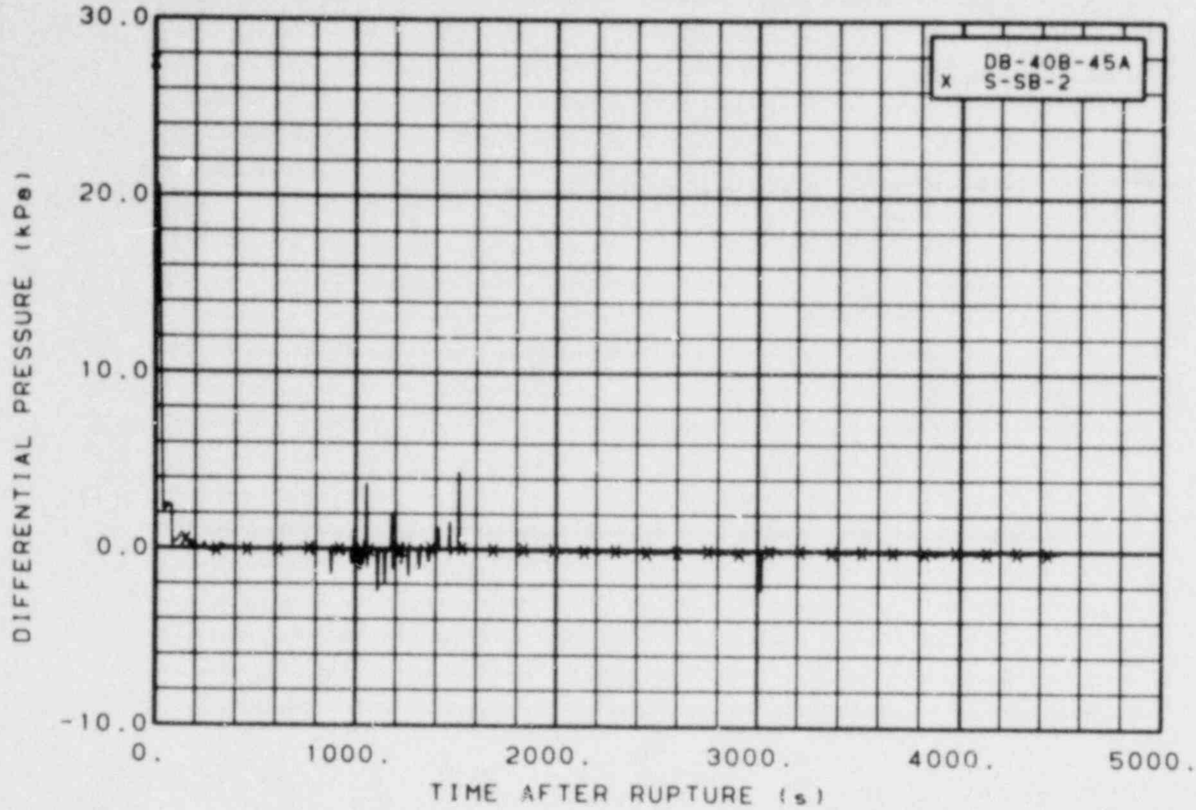

Figure 213. Differential pressure in broken loop, Test S-SB-2 (DB-40B-45A), from 0 to 4500 s.

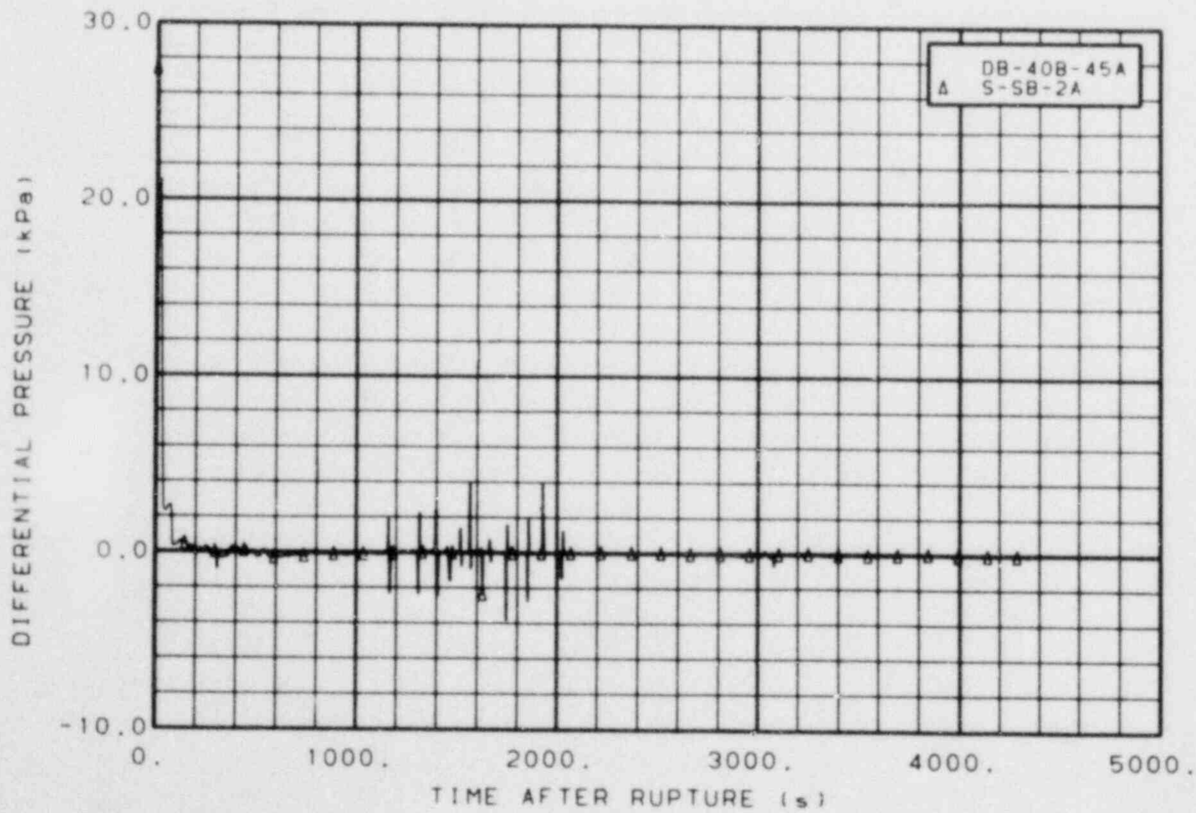

Figure 214. Differential pressure in broken loop, Test S-SB-2A (DB-40B-45A), from 0 to 4390 s.

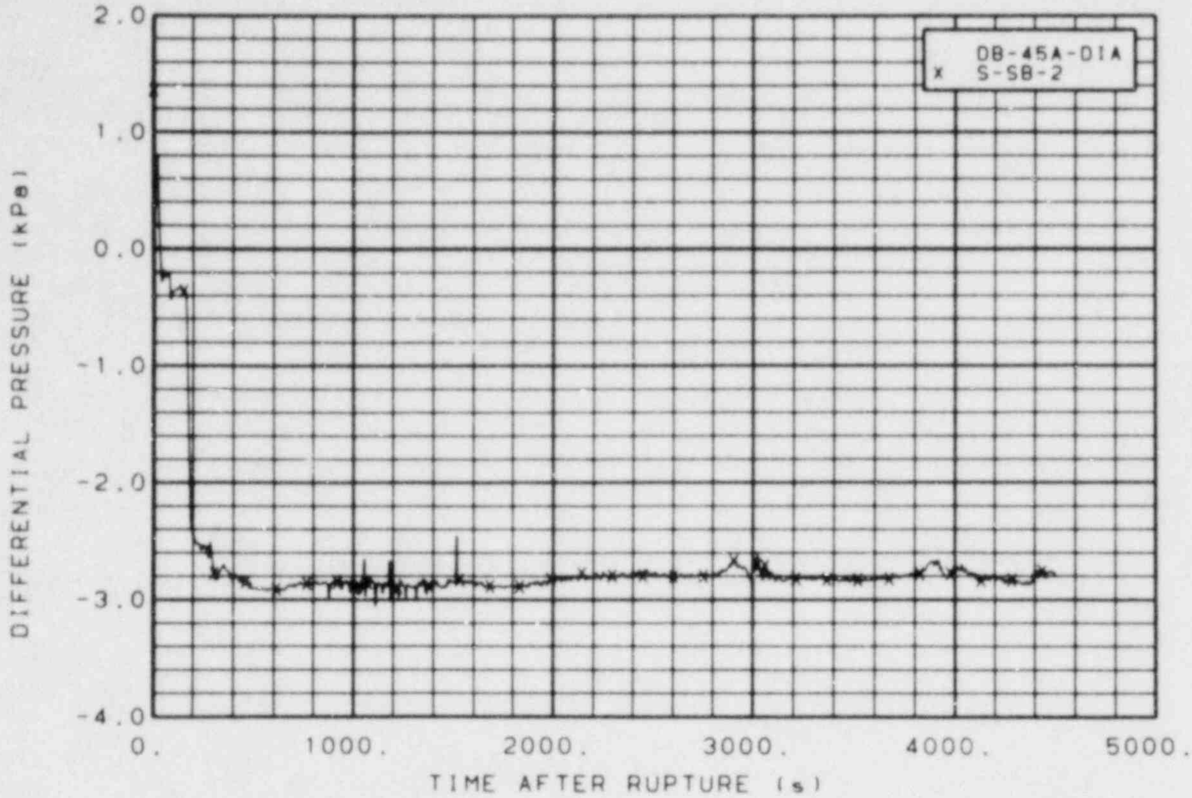

Figure 215. Differential pressure in broken loop, Test S-SB-2 (DB-45A-DIA), from 0 to 4500 s.

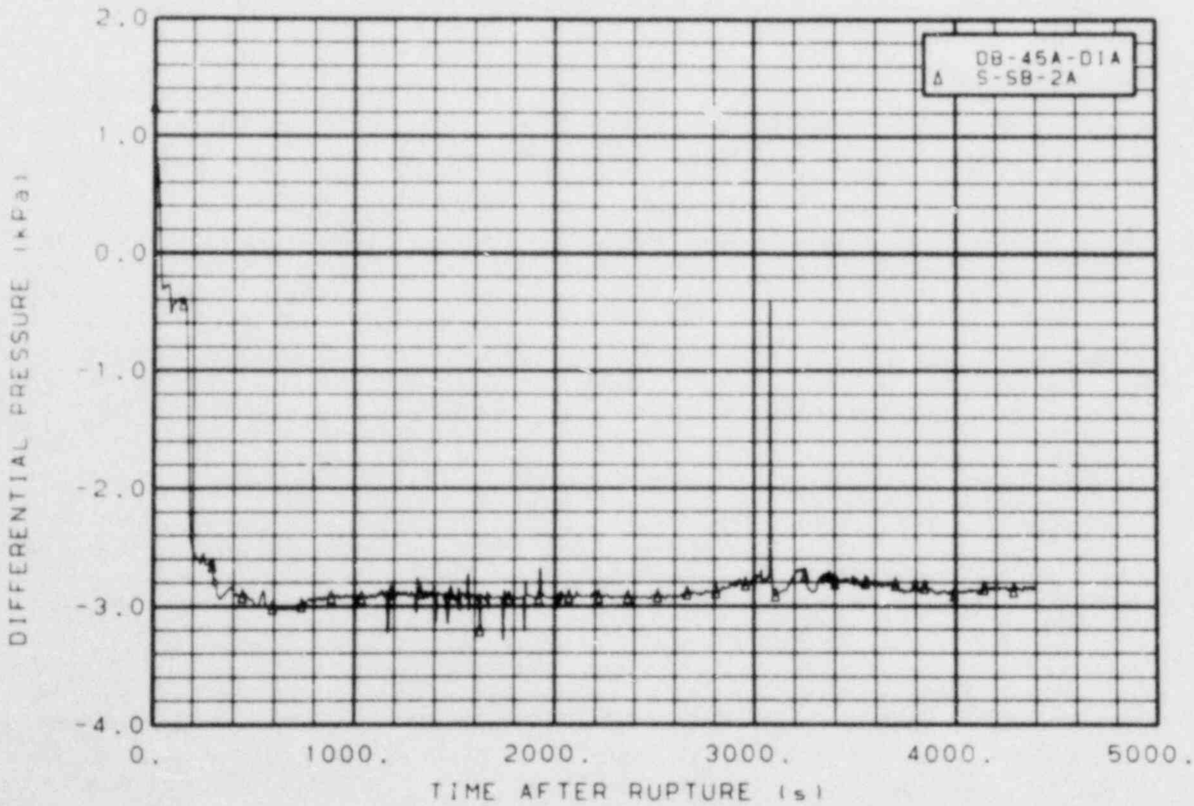

Figure 216. Differential pressure in broken loop, Test S-SB-2A (DB-45A-DIA), from 0 to 4390 s.

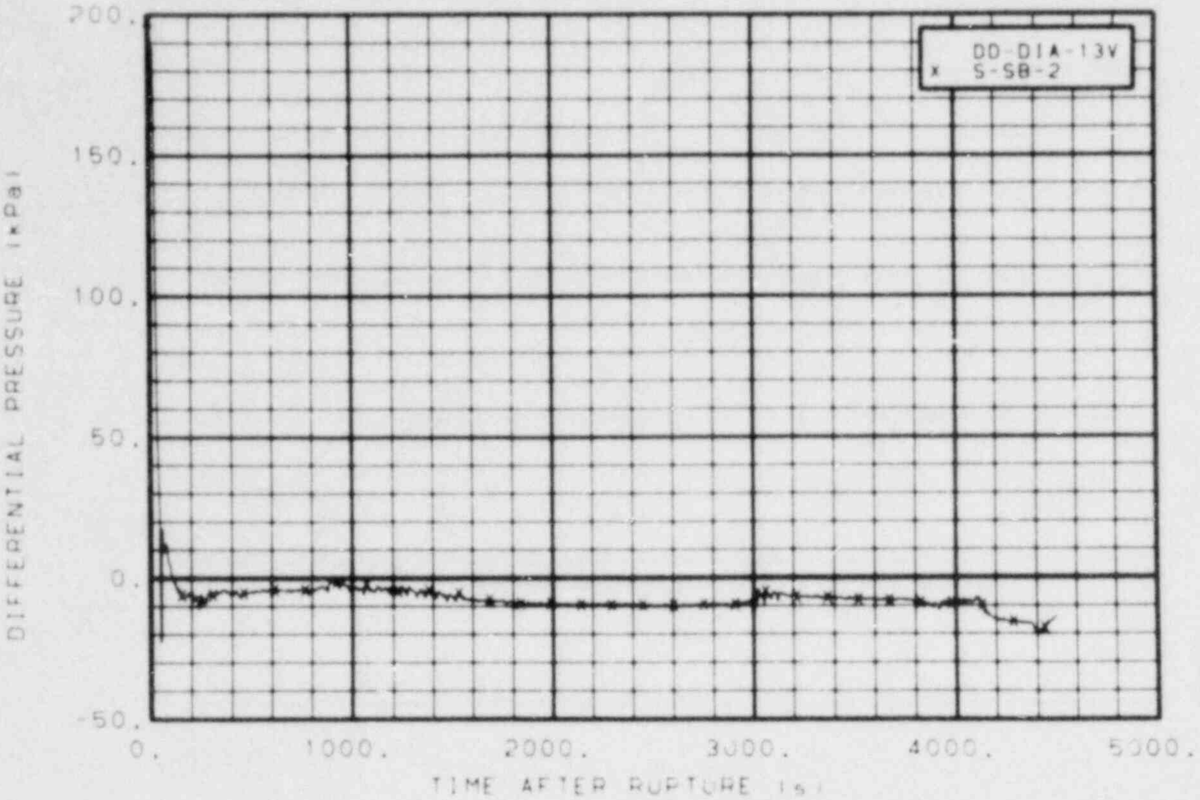

Figure 217. Differential pressure in downcomer, Test S-SB-2 (DD-DIA-13V), from 0 to 4500 s.

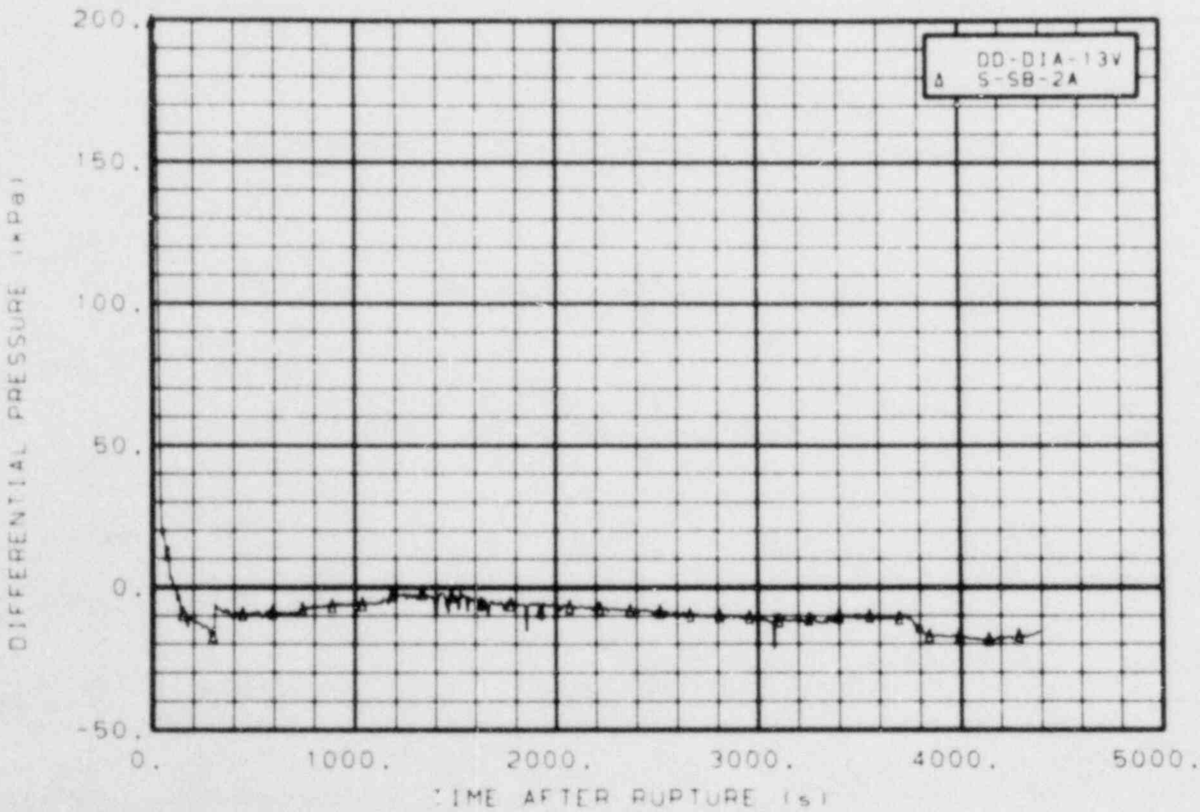

Figure 218. Differential pressure in downcomer, Test S-SB-2A (DD-DIA-13V), from 0 to 43[illegible]

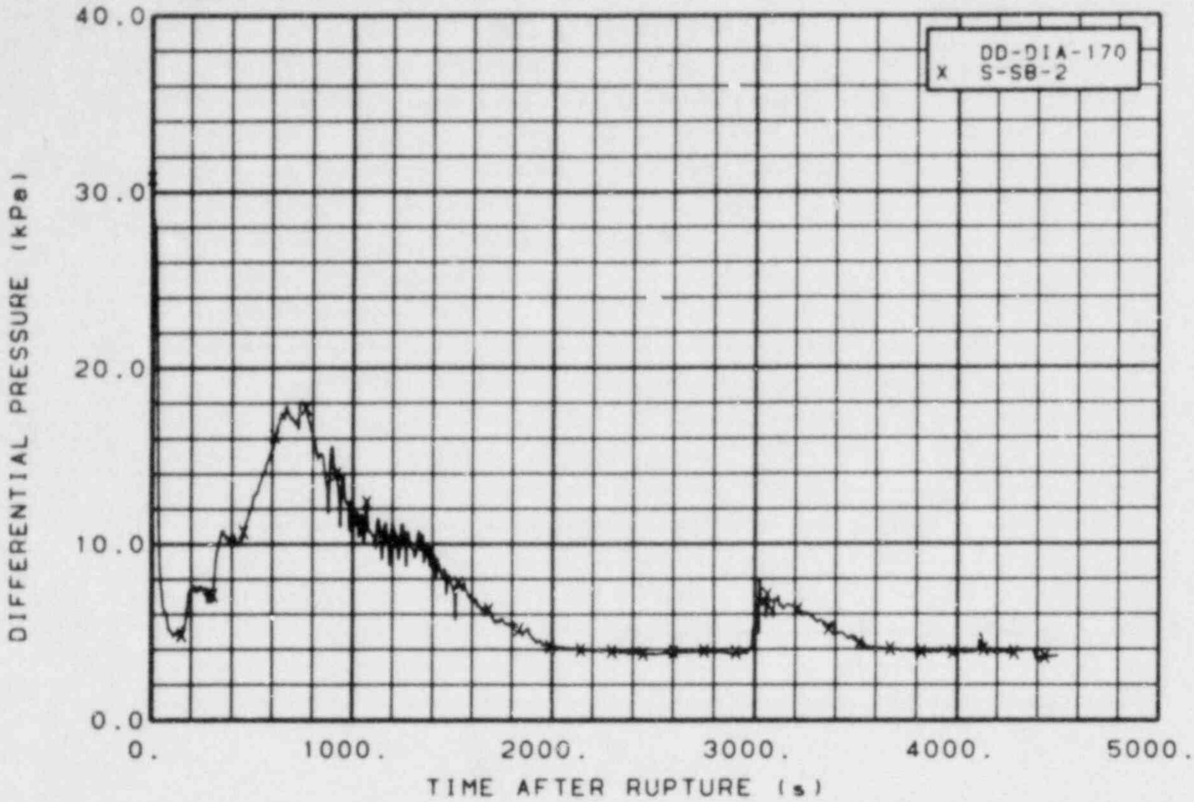

Figure 219. Differential pressure in downcomer, Test S-SB-2 (DD-DIA-170), from 0 to 4500 s.

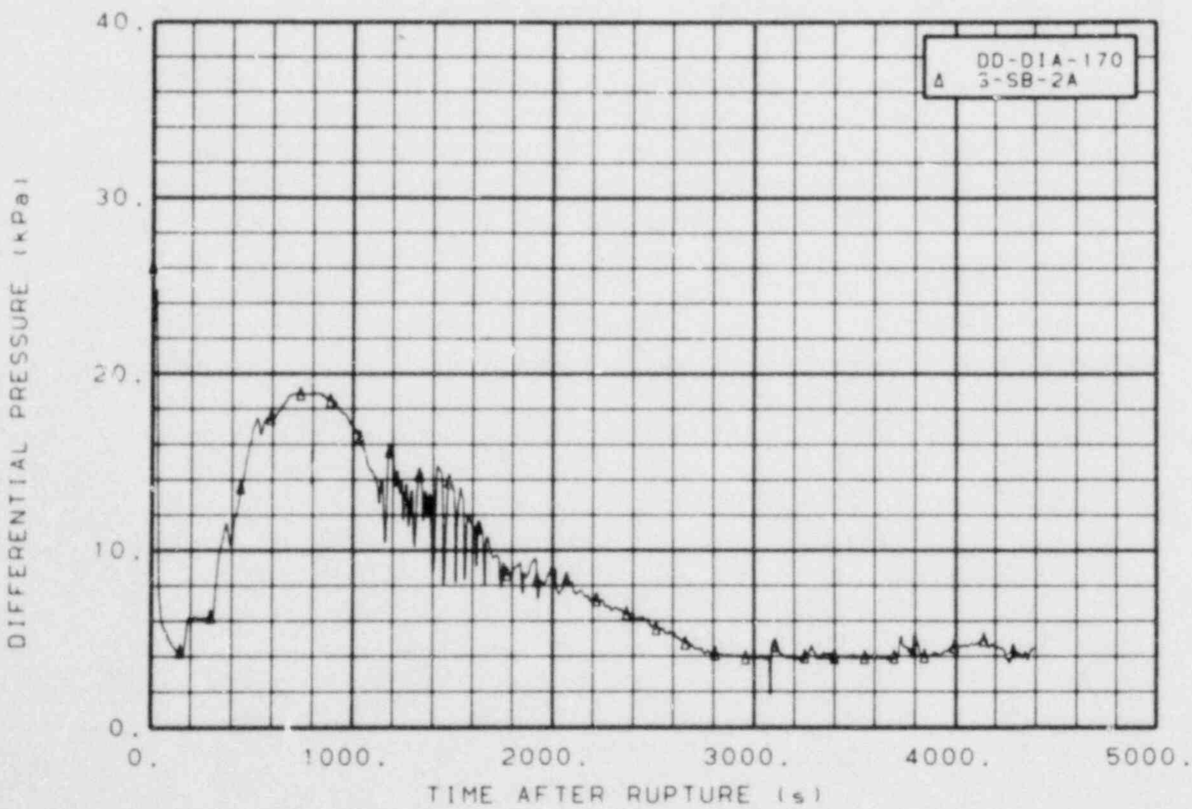

Figure 220. Differential pressure in downcomer, Test S-SB-2A (DD-DIA-170), from 0 to 4390 s.

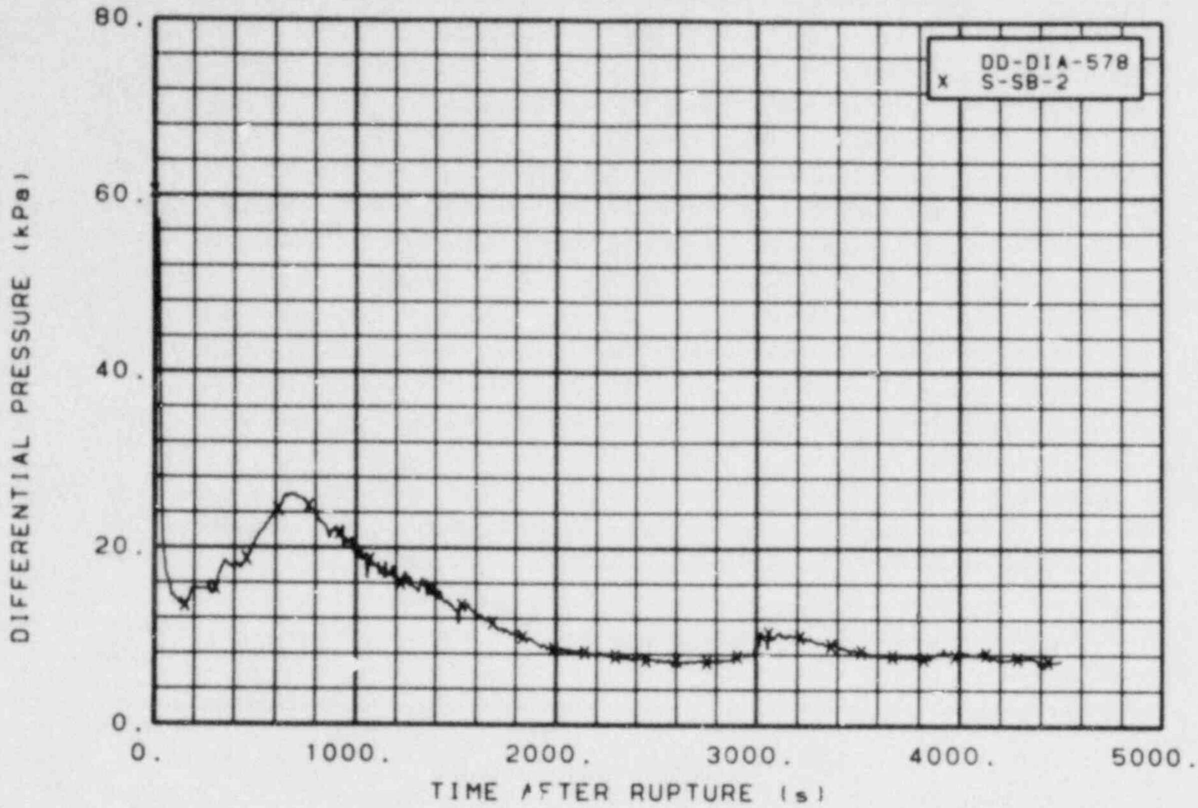

Figure 221. Differential pressure in downcomer, Test S-SB-2 (DD-DIA-578), from 0 to 4500 s.

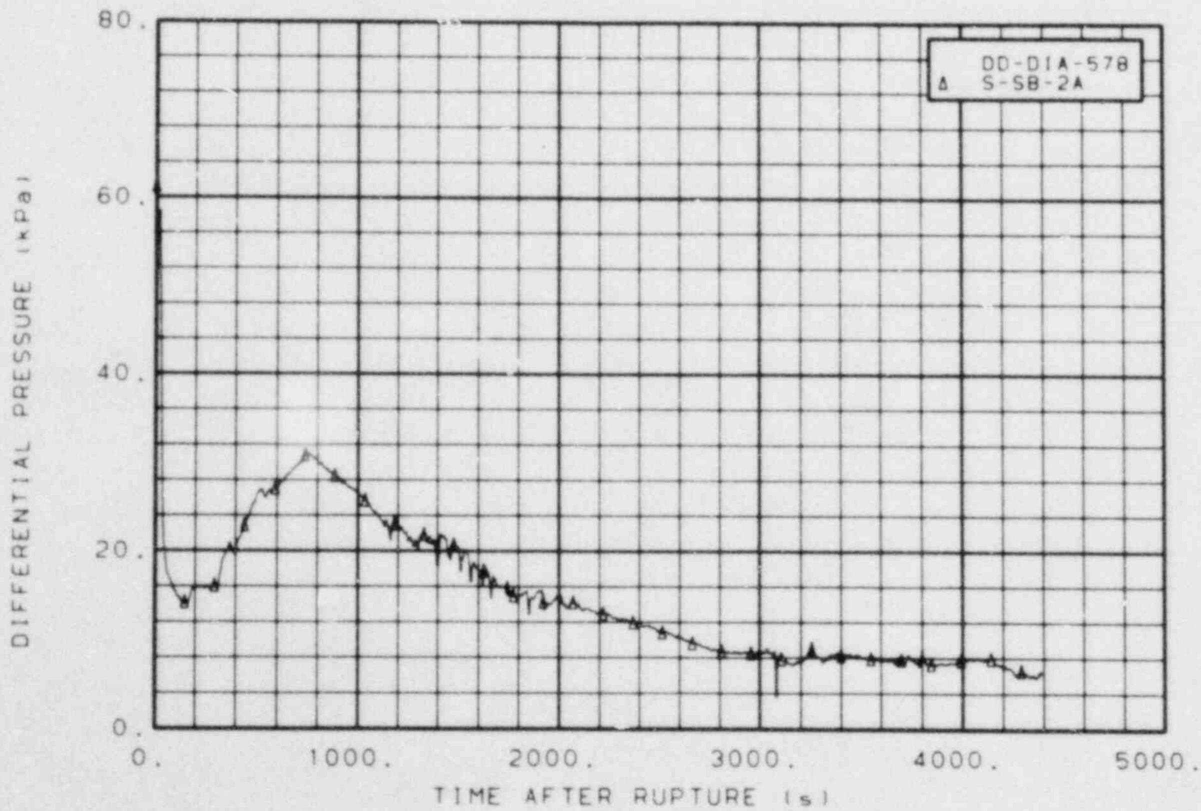

Figure 222. Differential pressure in downcomer, Test S-SB-2A (DD-DIA-578), from 0 to 4390 s.

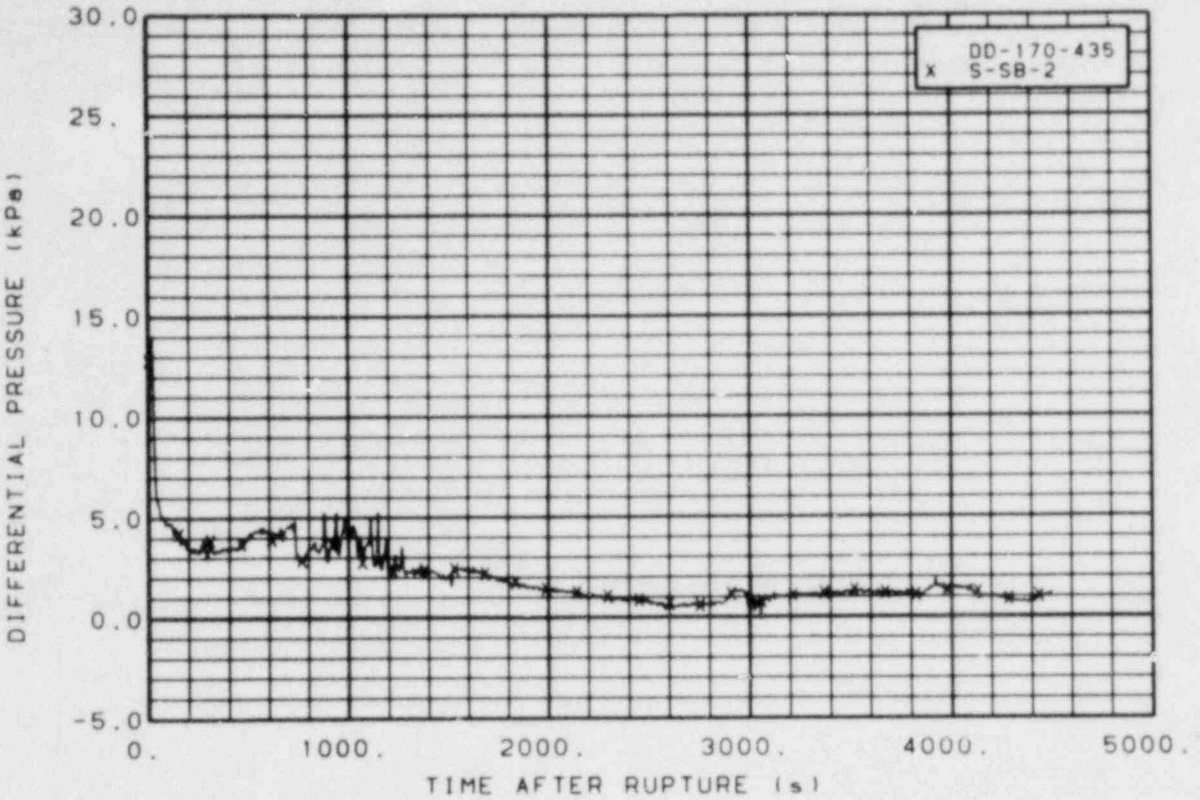

Figure 223. Differential pressure in downcomer, Test S-SB-2 (DD-170-435), from 0 to 4500 s.

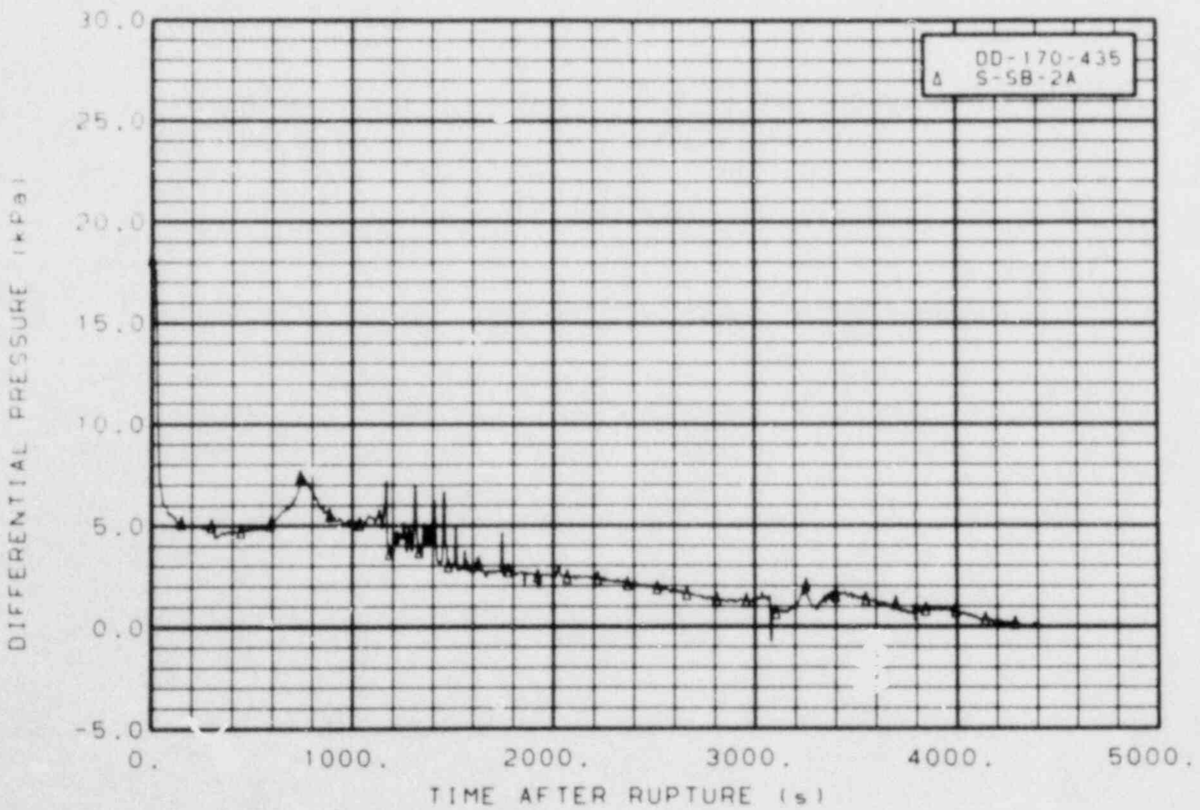

Figure 224. Differential pressure in downcomer, Test S-SB-2A (DD-170-435), from 0 to 4390 s.

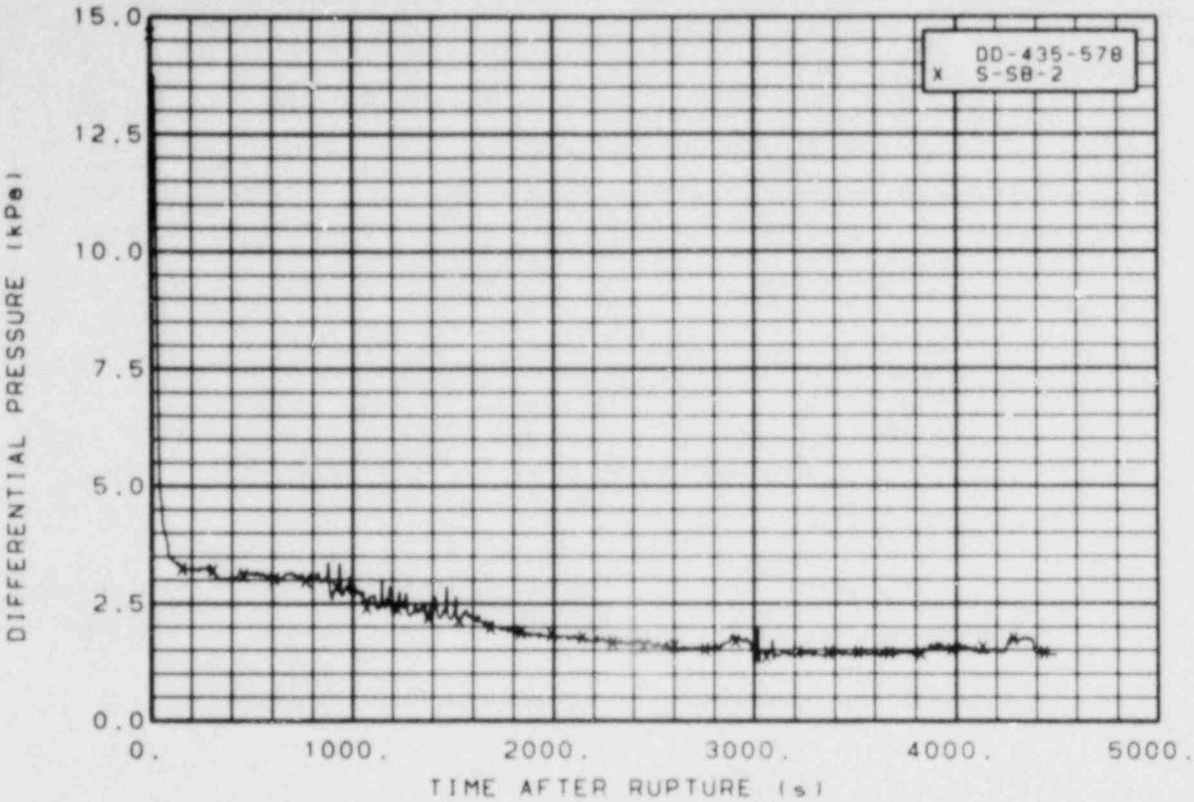

Figure 225. Differential pressure in downcomer, Test S-SB-2 (DD-435-578), from 0 to 4500 s.

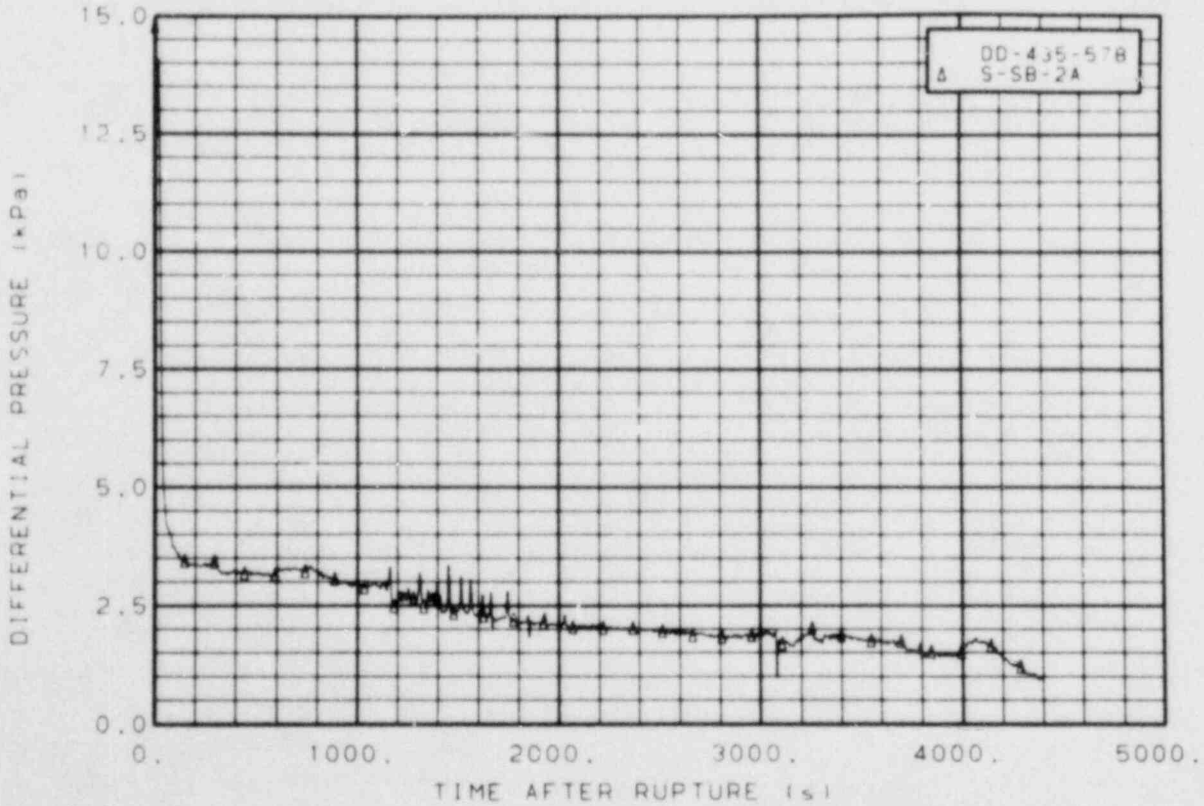

Figure 226. Differential pressure in downcomer, Test S-SB-2A (DD-435-578), from 0 to 4390 s.

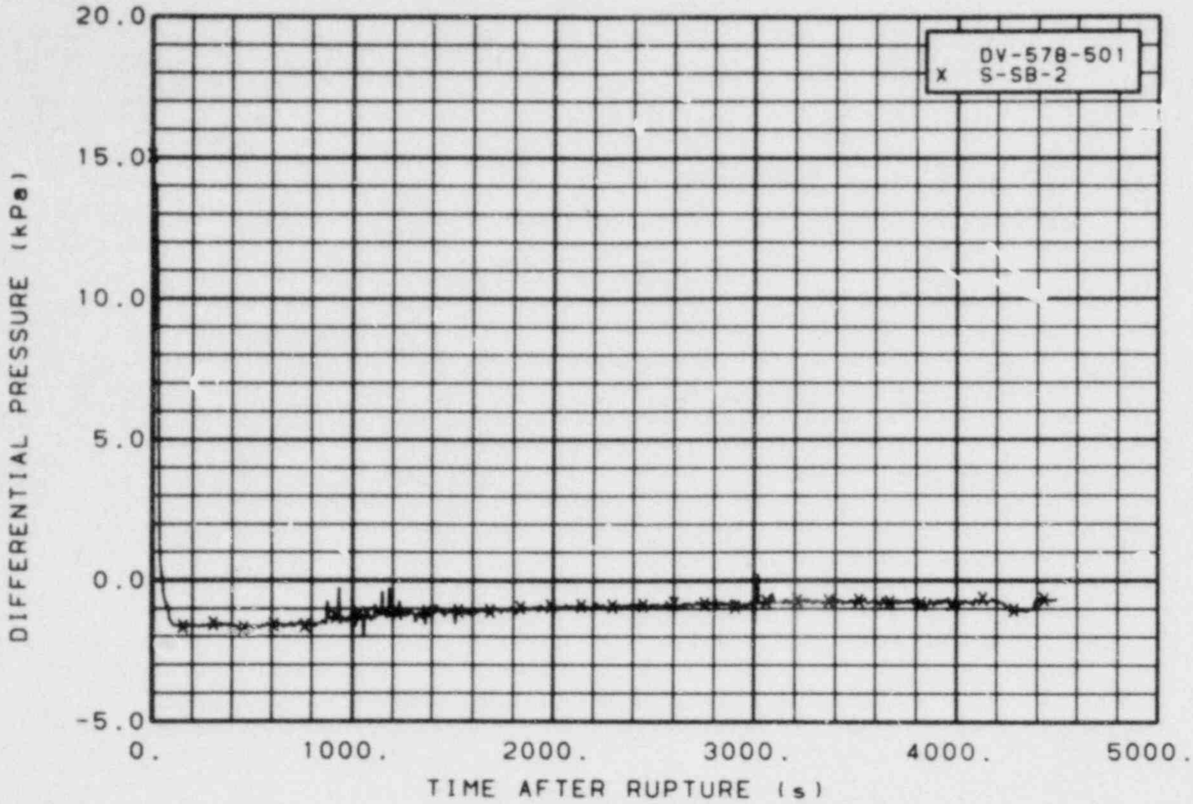

Figure 227. Differential pressure in downcomer, Test S-SB-2 (DV-578-501), from 0 to 4500 s.

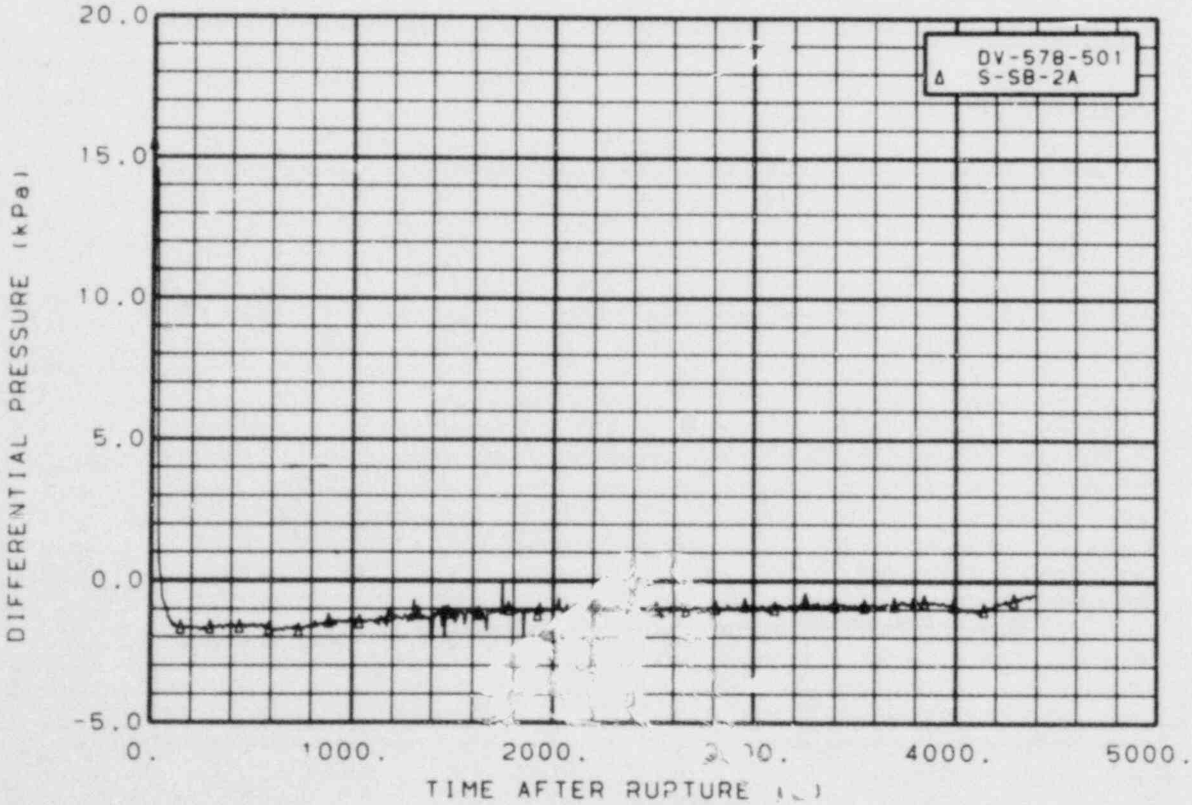

Figure 228. Differential pressure in downcomer, Test S-SB-2A (DV-578-501), from 0 to 4390 s.

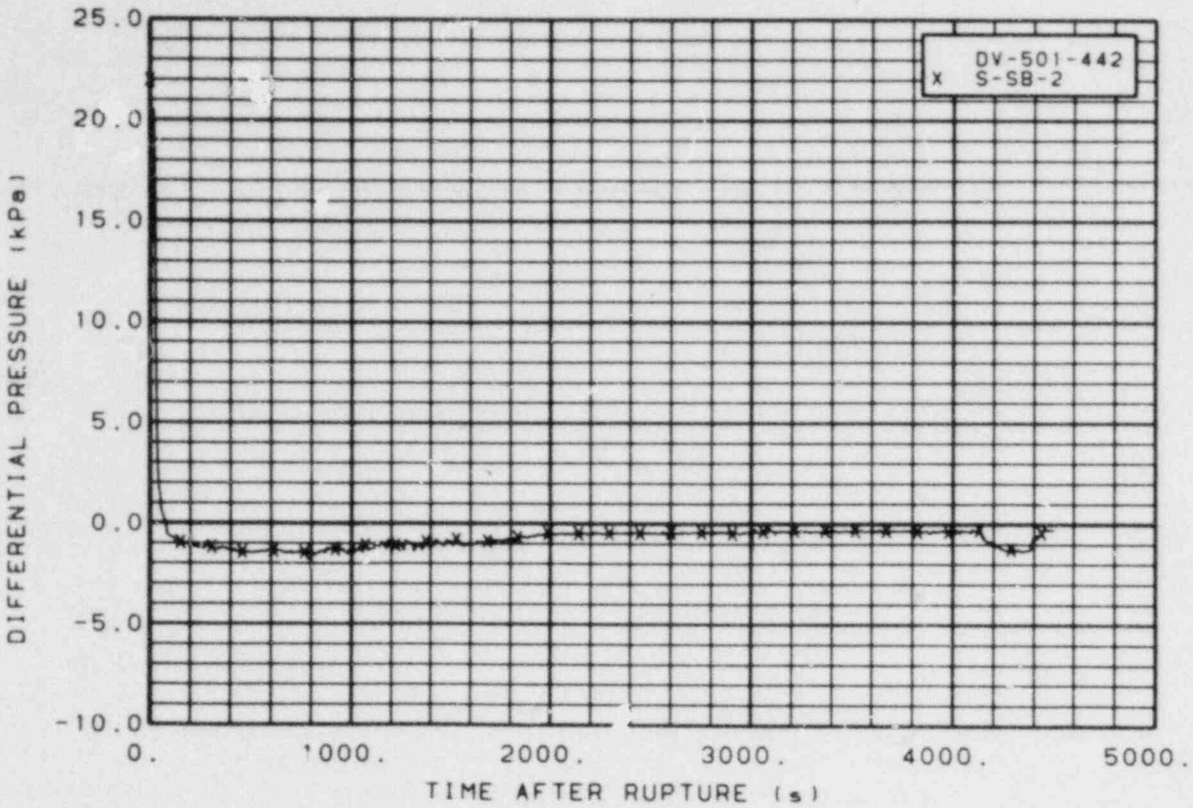

Figure 229. Differential pressure in vessel, Test S-SB-2 (DV-501-442), from 0 to 4500 s.

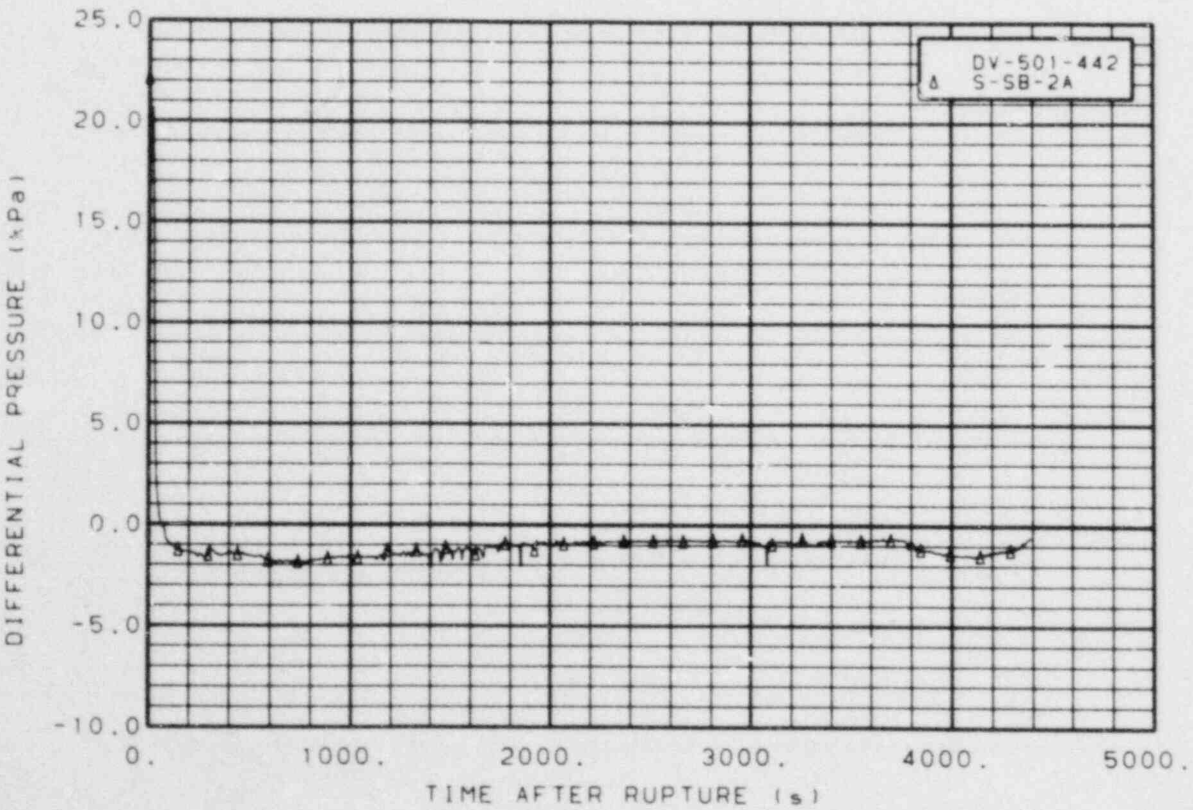

Figure 230. Differential pressure in vessel, Test S-SB-2A (DV-501-442), from 0 to 4390 s.

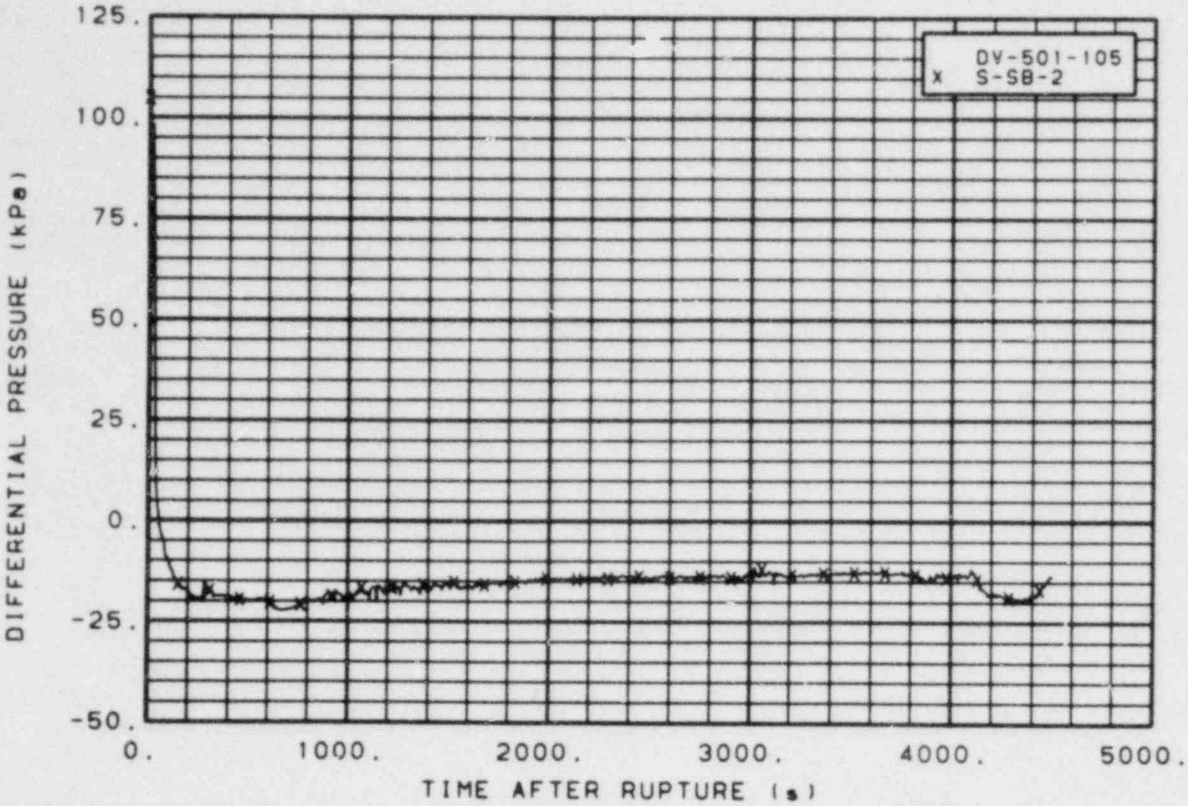

Figure 231. Differential pressure in vessel, Test S-SB-2 (DV-501-105), from 0 to 4500 s.

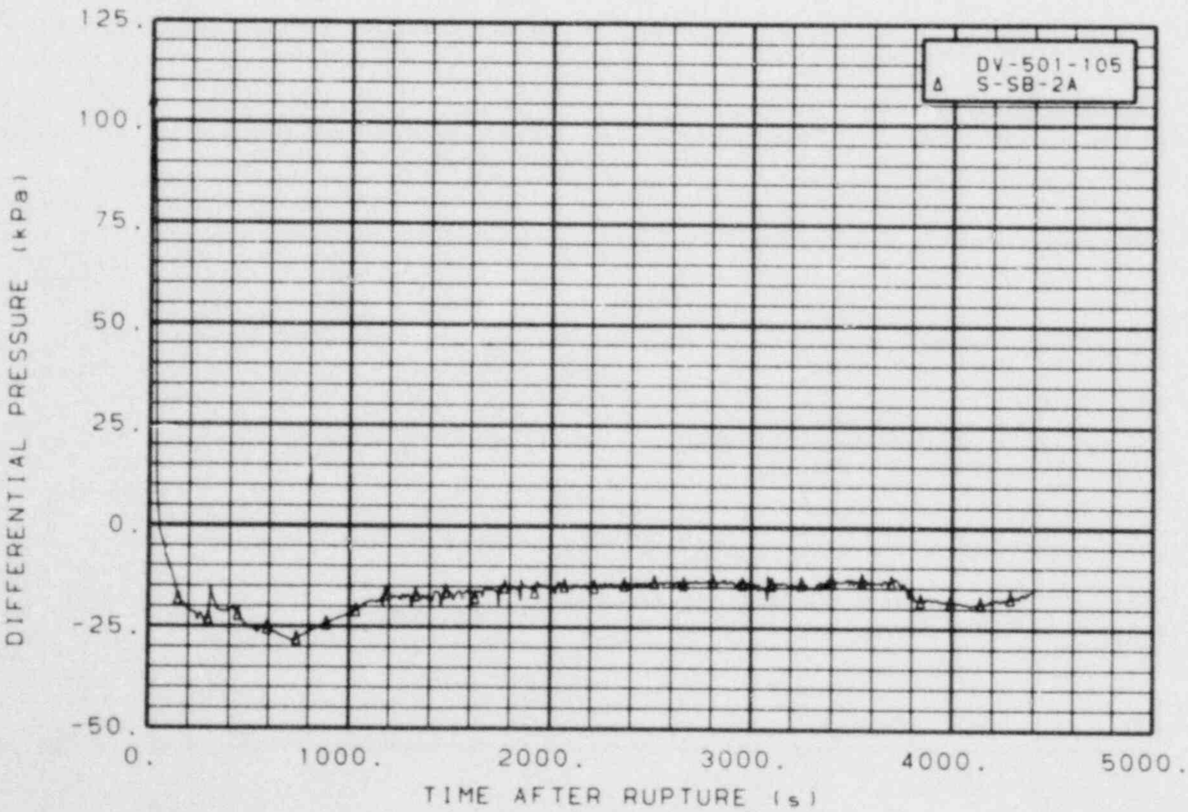

Figure 232. Differential pressure in vessel, Test S-SB-2A (DV-501-105), from 0 to 4390 s.

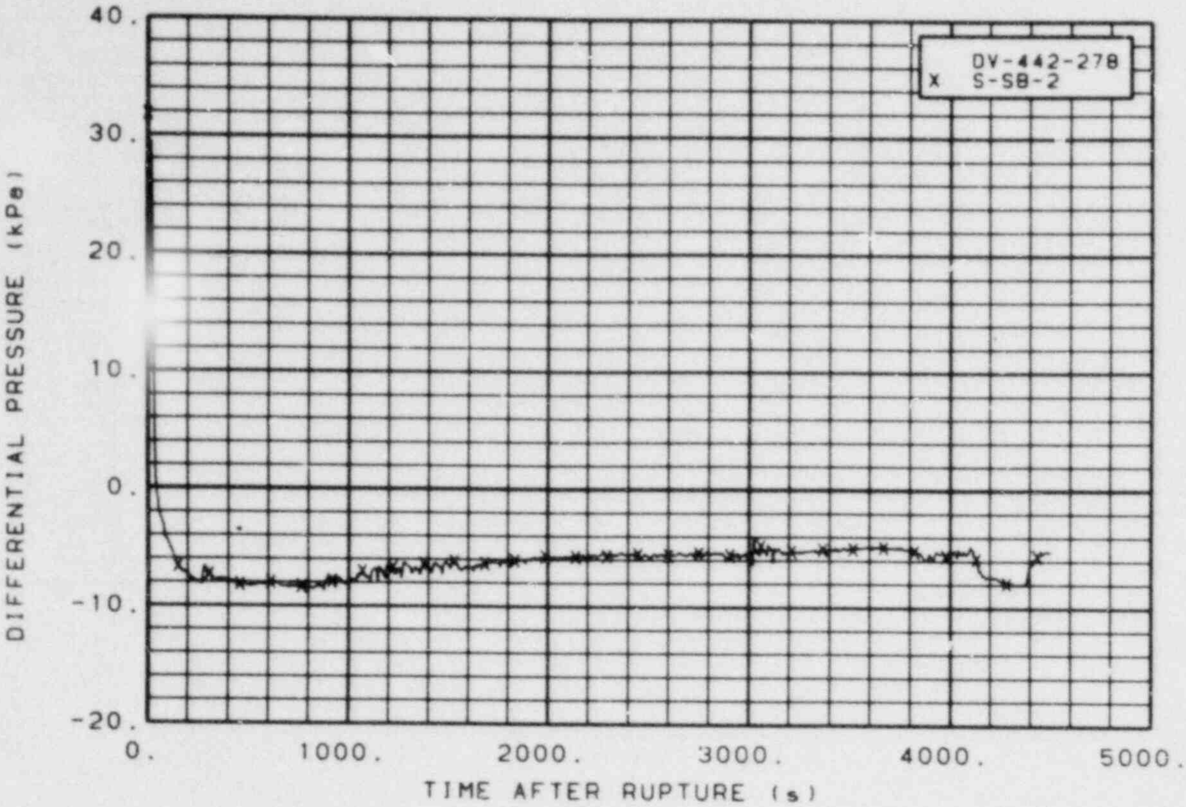

Figure 233. Differential pressure in vessel, Test S-SB-2 (DV-442-278), from 0 to 4500 s.

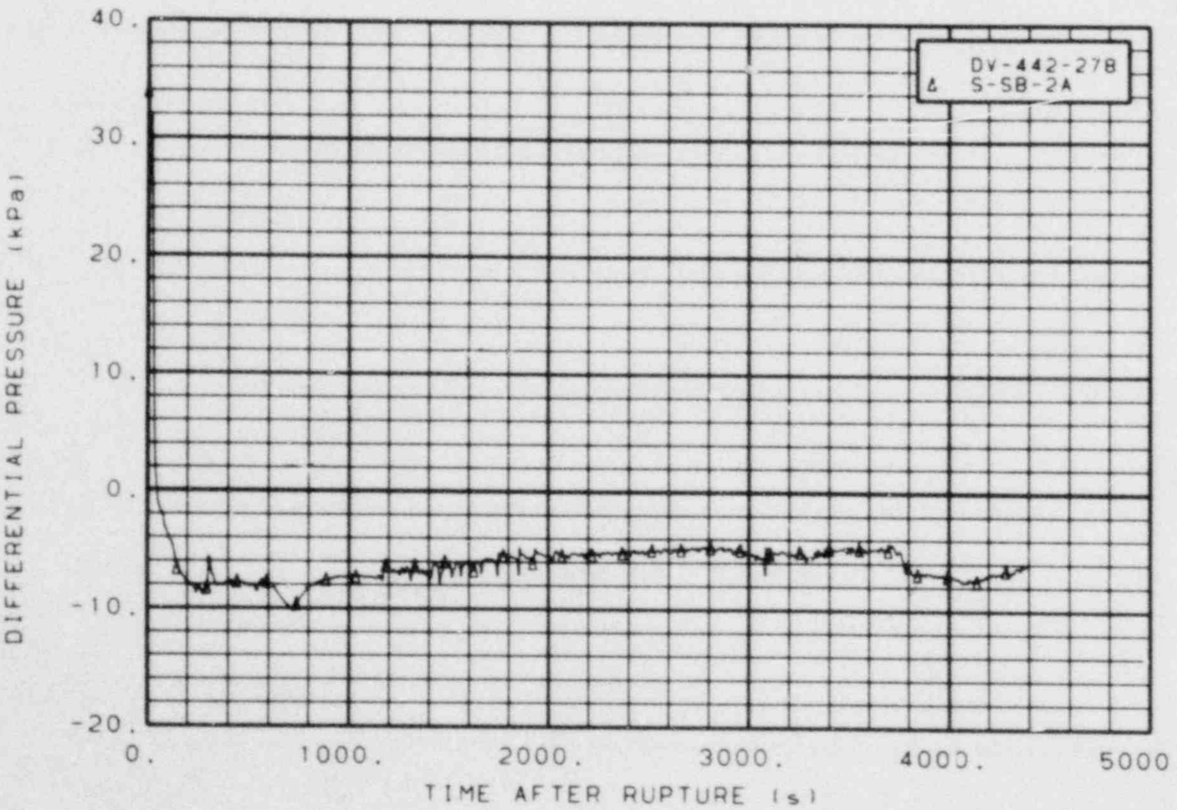

Figure 234. Differential pressure in vessel, Test S-SB-2A (DV-442-278), from 0 to 4390 s.

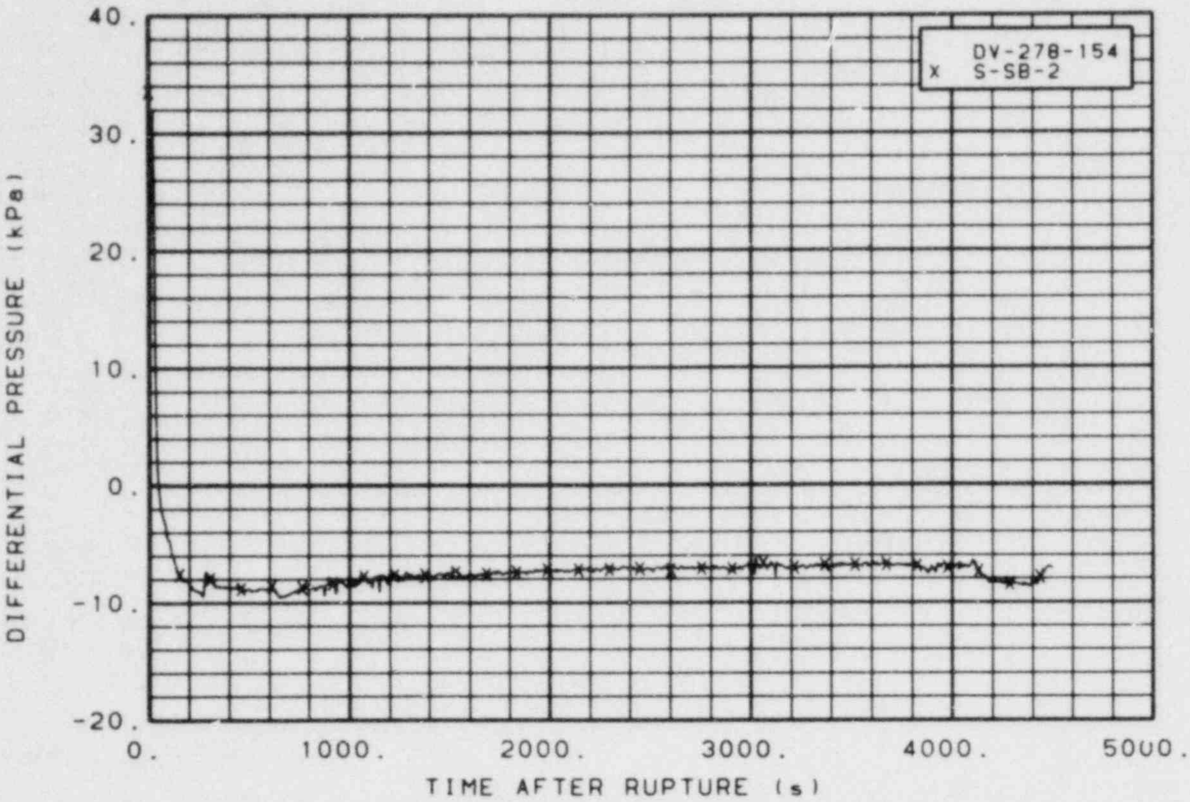

Figure 235. Differential pressure in vessel, Test S-SB-2 (DV-278-154), from 0 to 4500 s.

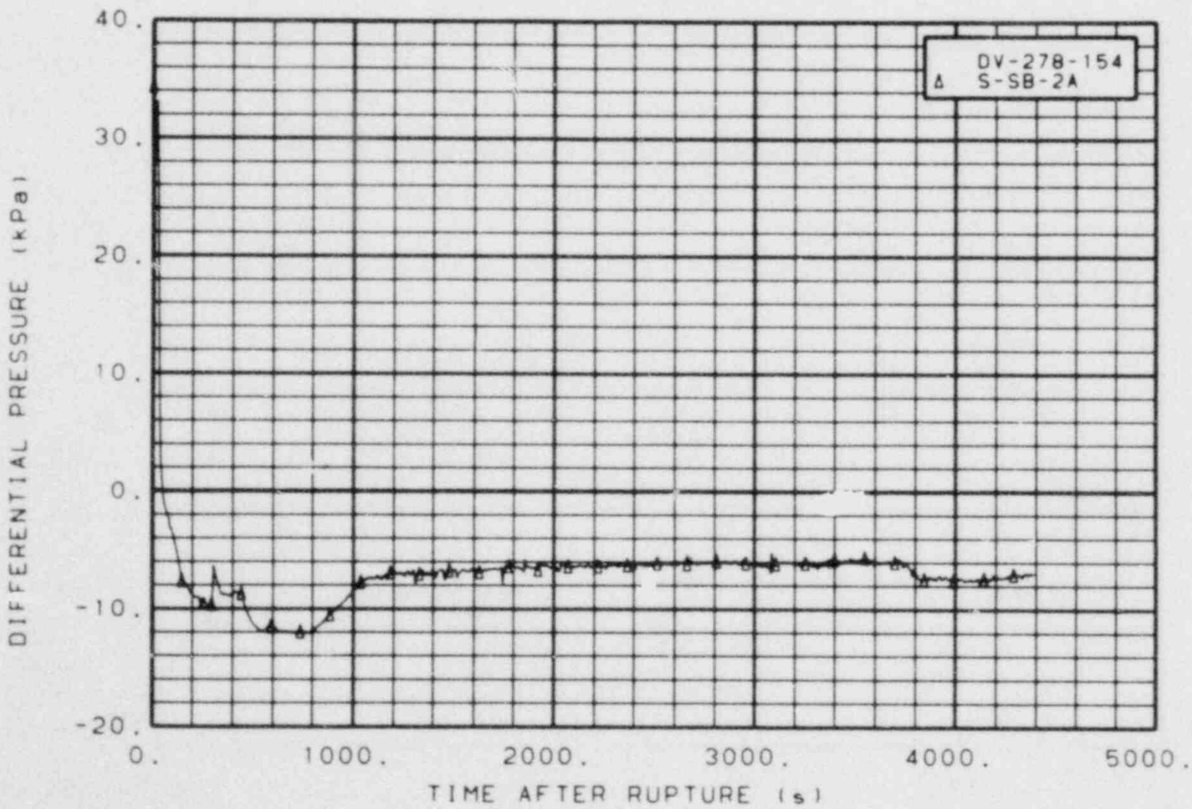

Figure 236. Differential pressure in vessel, Test S-SB-2A (DV-278-154), from 0 to 4390 s.

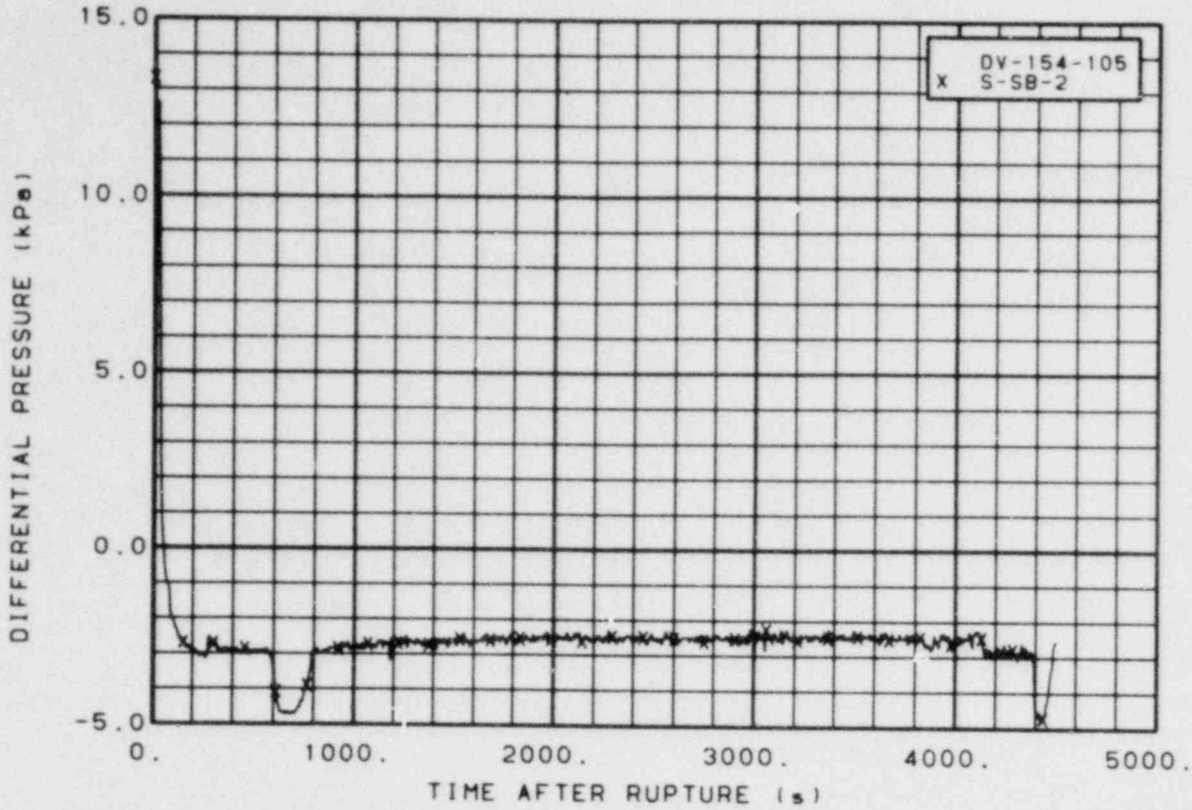

Figure 237. Differential pressure in vessel, Test S-SB-2 (DV-154-105), from 0 to 4500 s.

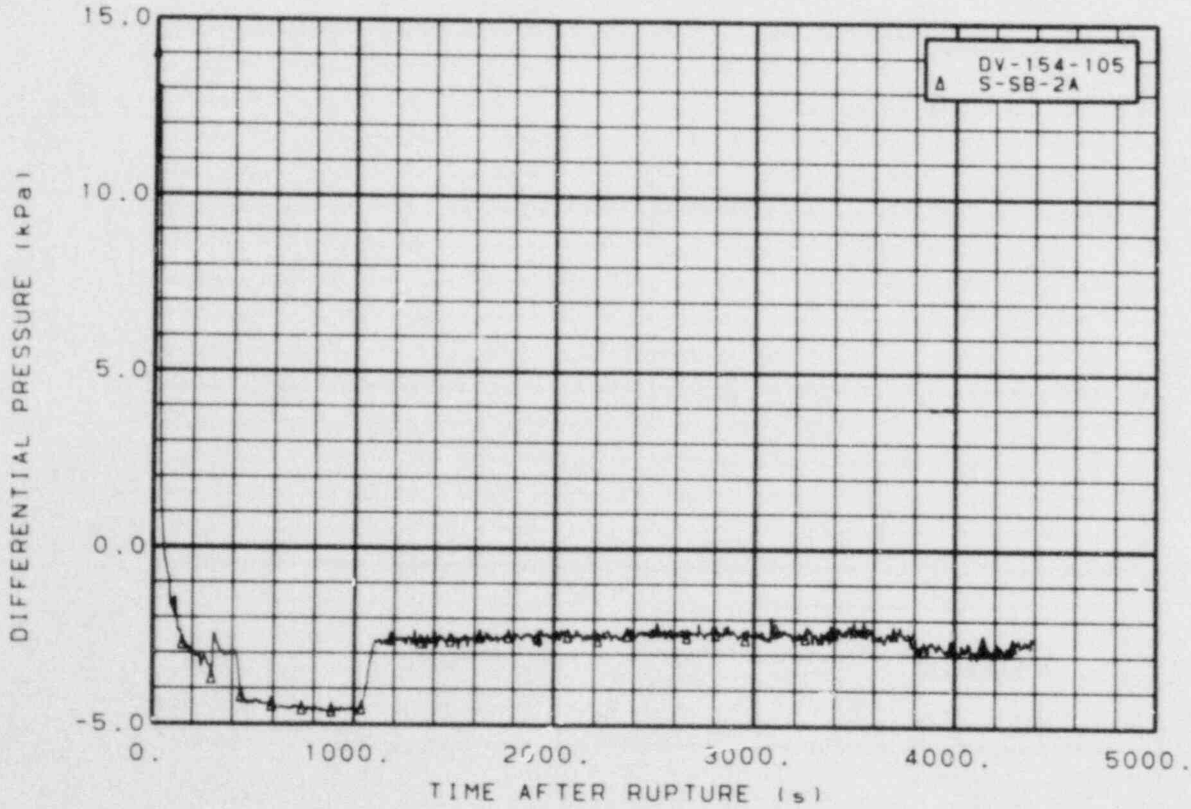

Figure 238. Differential pressure in vessel, Test S-SB-2A (DV-154-105), from 0 to 4390 s.

Figure 239. Differential pressure in vessel, Test S-SB-2A (DV-154 + 154), from 0 to 4390 s.

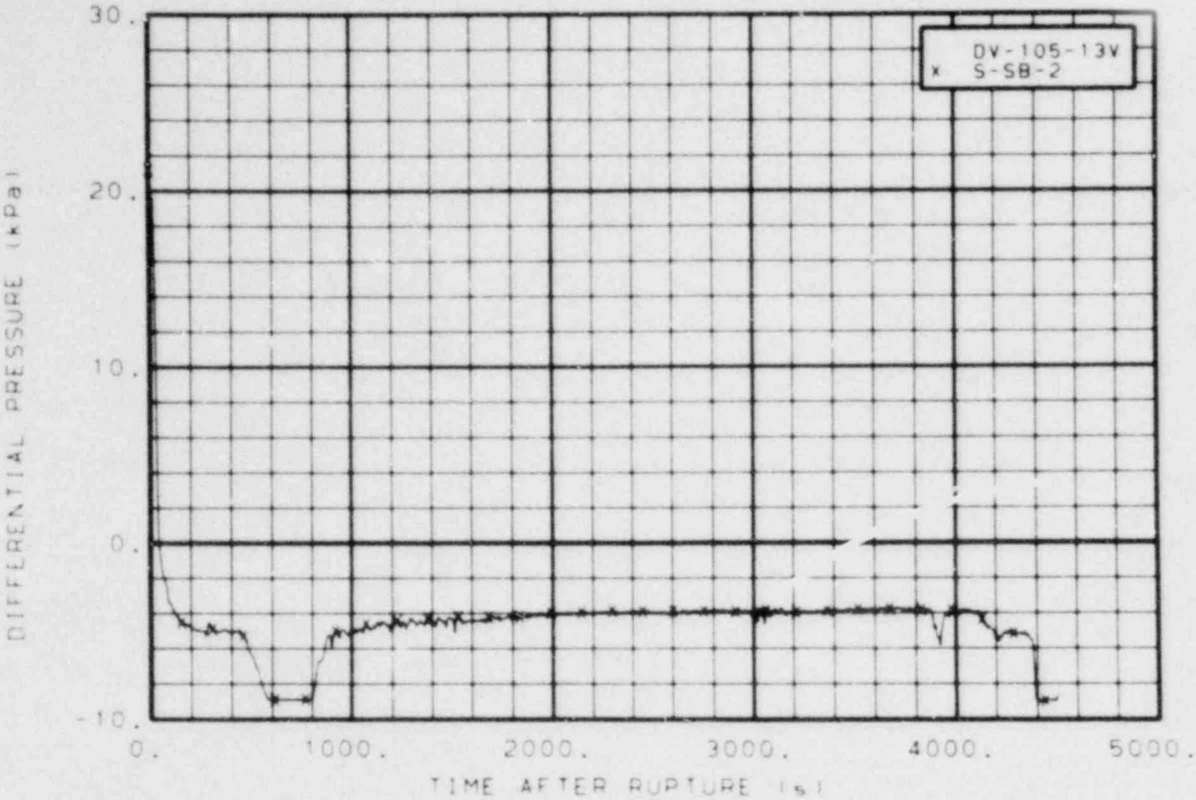

Figure 240. Differential pressure in vessel, Test S-SB-2 (DV-105-13V), from 0 to 4500 s.

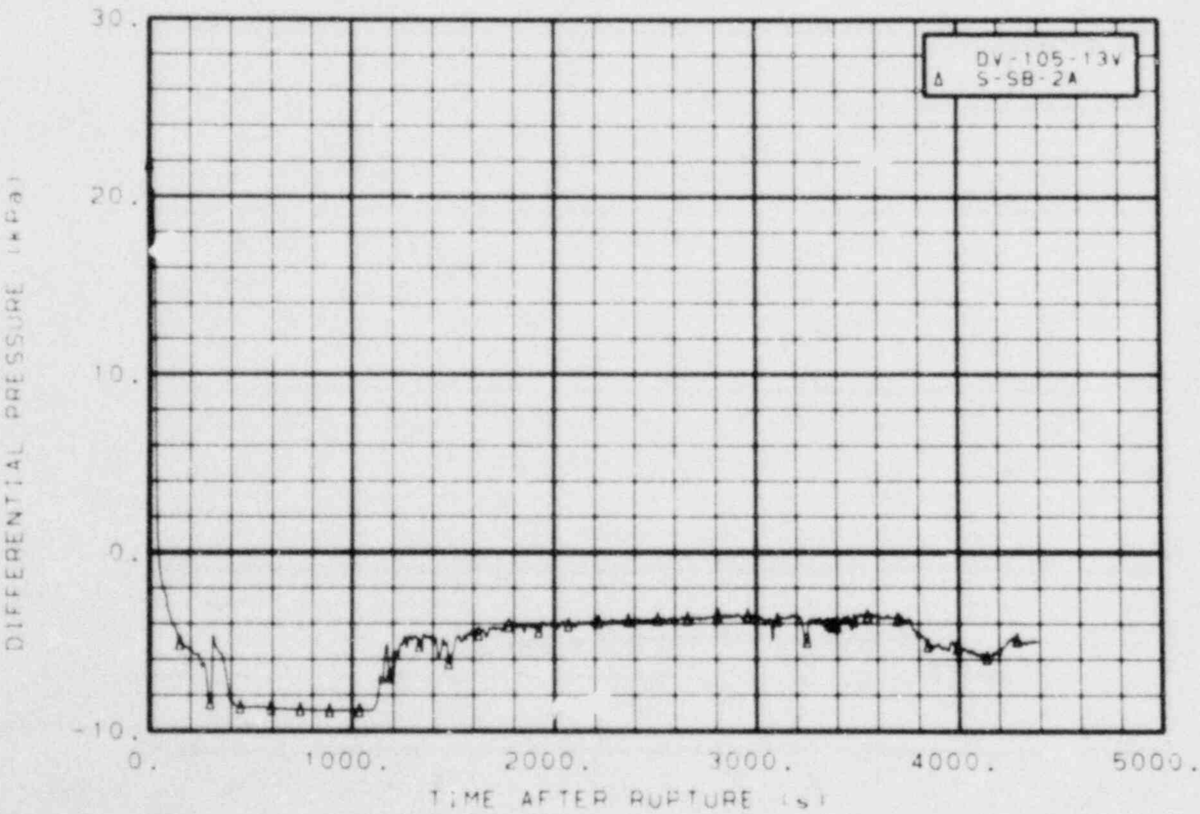

Figure 241. Differential pressure in vessel, Test S-SB-2A (DV-105-13V), from 0 to 4390 s.

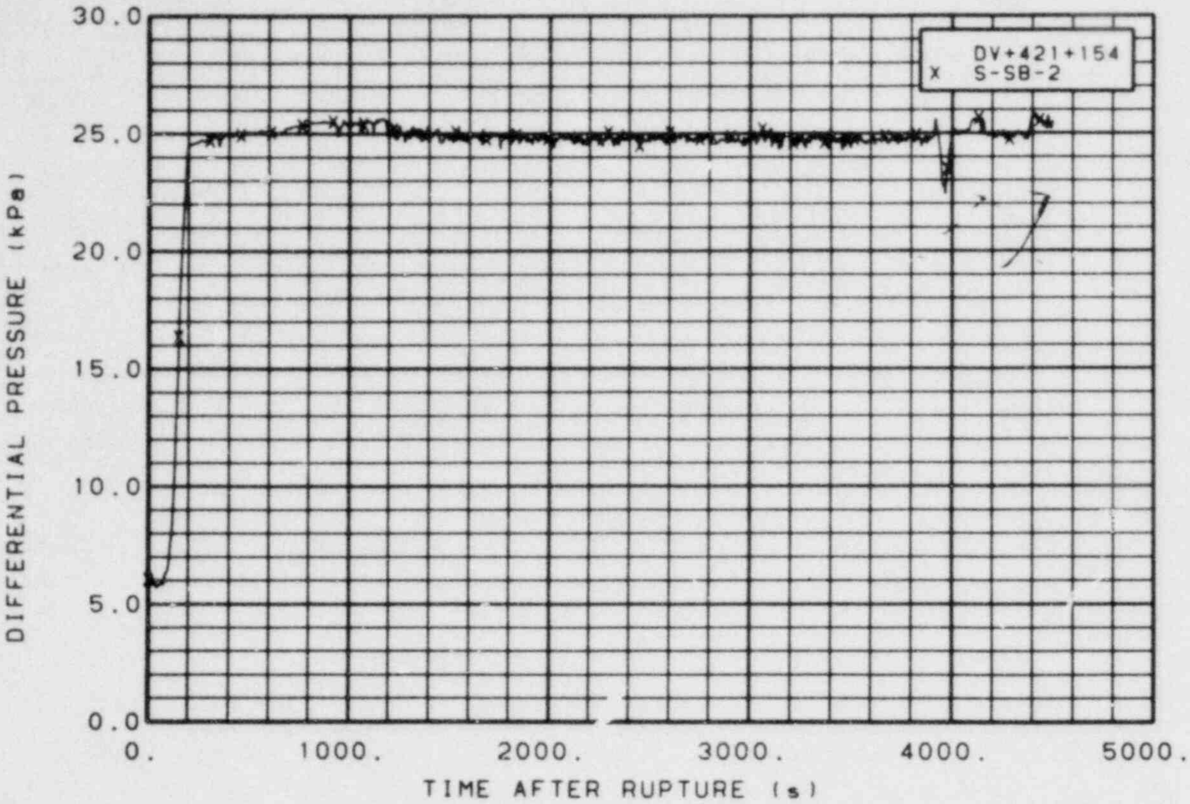

Figure 242. Differential pressure in vessel, Test S-SB-2 (DV + 421 + 154), from 0 to 4500 s.

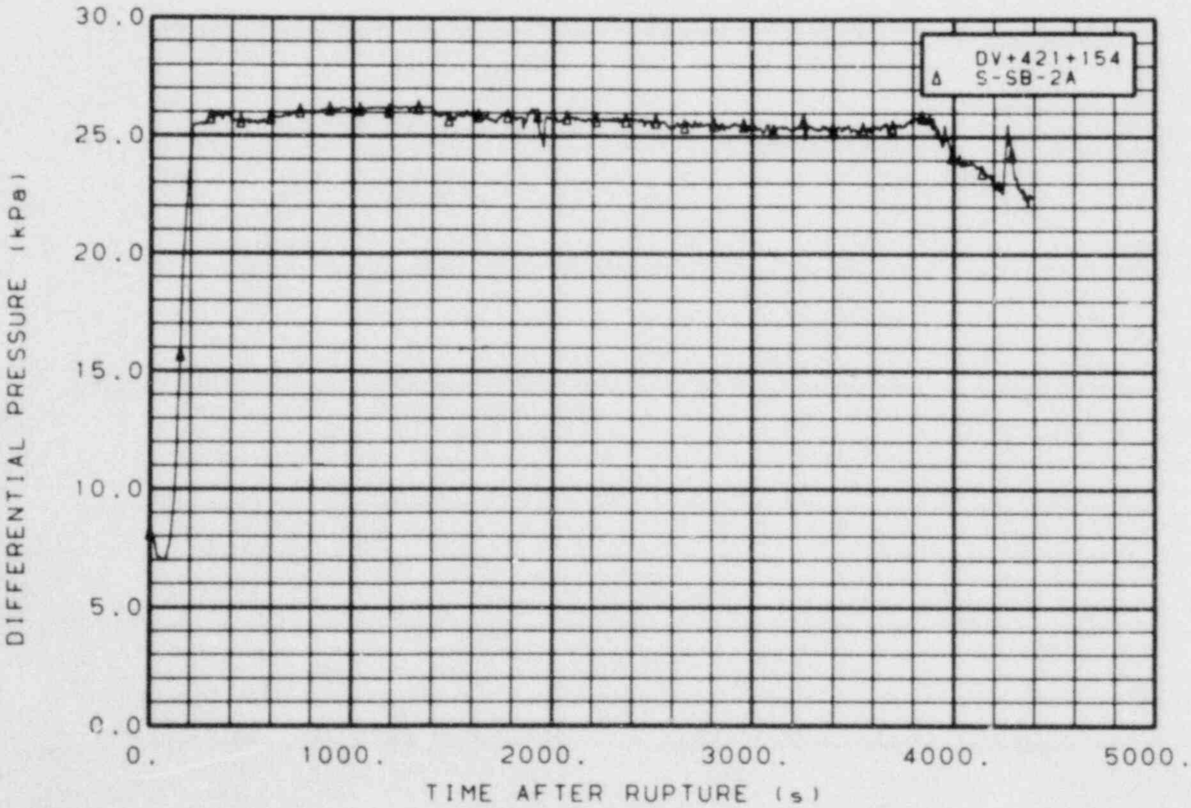

Figure 243. Differential pressure in vessel, Test S-SB-2A (DV + 421 + 154), from 0 to 4390 s.

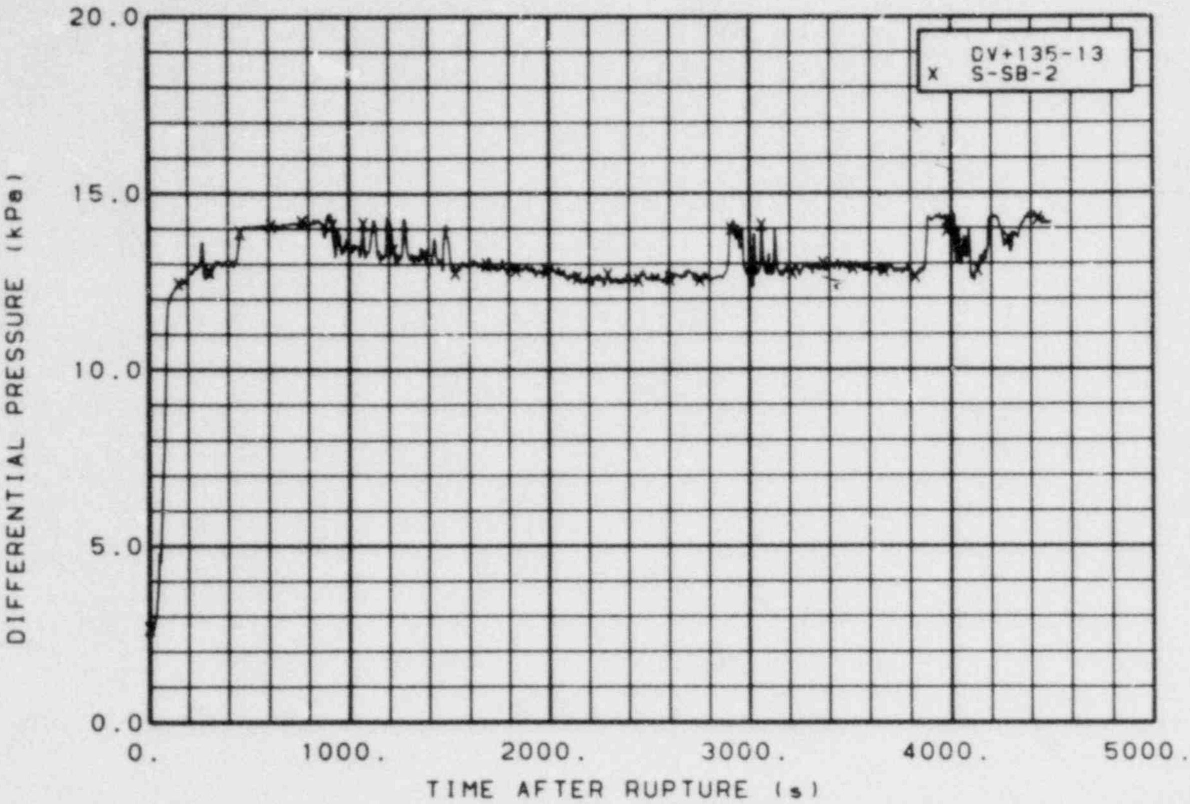

Figure 244. Differential pressure in vessel, Test S-SB-2 (DV + 135-13), from 0 to 4500 s.

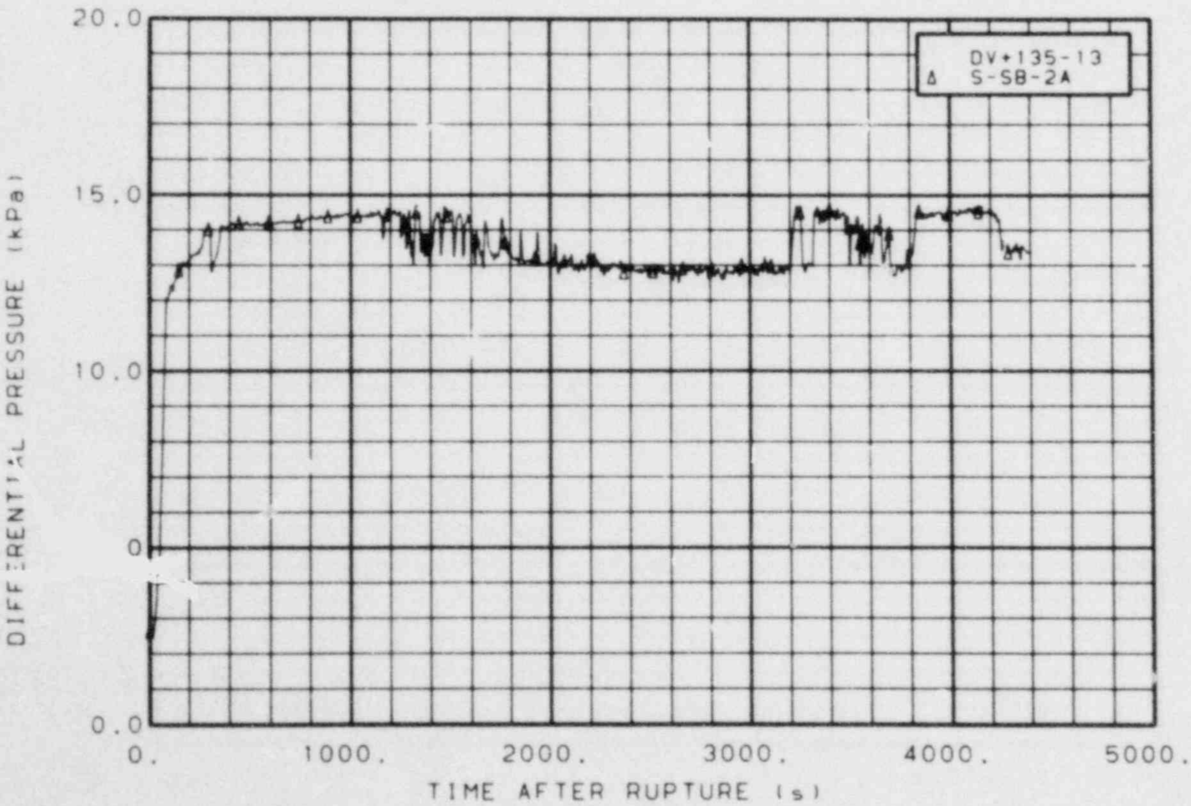

Figure 245. Differential pressure in vessel, Test S-SB-2A (DV + 135-13), from 0 to 4390 s.

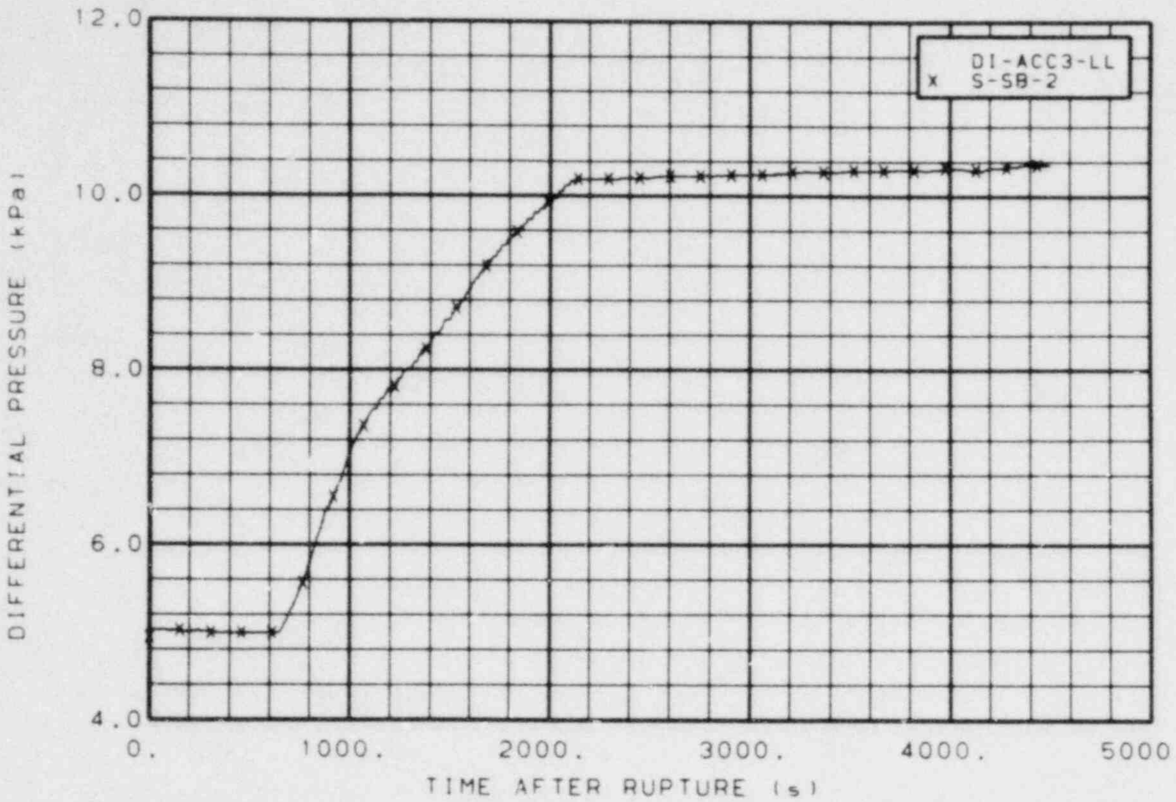

Figure 246. Differential pressure in intact loop ECC injection accumulator, Test S-SB-2 (DI-ACC3-LL), from 0 to 4500 s.

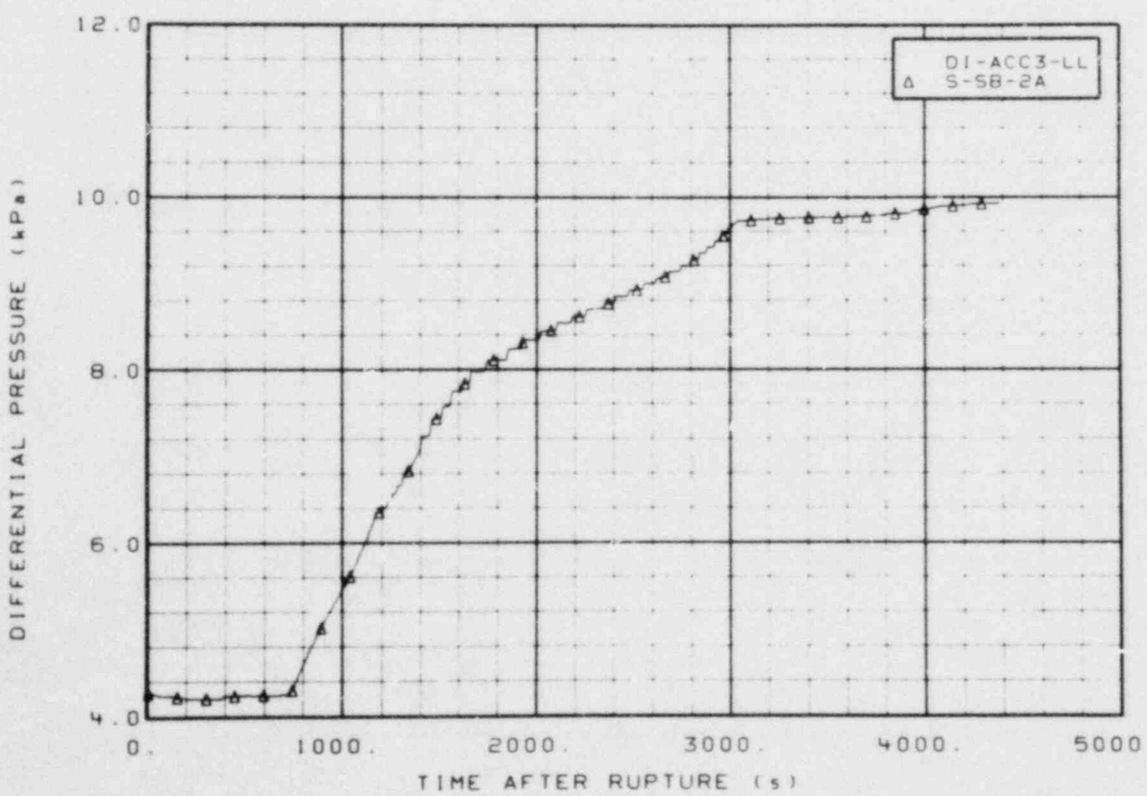

Figure 247. Differential pressure in intact loop ECC injection accumulator, Test S-SB-2A (DI-ACC3-LL), from 0 to 4390 s.

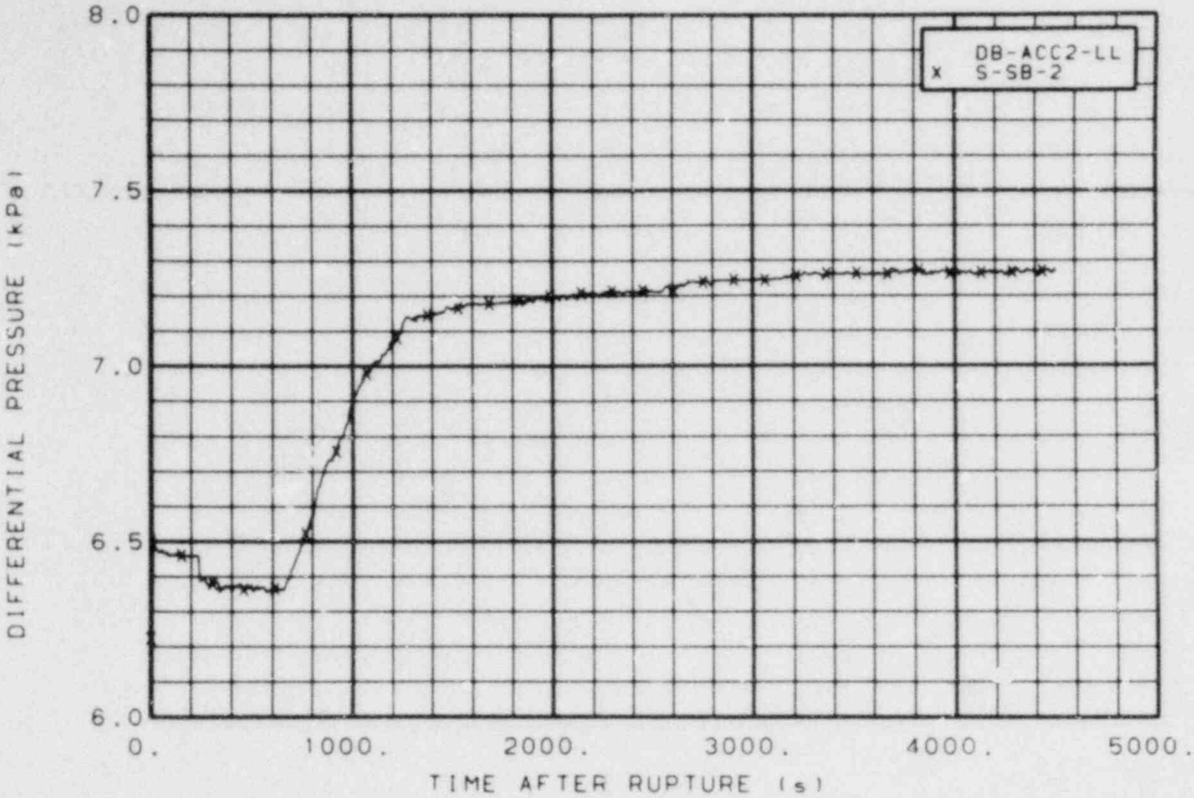

Figure 248. Differential pressure in broken loop ECC injection accumulator, Test S-SB-2 (DB-ACC2-LL), from 0 to 4500 s.

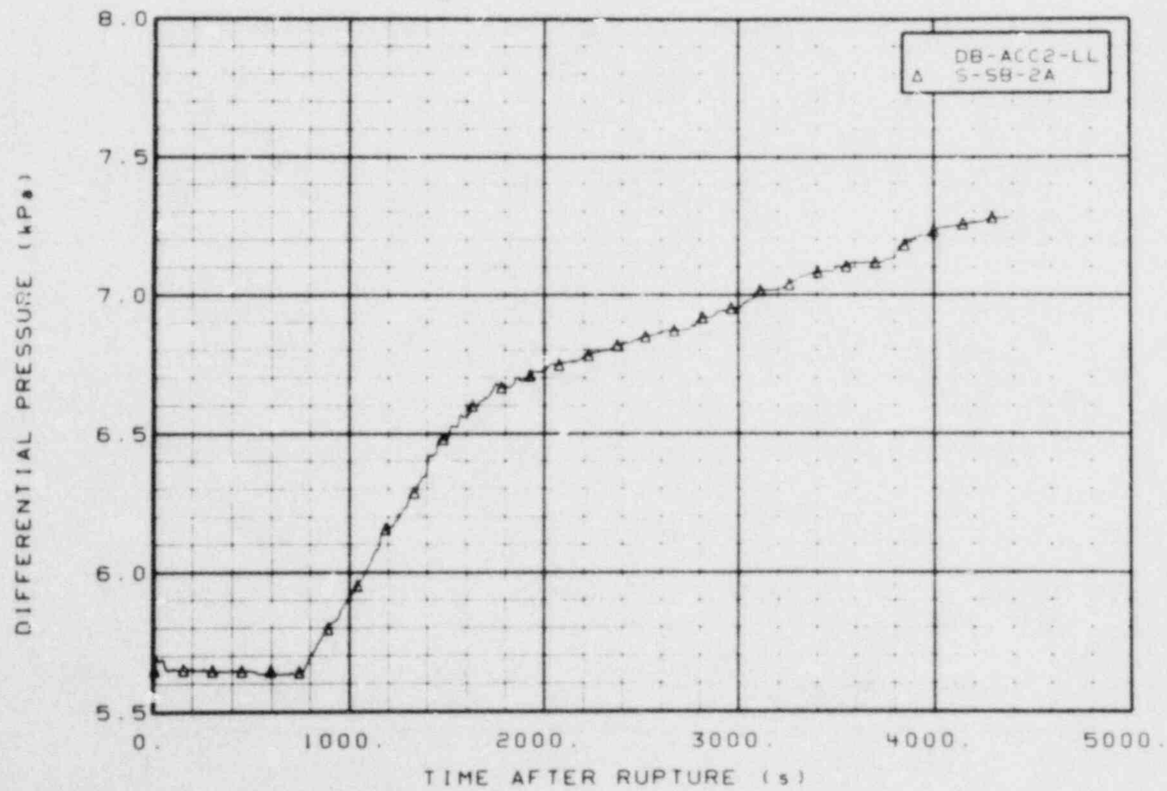

Figure 249. Differential pressure in broken loop ECC injection accumulator, Test S-SB-2A (DB-ACC2-LL), from 0 to 4390 s.

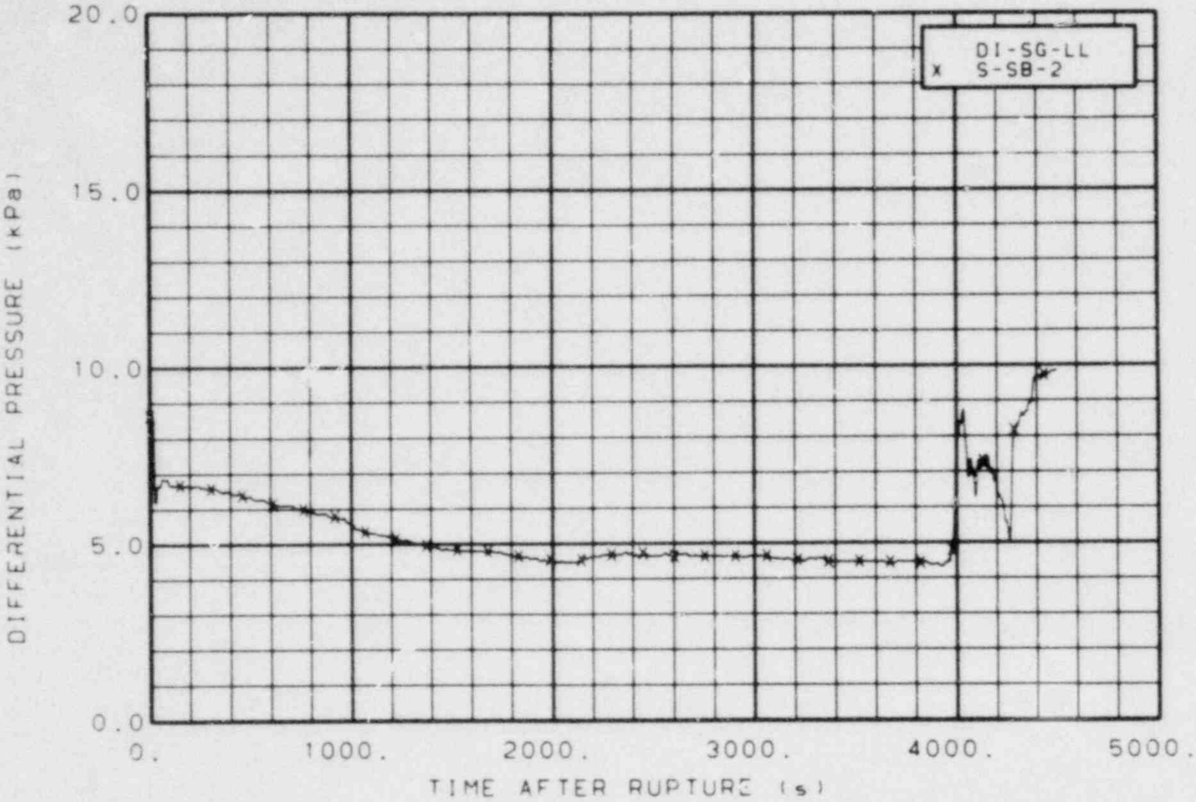

Figure 250. Differential pressure in intact loop steam generator, secondary side, liquid level, Test S-SB-2 (DI-SG-LL), from 0 to 4500 s.

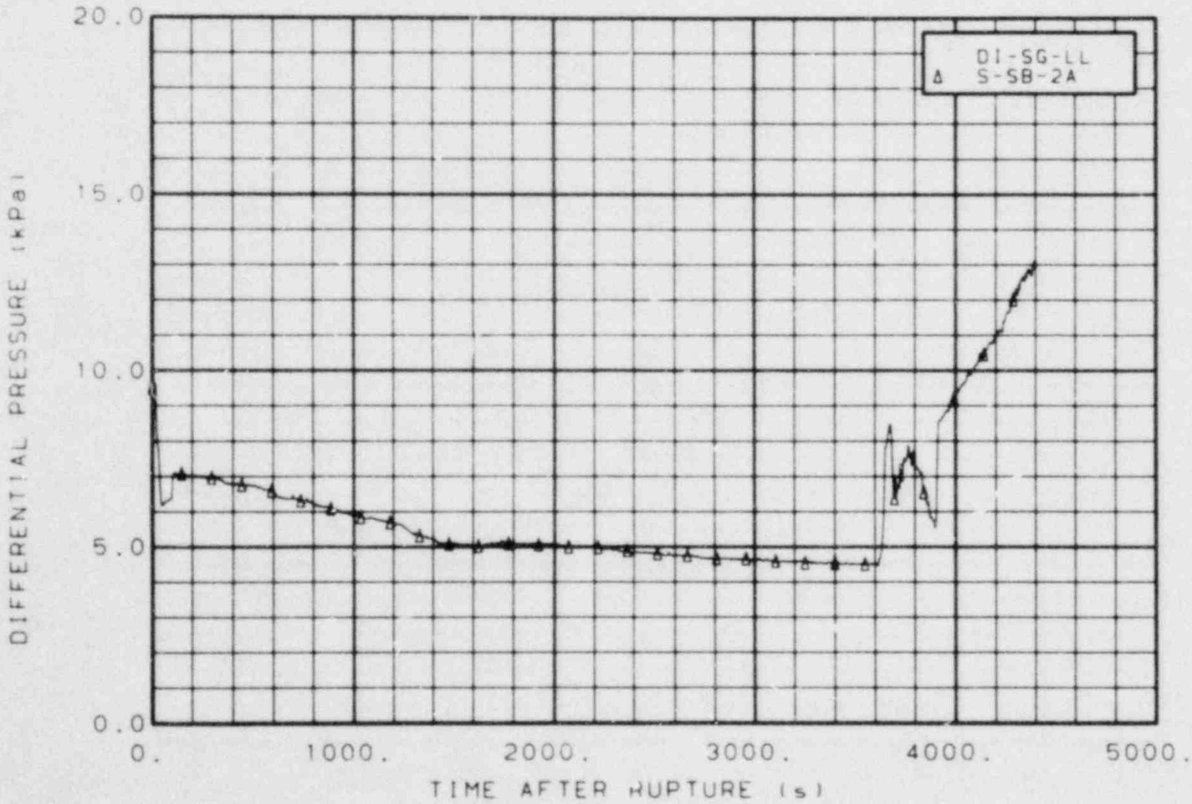

Figure 251. Differential pressure in intact loop steam generator, secondary side, liquid level, Test S-SB-2A (DI-SG-LL), from 0 to 4390 s.

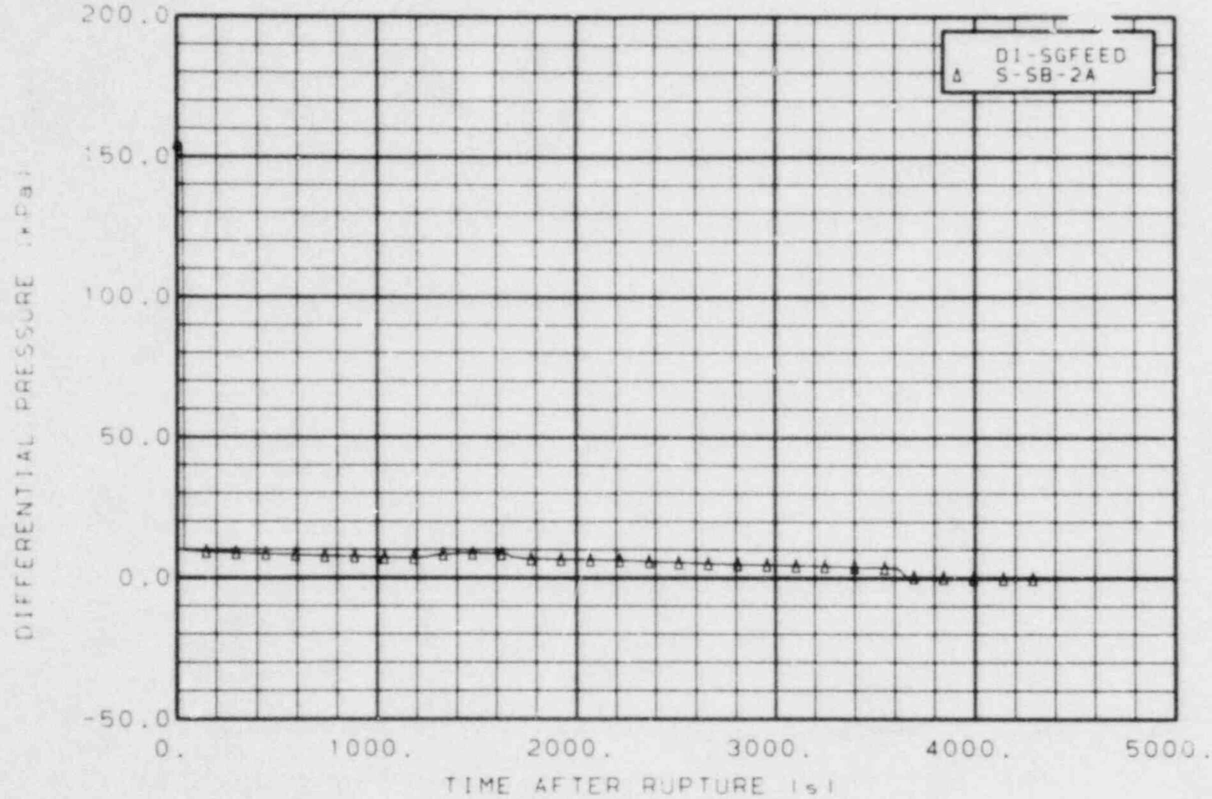

Figure 252. Differential pressure in intact loop steam generator, feedwater line, Test S-SB-2A (DI-SGFEED), from 0 to 4390 s.

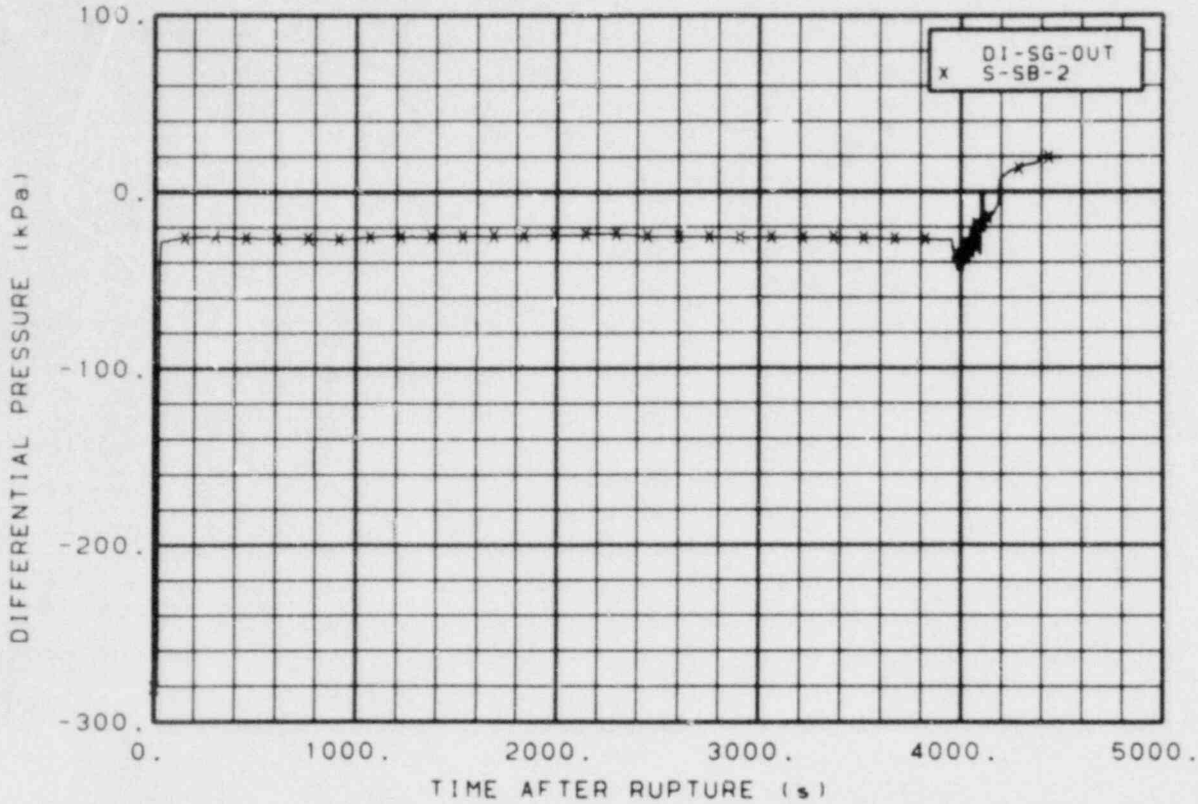

Figure 253. Differential pressure in intact loop steam generator, discharge line, Test S-SB-2 (DI-SG-OUT), from 0 to 4500 s.

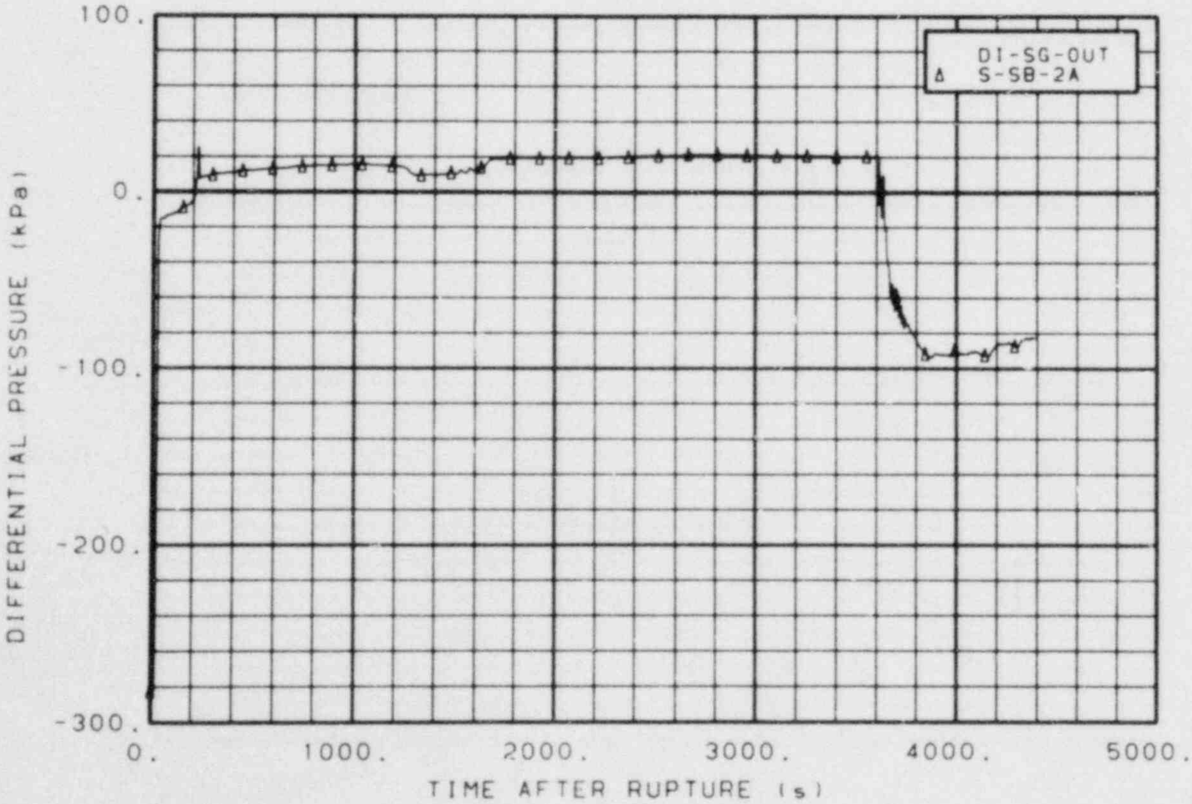

Figure 254. Differential pressure in intact loop steam generator, discharge line, Test S-SB-2A (DI-SG-OUT), from 0 to 4390 s.

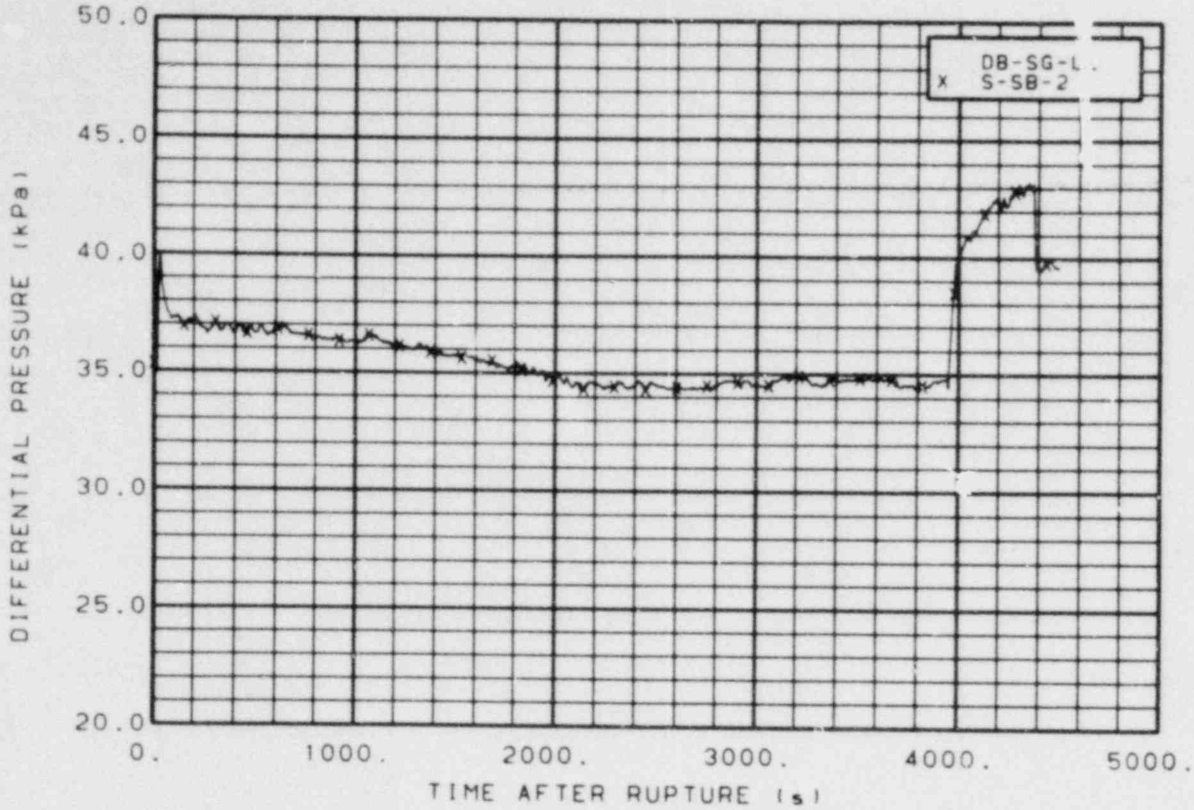

Figure 255. Differential pressure in broken loop steam generator, secondary side, liquid level, Test S-SB-2 (DB-SG-LL), from 0 to 4500 s.

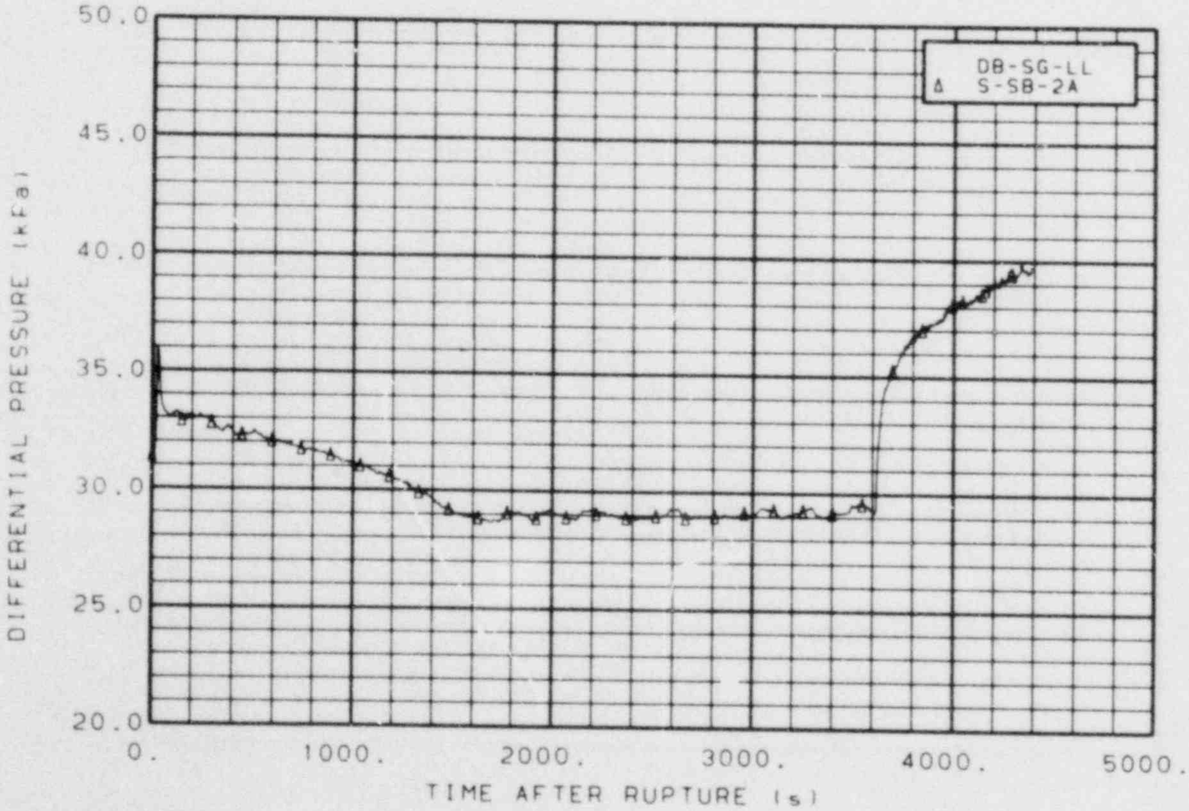

Figure 256. Differential pressure in broken loop steam generator, secondary side, liquid level, Test S-SB-2A (DB-SG-LL), from 0 to 4390 s.

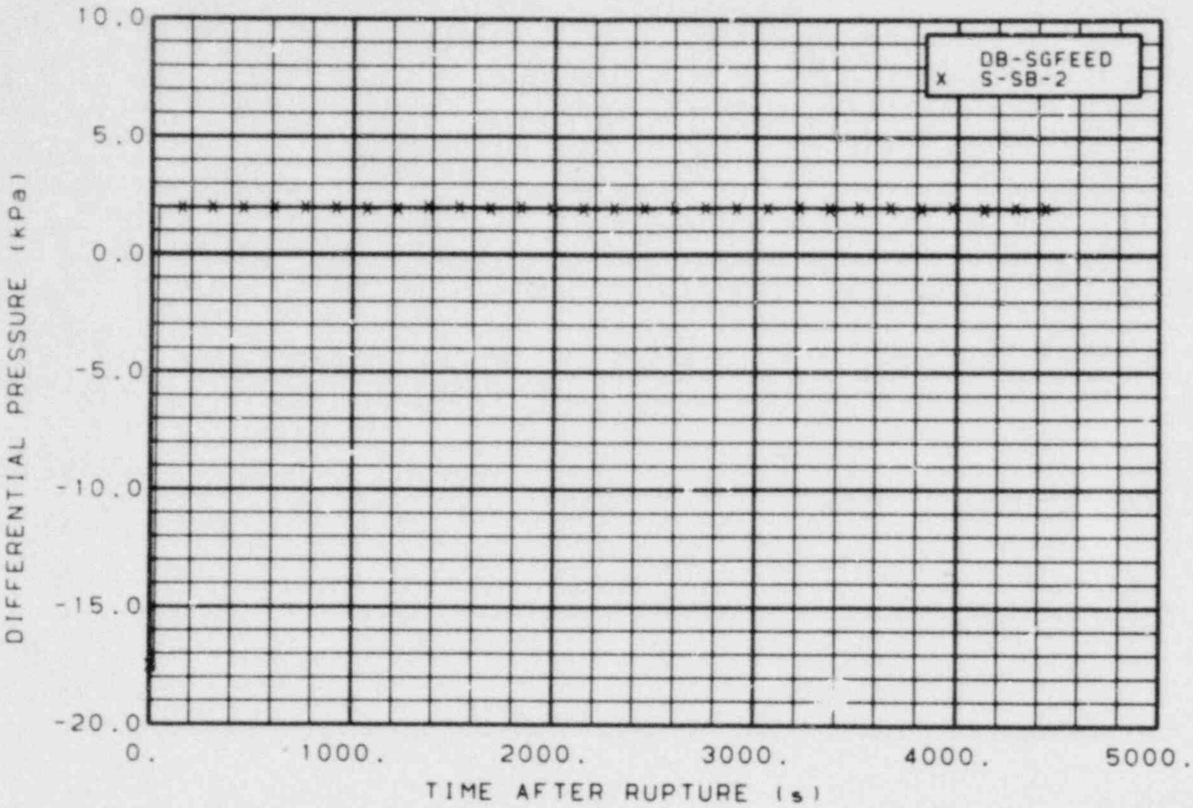

Figure 257. Differential pressure in broken loop steam generator, feedwater line, Test S-SB-2 (DB-SGFEED), from 0 to 4500 s.

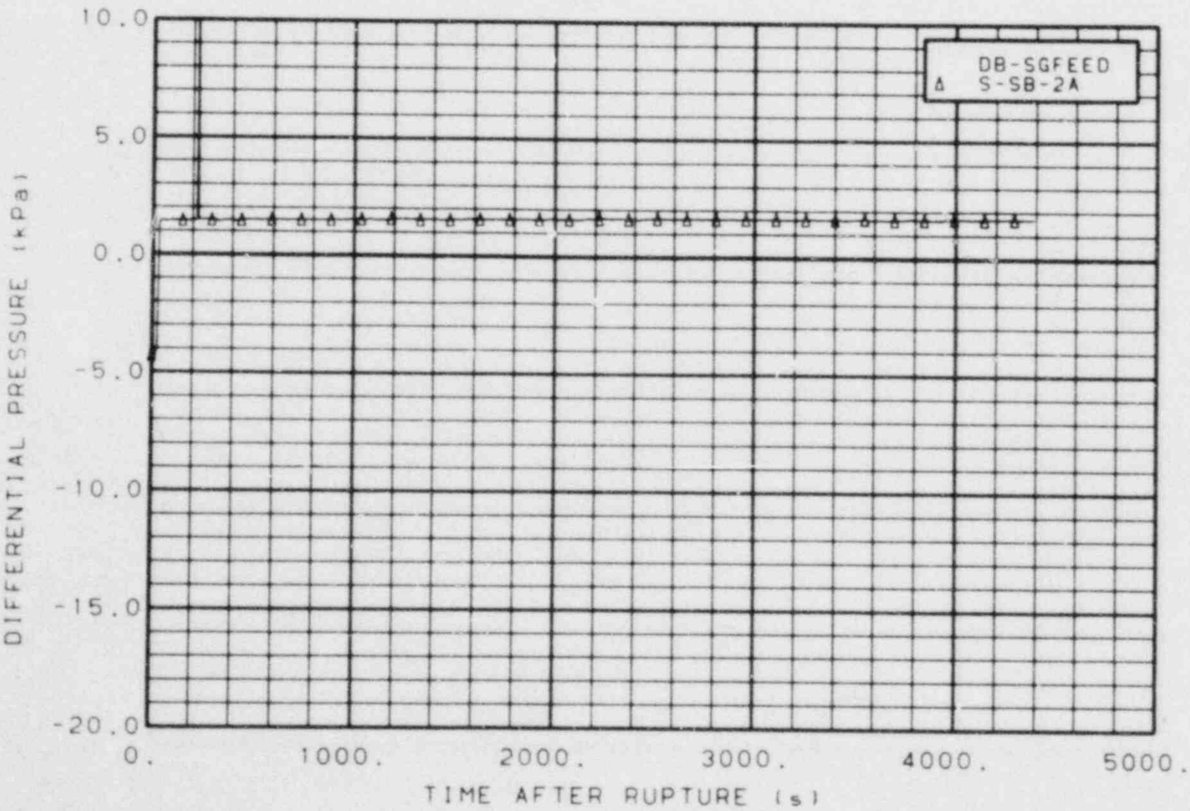

Figure 258. Differential pressure in broken loop steam generator, feedwater line, Test S-SB-2A (DB-SGFEED), from 0 to 4390 s.

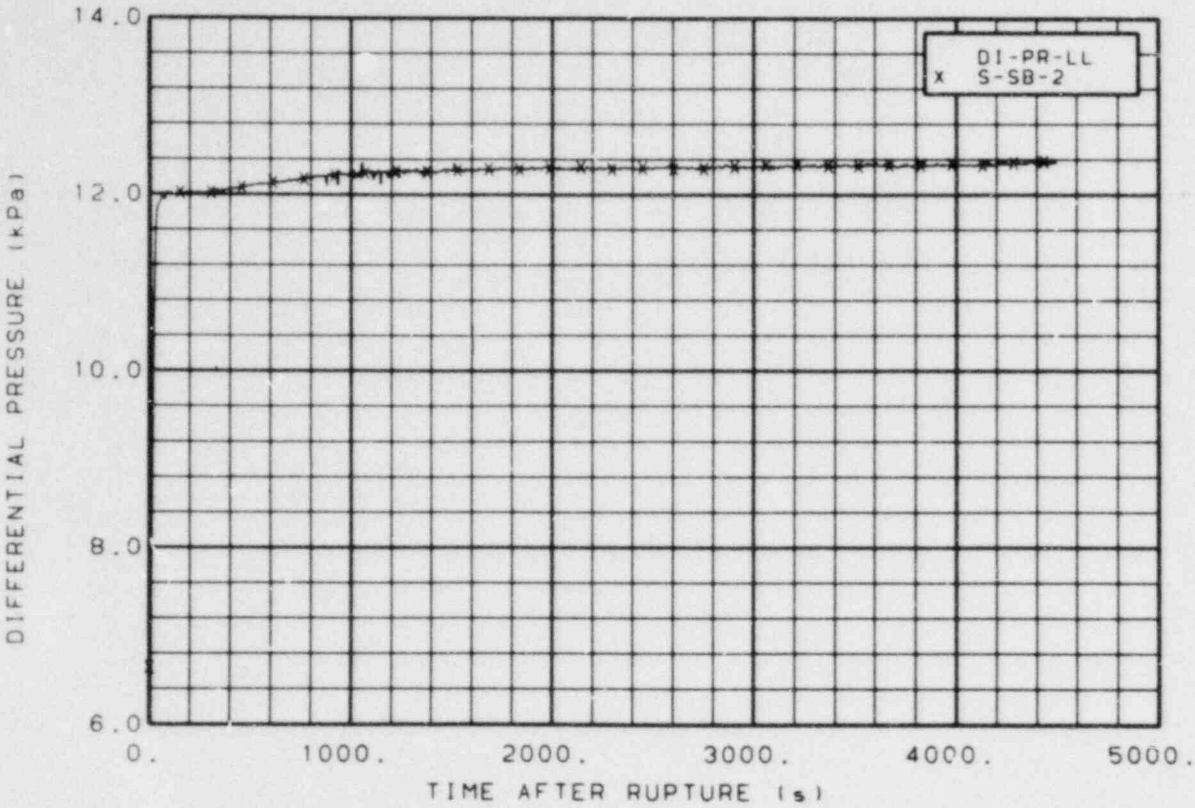

Figure 259. Differential pressure in pressurizer, liquid level, Test S-SB-2 (DI-PR-LL), from 0 to 4500 s.

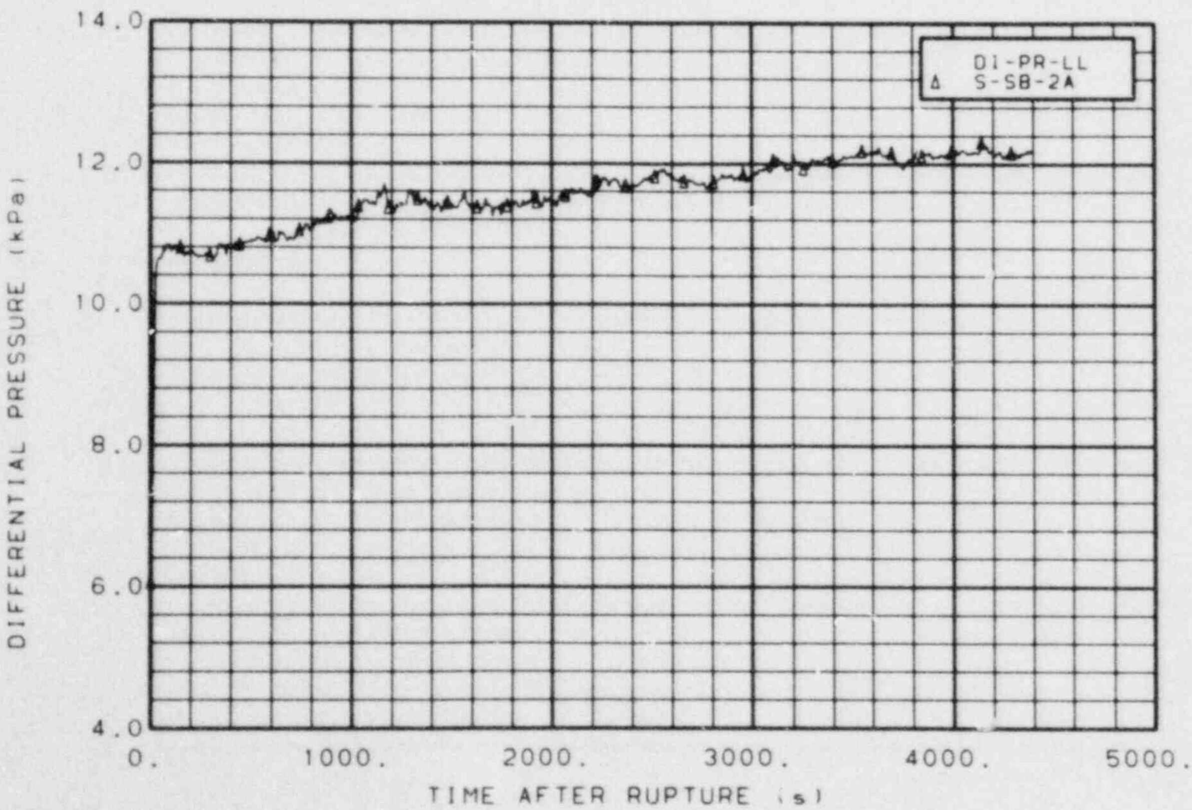

Figure 260. Differential pressure in pressurizer, liquid level, Test S-SB-2A (DI-PR-LL), from 0 to 4390 s.

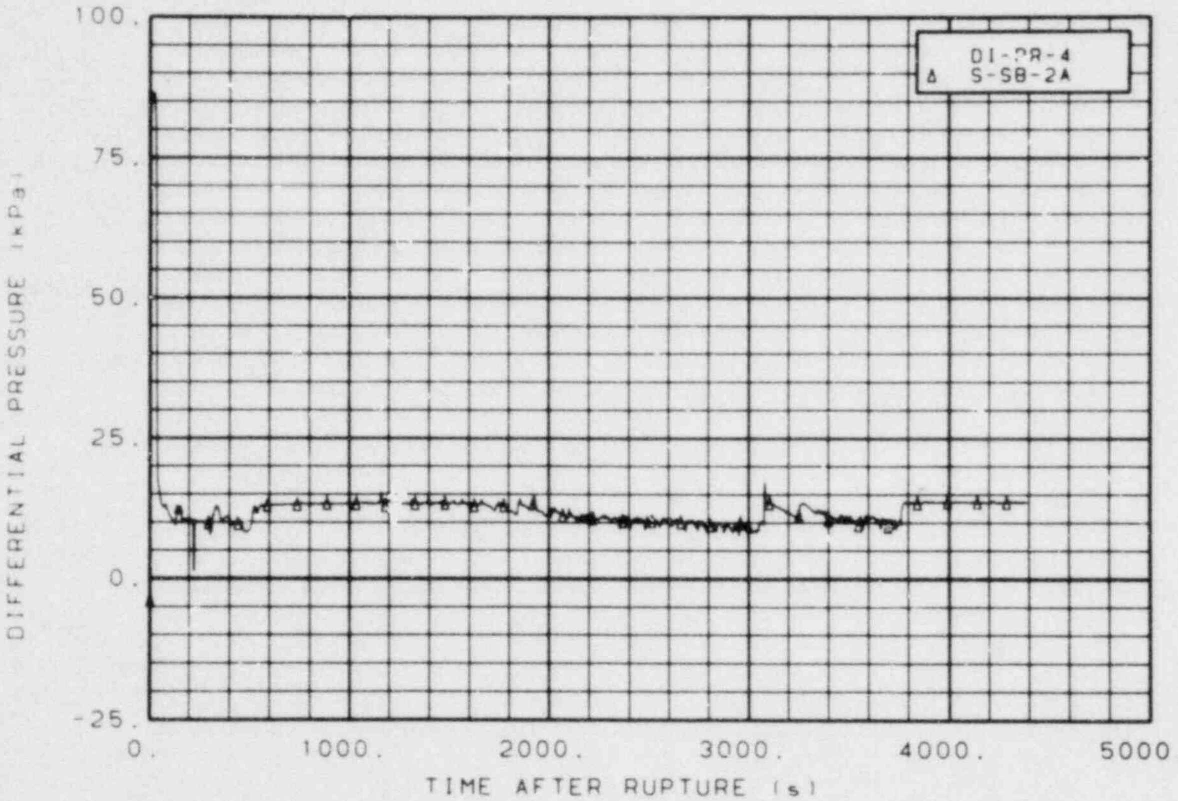

Figure 261. Differential pressure in pressurizer, Test S-SB-2A (DI-PR-4), from 0 to 4390 s.

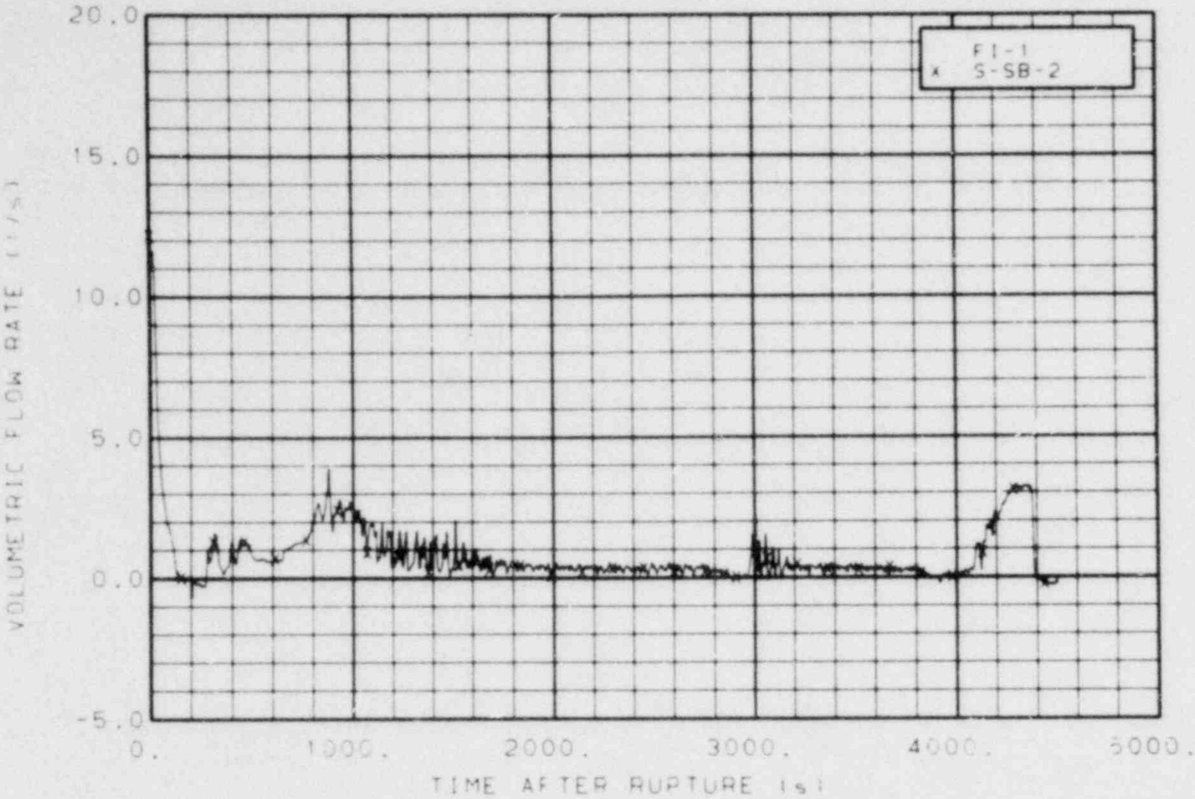

Figure 262. Volumetric Flow rate in intact loop hot leg, Test S-SB-2 (FI-1), from 0 to 4500 s.

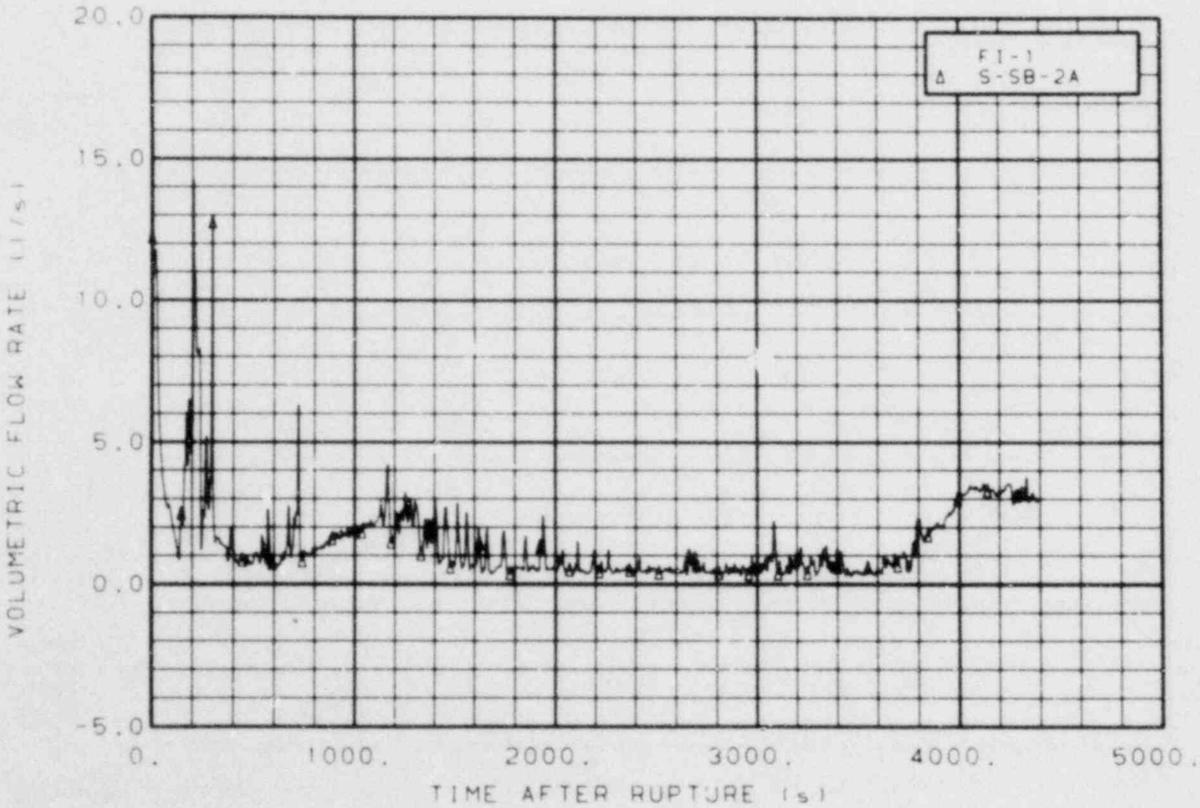

Figure 263. Volumetric Flow rate in intact loop hot leg, Test S-SB-2A (FI-1), from 0 to 4390 s.

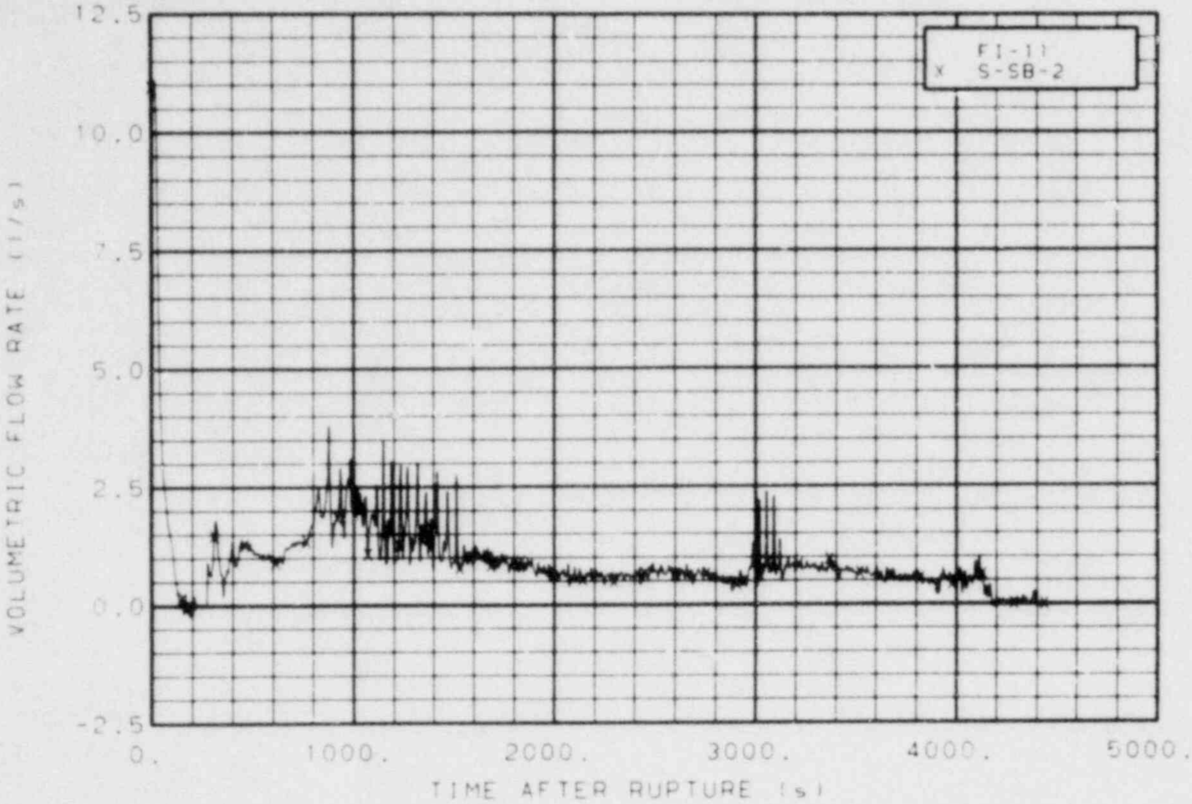

Figure 264. Volumetric Flow rate in intact loop cold leg, Test S-SB-2 (FI-11), from 0 to 4500 s.

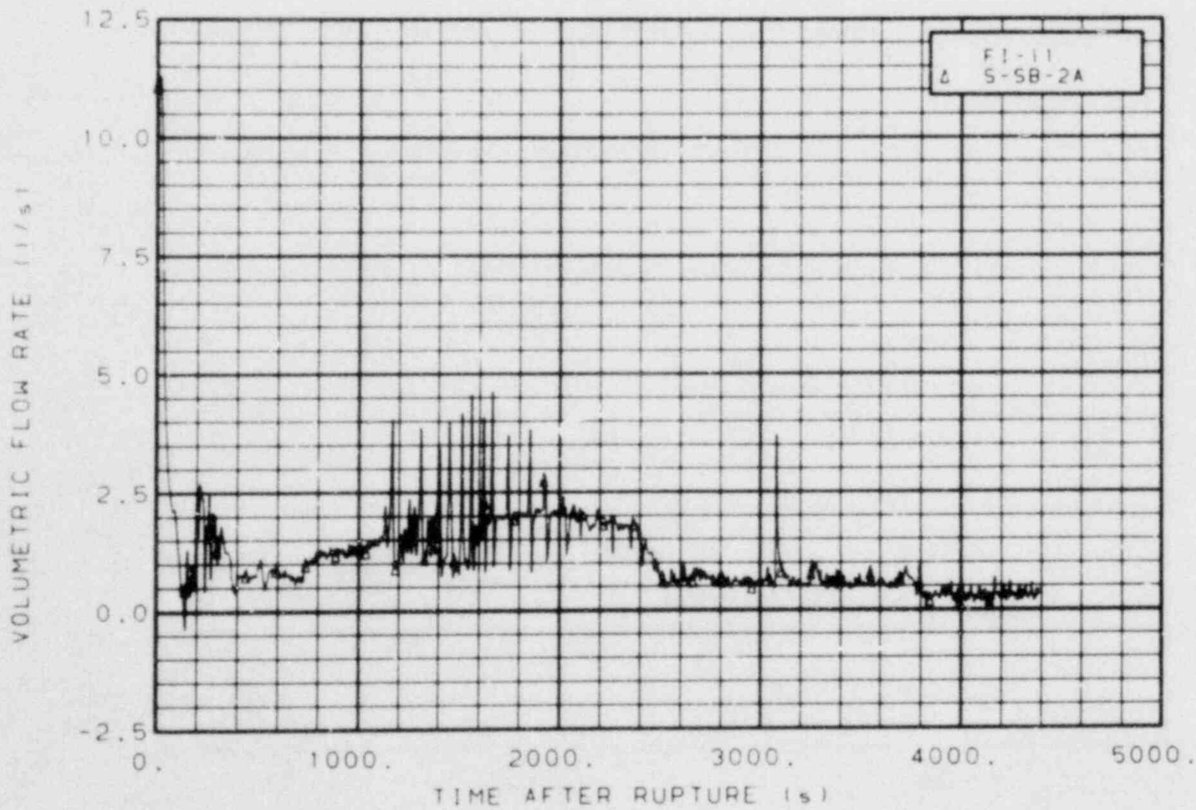

Figure 265. Volumetric Flow rate in intact loop cold leg, Test S-SB-2A (FI-11), from 0 to 4390 s.

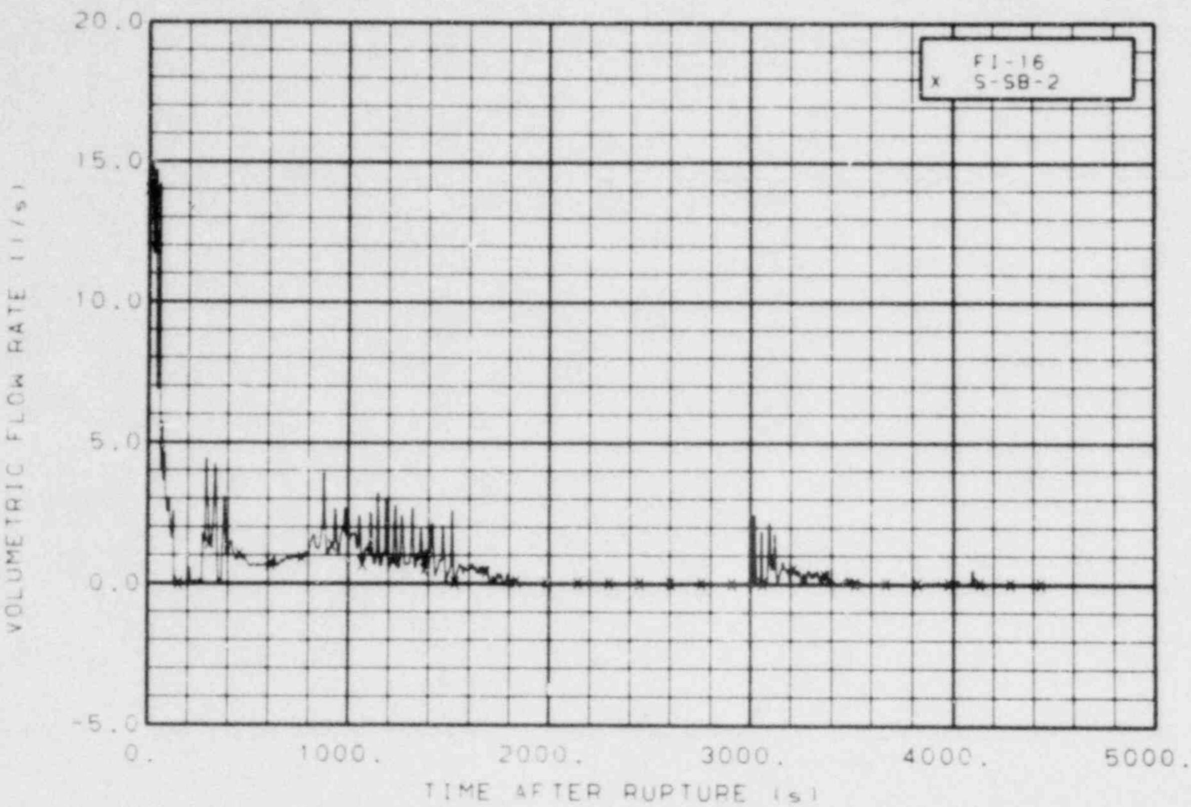

Figure 266. Volumetric Flow rate in intact loop cold leg, Test S-SB-2 (FI-16), from 0 to 4500 s.

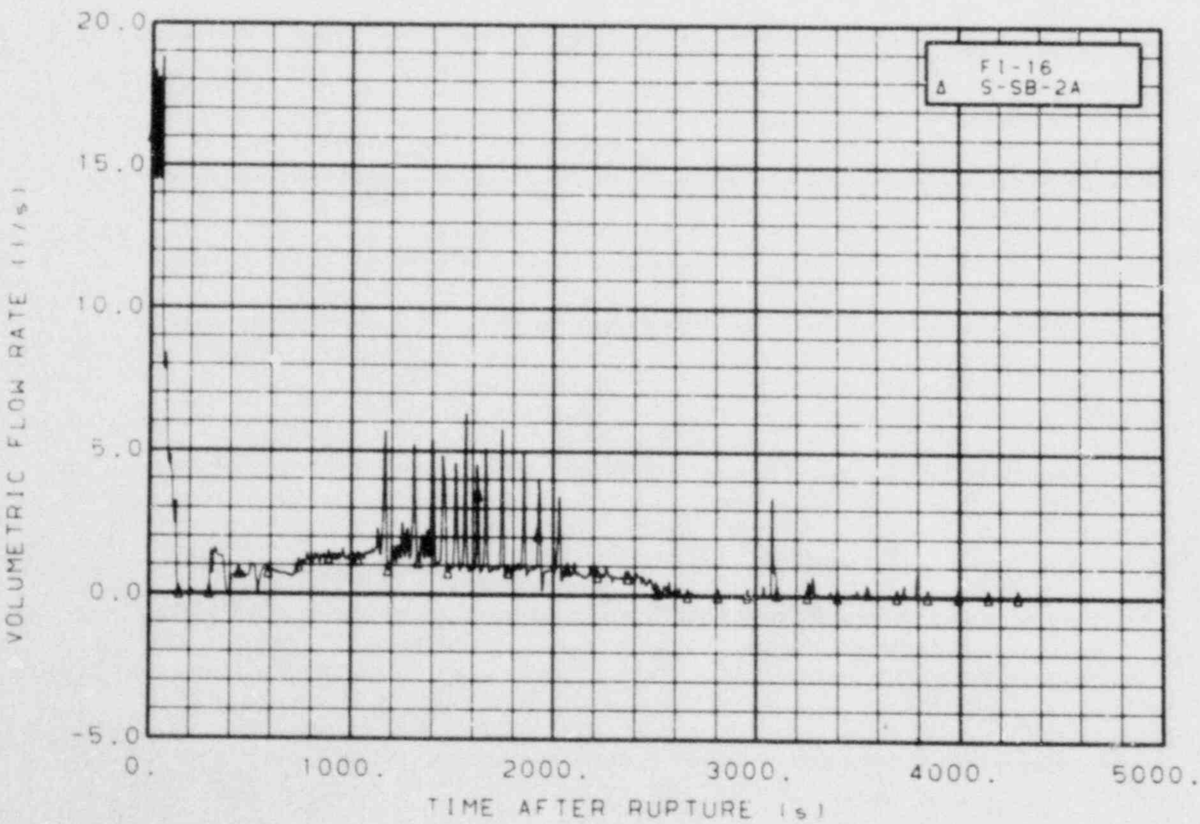

Figure 267. Volumetric Flow rate in intact loop cold leg, Test S-SB-2A (FI-16), from 0 to 4390 s.

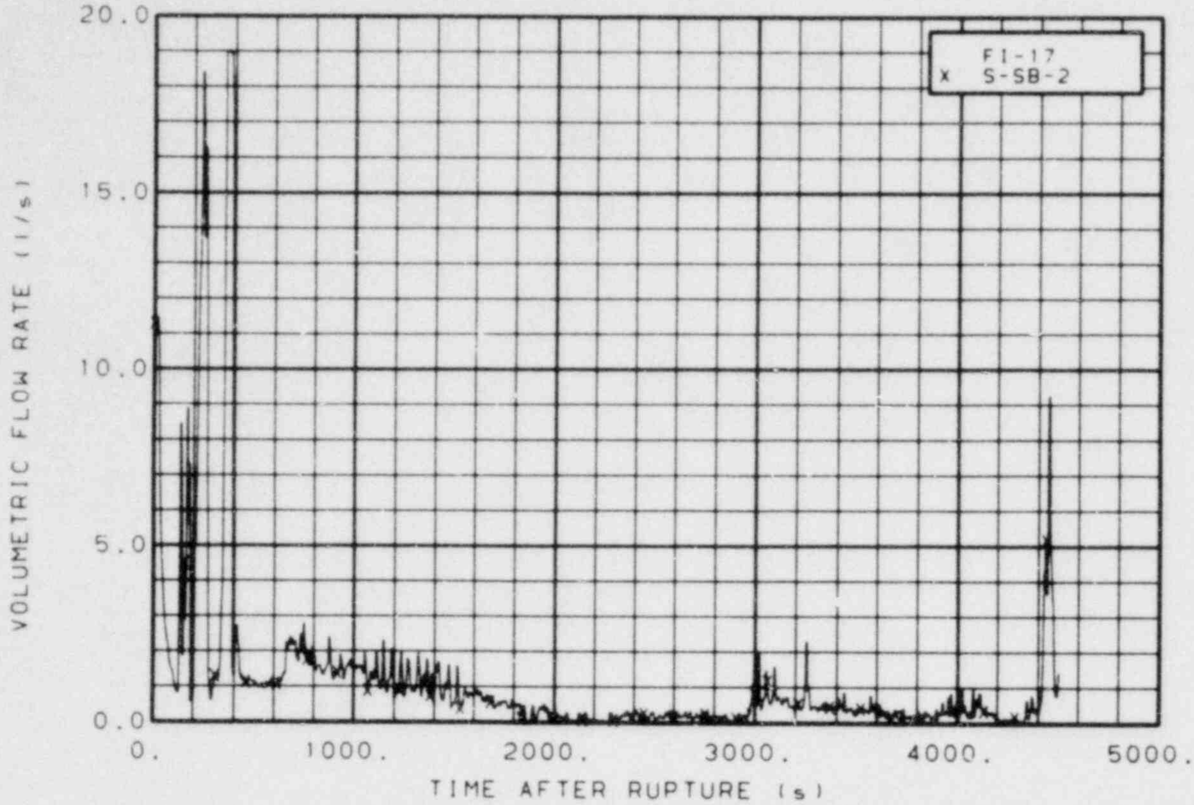

Figure 268. Volumetric Flow rate in intact loop cold leg, Test S-SB-2 (FI-17), from 0 to 4500 s.

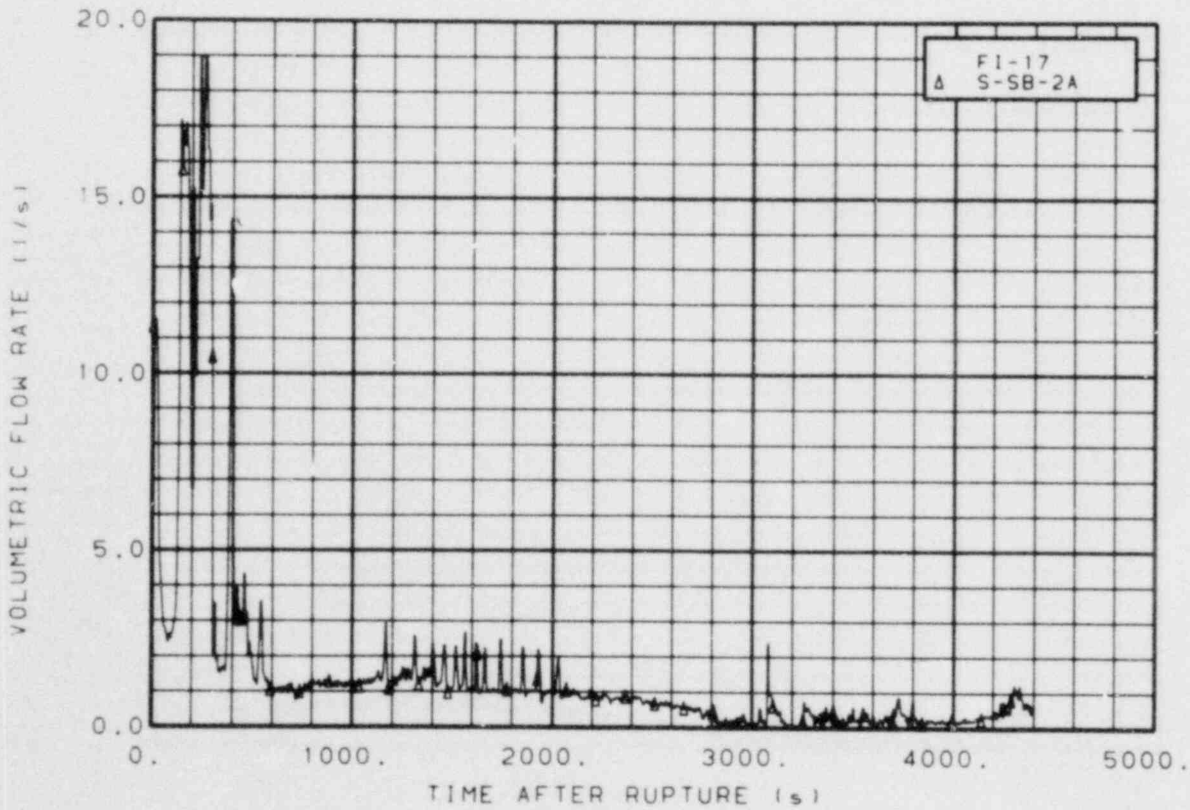

Figure 269. Volumetric Flow rate in intact loop cold leg, Test S-SB-2A (FI-17), from 0 to 4390 s.

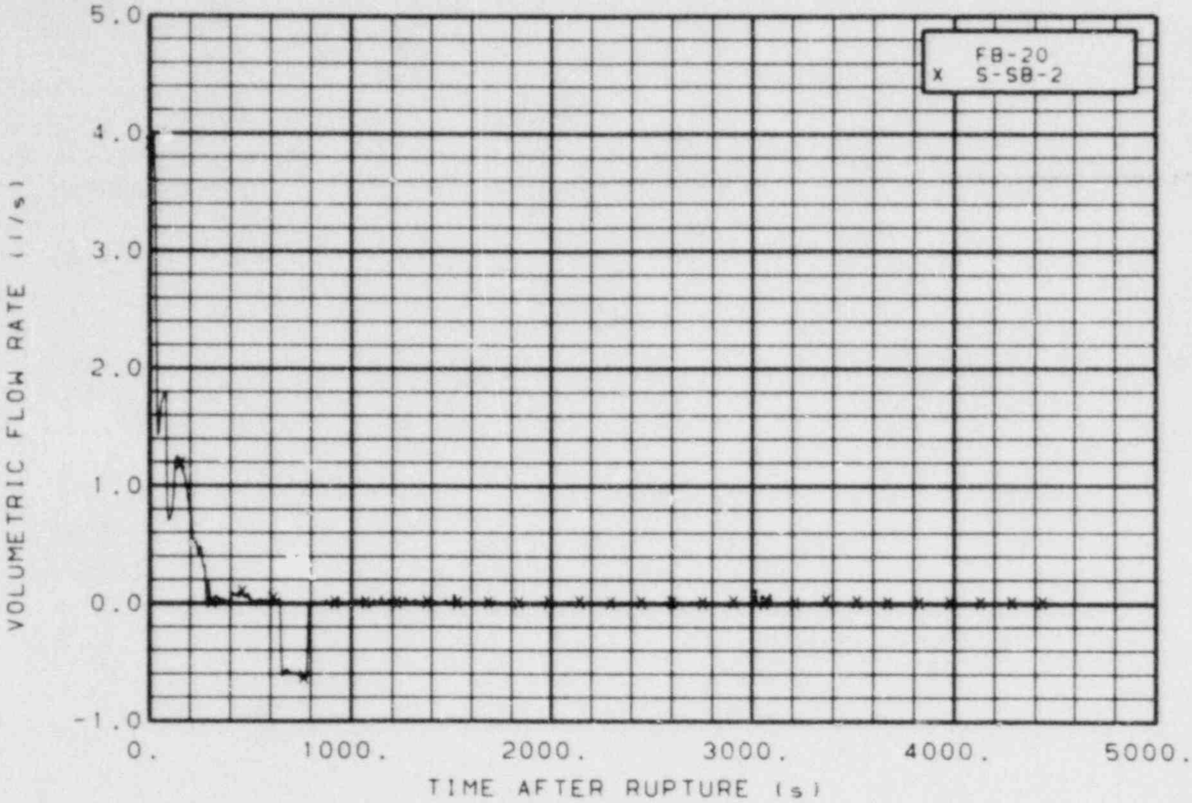

Figure 270. Volumetric Flow rate in intact loop hot leg, Test S-SB-2 (FB-20), from 0 to 4500 s.

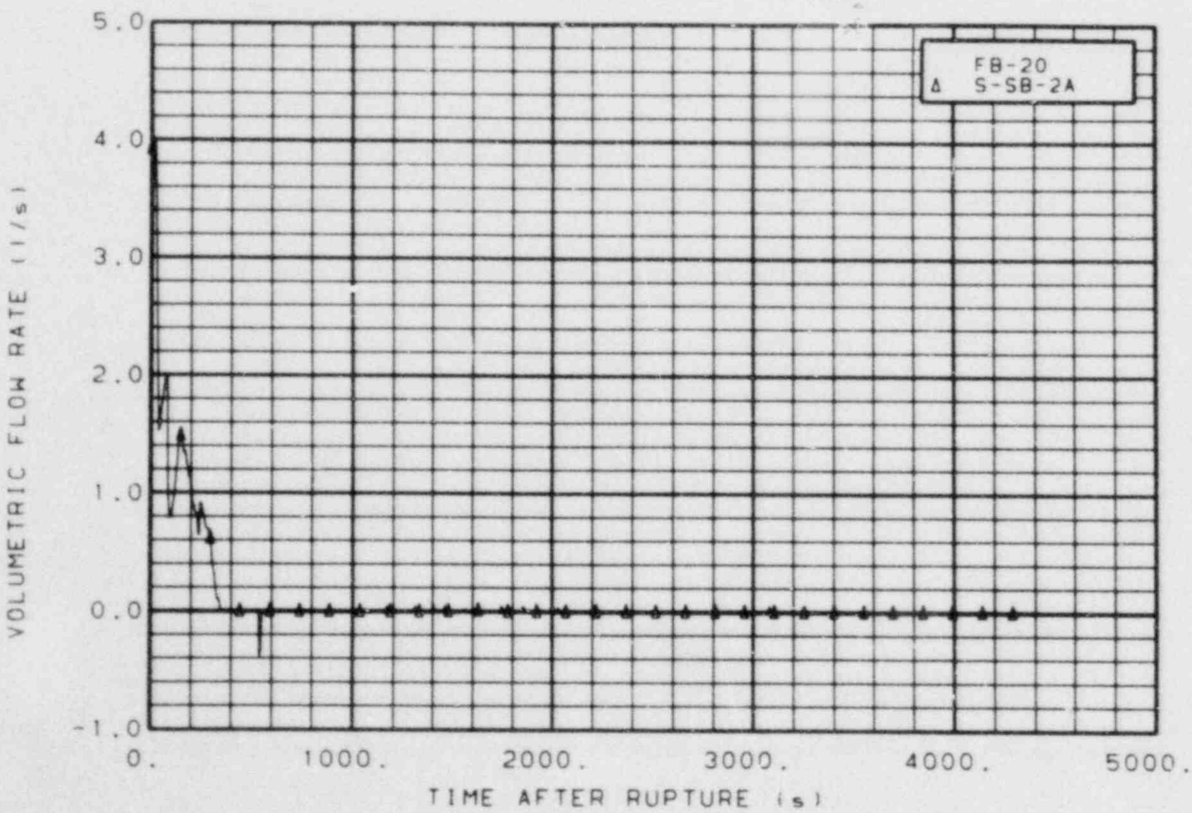

Figure 271. Volumetric Flow rate in intact loop hot leg, Test S-SB-2A (FB-20), from 0 to 4390 s.

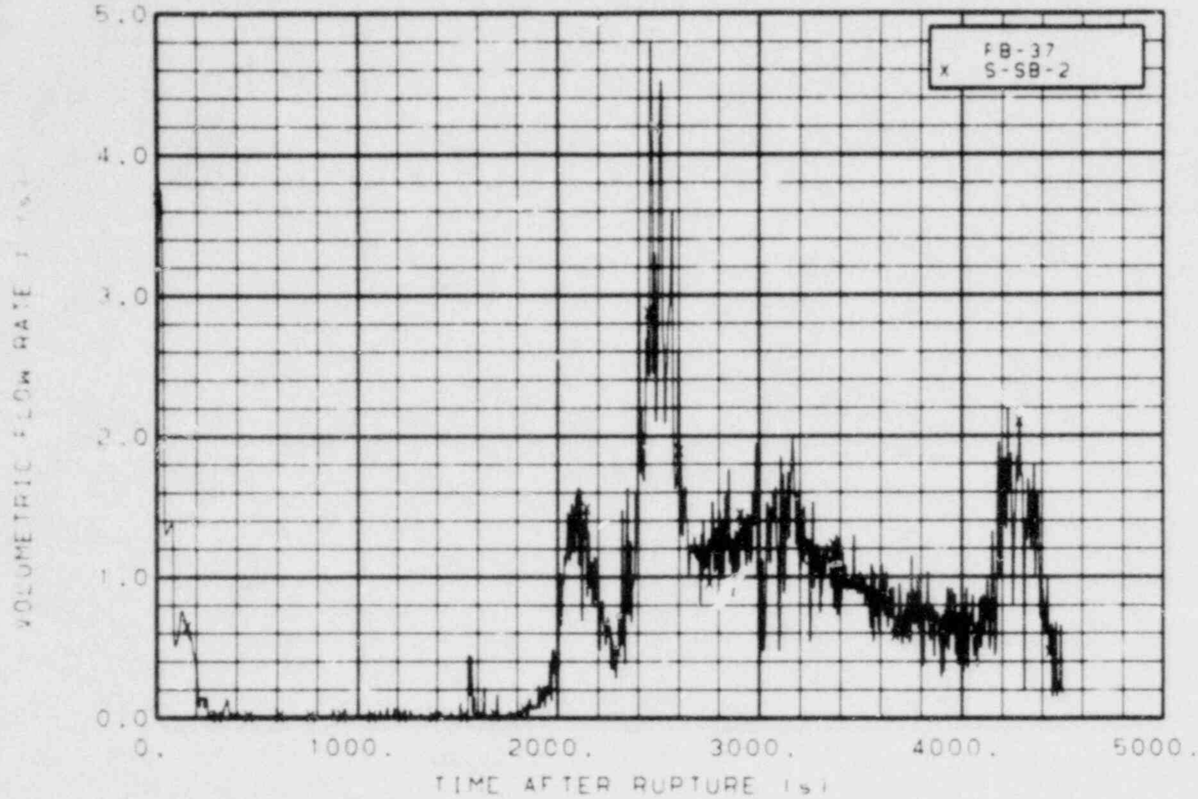

Figure 272. Volumetric Flow rate in broken loop cold leg, Test S-SB-2 (FB-37), from 0 to 4500 s.

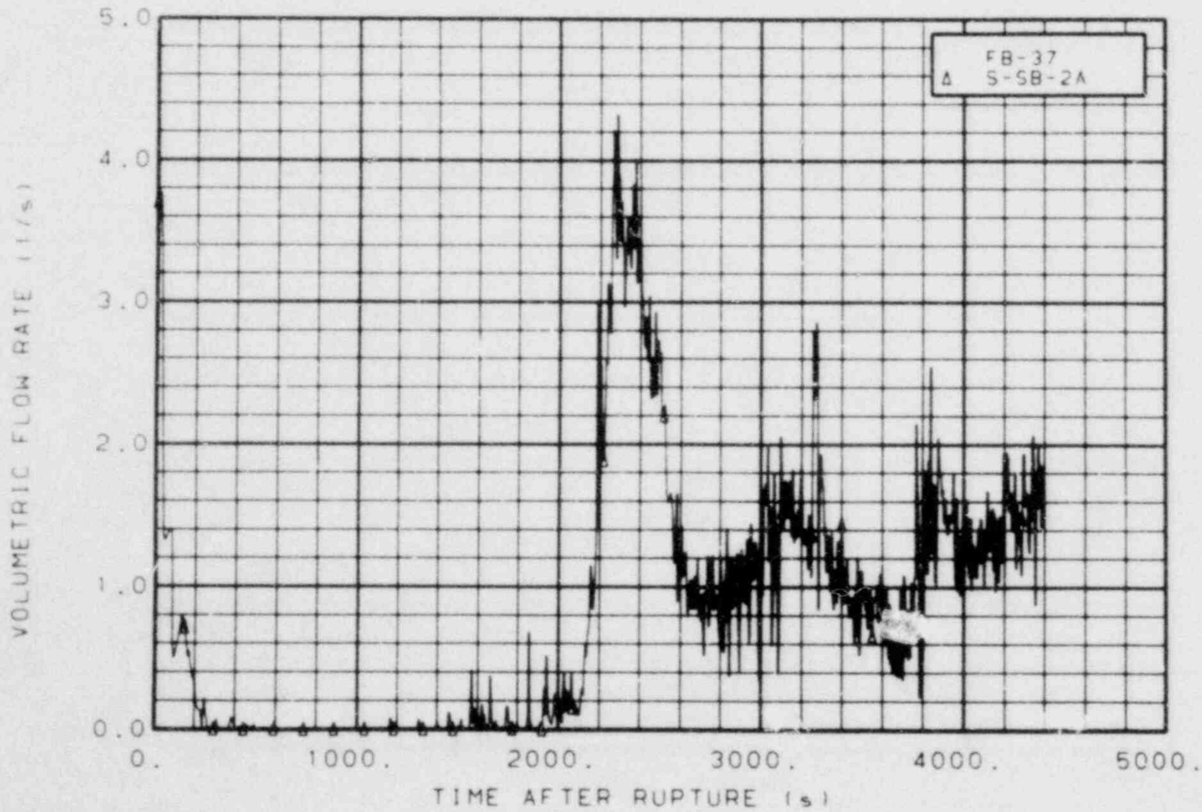

Figure 273. Volumetric Flow rate in broken loop cold leg, Test S-SB-2A (FB-37), from 0 to 4390 s.

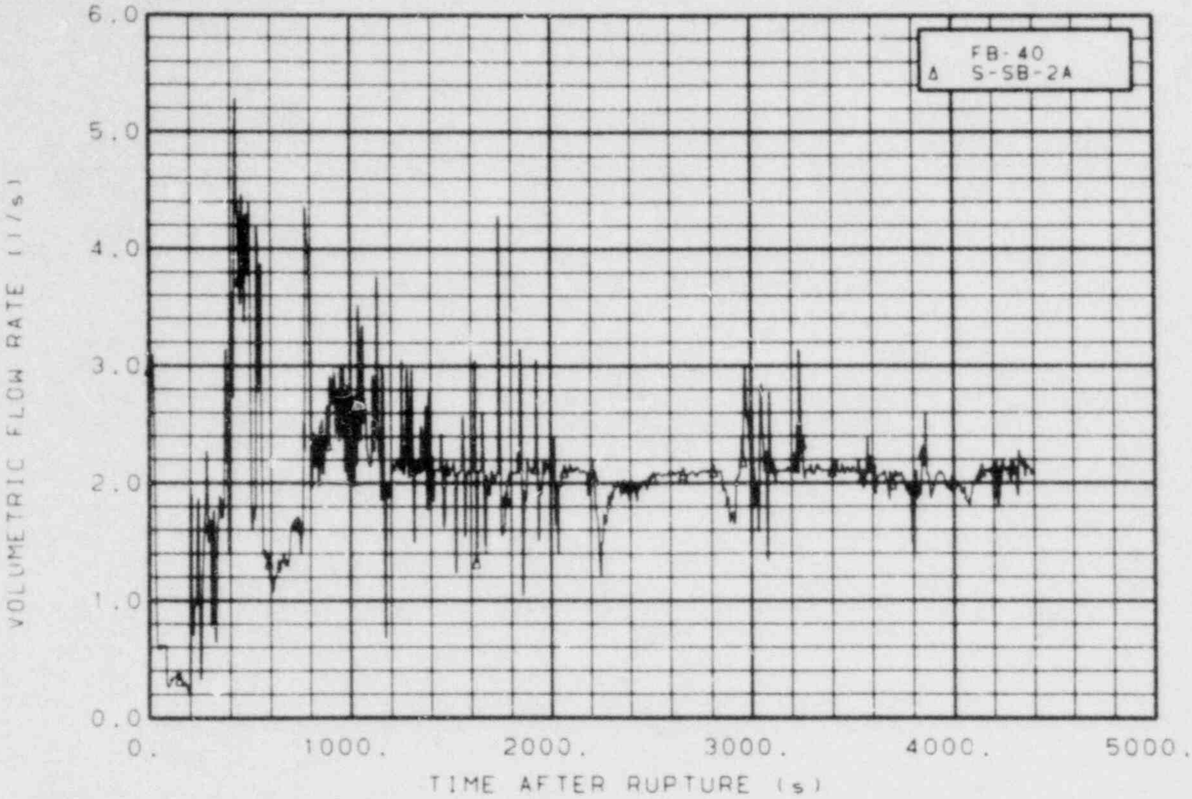

Figure 274. Volumetric Flow rate in broken loop cold leg, Test S-SB-2A (FB-40), from 0 to 4390 s.

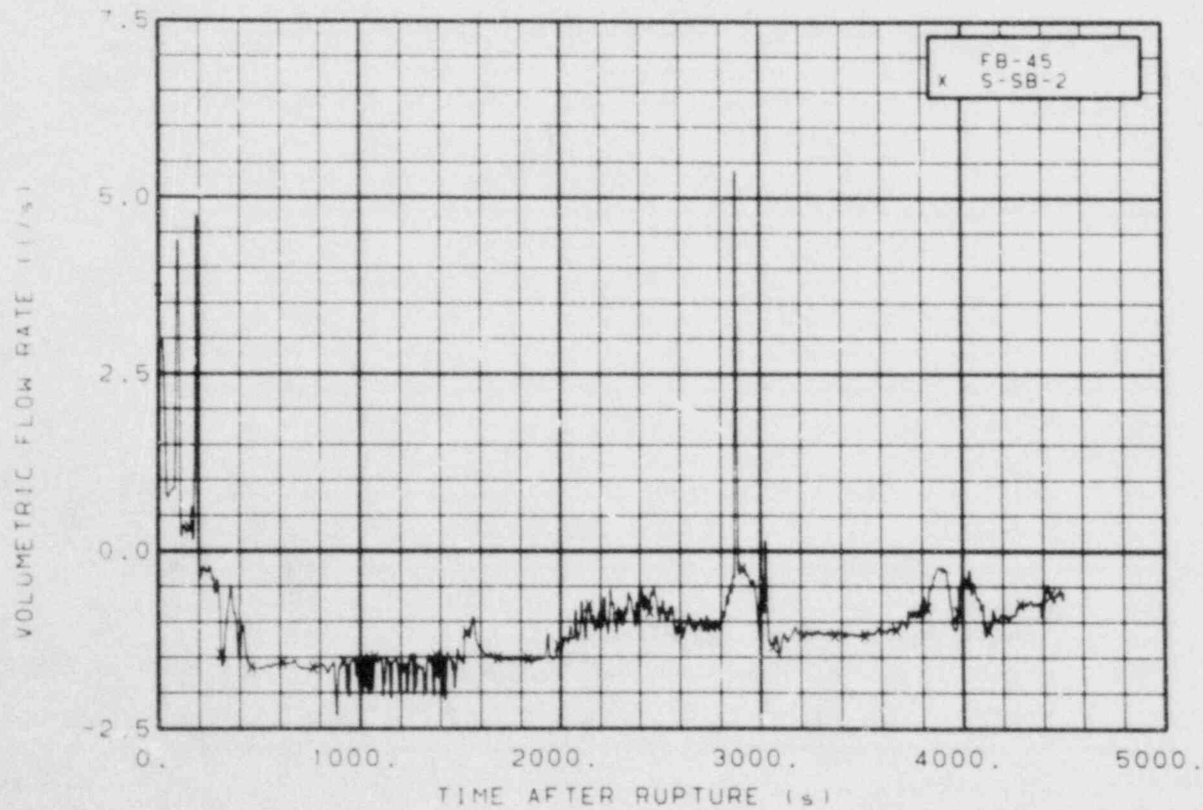

Figure 275. Volumetric Flow rate in broken loop cold leg, Test S-SB-2 (FB-45), from 0 to 4500 s.

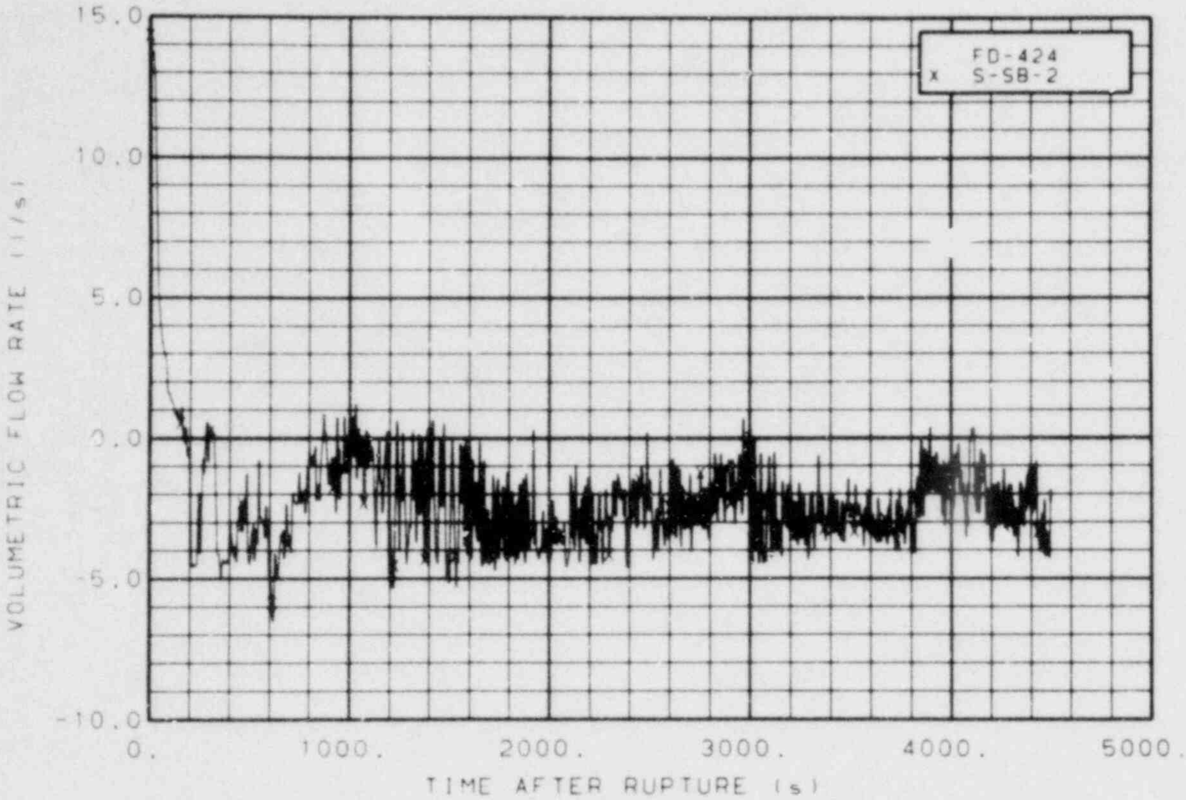

Figure 276. Volumetric Flow rate in downcomer, Test S-SB-2 (FD-424), from 0 to 4500 s.

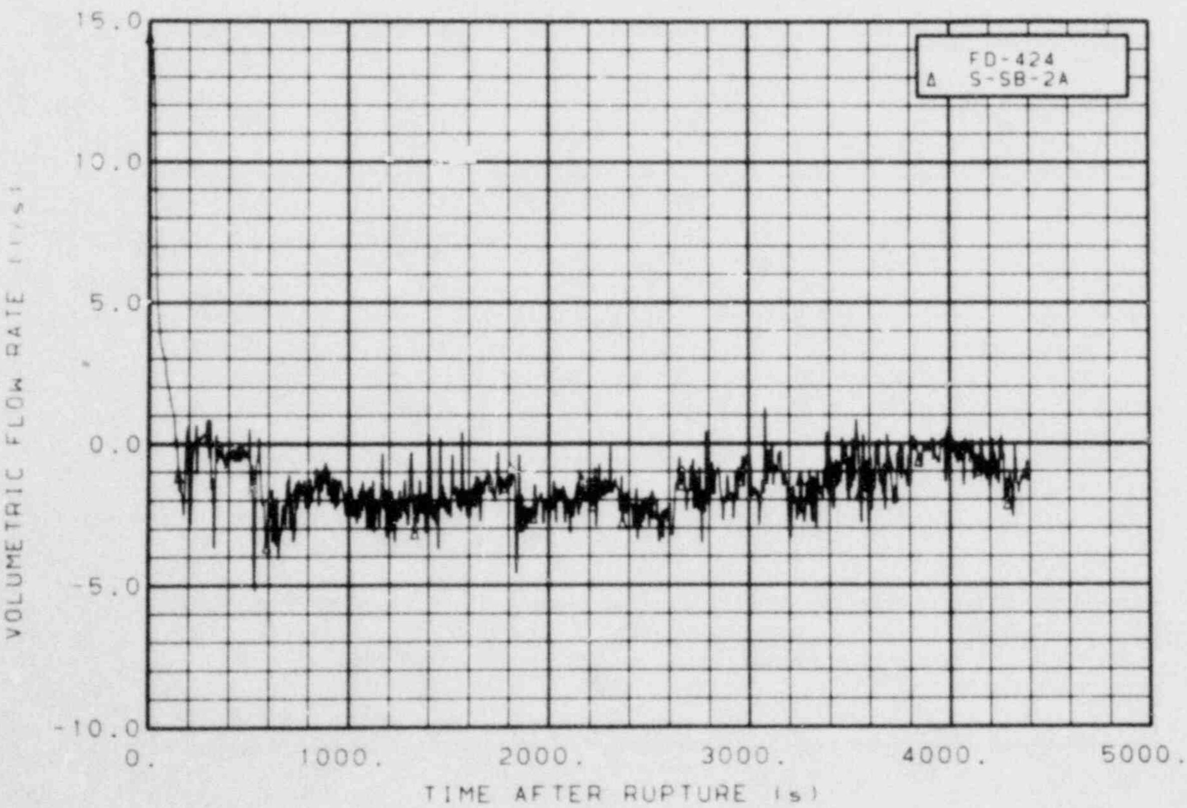

Figure 277. Volumetric Flow rate in downcomer, Test S-SB-2A (FD-424), from 0 to 4390 s.

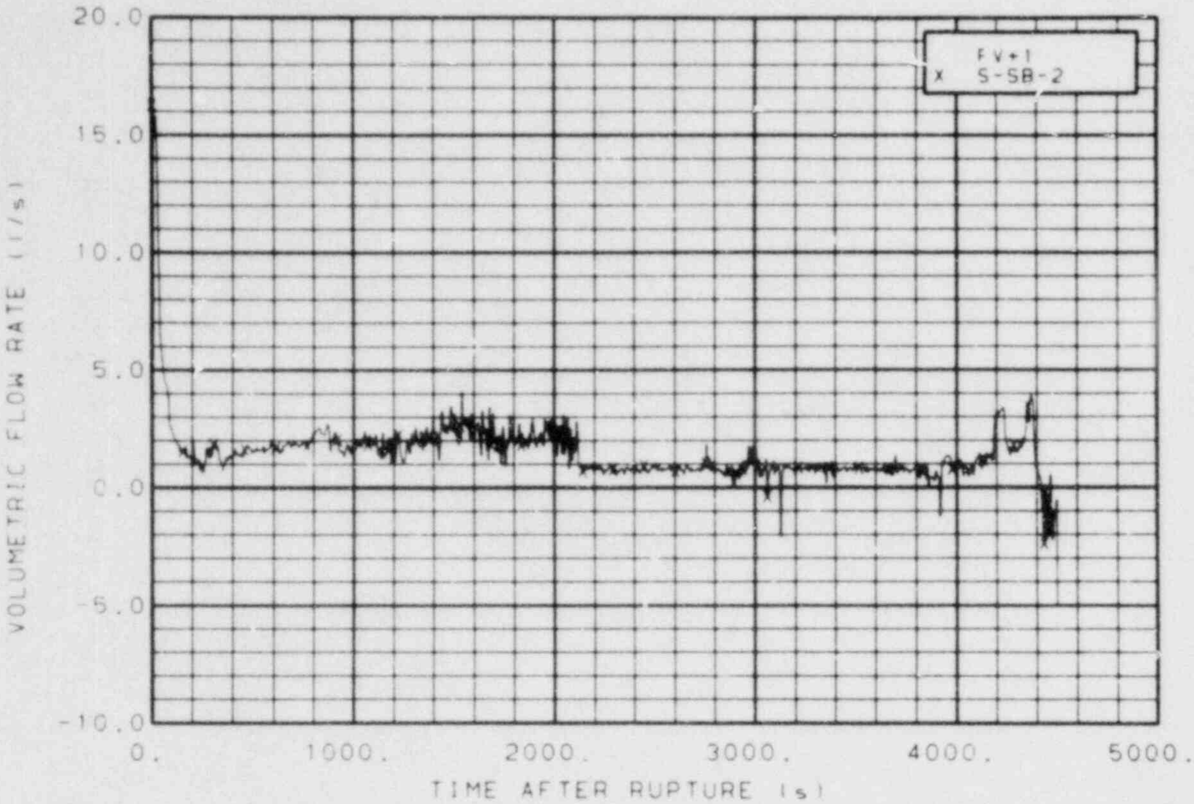

Figure 278. Volumetric Flow rate in vessel upper plenum, Test S-SB-2 (FV + 1), from 0 to 4500 s.

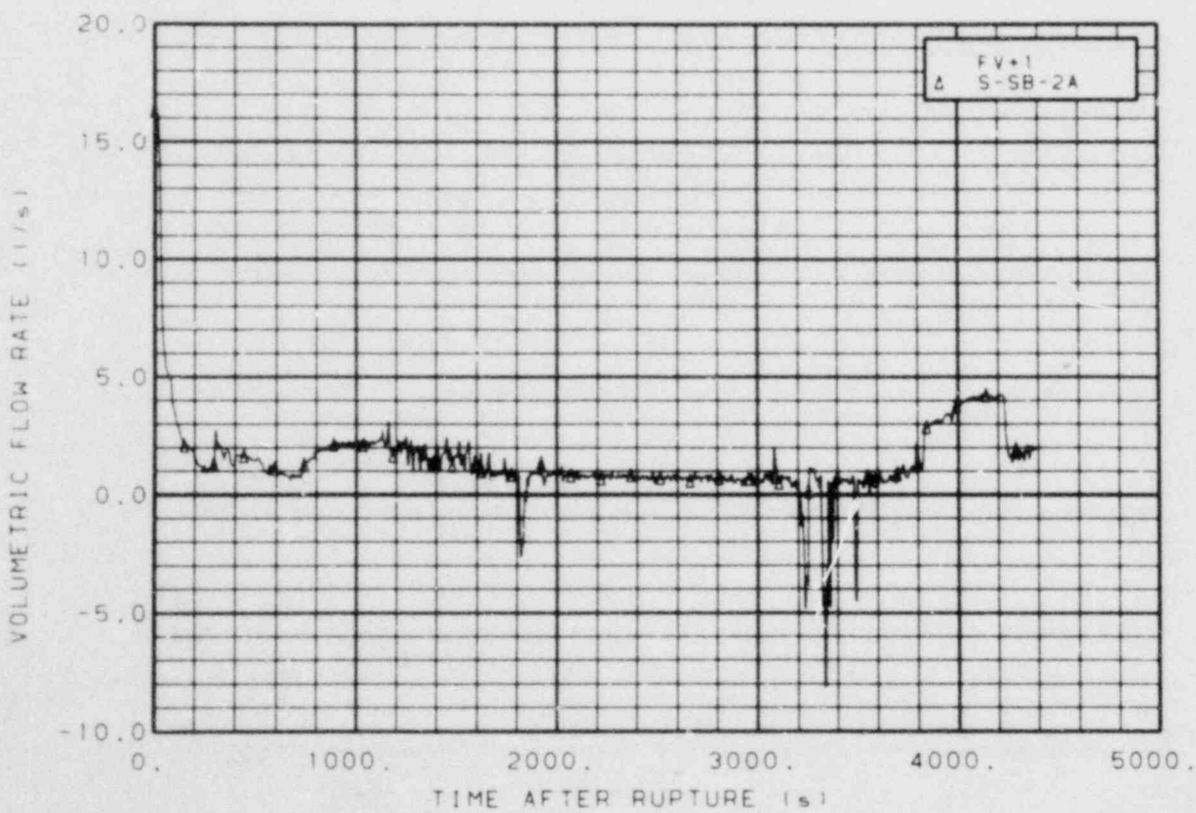

Figure 279. Volumetric Flow rate in vessel upper plenum, Test S-SB-2A (FV + 1), from 0 to 4390 s.

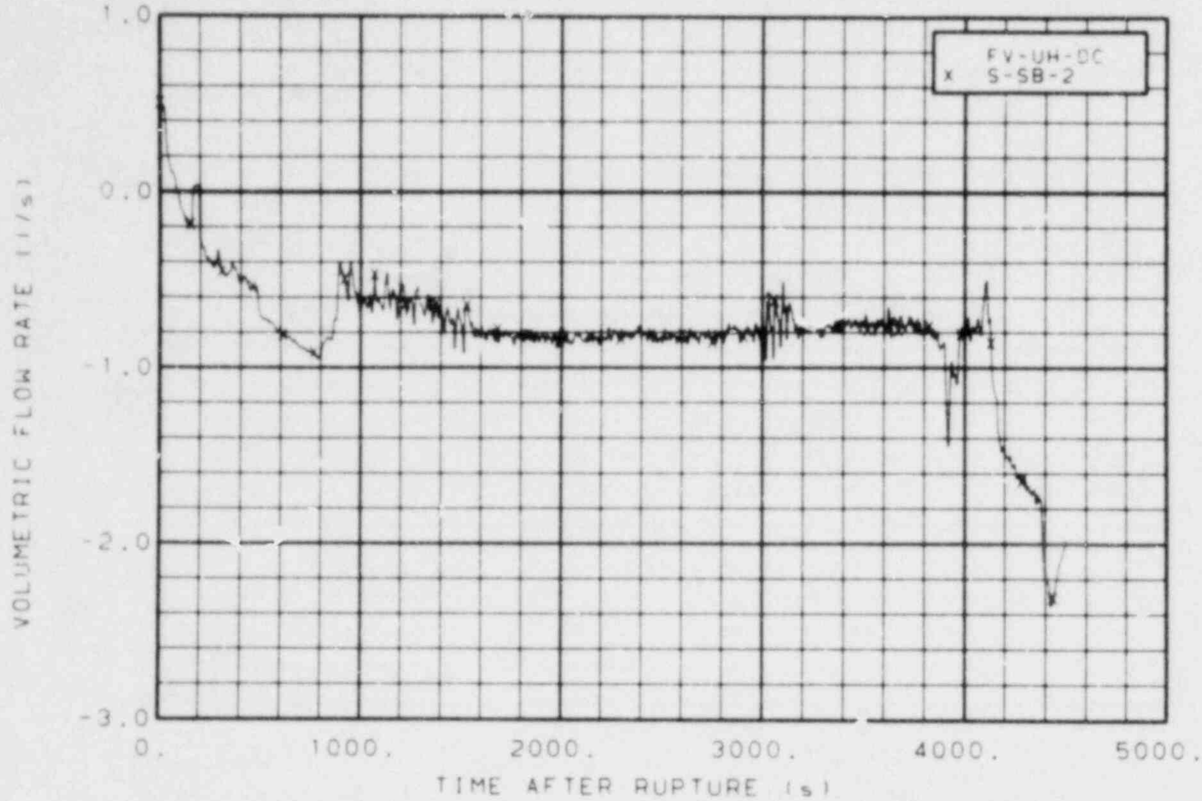

Figure 280. Volumetric Flow rate in upper head heat-up by-pass line, Test S-SB-2 (FV-UH-DC), from 0 to 4500 s.

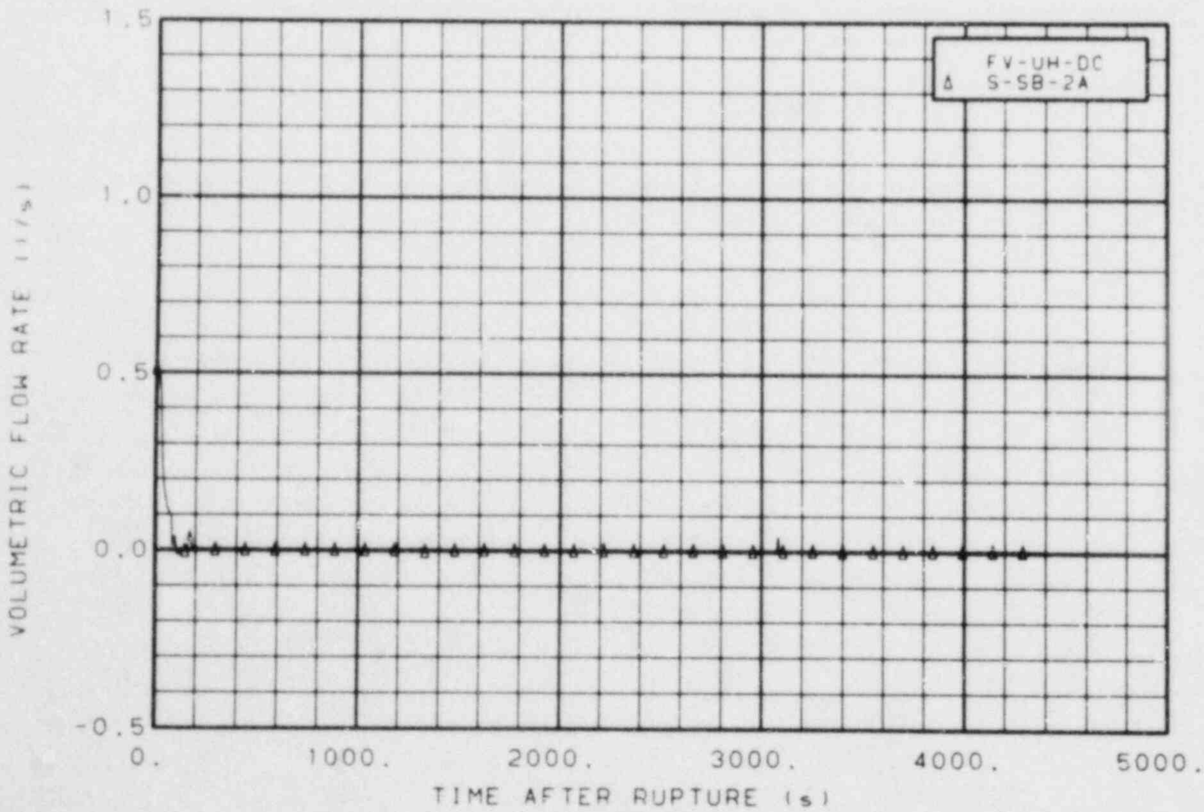

Figure 281. Volumetric Flow rate in upper head heat-up by-pass line, Test S-SB-2A (FV-UH-DC), from 0 to 4390 s.

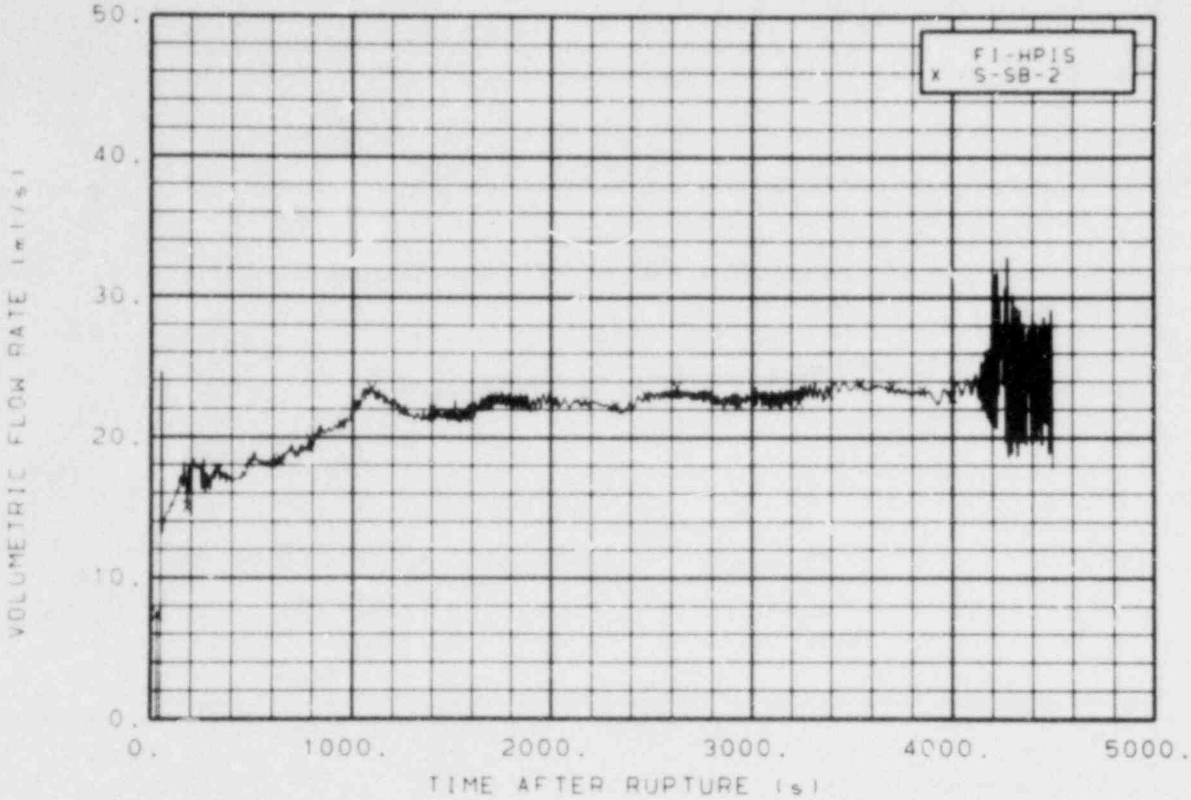

Figure 282. Volumetric Flow rate in intact loop high pressure injection system, Test S-SB-2 (FI-HPIS), from 0 to 4500 s.

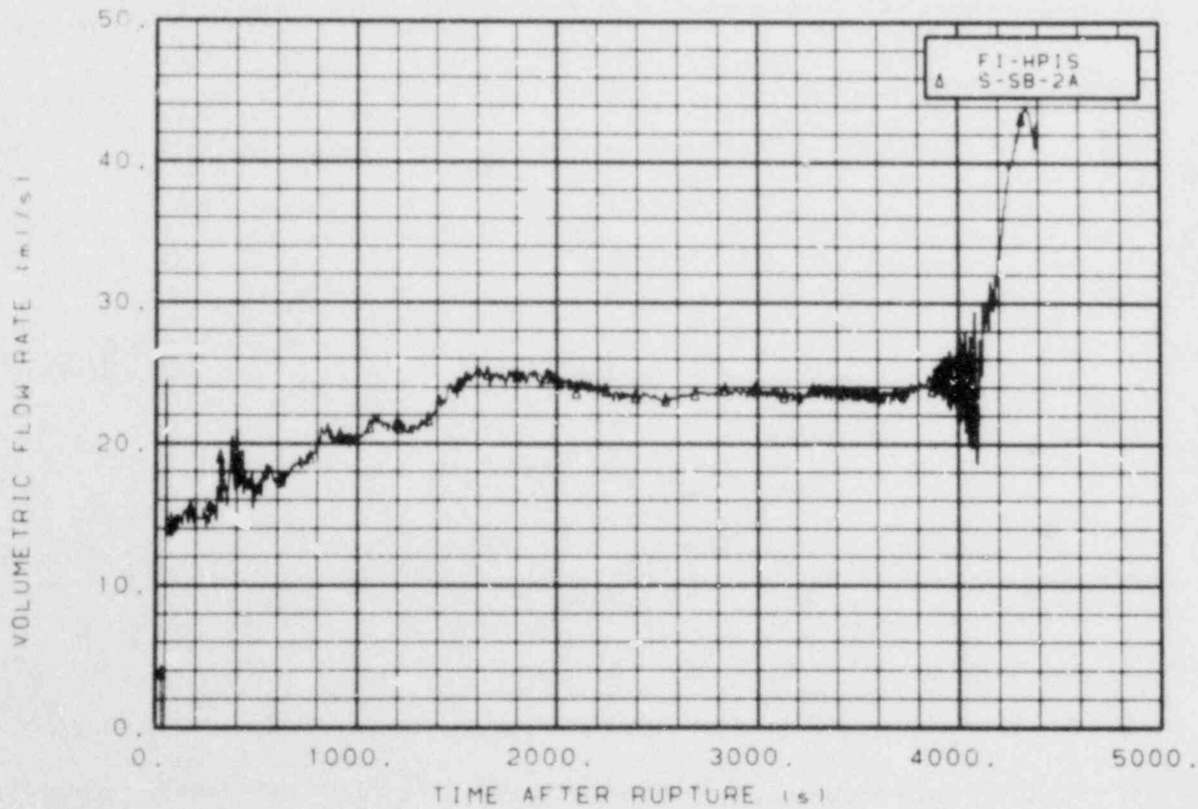

Figure 283. Volumetric Flow rate in intact loop high pressure injection system, Test S-SB-2A (FI-HPIS), from 0 to 4390 s.

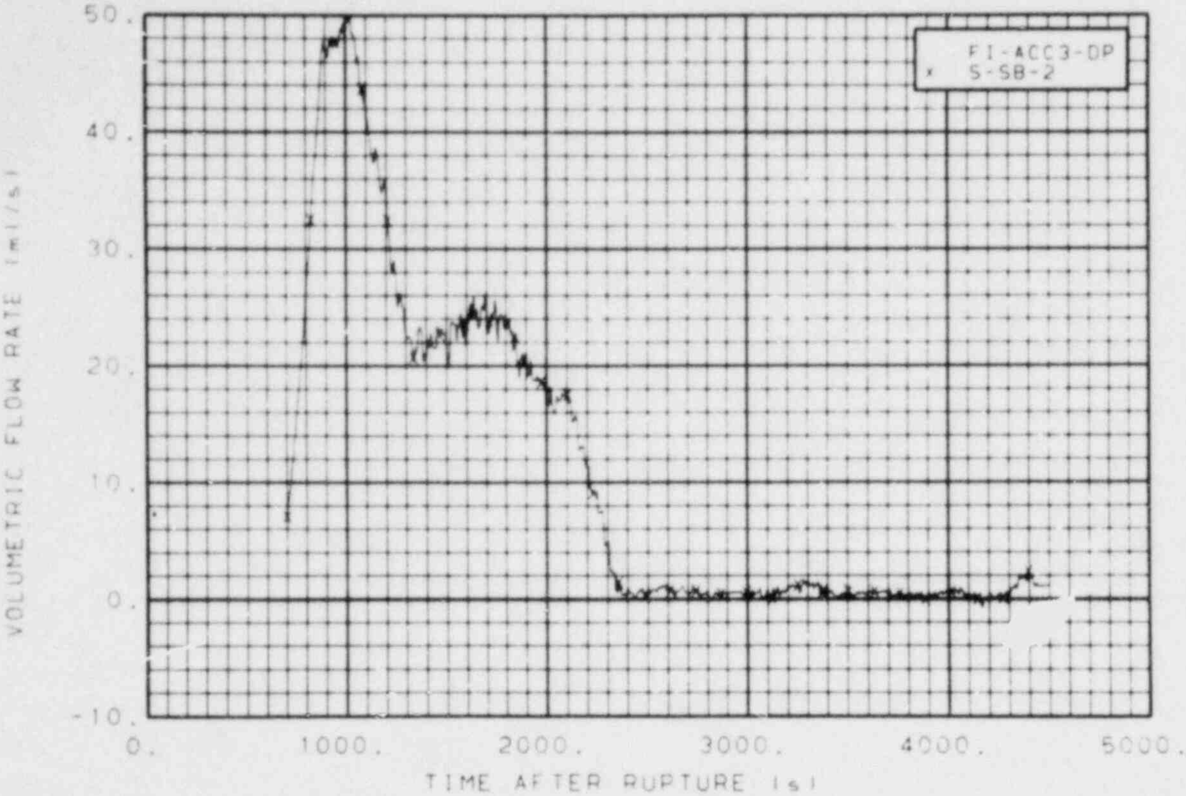

Figure 284. Calculated Volumetric Flow rate from measurement DI-ACC3-LL in intact loop, ECC accumulator, Test S-SB-2 (FI-ACC3-DP), from 700 to 4500 s.

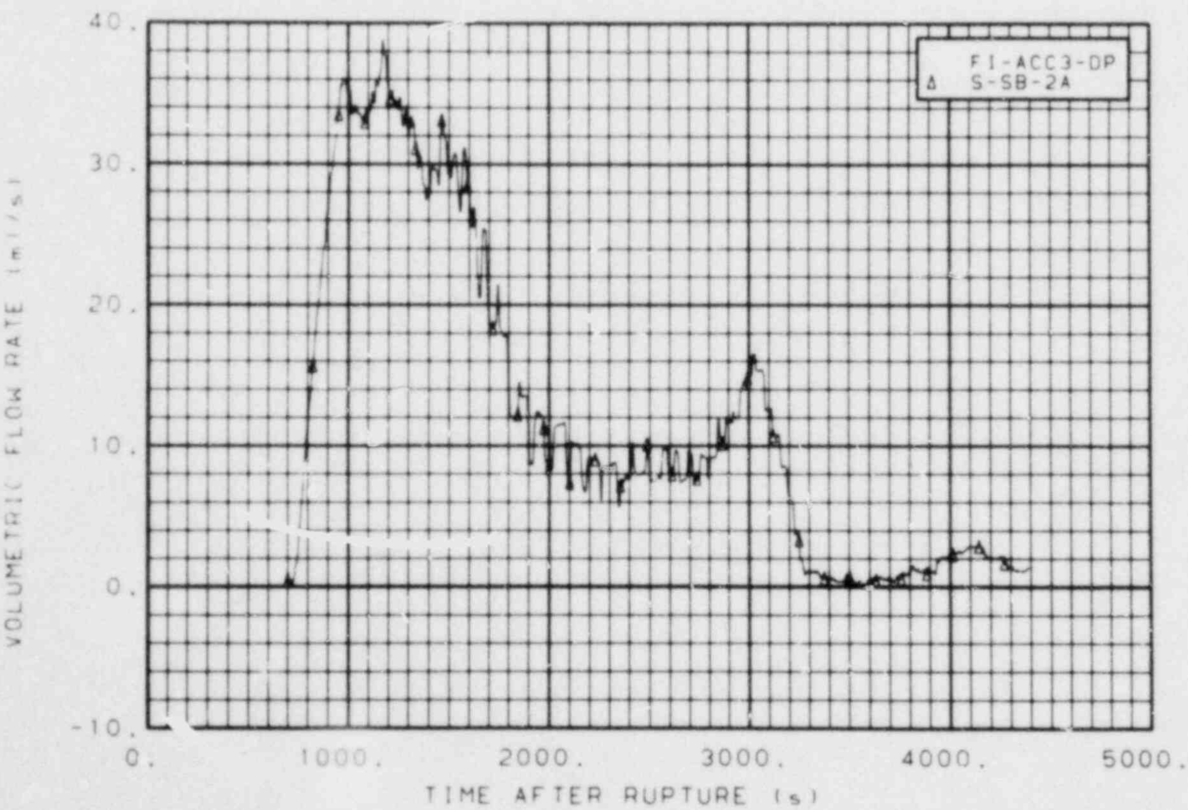

Figure 285. Calculated Volumetric Flow rate from measurement DI-ACC3-LL in intact loop, ECC accumulator, Test S-SB-2A (FI-ACC3-DP), from 700 to 4390 s.

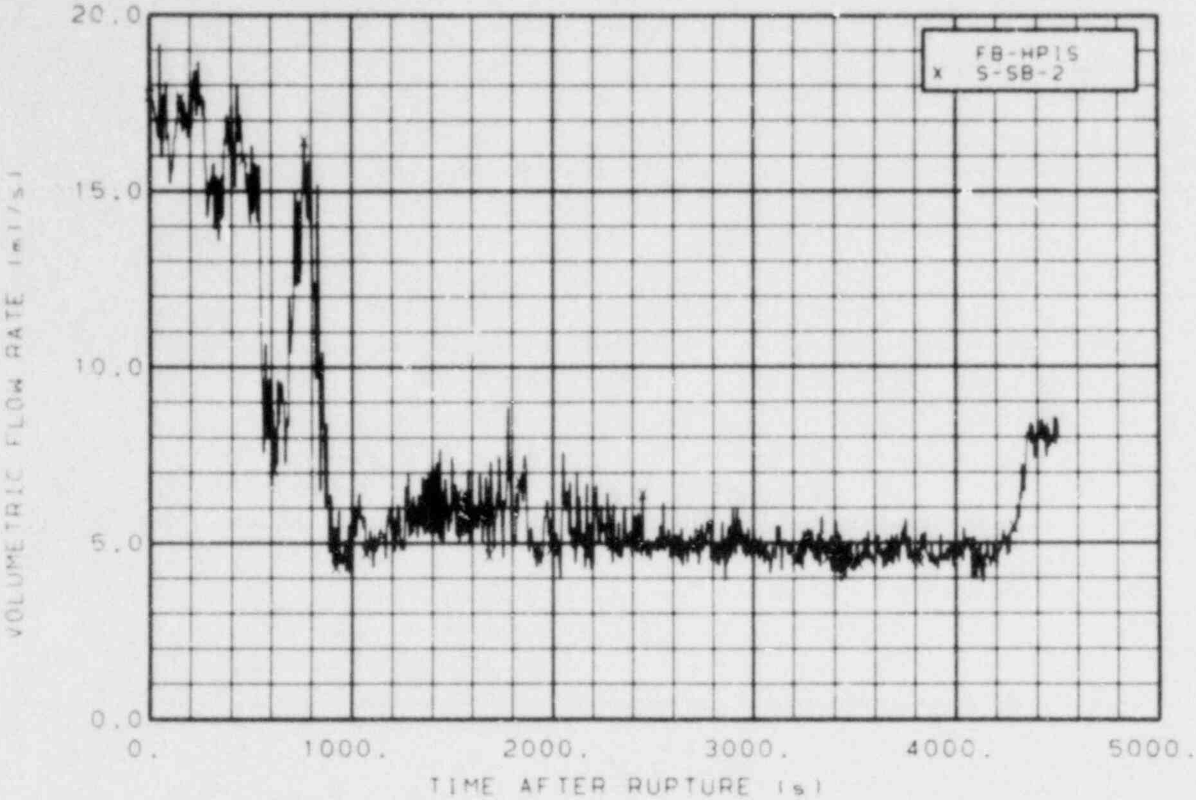

Figure 286. Volumetric Flow rate in broken loop high pressure injection system, Test S-SB-2 (FB-HPIS), from 0 to 4500 s.

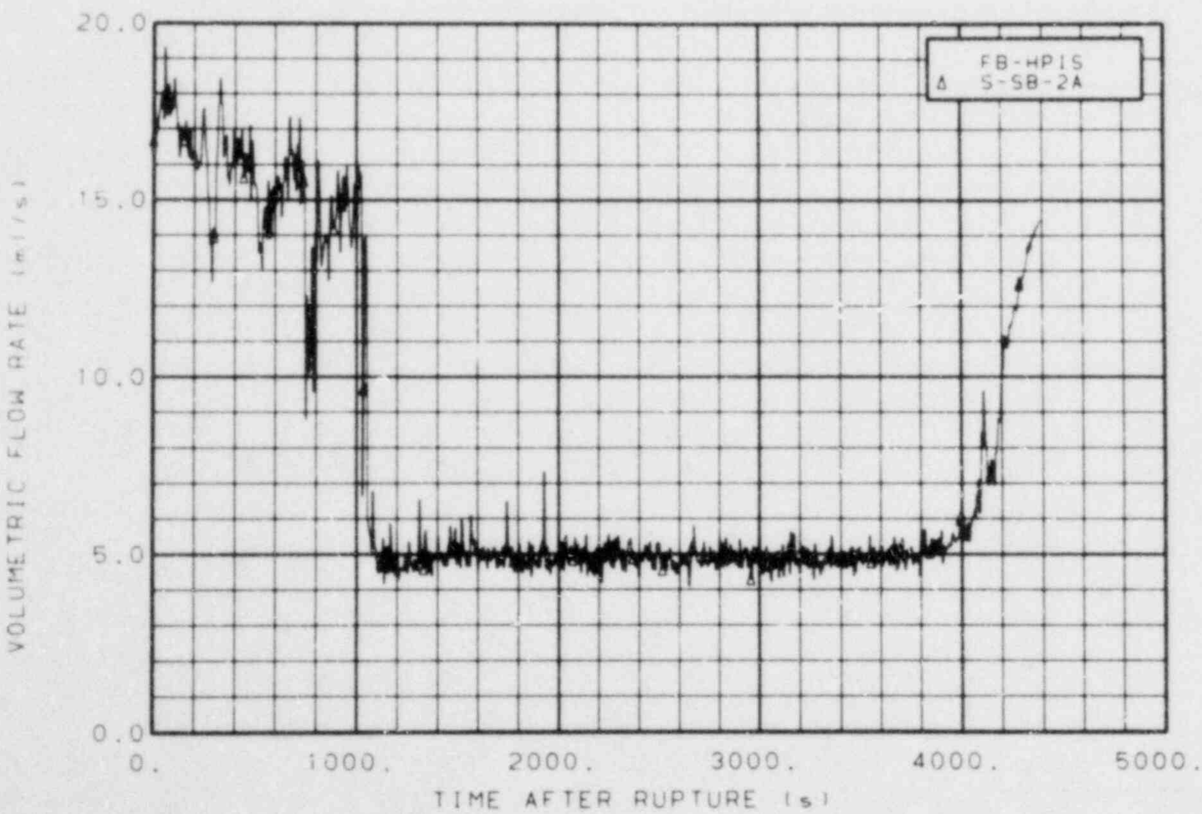

Figure 287. Volumetric Flow rate in broken loop high pressure injection system, Test S-SB-2A (FB-HPIS), from 0 to 4390 s.

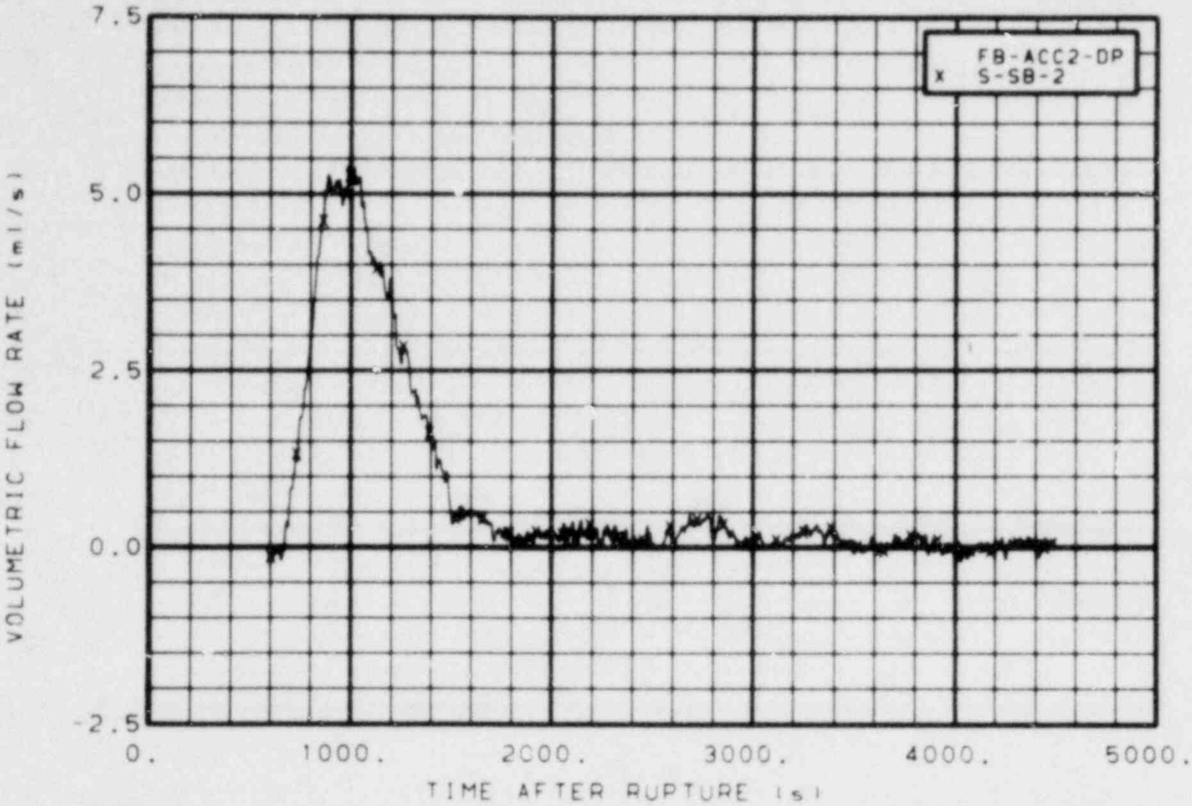

Figure 288. Calculated Volumetric Flow rate from measurement DB-ACC2-LL in broken loop, ECC accumulator, Test S-SB-2 (FB-ACC2-DP), from 700 to 4500 s.

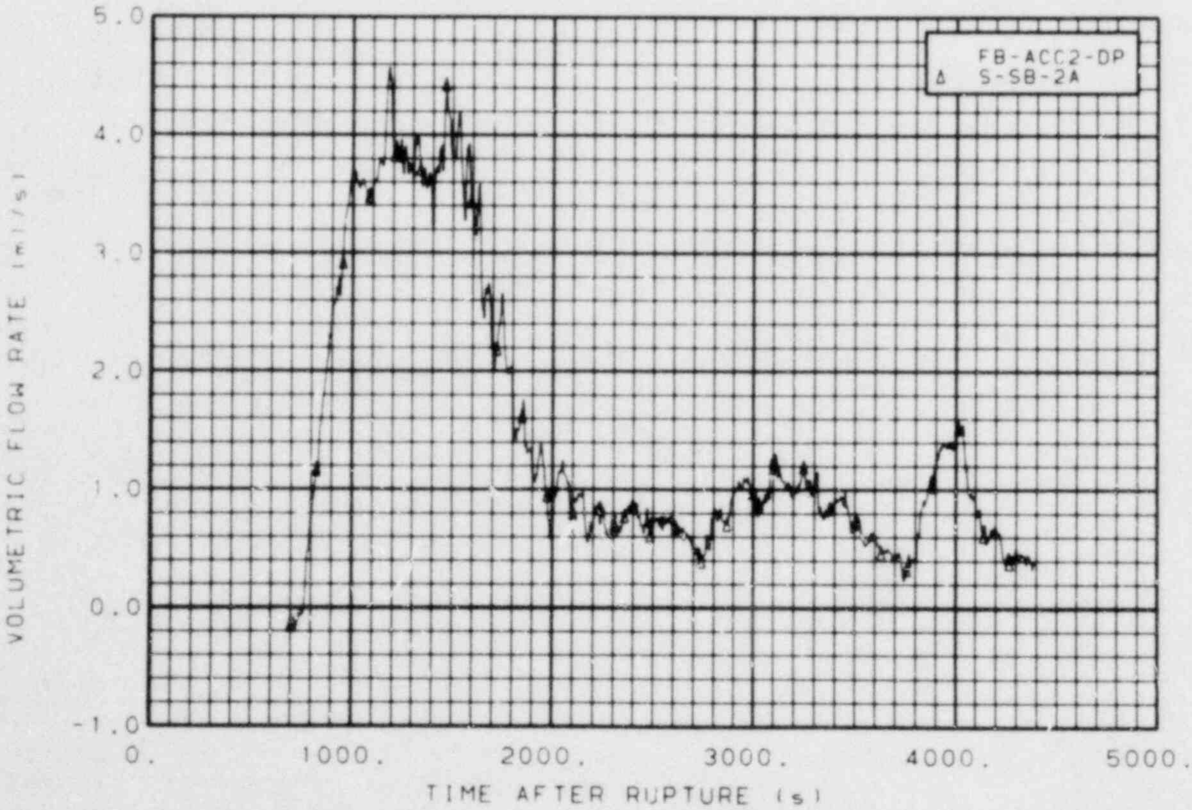

Figure 289. Calculated Volumetric Flow rate from measurement DB-ACC2-LL in broken loop, ECC accumulator, Test S-SB-2A (FB-ACC2-DP), from 700 to 4390 s.

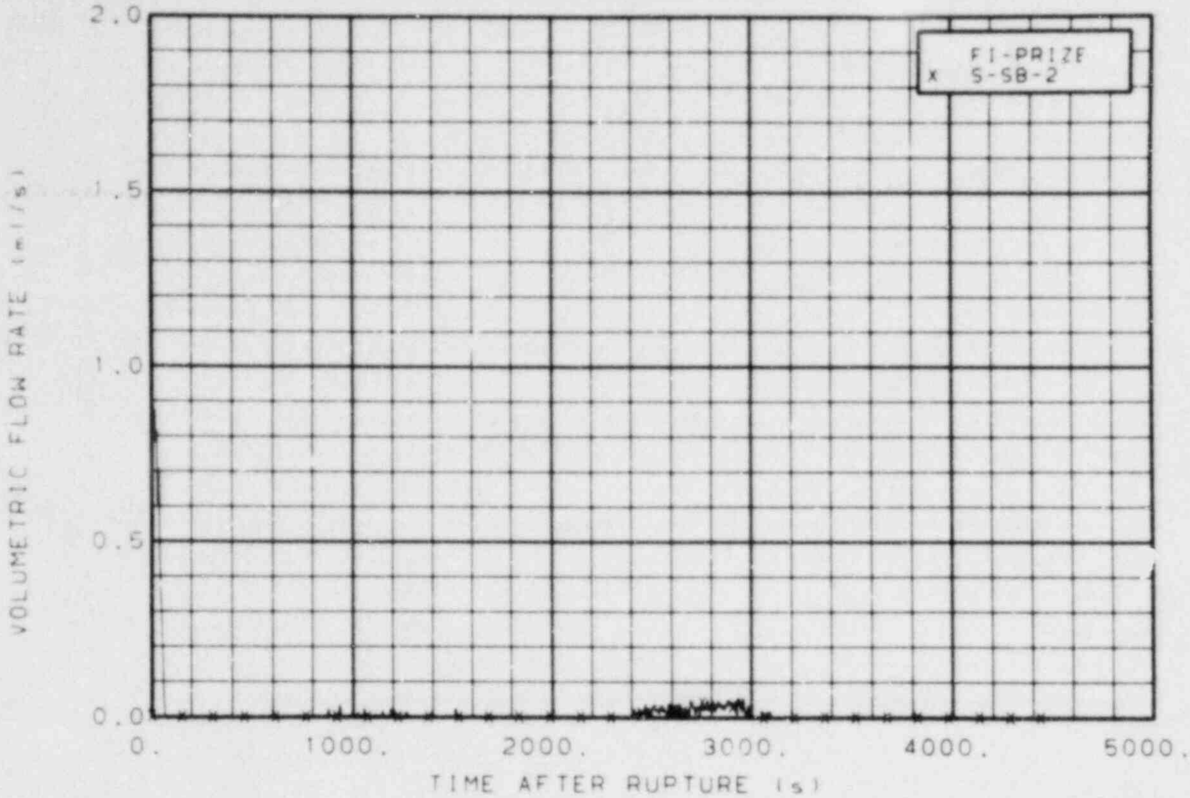

Figure 290. Volumetric Flow rate in intact loop, pressurizer surge line, Test S-SB-2 (FI-PRIZE), from 0 to 4500 s.

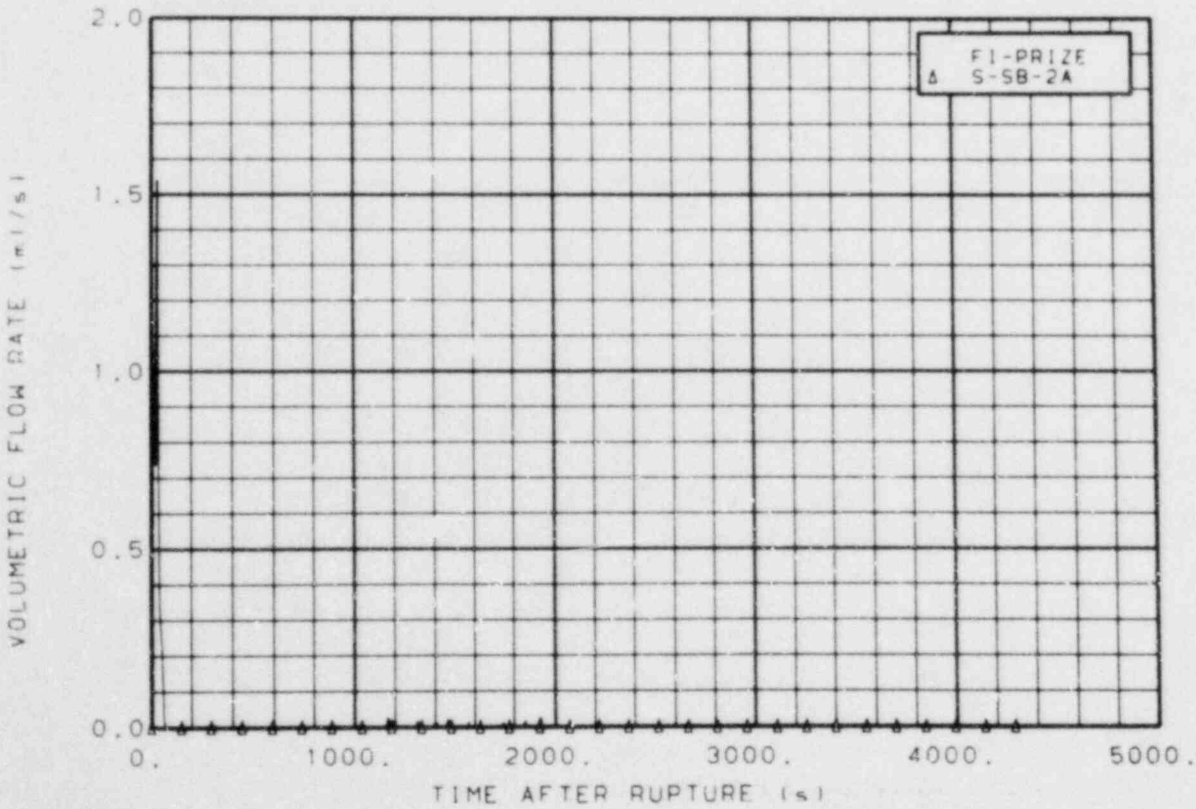

Figure 291. Volumetric Flow rate in intact loop, pressurizer surge line, Test S-SB-2A (FI-PRIZE), from 0 to 4390 s.

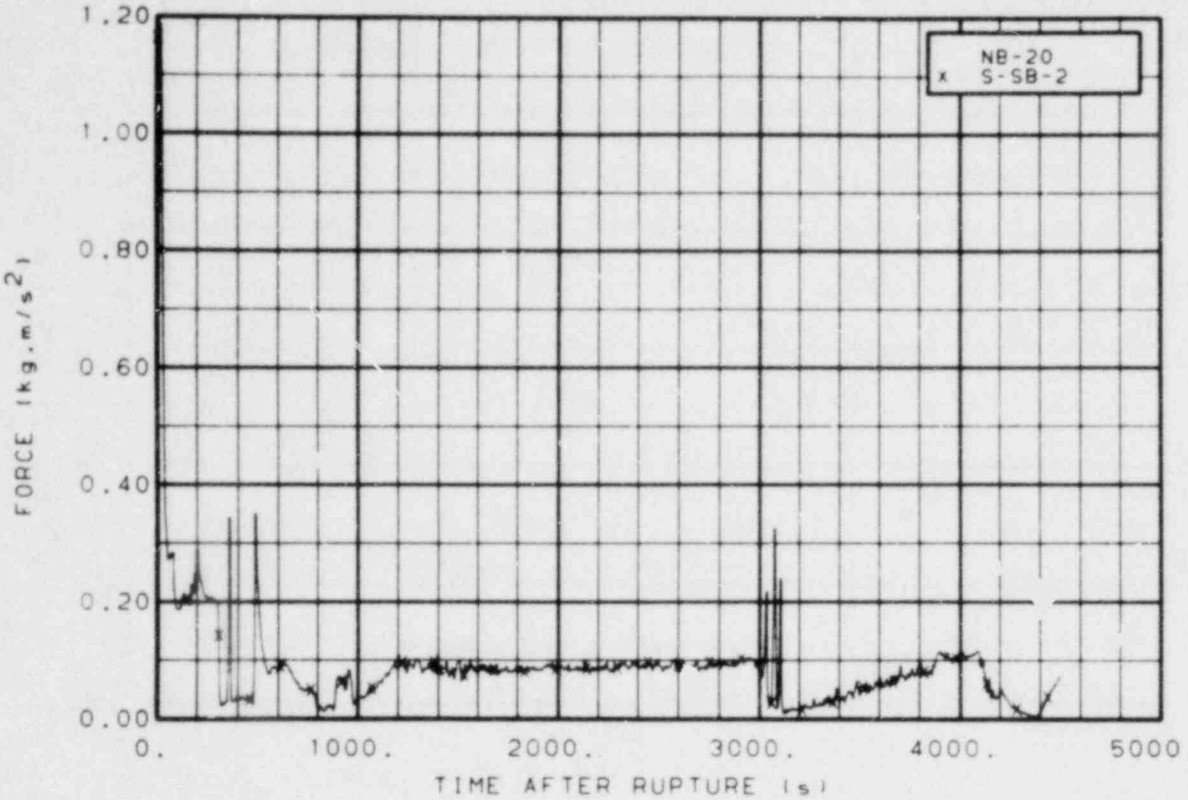

Figure 292. Momentum flux in broken loop hot leg, Test S-SB-2 (NB-20), from 0 to 4500 s.

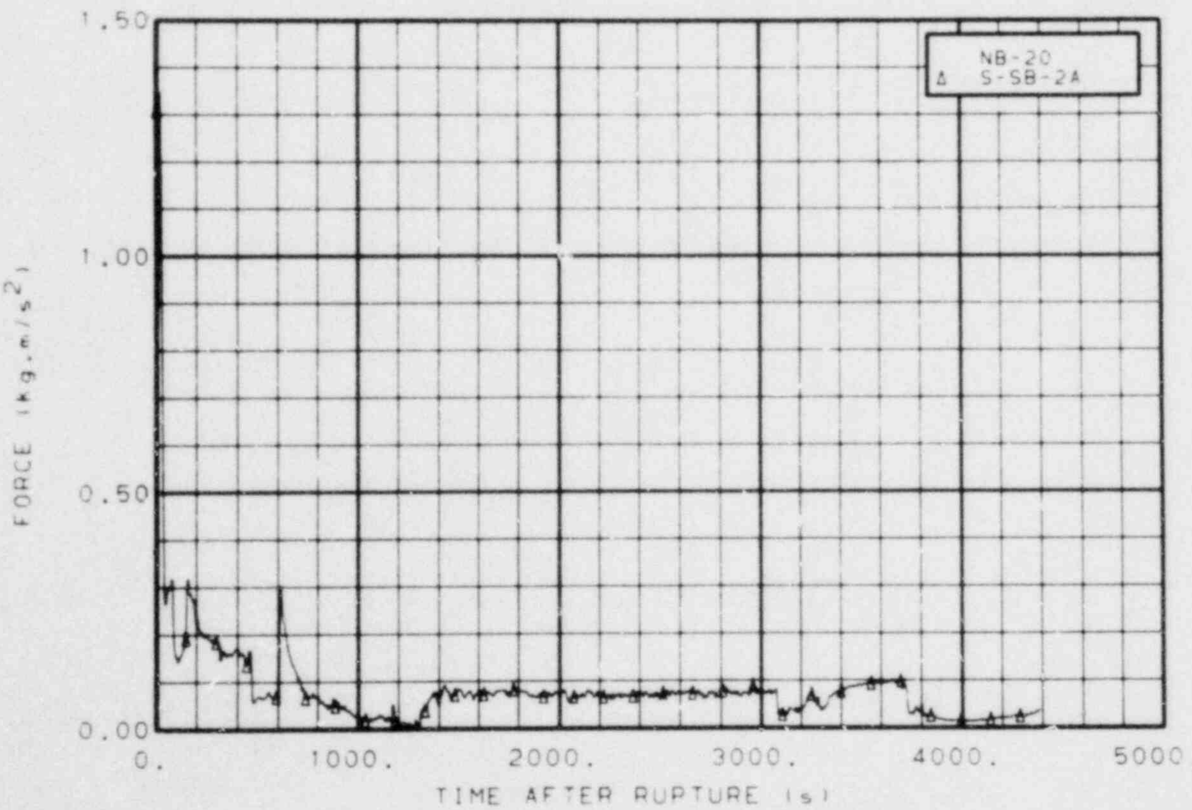

Figure 293. Momentum flux in broken loop hot leg, Test S-SB-2A (NB-20), from 0 to 4390 s.

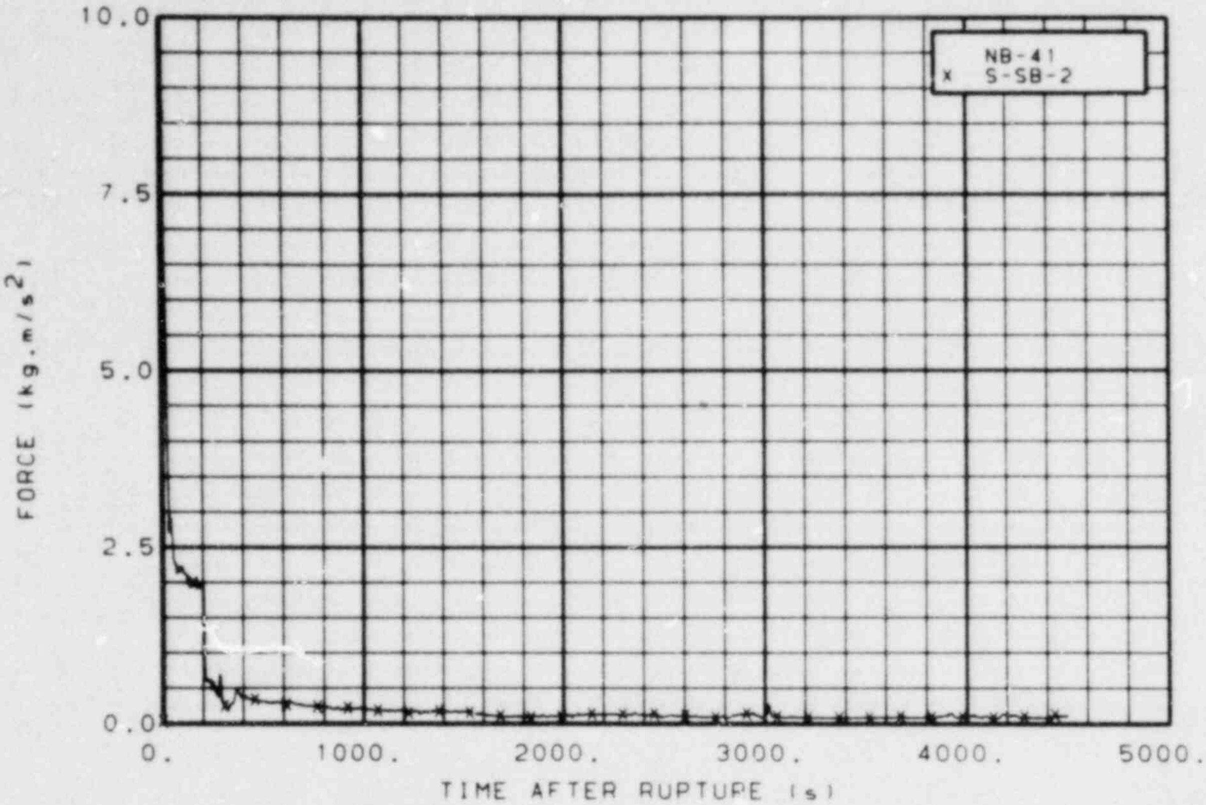

Figure 294. Momentum flux in broken loop cold leg, Test S-SB-2 (NB-41), from 0 to 4500 s.

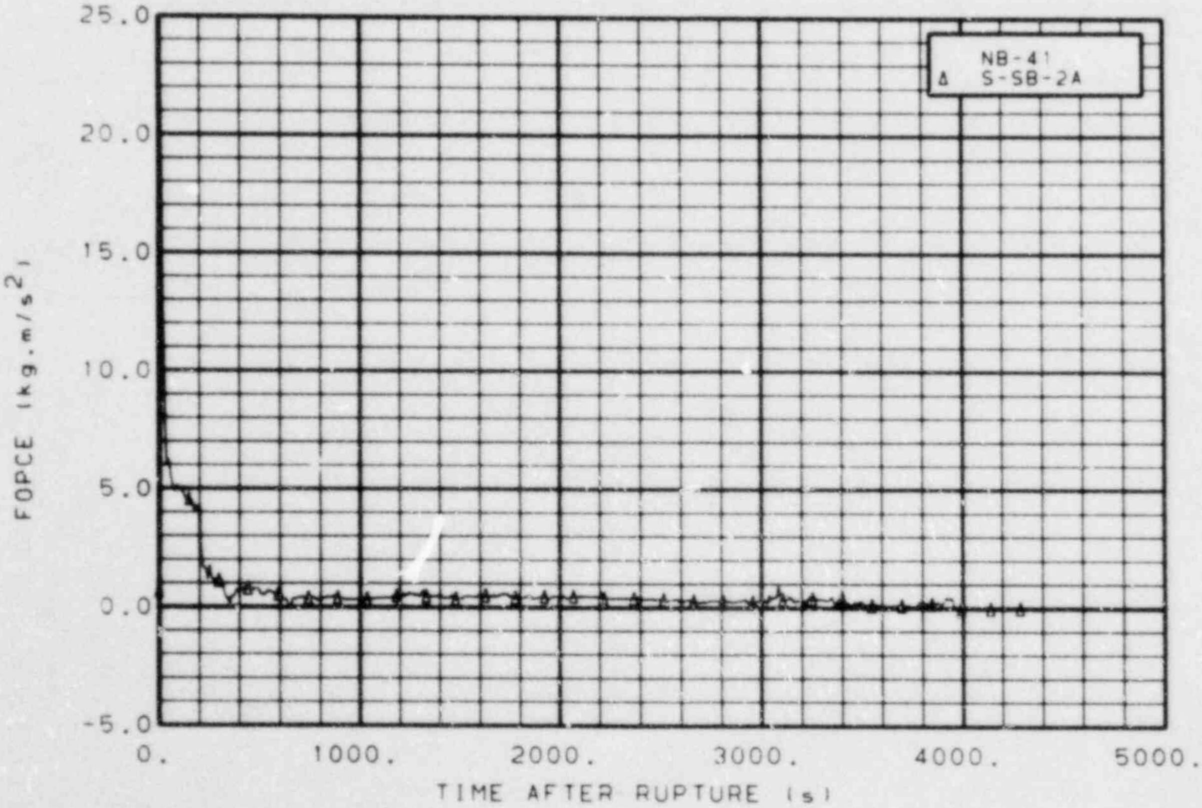

Figure 295. Momentum flux in broken loop cold leg, Test S-SB-2A (NB-41), from 0 to 4390 s.

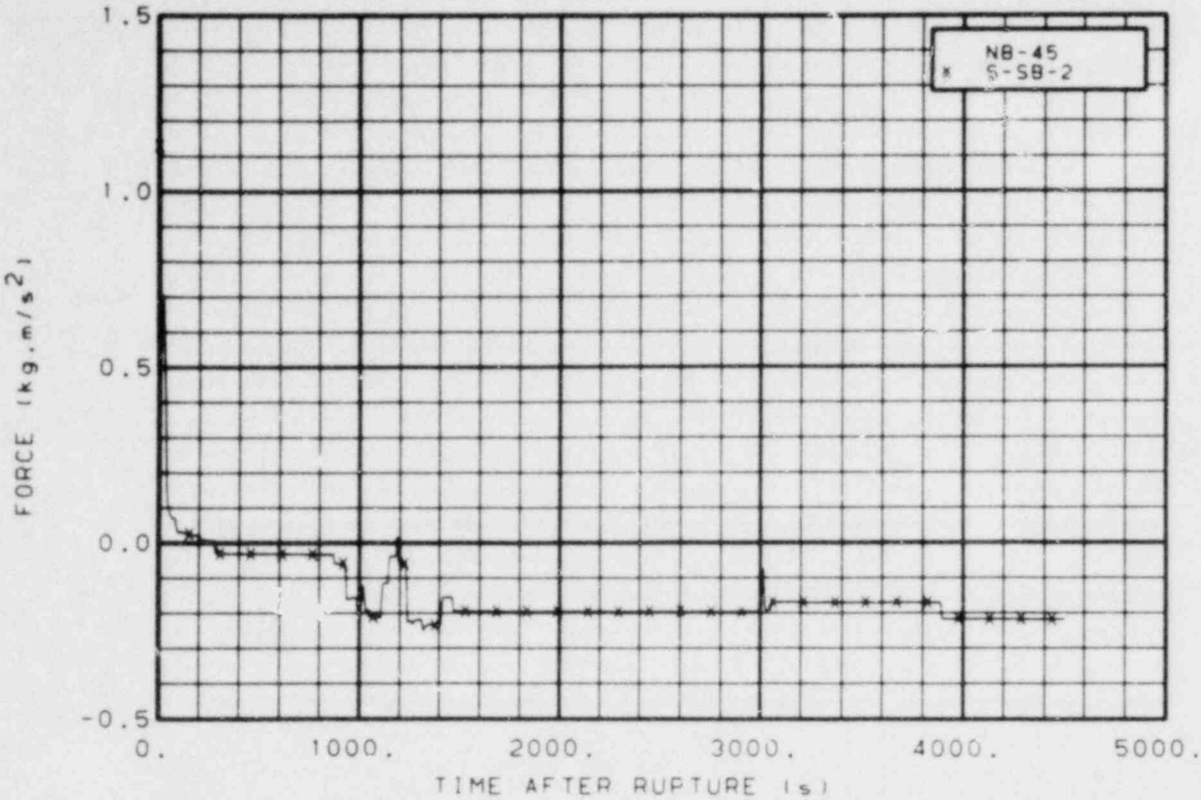

Figure 296. Momentum flux in broken loop cold leg, Test S-SB-2 (NB-45), from 0 to 4500 s.

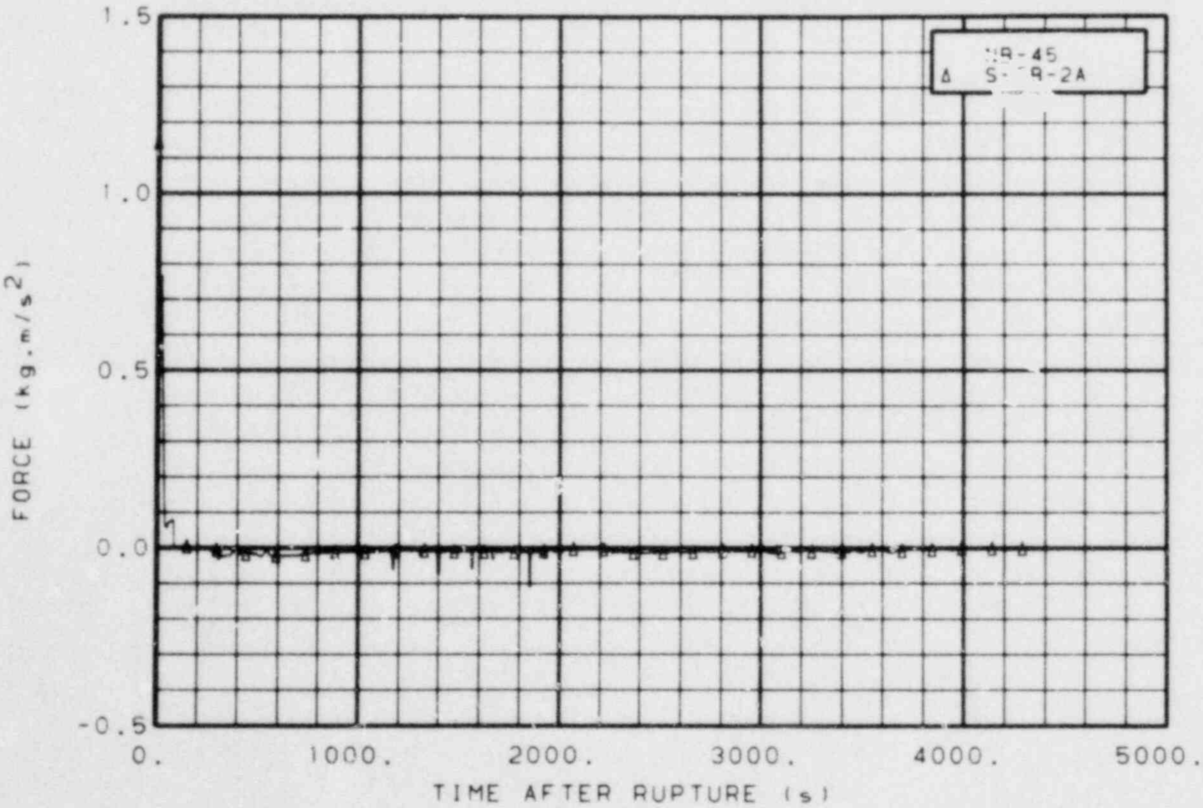

Figure 297. Momentum flux in broken loop cold leg, Test S-SB-2A (NB-45), from 0 to 4390 s.

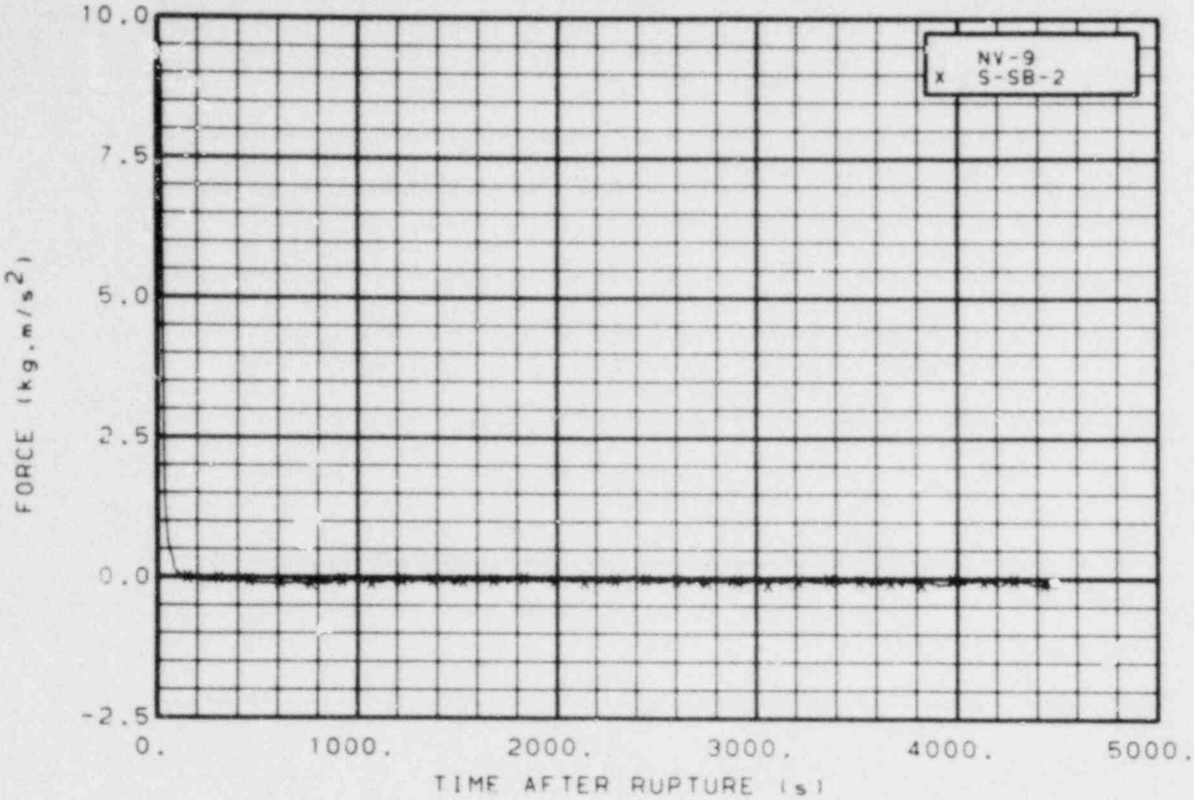

Figure 298. Momentum flux in core outlet, Test S-SB-2 (NV-9), from 0 to 4500 s.

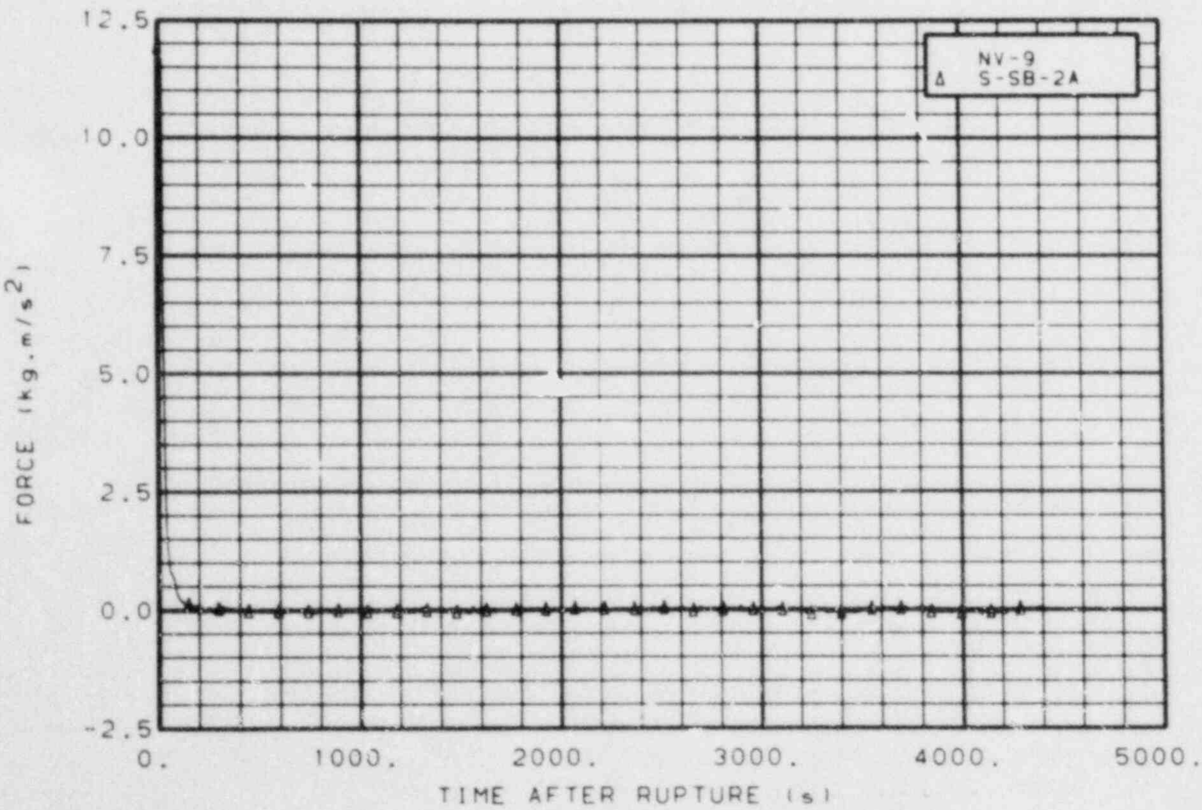

Figure 299. Momentum flux in core outlet, Test S-SB-2A (NV-9), from 0 to 4390 s.

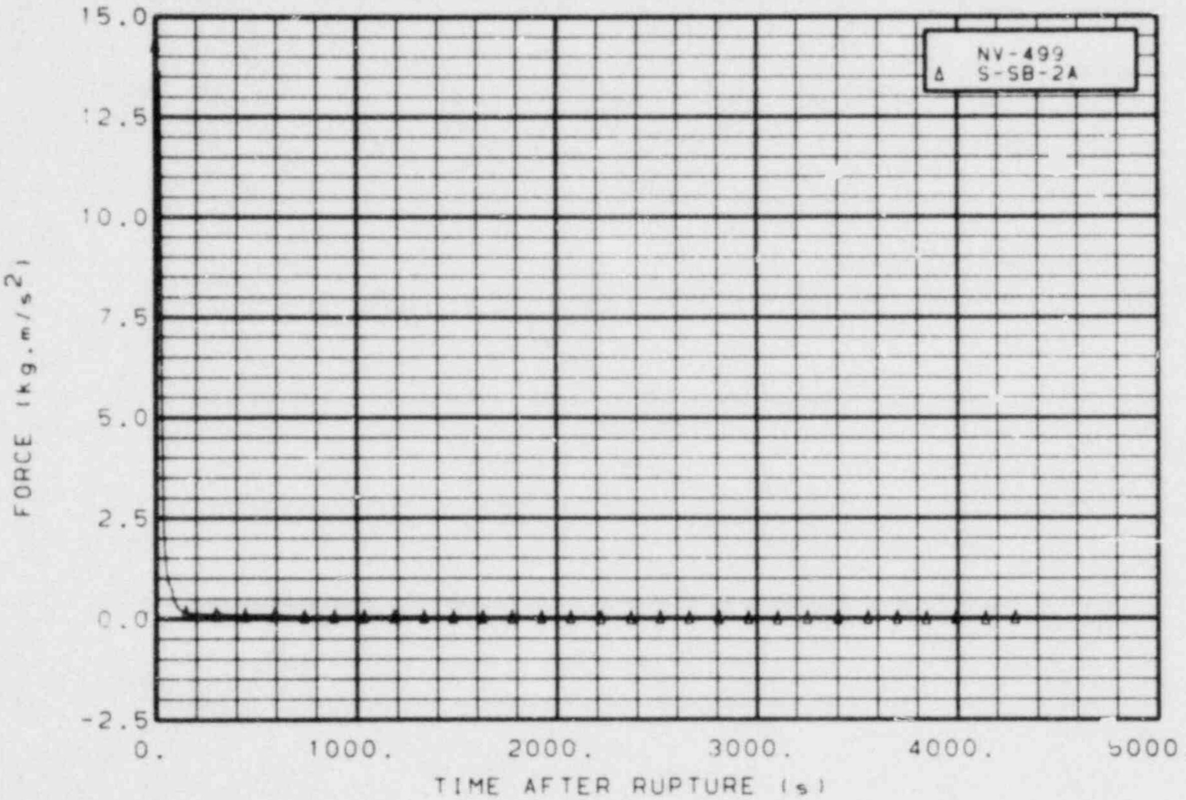

Figure 300. Momentum flux in core outlet, Test S-SB-2A (NV-499), from 0 to 4390 s.

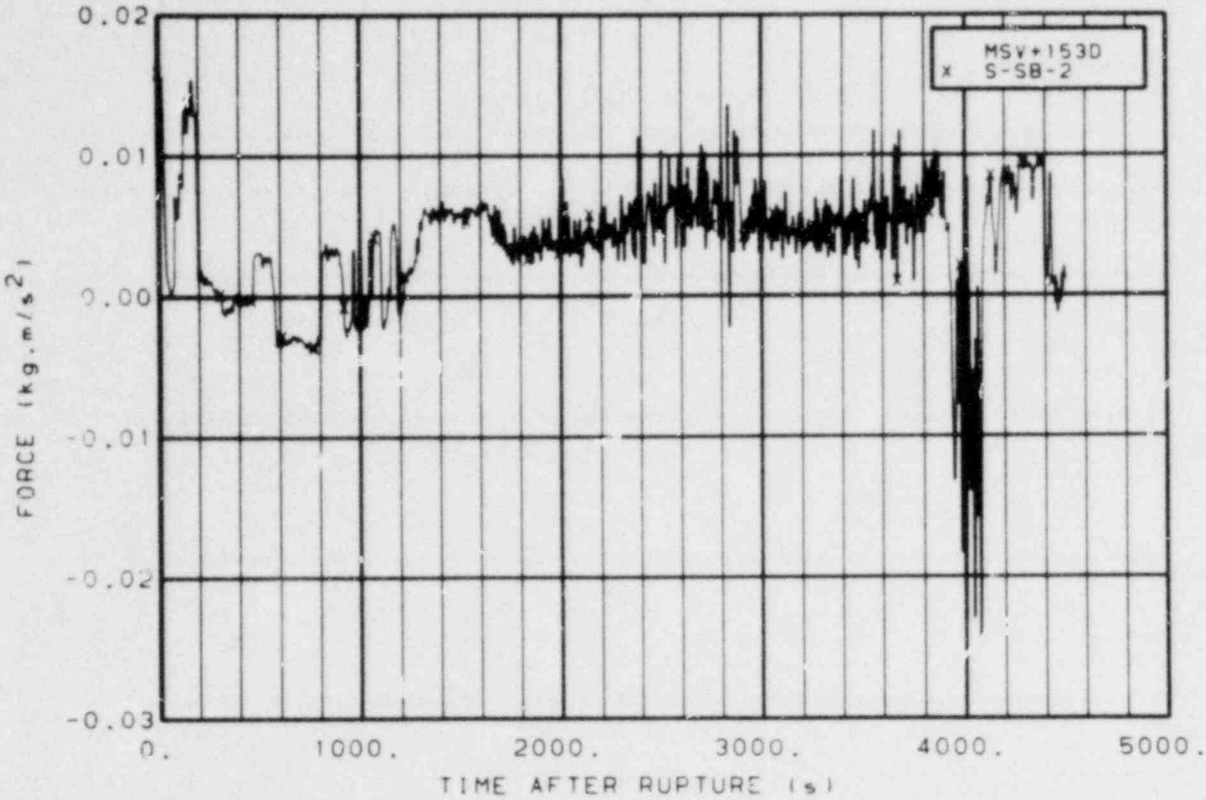

Figure 301. Momentum flux in vessel support tube, Test S-SB-2 (MSV + 153D), from 0 to 4500 s.

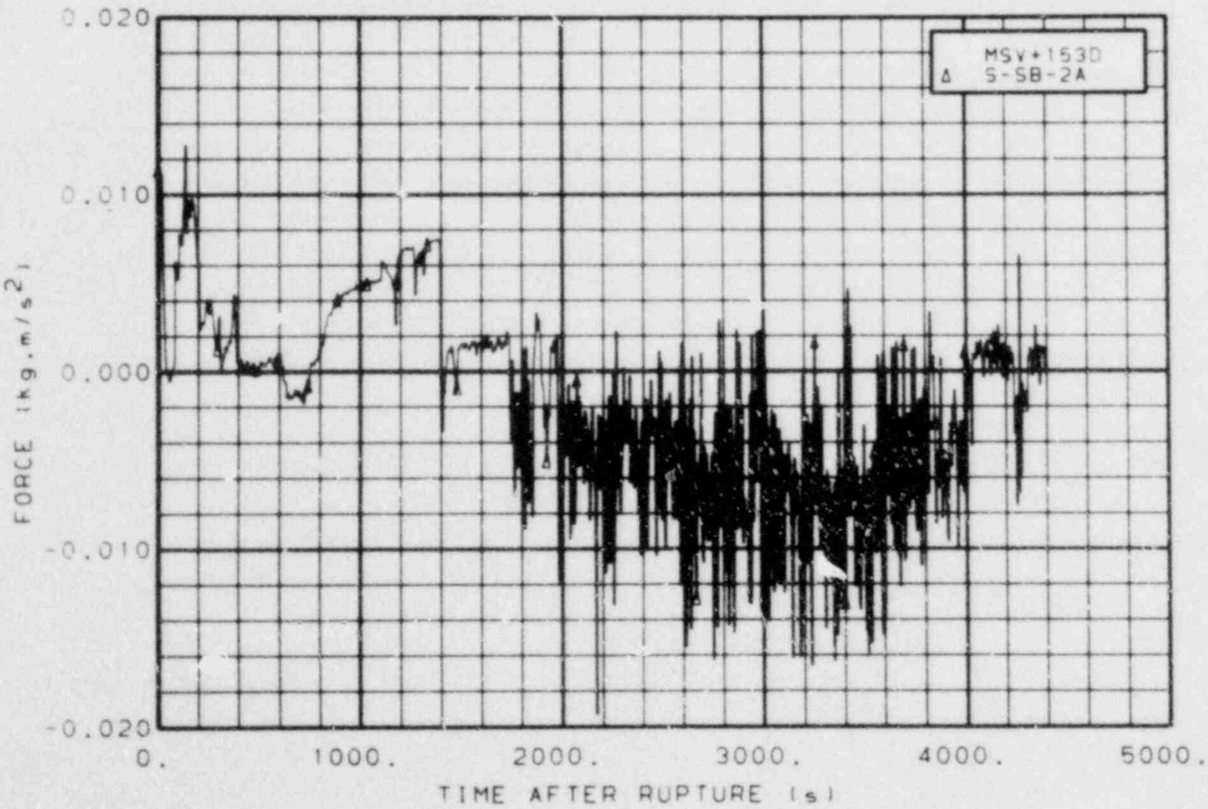

Figure 302. Momentum flux in vessel support tube, Test S-SB-2A (MSV + 153D), from 0 to 4390 s.

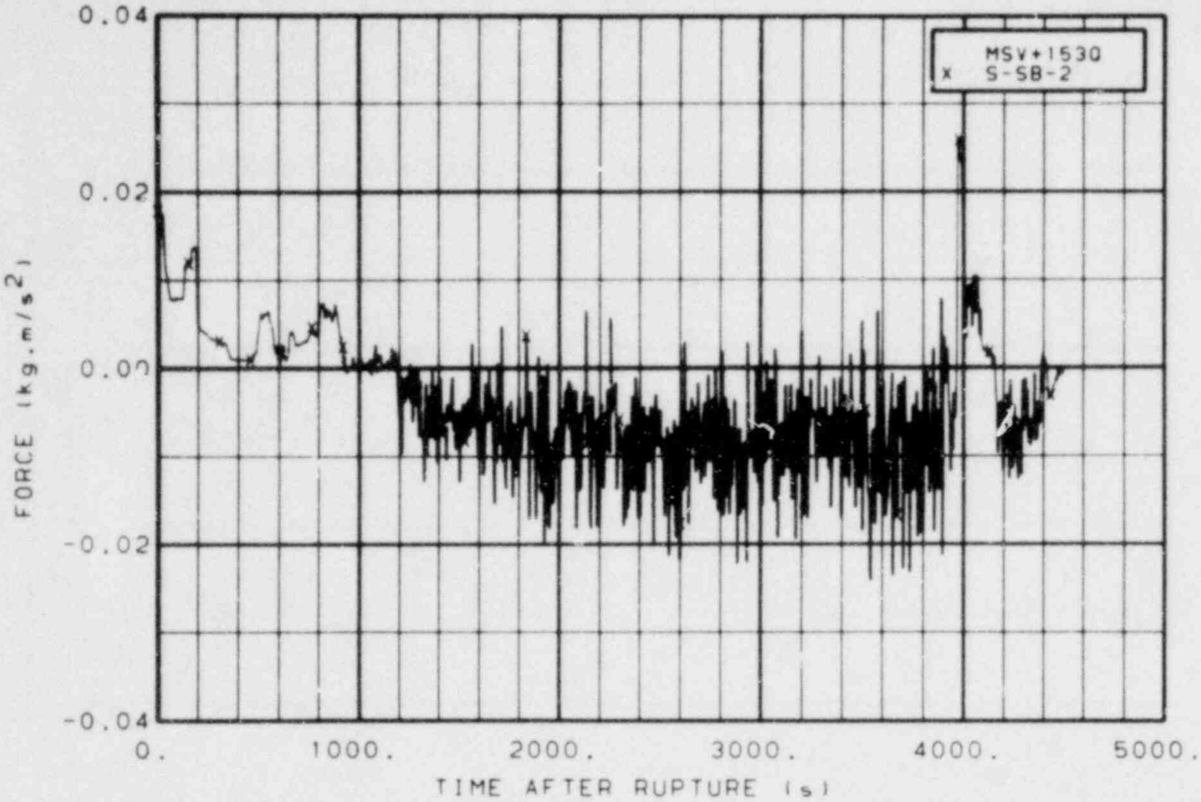

Figure 303. Momentum flux in vessel support tube, Test S-SB-2 (MSV + 153Q), from 0 to 4500 s.

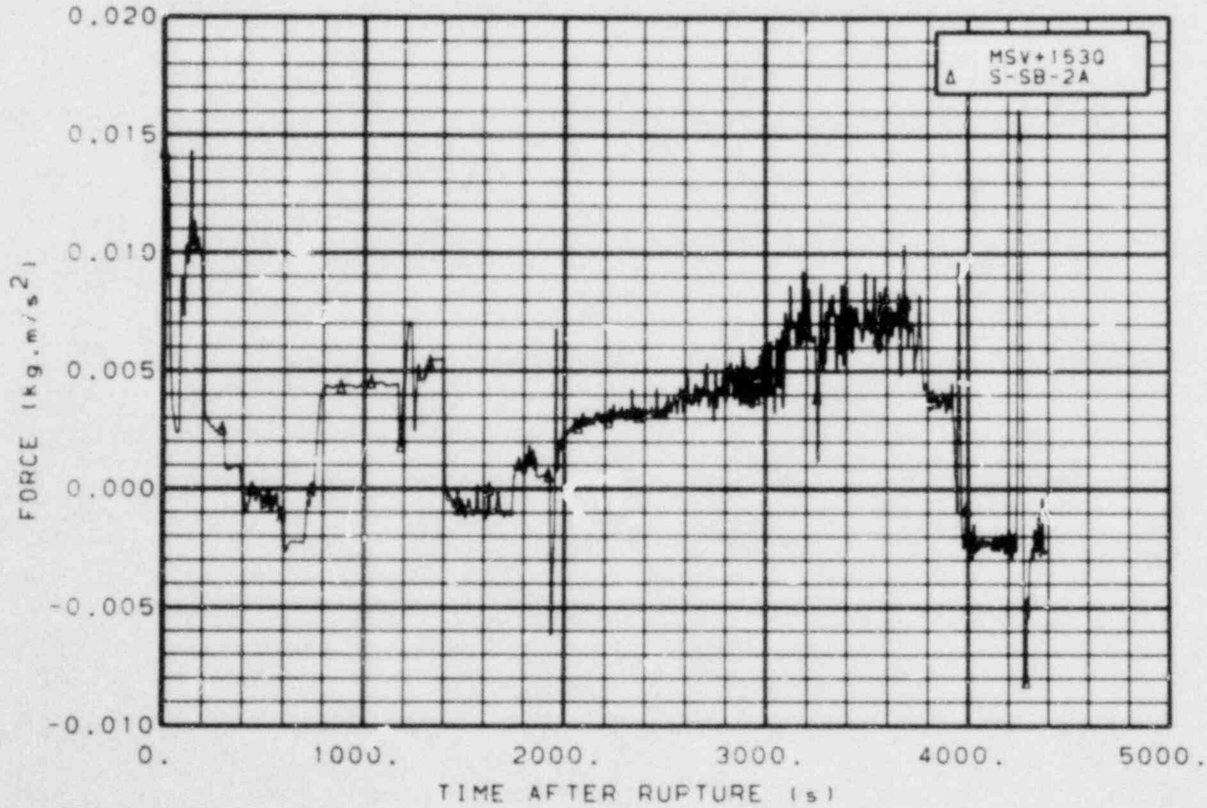

Figure 304. Momentum flux in vessel support tube, Test S-SB-2A (MSV + 153Q), from 0 to 4390 s.

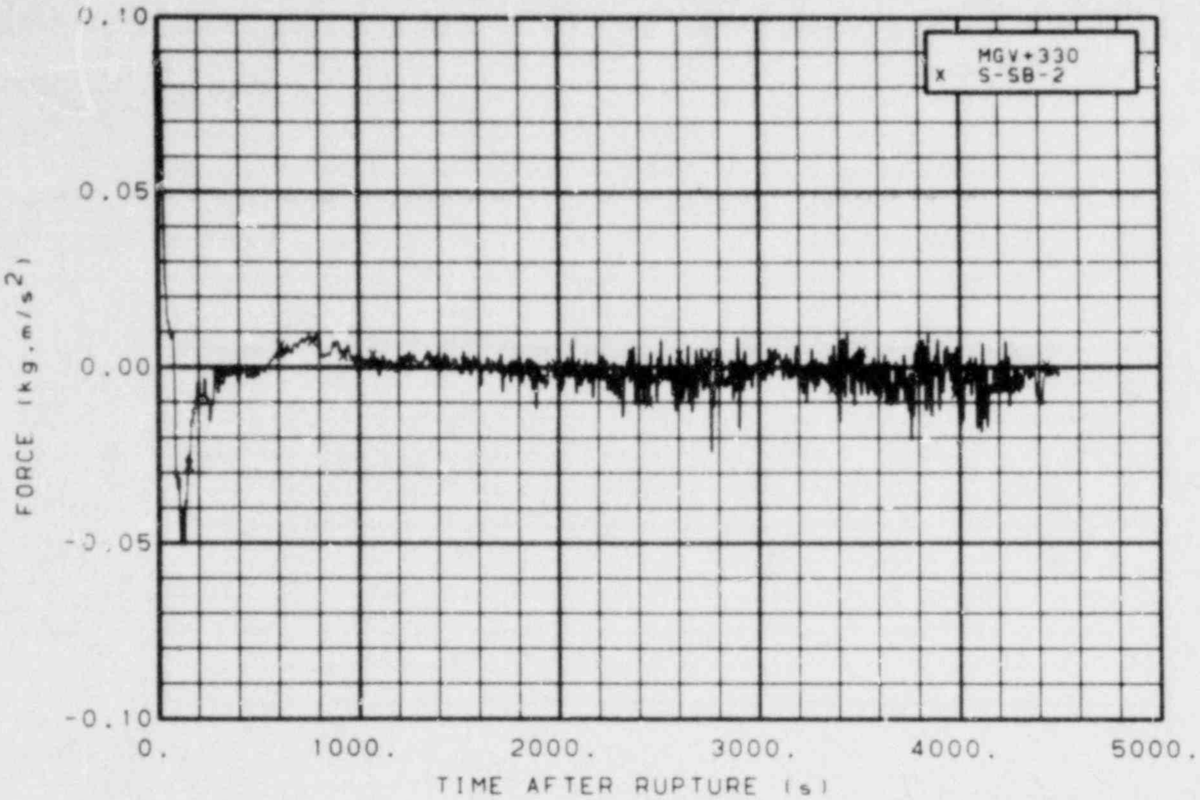

Figure 305. Momentum flux in vessel guide tube, Test S-SB-2 (MGV + 330), from 0 to 4500 s.

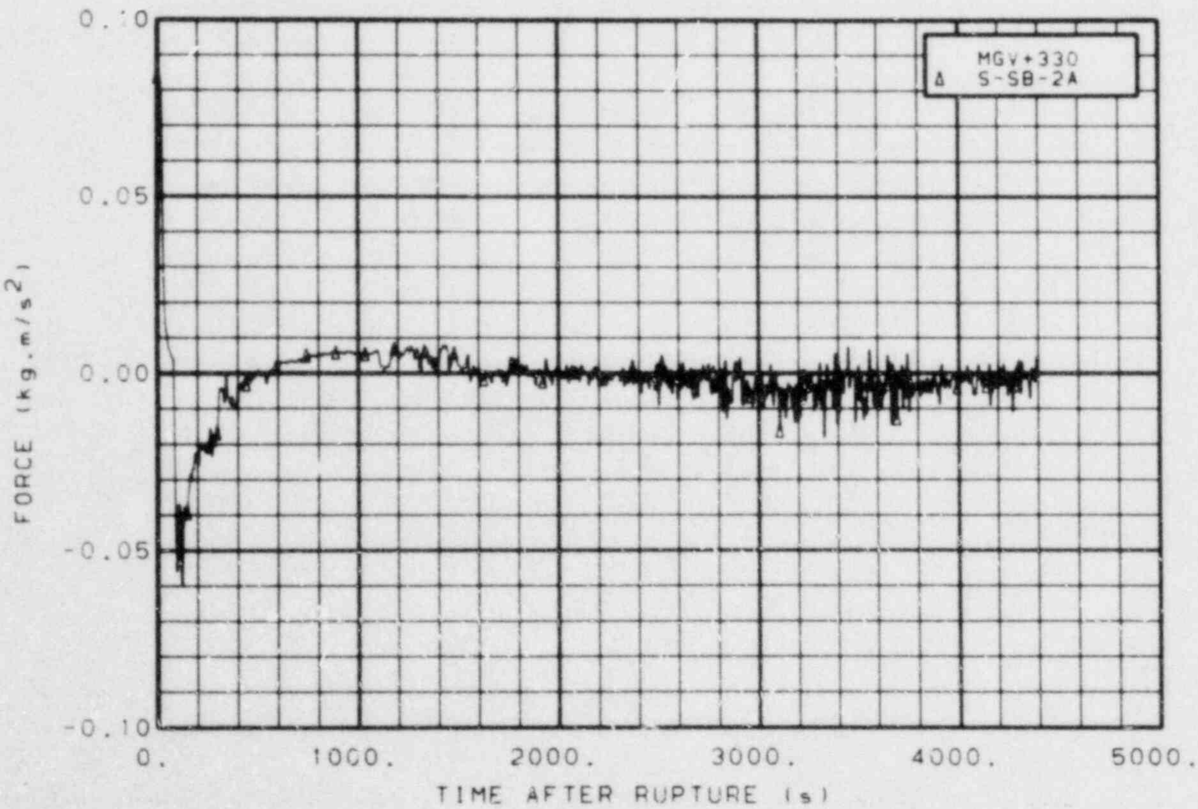

Figure 306. Momentum flux in vessel guide tube, Test S-SB-2A (MGV + 330), from 0 to 4390 s.

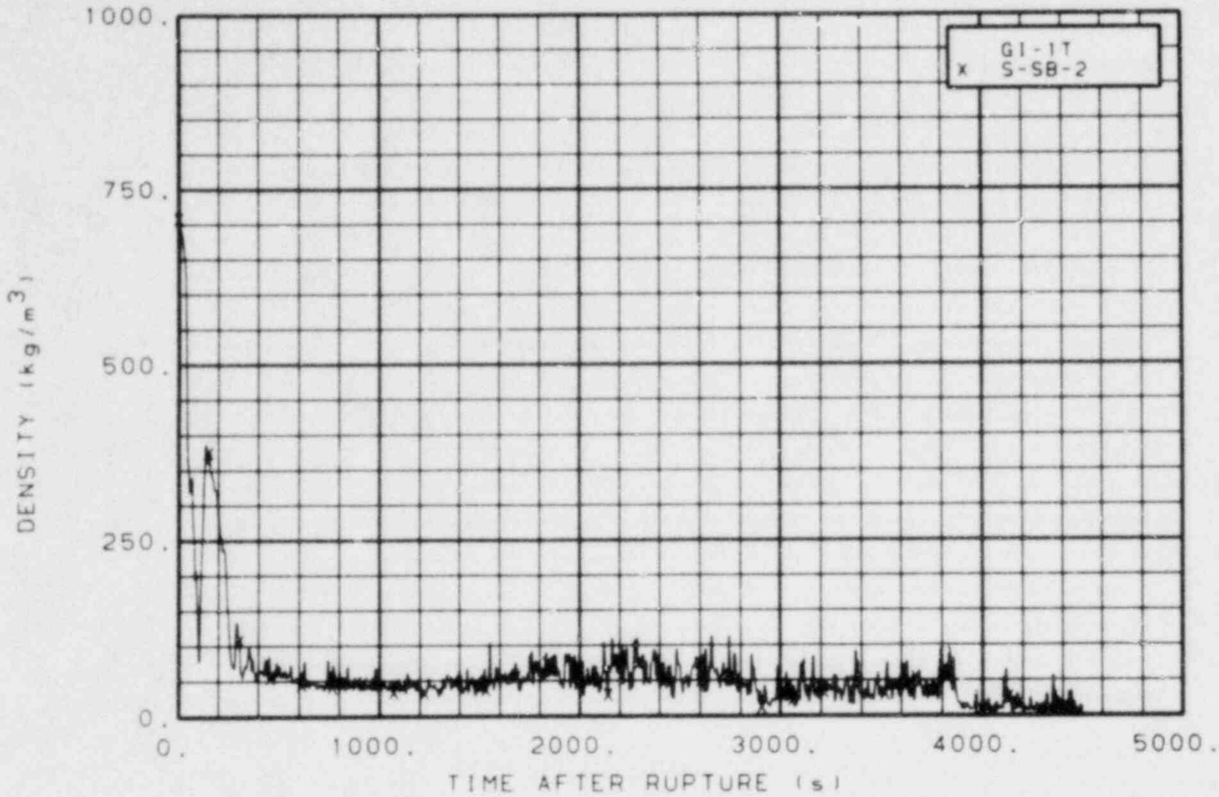

Figure 307. Density in intact loop hot leg, Test S-SB-2 (GI-1T), from 0 to 4500 s.

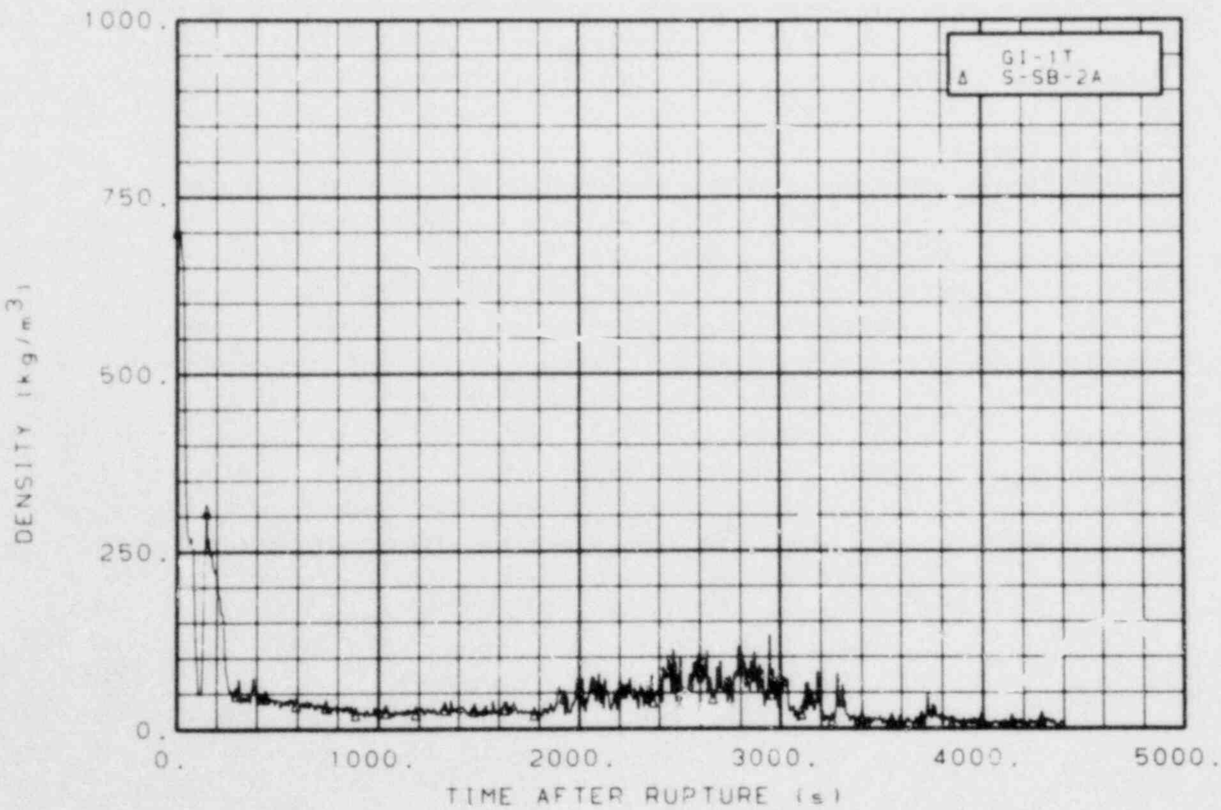

Figure 308. Density in intact loop hot leg, Test S-SB-2A (GI-1T), from 0 to 4390 s.

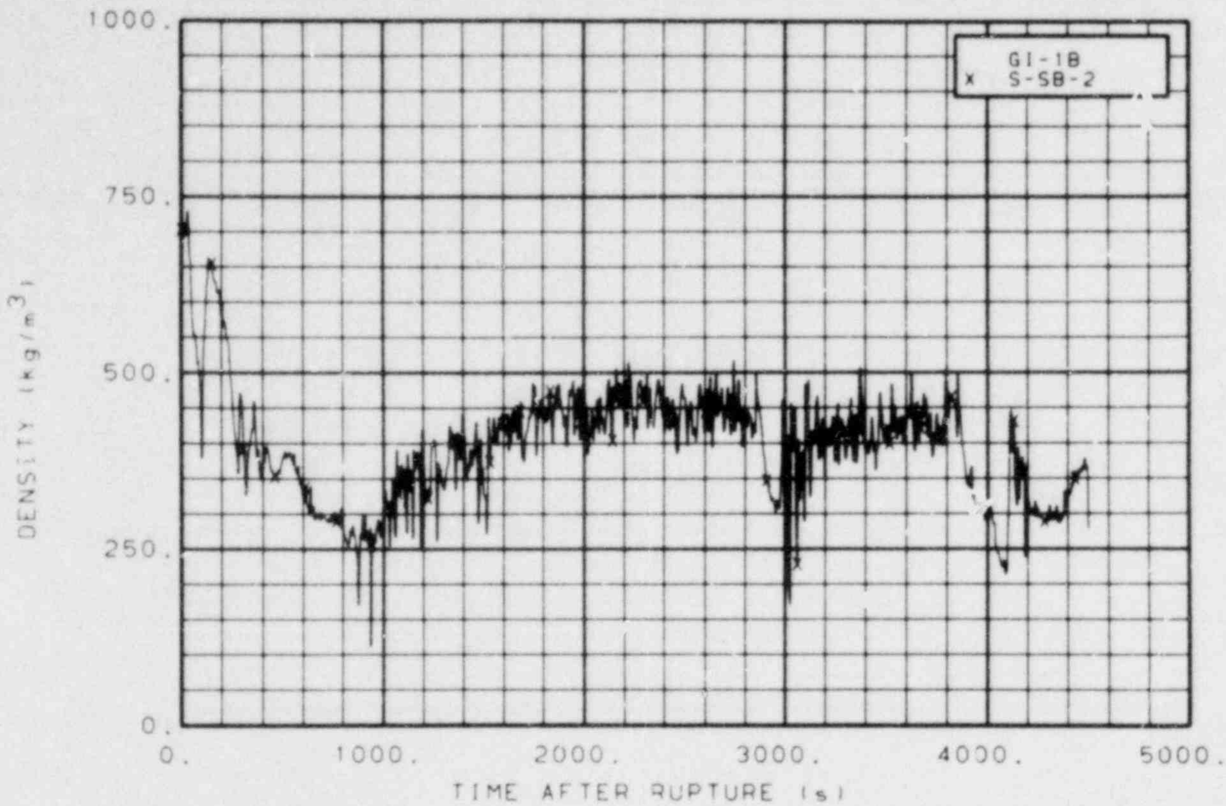

Figure 309. Density in intact loop hot leg, Test S-SB-2 (GI-1B), from 0 to 4500 s.

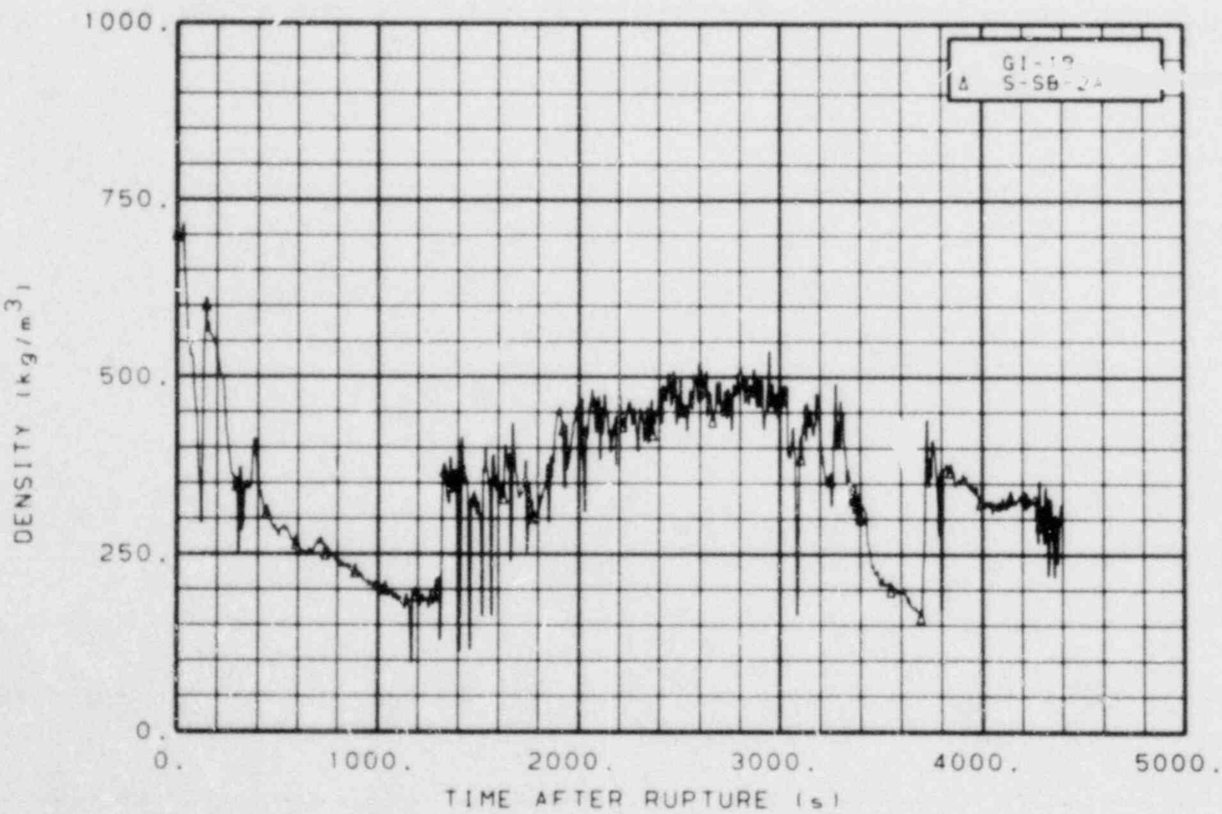

Figure 310. Density in intact loop hot leg, Test S-SB-2A (GI-1B), from 0 to 4390 s.

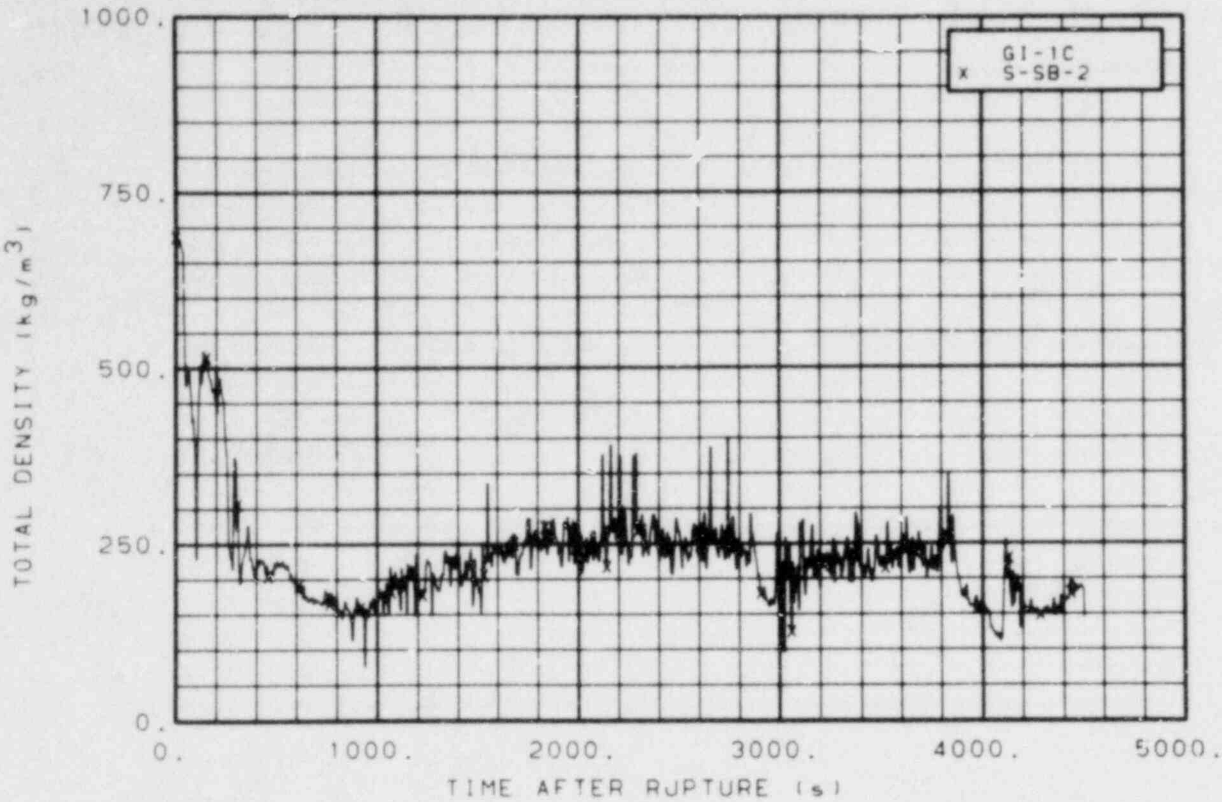

Figure 311. Density in intact loop hot leg, Test S-SB-2 (GI-1C), from 0 to 4500 s.

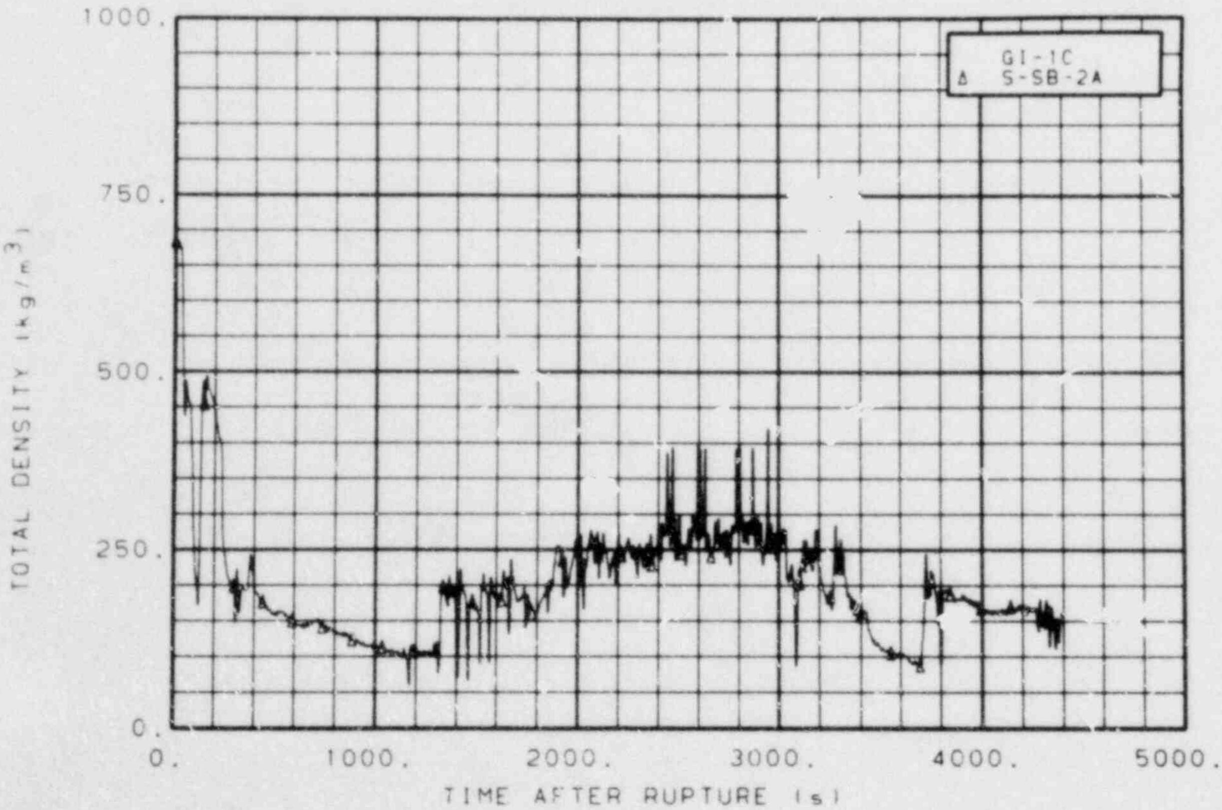

Figure 312. Density in intact loop hot leg, Test S-SB-2A (GI-1C), from 0 to 4390 s.

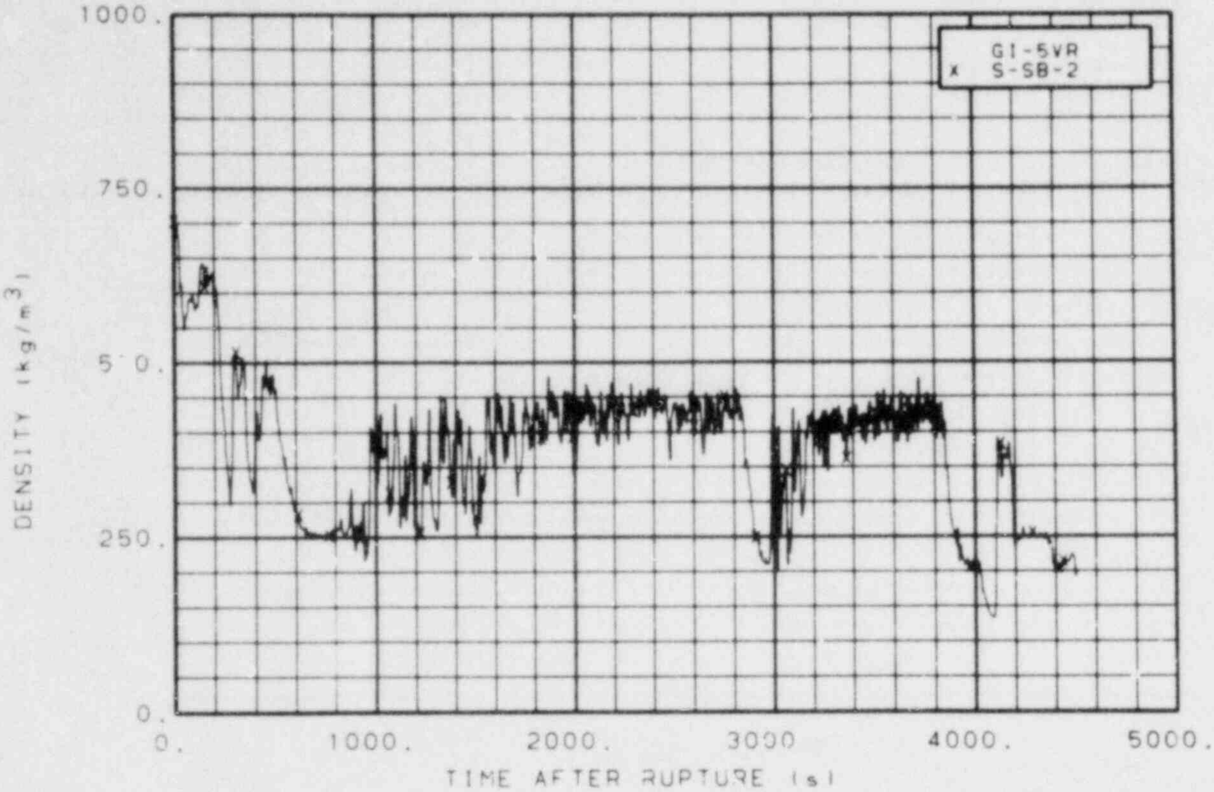

Figure 313. Density in intact loop hot leg, Test S-SB-2 (GI-5VR), from 0 to 4500 s.

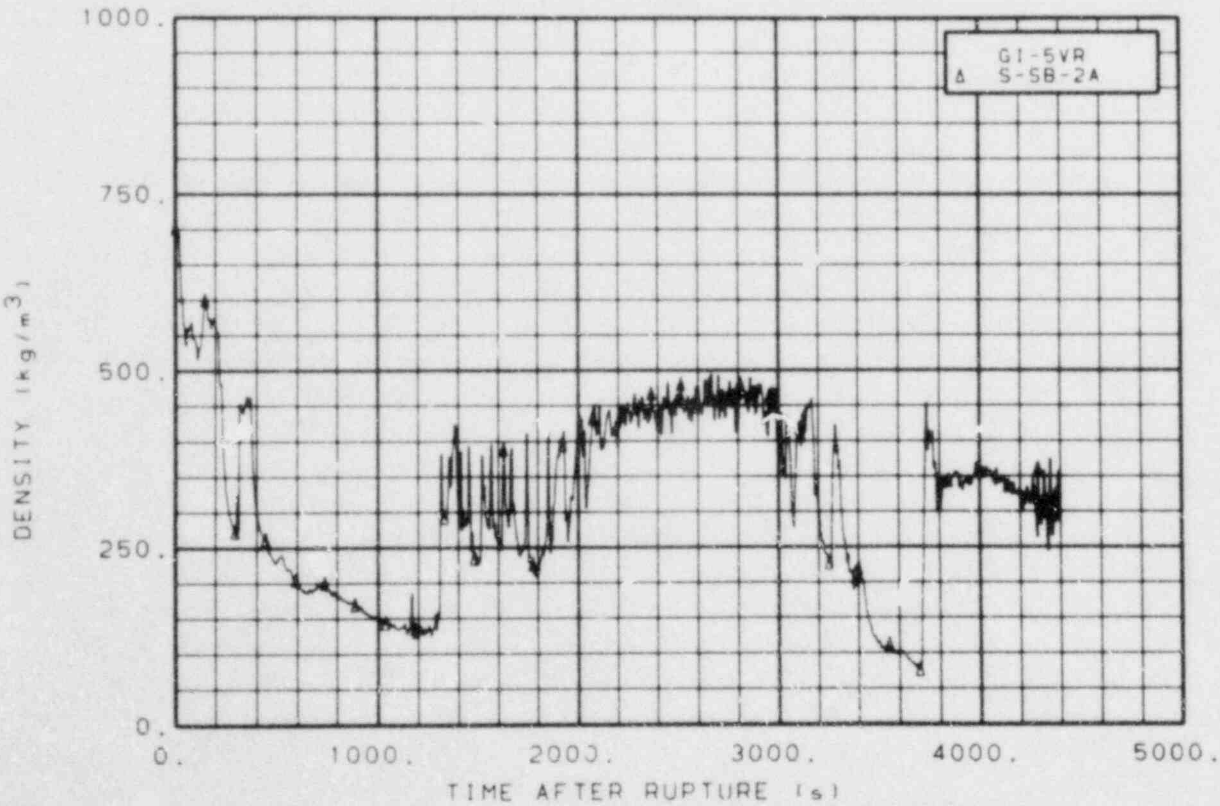

Figure 314. Density in intact loop hot leg, Test S-SB-2A (GI-5VR), from 0 to 4390 s.

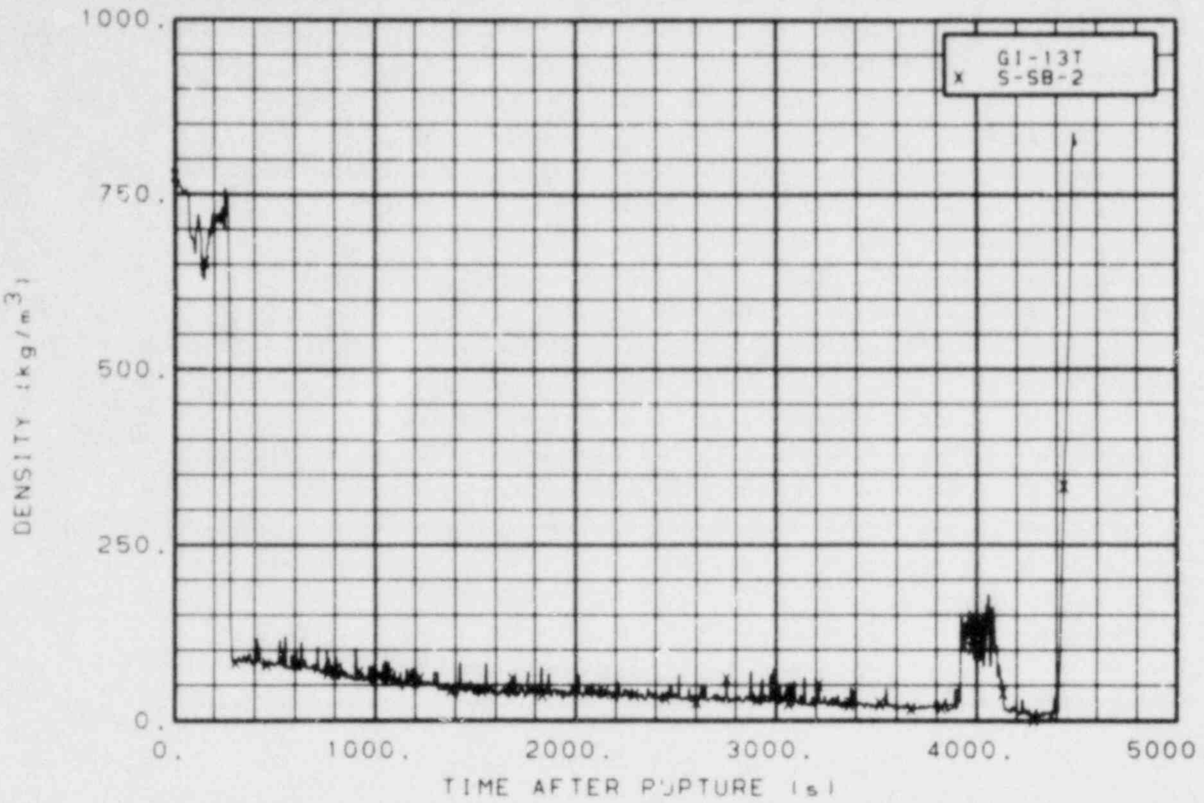

Figure 315. Density in intact loop cold leg, Test S-SB-2 (GI-13T), from 0 to 4500 s.

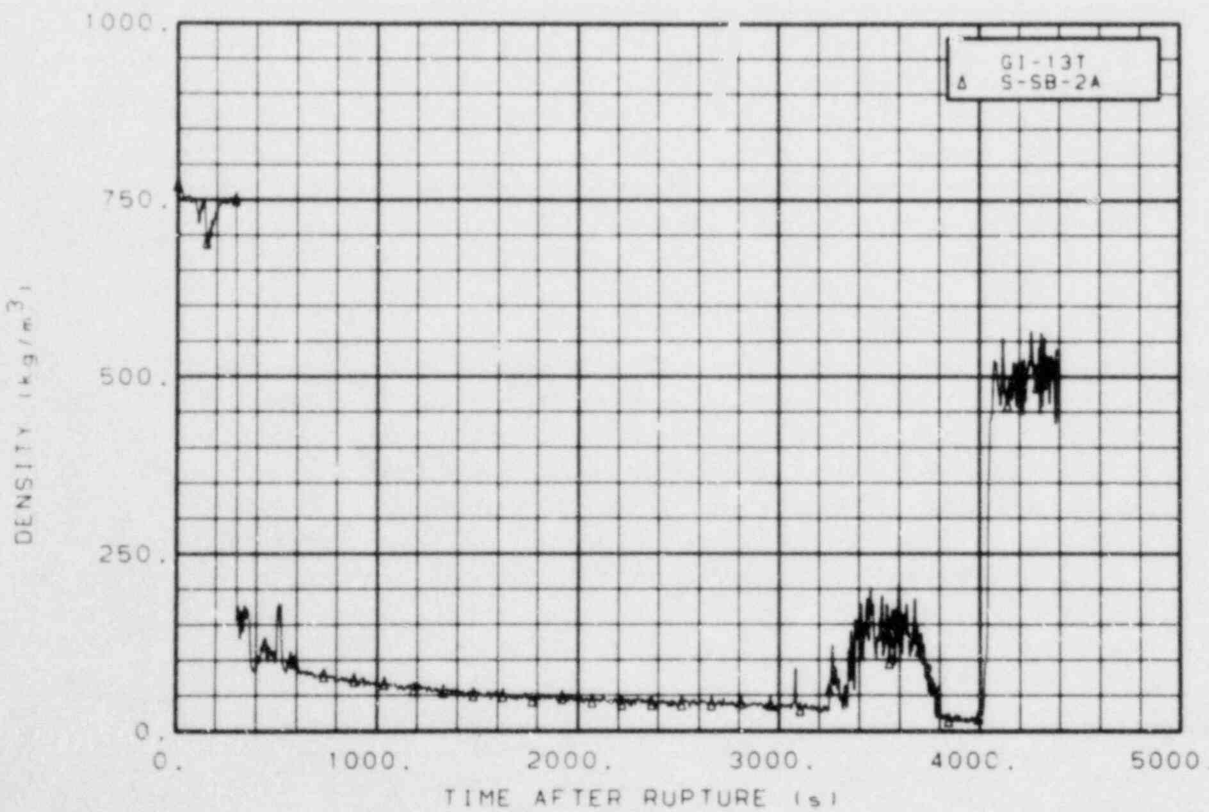

Figure 316. Density in intact loop cold leg, Test S-SB-2A (GI-13T), fro. J to 4390 s.

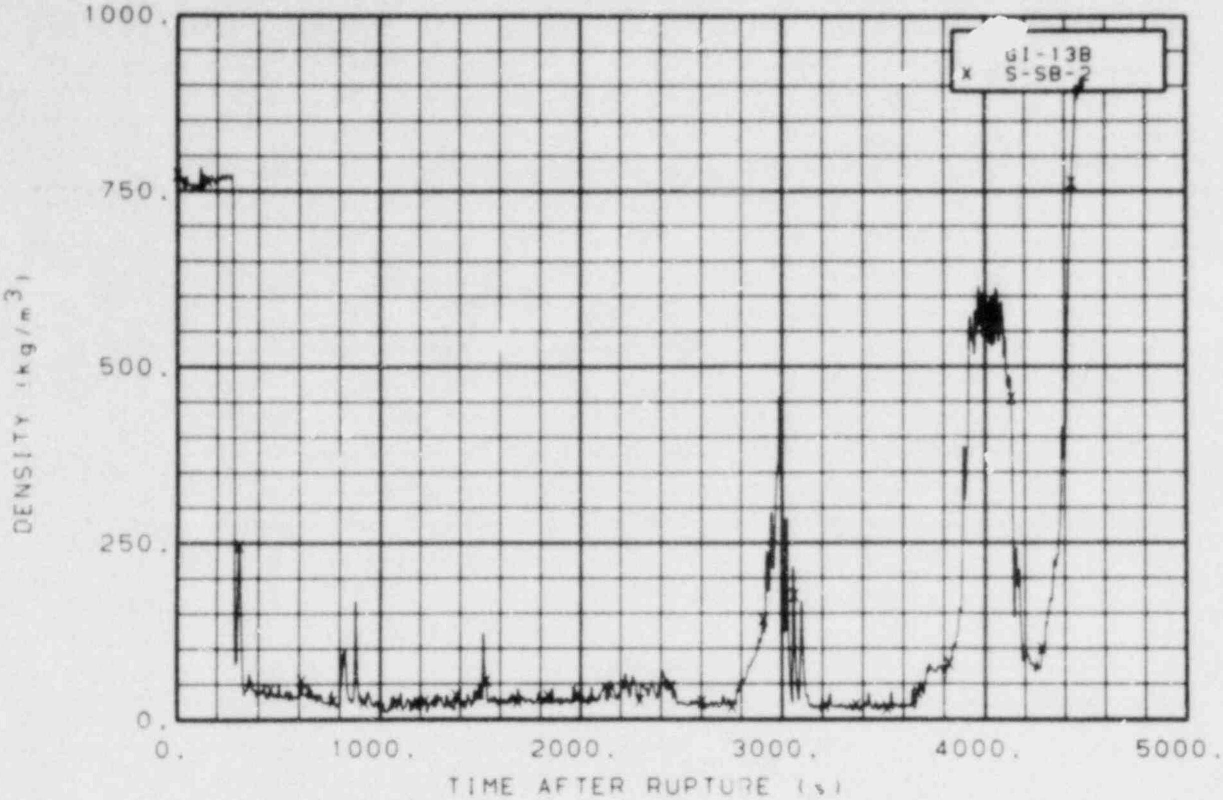

Figure 317. Density in intact loop cold leg, Test S-SB-2 (GI-13B), from 0 to 4500 s.

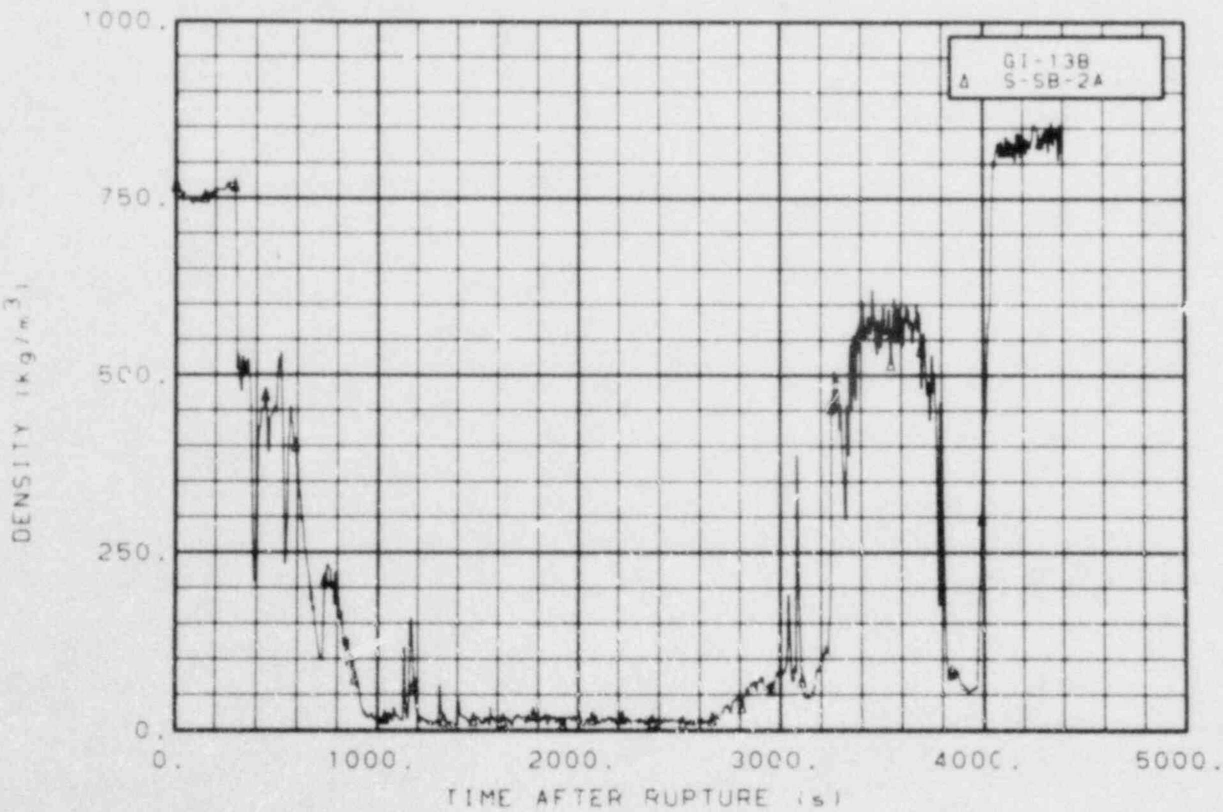

Figure 318. Density in intact loop cold leg, Test S-SB-2A (GI-13B), from 0 to 4390 s.

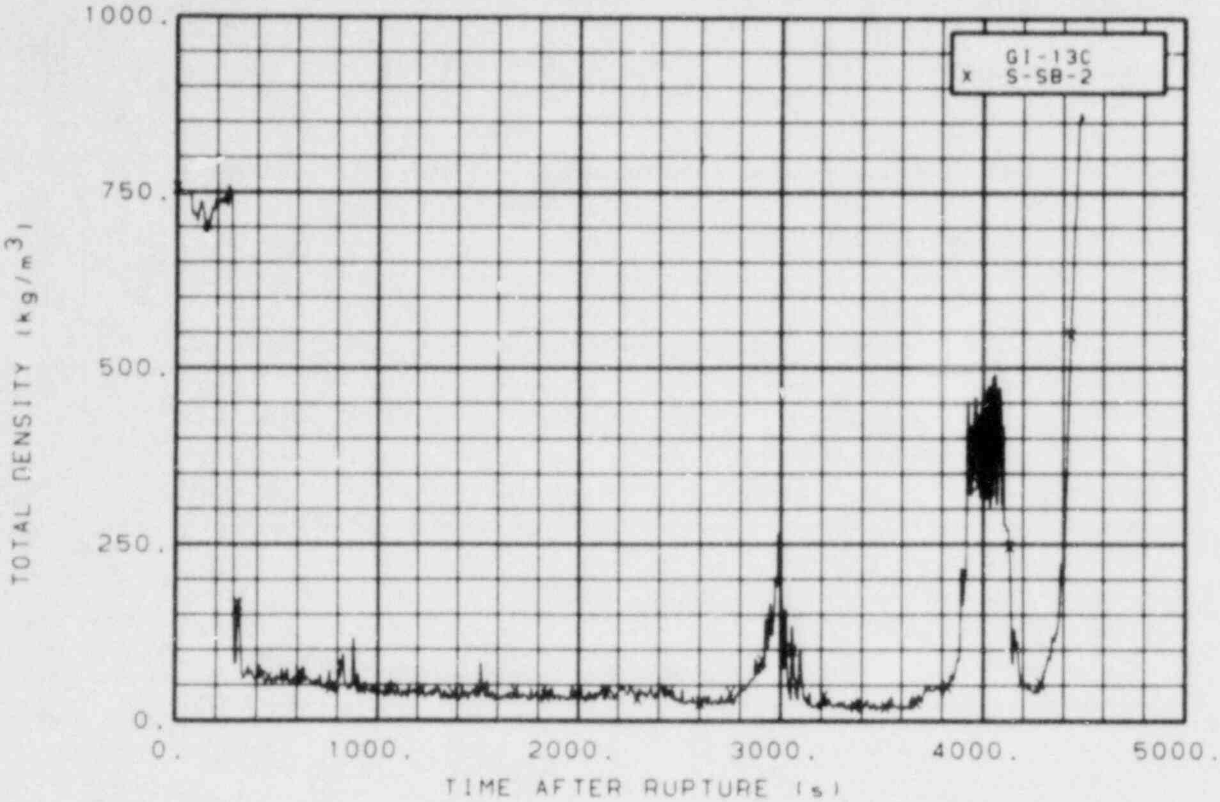

Figure 319. Density in intact loop cold leg, Test S-SB-2 (GI-13C), from 0 to 4500 s.

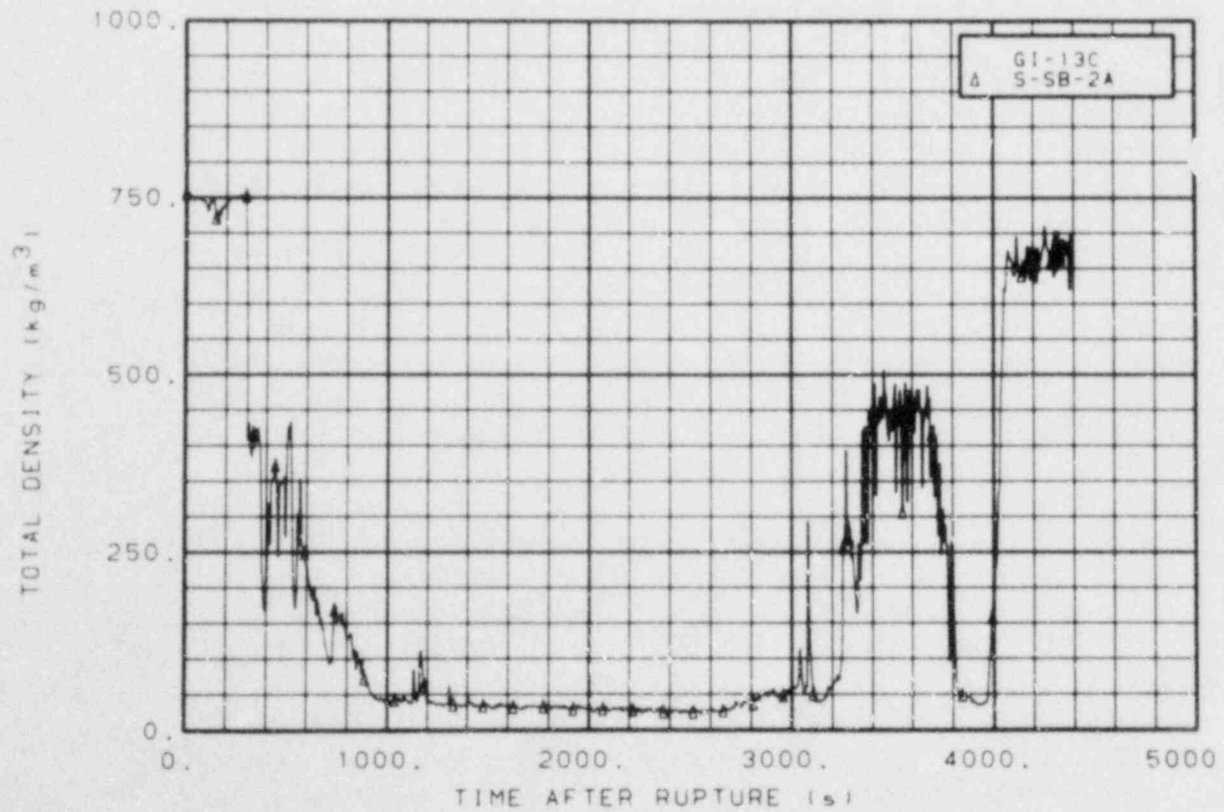

Figure 320. Density in intact loop cold leg, Test S-SB-2A (GI-13C), from 0 to 4390 s.

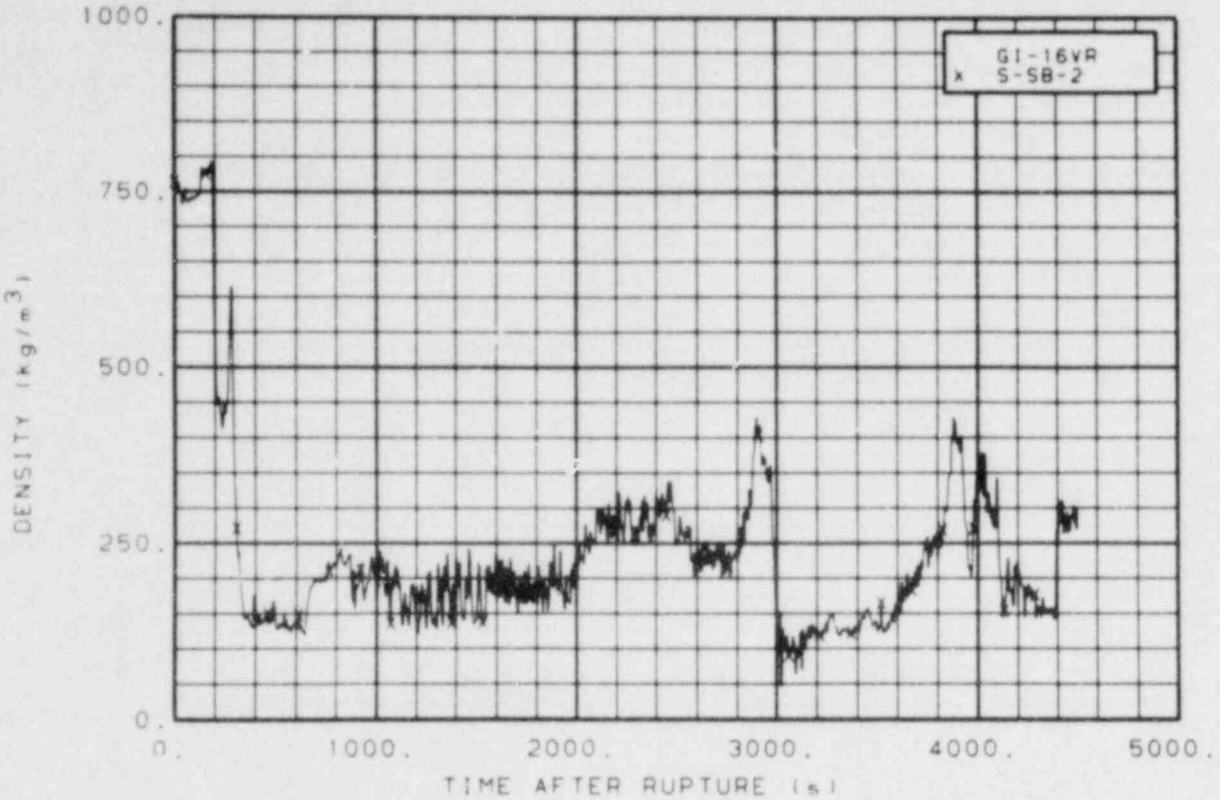

Figure 321. Density in intact loop cold leg, Test S-SB-2 (GI-16VR), from 0 to 4500 s.

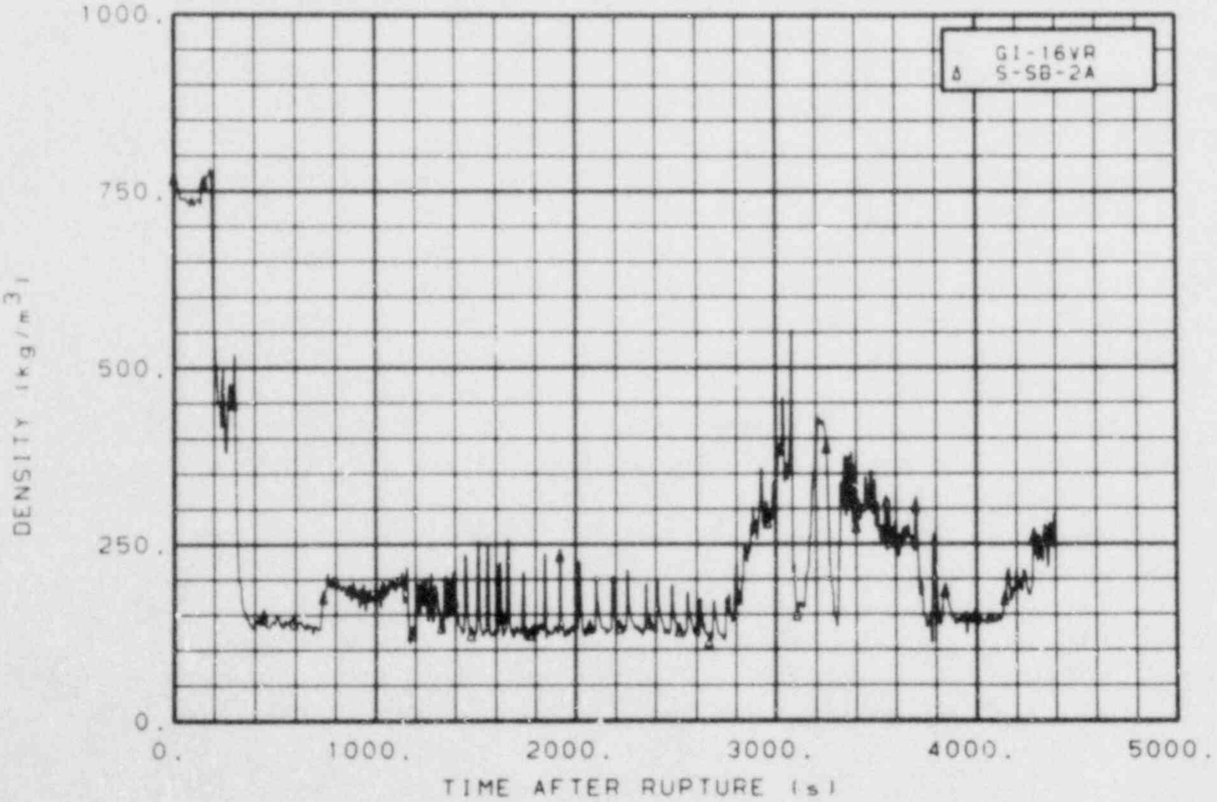

Figure 322. Density in intact loop cold leg, Test S-SB-2A (GI-16VR), from 0 to 4390 s.

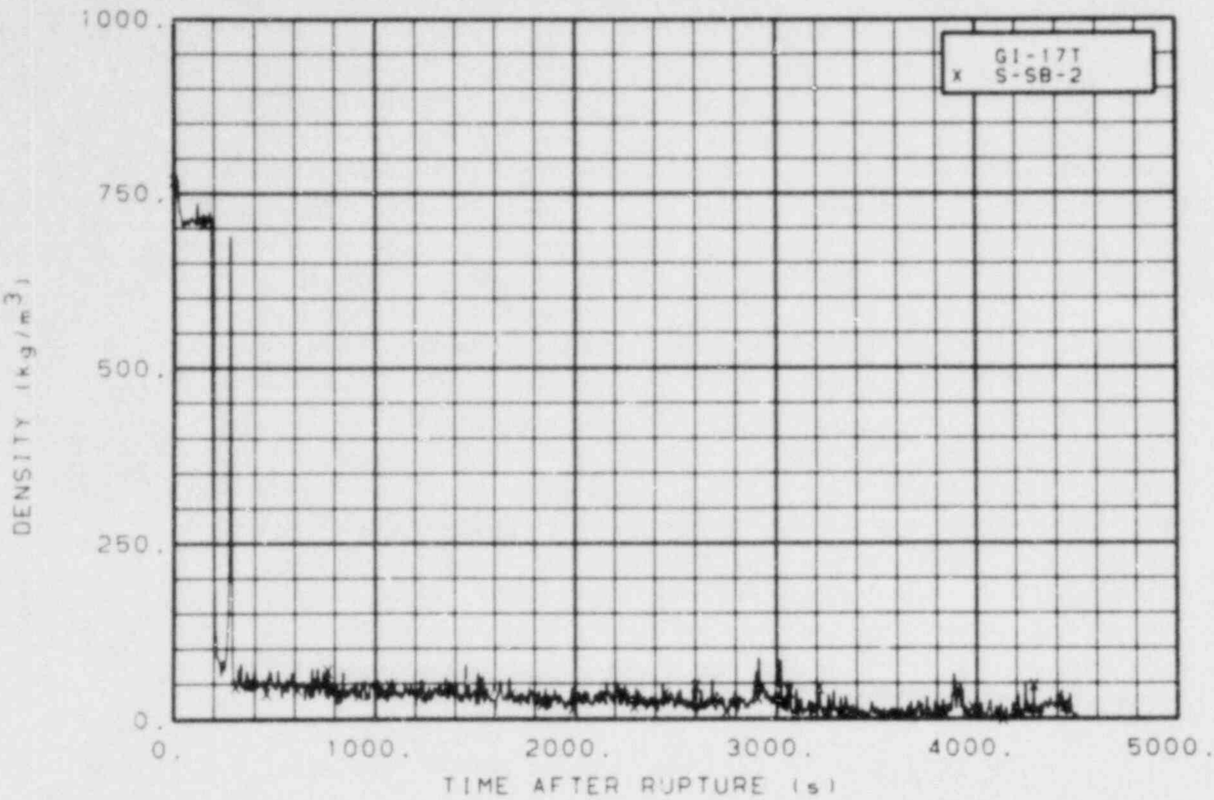

Figure 323. Density in intact loop cold leg, Test S-SB-2 (GI-17T), from 0 to 4500 s.

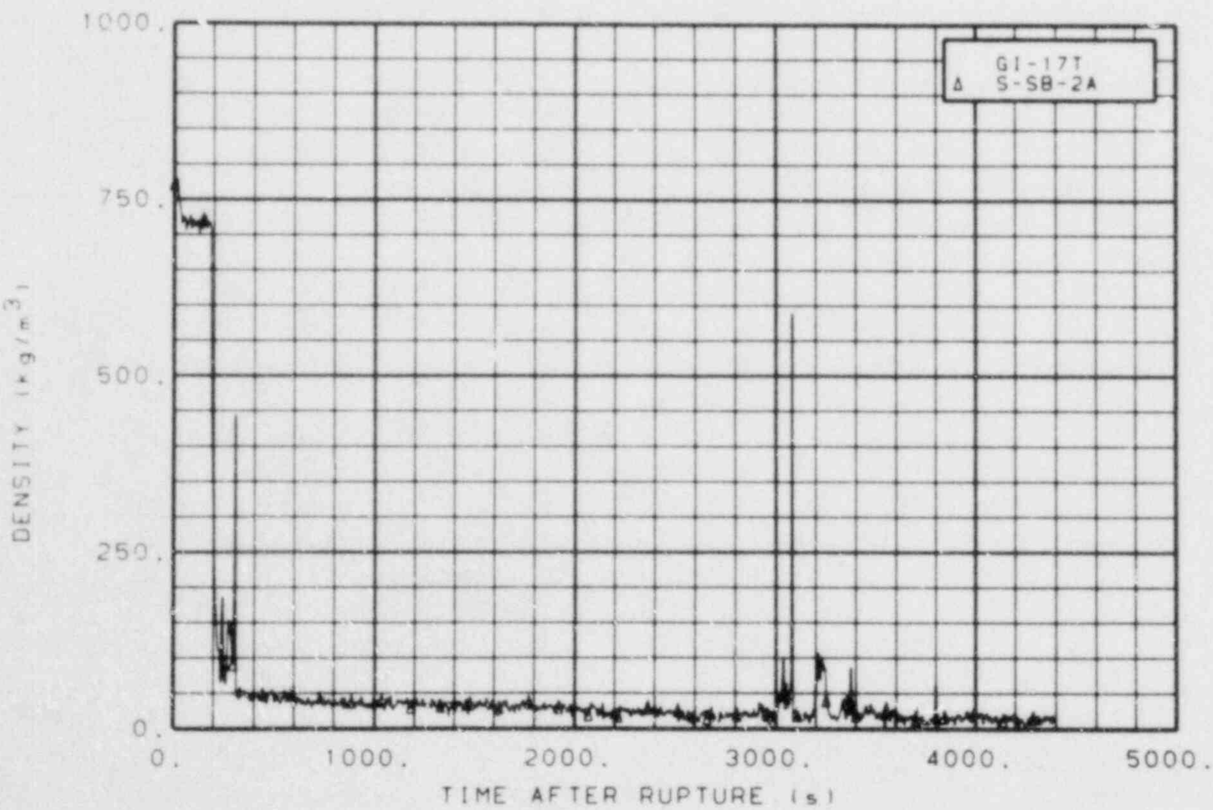

Figure 324. Density in intact loop cold leg, Test S-SB-2A (GI-17T), from 0 to 4390 s.

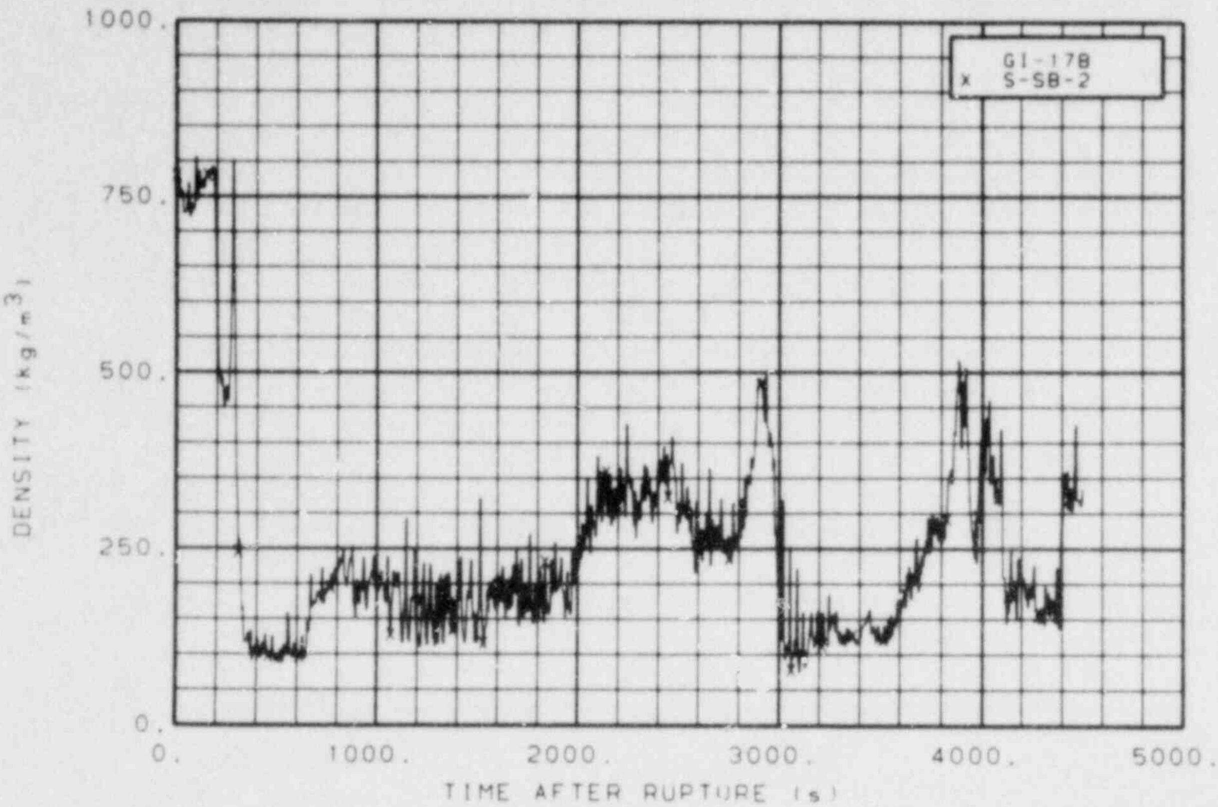

Figure 325. Density in intact loop cold leg, Test S-SB-2 (GI-17B), from 0 to 4500 s.

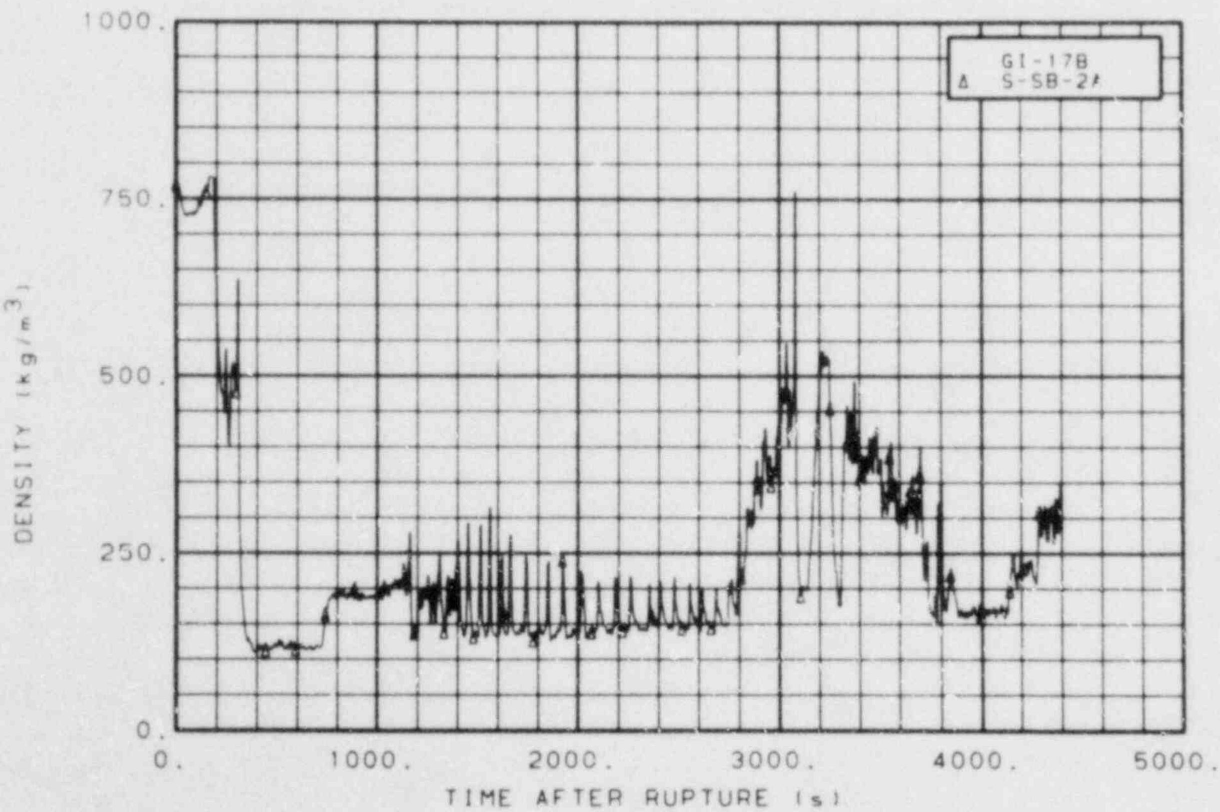

Figure 326. Density in intact loop cold leg, Test S-SB-2A (GI-17B), from 0 to 4390 s.

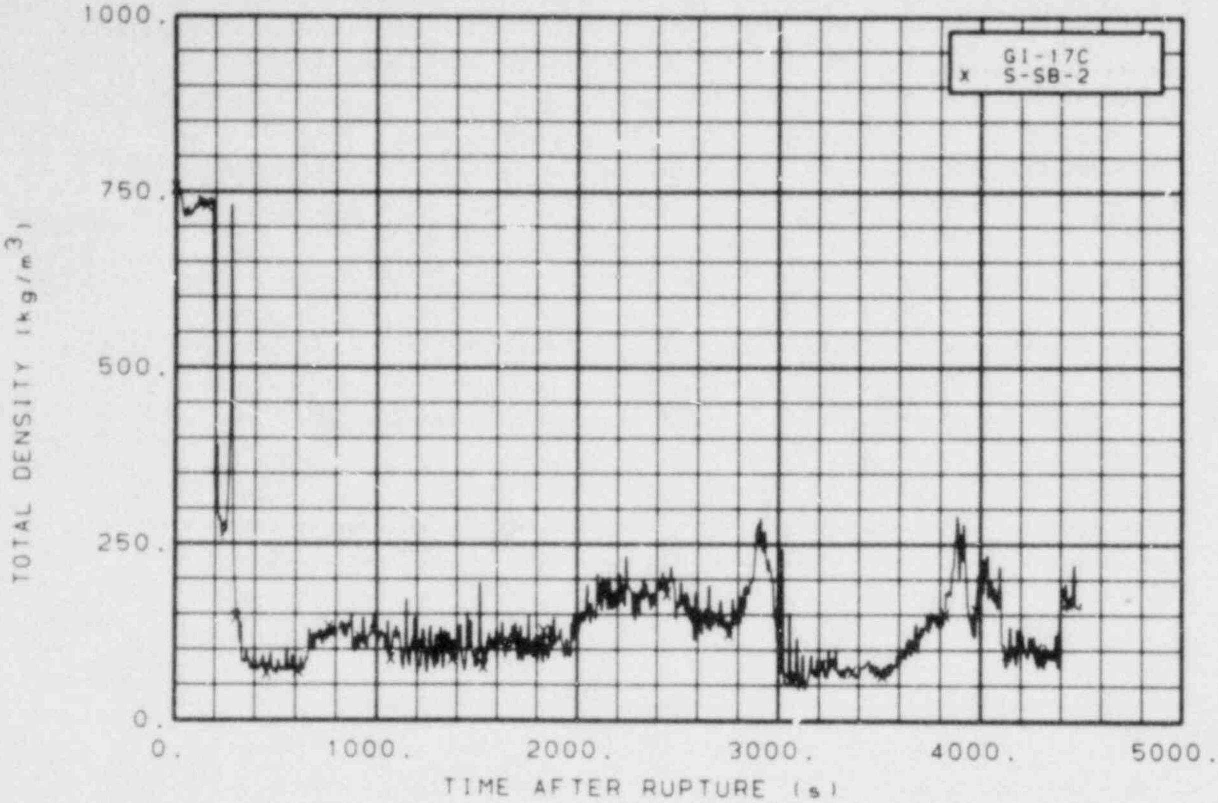

Figure 327. Density in intact loop cold leg, Test S-SB-2 (GI-17C), from 0 to 4500 s.

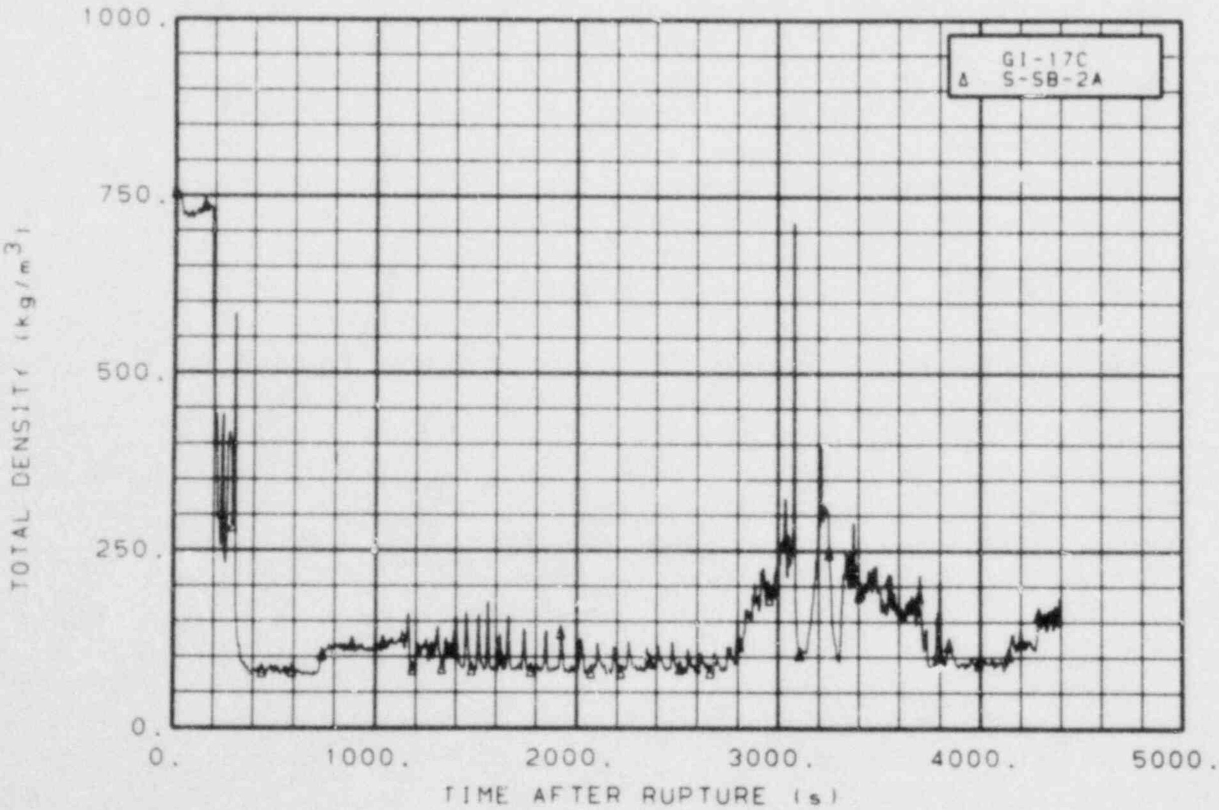

Figure 328. Density in intact loop cold leg, Test S-SB-2A (GI-17C), from 0 to 4390 s.

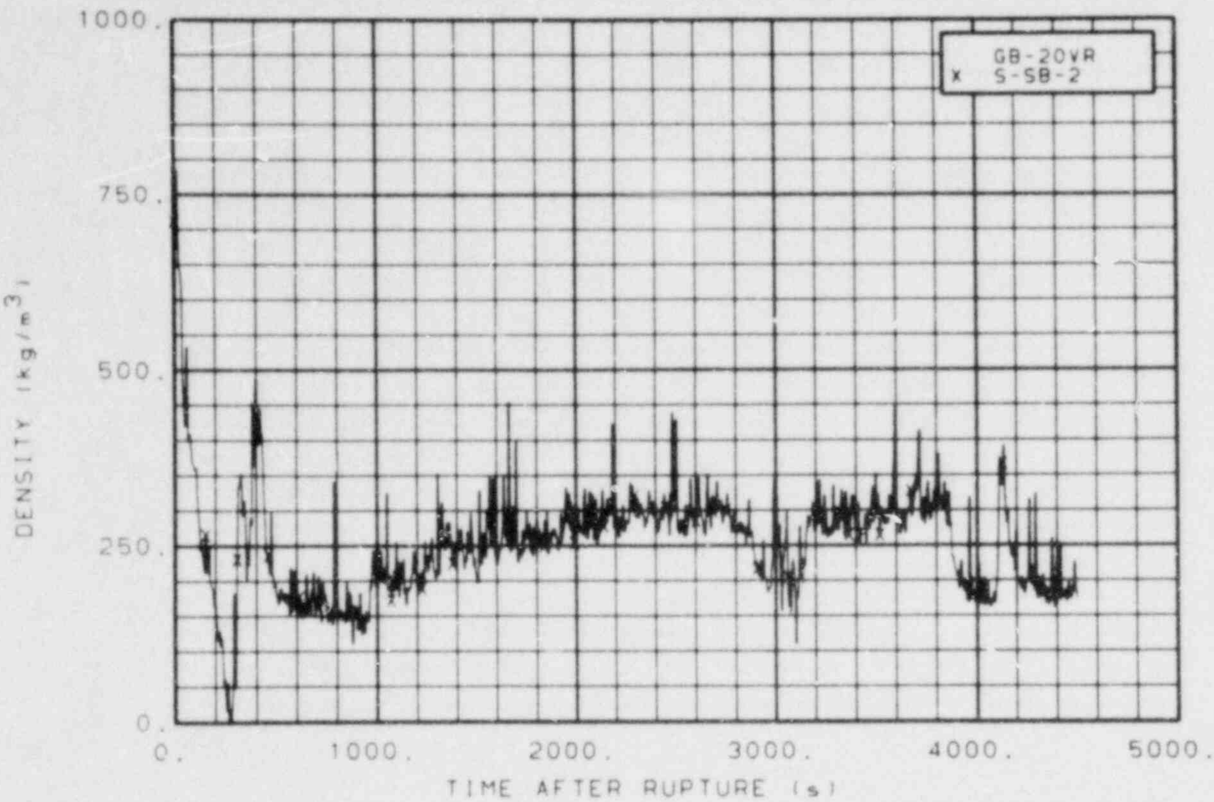

Figure 329. Density in broken loop hot leg, Test S-SB-2 (GB-20VR), from 0 to 4500 s.

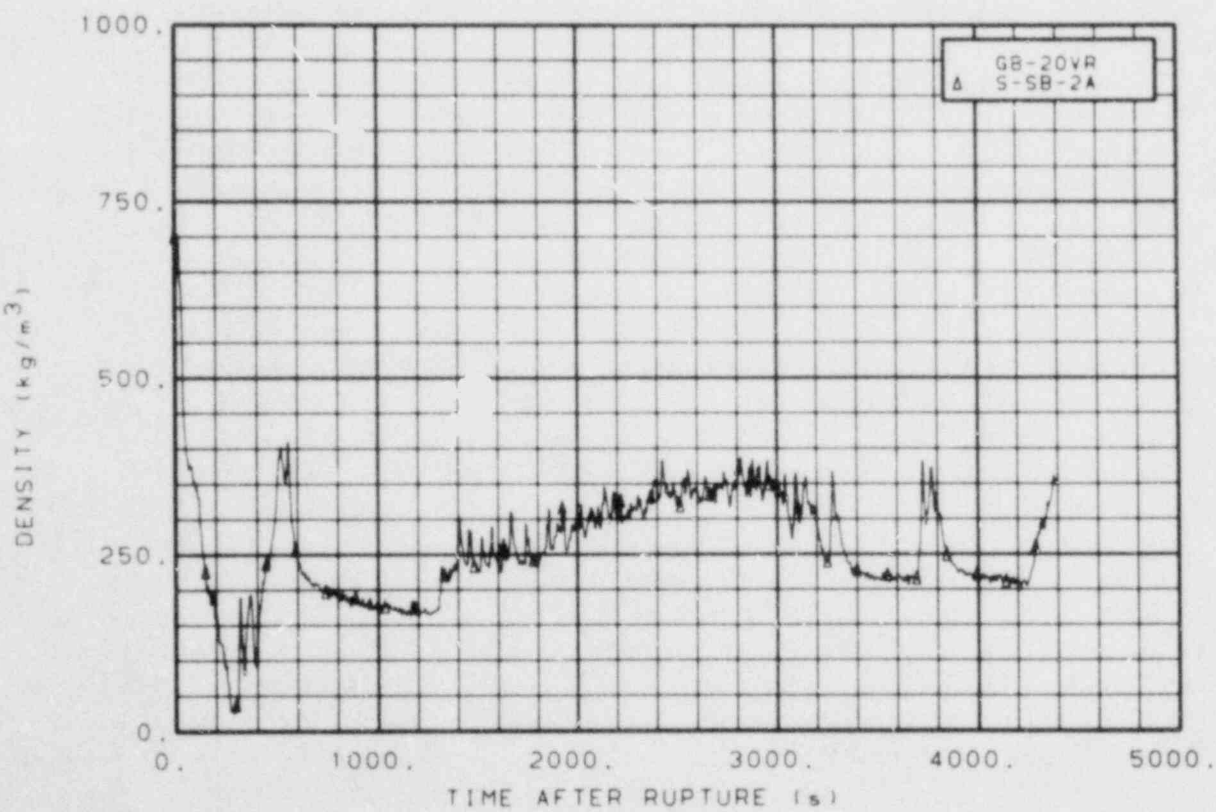

Figure 330. Density in broken loop hot leg, Test S-SB-2A (GB-20VR), from 0 to 4390 s.

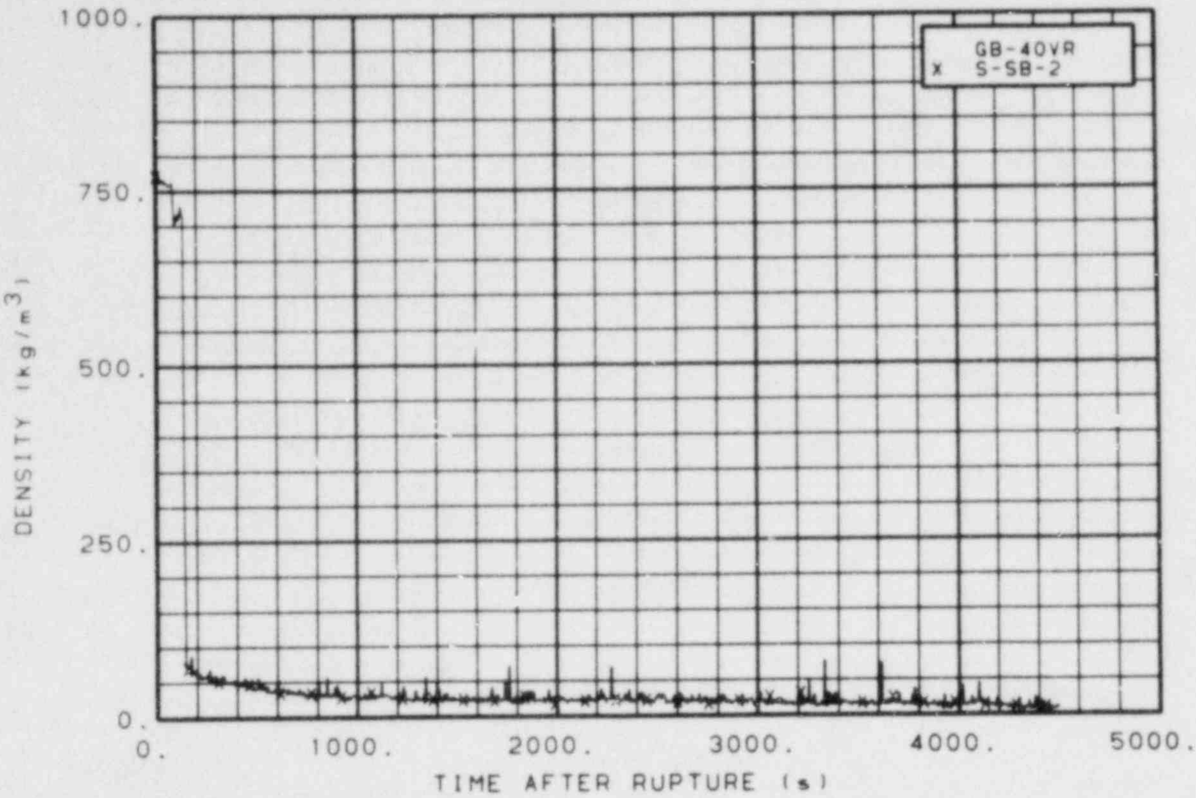

Figure 331. Density in broken loop cold leg, Test S-SB-2 (GB-40VR), from 0 to 4500 s.

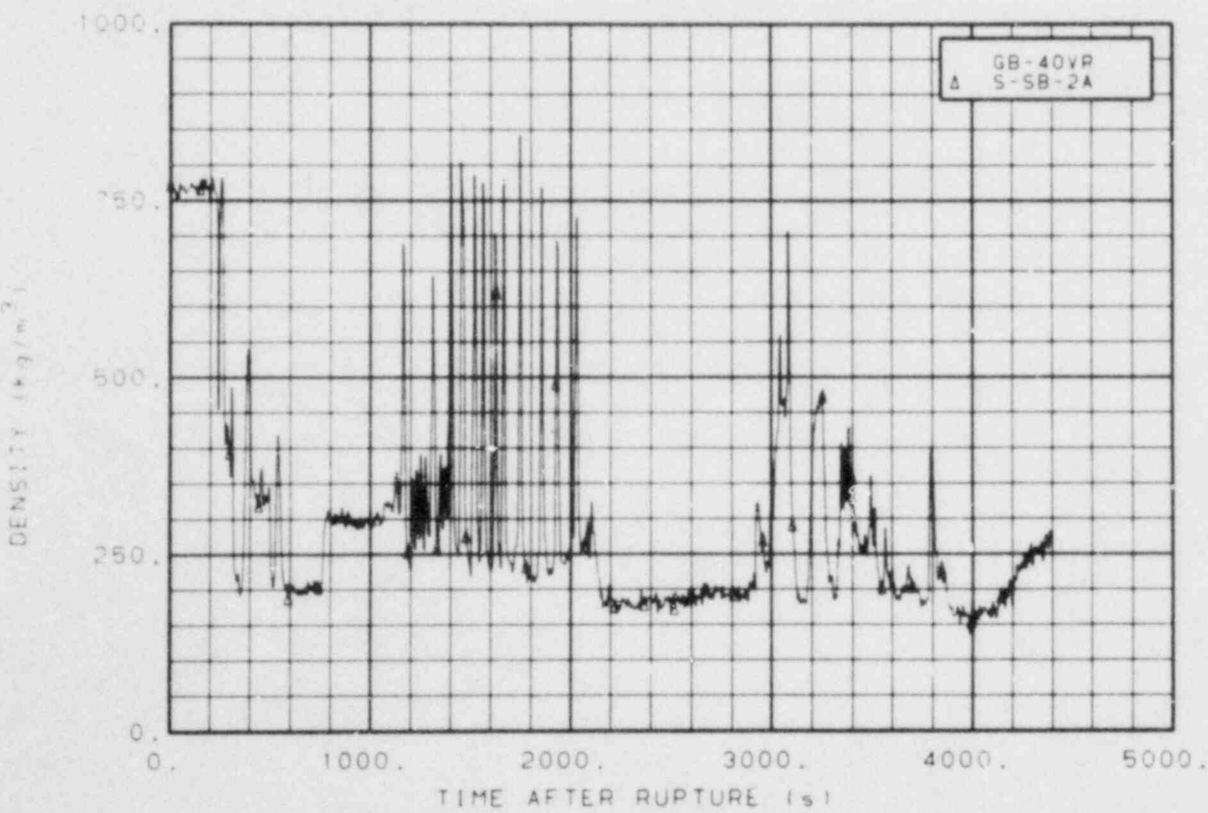

Figure 332. Density in broken loop cold leg, Test S-SB-2A (GB-40VR), from 0 to 4390 s.

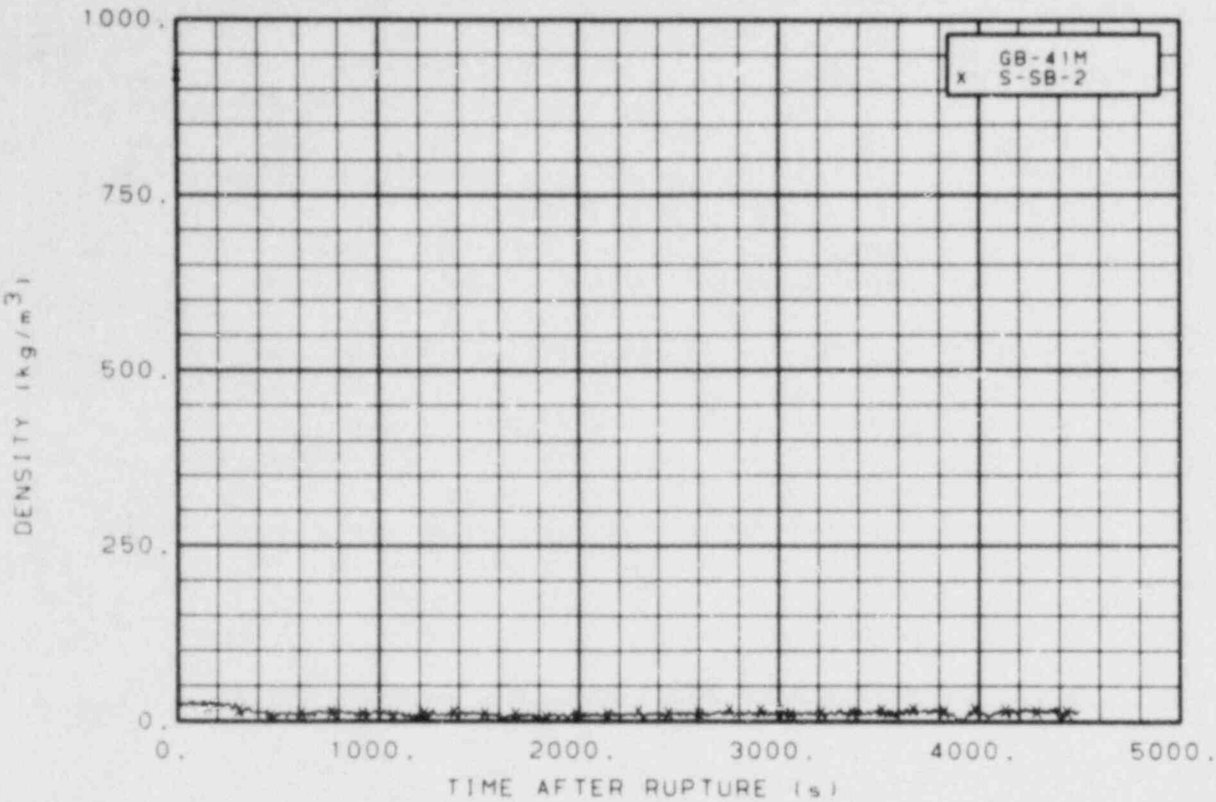

Figure 333. Density in broken loop cold leg, Test S-SB-2 (GB-41B), from 0 to 4500 s.

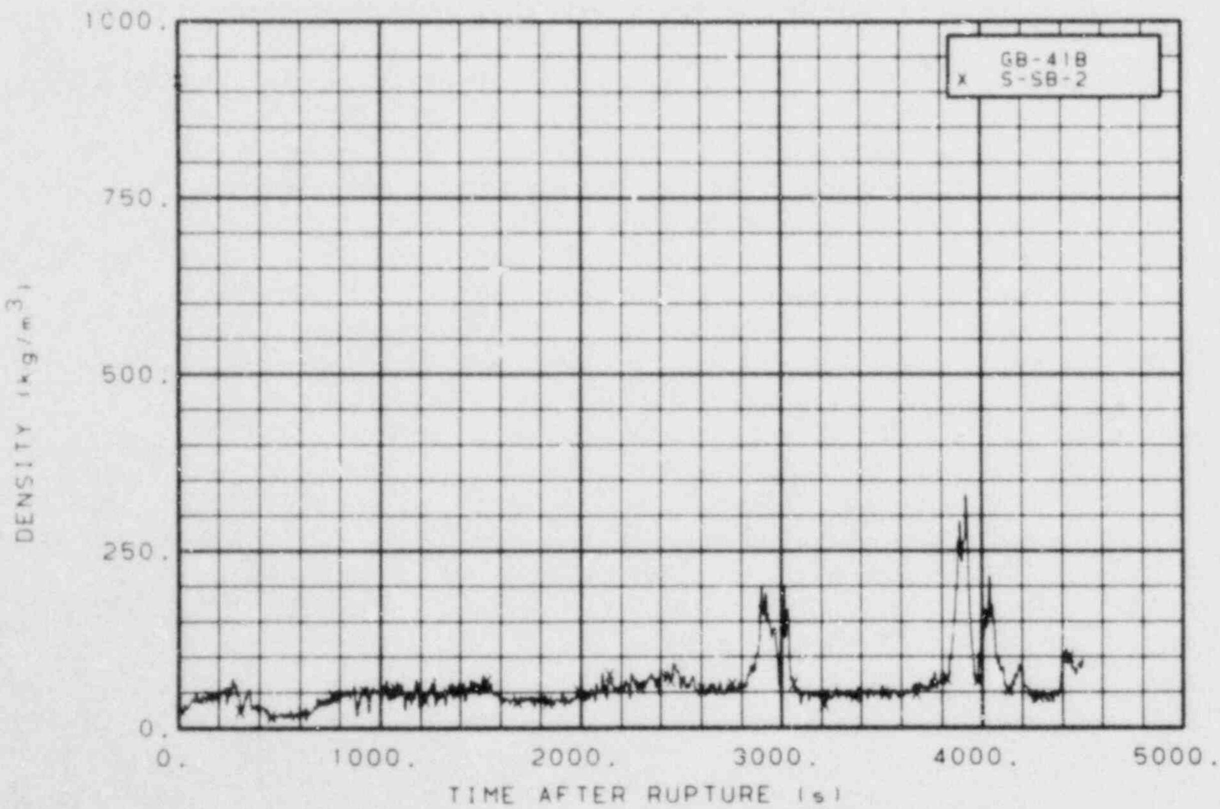

Figure 334. Density in broken loop cold leg, Test S-SB-2A (GB-41B), from 0 to 4390 s.

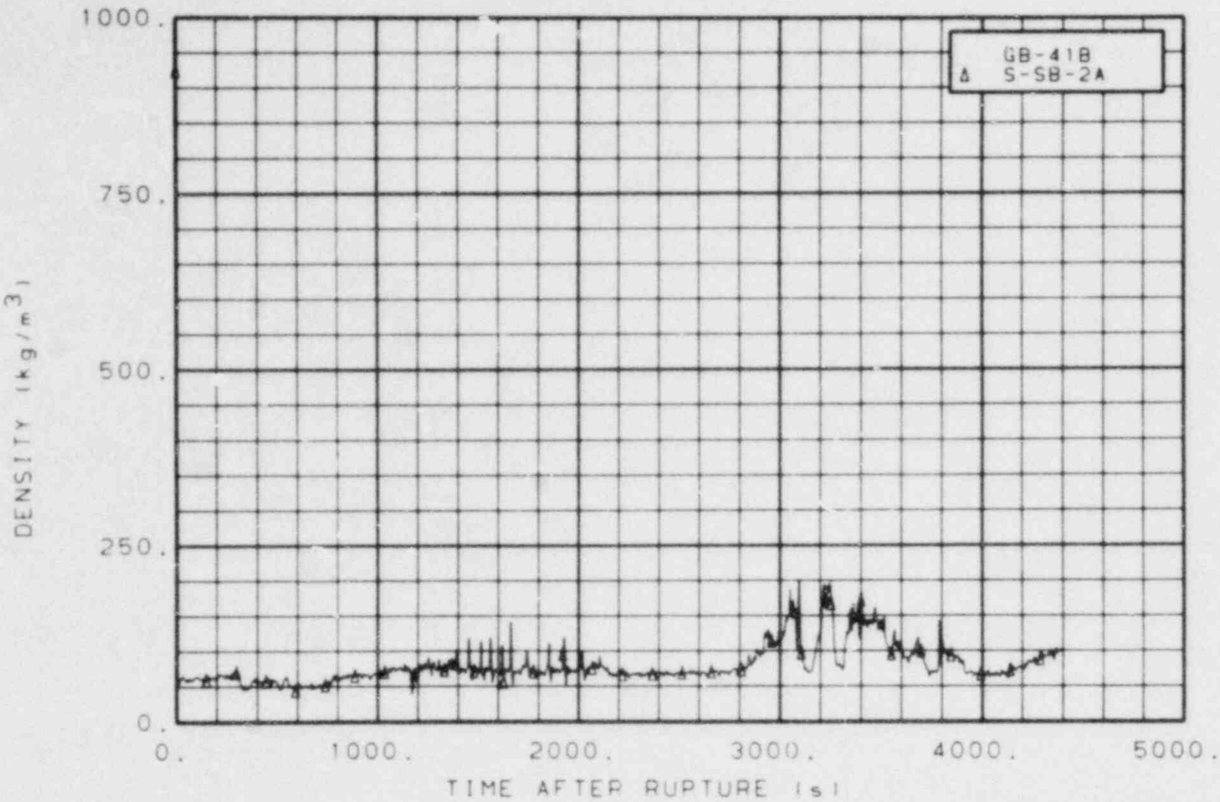

Figure 335. Density in broken loop cold leg, Test S-SB-2 (GB-41M), from 0 to 4500 s.

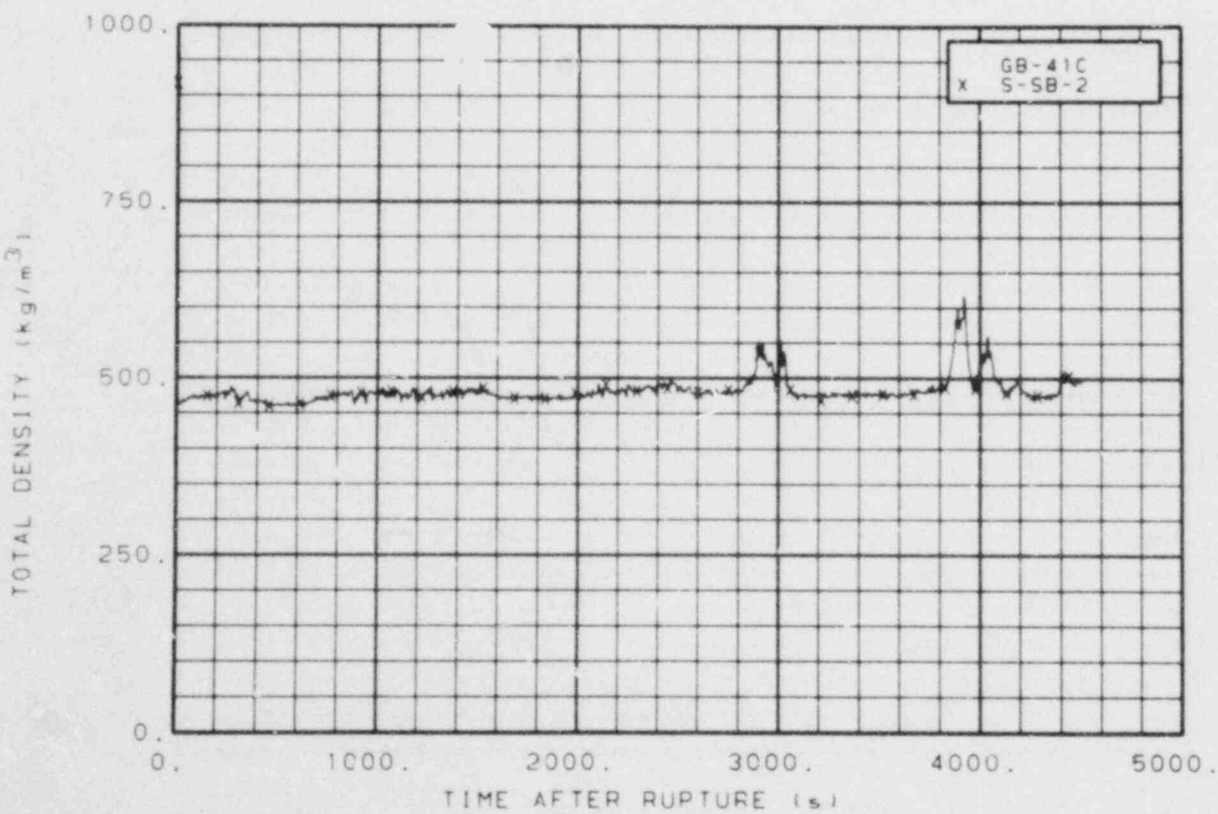

Figure 336. Density in broken loop cold leg, Test S-SB-2 (GB-41C), from 0 to 4500 s.

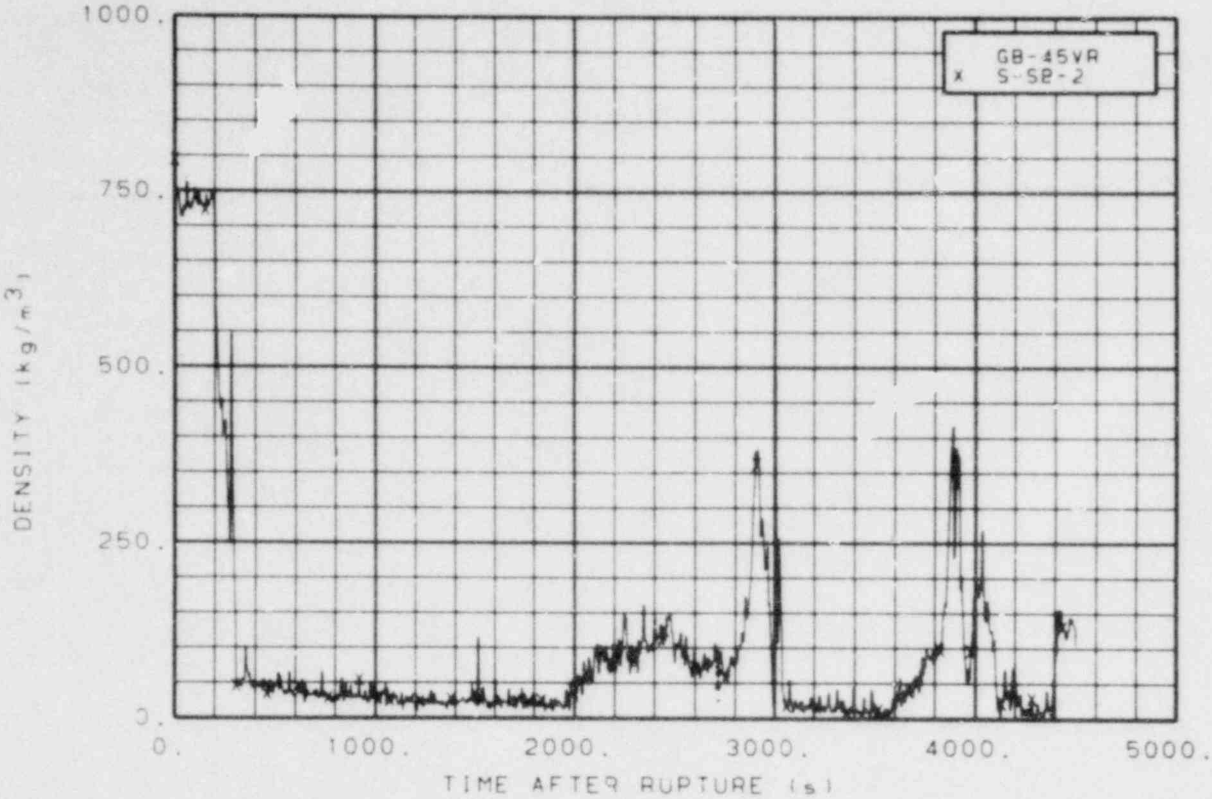

Figure 337. Density in broken loop cold leg, Test S-SB-2 (GB-45VR), from 0 to 4500 s.

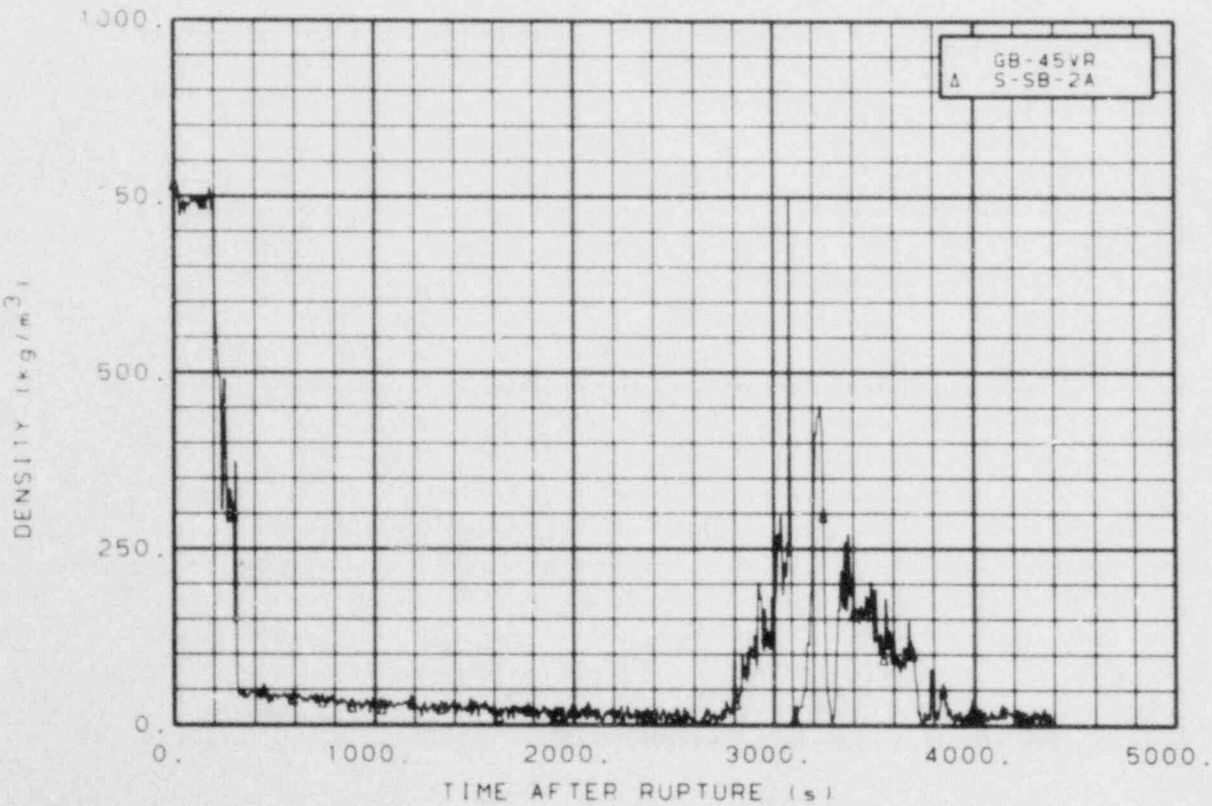

Figure 338. Density in broken loop cold leg, Test S-SB-2A (GB-45VR), from 0 to 4390 s.

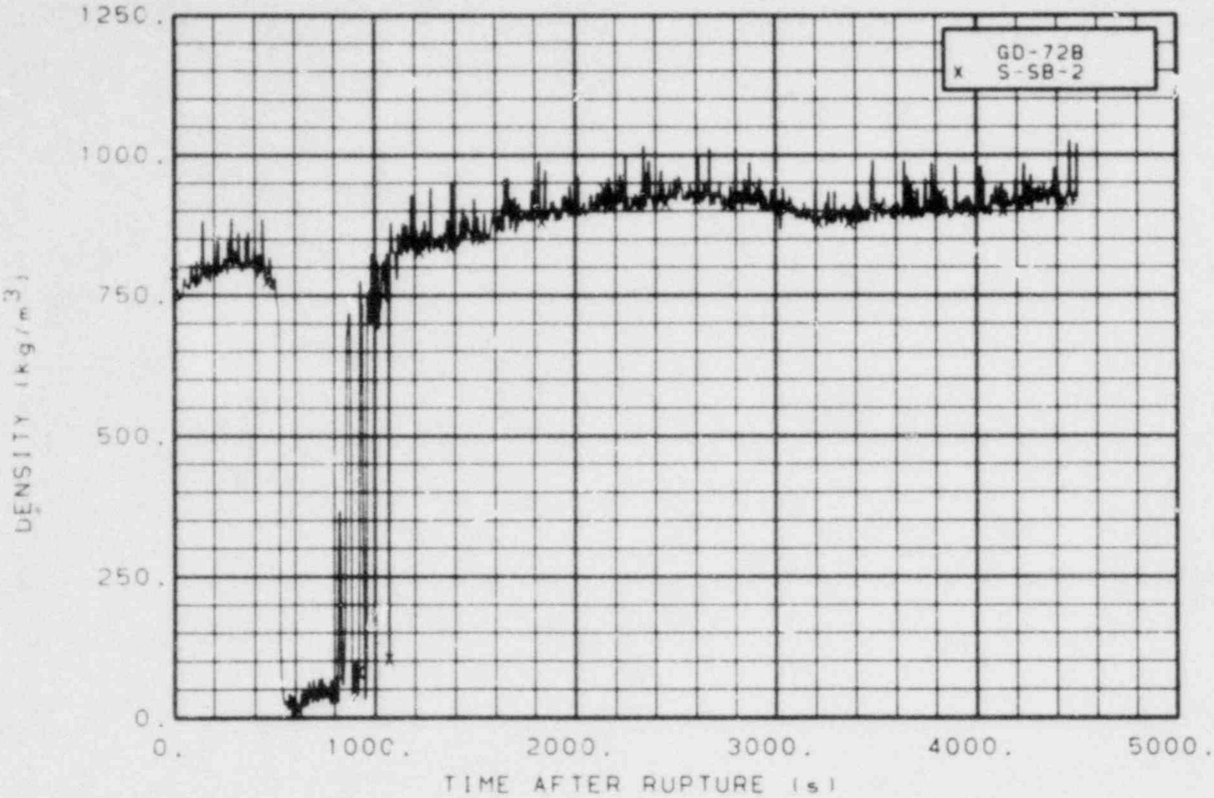

Figure 339. Density in downcomer, Test S-SB-2 (GD 72B), from 0 to 4500 s.

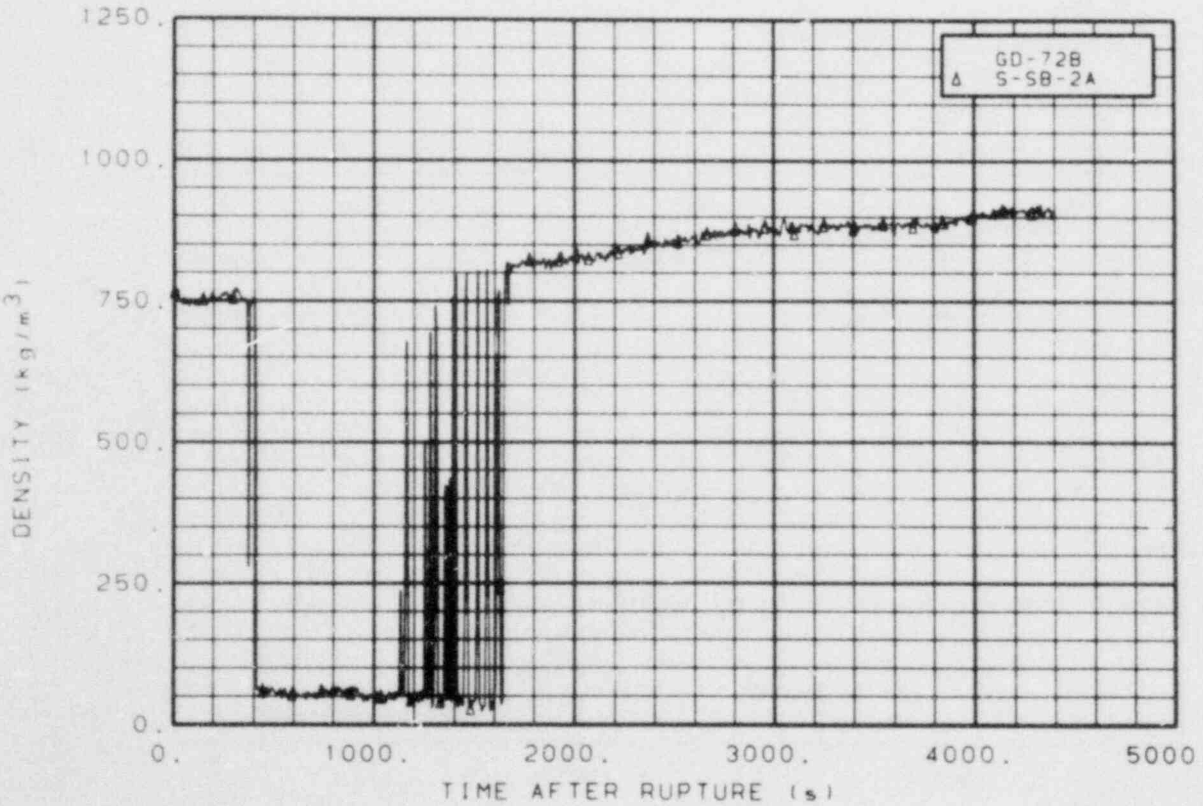

Figure 340. Density in downcomer, Test S-SB-2A (GD-72B), from 0 to 4390 s.

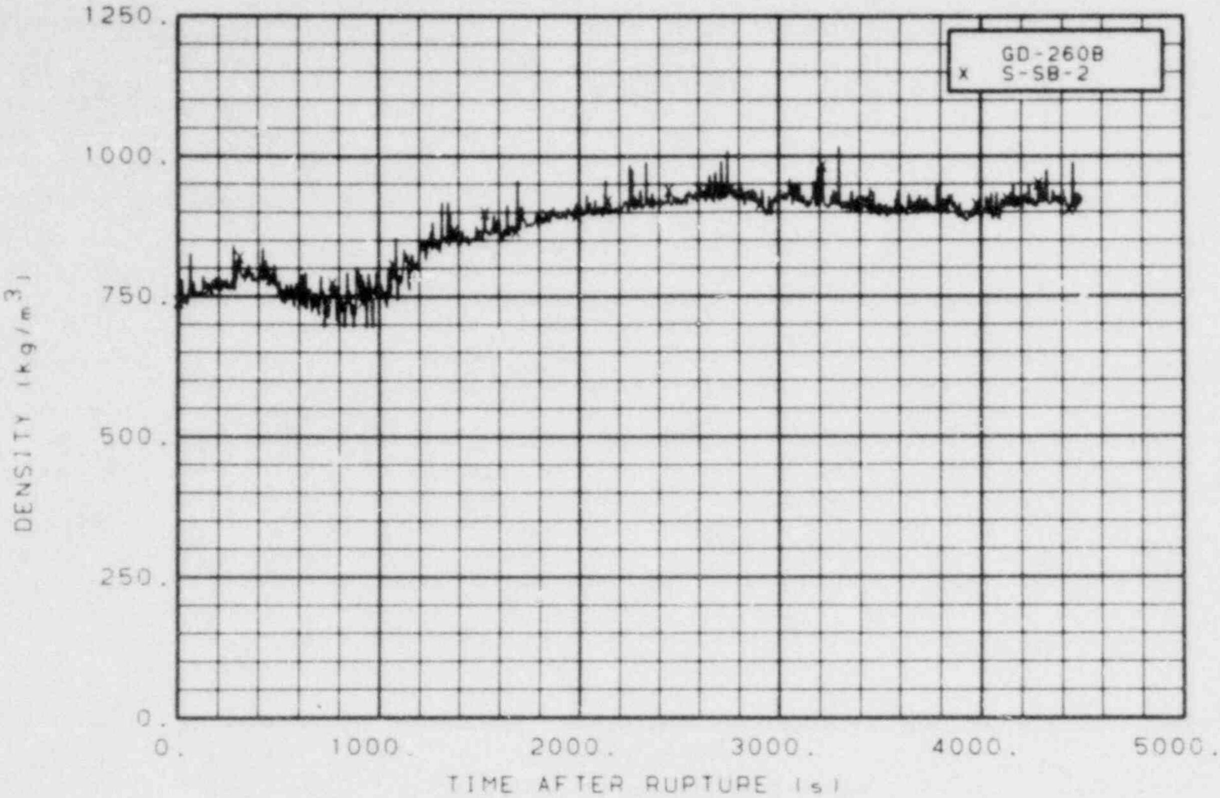

Figure 341. Density in downcomer, Test S-SB-2 (GD-260B), from 0 to 4500 s.

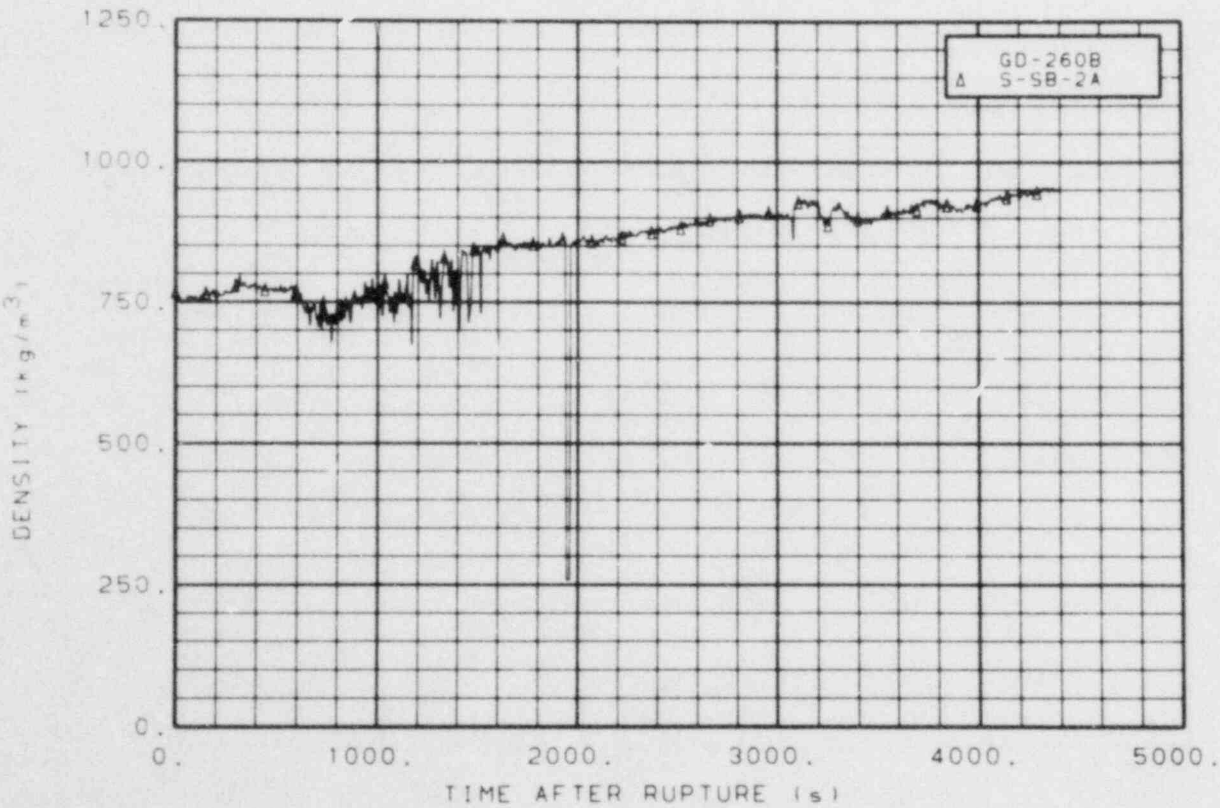

Figure 342. Density in downcomer, Test S-SB-2A (GD-260B), from 0 to 4390 s.

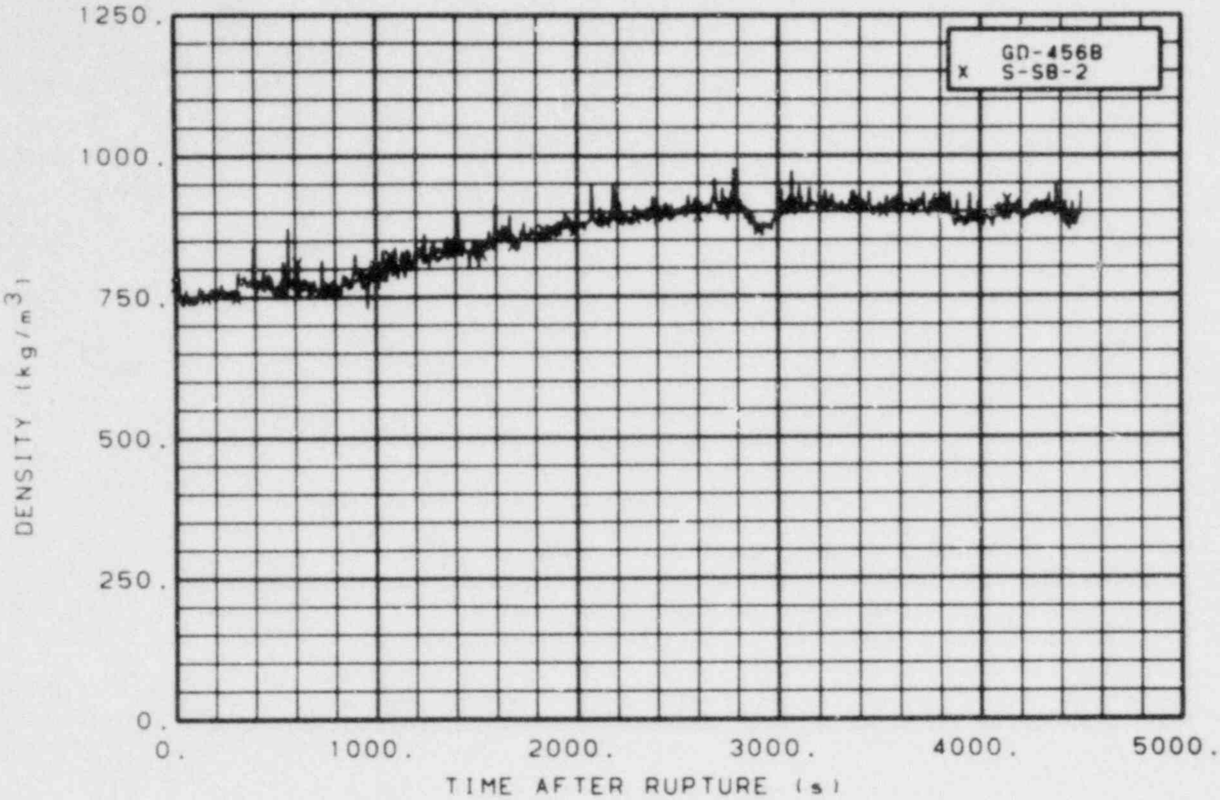

Figure 343. Density in downcomer, Test S-SB-2 (GD-456B), from 0 to 4500 s.

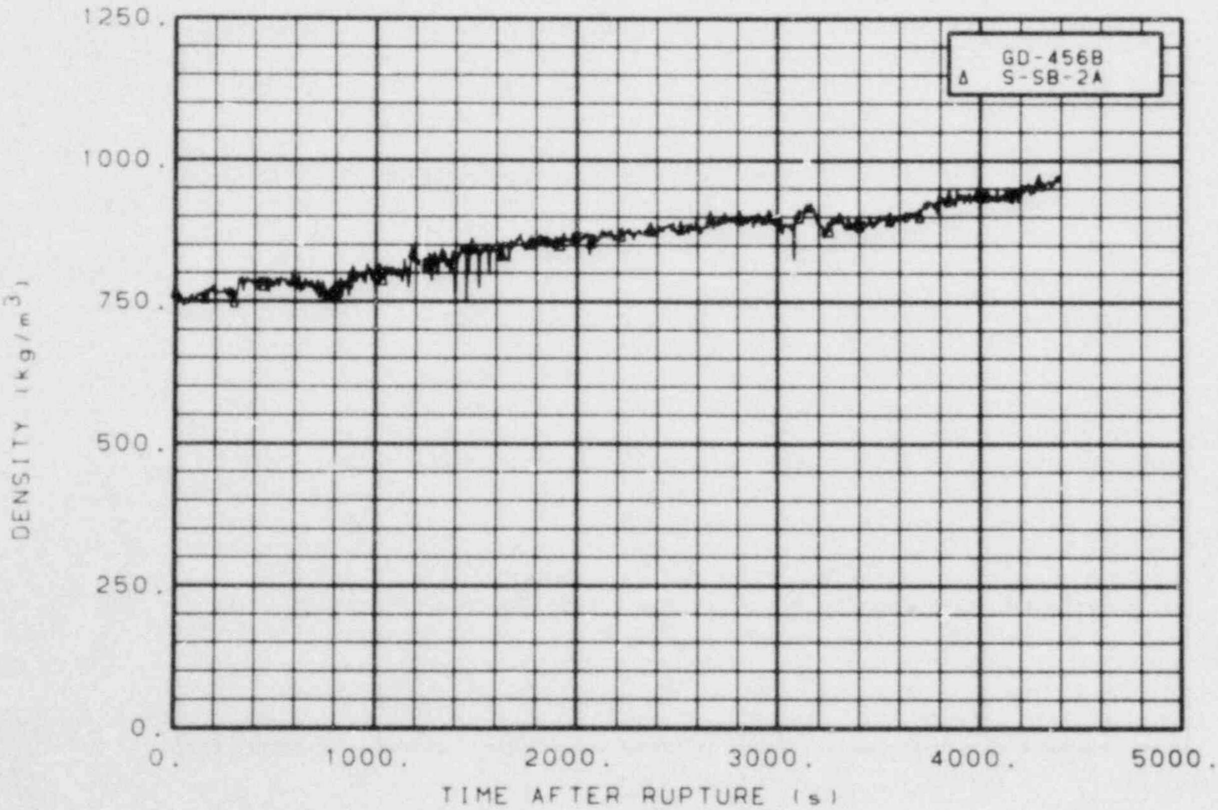

Figure 344. Density in downcomer, Test S-SB-2A (GD-456B), from 0 to 4390 s.

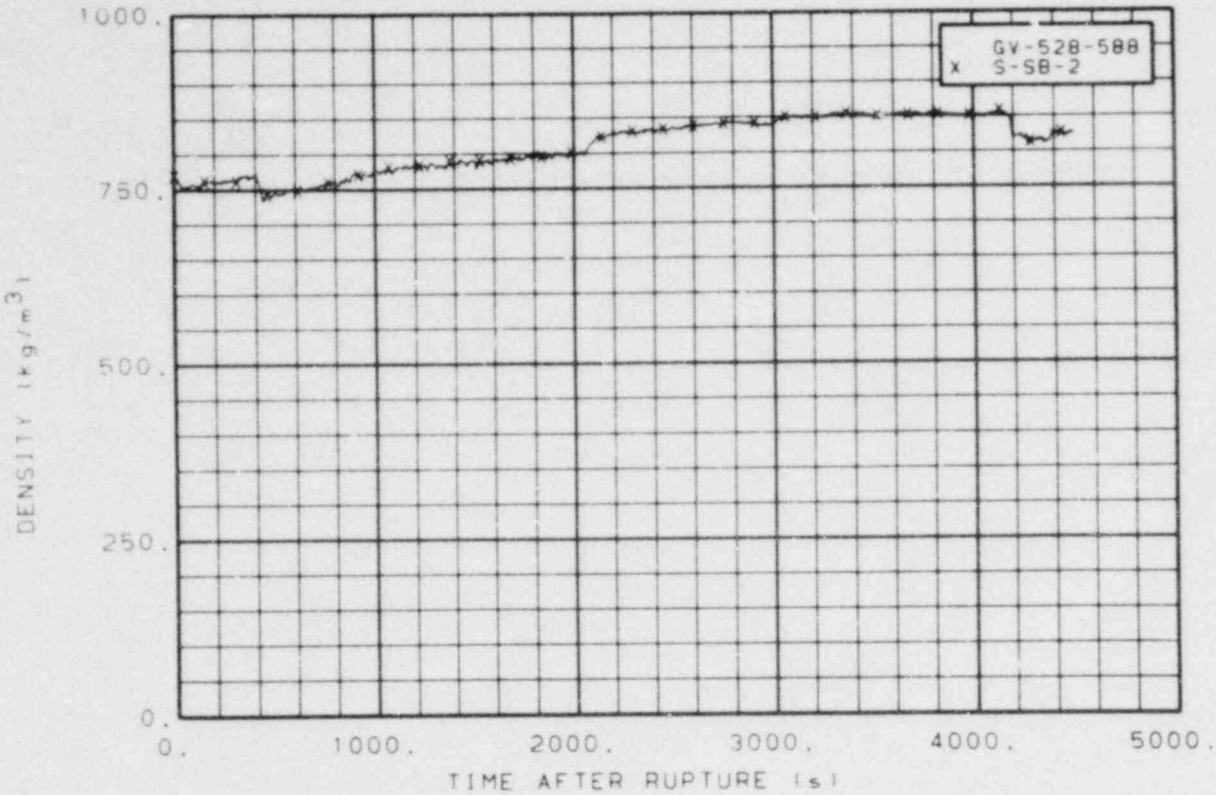

Figure 345. Density in vessel, Test S-SB-2 (GV-528-588), from 0 to 4500 s.

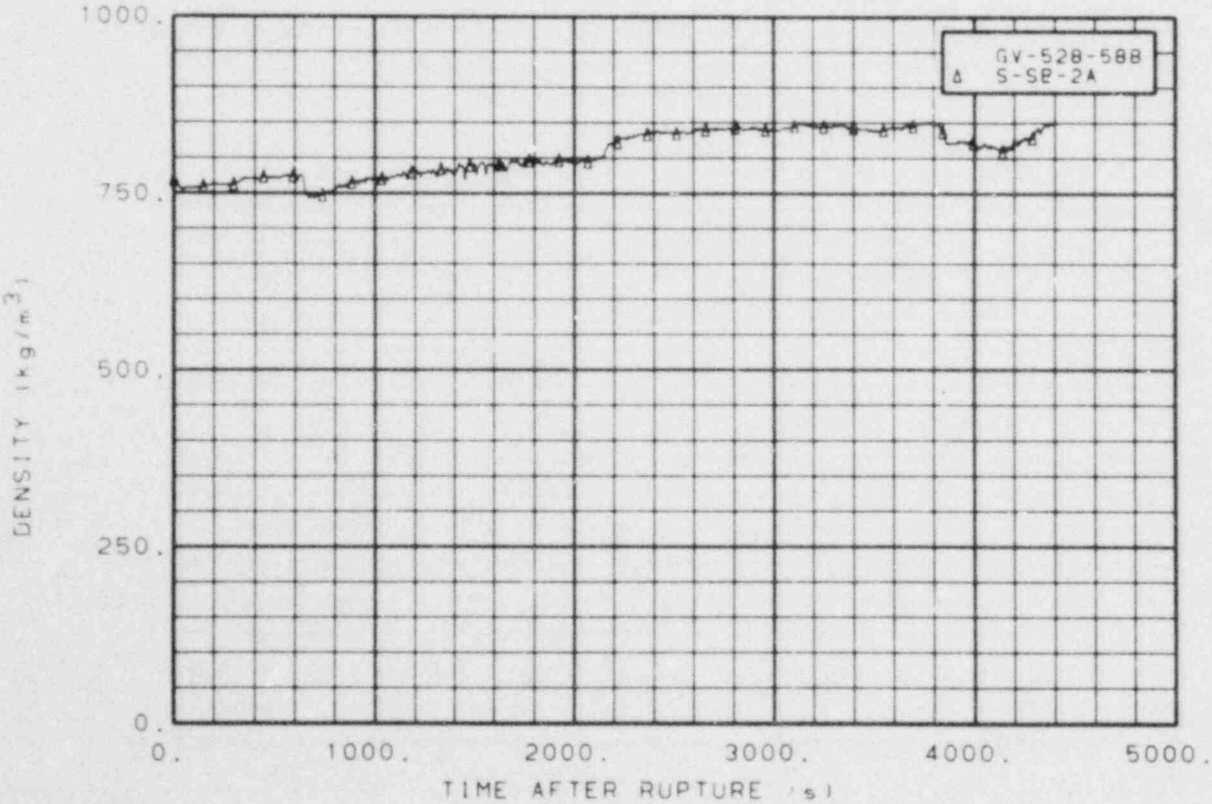

Figure 346. Density in vessel, Test S-SB-2A (GV-528-588), from 0 to 4390 s.

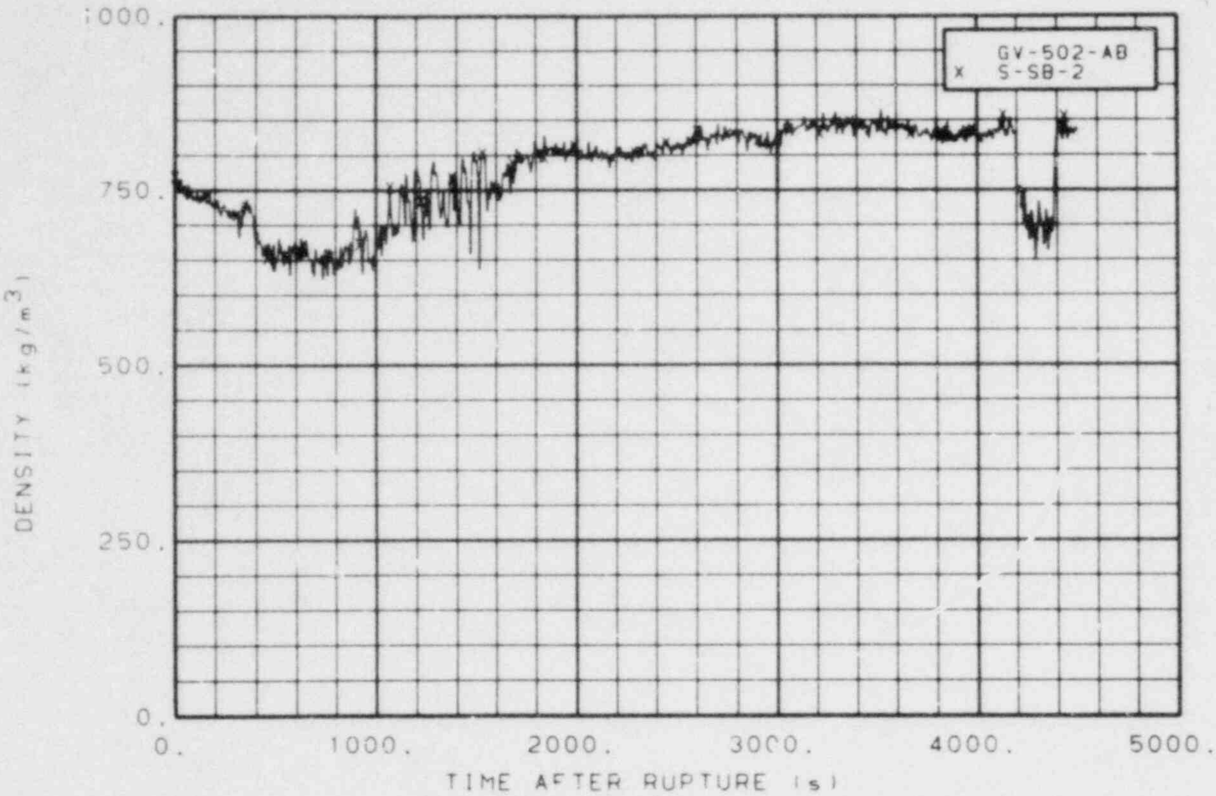

Figure 347. Density in vessel, Test S-SB-2 (GV-502-AB), from 0 to 4500 s.

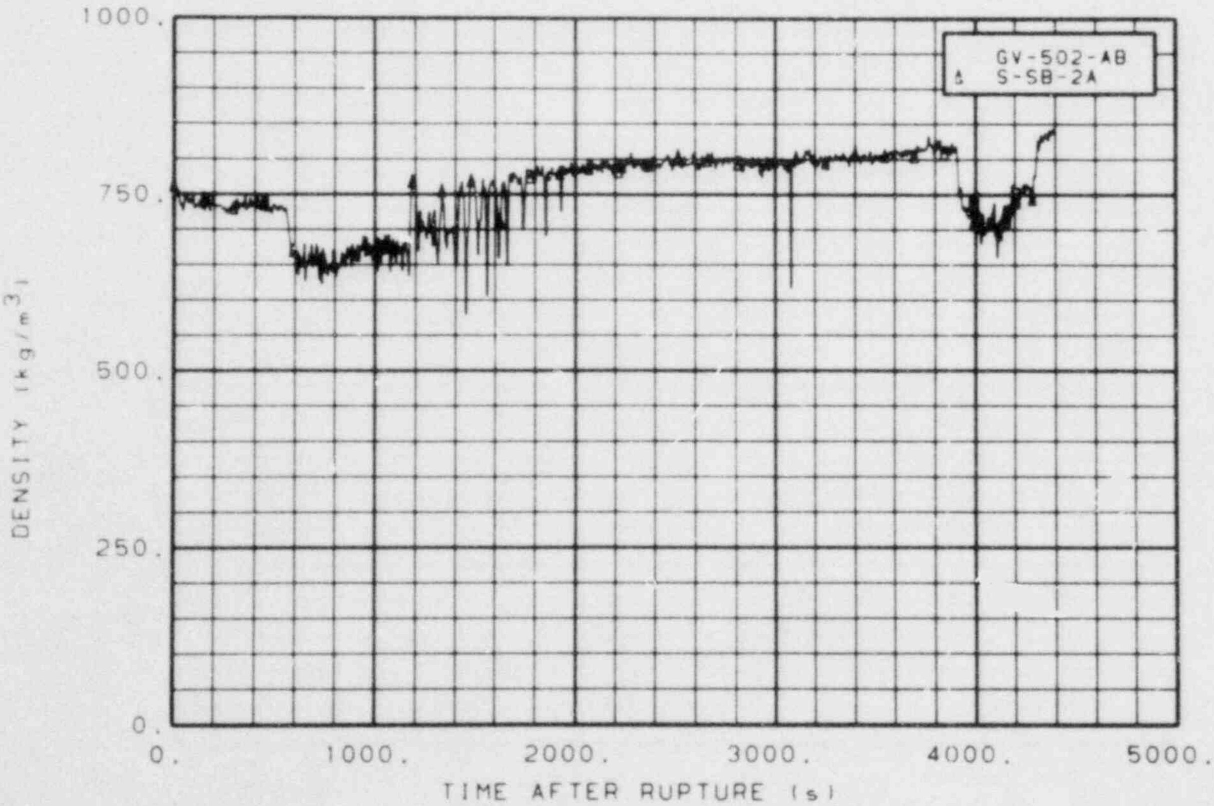

Figure 348. Density in vessel, Test S-SB-2A (GV-502-AB), from 0 to 4390 s.

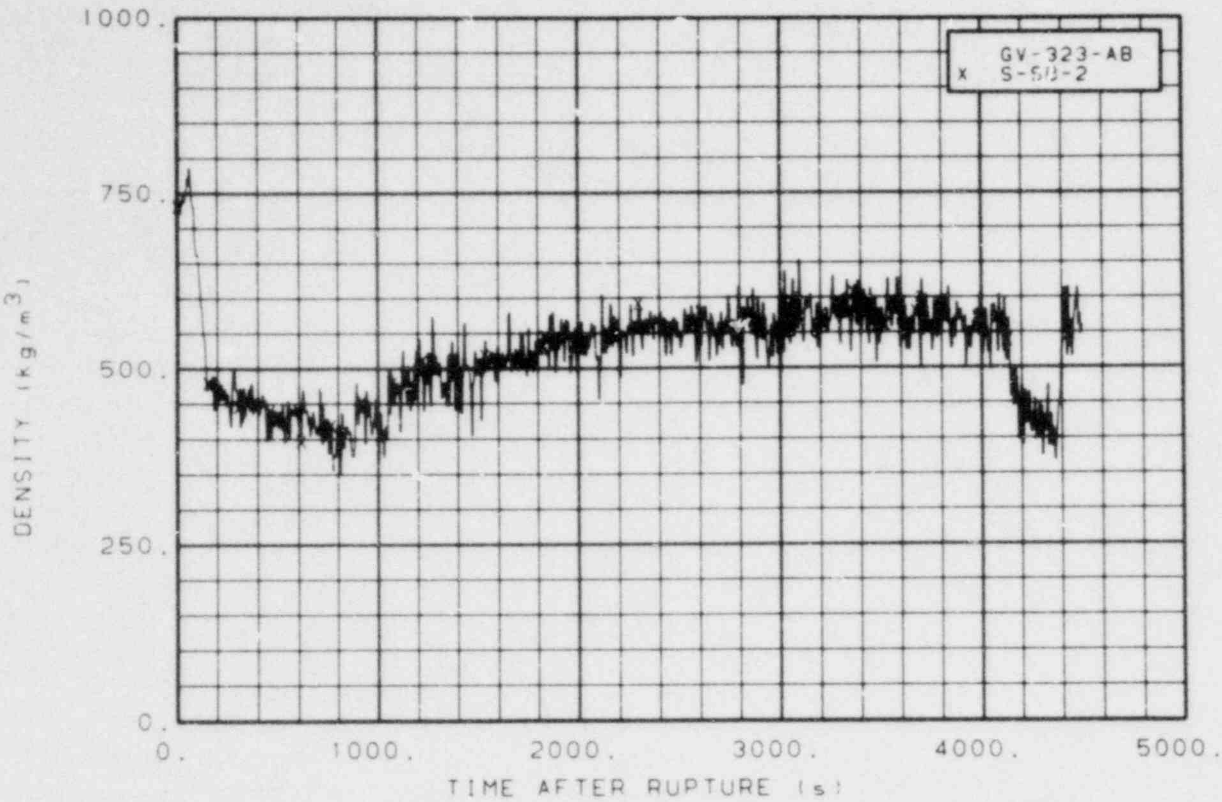

Figure 349. Density in vessel, Test S-SB-2 (GV-323-AB), from 0 to 4500 s.

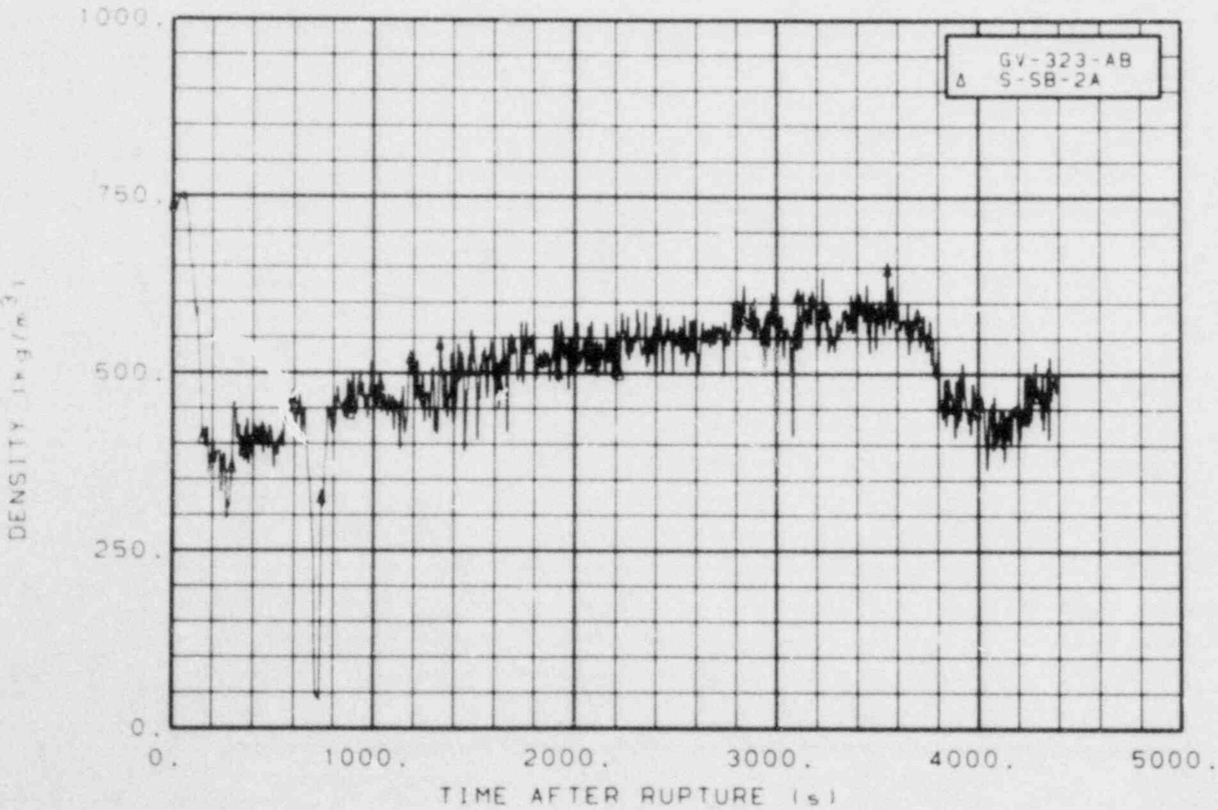

Figure 350. Density in vessel, Test S-SB-2A (GV-323-AB), from 0 to 4390 s.

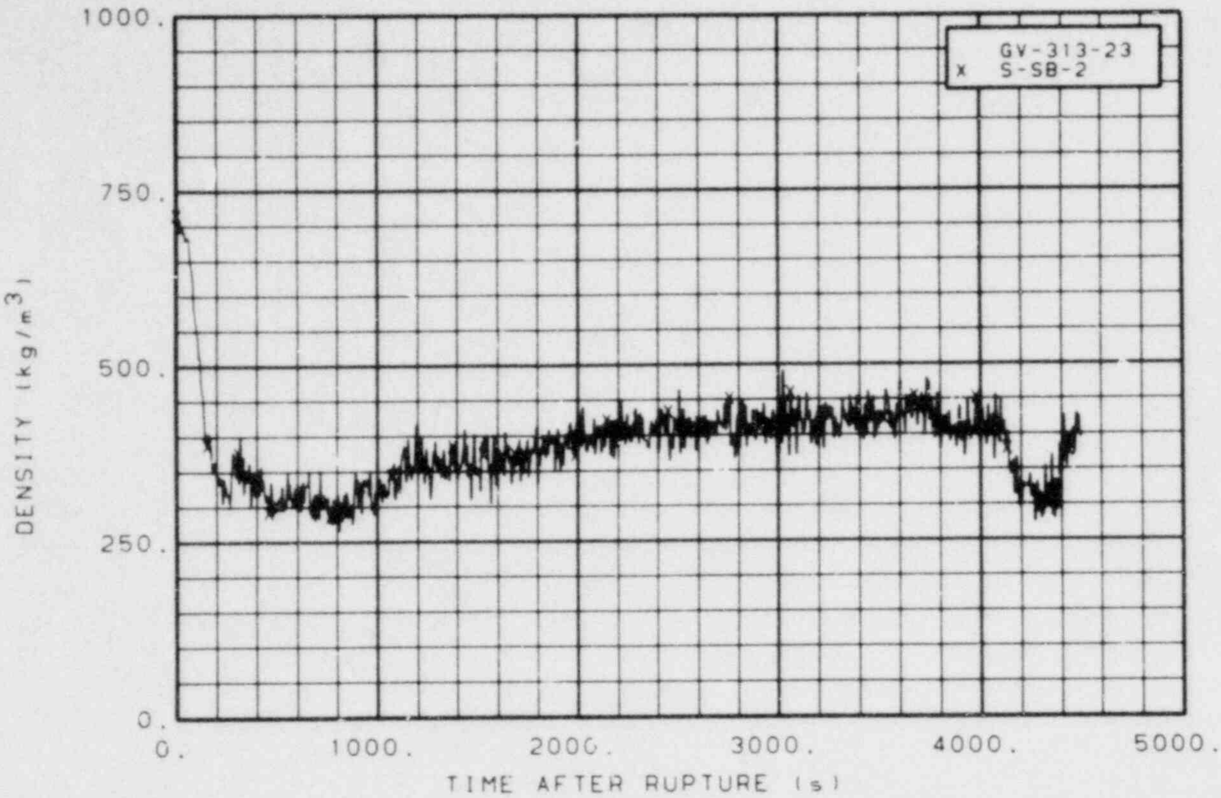

Figure 351. Density in vessel, Test S-SB-2 (GV-313-23), from 0 to 4500 s.

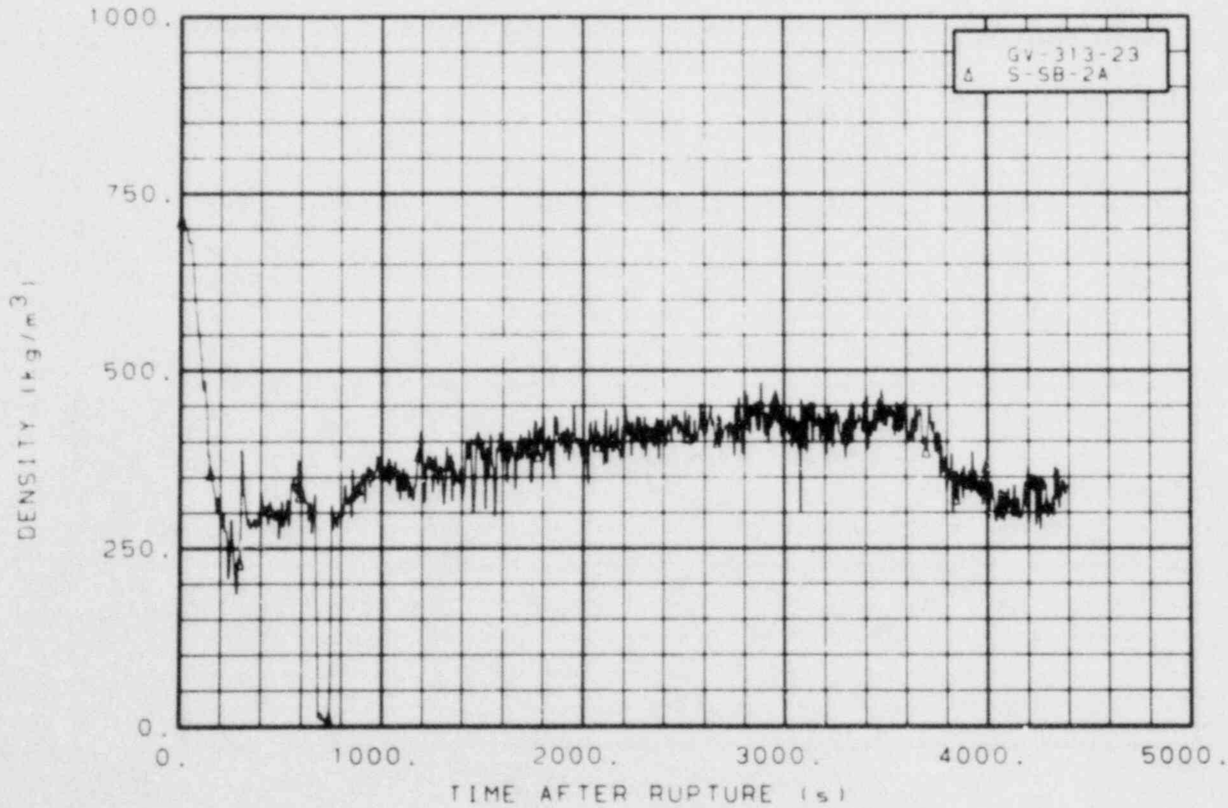

Figure 352. Density in vessel, Test S-SB-2A (GV-313-23), from 0 to 4390 s.

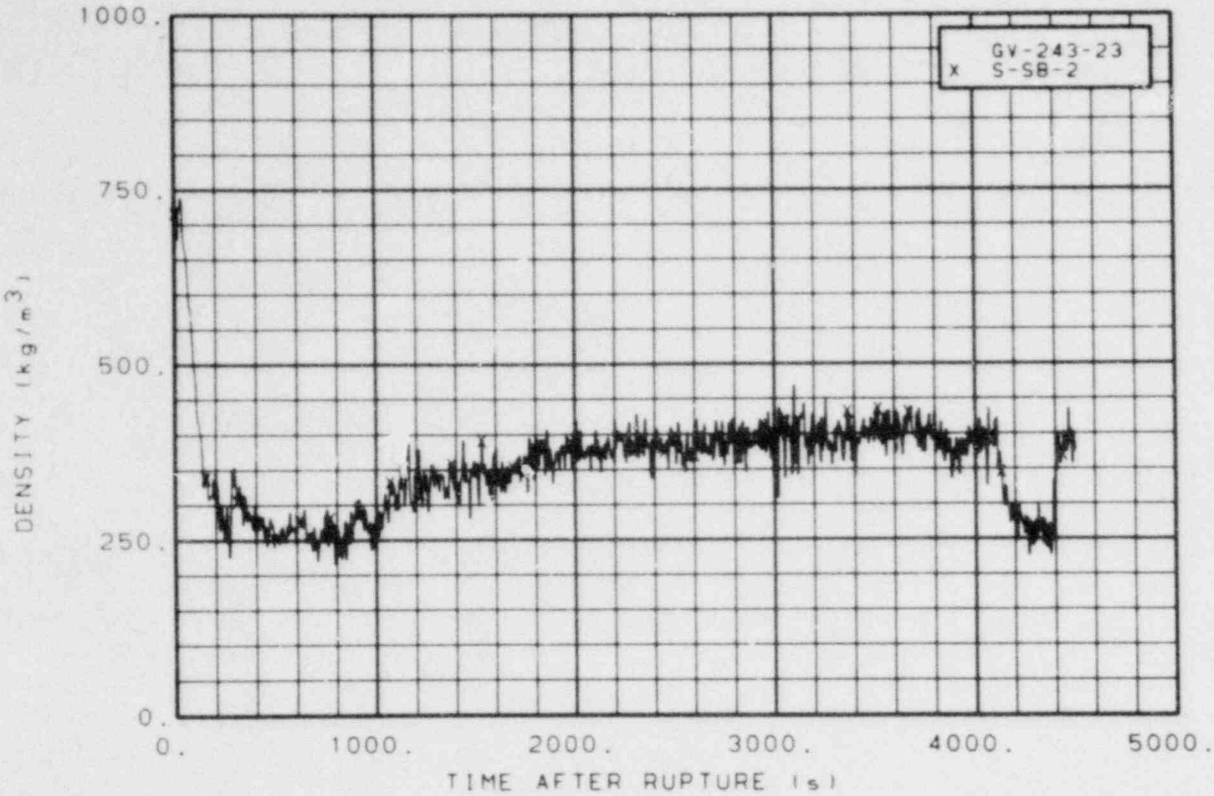

Figure 353. Density in vessel, Test S-SB-2 (GV-243-23), from 0 to 4500 s.

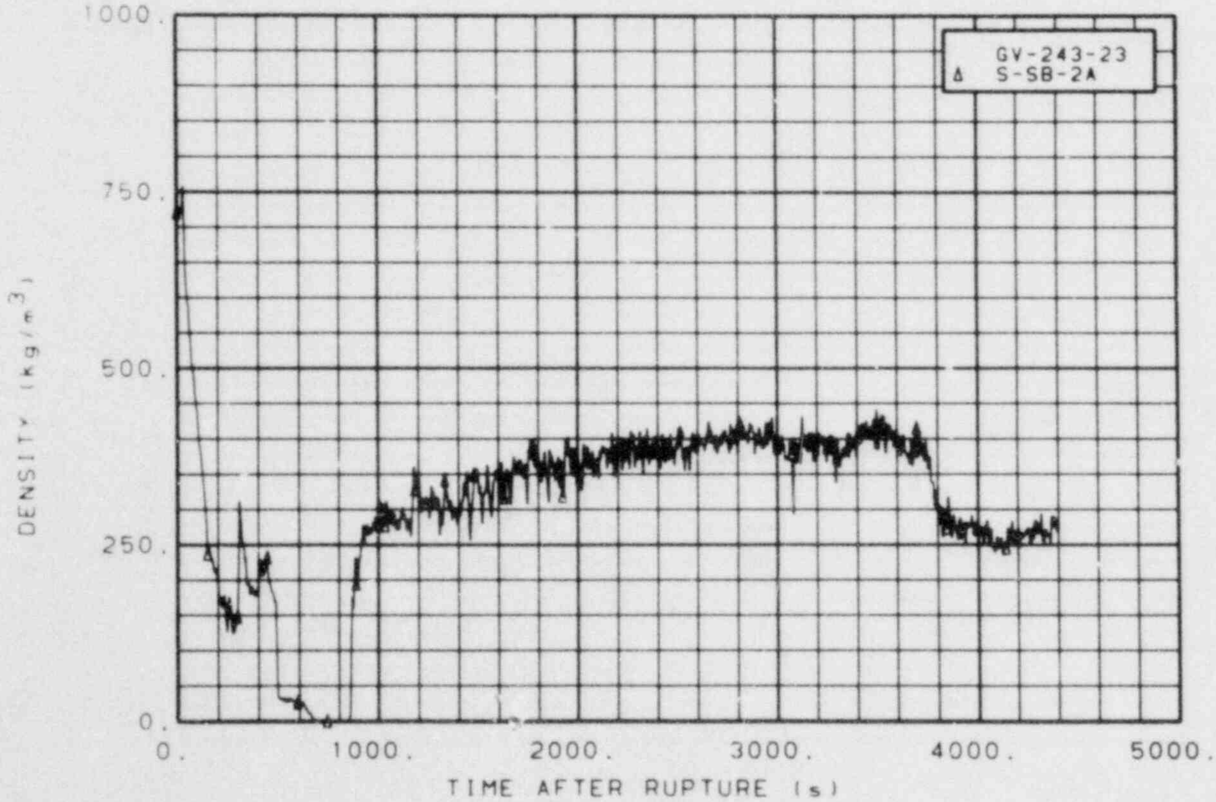

Figure 354. Density in vessel, Test S-SB-2A (GV-243-23), from 0 to 4390 s.

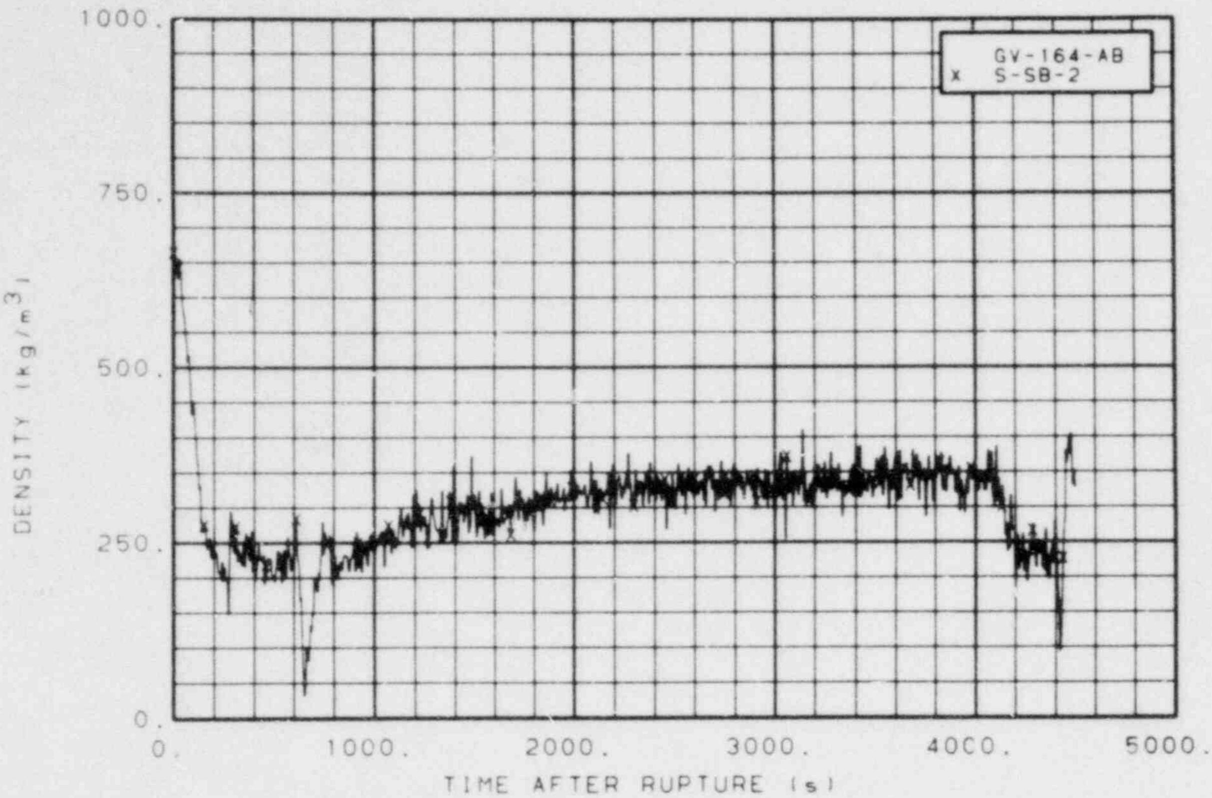

Figure 355. Density in vessel, Test S-SB-2 (GV-164-AB), from 0 to 4500 s.

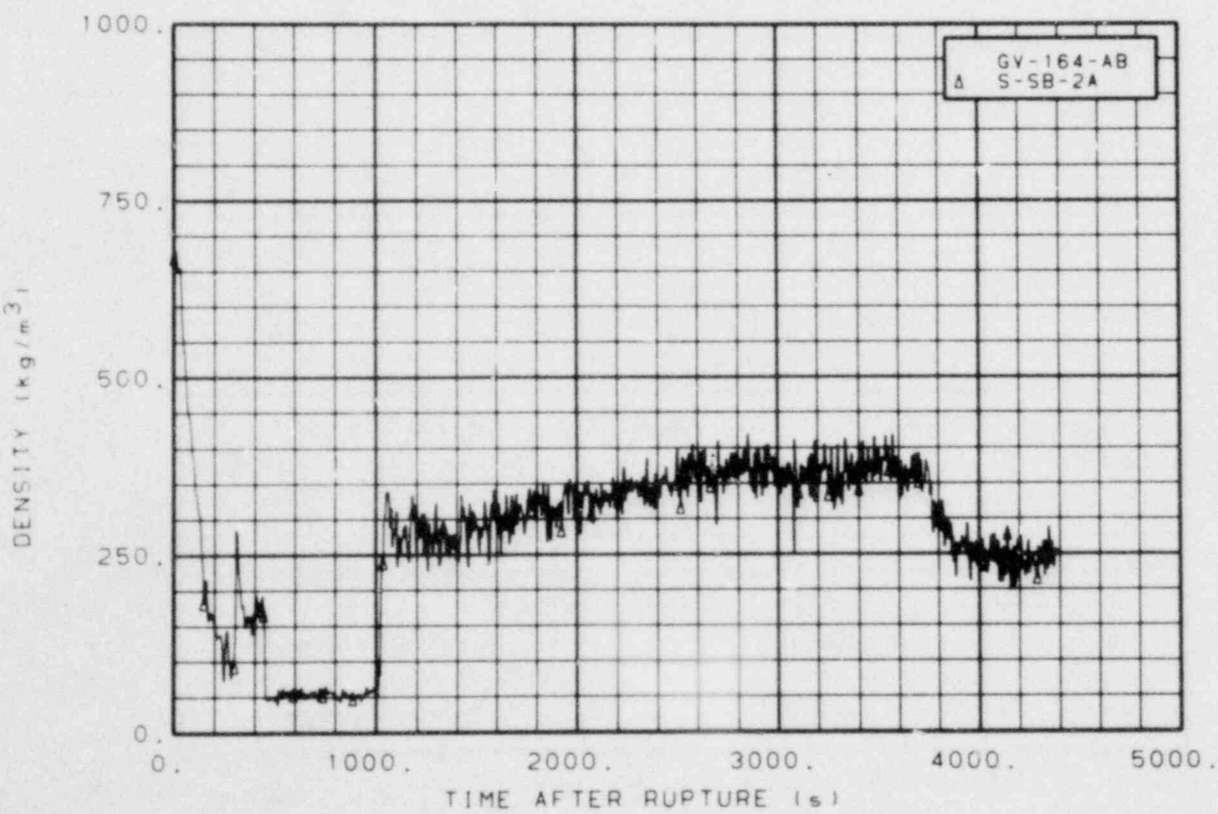

Figure 356. Density in vessel, Test S-SB-2A (GV-164-AB), from 0 to 4390 s.

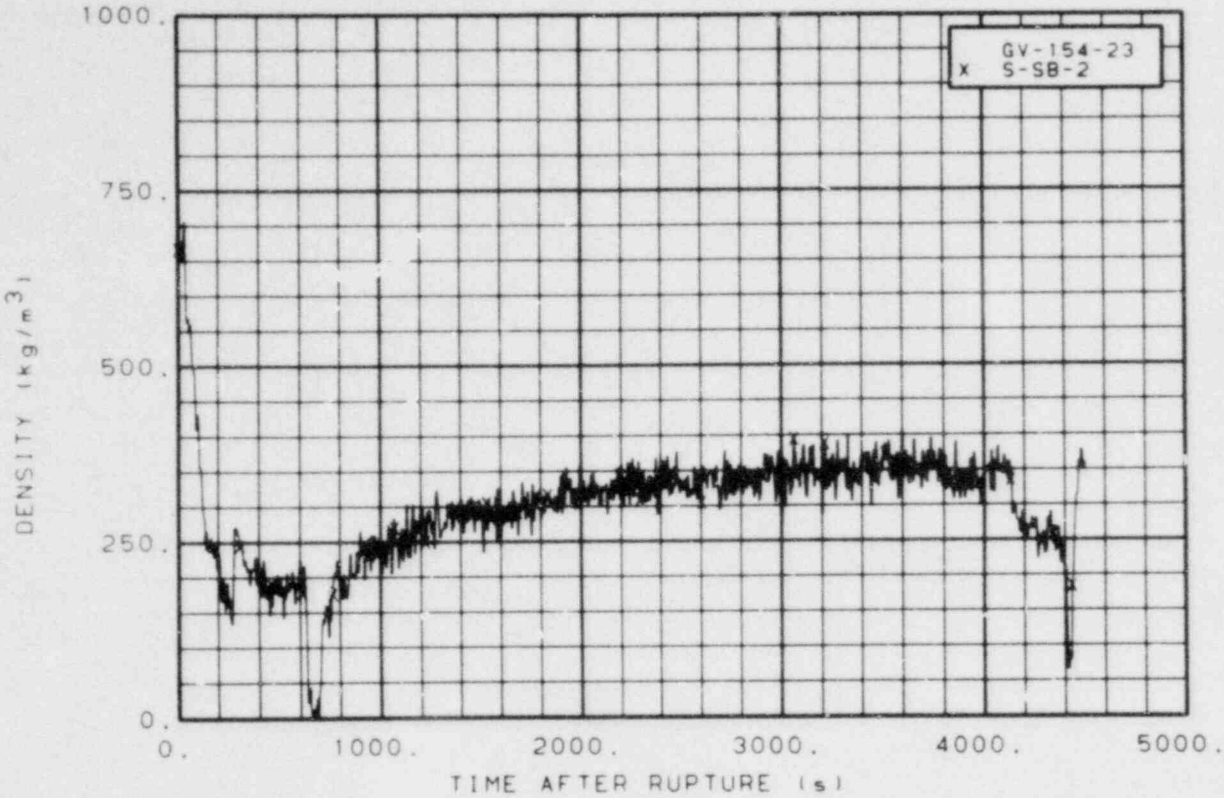

Figure 357. Density in vessel, Test S-SB-2 (GV-154-23), from 0 to 4500 s.

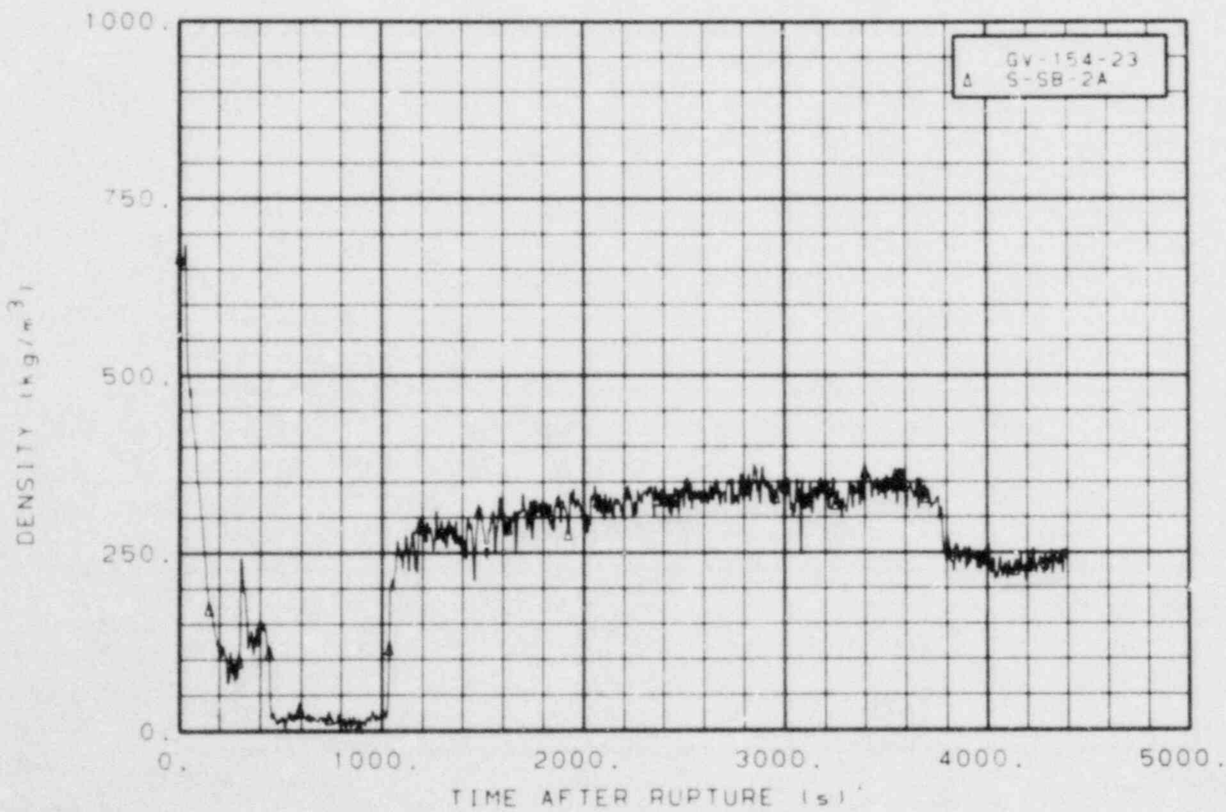

Figure 358. Density in vessel, Test S-SB-2A (GV-154-23), from 0 to 4390 s.

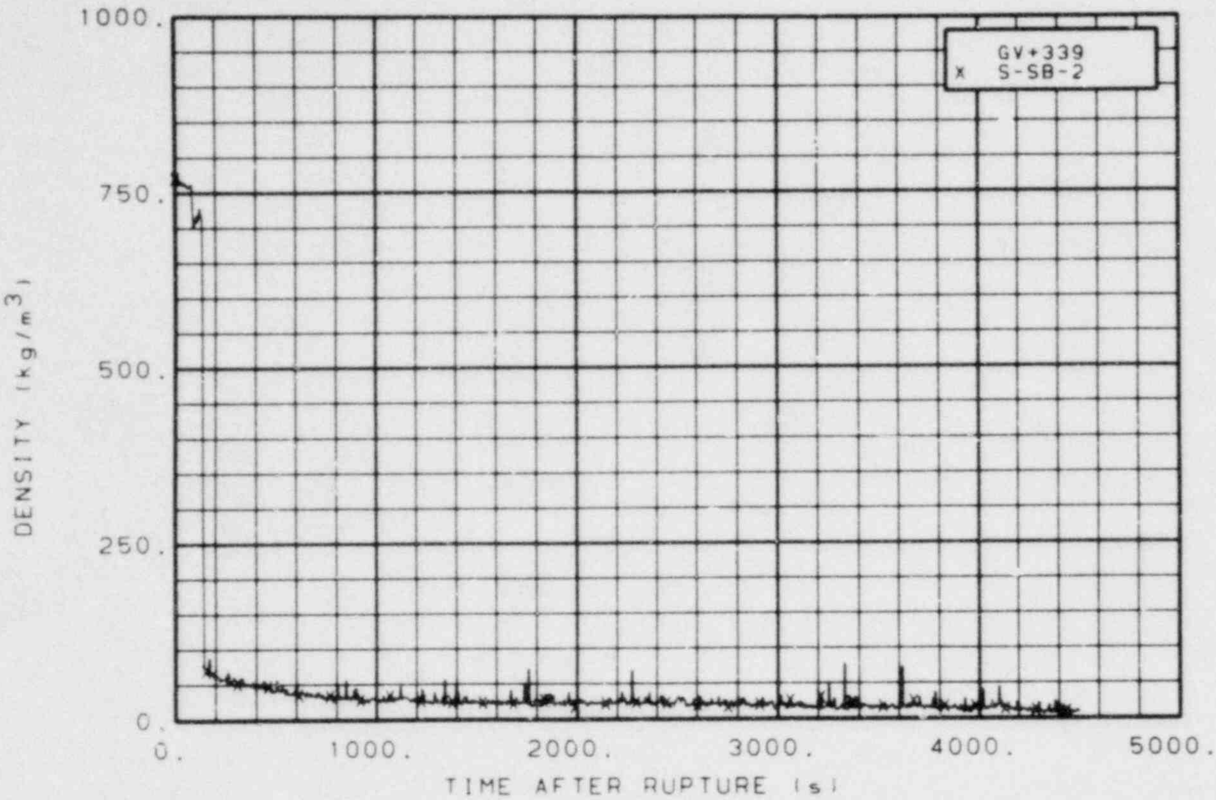

Figure 359. Density in vessel, Test S-SB-2 (GV + 339), from 0 to 4500 s.

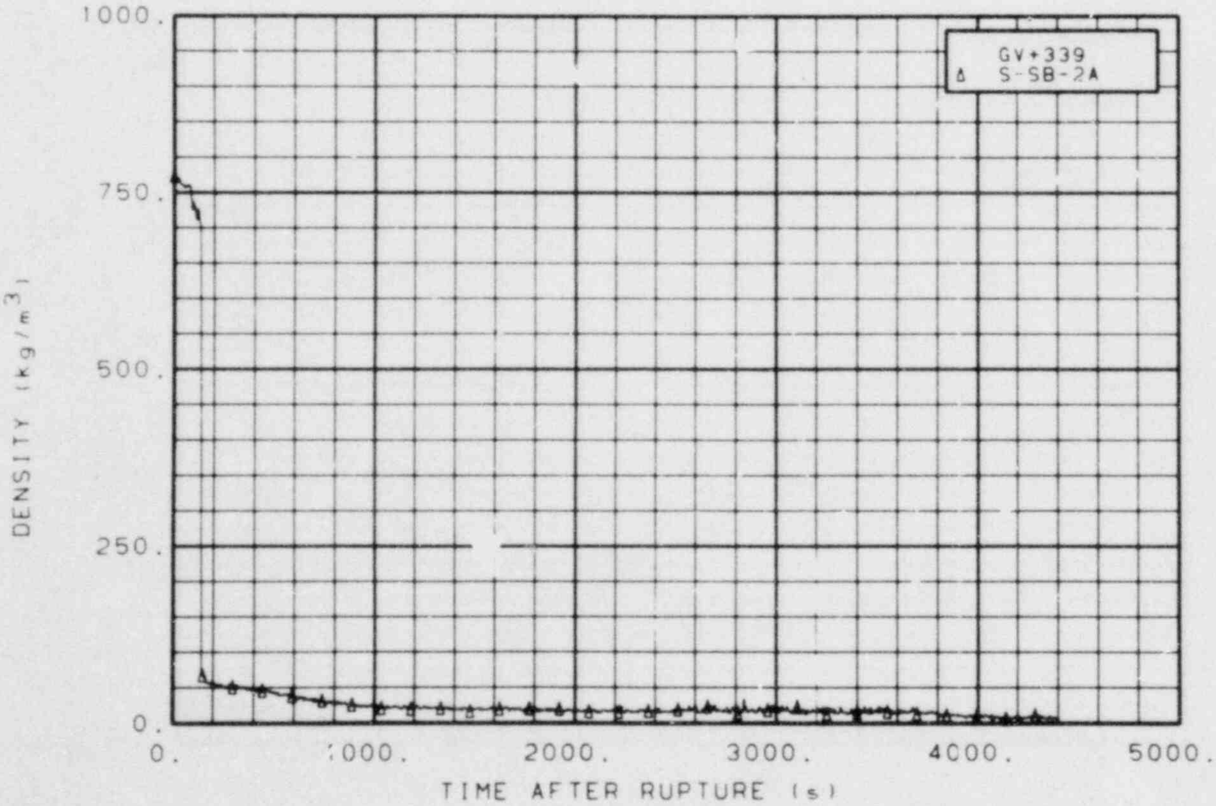

Figure 360. Density in vessel, Test S-SB-2A (GV + 339), from 0 to 4390 s.

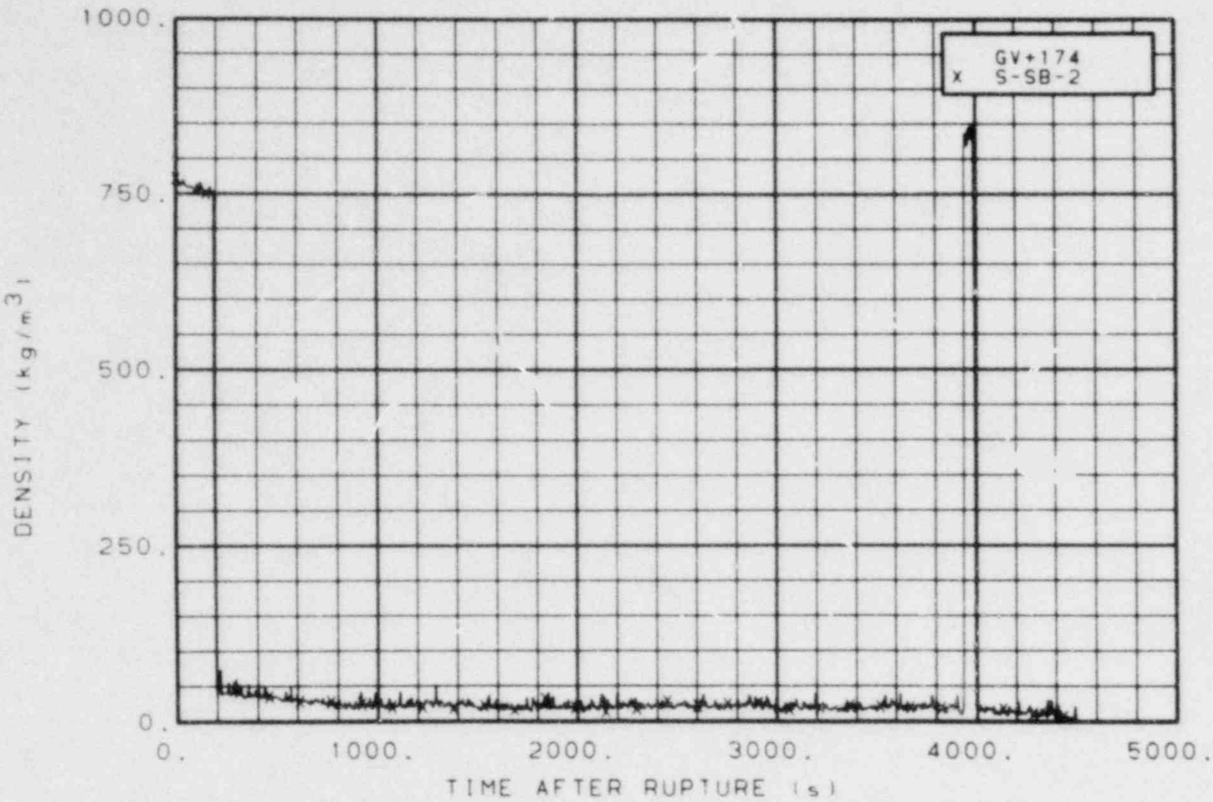

Figure 361. Density in vessel, Test S-SB-2 (GV + 174), from 0 to 4500 s.

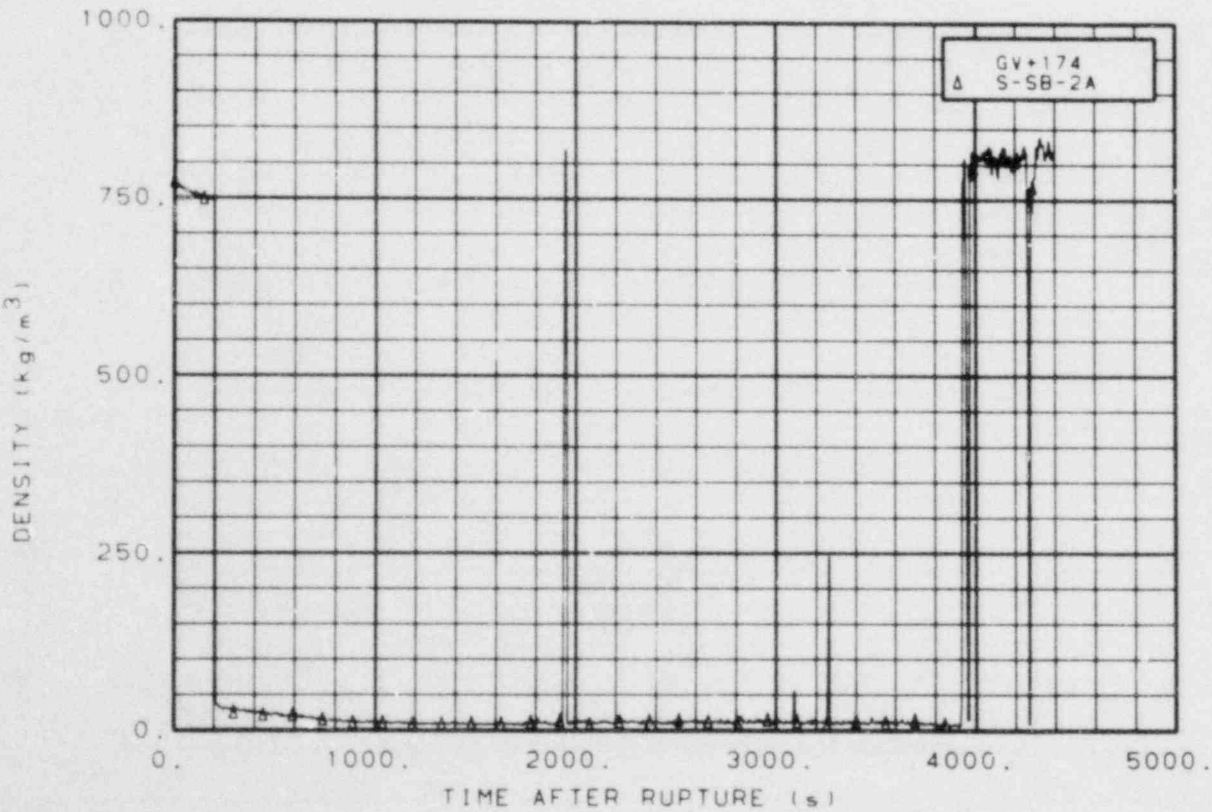

Figure 362. Density in vessel, Test S-SB-2A (GV + 174), from 0 to 4390 s.

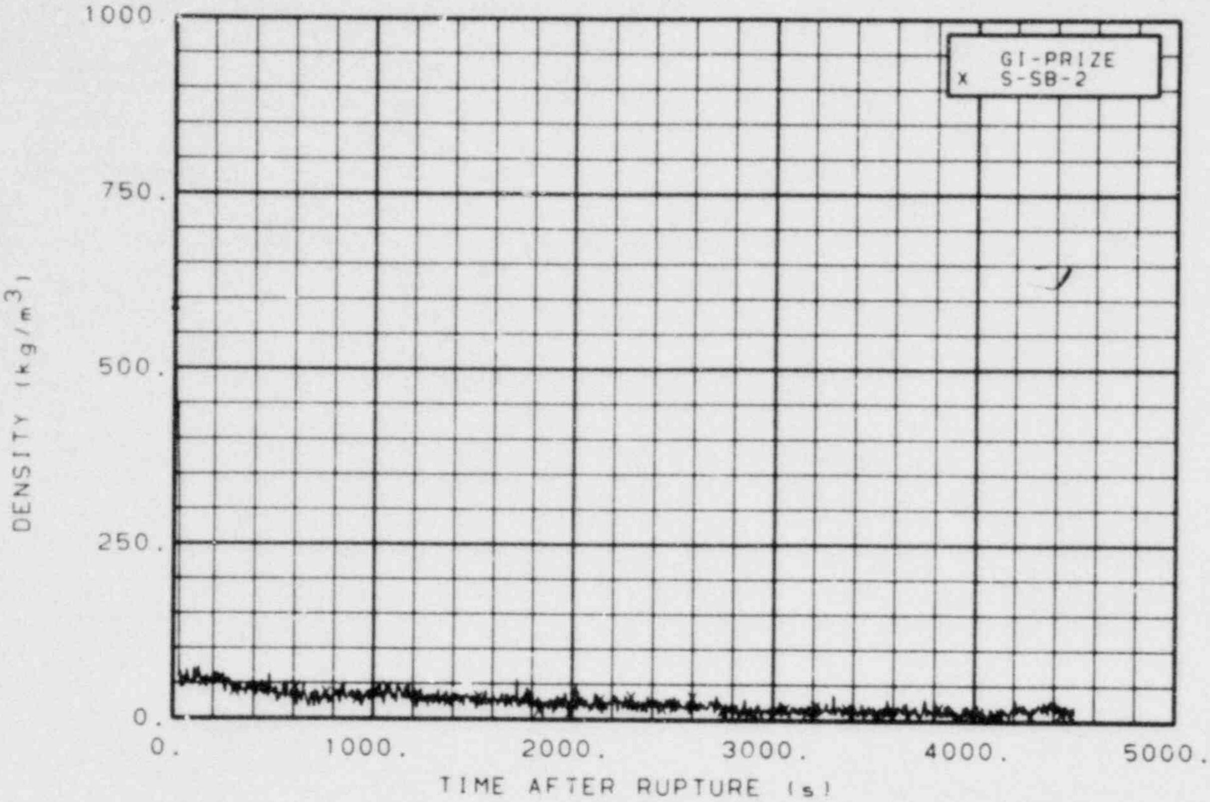

Figure 363. Density in intact loop pressurizer, Test S-SB-2 (GI-PRIZE), from 0 to 4500 s.

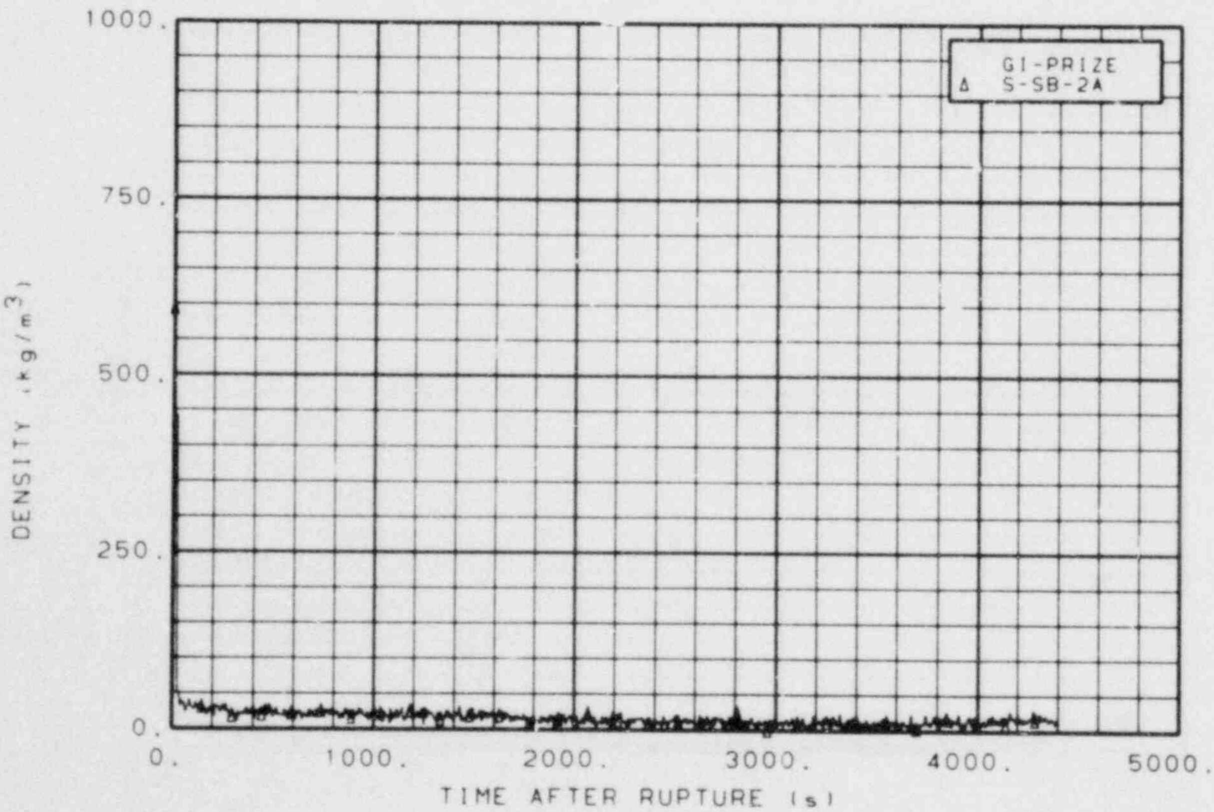

Figure 364. Density in intact loop pressurizer, Test S-SB-2A (GI-PRIZE), from 0 to 4390 s.

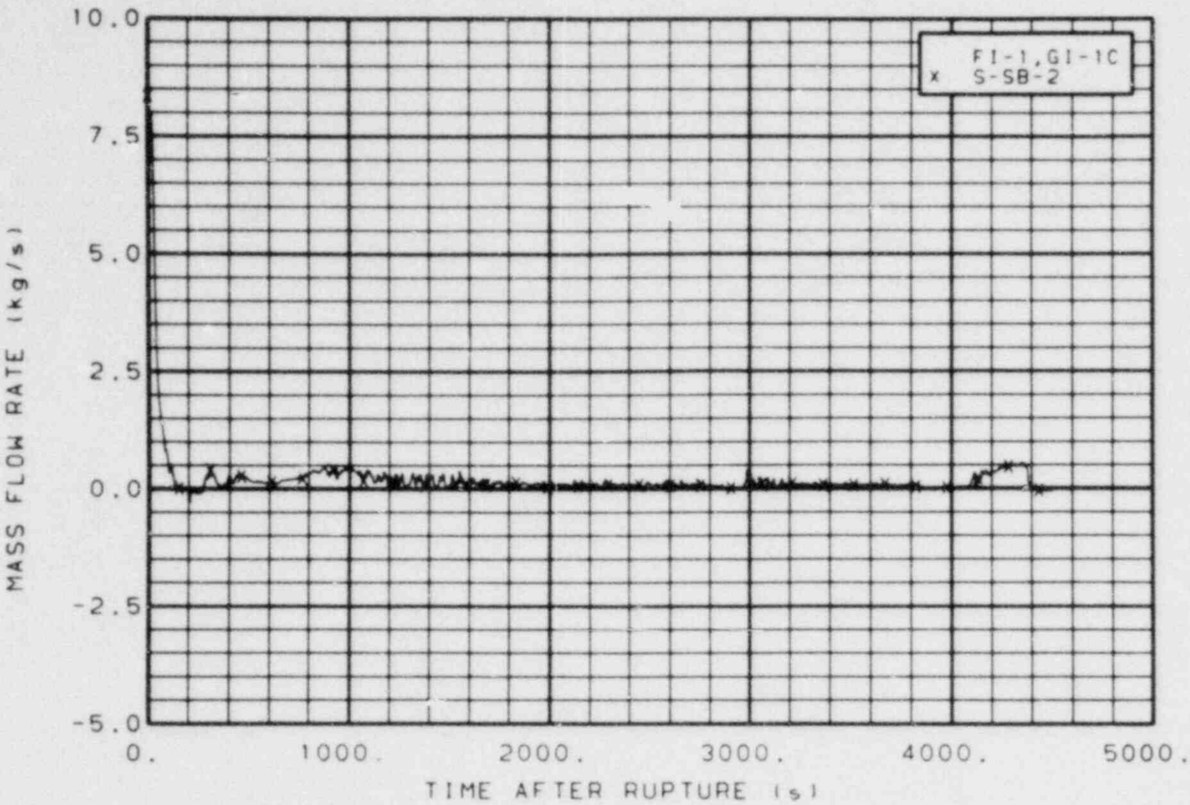

Figure 365. Mass Flow in intact loop hot leg, Test S-SB-2 (FI-1 and GI-1C), from 0 to 4500 s.

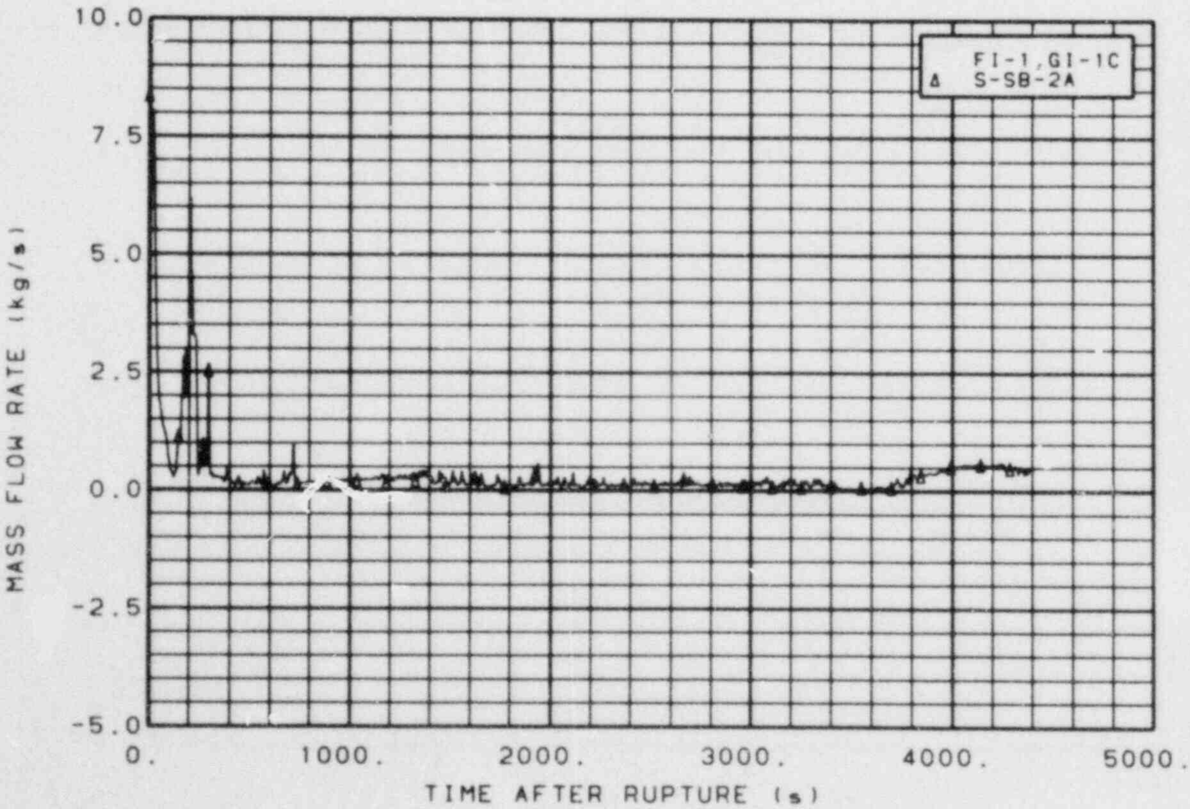

Figure 366. Mass Flow in intact loop hot leg, Test S-SB-2A (FI-1 and GI-1C), from 0 to 4390 s.

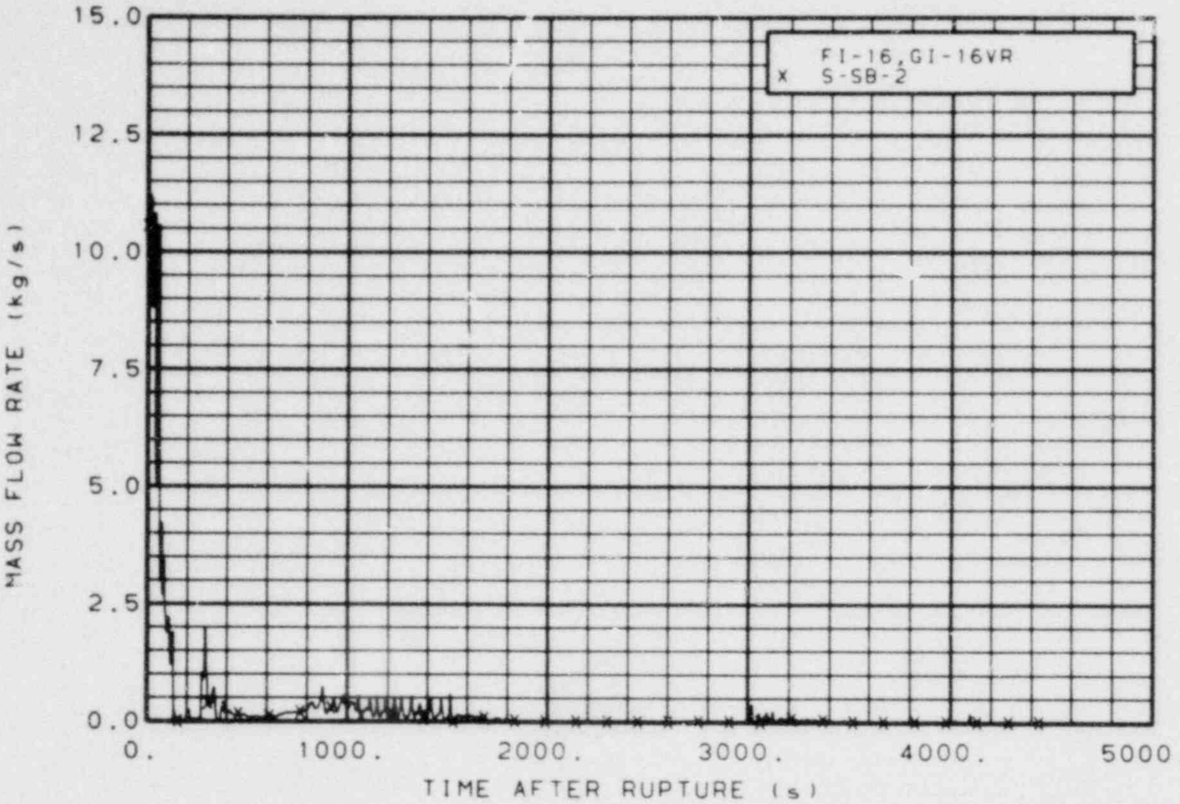

Figure 367. Mass Flow in intact loop cold leg, Test S-SB-2 (FI-16 and GI-16VR), from 0 to 4500 s.

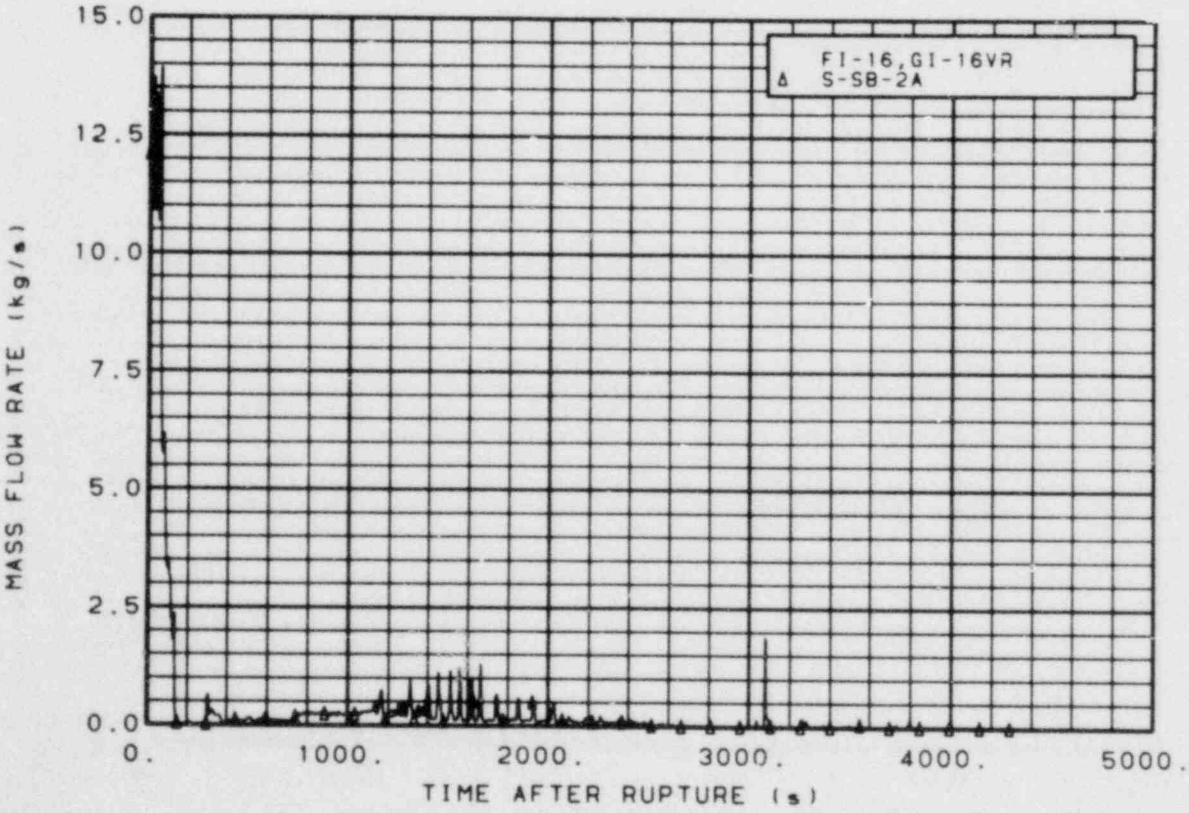

Figure 368. Mass Flow in intact loop cold leg, Test S-SB-2A (FI-16 and GI-16VR), from 0 to 4390 s.

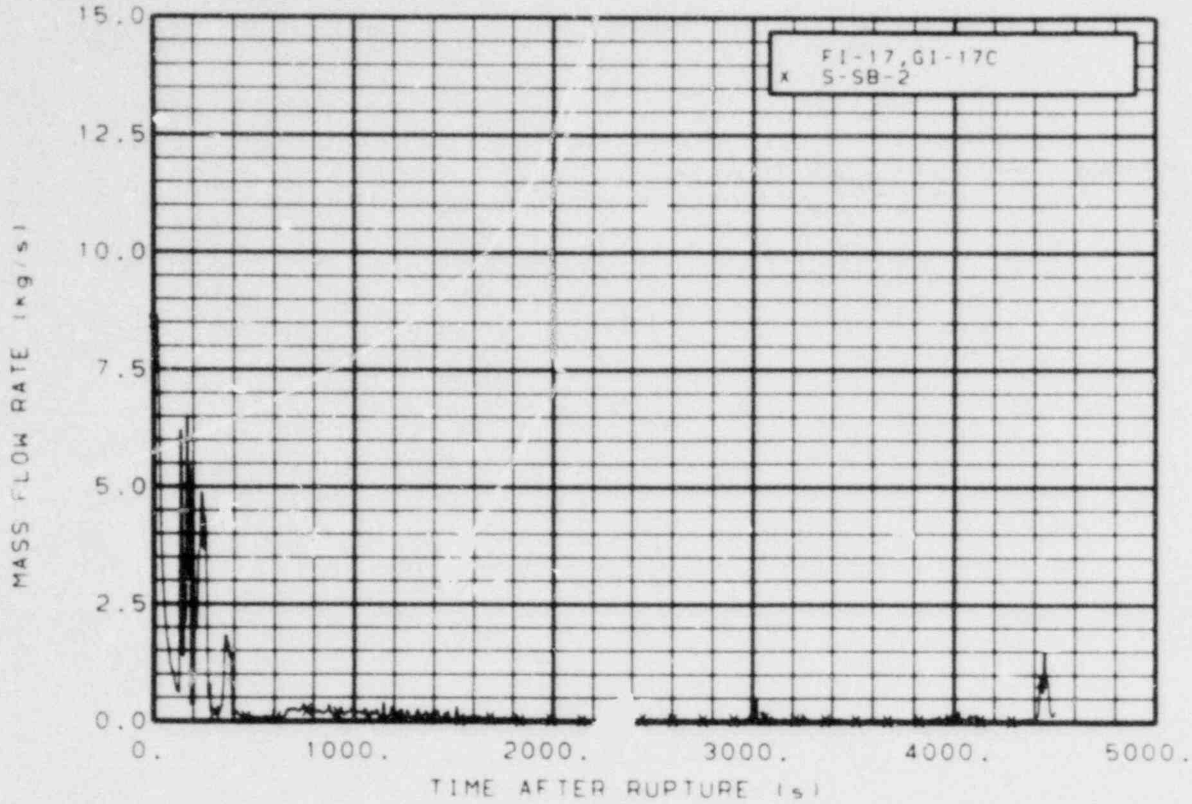

Figure 369. Mass Flow in intact loop cold leg, Test S-SB-2 (FI-17 and GI-17C), from 0 to 4500 s.

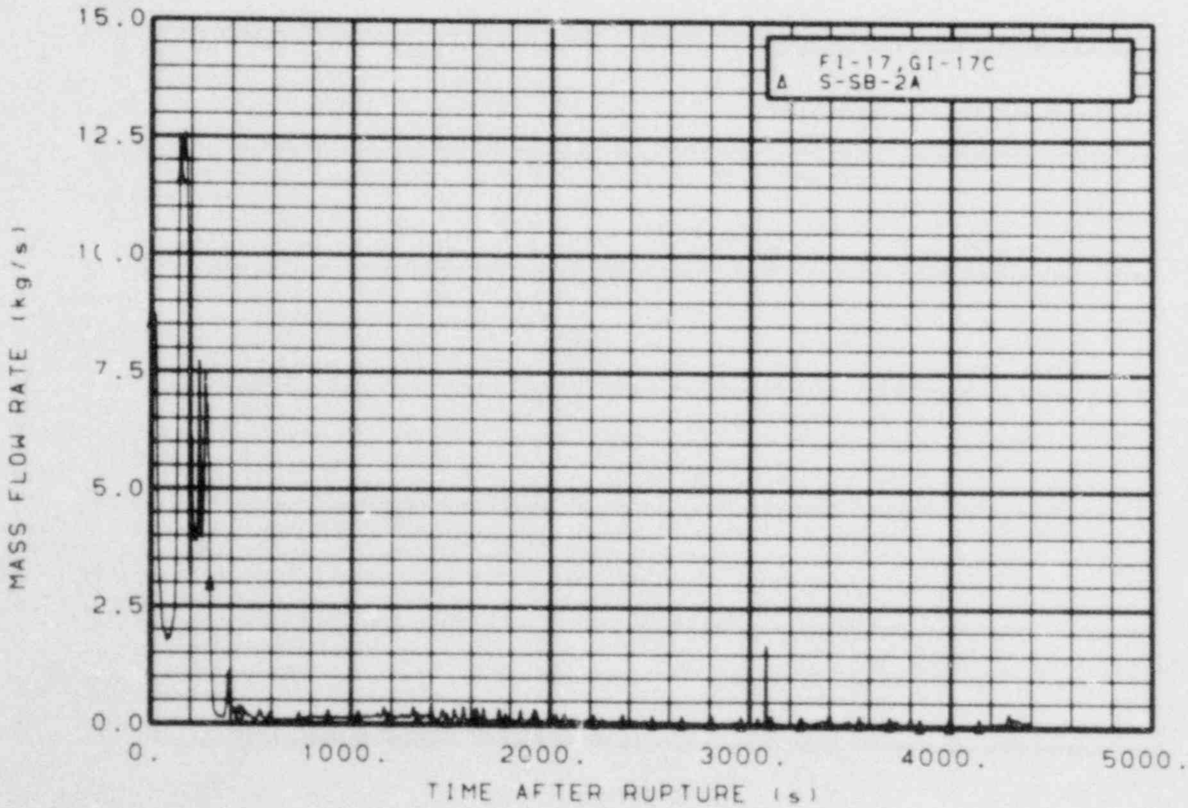

Figure 370. Mass Flow in intact loop cold leg, Test S-SB-2A (FI-17 and GI-17C), from 0 to 4390 s.

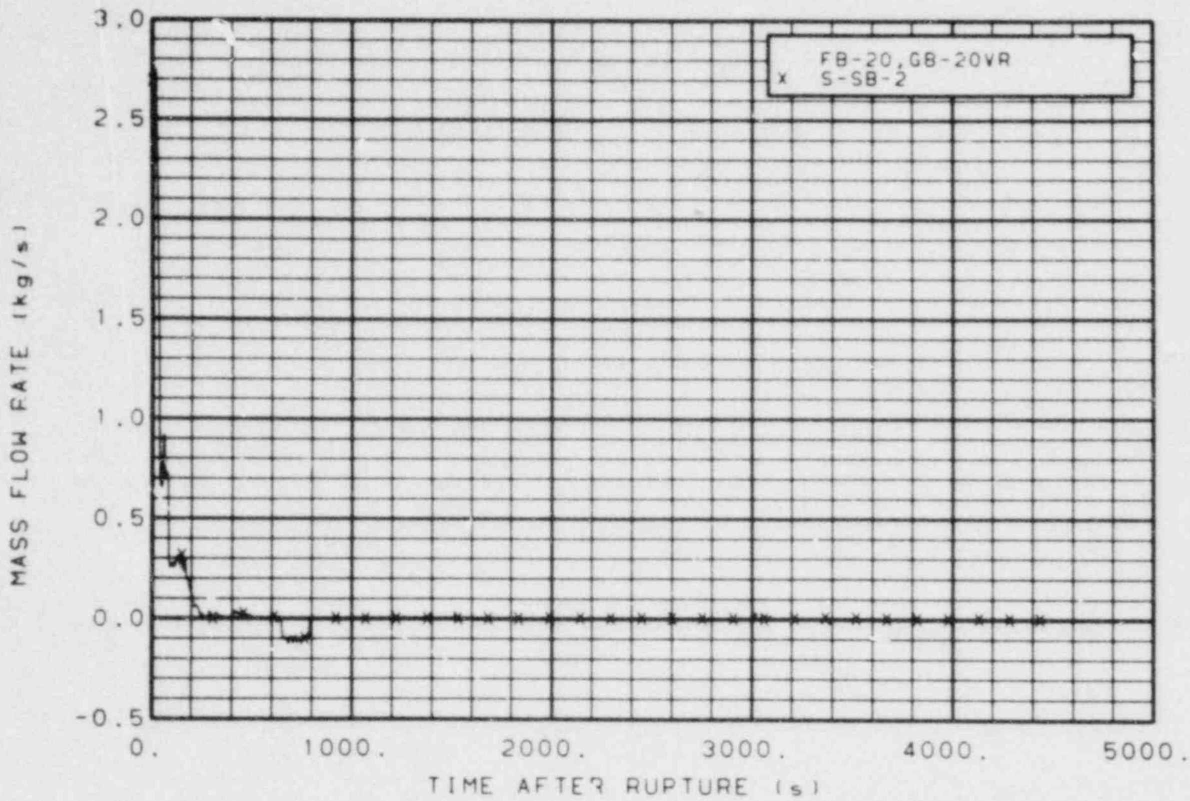

Figure 371. Mass Flow in intact loop hot leg, Test S-SB-2 (FB-20 and GB-20VR), from 0 to 4500 s.

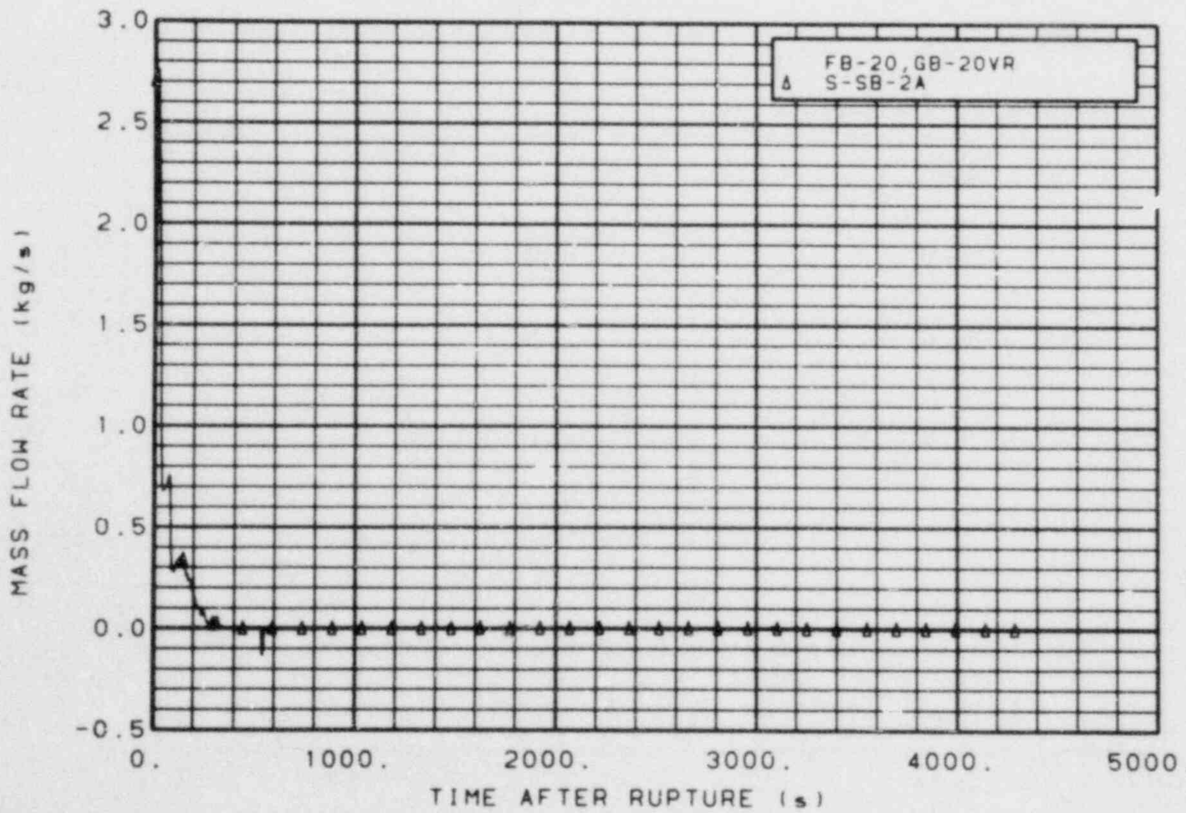

Figure 372. Mass Flow in intact loop hot leg, Test S-SB-2A (FB-20 and GB-20VR), from 0 to 4390 s.

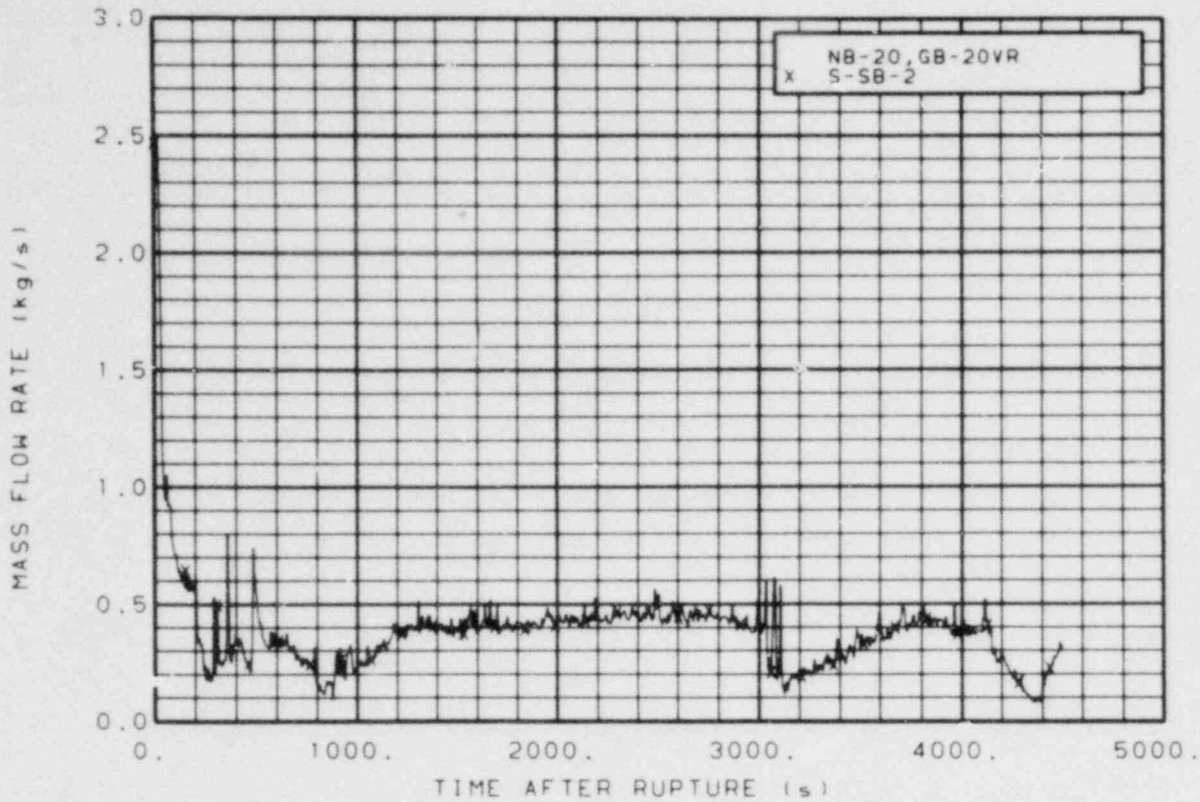

Figure 373. Mass Flow in intact loop hot leg, Test S-SB-2 (NB-20 and GB-20VR), from 0 to 4500 s.

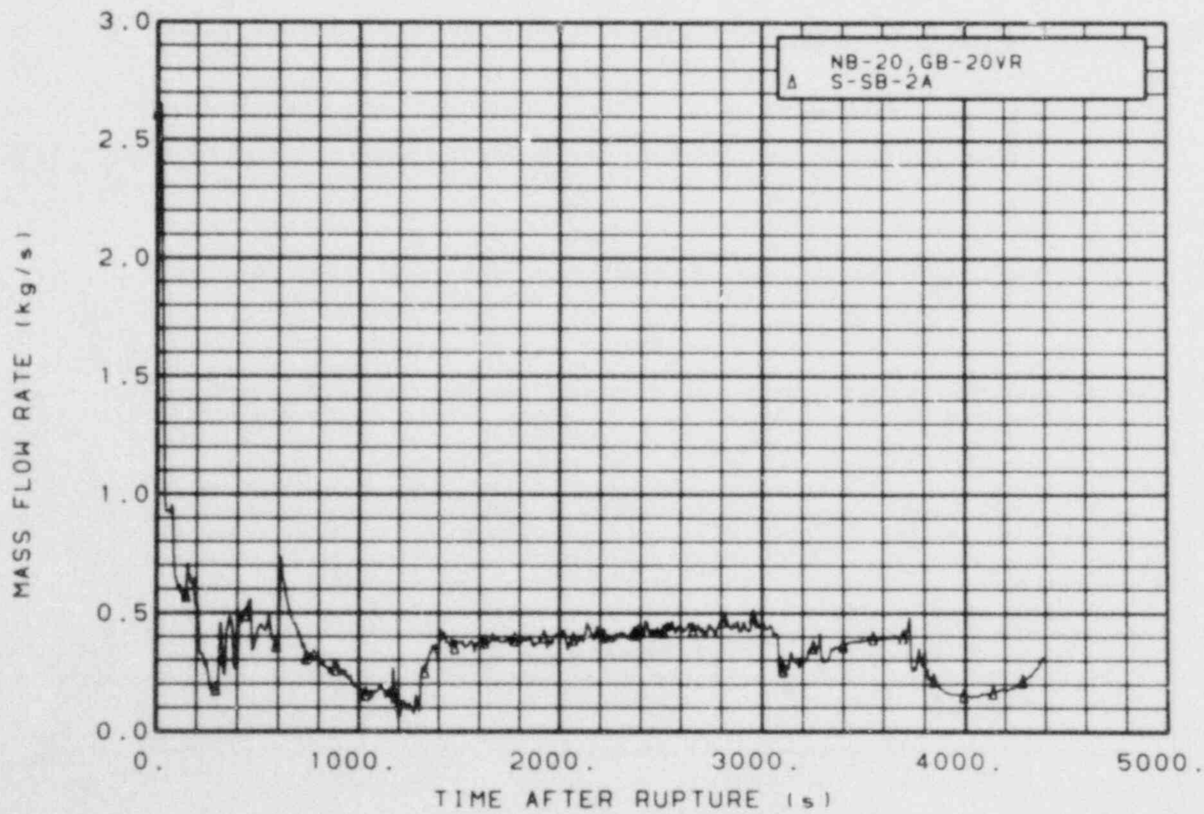

Figure 374. Mass Flow in intact loop hot leg, Test S-SB-2A (NB-20 and GB-20VR), from 0 to 4390 s.

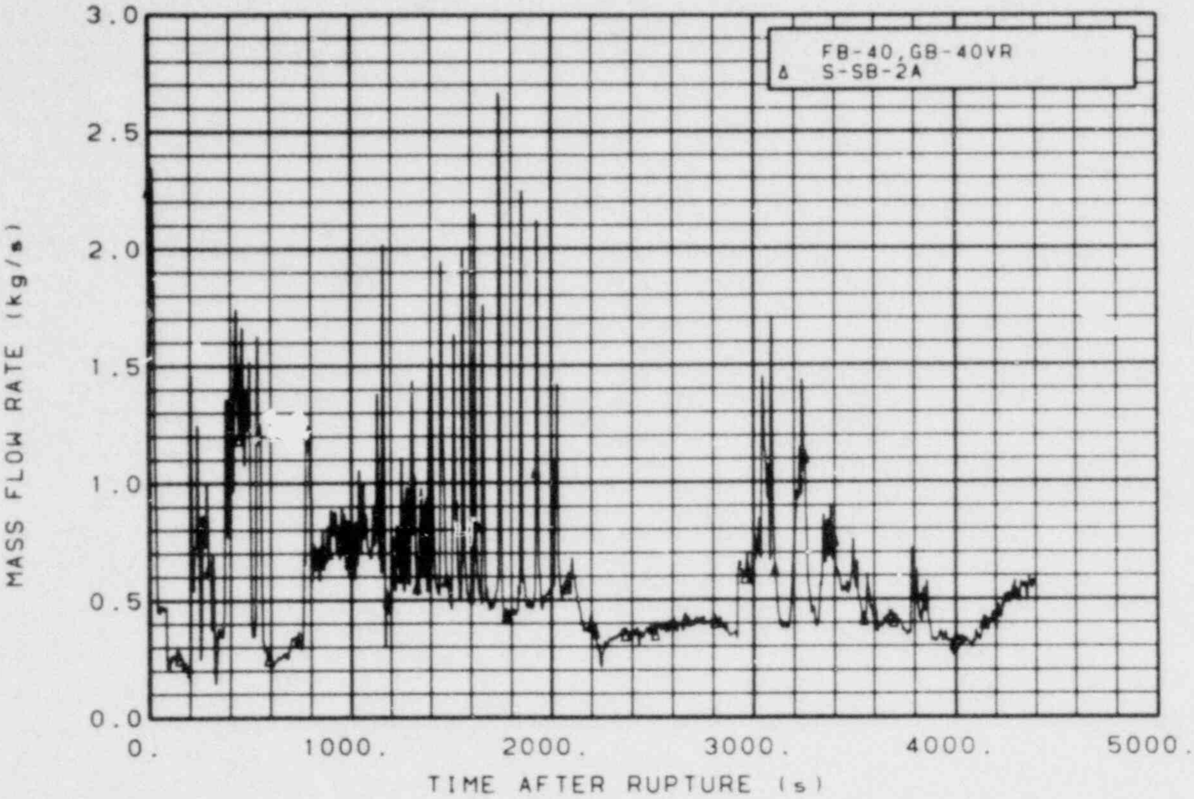

Figure 375. Mass Flow in broken loop cold leg, Test S-SB-2A (FB-40 and GB-40VR), from 0 to 4390 s.

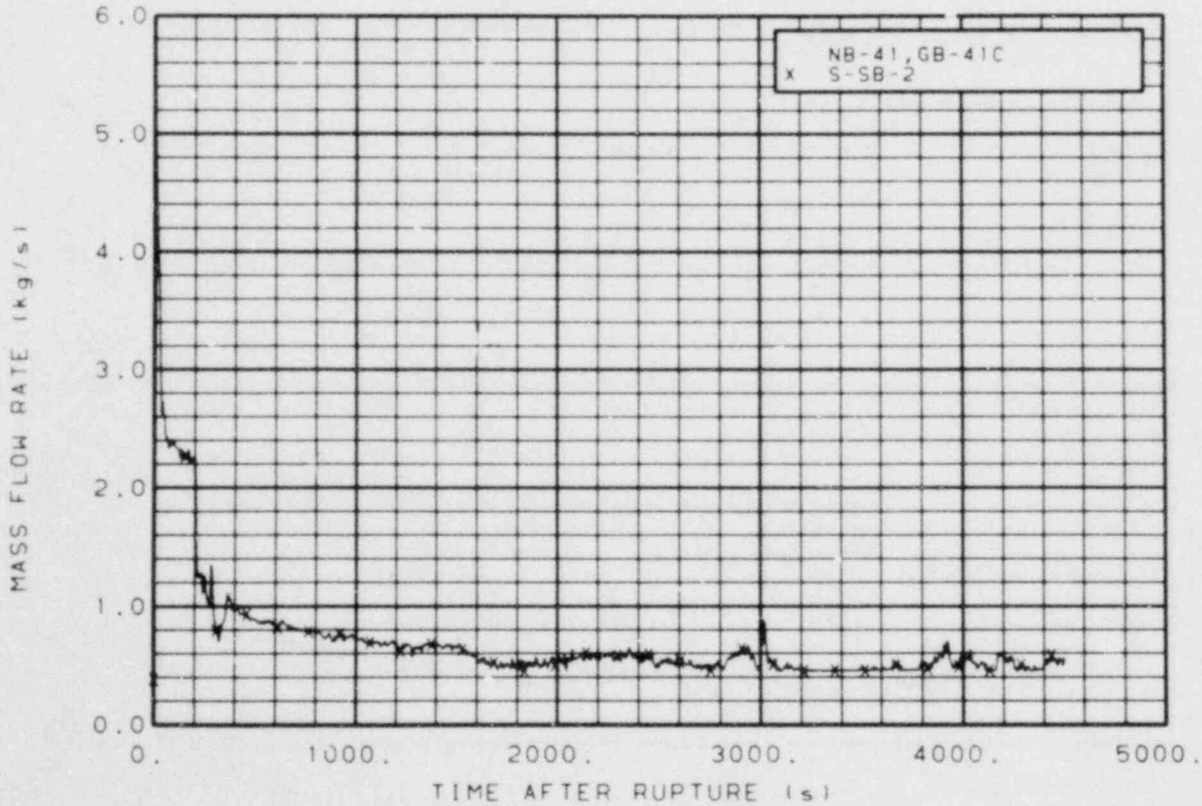

Figure 376. Mass Flow in broken loop cold leg, Test S-SB-2 (NB-41 and GB-41C), from 0 to 4500 s.

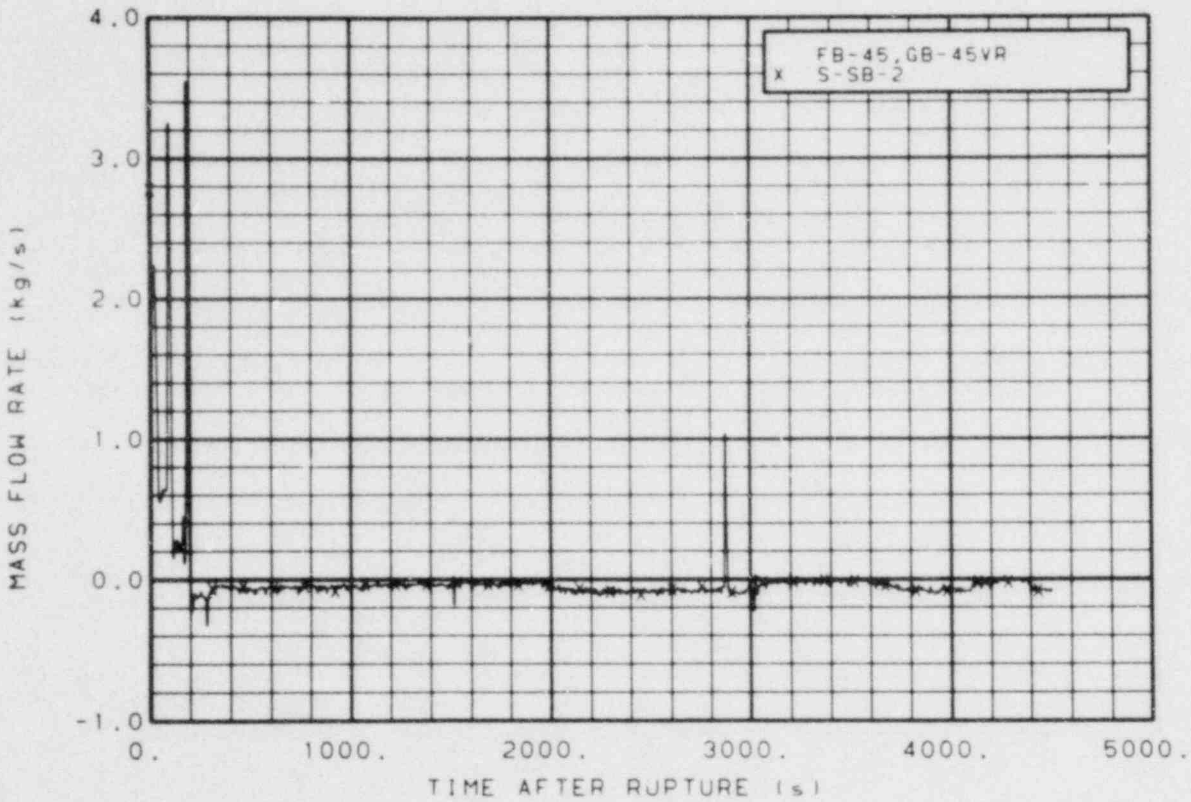

Figure 377. Mass Flow in broken loop c ld leg, Test S-SB-2 (FB-45 and GB-45VR), from 0 to 4500 s.

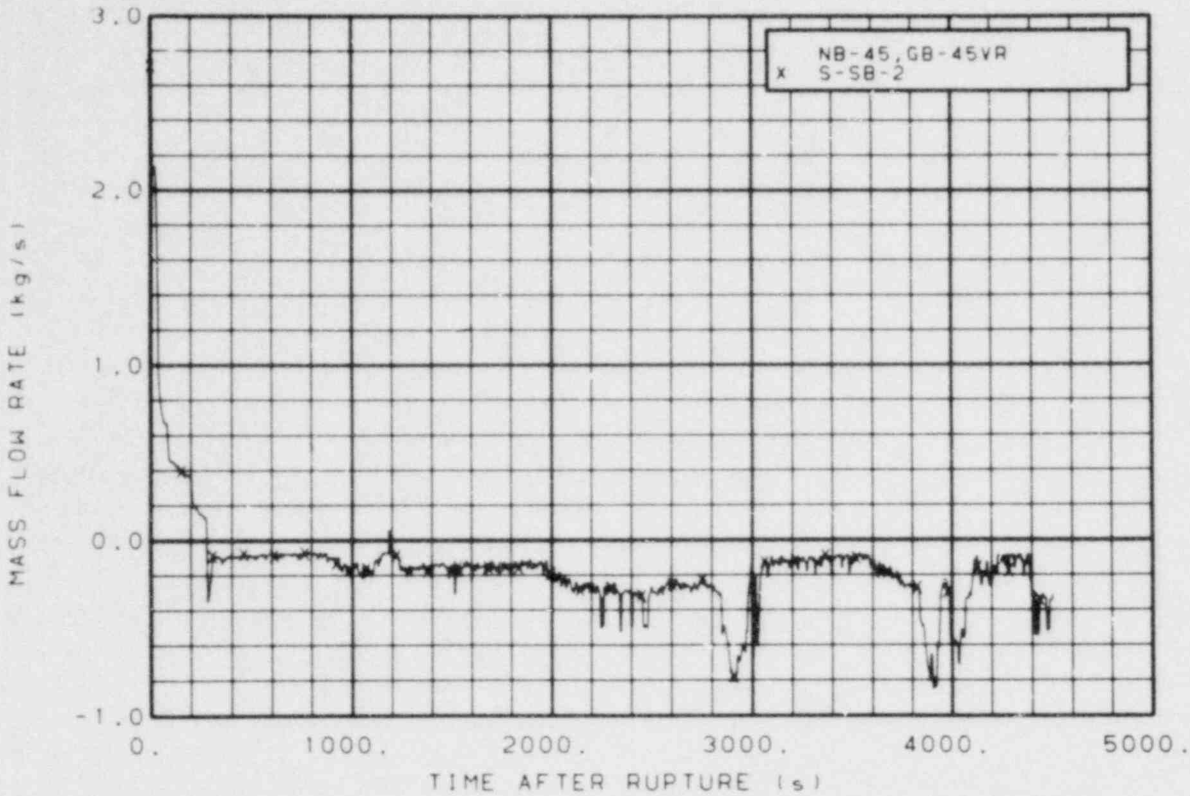

Figure 378. Mass Flow in broken loop cold leg, Test S-SB-2 (NB-45 and GB-45VR), from 0 to 4500 s.

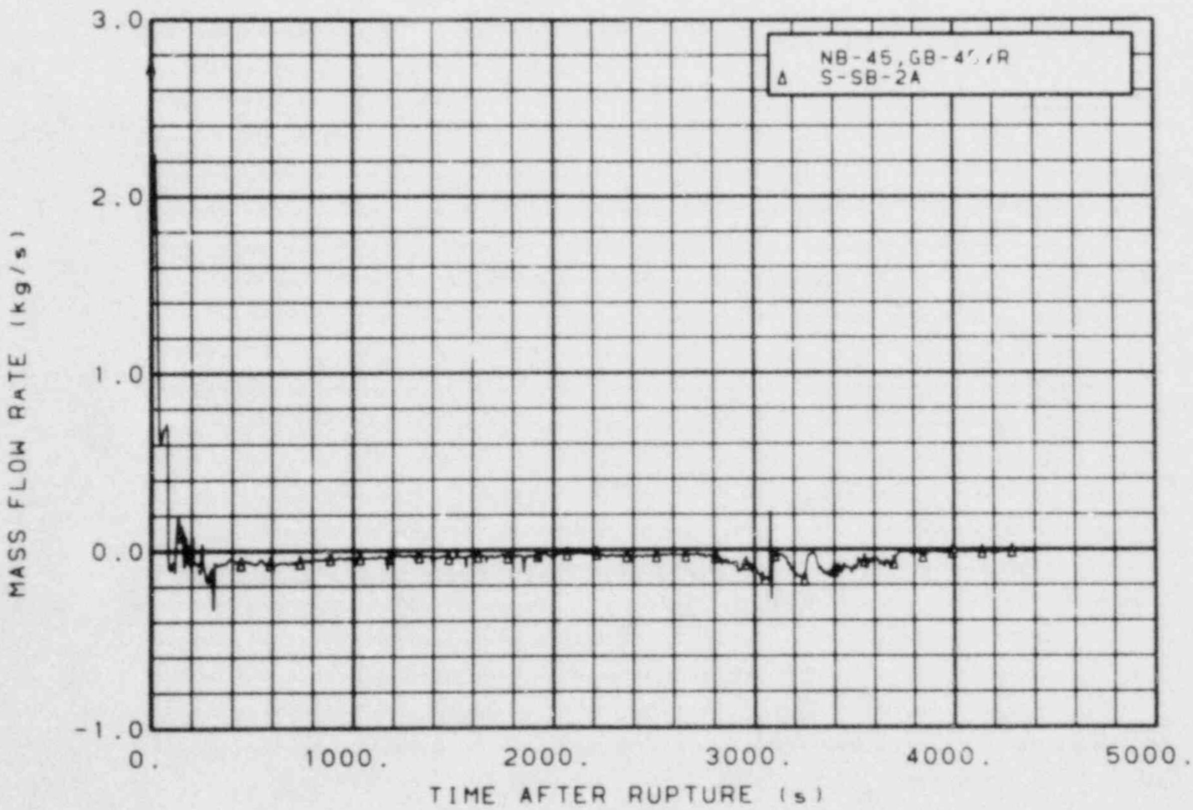

Figure 379. Mass Flow in broken loop cold leg, Test S-SB-2A (NB-45 and GB-45VR), from 0 to 4390 s.

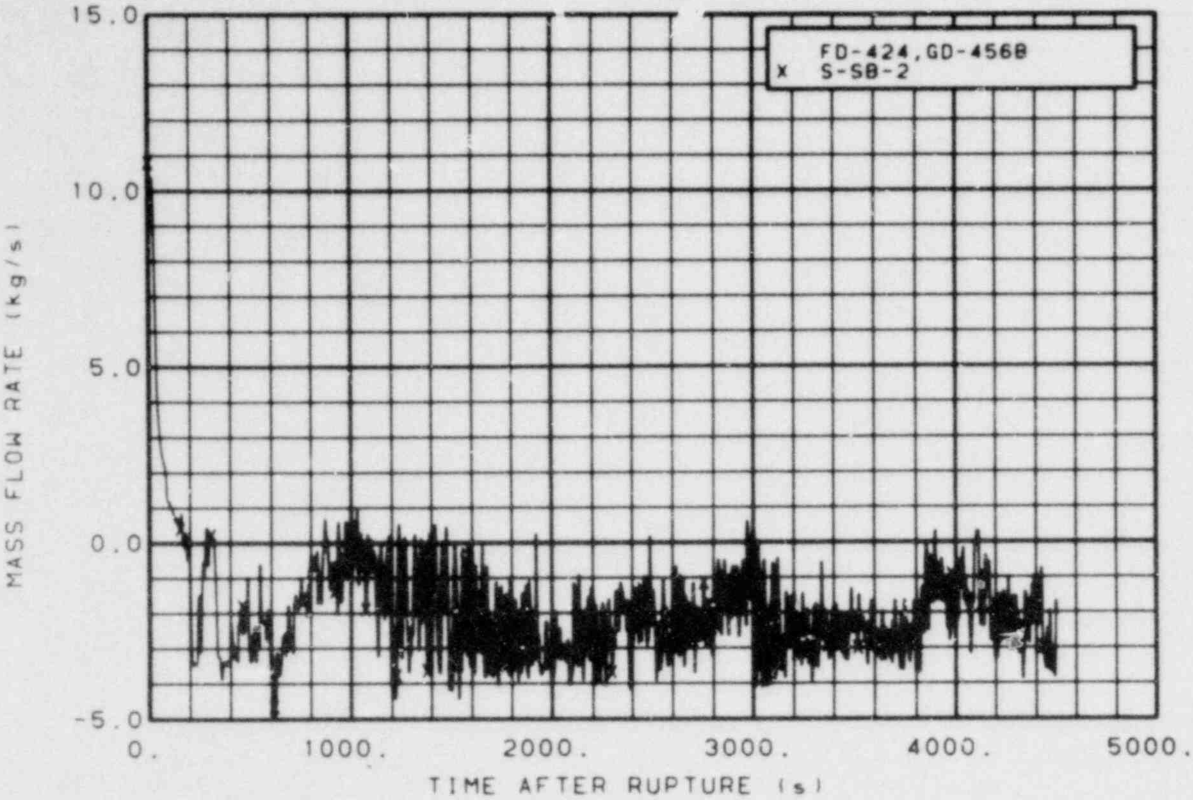

Figure 380. Mass Flow in downcomer, Test S-SB-2 (FD-424 and GD-456B), from 0 to 4500 s.

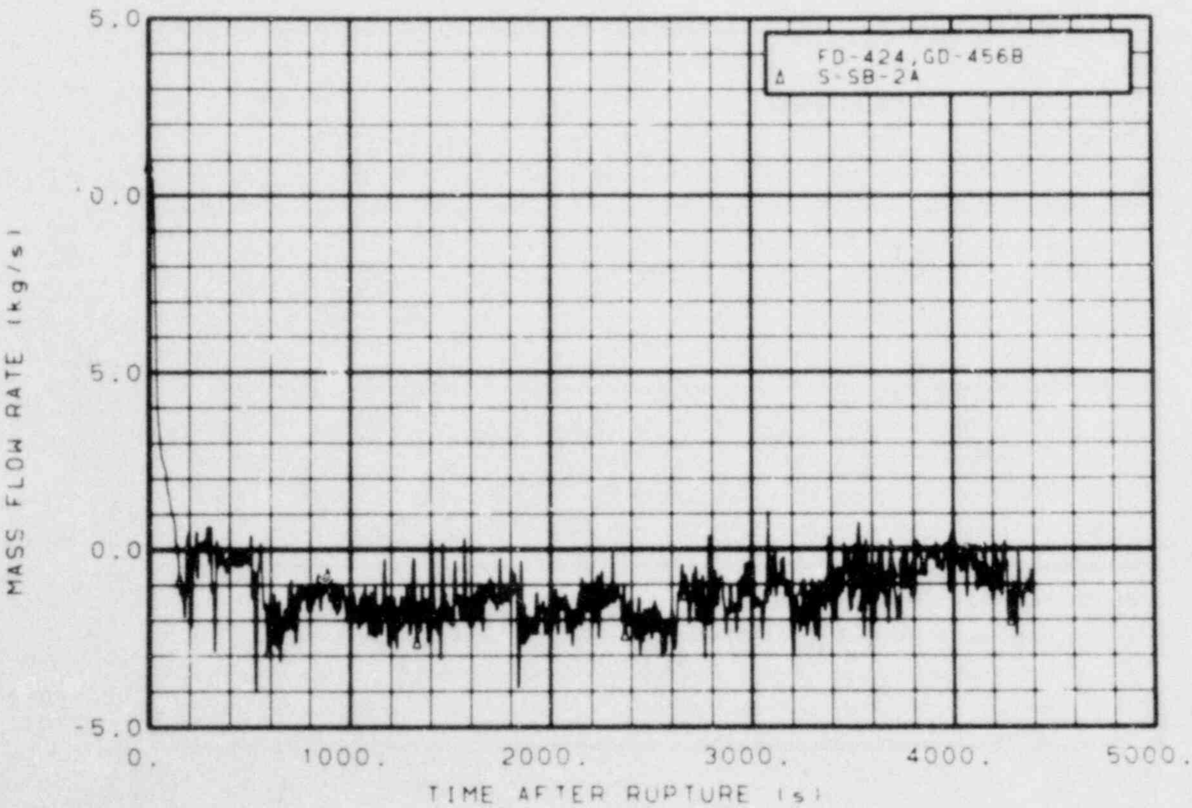

Figure 381. Mass Flow in downcomer, Test S-SB-2A (FD-424 and GD-456B), from 0 to 4390 s.

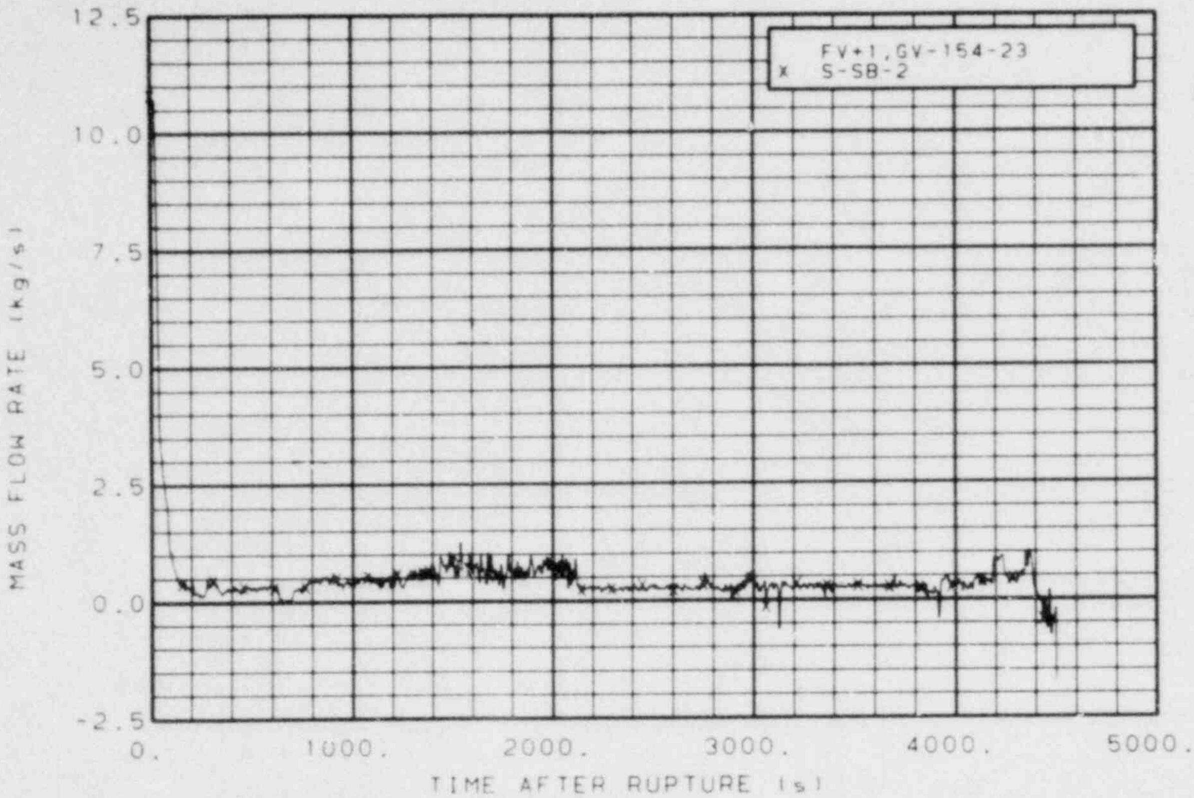

Figure 382. Mass Flow in vessel, Test S-SB-2 (FV + 1 and GV -154-23), from 0 to 4500 s.

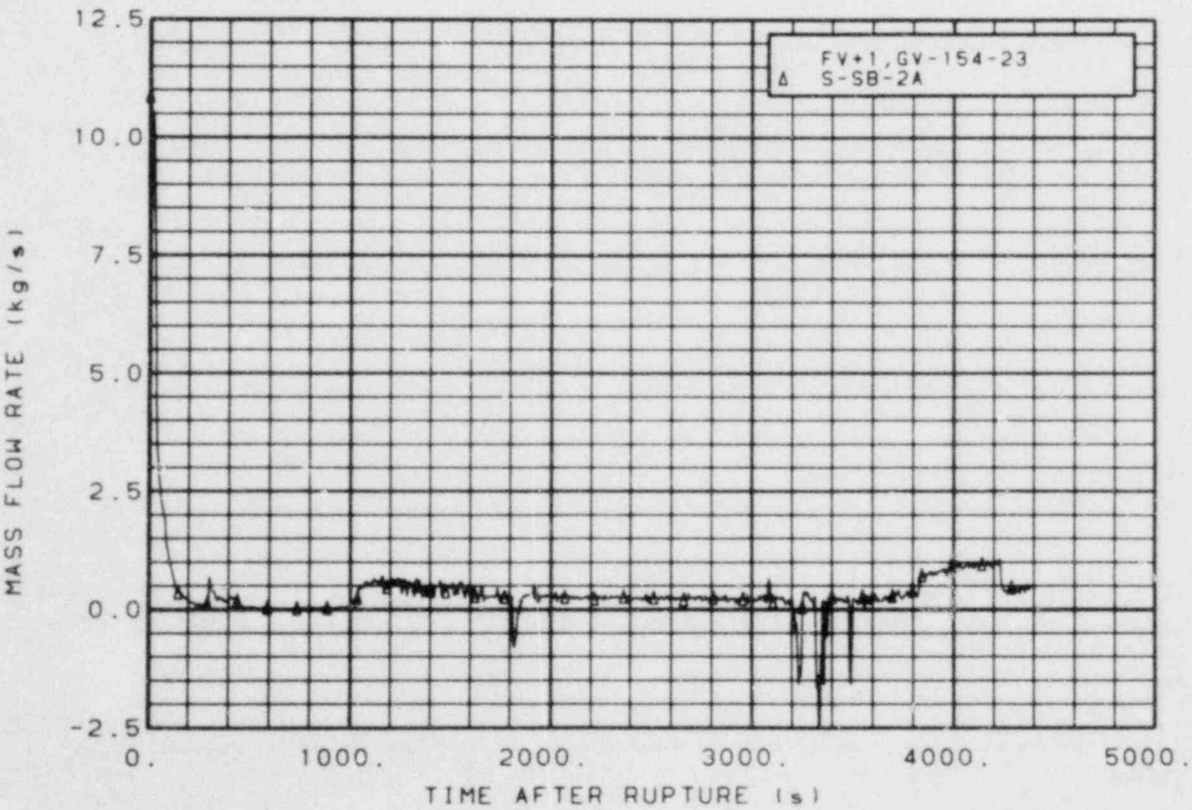

Figure 383. Mass Flow in vessel, Test S-SB-2A (FV + 1 and GV -154-23), from 0 to 4390 s.

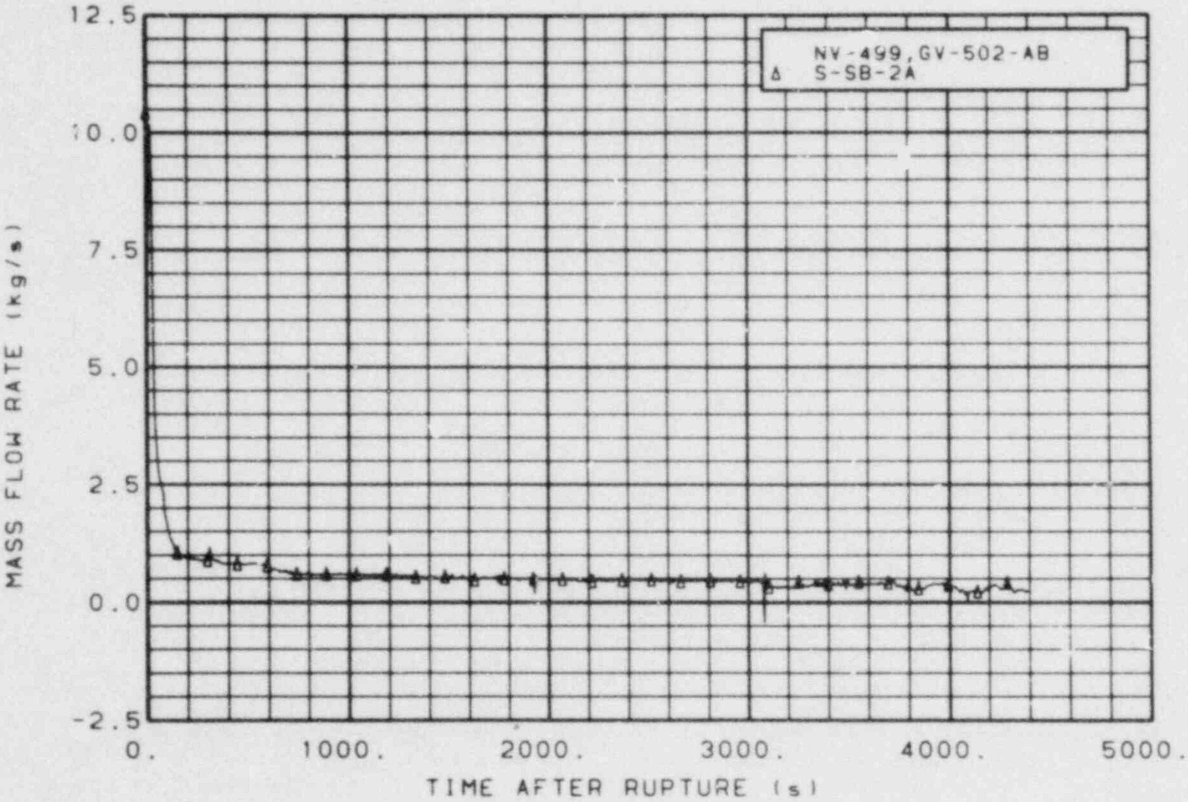

Figure 384. Mass Flow in vessel, Test S-SB-2A (NV-499 and GV-502-AB), from 0 to 4390 s.

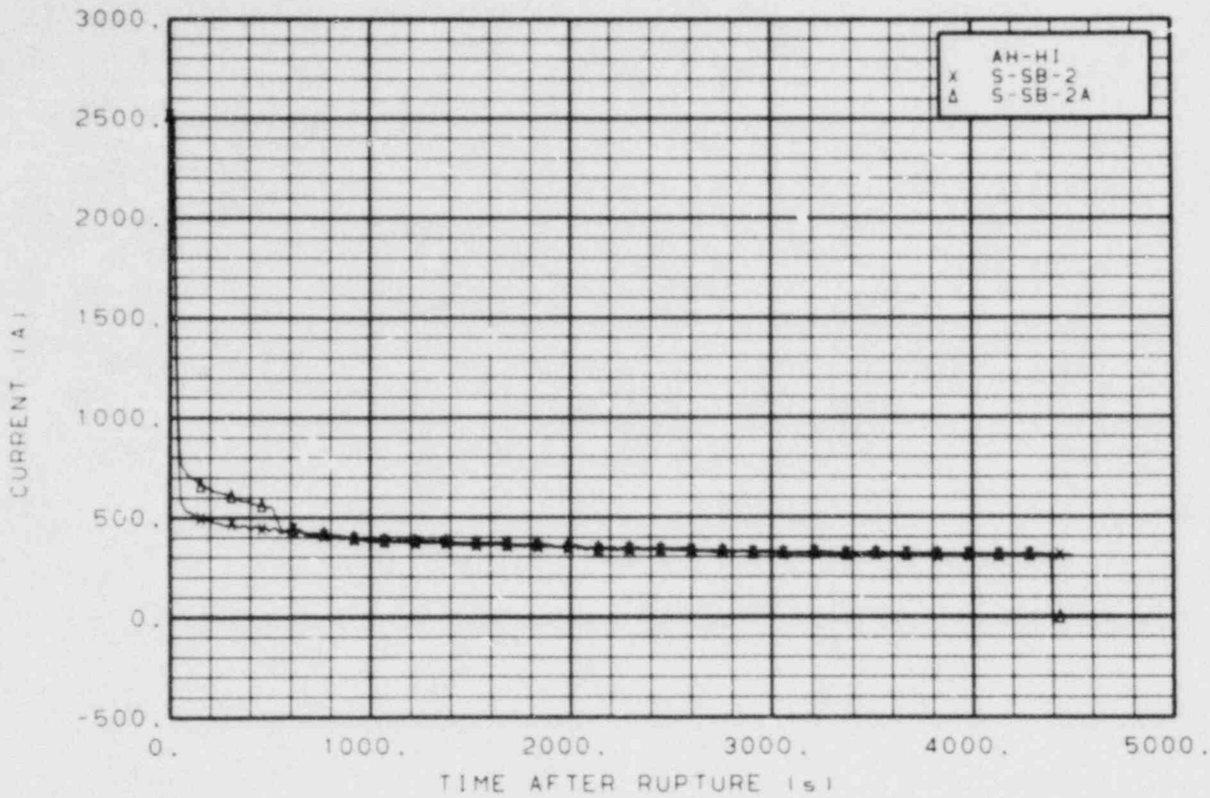

Figure 385. Core heater high power bus amperage (AH-HI), from 0 to 4500 s.

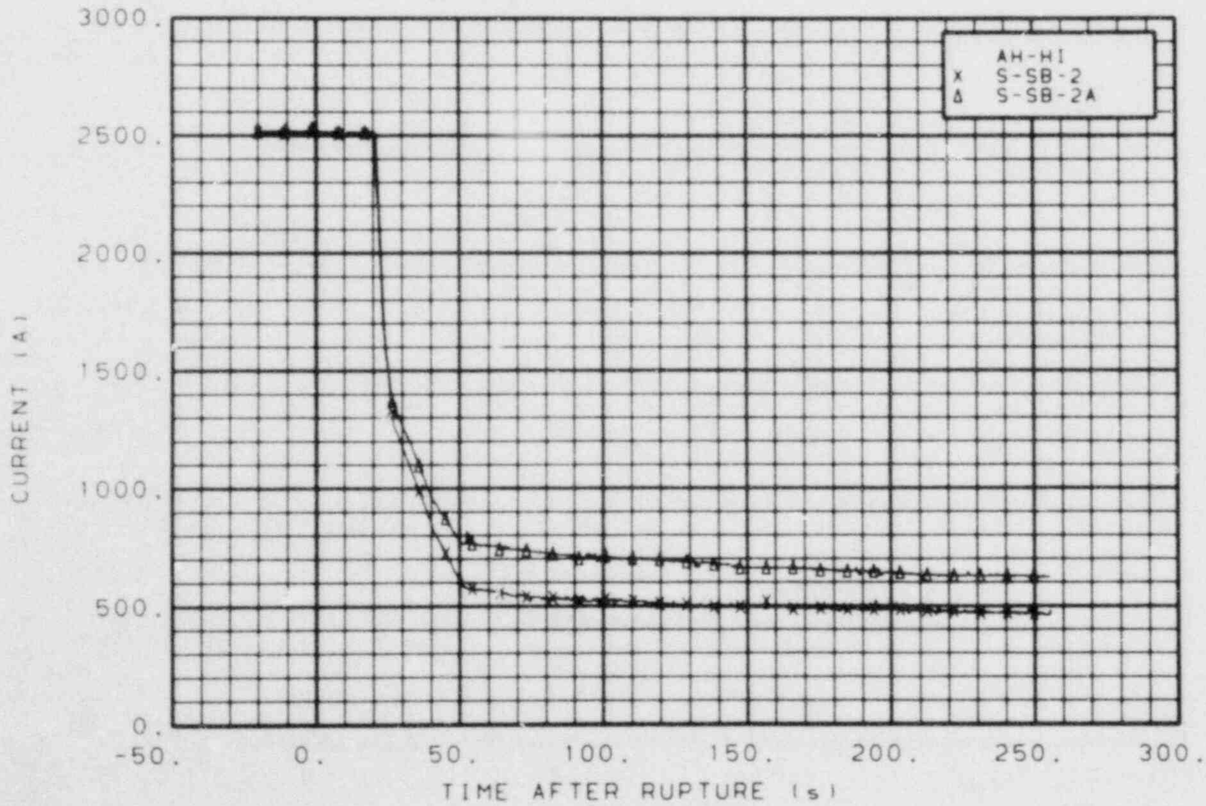

Figure 386. Core heater high power bus amperage (AH-HI), from -20 to 256 s.

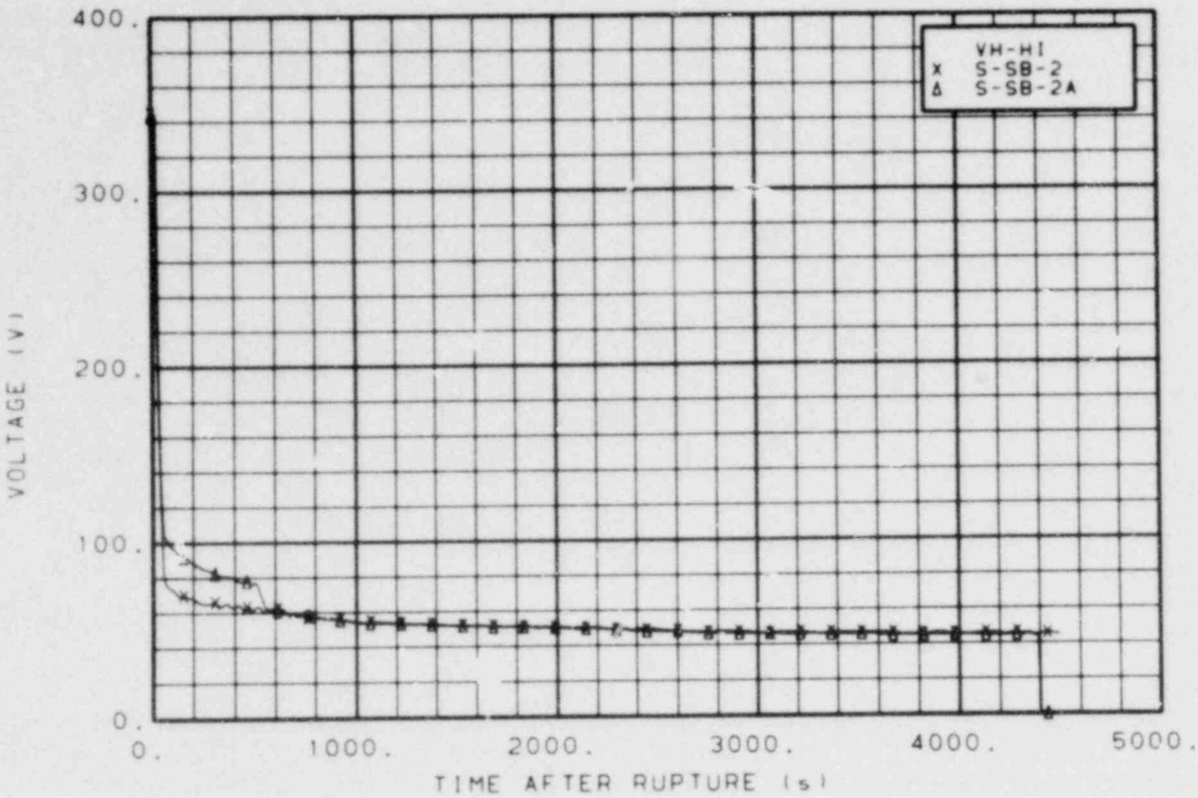

Figure 387. Core heater high power bus voltage (VH-HI), from 0 to 4500 s.

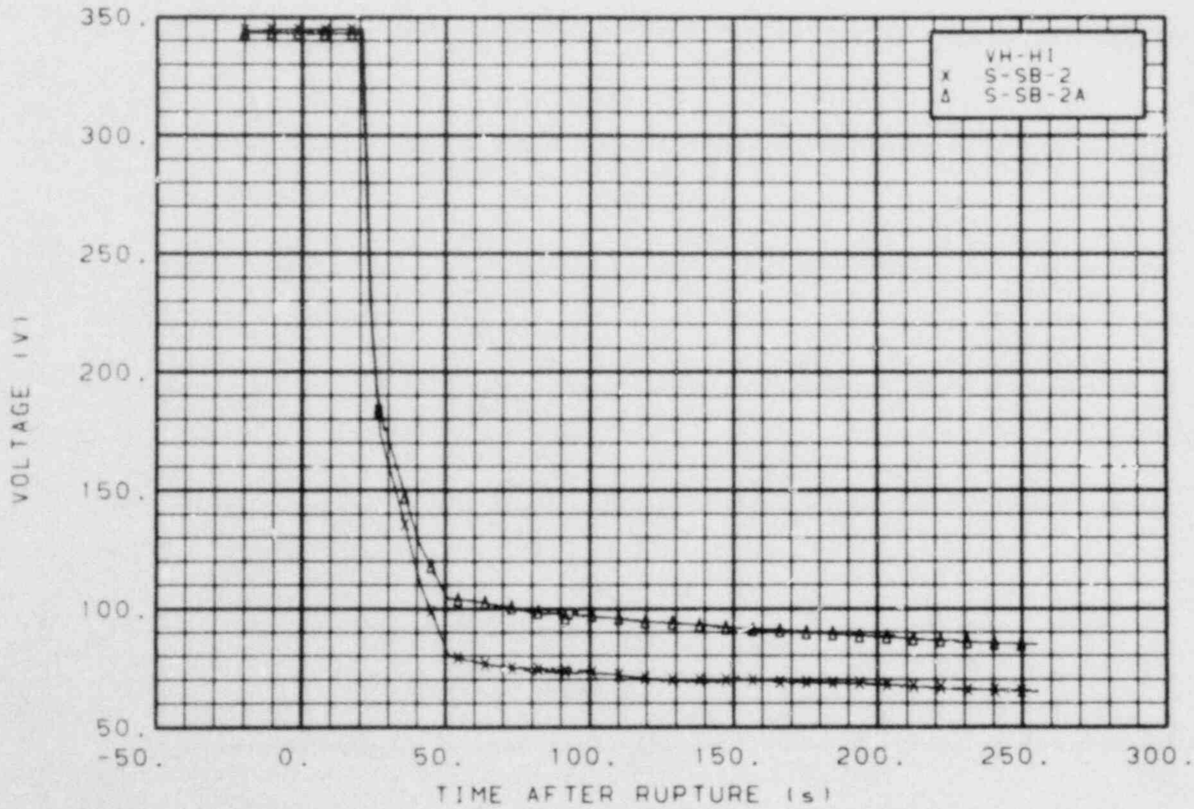

Figure 388. Core heater high power bus voltage (VH-HI), from -20 to 256 s.

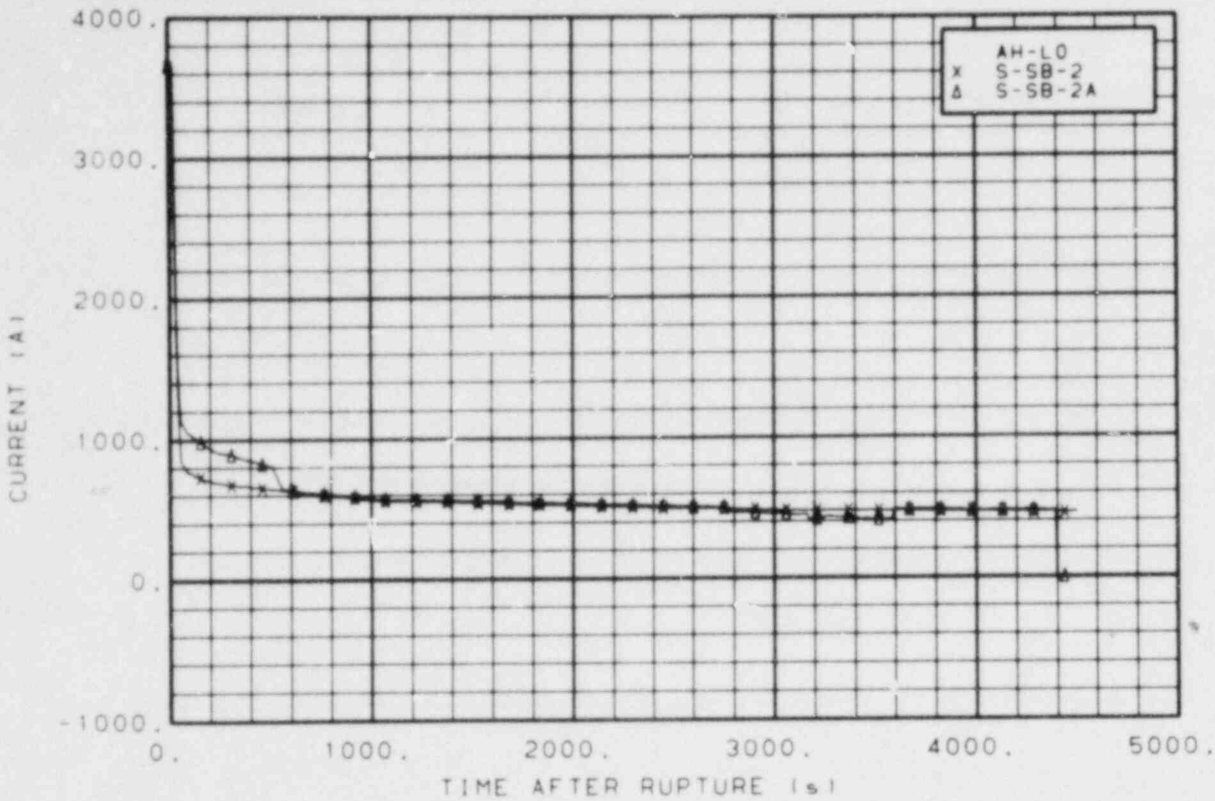

Figure 389. Core heater low power bus amperage (AH-LO), from 0 to 4500 s.

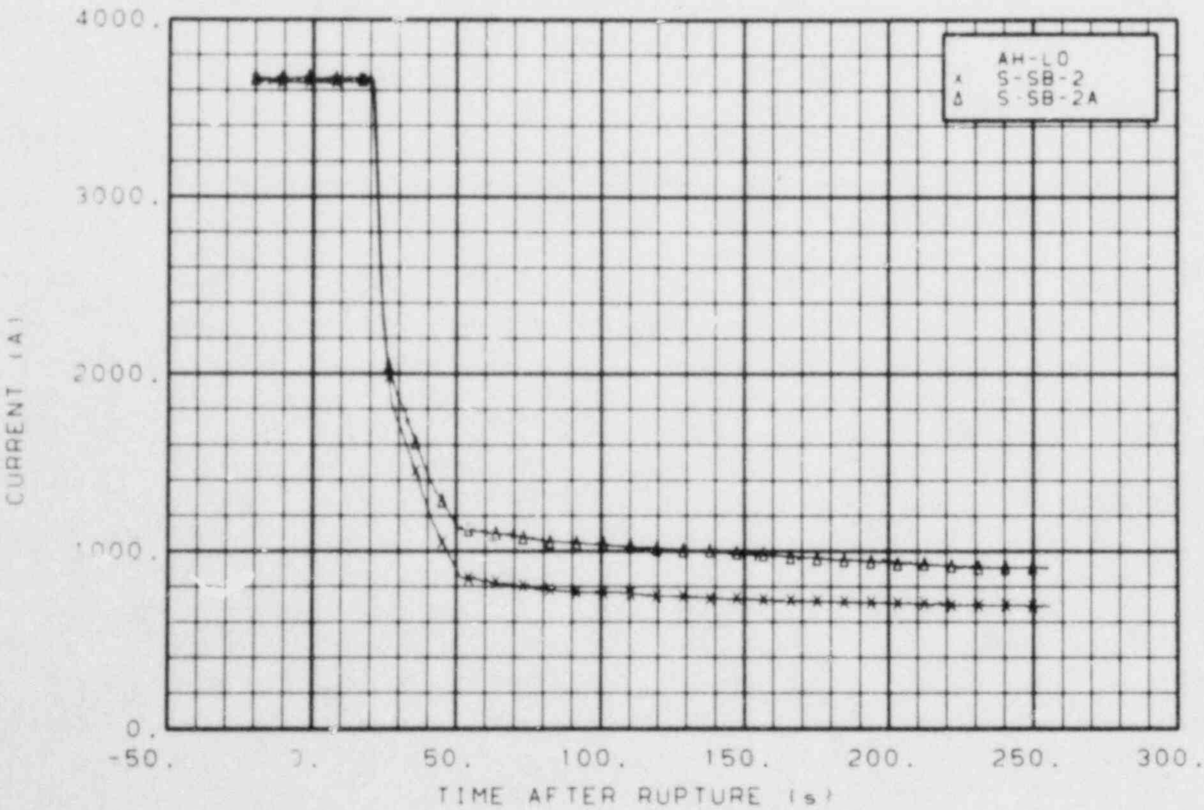

Figure 390. Core heater low power bus amperage (AH-LO), from-20 to 256 s.

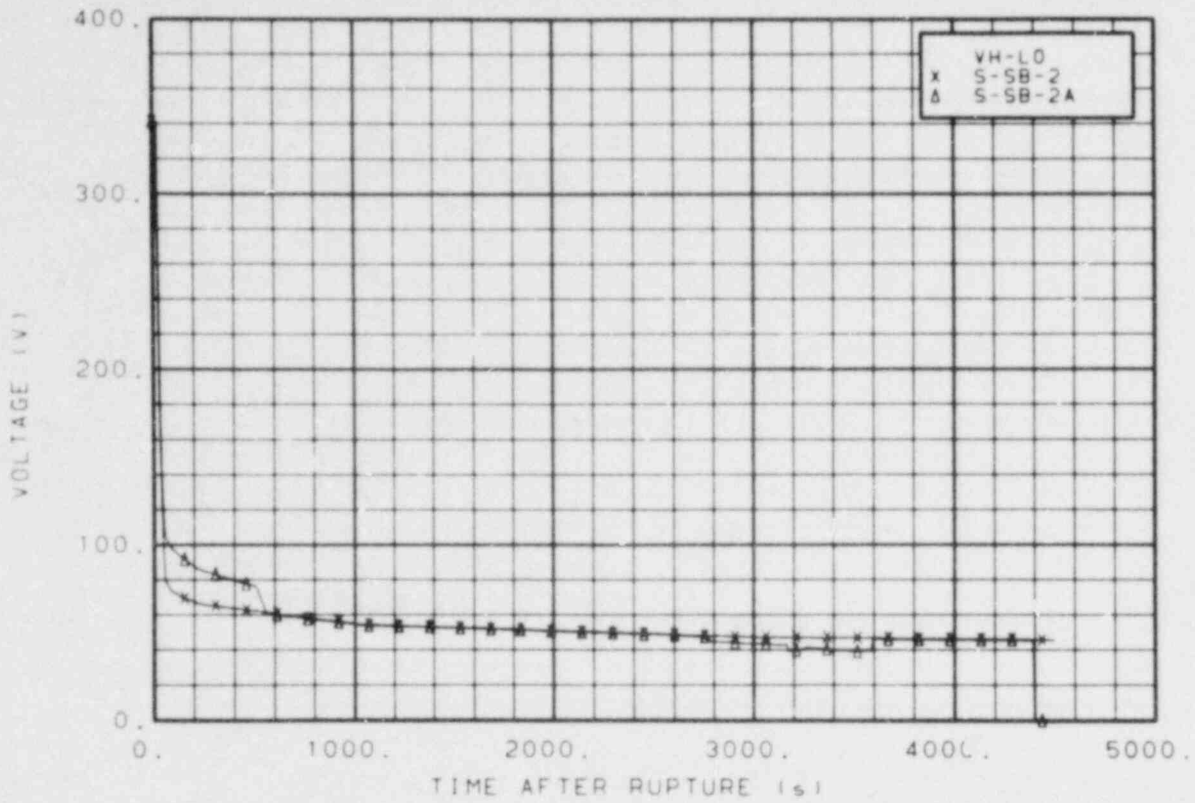

Figure 391. Core heater low power bus voltage (VH-LO), from 0 to 4500 s.

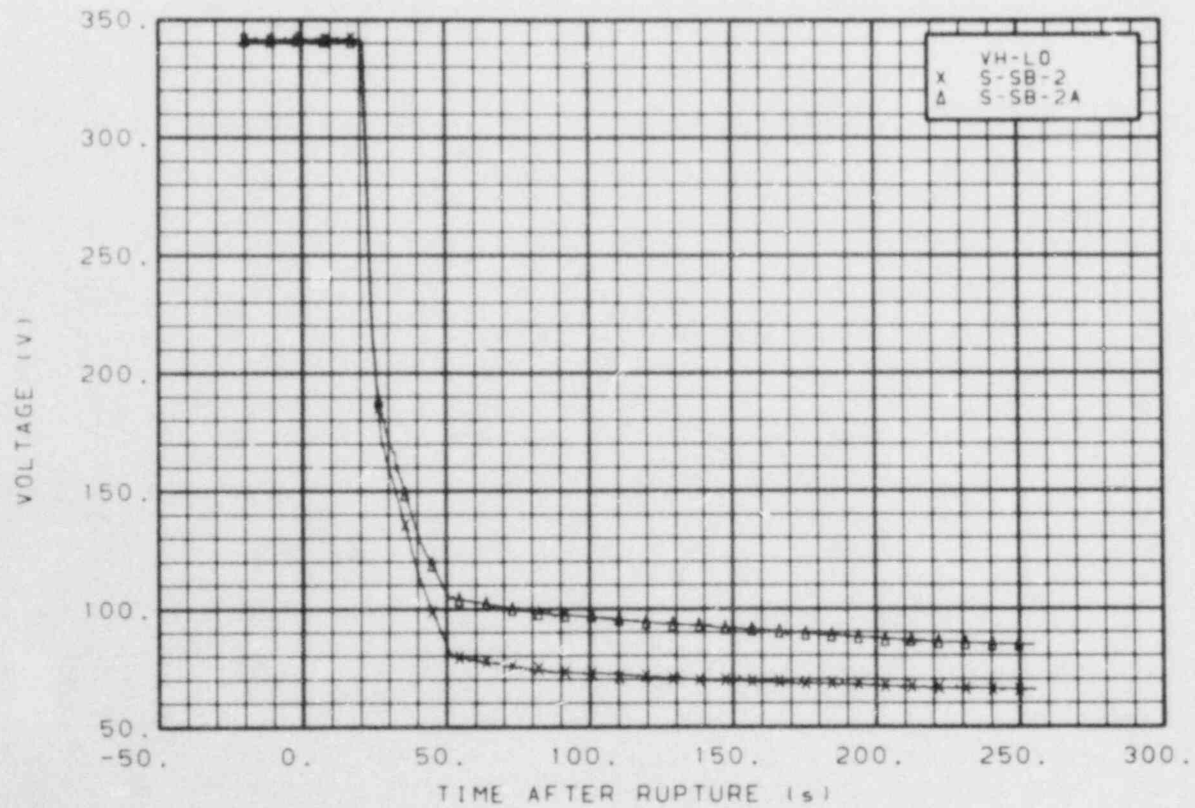

Figure 392. Core heater low power bus voltage (VH-LO), from -20 to 256 s.

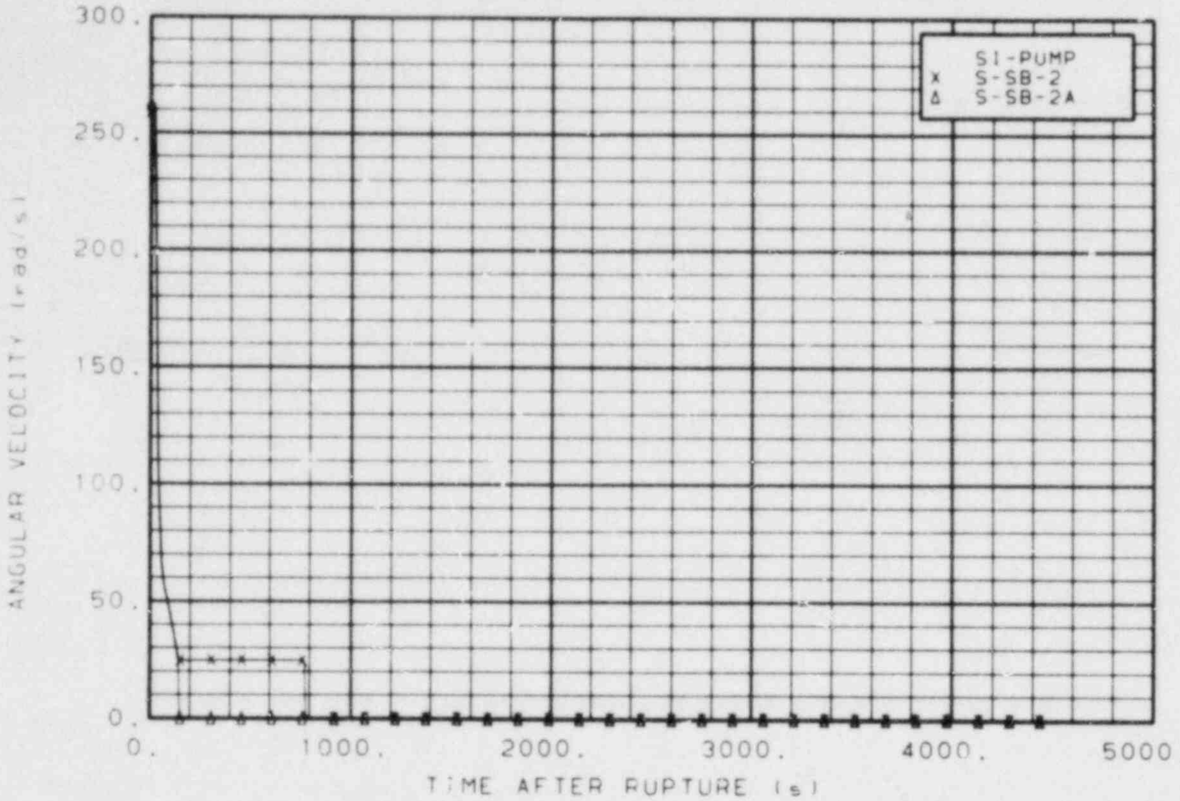

Figure 393. Intact loop pump speed (SI-PUMP), from 0 to 4500 s.

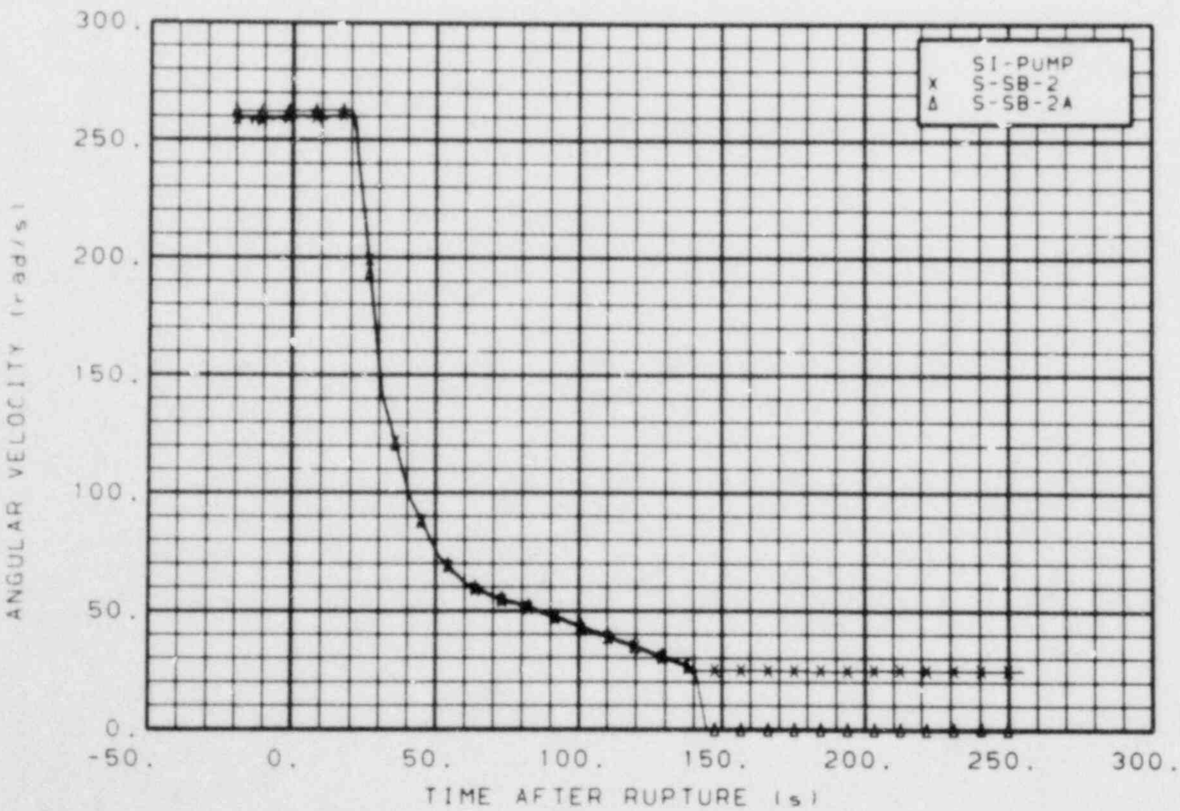

Figure 394. Intact loop pump speed (SI-PUMP), from -20 to 256 s.

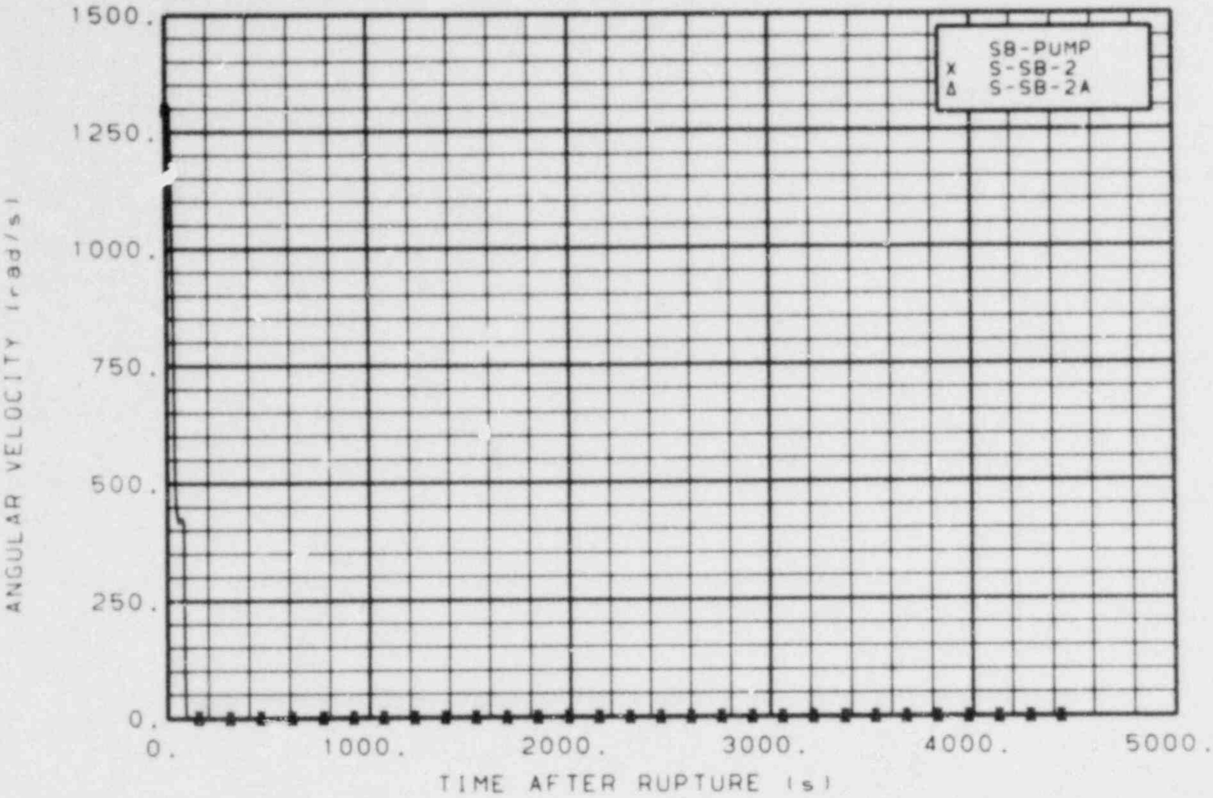

Figure 395. Broken loop pump speed (SB-PUMP), from 0 to 4500 s.

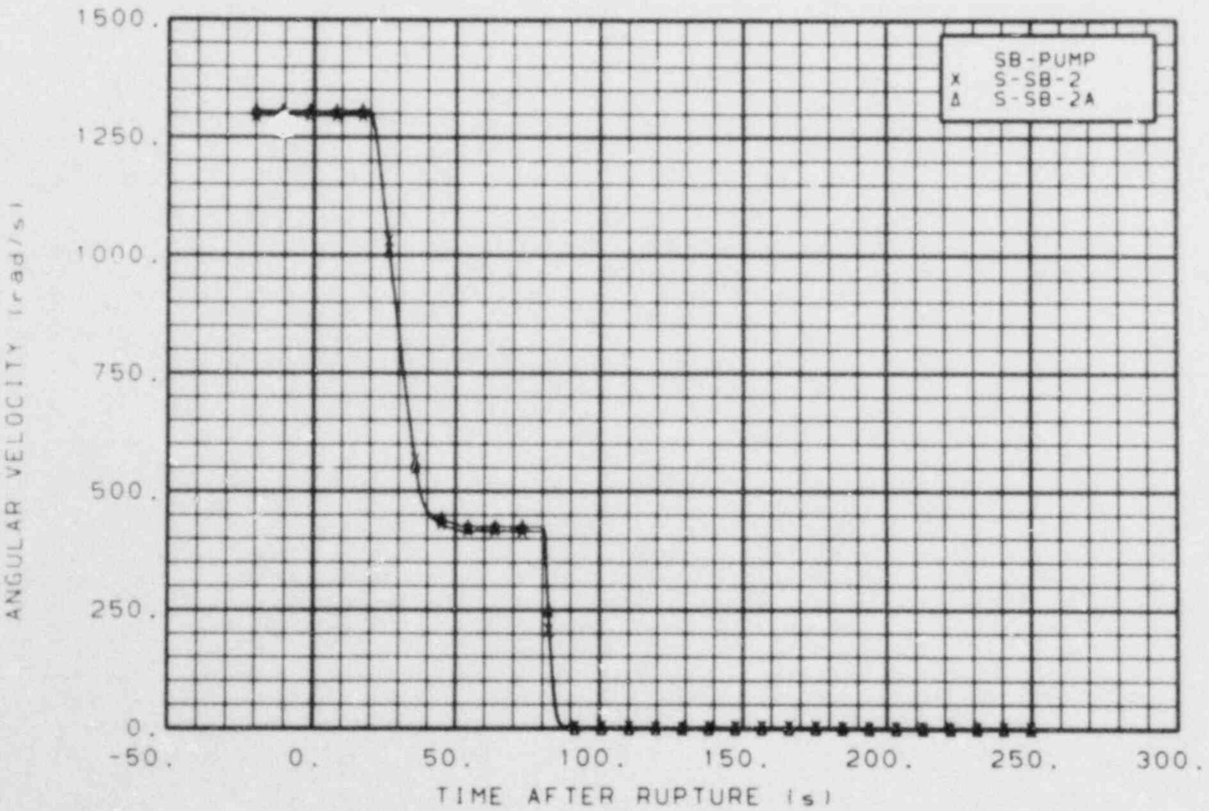

Figure 396. Broken loop pump speed (S.. . UMP), from -20 to 256 s.

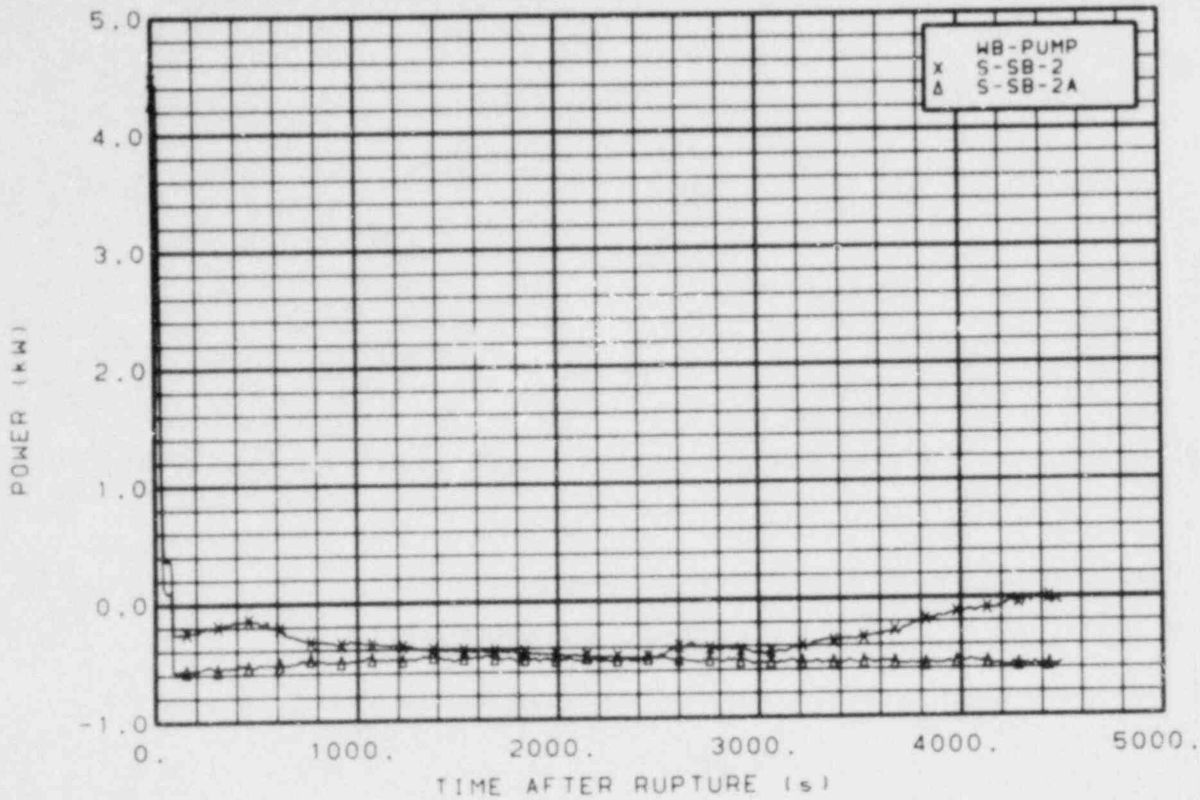

Figure 397. Broken loop pump power (WB-PUMP), from 0 to 4500 s.

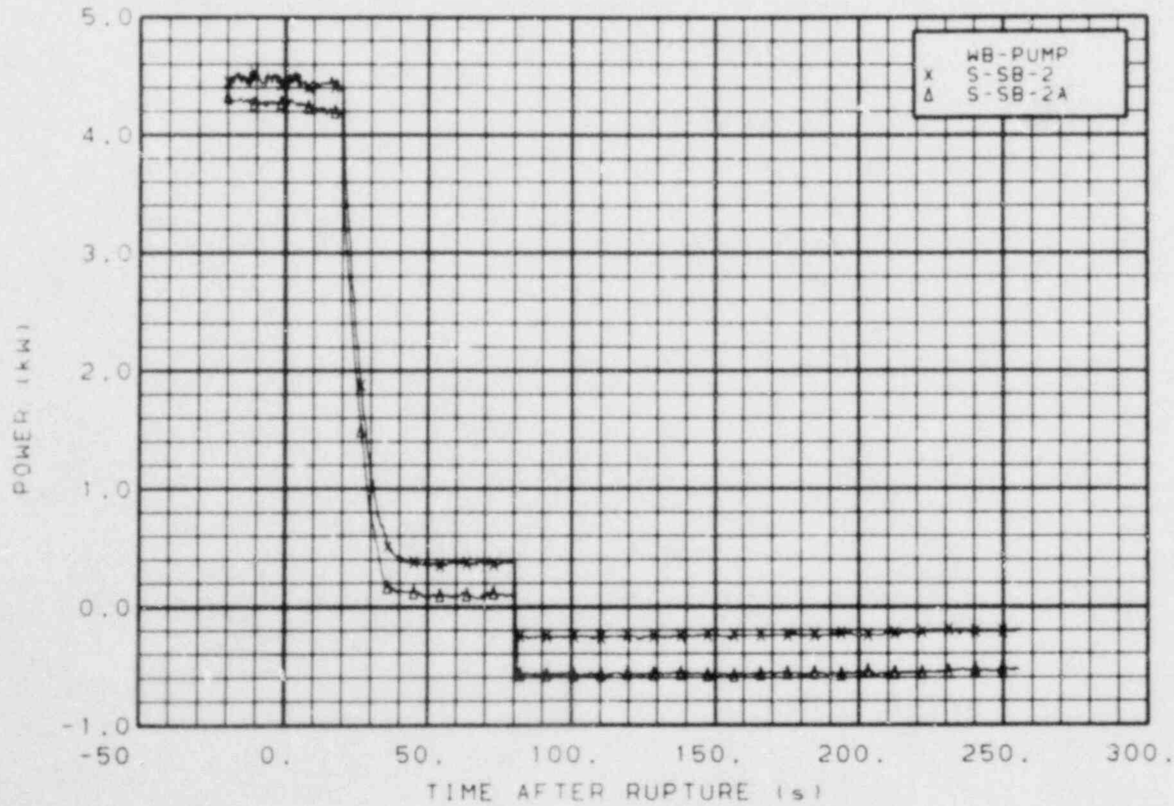

Figure 398. Broken loop pump power (WB-PUMP), from -20 to 256 s.

IV. REFERENCES

1. L. J. Ball et al., *Semiscale Program Description*, TREE-NUREG-1210, May 1978.

2. M. L. Patton, *Semiscale Mod-3 Test Program and System Description*, NUREG/CR-0239, TREE-NUREG-1212, July 1978.

APPENDIX A

DATA ACQUISITION SYSTEM CAPABILITIES

APPENDIX A

DATA ACQUISITION SYSTEM CAPABILITIES

The Semiscale Mod-3 system provides for the acquiring, processing, and presenting of test data. The test data system comprises detectors, signal conditioners, signal processors, and recording and display equipment. The data obtained are principally recorded on an on-line digital system.

The on-line digital system is called the digital data acquisition and processing system (DDAPS). There are two separate DDAPS providing capability for 240 channels on DDAPS I and 120 channels on DDAPS II. Both systems comprise the following hardware:

- A central processing unit computer
- A 256 channel multiplexer and a 12 bit analog-to-digital convertor
- A five megaword, moving head, disk unit
- A digital, nine track 800 bit per inch, magnetic tape unit
- A cathode-ray-tube terminal with a hard copy unit for subsystem control and for graphics and alphanumeric data output.

These DDAPS have dual and single speed capabilities with identical storage and data output limitations. The dual speed mode provides the capability of extending the recording time during a test. The maximum measured throughput rate for the system is 24 000 words per second. This throughput rate can be reduced in increments of 100 words per second. The throughput rate, the number of data channels recorded, and the fixed display of 920 points per graph determine the time base for displaying the data.

After the data have been stored, data reduction can be made for presentation and analysis purposes. Because of hardware limitations and aesthetic considerations of data presentation, only certain time bases are used when the data are reduced. For data displayed from 0 to 4500 s, the recorded data are made to occupy a 4500 s span with an uncompressed time base of 276 s.

Generally, 920 points from a given data channel are displayed in the nominal time base of 276 s. Integral (1 to 20) multiples of 276 s may be used as variations on the nominal time base. Because the output is fixed at 920 points, data compression is accomplished by averaging adjacent data points to give the desired compression.

APPENDIX B

POSTTEST ADJUSTMENTS TO DATA FROM SEMISCALE MOD-3 TESTS S-SB-2 AND S-SB-2A

APPENDIX B

POSTTEST ADJUSTMENTS TO DATA FROM SEMISCALE MOD-3 TESTS S-SB-2 AND S-SB-2A

Many of the transducers used in the Semiscale Mod-3 system exhibit significant sensitivity to one or more spurious inputs. Strain gage bridge circuits used in pressure transducers, differential pressure transducers, and drag discs are sensitive to changes in ambient temperature. Differential pressure cells are also sensitive to changes in system pressure. Photomultiplier tubes used as gamma-ray detectors in the density transducers are sensitive to temperature changes, as well as to random variations in the locations of the radiation sources. Core power measurements depend on a calibrated resistor, whose resistance changes in value as a function of time and power level as it heats up.

Although the uncertainties introduced into the data by spurious secondary inputs generally do not exceed the specified uncertainty ranges of the transducers, significant improvement in measurement accuracy can be achieved if the secondary sensitivity can be identified and removed. Since the exact values of the spurious inputs to which different transducers might be sensitive cannot often be easily predicted and are sometimes inconvenient to measure, secondary effects have been accounted for by correcting the data after the test rather than by using elaborate real time programs in the data acquisition system computer. The methods and results of the posttest data correction analysis for Tests S-SB-2 and S-SB-2A are presented in the following paragraphs and tables.

Differential Pressure Measurements

Pressure sensitivity in the differential pressure cells in the main system loop is determined from the pretest system pressure check. Digital data are recorded for all measurements at ambient temperature, with no flow, and a continually increasing system pressure from 0.7 to 15.5 MPa. The output of the differential pressure cell is plotted against system pressure, with the resulting plots used to describe the pressure response of the transducer.

Corrections to differential pressure data were made using the following equation:

$$F'(t) = F(t) + P_1 P(t) \quad \text{(B-1)}$$

where

$F'(t)$ = corrected data, kPa

$F(t)$ = raw data (kPa)

P_1 = pressure sensitivity (kPa/MPa)

$P(t)$ = pressure data from indicated transducer used for pressure correction sensitivity (MPa).

Density Measurements

Density calculations are based on the voltage output of the photomultiplier tubes in gamma-attenuation densitometer assemblies. The equation used for converting voltage to density is as follows:

$$\rho = C_o + C_1 F(t) \quad \text{(B-2)}$$

where

ρ = the density (kg/m^3)

C_o = offset (kg/m^3)

C_1 = conversion factor (kg/m^3)/v

$F(t)$ = transducer output (v).

Constants C_o and C_1 are adjusted to match the final data to density values calculated from measured pressure and temperature values at the preblowdown and postdrain conditions, effectively giving the data an in-place calibration. These calculations are made in the Mod-3 system prior to initial data release and are not considered posttest adjustments.

Some density measurements are obtained using a two-beam gamma densitometer which operates on the same basic principle of gamma attenuation as does the single-beam gamma densitometer. Each beam originates from the same gamma source and is allowed to pass through separate portions of the piping cross-sectional flow area to obtain an average density measurement in that particular region. The geometrical relationship of the gamma beam path through the piping and geometrically related variables used for processing of data from a two-beam gamma densitometer are shown in Figure B-1. The average density measured by each individual gamma beam is obtained using the same equation as is used for the single-beam densitometers.

In the Semiscale Mod-3 system, two-beam gamma densitometers provide information which allows the calculation of a better average density than that obtained from a single beam in a horizontal pipe. A mathematical model is used for processing the two-beam data to obtain the improved average density information. The processing method used is based on a froth-water model coupled with information from the two individual gamma beams and related beam path and piping cross-sectional geometry. The resulting information is recorded and reported under the density measurement identification ending with a "C," for example, GI-17C.

The use of the froth-water model for obtaining average density from a two-beam gamma densitometer in a horizontal pipe is based on observations indicating that flow regimes in the Semiscale Mod-3 system can be modeled by a layer of water on the bottom of the pipe with a degree of froth on the surface. For homogeneous flow conditions, such as all froth or all liquid, the model remains valid. At any point in time, slug flow is also modeled. The froth-water model does not model annular or inverted annular flows very well. However, these flows are not expected to exist for significant portions of a Semiscale Mod-3 system blowdown in horizontal piping. Density gradients from the top to the bottom of the pipe may exist showing no distinct location change from water to froth. This flow is neither totally homogeneous nor stratified, but the froth-water model does provide an adequate approximation of the average density characteristic of this flow pattern.

The average density obtained by using the gamma beam geometry shown in Figure B-1 and by applying the froth-water model is given by

$$\bar{\rho} = \alpha_f \rho_1 + (1 - \alpha_f)\rho_w \ \text{kg/m}^3 \qquad \text{(B-3)}$$

where

$\bar{\rho}$ = average cross-sectional density

ρ_1 = average density measured by the upper beam (measures the froth density)

ρ_w = density of liquid water (at local system conditions)

α_f = $1 + [1/(2\pi)]\ (\sin\beta - \beta)$ = volumetric fraction containing froth.

The angle which β represents is shown in Figure B-1. Values for β are obtained as follows:

$$\beta = 2\cos^{-1}(1 - 2h) \qquad \text{(B-4)}$$

where

$$h = \frac{H}{D} = \cos^2\theta\left(\frac{\rho_2 - \rho_1}{\rho_w - \rho_1}\right)$$

where

H = $\ell_w \cos\theta$ (ℓ_w and θ are defined in Figure B-1)

D = piping inside diameter

ρ_2 = the average density measured by the lower gamma beam.

Average density is not calculated using the two-beam froth-water model when the angle is not favorable due to system hardware restrictions in positioning the source. The froth-water model requires separate density sampling in both the upper and lower portions of the piping cross section.

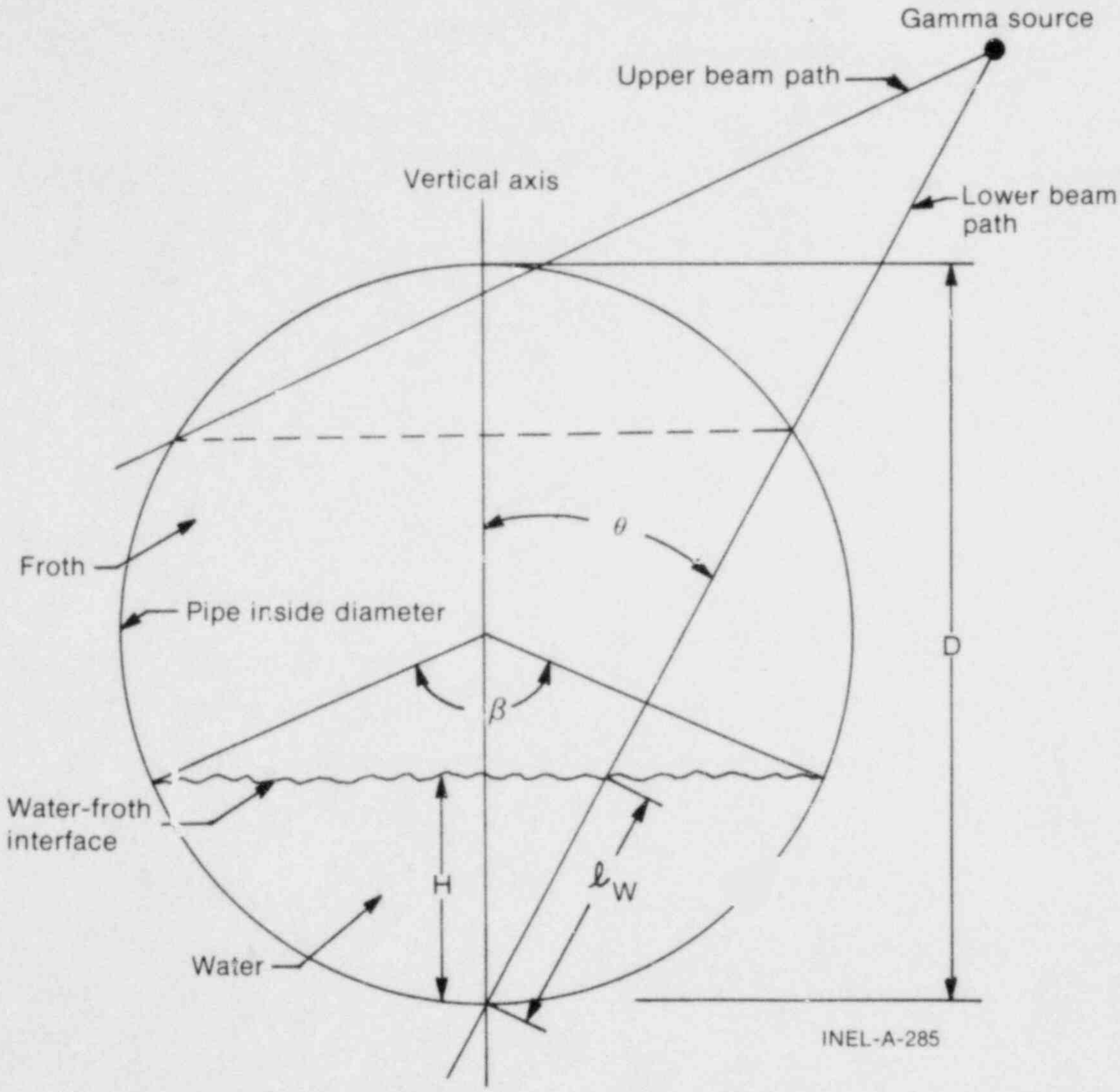

Figure B-1. Geometry used for processing of density data obtained from two-beam gamma densitometers.

APPENDIX C

SELECTED DATA WITH ESTIMATED TOTAL UNCERTAINTY BANDS FROM SEMISCALE MOD-3 TESTS S-SB-2 AND S-SB-2A

APPENDIX C

SELECTED DATA WITH ESTIMATED TOTAL UNCERTAINTY BANDS FROM SEMISCALE MOD-3 TESTS S-SB-2 AND S-SB-2A

Analysis has been performed on selected data from tests to provide a guide to the uncertainty associated with data measurements in the Semiscale Mod-3 system. The end result of the analysis is presented as uncertainty bands about the measured data which represent a 95% confidence level.

The uncertainty bands are obtained by combining uncertainties obtained from analysis of the data itself (random uncertainty) and engineering analysis of the measurement system (engineering uncertainty). The procedure by which uncertainty bands were established for the data presented in this appendix is described in the following paragraphs.

The data trace under analysis was empirically fitted with a linear difference equation, which was subject to a white noise input at each sampling time point. The objective of the empirical fitting procedure was to characterize the white noise, which was taken to represent the random uncertainty. The procedures for fitting the difference equation are discussed in depth in Reference C-1. A data trace was often segmented, and different equations were fitted to each segment with statistical correlations between successive observations accounted for by the fitting procedure. The white noise input was assumed to arise from a normally distributed population. The standard deviation of the white noise, as found during the fitting procedures, was taken as an estimate of the random uncertainty standard deviation and is shown in Table C-1 in appropriate engineering units. (Tables are presented consecutively starting on page 245.) The traces of the uncertainty band analysis are shown in Figures C-1 through C-78. (Figures are presented consecutively starting on page 255.)

Other uncertainties in the data exist because of such factors as variability in installation procedures and techniques, calibration uncertainties, variability in materials, and temperature and pressure sensitivities. These uncertainties and the procedures for estimating them are discussed in Reference C-2. They are referred to as engineering uncertainties, and the estimates are largely subjective. Because of the continuing effort to improve the accuracy of the measured data, such as through the use of better transducers, better signal conditioning and processing equipment, and better calibration and installation techniques, the engineering uncertainties for data from most of the transducer systems have changed from those published in Reference C-2. Table C-2 provides a summary of engineering uncertainty values obtained from current analysis techniques as applied to the data presented herein.

In addition to the normal hardware and installation related sources of engineering uncertainty, a significant measurement uncertainty results when the current transducer systems are subjected to separated two-phase flow regimes during the course of the blowdown transient. Accordingly, for those data affected (fluid density, volumetric flow, and mass flow), which are presented in this appendix, a more extensive assessment was conducted of additional engineering uncertainty due to flow regime effects. Table C-3 identifies the data analyzed and the period in the blowdown process for which flow regime uncertainties were included as a part of the total engineering uncertainty. The time of occurrence of separated two-phase flow and the resulting effect on the uncertainty of the data were evaluated by considering, on an individual basis, each detector output with reference to indications by other auxiliary measurements.

The gamma densitometer density measurement data are affected by two-phase separated flow regimes. The resulting transducer output is a measurement of the average attenuation of the gamma beam through the measured medium. The beam attenuation, in turn, is interpreted through physical relationship to be a measure of the average density along the beam path. When stratified type flow was considered present, the gamma beam attenuation was considered to be a result of a liquid layer and steam at system conditions.

The flow regime uncertainties of the turbine flowmeter were estimated by calculating a void fraction and the cross-sectional liquid and steam flow area for stratified flow. This calculation was accomplished using methods similar to those used to calculate the average density for stratified flows. A simple model was used to equate the forces on the turbine with the assumption of a known void fraction, stratified flow, known component sities, and slip ratio greater than unity. This process provided phase velocities. With the phase densities, velocities, and void fraction, a volumetric flow rate could be calculated. The difference between this value and the measured value was considered to be the uncertainty.

The overall standard deviation of a data point is taken as the root of the sum of the random uncertainty variance and the total engineering uncertainty variance; that is,

$$\sigma_o = \sqrt{\sigma_R^2 + \sigma_E^2} \qquad \text{(C-1)}$$

where

σ_o = overall standard deviation of a data point

σ_R^2 = random uncertainty variance

σ_E^2 = engineering uncertainty variance.

The uncertainty bands for the data are computed about the value given by the fitted difference equation y_i at time point i; that is,

$$\text{uncertainty band} = y_i \pm 1.96\sigma_o. \qquad \text{(C-2)}$$

With due regard to the fact that σ_E has been estimated subjectively, the uncertainty band may be interpreted as an approximate 95% confidence interval within which any true value of the measured variable is consistent with the data.

On certain occasions, the symmetrical uncertainty band given by Equation (C-2) is not appropriate. On those occasions, asymmetrical uncertainty bands were computed; that is, with the width being greater on one side of y_i than on the other.

Finally, the original data trace, along with its uncertainty band from Equation (C-2), was input to a computer plot package. The resulting plot contained the actual data trace surrounded by an uncertainty band derived both from random uncertainty and engineering uncertainty considerations. If thermocouple dryout occurred, the indicated uncertainty bands for the fluid temperature measurements are invalid and should be ignored.

TABLE C-1. RANDOM UNCERTAINTY STANDARD DEVIATION (TESTS S-SB-2 AND S-SB-2A)

Measurement	Test	Random Uncertainty Standard Deviation σ_R	Period of Application (s)	Figure
TFI-1	S-SB-2	0.17	-20 to 255	C-1
	S-SB-2A	0.12	-20 to 255	C-2
TFB-45	S-SB-2	0.25	-20 to 255	C-3
	S-SB-2A	0.11 0.35	-20 to 160 160 to 255	C-4
TFD-2[illegible]9	S-SB-2	0.20	-20 to 255	C-5
	S-SB-2A	0.19	-20 to 255	C-6
TFV-572W	S-SB-2	0.13	-20 to 255	C-7
	S-SB-2A	0.14	-20 to 255	C-8
TFG-7AB-34	S-SB-2	0.66 0.48 0.23	-20 to 25 25 to 30 30 to 255	C-9
	S-SB-2A	0.38 0.76 0.30	-20 to 20 20 to 26 26 to 255	C-10
TMI-1T	S-SB-2	0.13	-20 to 255	C-11
	S-SB-2A	0.12	-20 to 255	C-12
TMB-45T	S-SB-2	0.10	-20 to 255	C-13
	S-SB-2A	0.33	-20 to 255	C-14
TMB-294	S-SB-2	0.09	-20 to 255	C-15
	S-SB-2A	0.11	-20 to 255	C-16
TIMD-294	S-SB-2	0.21	-20 to 255	C-17
	S-SB-2A	0.22	-20 to 255	C-18
TIMV-572W	S-SB-2	0.10	-20 to 255	C-19
	S-SB-2A	0.10	-20 to 255	C-20
TH-C2-08	S-SB-2	0.34 0.42 0.49	-20 to 25 25 to 30 30 to 255	C-21

TABLE C-1. (continued)

Measurement	Test	Random Uncertainty Standard Deviation σ_R	Period of Application (s)	Figure
TH-C2-08 (continued)	S-SB-2A	0.23	-20 to 20	C-22
		0.56	20 to 26	
		0.26	26 to 255	
TH-C2-321	S-SB-2	0.71	-20 to 25	C-23
		1.00	25 to 30	
		0.38	30 to 255	
	S-SB-2A	0.31	-20 to 20	C-24
		1.11	20 to 26	
		0.26	26 to 255	
PI-16	S-SB-2	0.02	-20 to 255	C-25
	S-SB-2A	0.01	-20 to 255	C-26
PB-45A	S-SB-2	0.02	-20 to 255	C-27
	S-SB-2A	0.02	-20 to 255	C-28
PI-PRIZE	S-SB-2	0.01	-20 to 255	C-29
	S-SB-2A	0.01	-20 to 255	C-30
PB-SD	S-SB-2	0.03	-20 to 255	C-31
	S-SB-2A	0.00	-20 to 255	C-32
DI-6-7	S-SB-2	13.68	-20 to 25	C-33
		10.79	25 to 30	
		1.31	30 to 255	
	S-SB-2A	9.21	-20 to 20	C-34
		12.30	20 to 26	
		4.37	26 to 255	
DI-13-15	S-SB-2	17.50	-20 to 25	C-[illegible]
		17.15	25 to 30	
		5.59	30 to 255	
	S-SB-2A	12.31	-20 to 20	C-36
		17.55	20 to 26	
		6.18	26 to 255	
DB-29-40B	S-SB-2	13.57	-20 to 25	C-37
		8.51	25 to 30	
		4.98	30 to 255	

TABLE C-1. (continued)

Measurement	Test	Random Uncertainty Standard Deviation σ_R	Period of Application (s)	Figure
DB-29-40B (continued)	S-SB-2A	7.26	-20 to 20	C-38
		13.47	20 to 26	
		4.26	26 to 255	
DD-DIA-578	S-SB-2	1.33	-20 to 25	C-39
		1.16	25 to 30	
		0.56	30 to 255	
	S-SB-2A	0.67	-20 to 255	C-40
DV-501-105	S-SB-2	1.65	-20 to 25	C-41
		2.14	25 to 30	
		0.79	30 to 255	
	S-SB-2A	0.89	-20 to 255	C-42
DI-SG-LL	S-SB-2	0.48	-20 to 16	C-43
		0.14	16 to 255	
	S-SB-2A	0.66	-20 to 26	C-44
		0.11	26 to 255	
FI-1	S-SB-2	0.26	-20 to 255	C-45
	S-SB-2A	0.10	-20 to 130	C-46
		2.68	130 to 255	
FI-16	S-SB-2	1.31	-20 to 61	C-47
		0.86	61 to 125	
		0.27	125 to 225	
	S-SB-2A	1.07	-20 to 136	C-48
		0.13	136 to 225	
FI-17	S-SB-2	0.40	-20 to 127	C-49
		3.86	127 to 255	
	S-SB-2A	0.40	-20 to 121	C-50
		3.86	121 to 255	
FD-424	S-SB-2	0.10	-20 to 91	C-51
		0.58	91 to 151	
		2.47	151 to 205	
		0.85	205 to 235	
		2.47	235 to 255	
	S-SB-2A	0.13	-20 to 121	C-52
		1.41	121 to 255	

TABLE C-1. (continued)

Measurement	Test	Random Uncertainty Standard Deviation σ_R	Period of Application (s)	Figure
FV+1	S-SB-2	0.14	-20 to 185	C-53
		0.50	185 to 255	
	S-SB-2A	0.07	-20 to 61	C-54
		0.14	61 to 255	
FI-HPIS	S-SB-2	14.32	-20 to 50	C-55
		1.85	50 to 255	
	S-SB-2A	13.73	-20 to 23	C-56
		6.81	23 to 255	
GI-IT	S-SB-2	21.87	-20 to 47	C-57
		112.42	47 to 53	
		24.97	53 to 255	
	S-SB-2A	22.0	-20 to 255	C-58
GI-1B	S-SB-2	21.02	-20 to 255	C-59
	S-SB-2A	15.93	-20 to 124	C-60
		26.79	124 to 130	
		14.53	130 to 255	
GI-1C	S-SB-2	8.59	-20 to 46	C-61
		31.77	46 to 103	
		26.06	103 to 109	
		25.68	109 to 255	
	S-SB-2A	7.63	-20 to 40	C-62
		23.35	40 to 125	
		39.82	125 to 131	
		26.75	131 to 255	
GI-17T	S-SB-2	24.79	-20 to 181	C-63
		44.66	181 to 187	
		28.24	187 to 255	
	S-SB-2A	23.91	-20 to 182	C-64
		29.51	182 to 255	
GI-17B	S-SB-2	24.25	-20 to 181	C-65
		32.23	181 to 255	
	S-SB-2A	16.04	-20 to 255	C-66

TABLE C-1. (continued)

Measurement	Test	Random Uncertainty Standard Deviation σ_R	Period of Application (s)	Figure
GI-17C	S-SB-2	14.07	-20 to 196	C-67
		31.64	196 to 255	
	S-SB-2A	10.92	-20 to 182	C-68
		35.83	182 to 255	
GB-45VR	S-SB-2	21.37	-20 to 196	C-69
		31.67	196 to 255	
	S-SB-2A	25.32	-20 to 200	C-70
		30.16	200 to 255	
GD-456B	S-SB-2	28.18	-20 to 255	C-71
	S-SB-2A	24.59	-20 to 255	C-72
FI-1, GI-1C	S-SB-2	0.14	-20 to 255	C-73
	S-SB-2A	0.11	-20 to 140	C-74
		1.21	140 to 255	
FI-17, GI-17C	S-SB-2	0.18	-20 to 127	C-75
		1.70	127 to 255	
	S-SB-2A	0.29	-20 to 121	C-76
		2.26	121 to 255	
FD-424, GD-456B	S-SB-2	0.26	-20 to 140	C-77
		1.71	140 to 205	
		0.64	205 to 235	
		1.78	235 to 255	
	S-SB-2A	0.19	-20 to 130	C-78
		1.11	130 to 255	

TABLE C-2. GENERAL MEASUREMENT ENGINEERING UNCERTAINTY SOURCES AND UNCERTAINTY VALUES (TESTS S-SB-2 AND S-SB-2A)

Measurement Category	Uncertainty Sources	Uncertainty Value	Expected Uncertainty Values
Fluid Temperature	Changes in homogeneity of the thermocouple wire due to cold working	±1.11 K	±1.66 K, R ≤ 550 K[a]
	Data interpretation from standard refererence tables	±1.11 K, R ≤ 550 K ±0.0021 R, R > 550 K	$\pm\left[1.42 + (0.0021\ R)^2\right]^{1/2}$, R 550 K[a]
	General data acquisition processing	±0.42 K	where
	Thermal aging of the thermocouples	±0.28 K	R = transducer reading (K)
Material Temperature	Changes in homogeneity of the thermocouple wire due to cold working	±1.11 K	
	Thermocouple radial position	±2.78 K	±3.33 K, R ≤ 550 K
	Data interpretation from standard refererence tables	±1.11 K, R ≤ 550 K ±0.0021, R, R > 550 K	$\pm\left[9.75 + (0.0021\ R)^2\right]^{1/2}$, R > 550 K
	General data acquisition and processing	±0.42 K	where
	Thermal aging of the thermocouples	±0.28 K	R = transducer reading (K)

TABLE C-2. (continued)

Measurement Category	Uncertainty Sources	Uncertainty Value	Expected Uncertainty Values
Pressure	Entrance effects	±0.3% of transducer full scale	±0.44% of transducer full scale
	Calibration	±0.26% of transducer full scale	
	Temperature sensitivity	±0.13% of transducer full scale	
	General data acquisition and processing	±0.15% of system full scale	
Differential Pressure	Installation	±0.03% of transducer full scale	±2% of transducer full scale[b]
	Calibration		
	Transducer ranges ±4.96 through ±199.26 KPa	$\pm\left[(0.05) + (0.5\ R/FS)^2\right]^{1/2}$ % of transducer full scale	
	Transducer ranges ±3.44.74, ±689.47, ±3447 kPa	$\pm\left[(0.03) + (0.5\ R/FS)^2\right]^{1/2}$ % of transducer full scale	
	Transducer ranges ±6894, ±10 342 kPa	$\pm\left[(0.02) + (0.5\ R/FS)^2\right]^{1/2}$ % of transducer full scale	
	Temperature sensitivity	±0.5% of transducer full scale	where R = transducer reading (kPa) FS = transducer range full scale (kPa)
	General data acquisition and processing	±0.15% of system full scale	
	Air entrapment	±0.069 kPa	

TABLE C-2. (continued)

Measurement Category	Uncertainty Sources	Uncertainty Value	Expected Uncertainty Values
Density	Calibration	±1.0% of reading (kg/m^3)	c
	Detector system uncertainty	±2.1 kg/m^3	
	General data acquisition and processing	±0.15% of system full scale (kg/m^3)	
	Flow regime	c	
Volumetric Flow (turbine flowmeter)	Calibration instrument reading	±0.25% of transducer full scale	c
	Calibration standards	±19.56 x 10^{-2} L/s	
	Velocity profile	±2.9% of reading	
	Frequency-to-voltage conversion	±0.25% of transducer full scale	
	General data acquisition and processing	±0.15% of system full scale	
	Dead bands	±5% of transducer full scale	
	Flow regimes	c	

TABLE C-2. (continued)

Measurement Category	Uncertainty Sources	Uncertainty Value	Expected Uncertainty Values
Mass Flow Rate (from volumetric flow and density data)	Combined results from individual uncertainty sources for volumetric flow and density data[d]	c	c

a. This value is no longer valid after thermocouple dryout occurs.

b. Value is based on observed system performance. It is more conservative than that obtained from the statistical summation of the identified engineering uncertainties.

c. Uncertainty value is time and flow regime dependent.

d. The general method for combining volumetric flow with density data to obtain mass flow rate and the resulting uncertainties in the data are explained in Reference C-2.

TABLE C-3. TIME PERIODS WHEN FLOW REGIME UNCERTAINTIES WERE APPLIED (TESTS S-SB-2 AND S-SB-2A)

Detector Identification	Test	Time During Which Flow Regime Uncertainties were applied (s)	Figure
FI-1	S-SB-2	25 to 4534	C-45
	S-SB-2A	20 to 4390	C-46
FI-17	S-SB-2	190 to 4534	C-49
	S-SB-2A	186 to 4390	C-50
FV+1	S-SB-2	40 to 4534	C-53
	S-SB-2A	40 to 440 1050 to 4390	C-54
GI-1C	S-SB-2	25 to 4534	C-61
	S-SB-2A	20 to 4390	C-62
GI-17C	S-SB-2	190 to 4534	C-67
	S-SB-2A	186 to 4390	C-68
GB-45VR	S-SB-2	197 to 310 1980 to 3040 3580 to 4120	C-69
	S-SB-2A	200 to 300 2750 to 3750	C-70
FI-1, GI-1C	S-SB-2	25 to 4534	C-73
	S-SB-2A	20 to 4390	C-74
FI-17, GI-17C	S-SB-2	190 to 4534	C-75
	S-SB-2A	186 to 4390	C-76

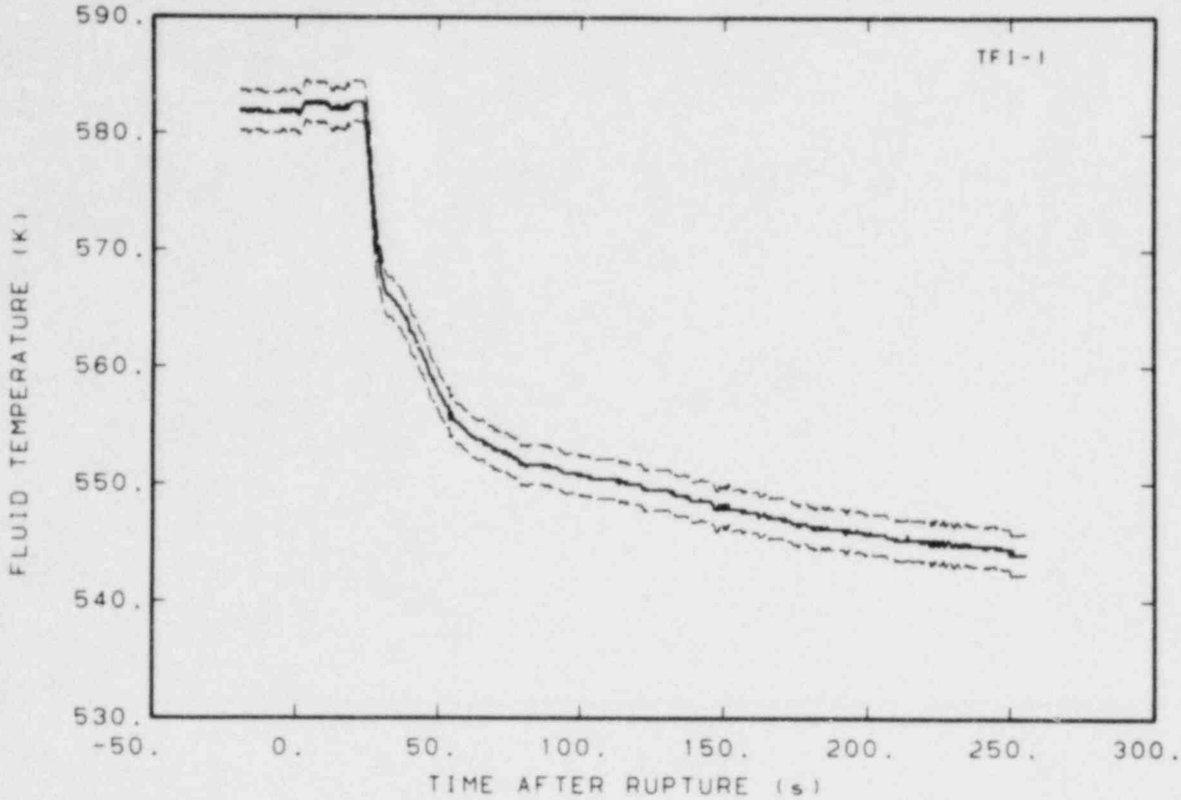

Figure C-1. Fluid temperature in intact loop hot leg, Test S-SB-2 (TFI-1).

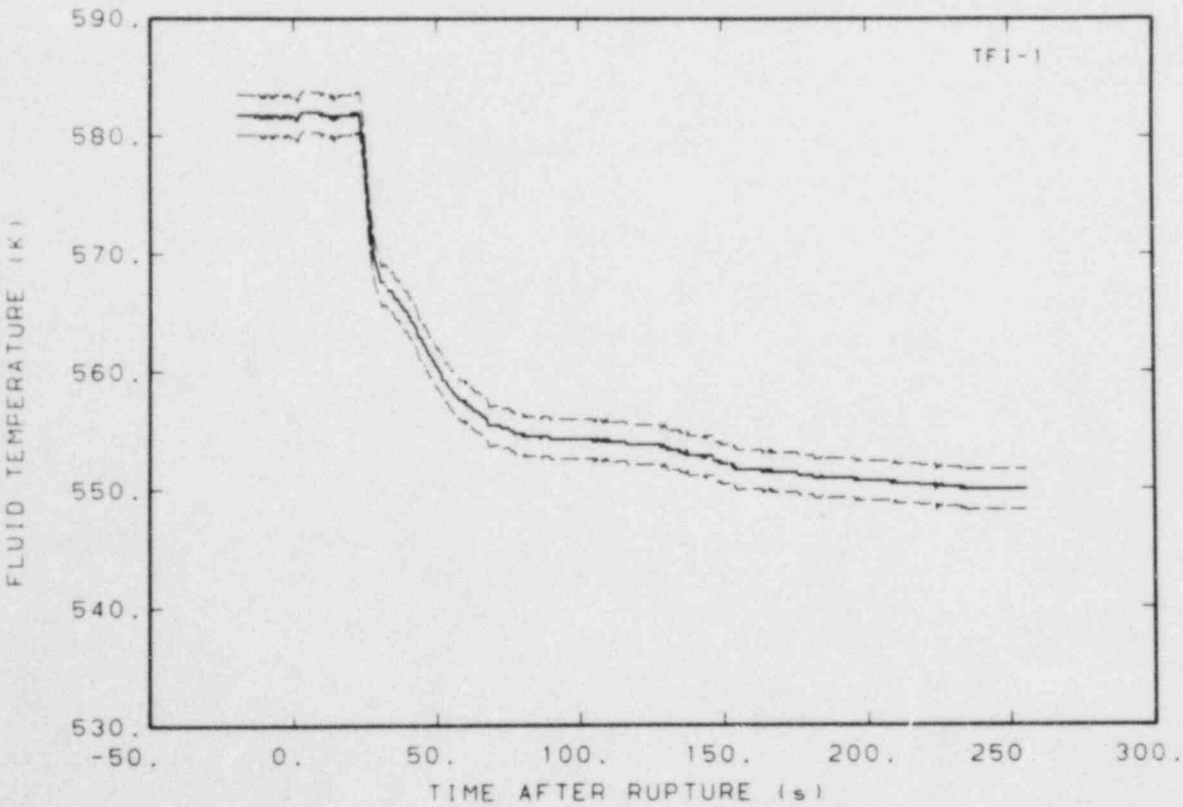

Figure C-2. Fluid temperature in intact loop hot leg, Test S-SB-2A (TFI-1).

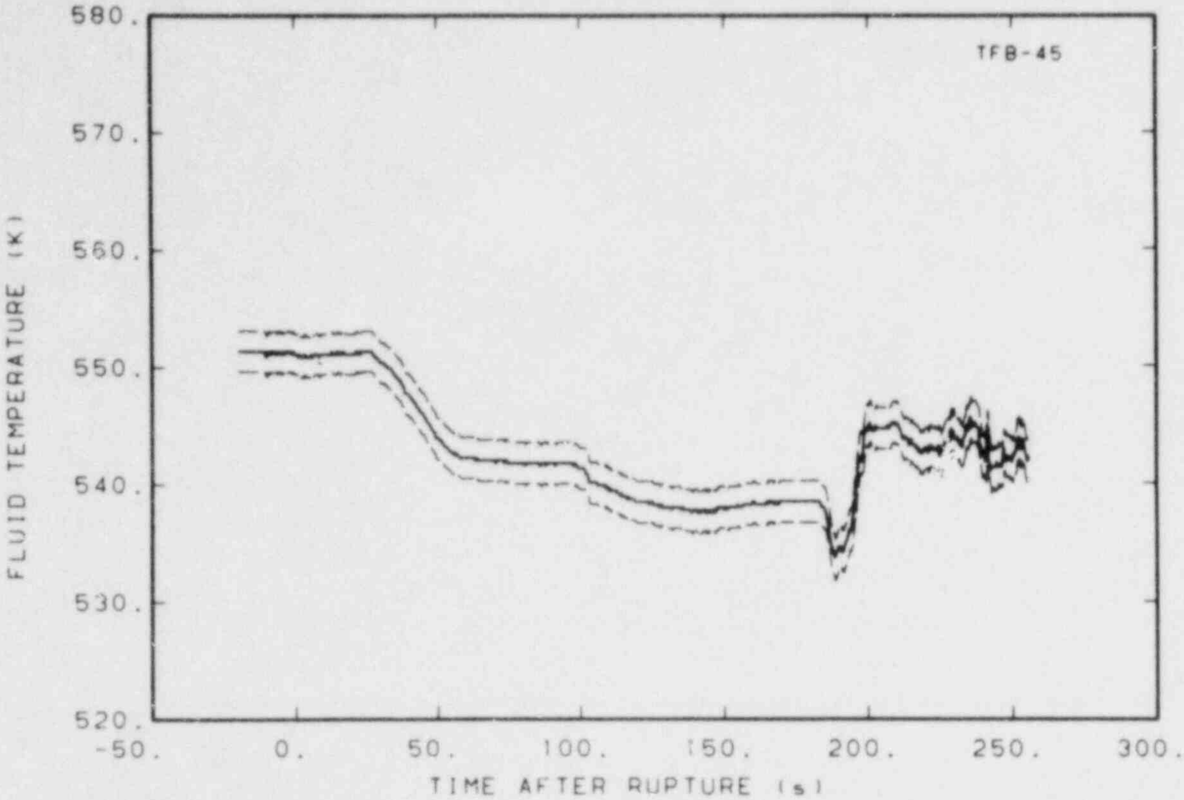

Figure C-3. Fluid temperature in broken loop cold leg, Test S-SB-2 (TFB-45).

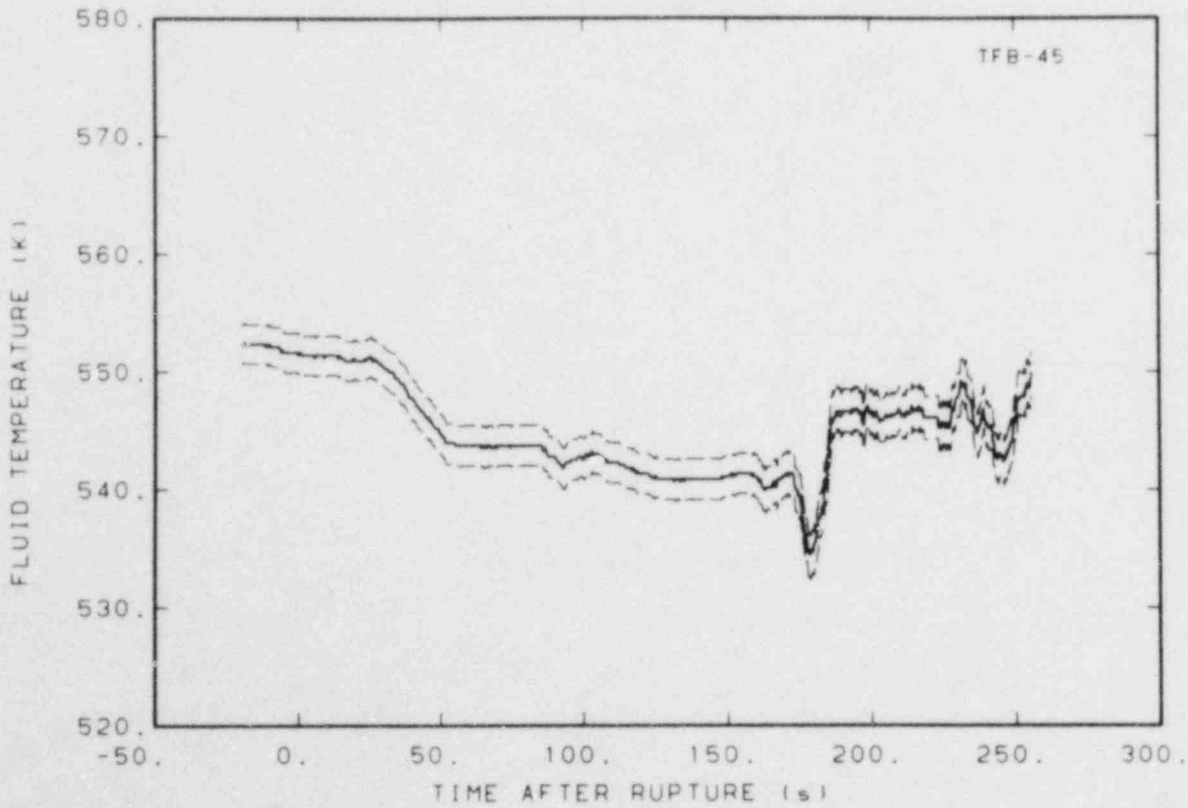

Figure C-4. Fluid temperature in broken loop cold leg, Test S-SB-2A (TFB-45).

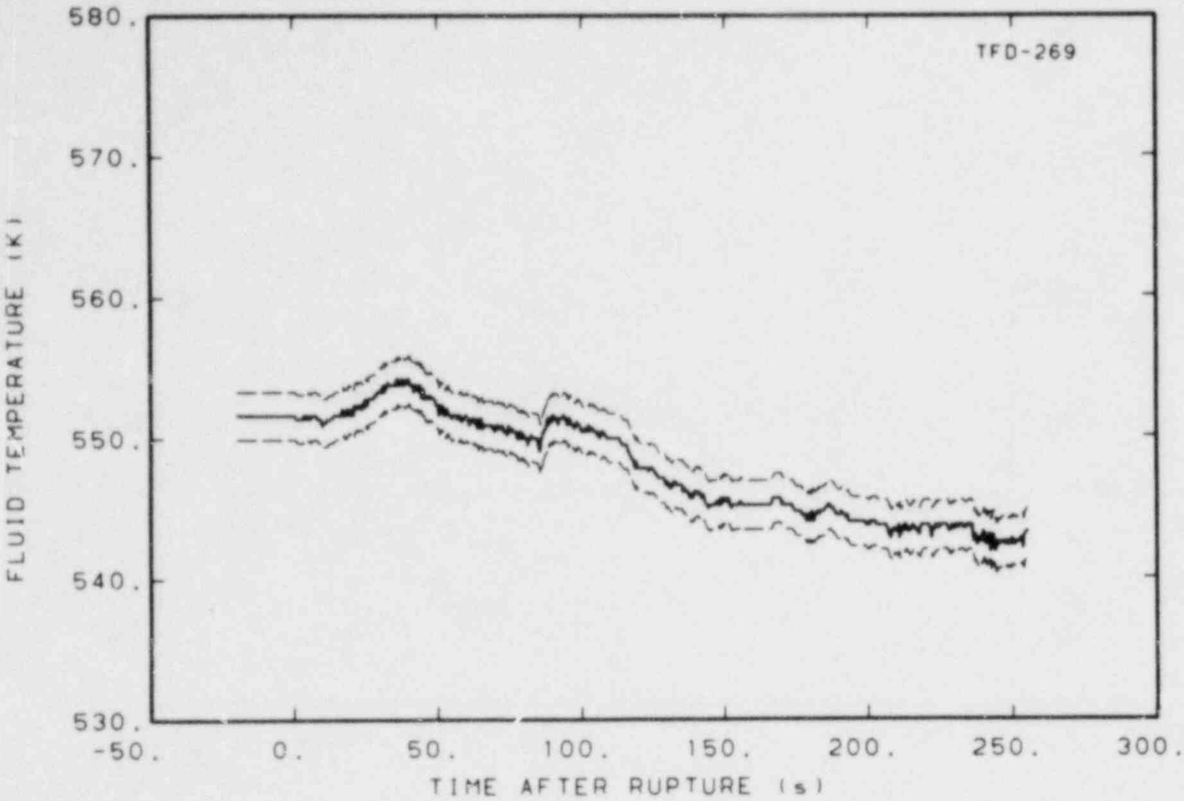

Figure C-5. Fluid temperature in downcomer, Test S-SB-2 (TFD-269).

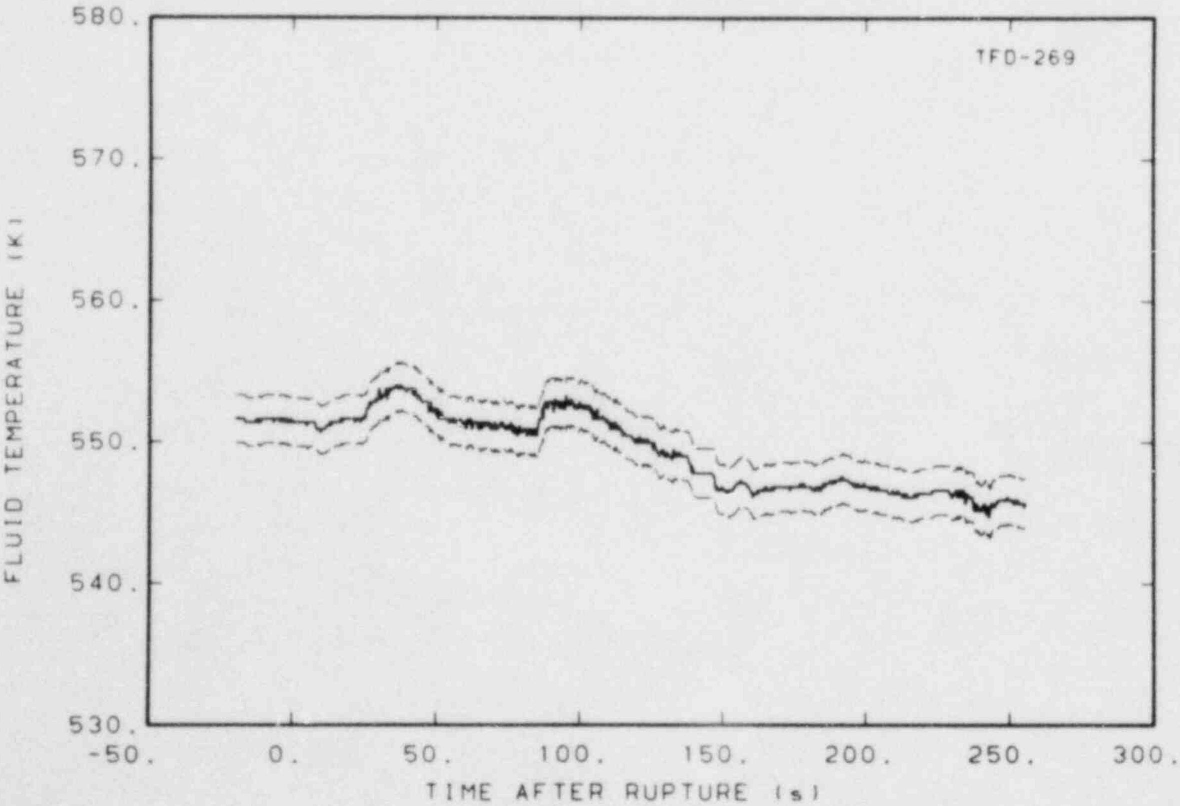

Figure C-6. Fluid temperature in downcomer, Test S-SB-2A (TFD-269).

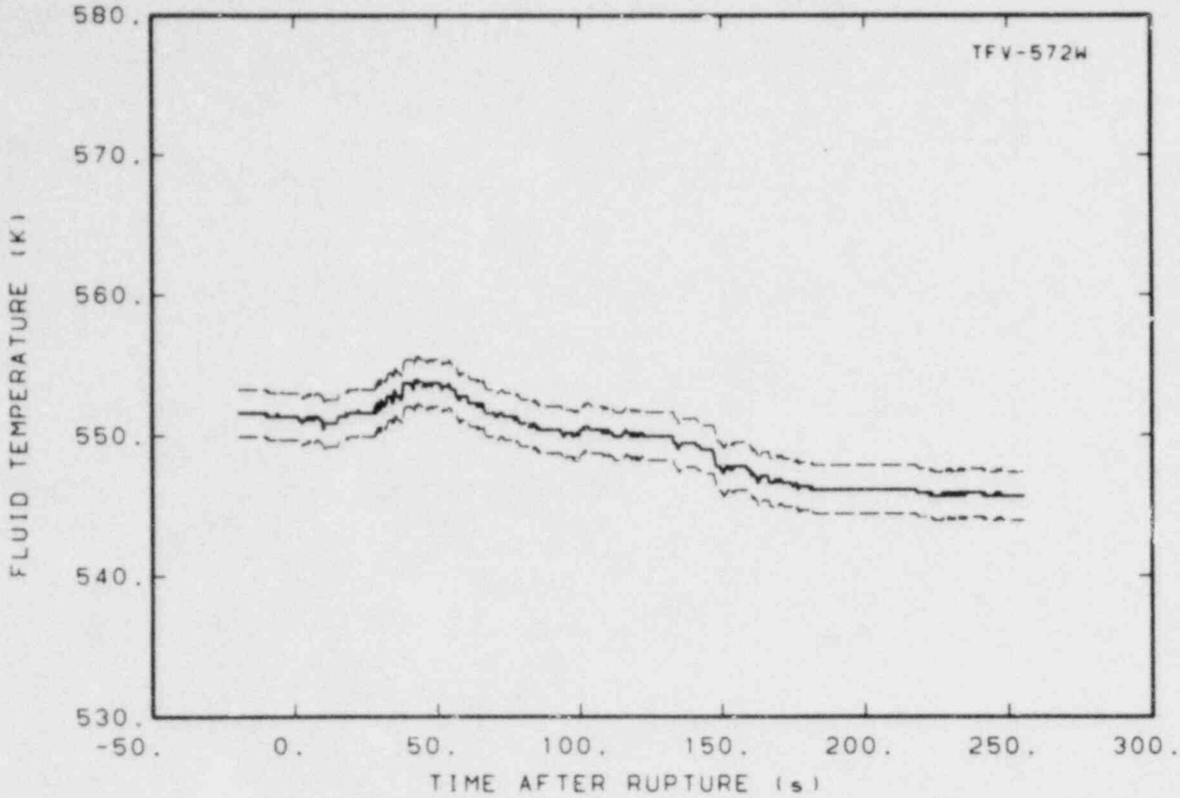

Figure C-7. Fluid temperature in vessel, Test S-SB-2 (TFV-572W).

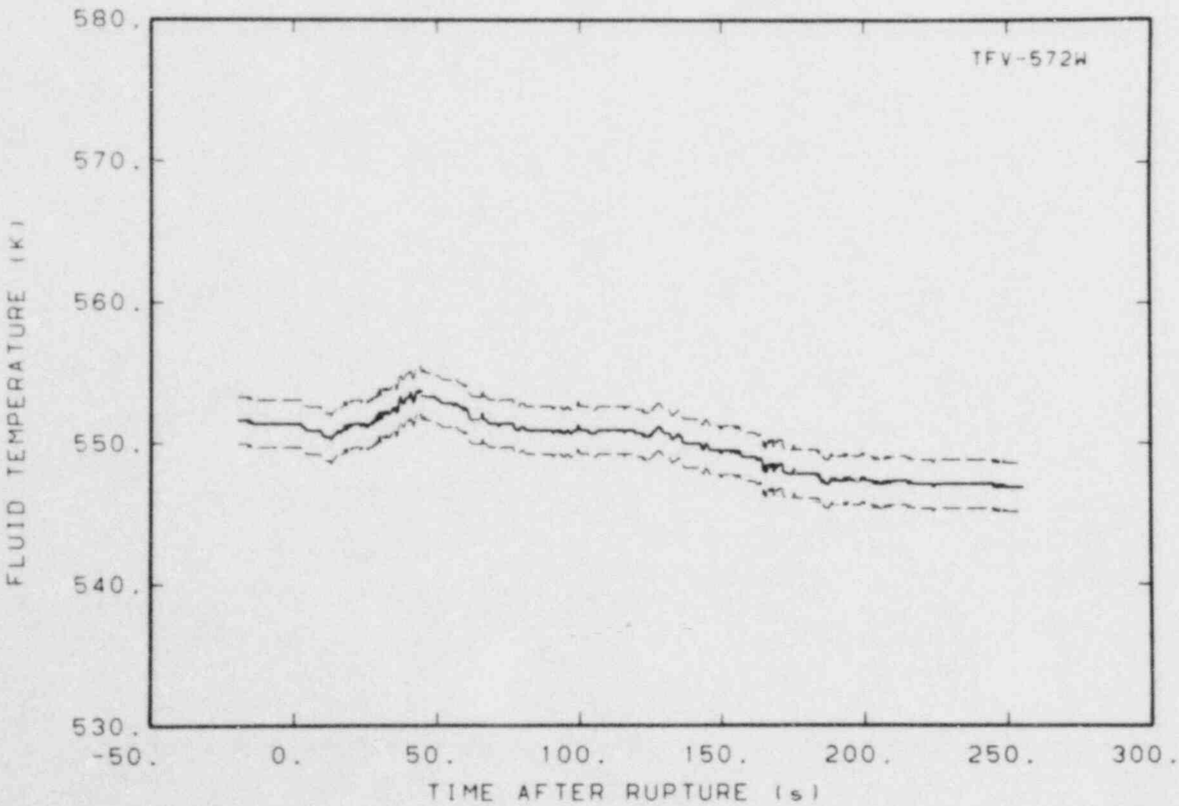

Figure C-8. Fluid temperature in vessel, Test S-SB-2A (TFV-572W).

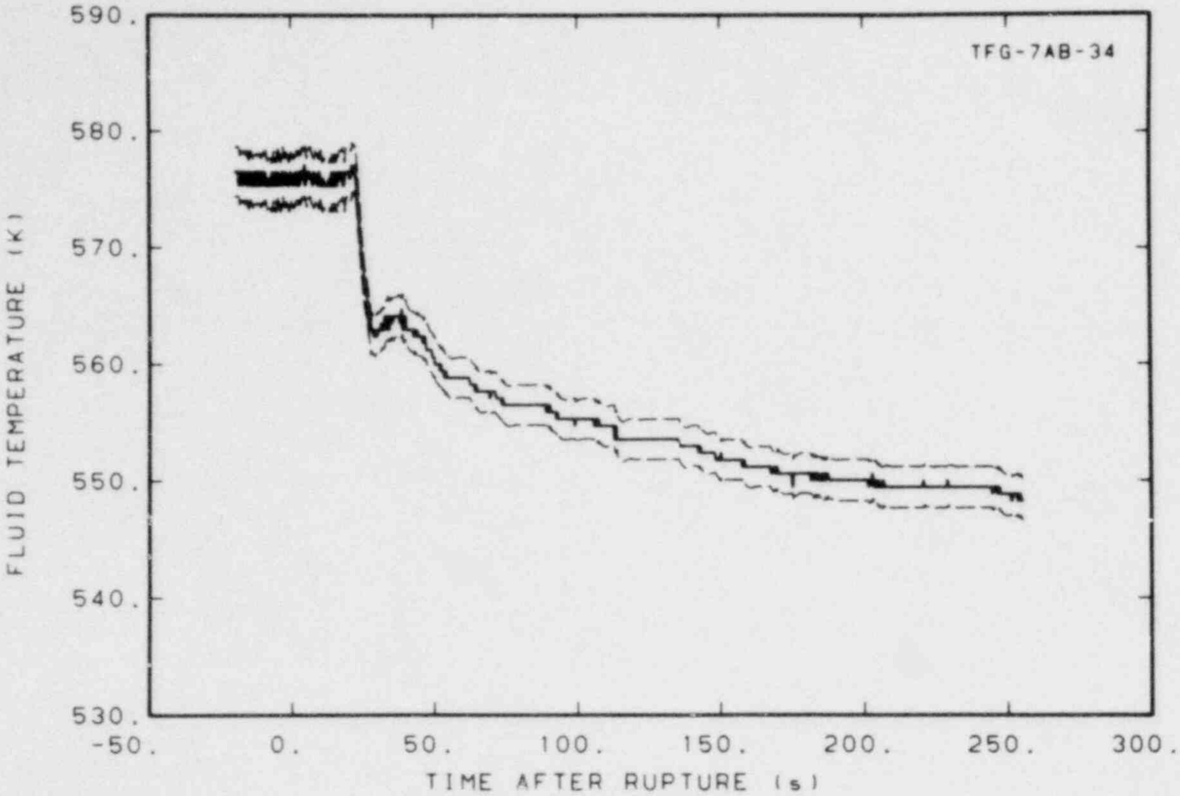

Figure C-9. Fluid temperature in core, Grid Spacer 7, Test S-SB-2 (TFG-7AB-34).

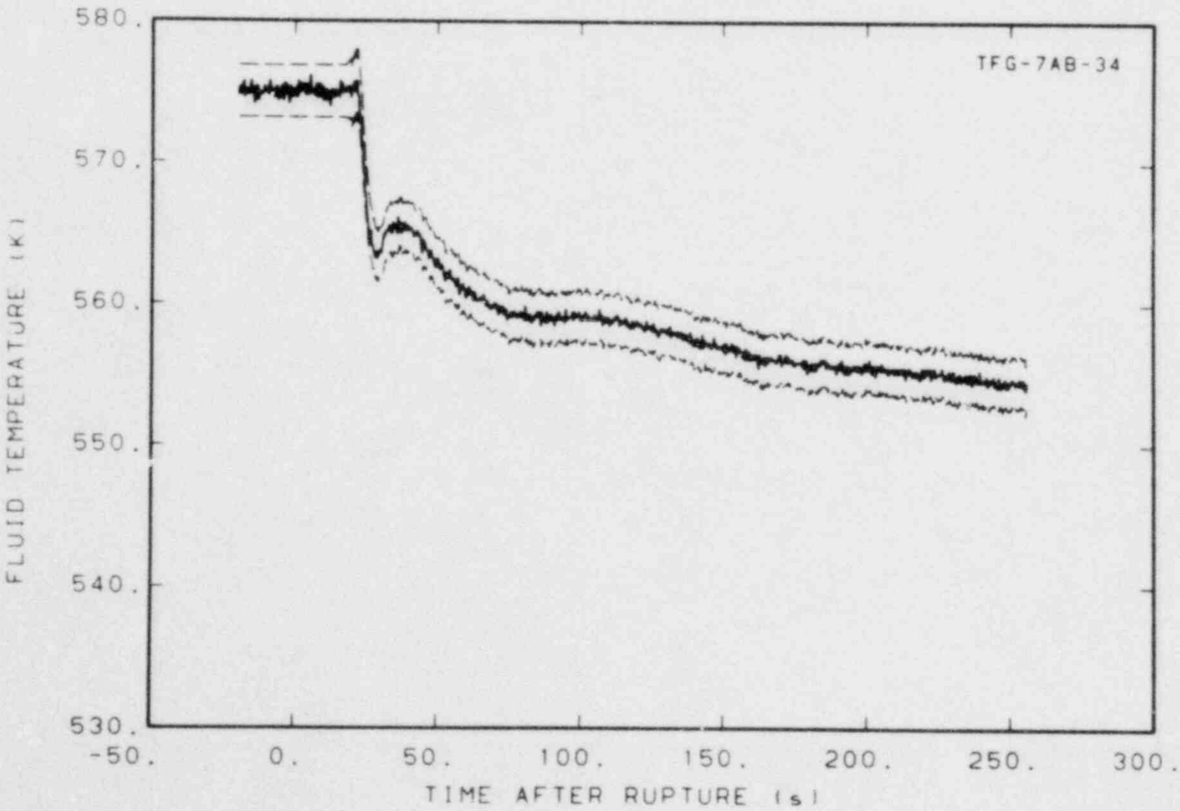

Figure C-10. Fluid temperature in core, Grid Spacer 7, Test i-SB-2A (TFG-7AB-34).

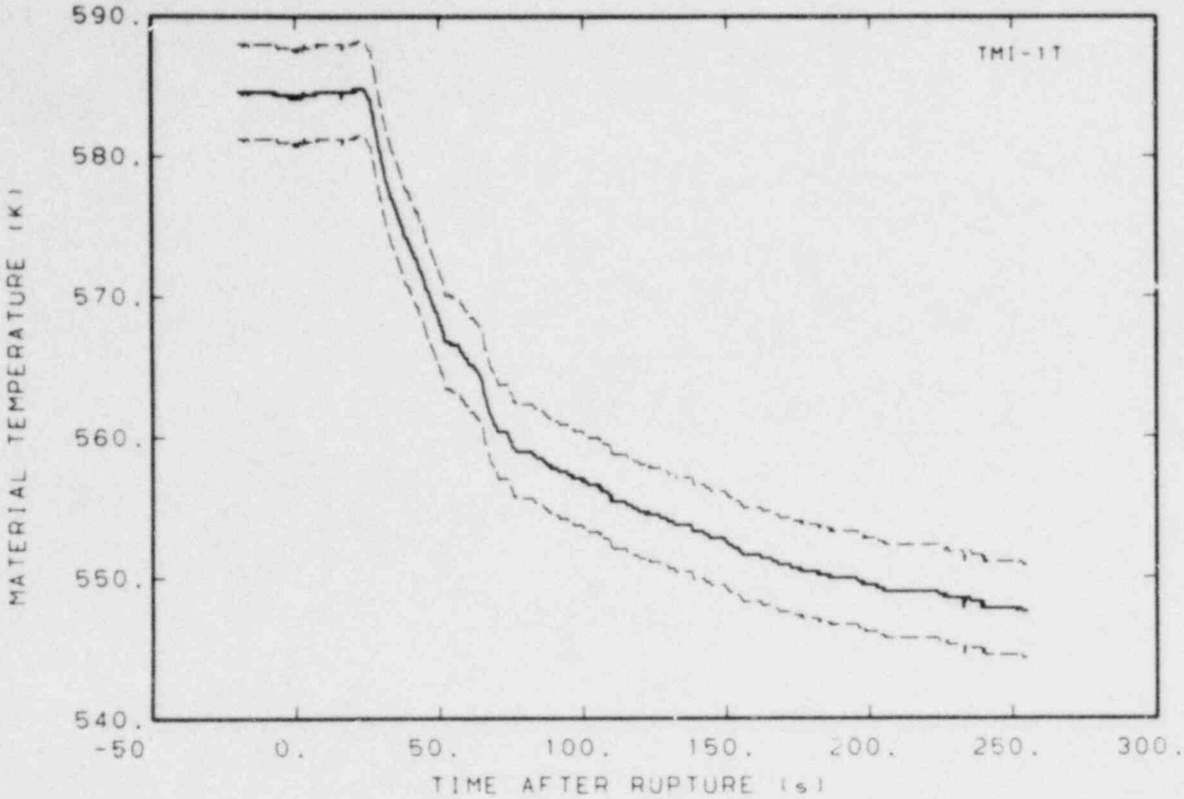

Figure C-11. Material temperature in intact loop hot leg, Test S-SB-2 (TMI-1T).

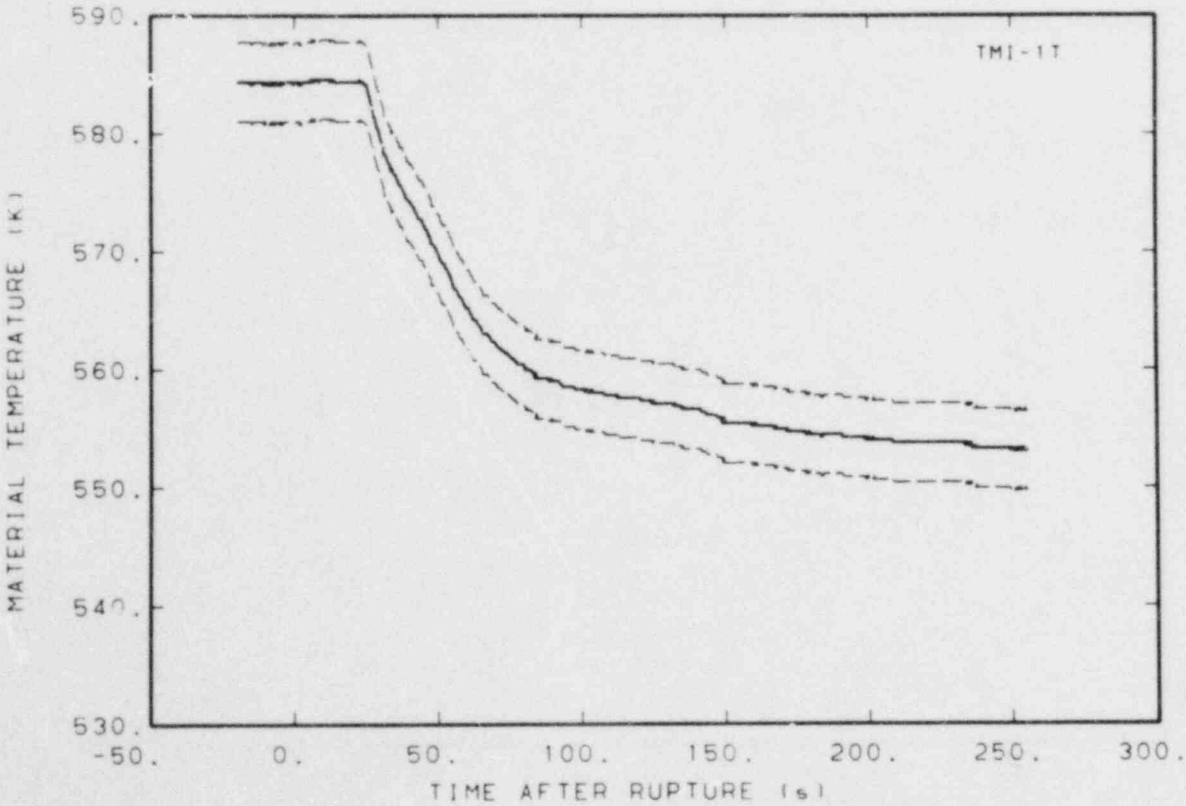

Figure C-12. Material temperature in intact loop hot leg, Test S-SB-2A (TMI-1T).

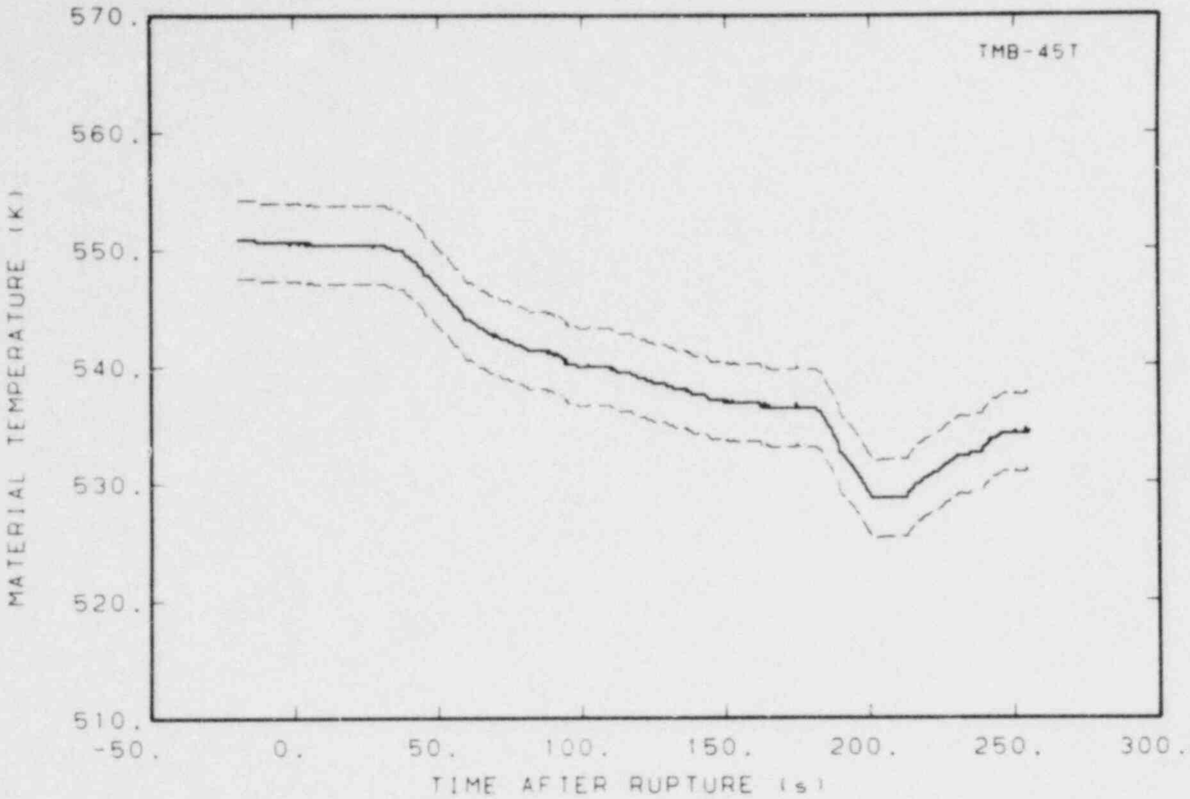

Figure C-13. Material temperature in broken loop cold leg, Test S-SP-2 (TMB-45T).

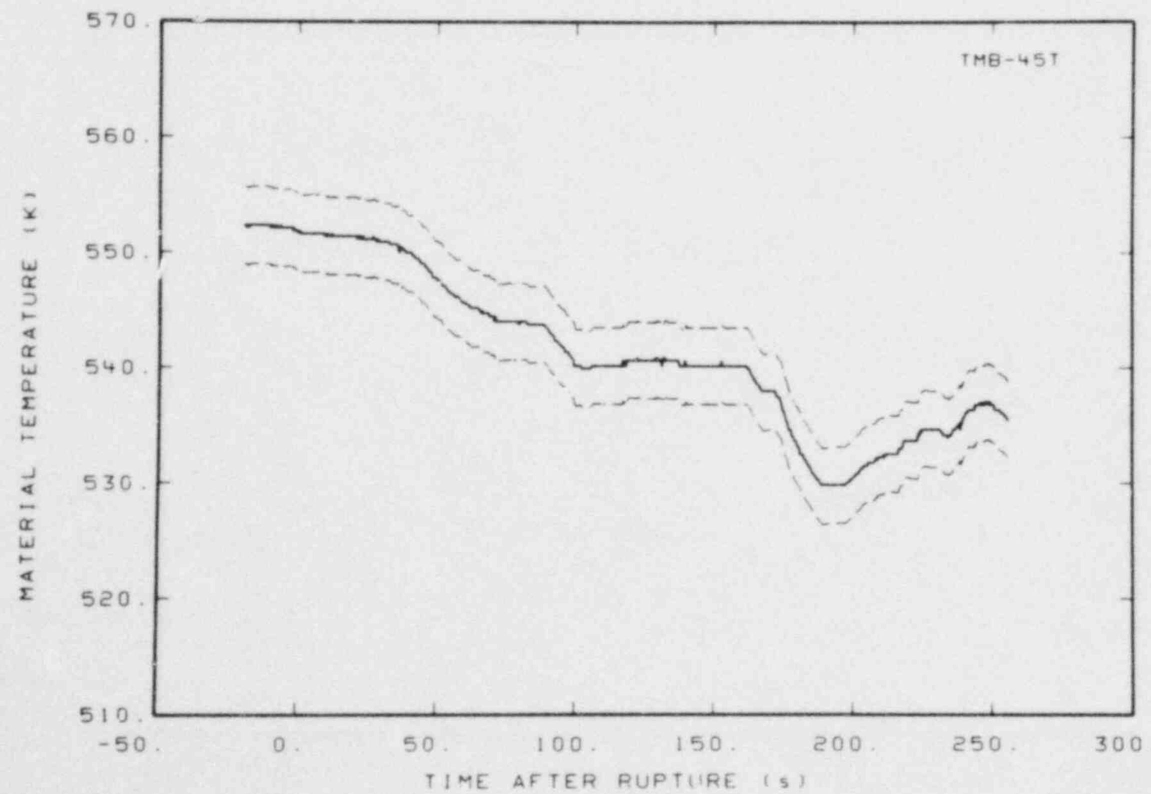

Figure C-14. Material temperature in broken loop cold leg, Test S-Sà-2A (TMB-45T).

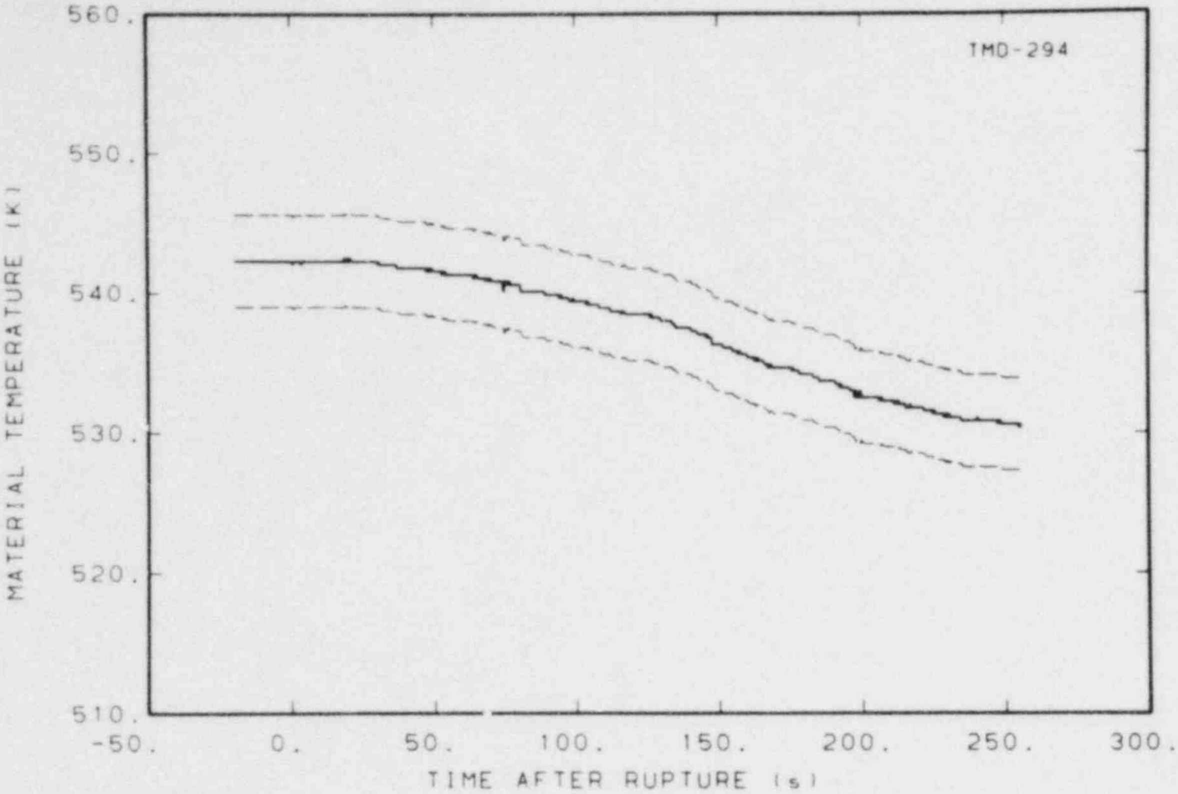

Figure C-15. Material temperature in downcomer, Test S-SB-2 (TMD-294).

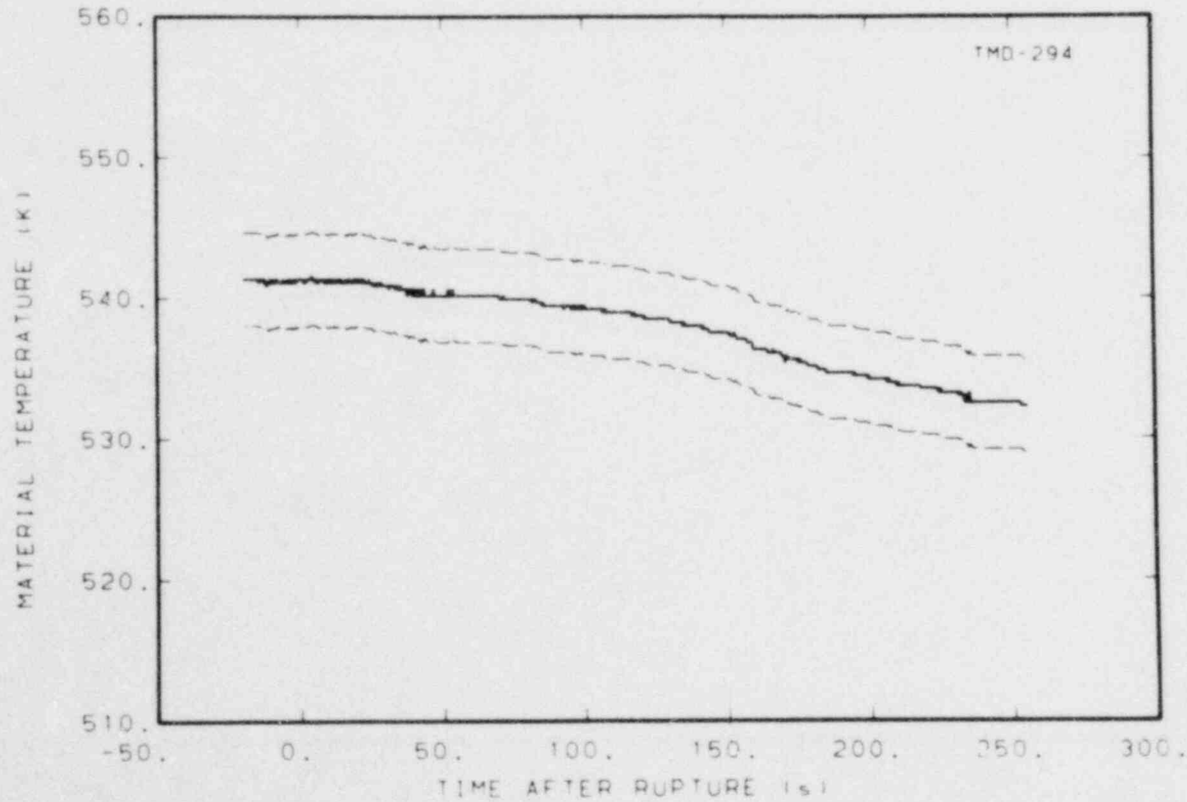

Figure C-16. Material temperature in downcomer, Test S-SB-2A (TMD-294).

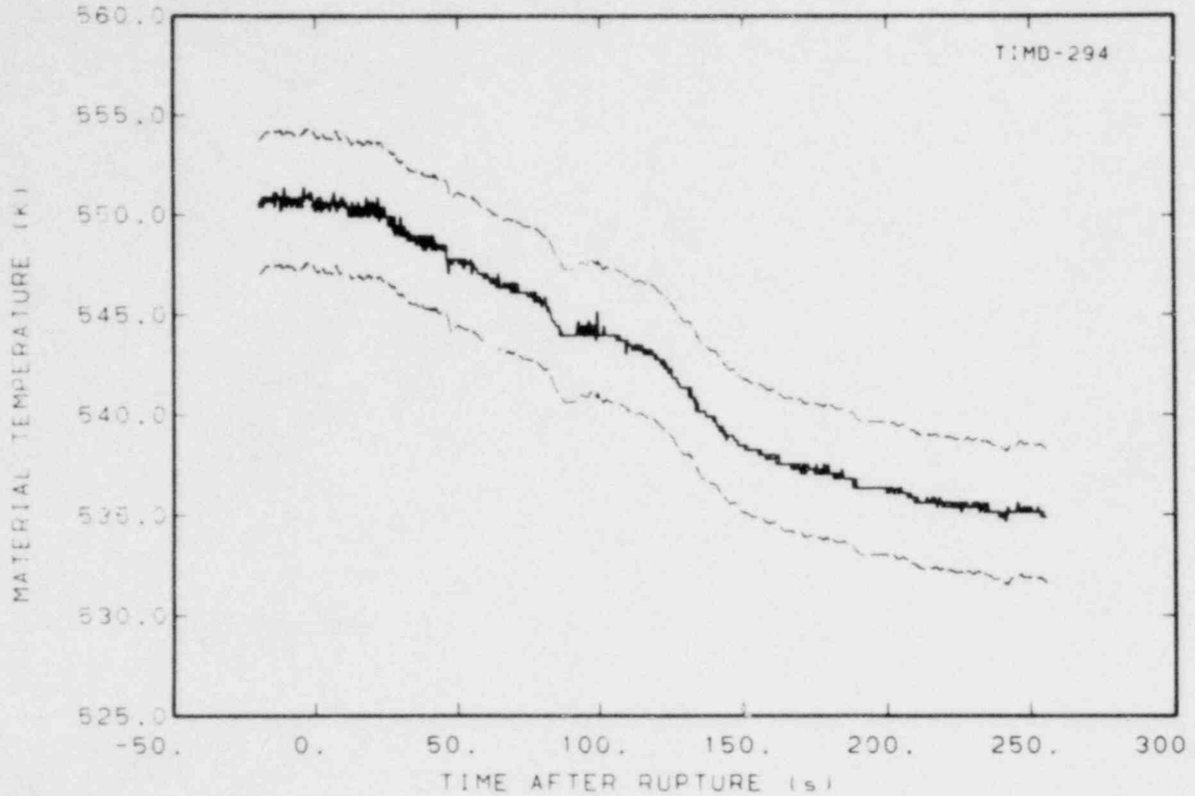

Figure C-17. Material temperature in downcomer insulator, Test S-SB-2 (TIMD-294).

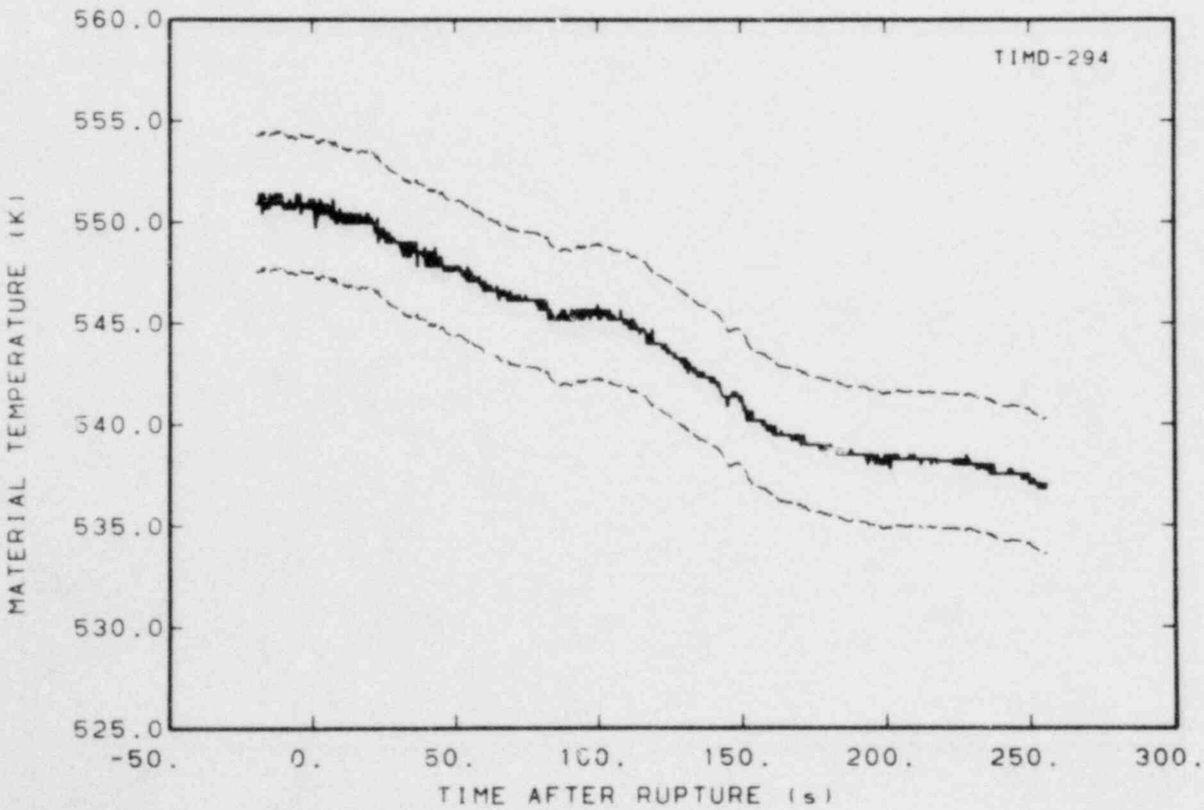

Figure C-18. Material temperature in downcomer insulator, Test S-SB-2A (TIMD-294).

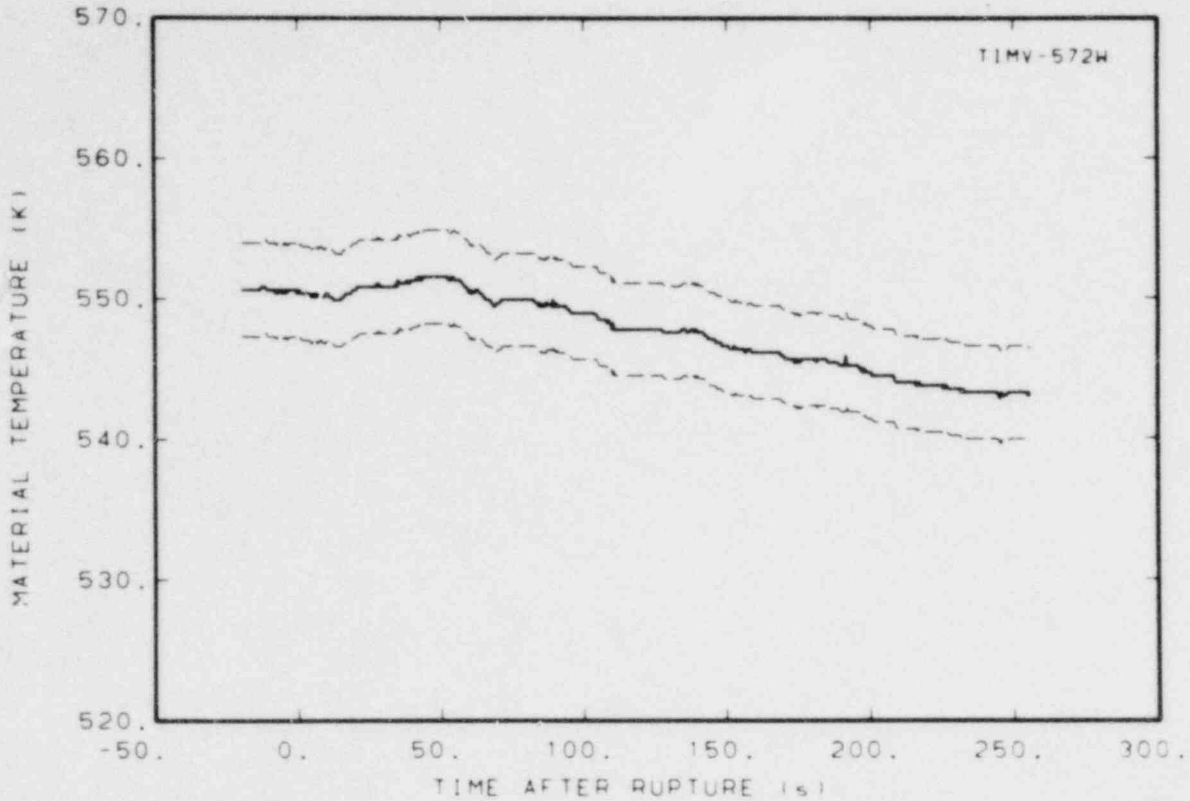

Figure C-19. Material temperaturc in vessel insulator, Test S-SB-2 (TIMV + 572W).

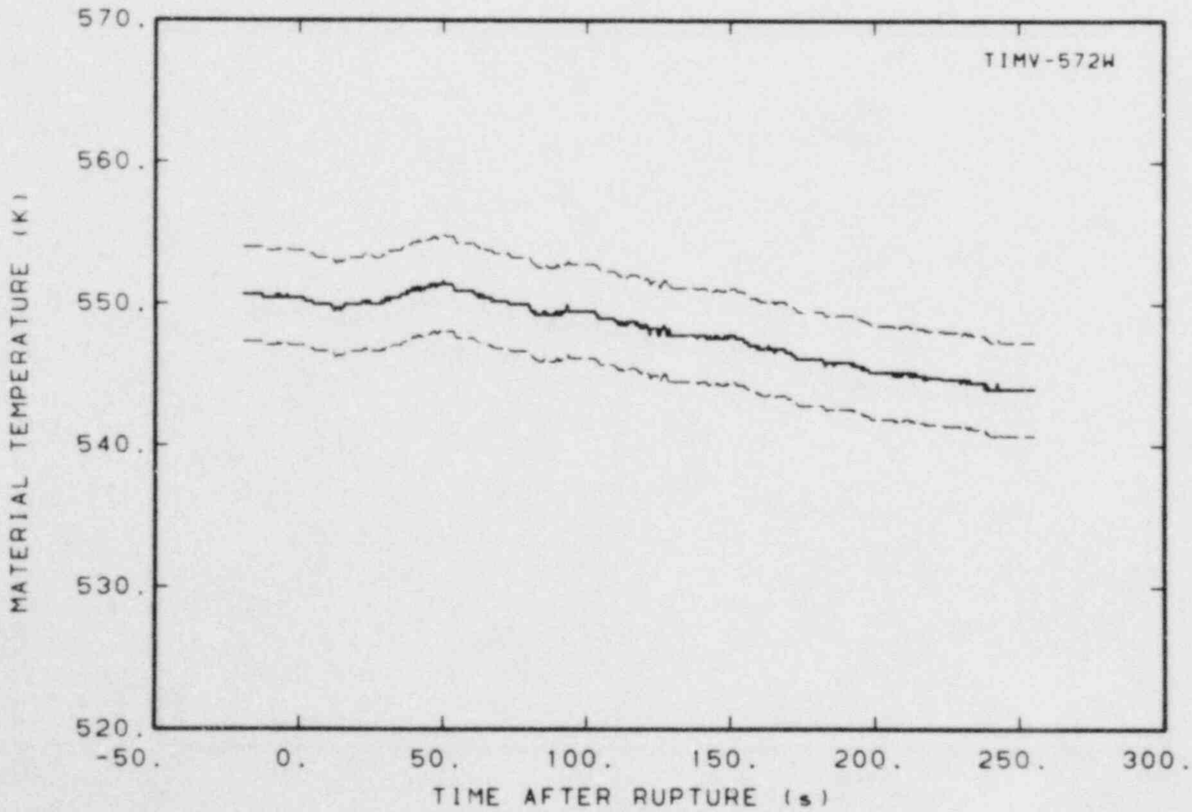

Figure C-20. Material temperature in vessel insulator, Test S-SB-2A (TIMV + 572W).

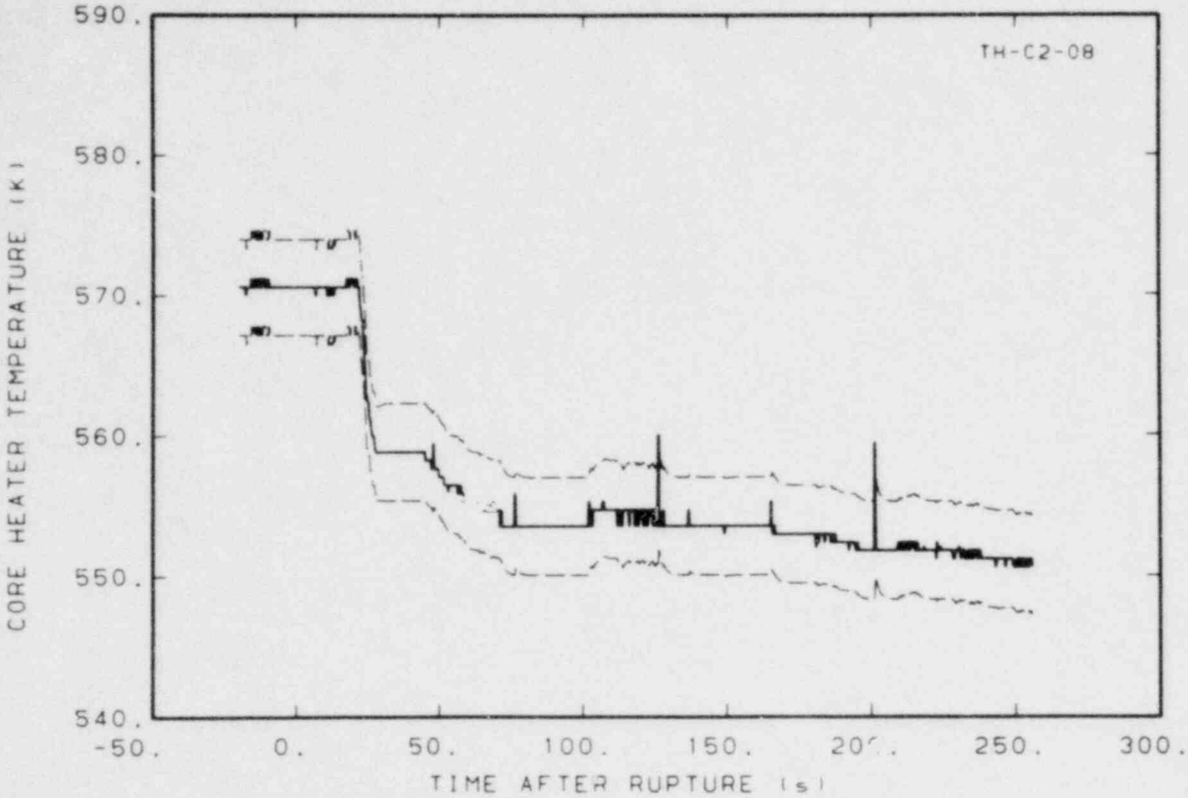

Figure C-21. Core heater temperature, Rod C-2, Test S-SB-2 (TH-C2-08).

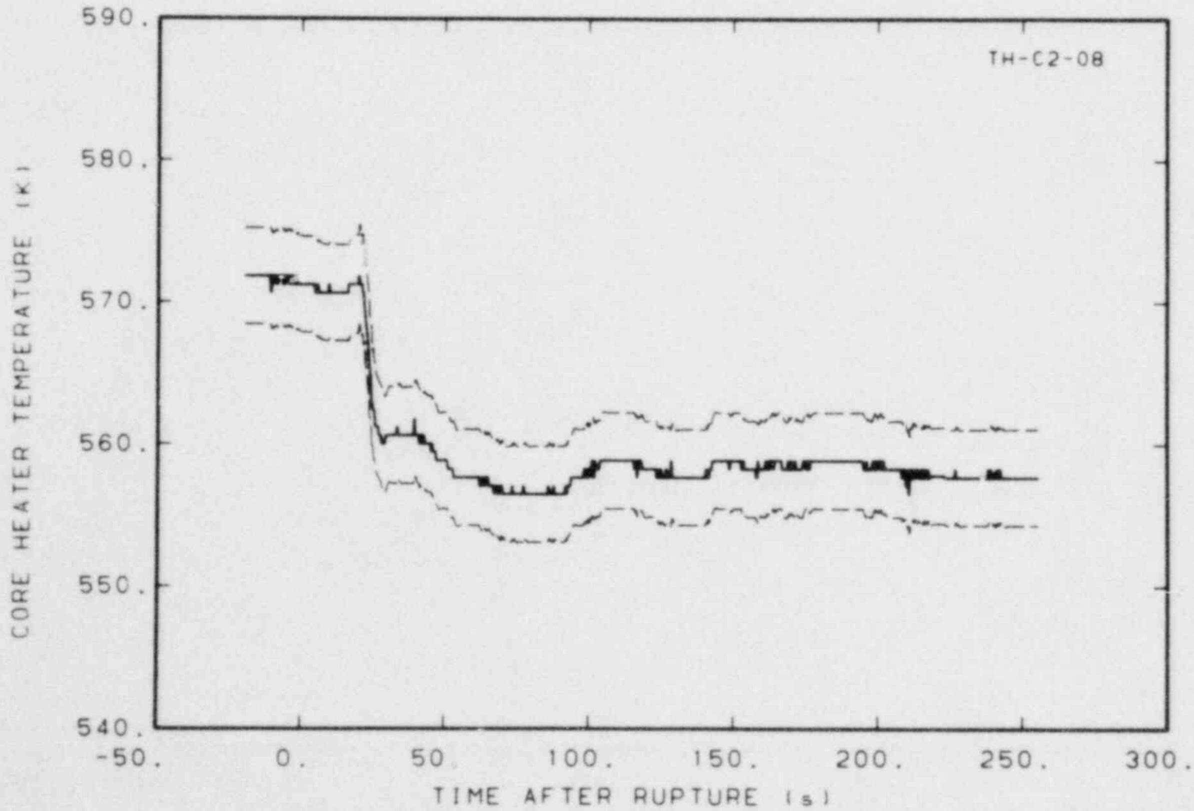

Figure C-22. Core heater temperature, Rod C-2, Test S-SB-2A (TH-C2-08).

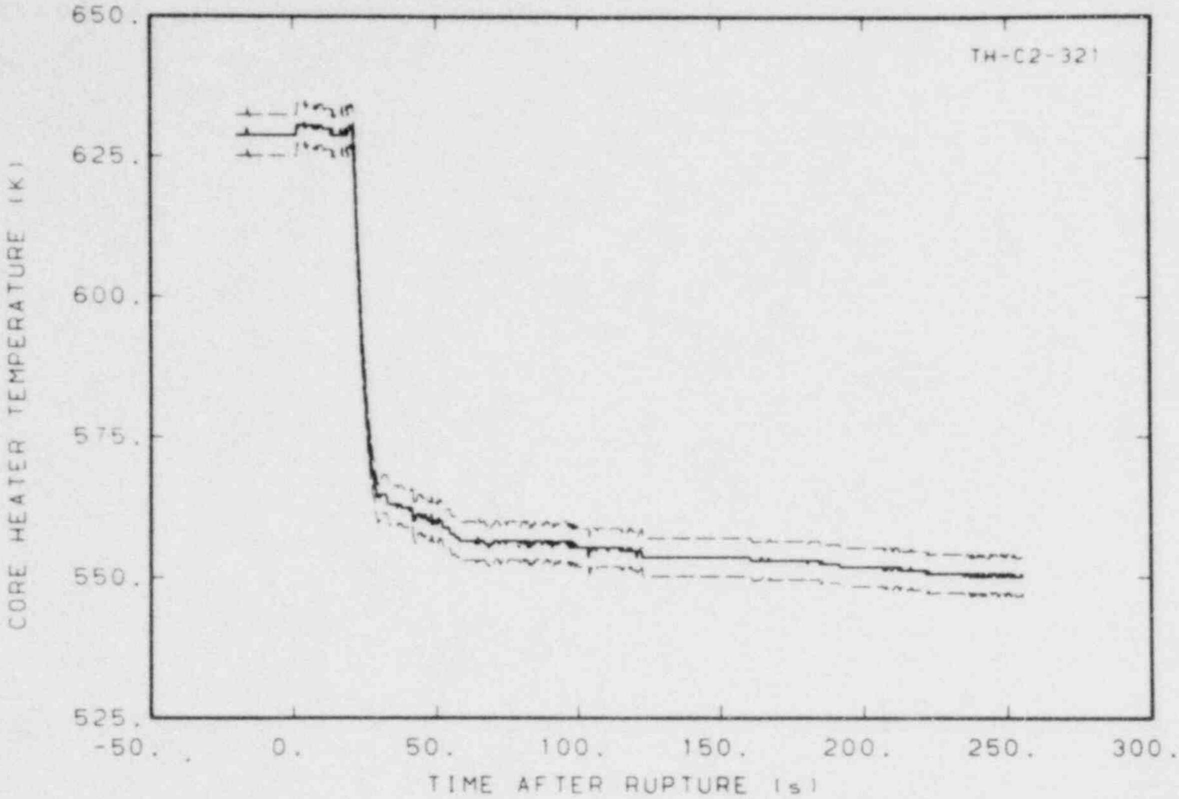

Figure C-23. Core heater temperature, Rod C-2, Test S-SB-2 (TH-C2-321).

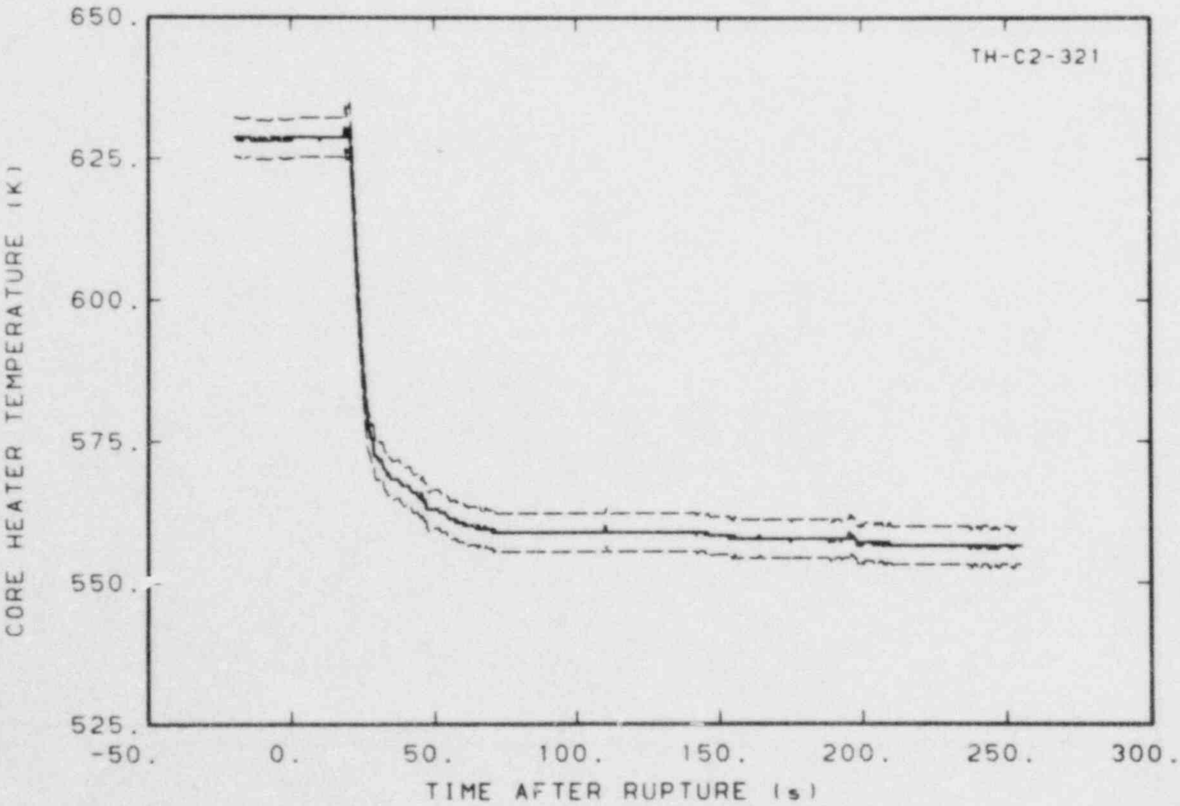

Figure C-24. Core heater temperature, Rod C-2, Test S-SB-2A (TH-C2-321).

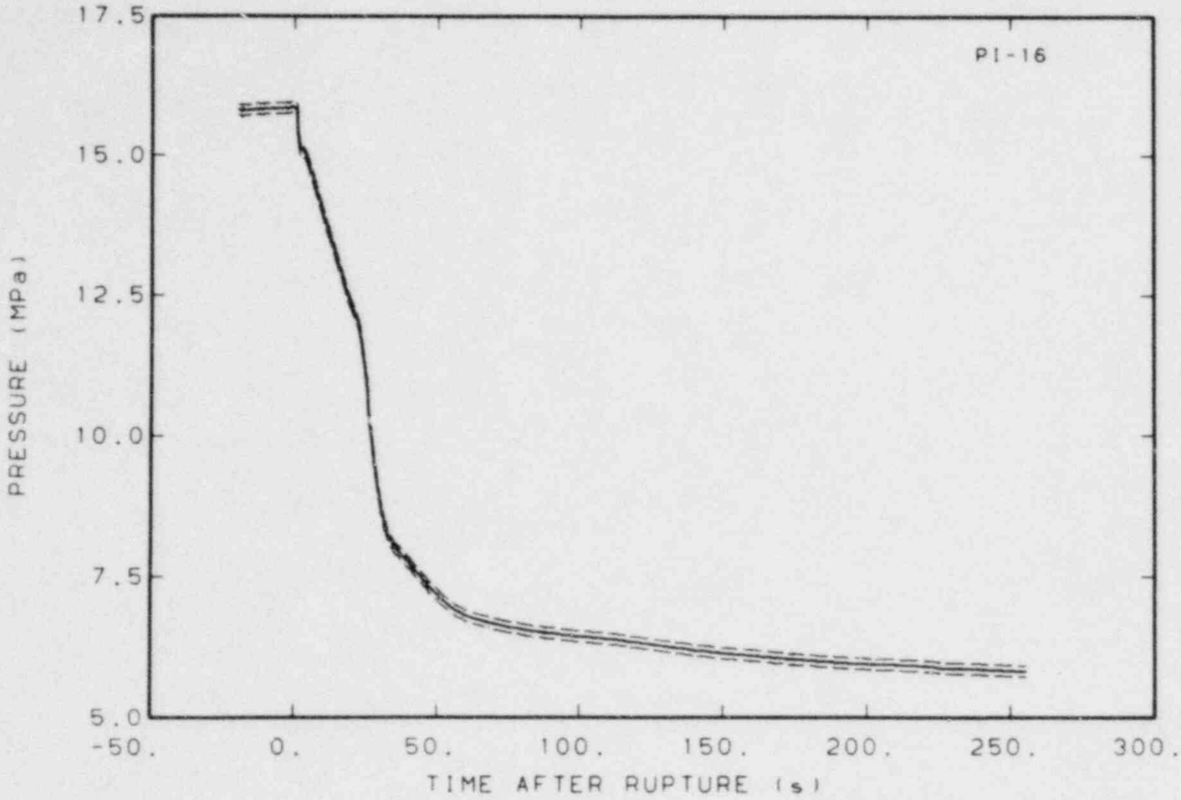

Figure C-25. Pressure in intact loop cold leg, Test S-SB-2 (PI-16).

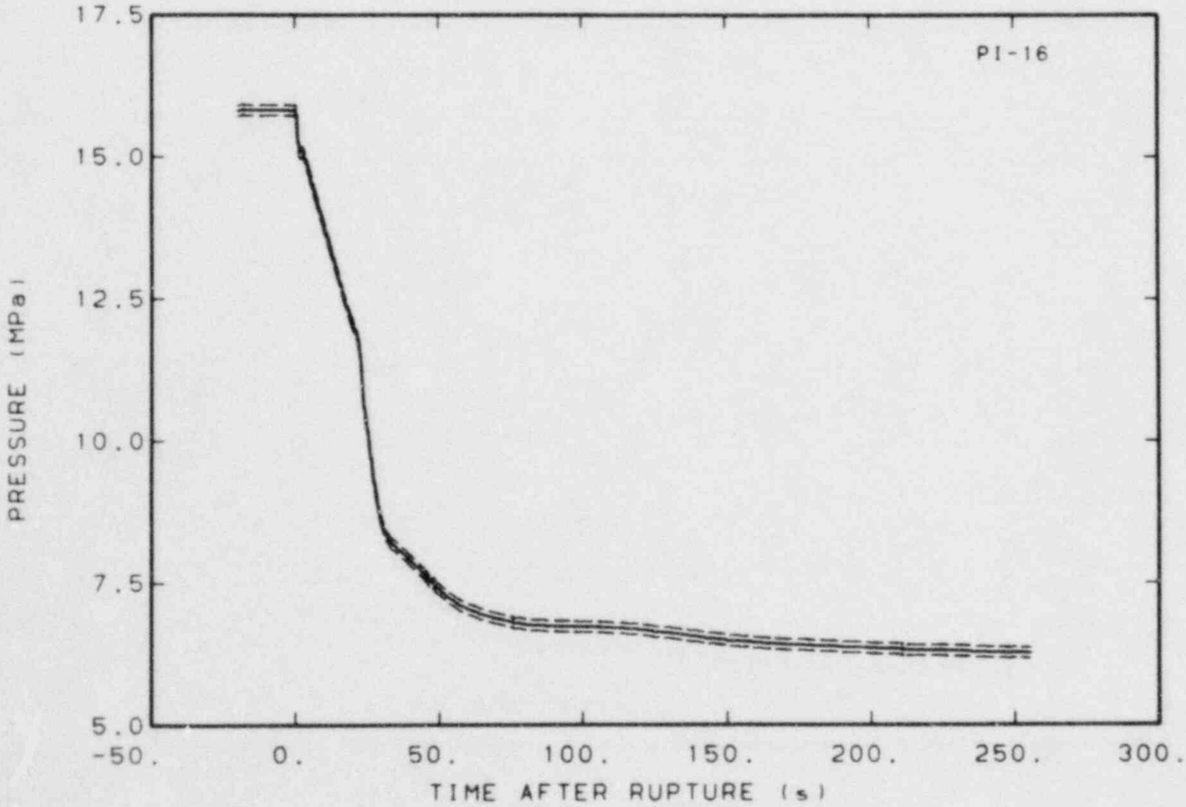

Figure C-26. Pressure in intact loop cold leg, Test S-SB-2A (PI-16).

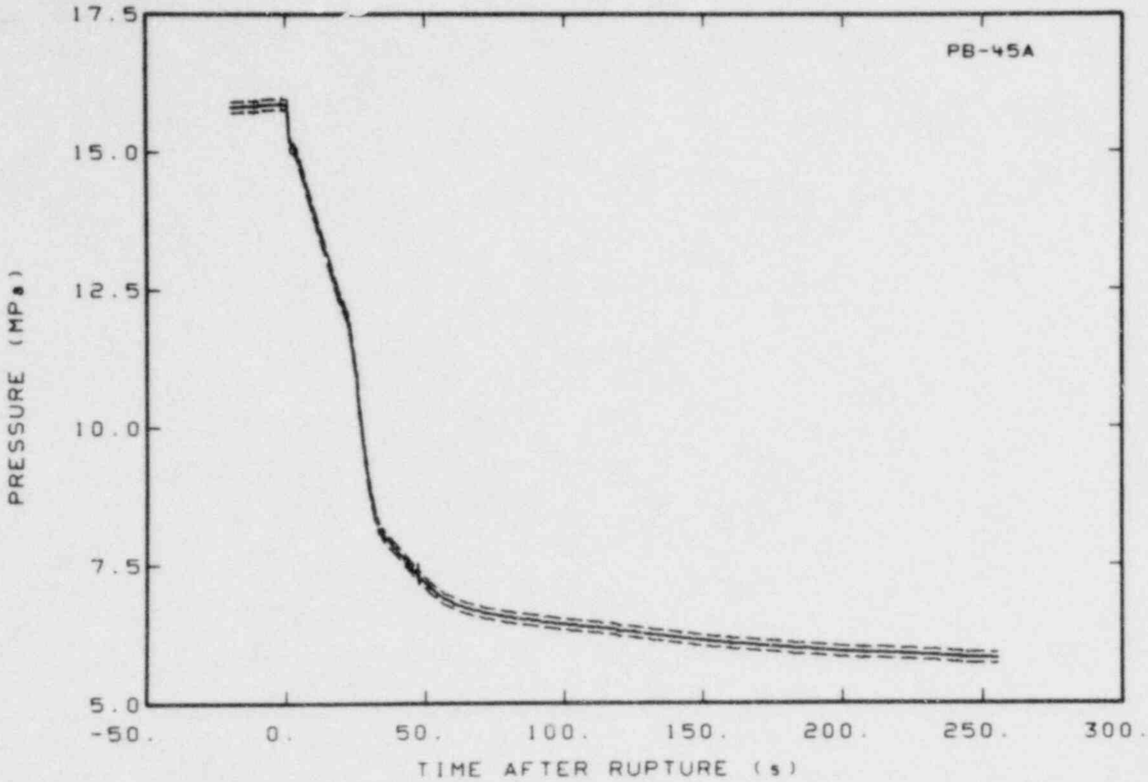

Figure C-27. Pressure in broken loop cold leg, Test S-SB-2 (PB-45A).

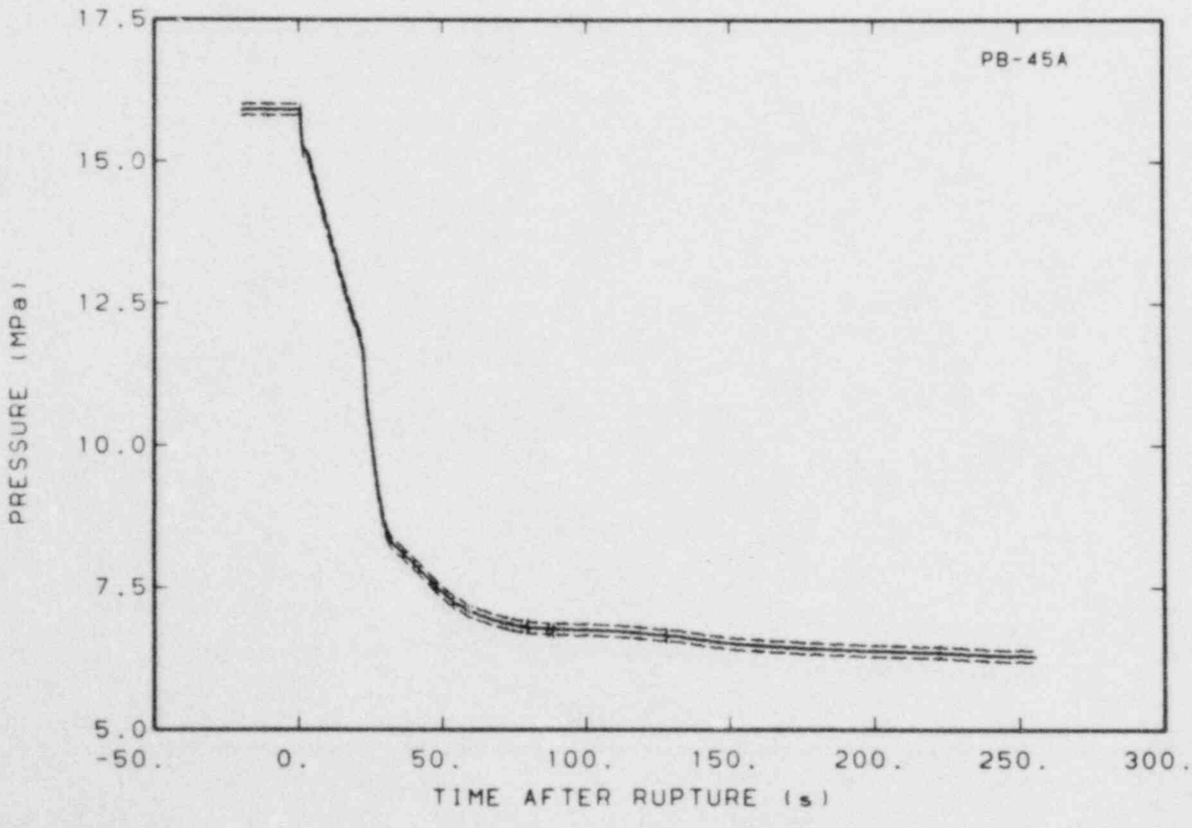

Figure C-28. Pressure in broken loop cold leg, Test S-SB-2A (PB-45A).

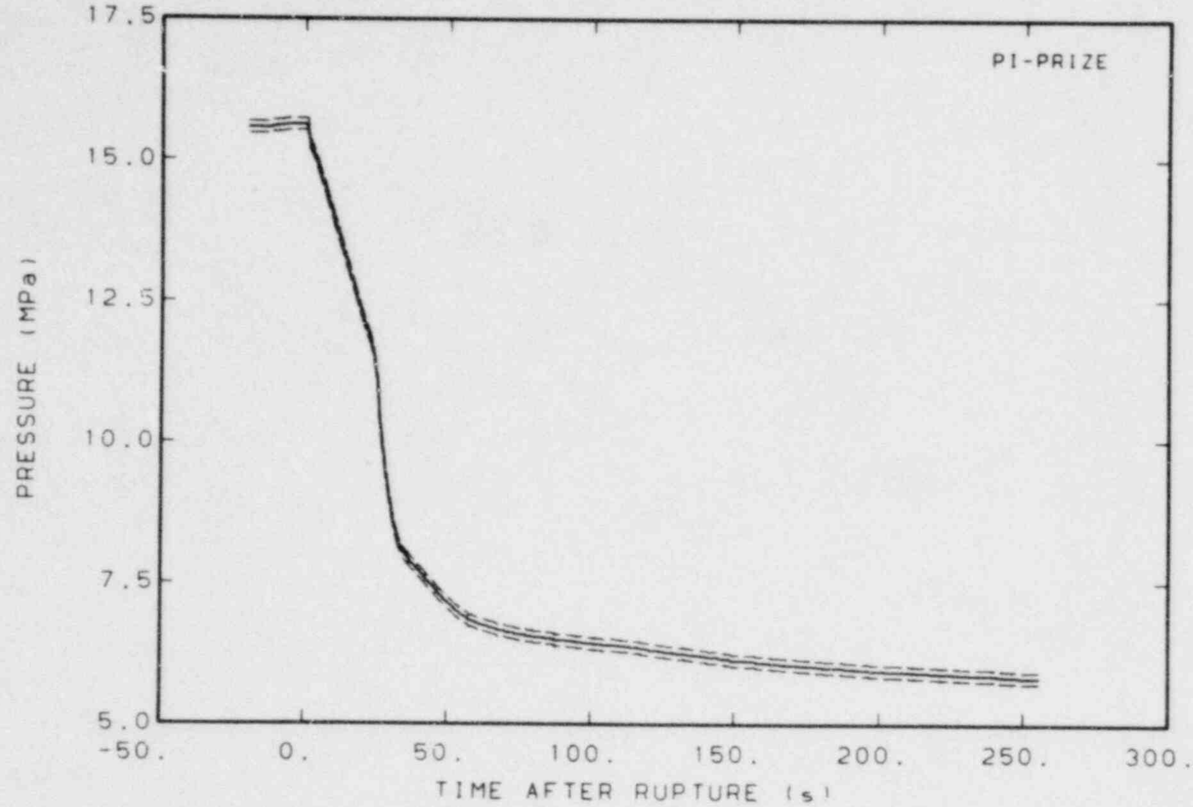

Figure C-29. Pressure in intact loop pressurizer, Test S-SB-2 (PI-PRIZE).

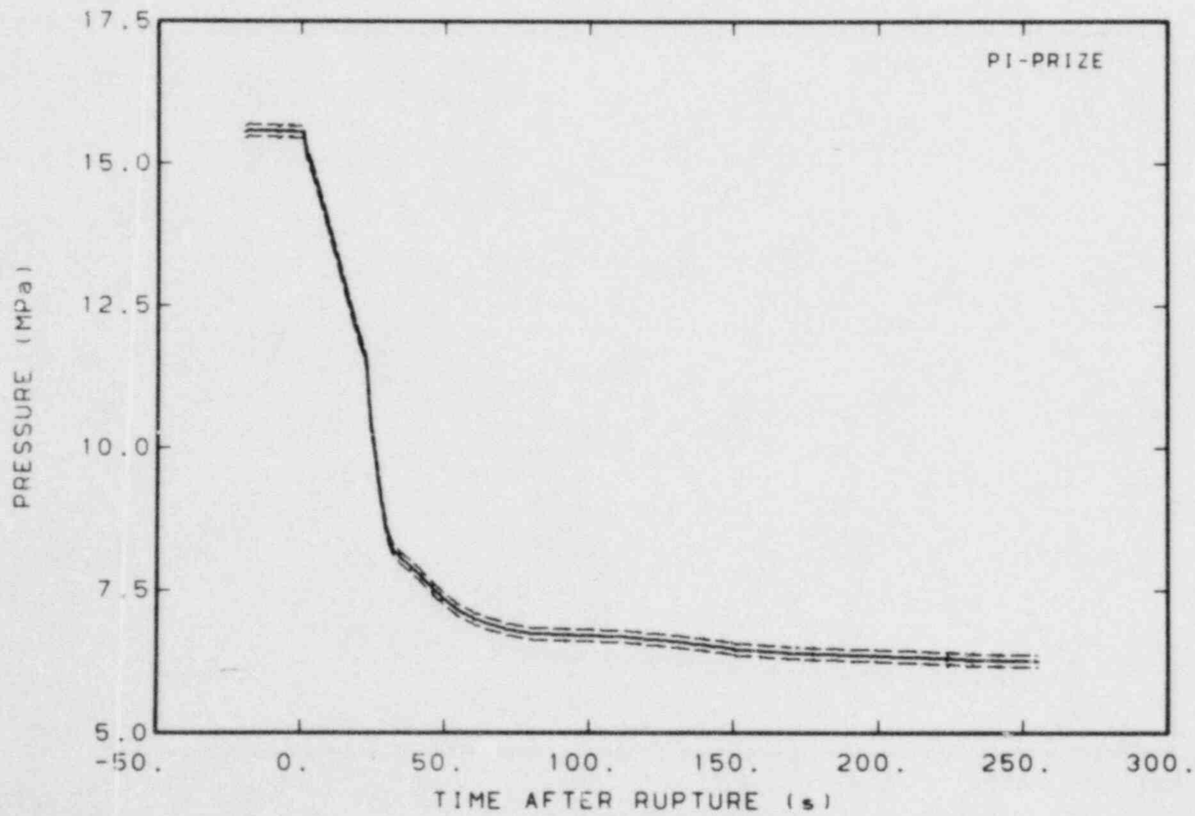

Figure C-30. Pressure in intact loop pressurizer, Test S-SB-2A (PI-PRIZE).

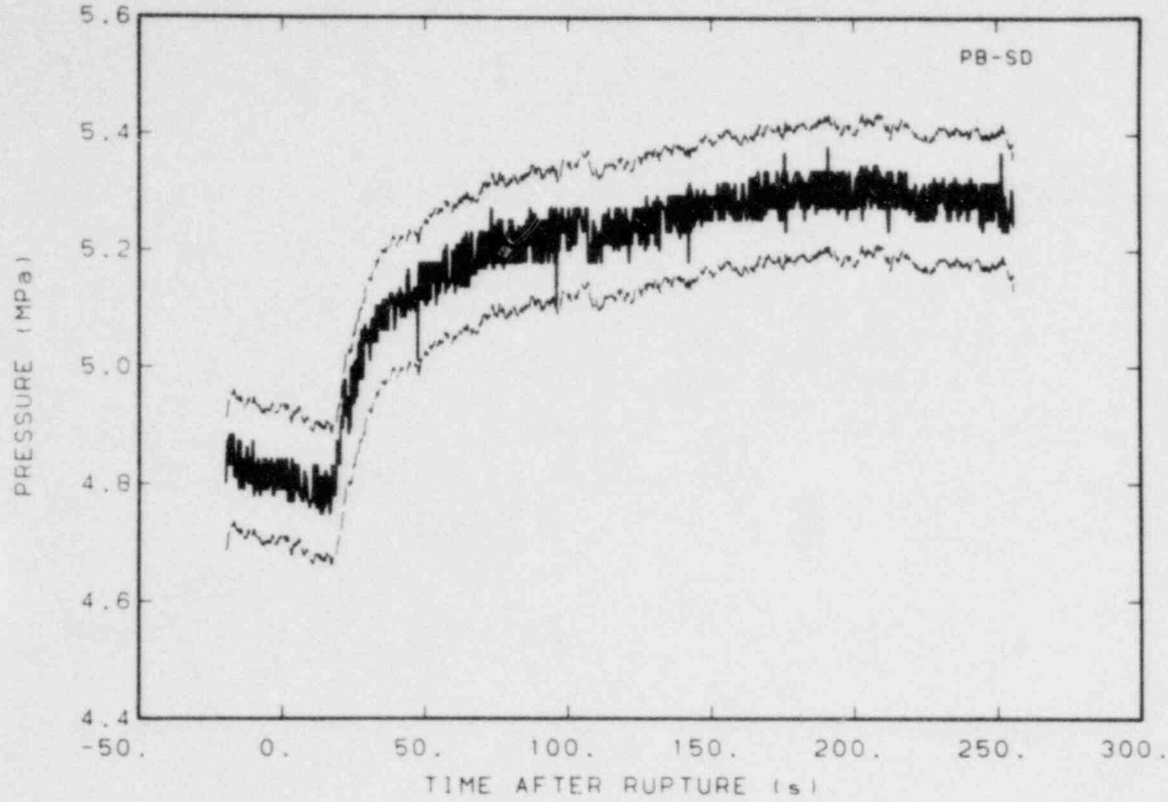

Figure C-31. Pressure in broken loop steam generator dome, Test S-SB-2 (PB-SD).

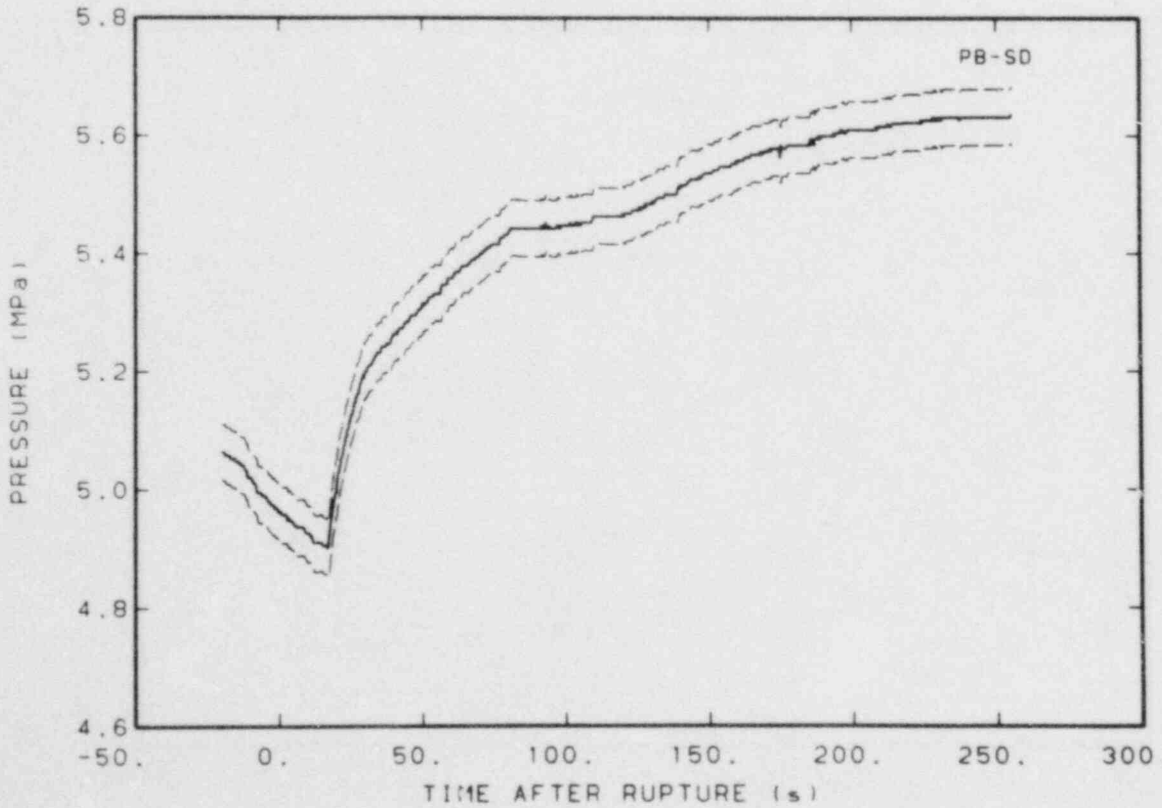

Figure C-32. Pressure in broken loop steam generator dome, Test S-SB-2A (PB-SD).

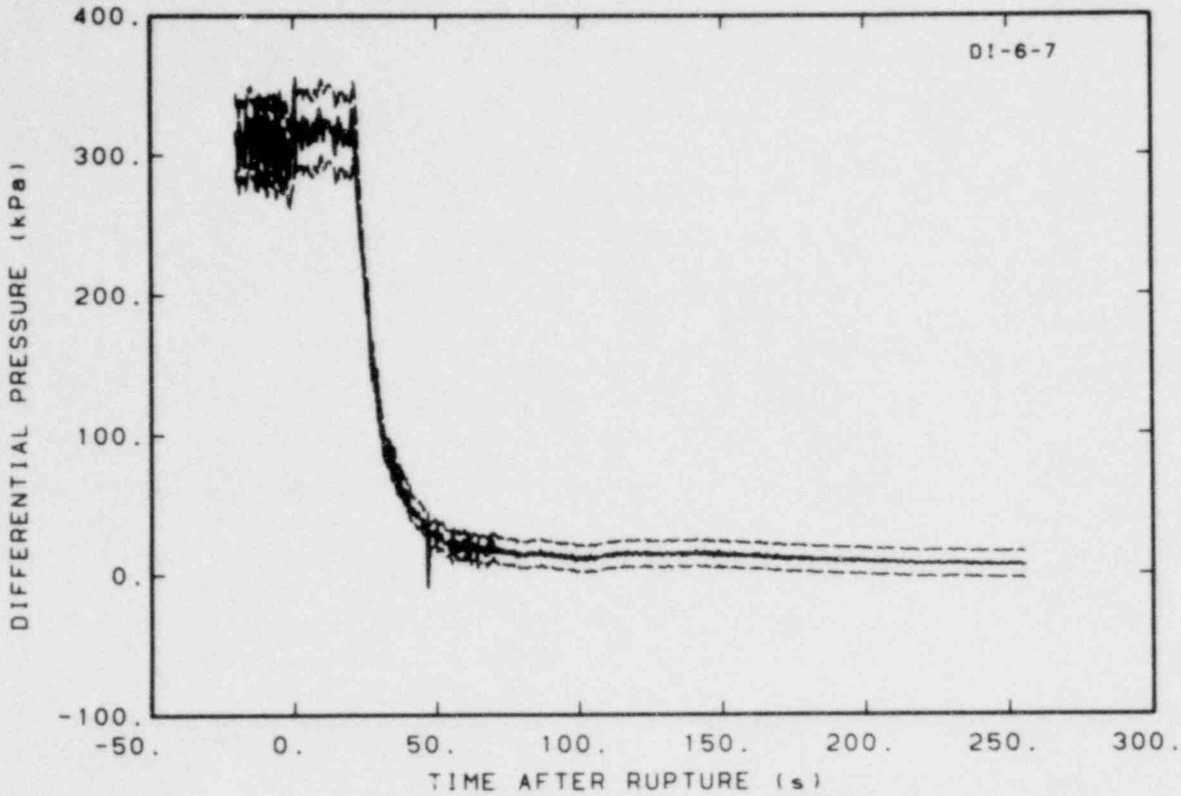

Figure C-33. Differential pressure across intact loop steam generator, Test S-SB-2 (DI-6-7).

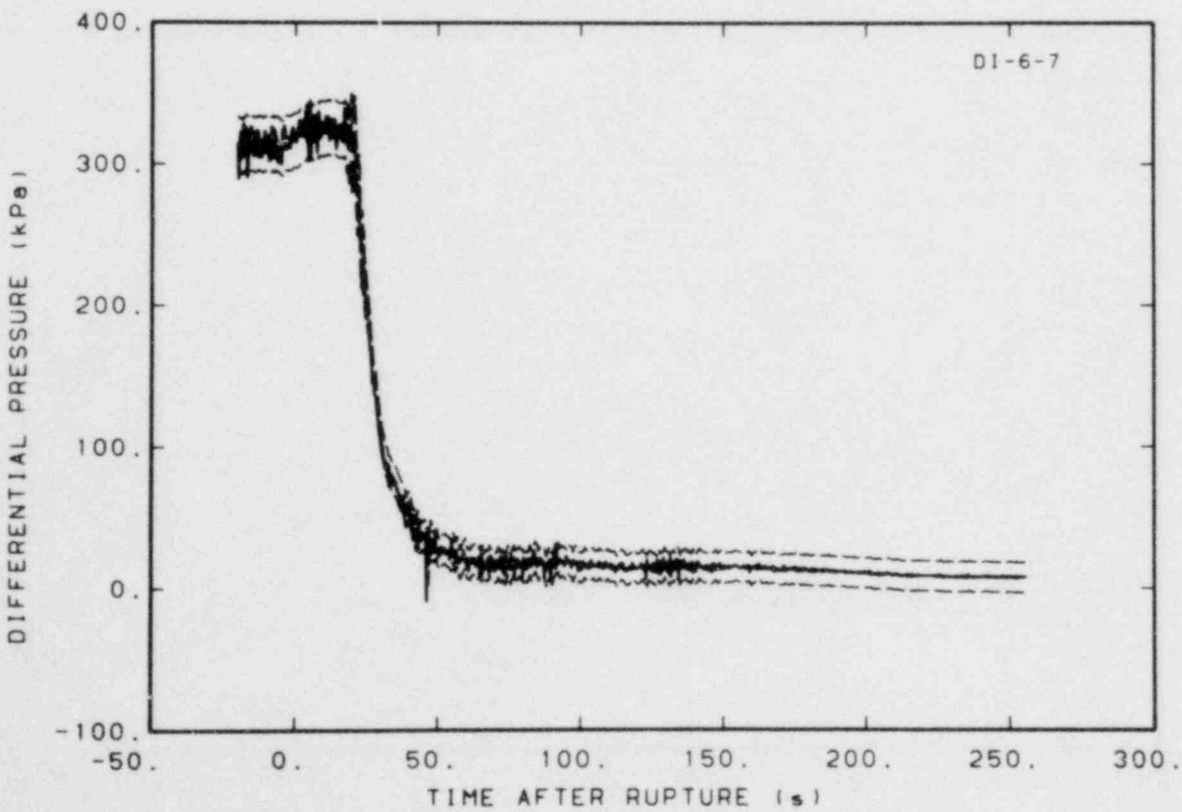

Figure C-34. Differential pressure across intact loop steam generator, Test S-SB-2A (DI-6-7).

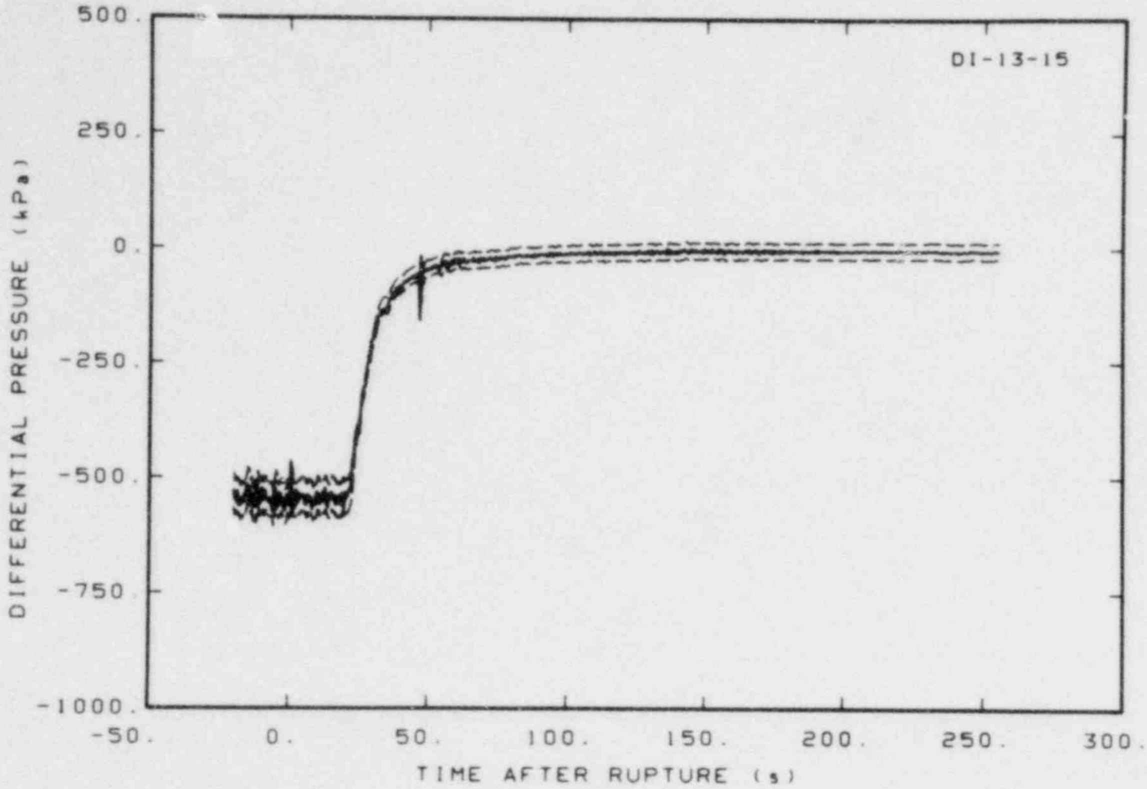

Figure C-35. Differential pressure across intact loop pump, Test S-SB-2 (DI-13-15).

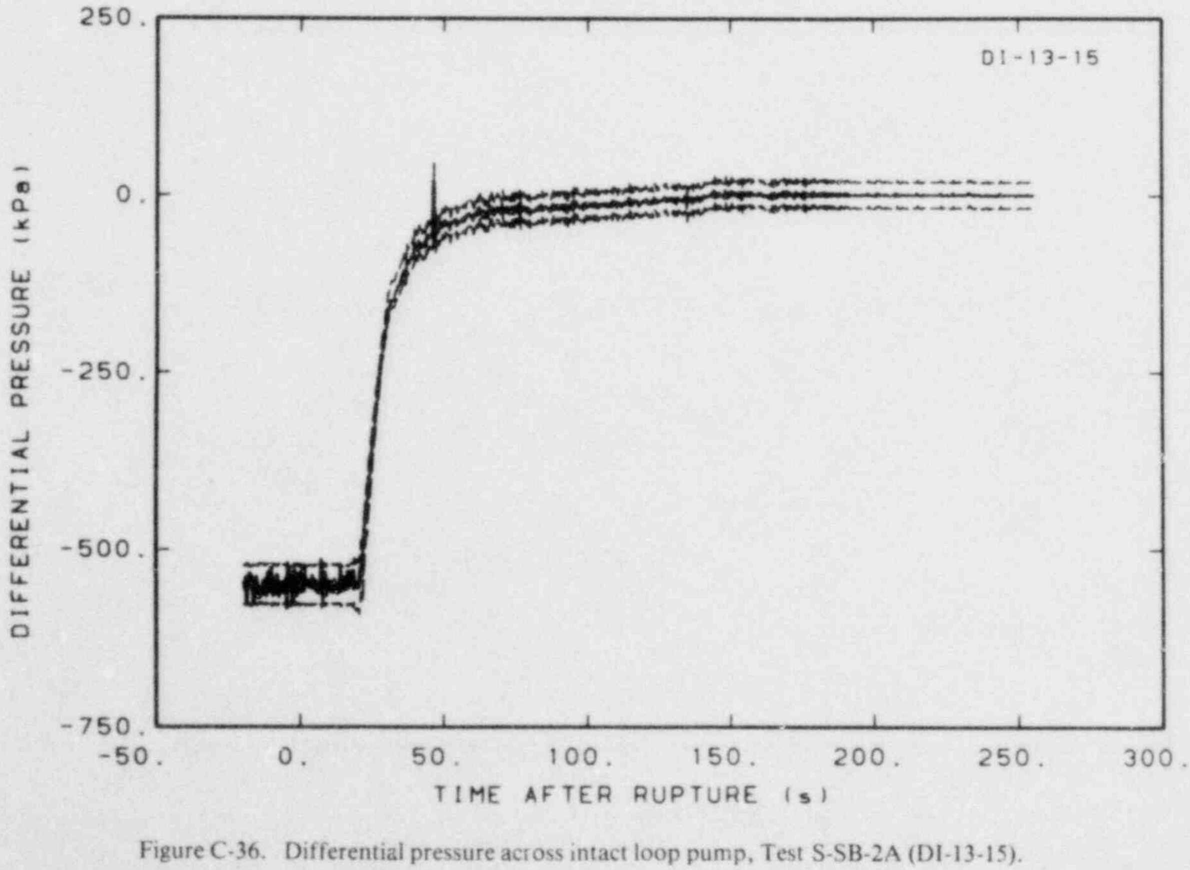

Figure C-36. Differential pressure across intact loop pump, Test S-SB-2A (DI-13-15).

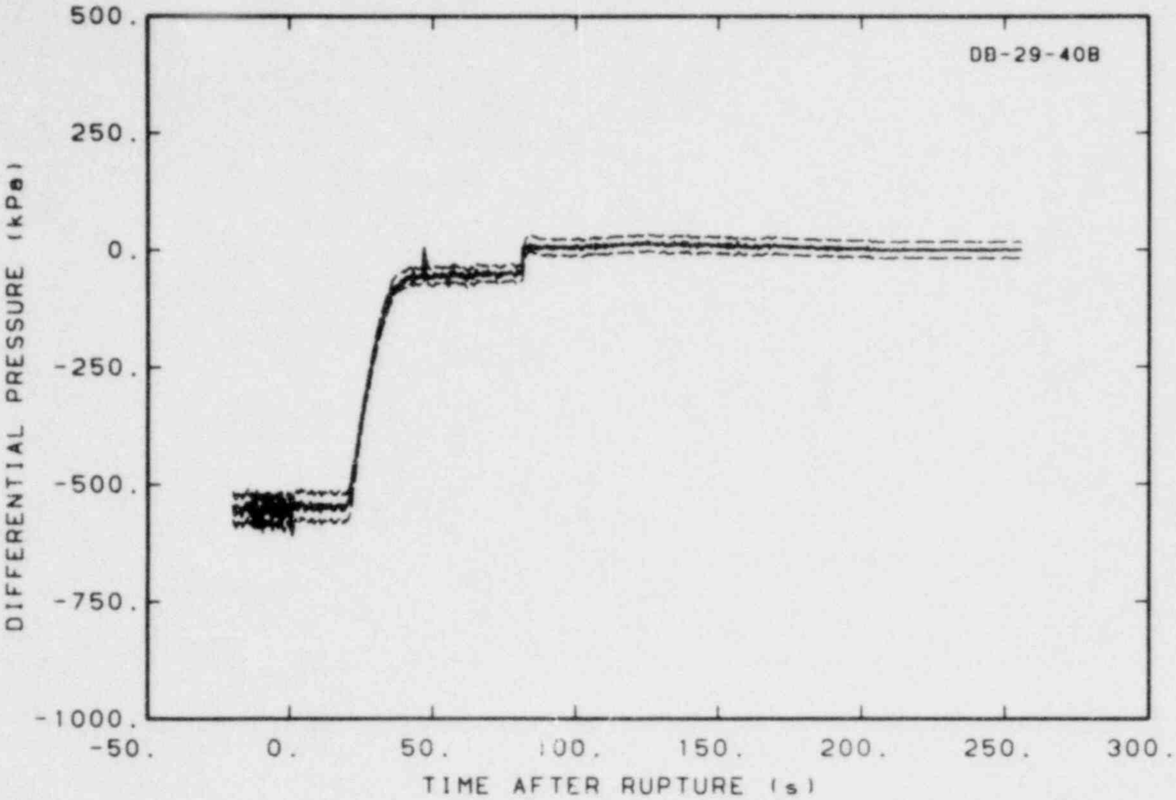

Figure C-37. Differential pressure across broken loop pump, Test S-SB-2 (DB-29-40B).

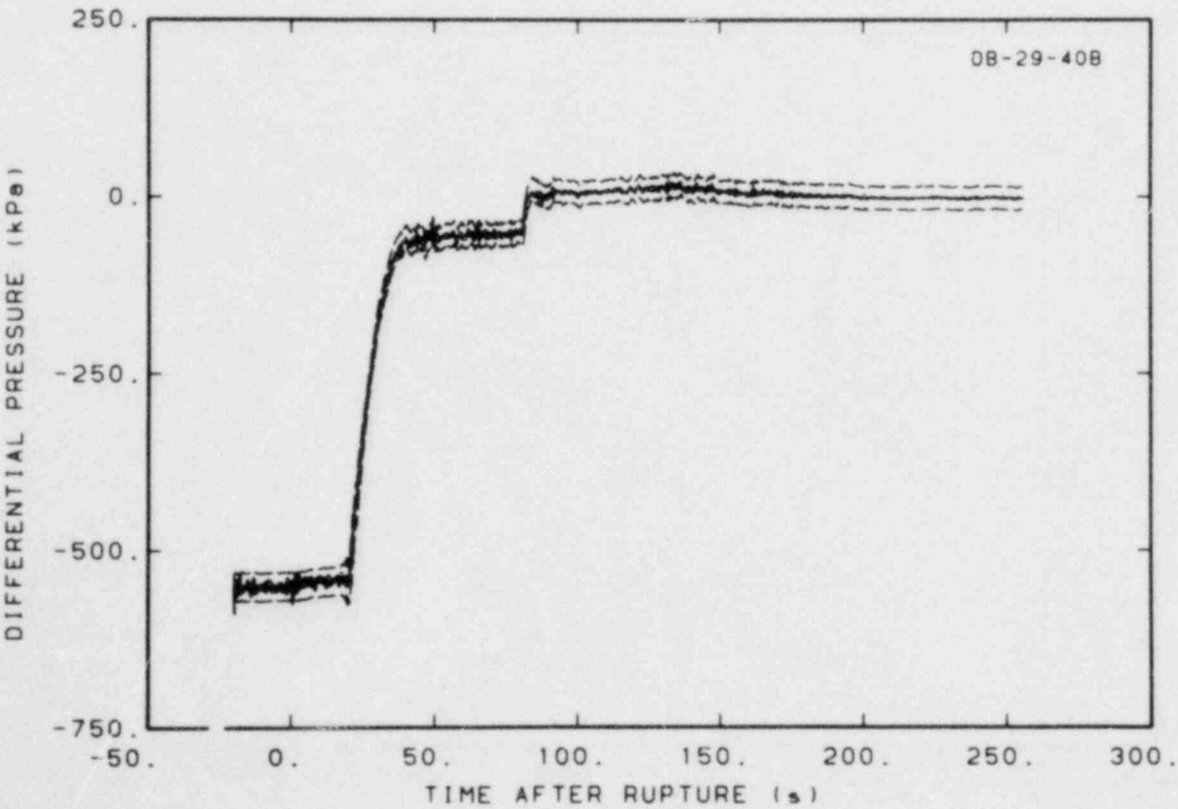

Figure C-38. Differential pressure across broken loop pump, Test S-SB-2A (DB-29-40B).

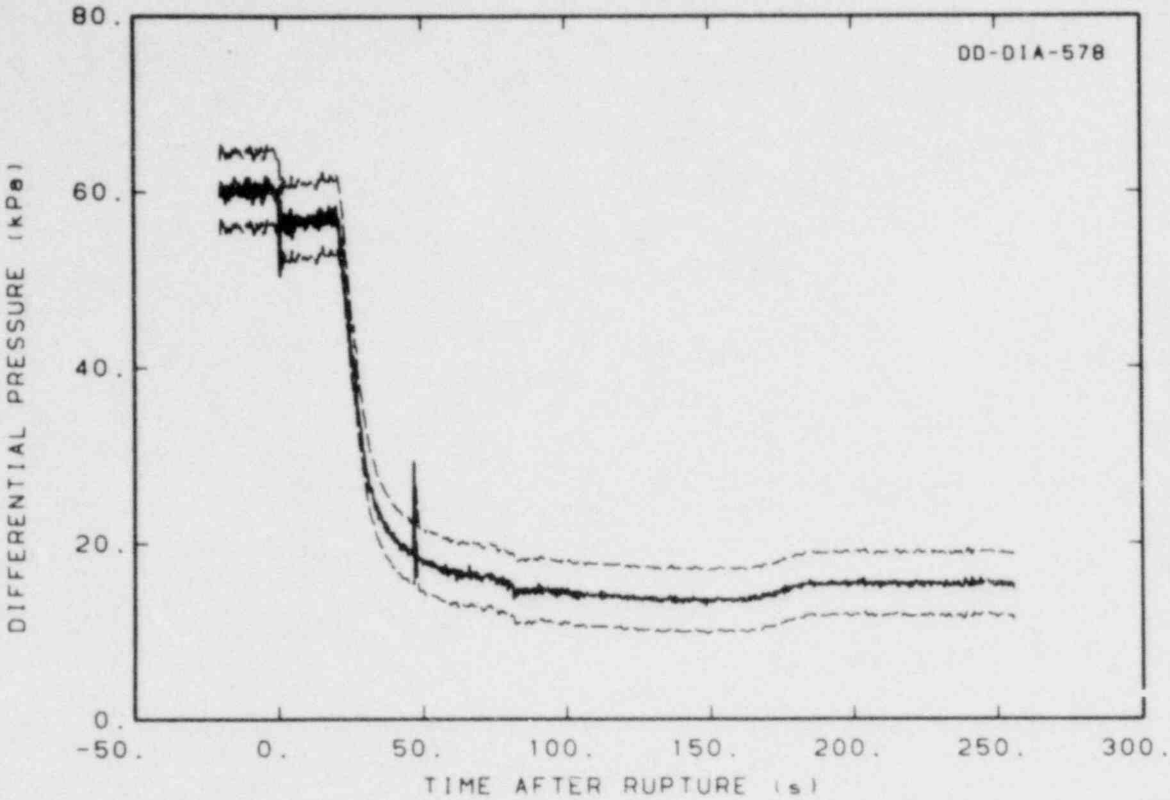

Figure C-39. Differential pressure in downcomer, Test S-SB-2 (DD-DIA-578).

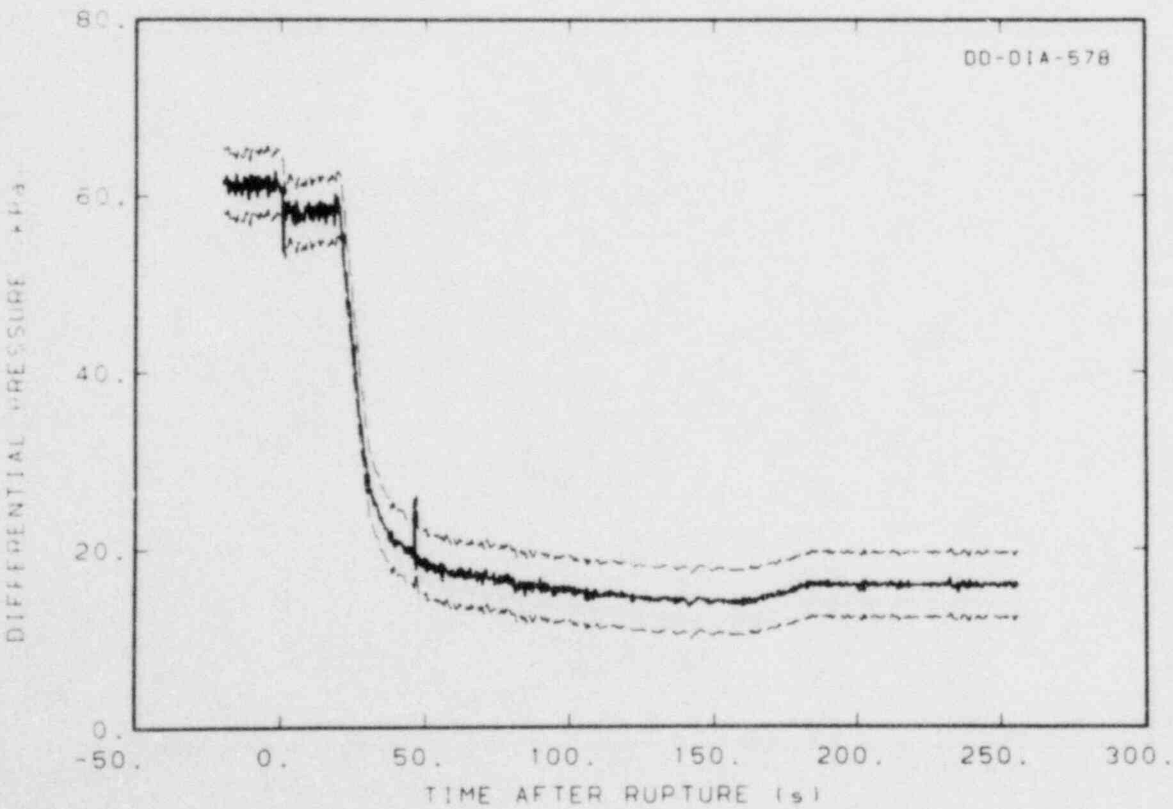

Figure C-40. Differential pressure in downcomer, Test S-SB-2A (DD-DIA-578).

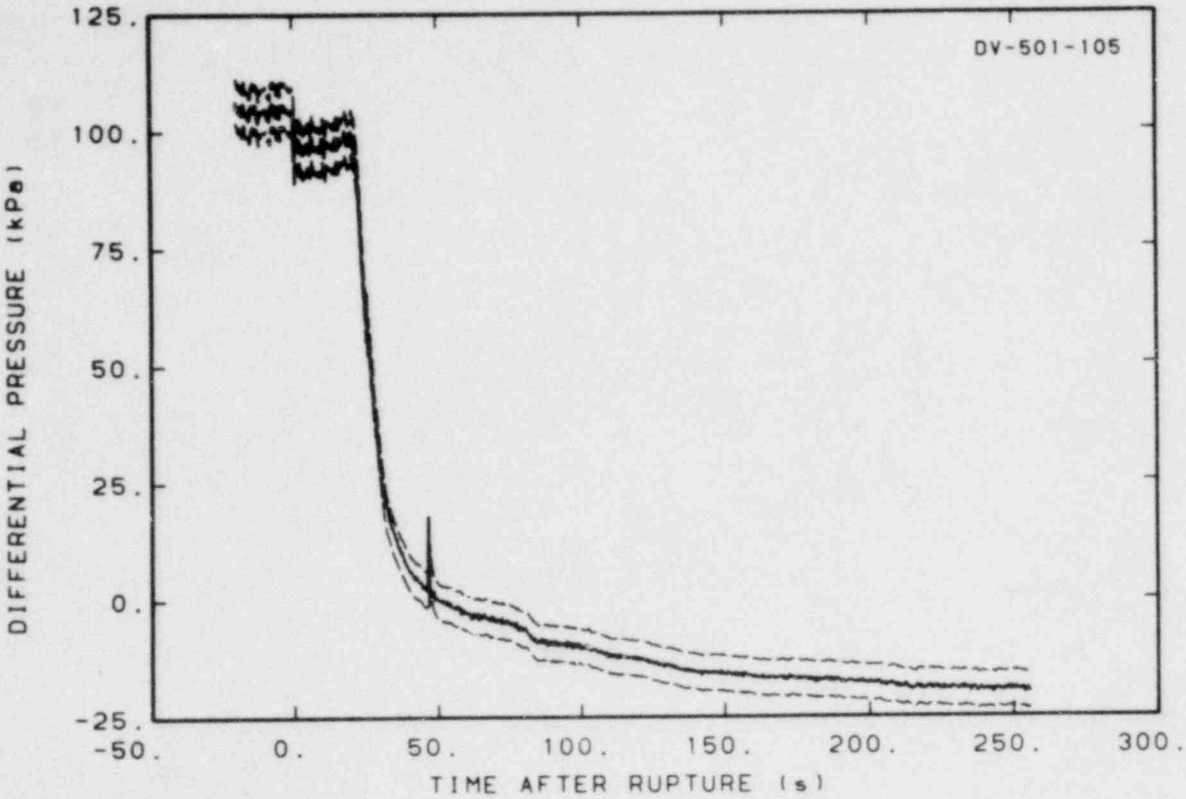

Figure C-41. Differential pressure in vessel, Test S-SB-2 (DV-501-105).

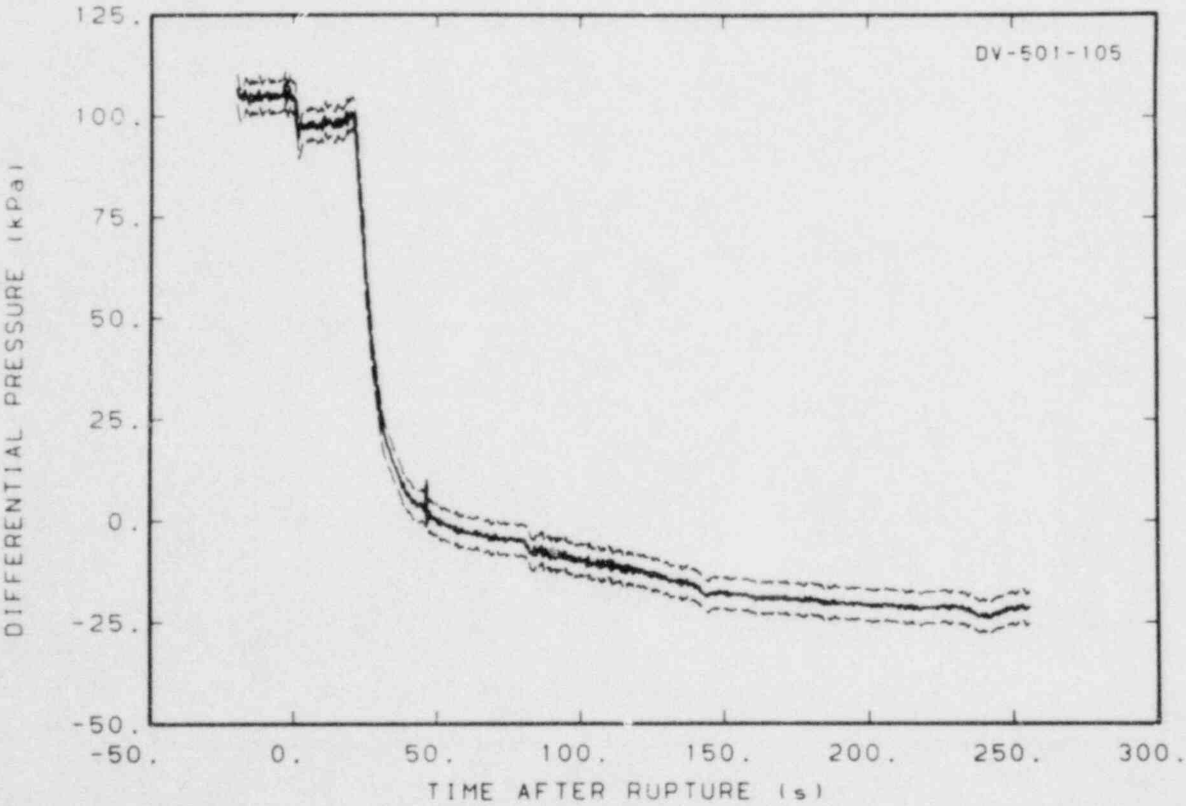

Figure C-42. Differential pressure in vessel, Test S-SB-2A (DV-501-105).

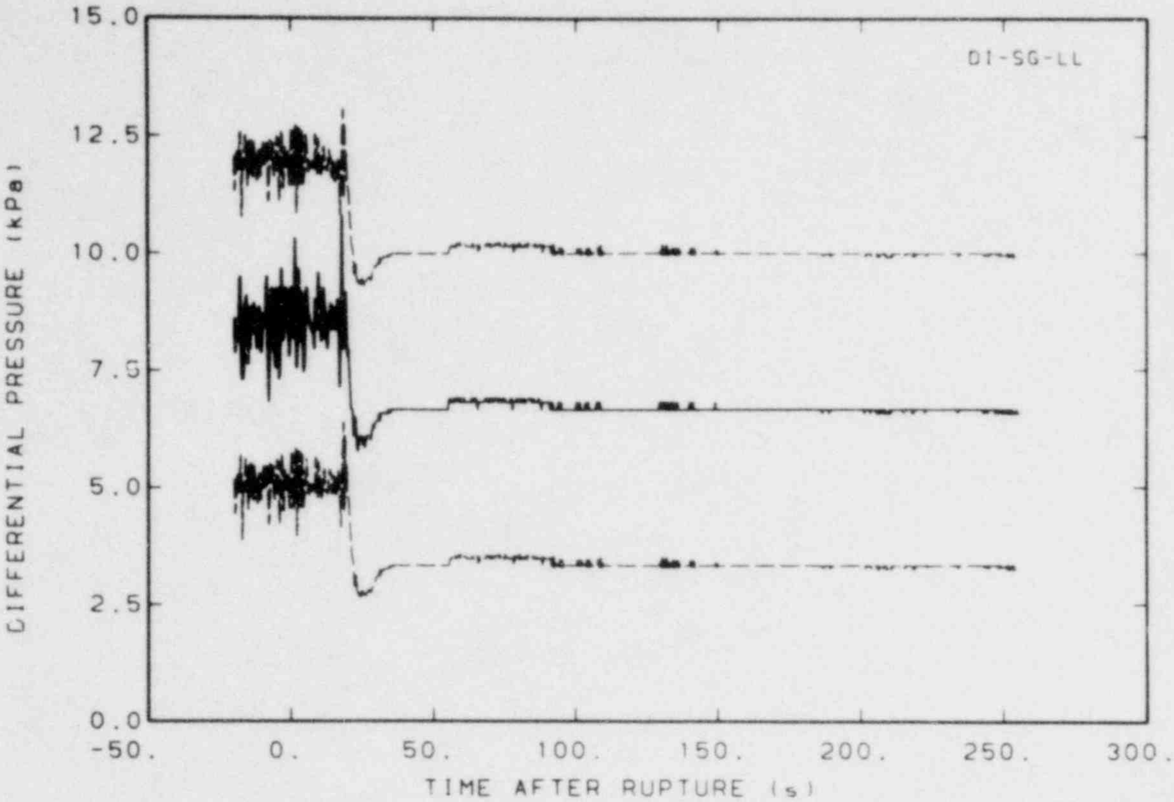

Figure C-43. Differential pressure, intact loop steam generator, secondary side, liquid level, Test S-SB-2 (DI-SG-LL).

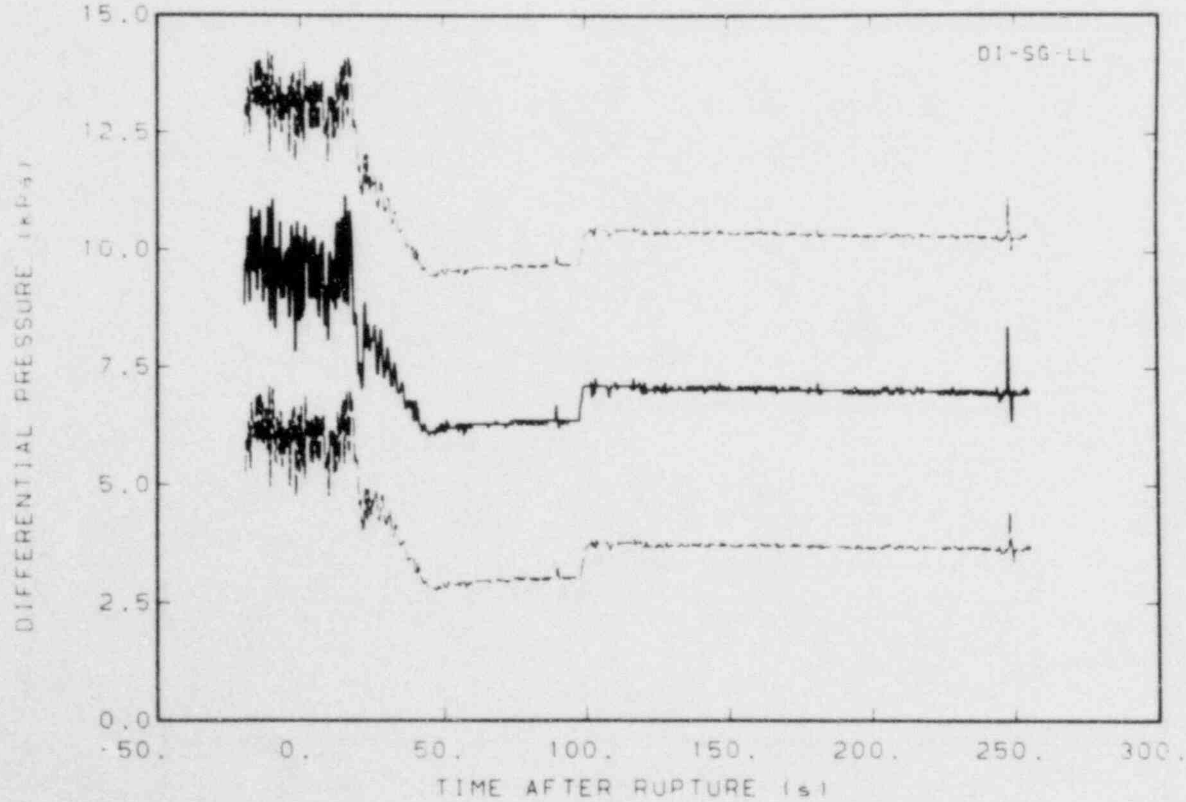

Figure C-44. Differential pressure, intact loop steam generator, secondary side, liquid level, Test S-SB-2A (DI-SG-LL).

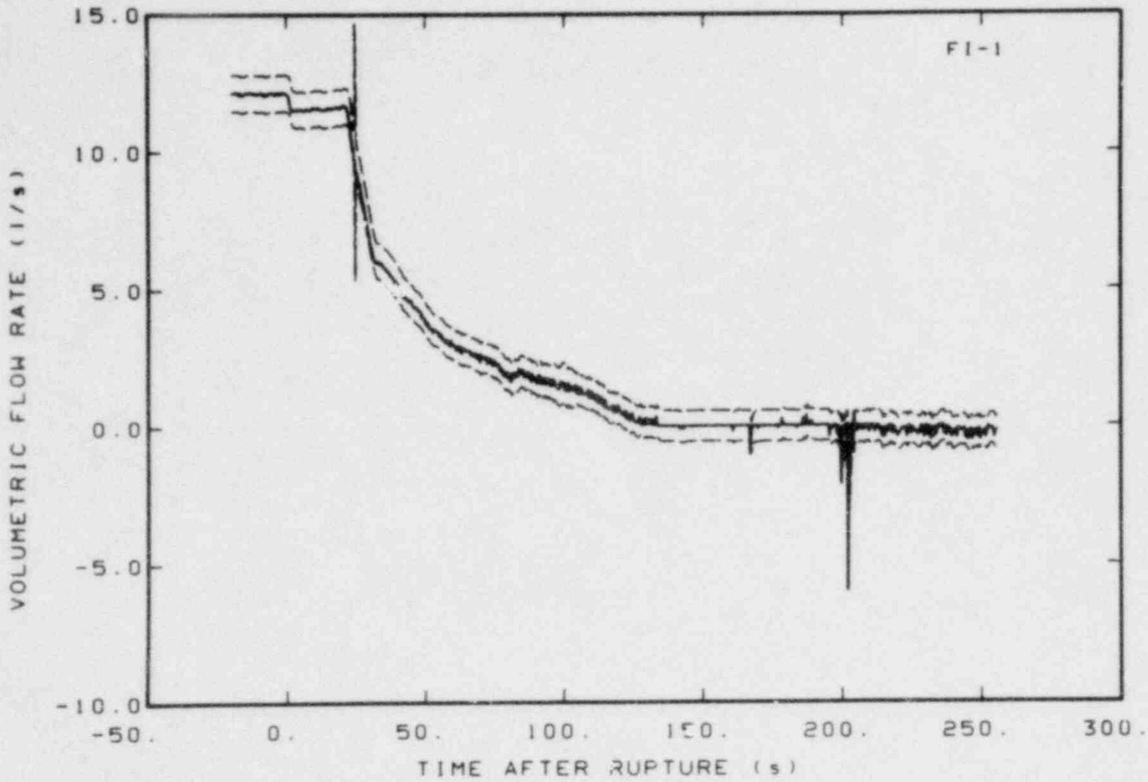

Figure C-45. Volumetric Flow rate in intact loop hot leg, Test S-SB-2 (FI-1).

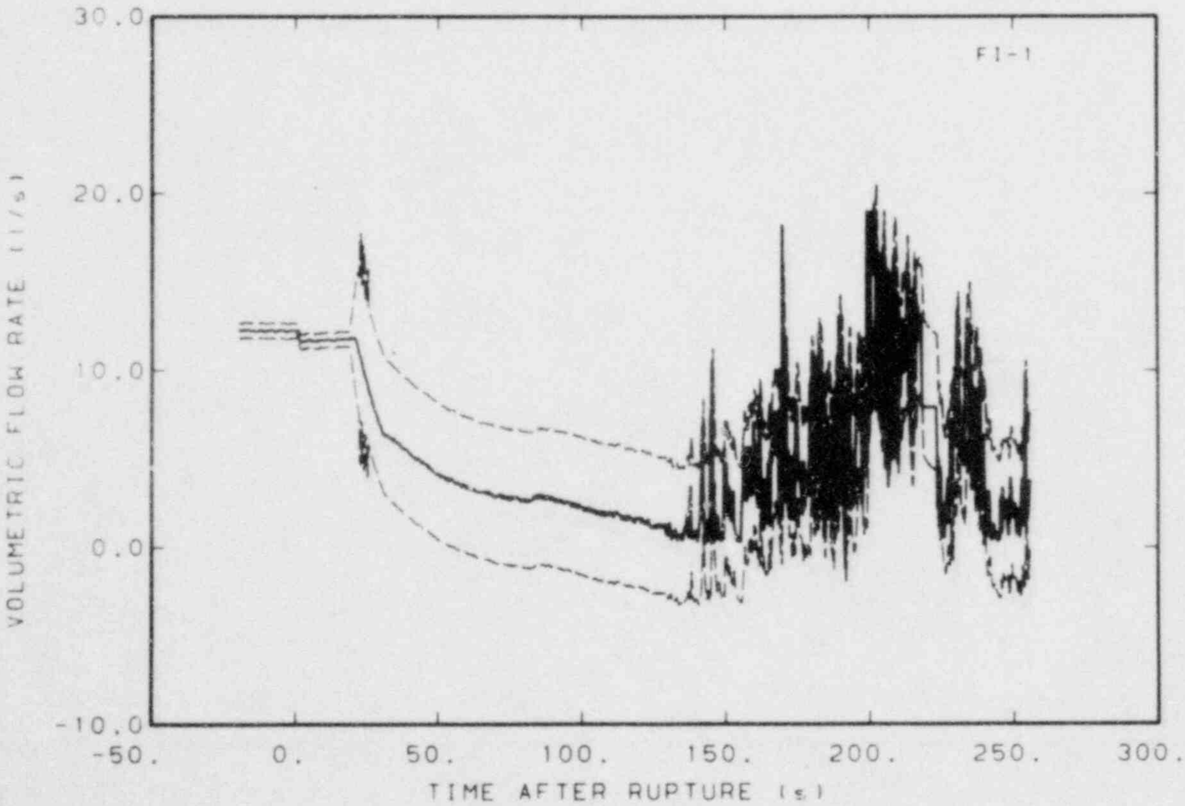

Figure C-46. Volumetric Flow rate in intact loop hot leg, Test S-SB-2A (FI-1).

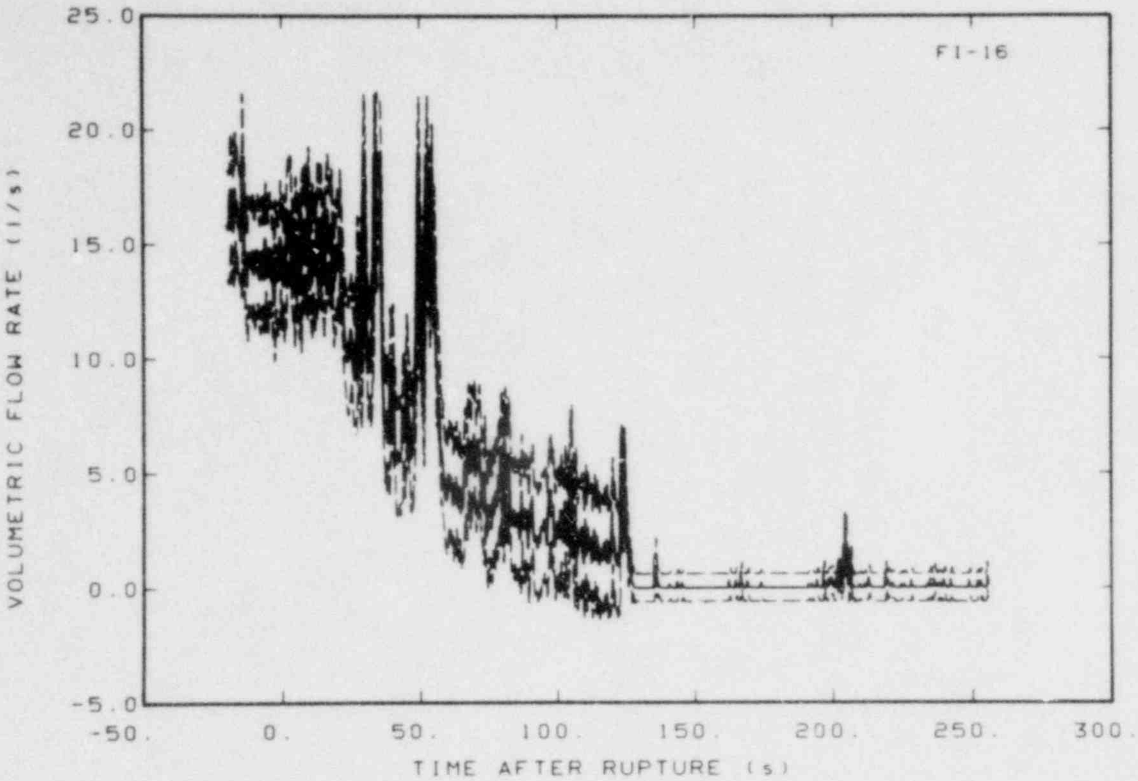

Figure C-47. Volumetric Flow rate in intact loop cold leg, Test S-SB-2 (FI-16).

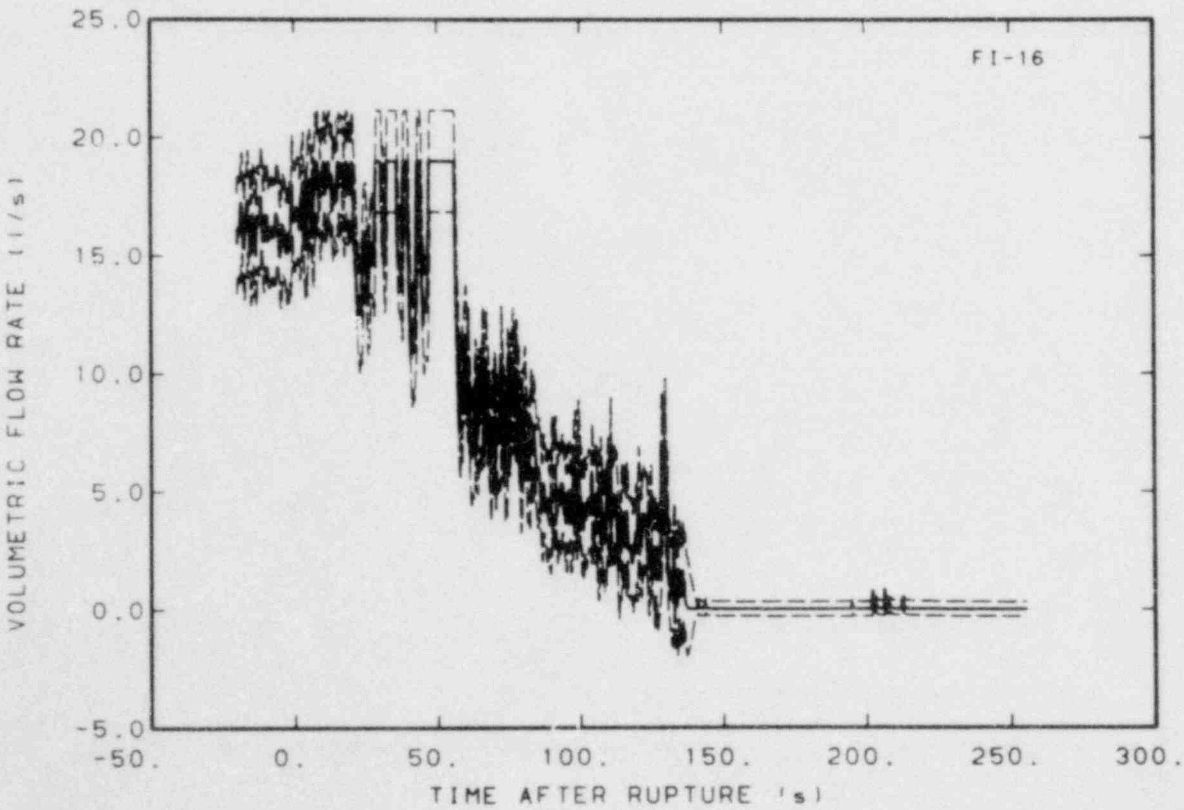

Figure C-48. Volumetric Flow rate in intact loop cold leg, Test S-SB-2A (FI-16).

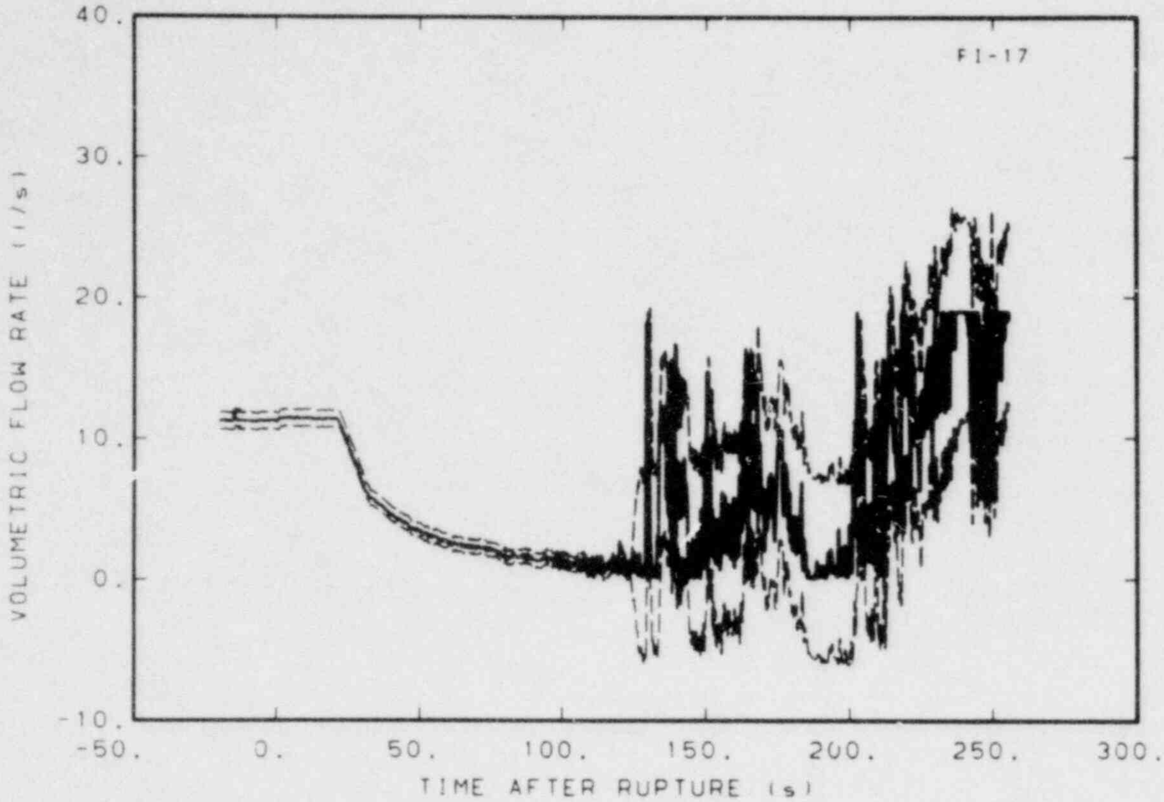

Figure C-49. Volumetric Flow rate in intact loop cold leg, Test S-SB-2 (FI-17).

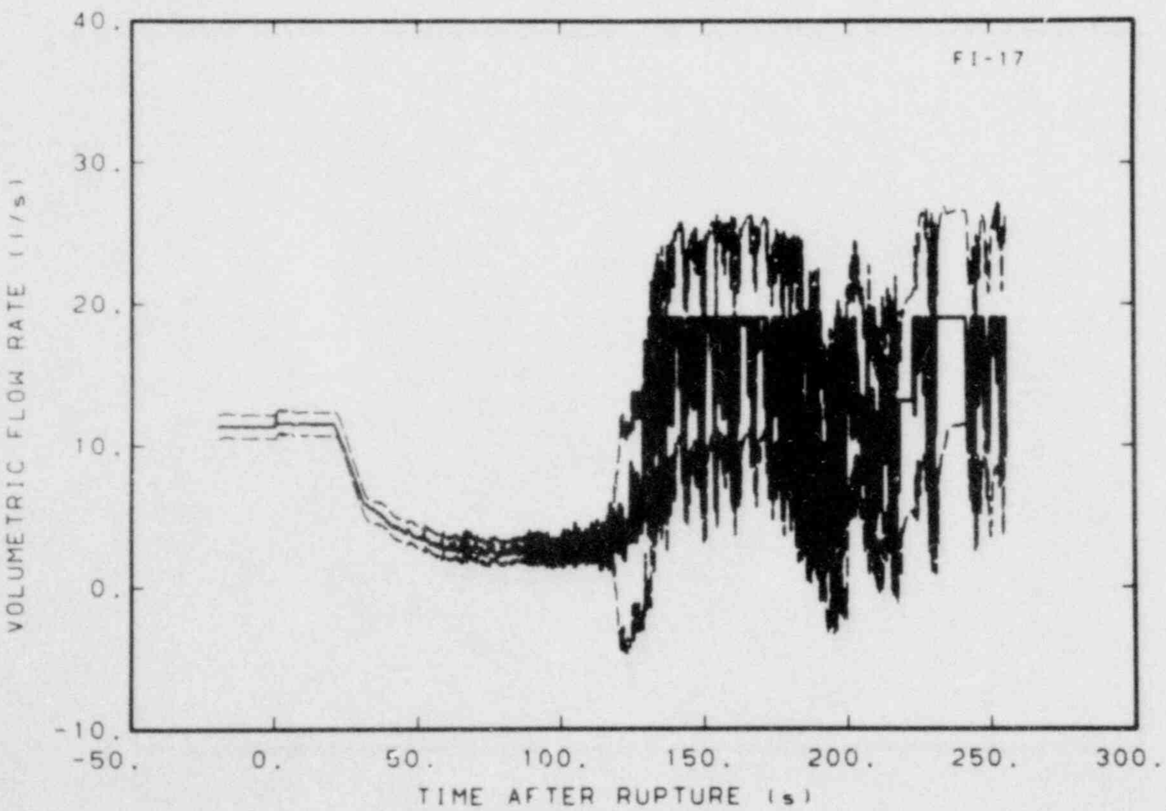

Figure C-50. Volumetric Flow rate in intact loop cold leg, Test S-SB-2A (FI-17).

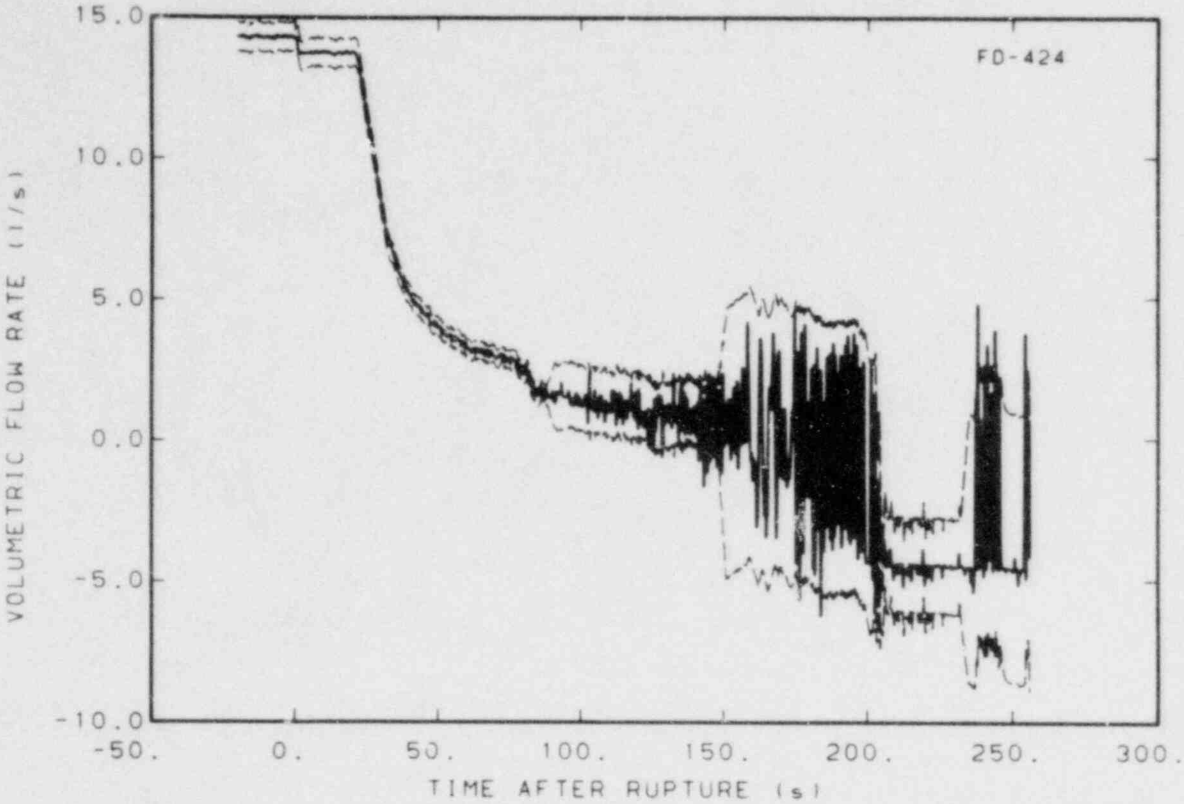

Figure C-51. Volumetric Flow rate in downcomer, Test S-SB-2 (FD-424).

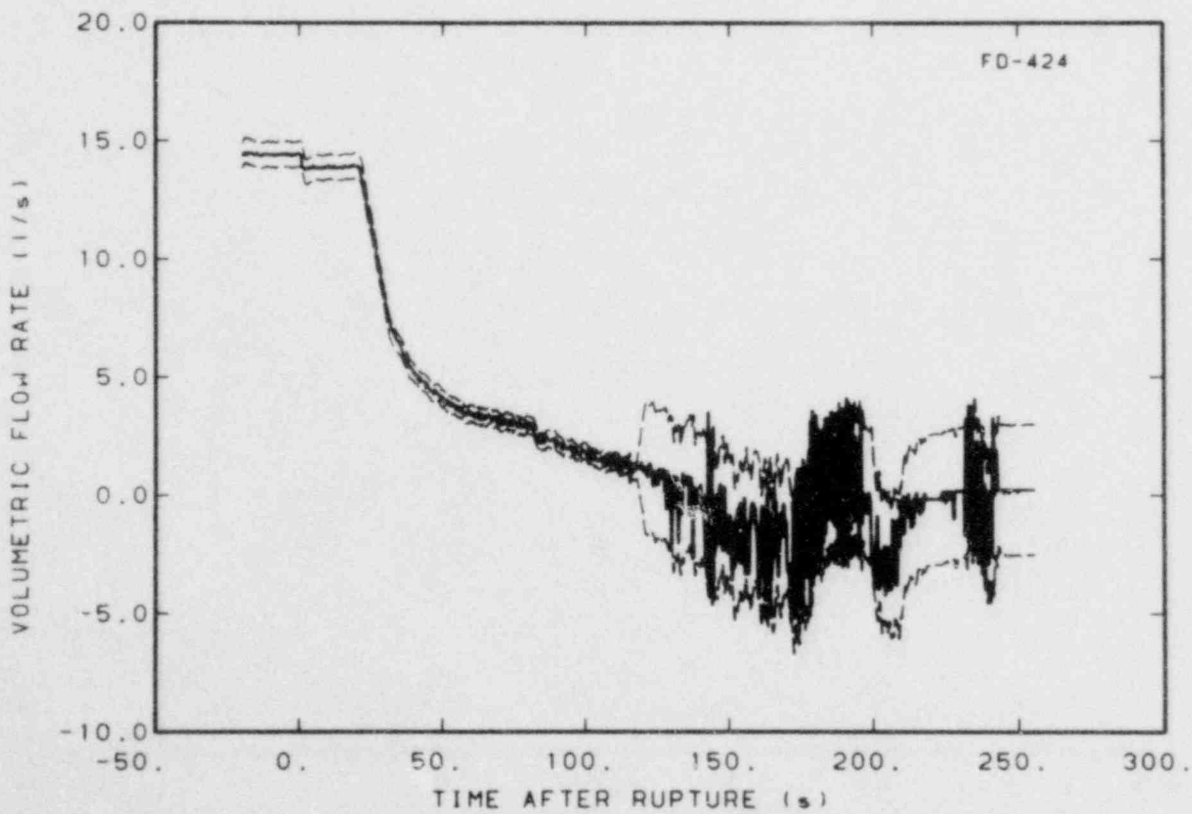

Figure C-52. Volumetric Flow rate in downcomer, Test S-SB-2A (FD-424).

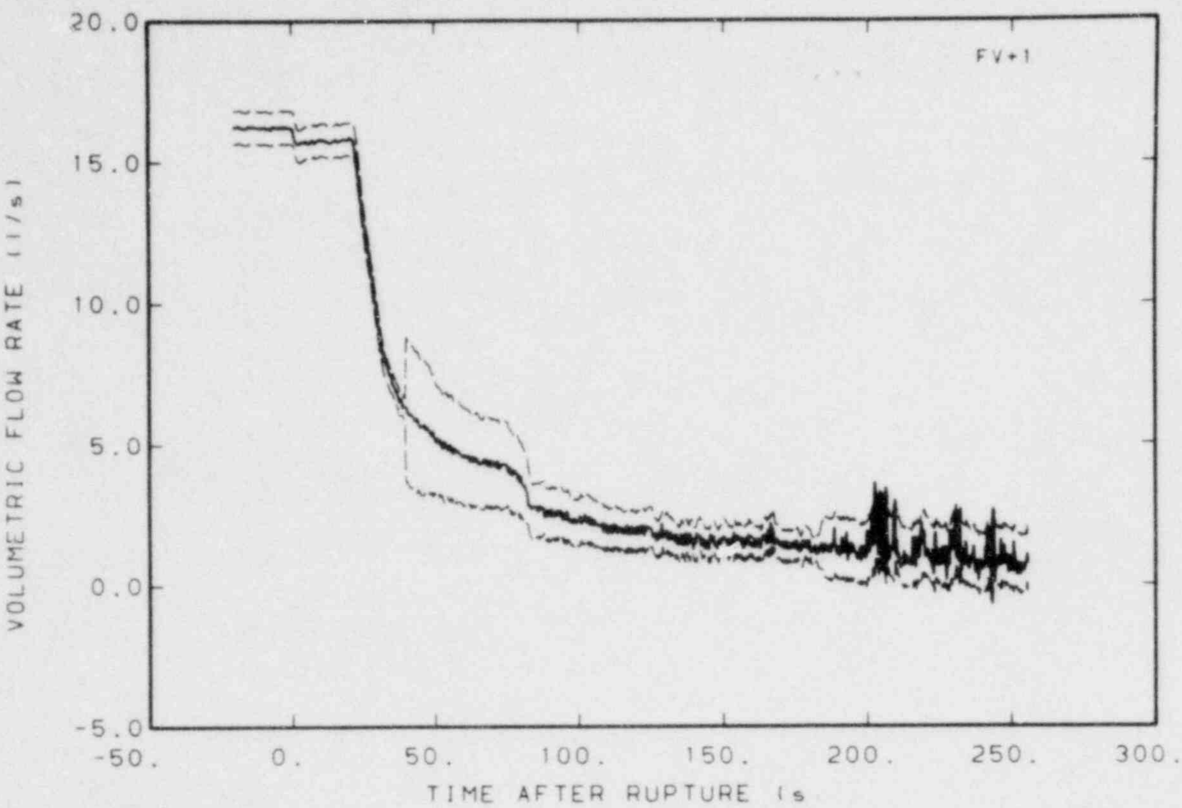

Figure C-53. Volumetric Flow rate in vessel upper plenum, Test S-SB-2 (FV + 1).

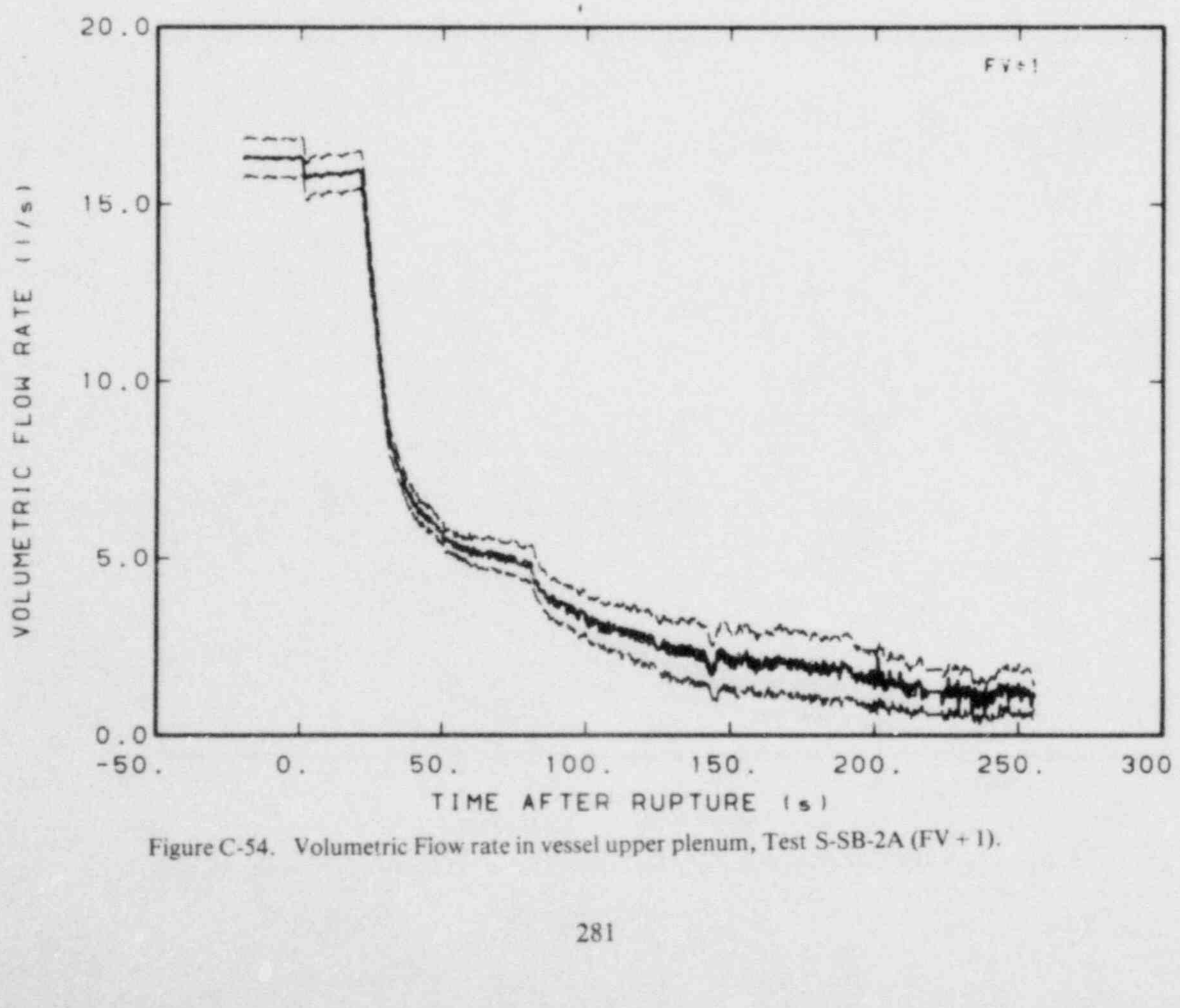

Figure C-54. Volumetric Flow rate in vessel upper plenum, Test S-SB-2A (FV + 1).

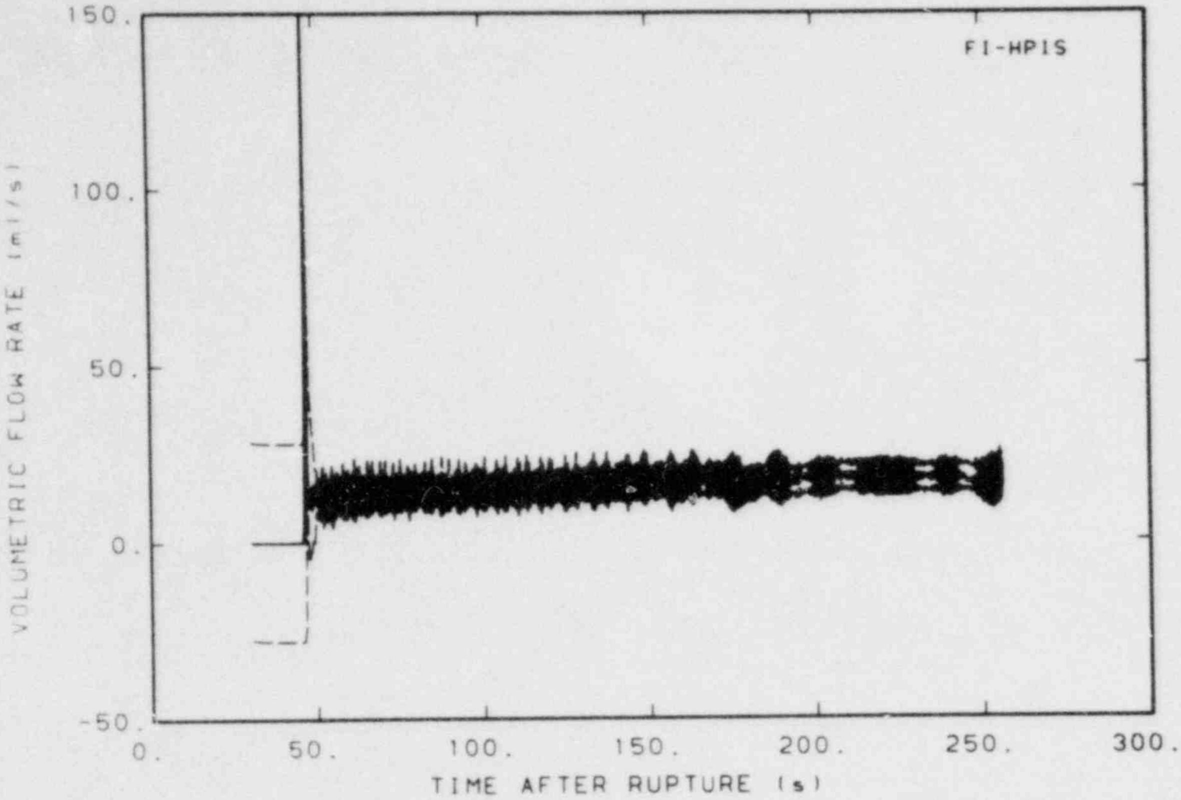

Figure C-55. Volumetric Flow rate in intact loop high pressure injection system, Test S-SB-2 (FI-HPIS).

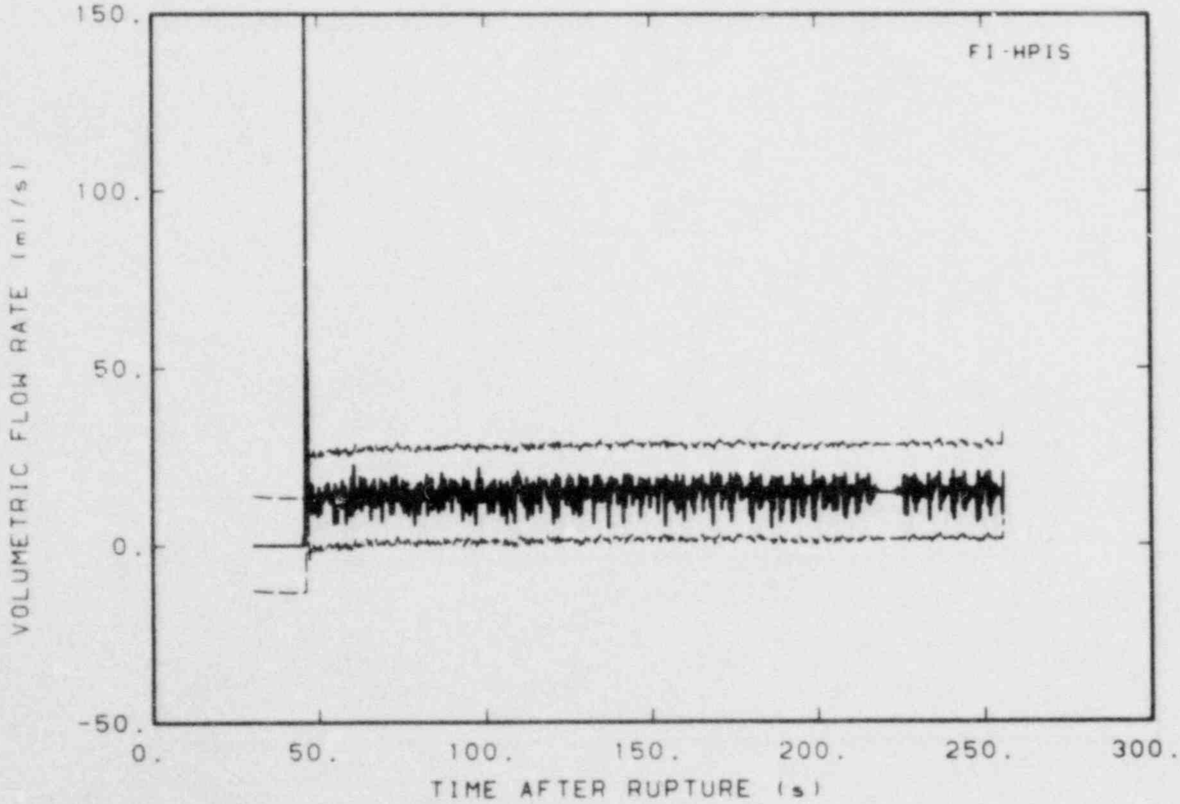

Figure C-56. Volumetric Flow rate in intact loop high pressure injection system, Test S-SB-2A (FI-HPIS).

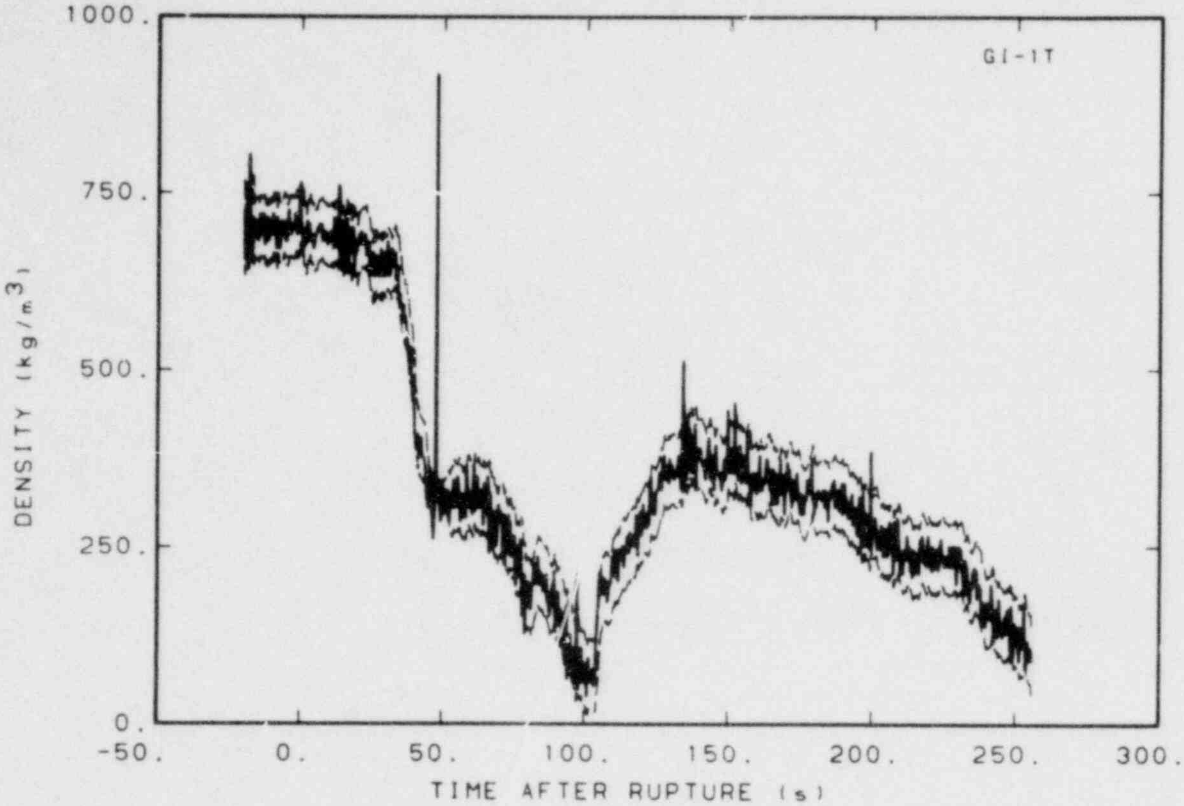

Figure C-57. Density in intact loop hot leg, Test S-SB-2 (GI-1T).

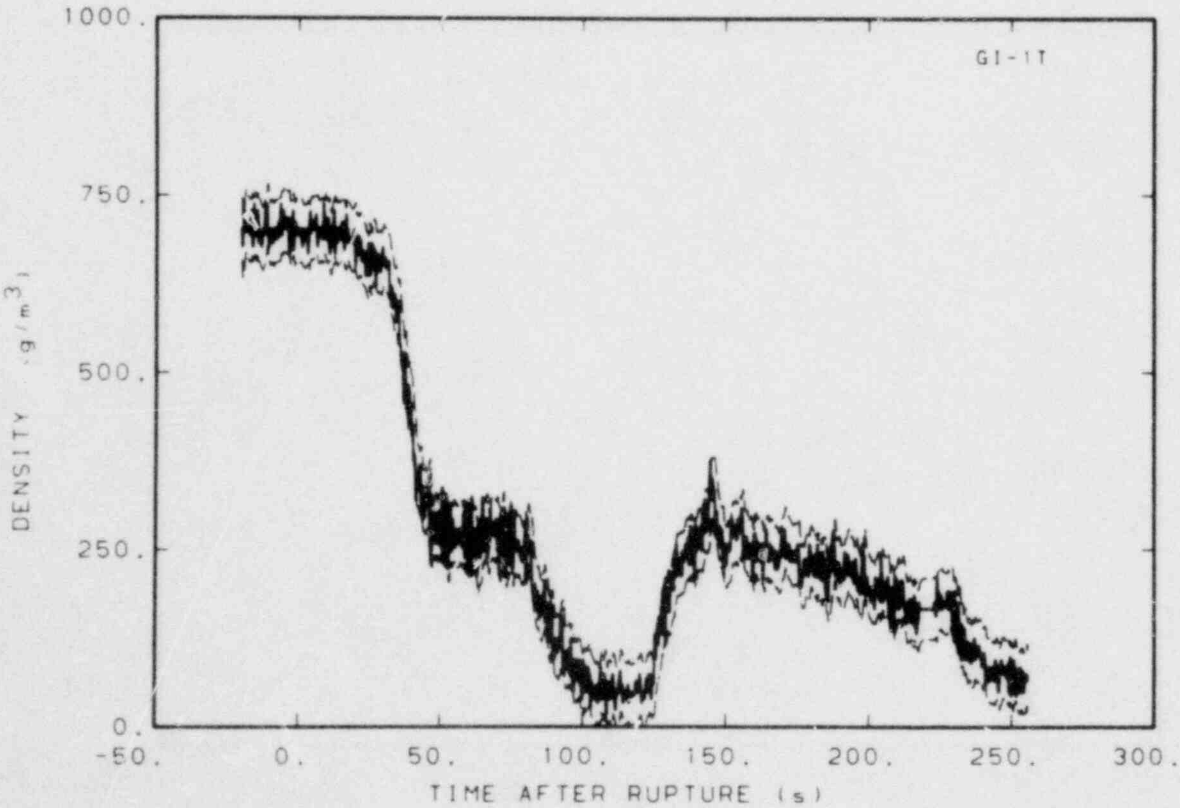

Figure C-58. Density in intact loop hot leg, Test S-SB-2A (GI-1T).

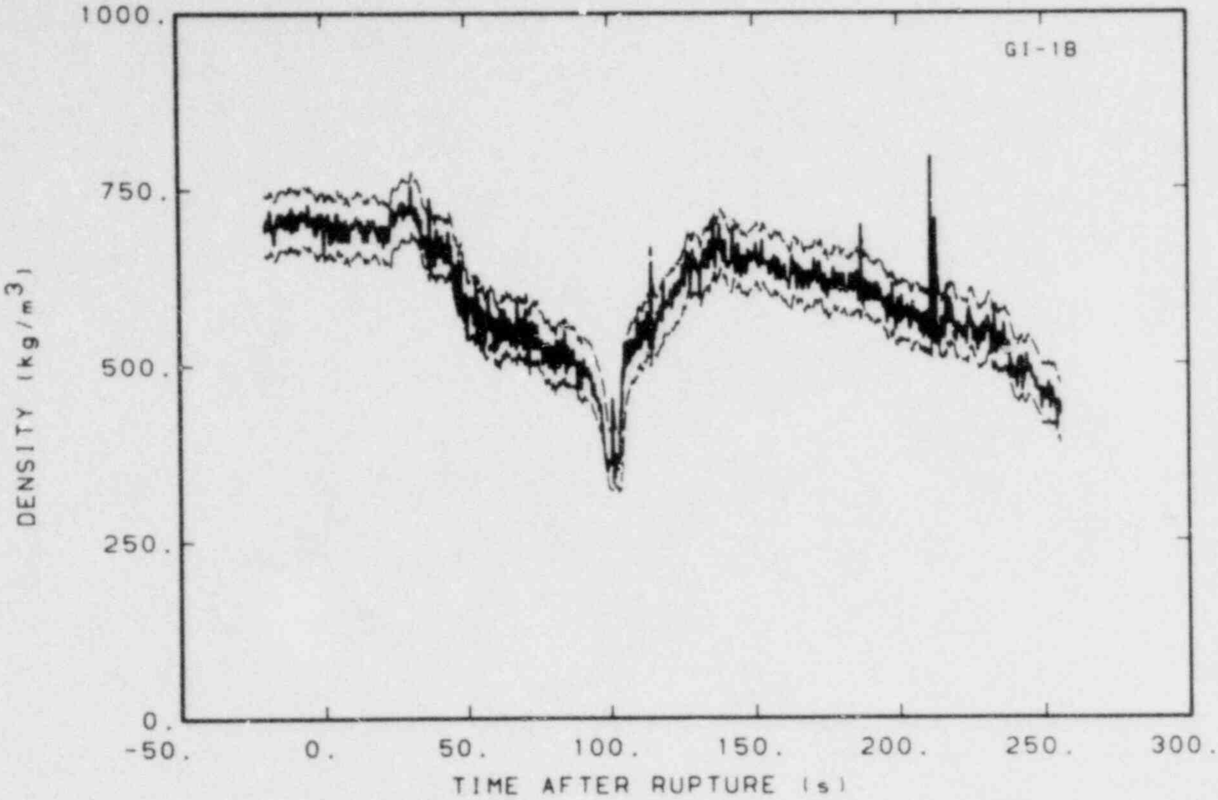

Figure C-59. Density in intact loop hot 'eg, Test S-SB-2 (GI-1B).

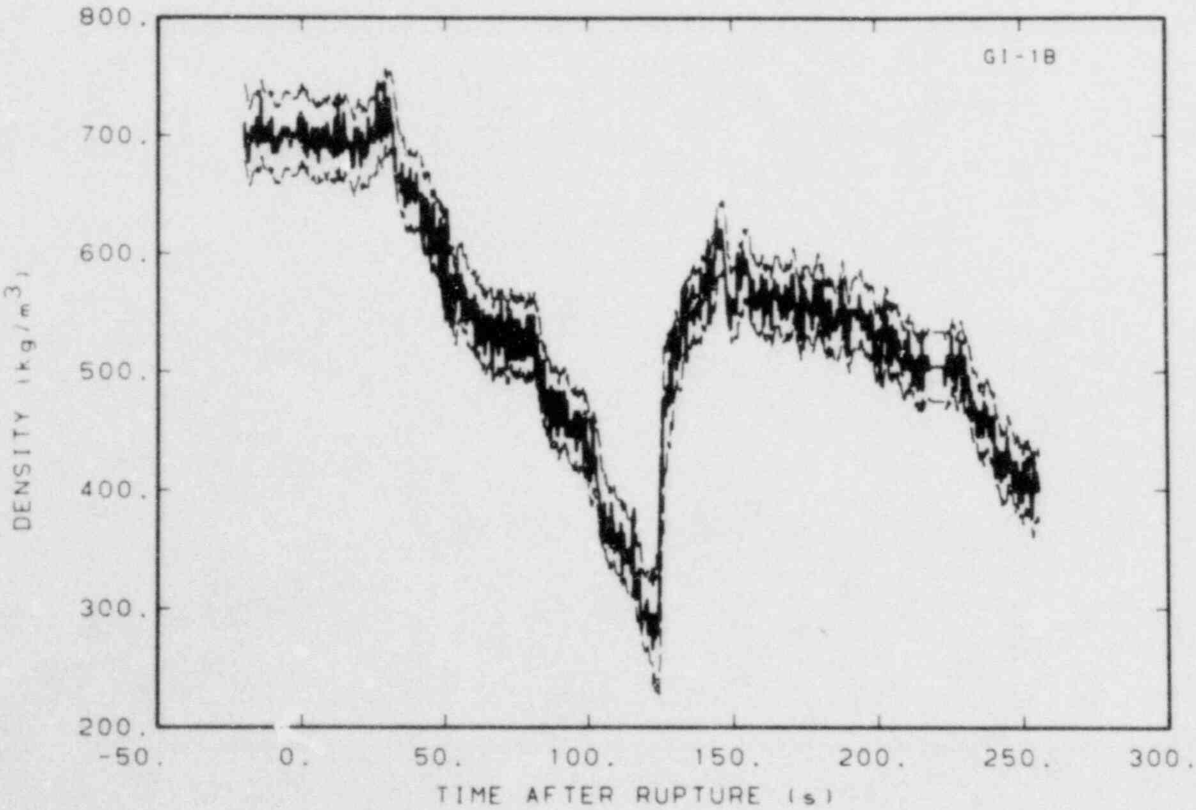

Figure C-60. Density in intact loop hot leg, Test S-SB-2A (GI-1B).

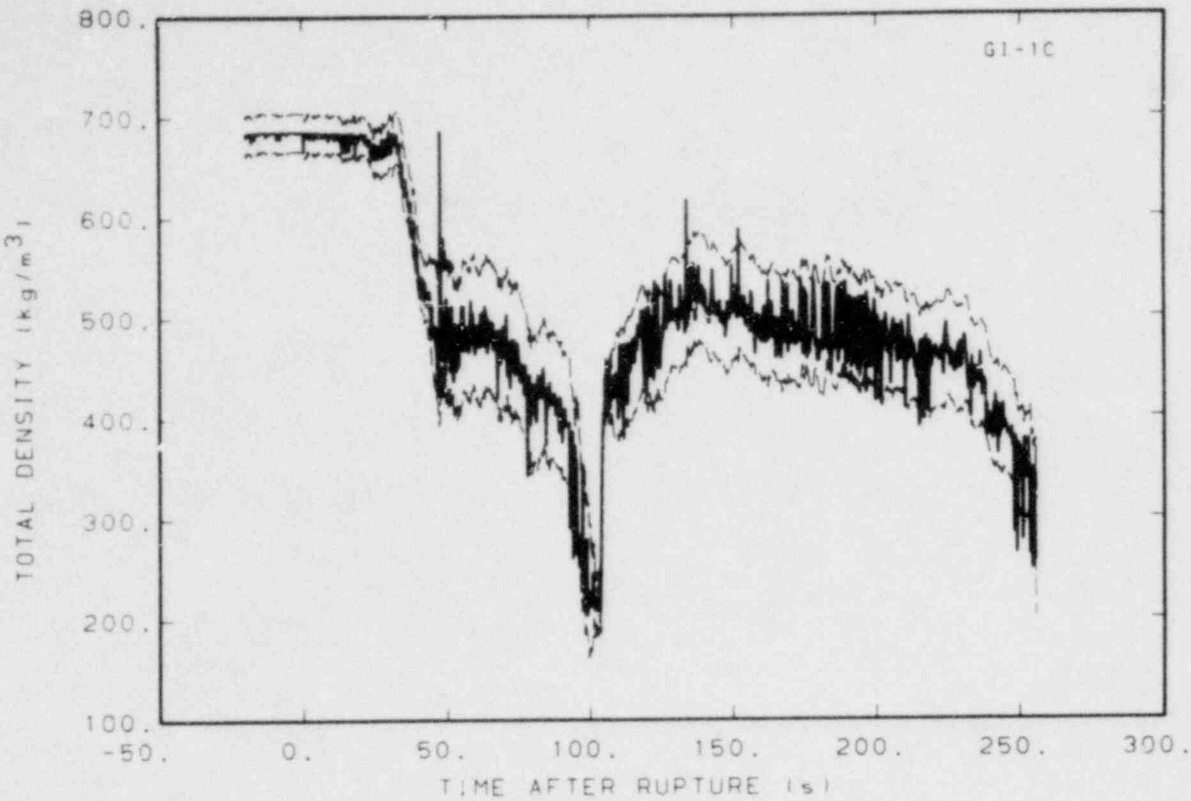

Figure C-61. Density in intact loop hot leg, Test S-SB-2 (GI-1C).

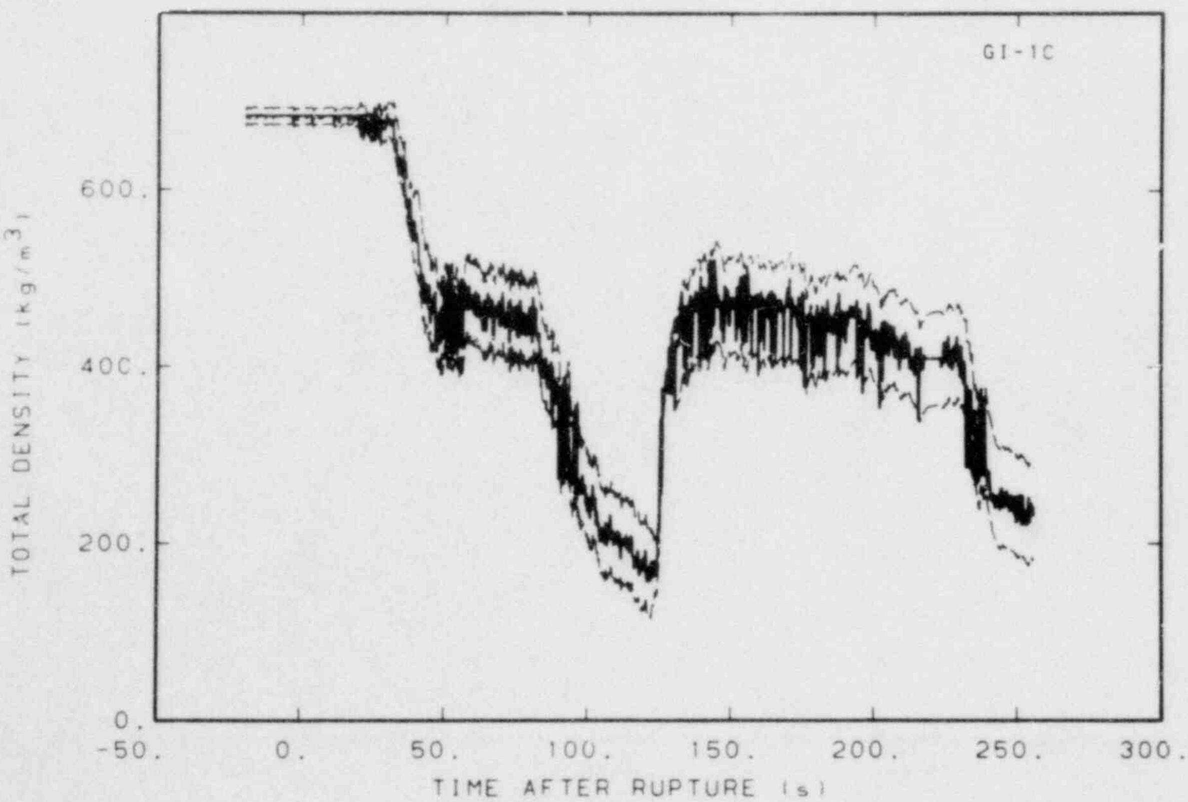

Figure C-62. Density in intact loop hot leg, Test S-SB-2A (GI-1C).

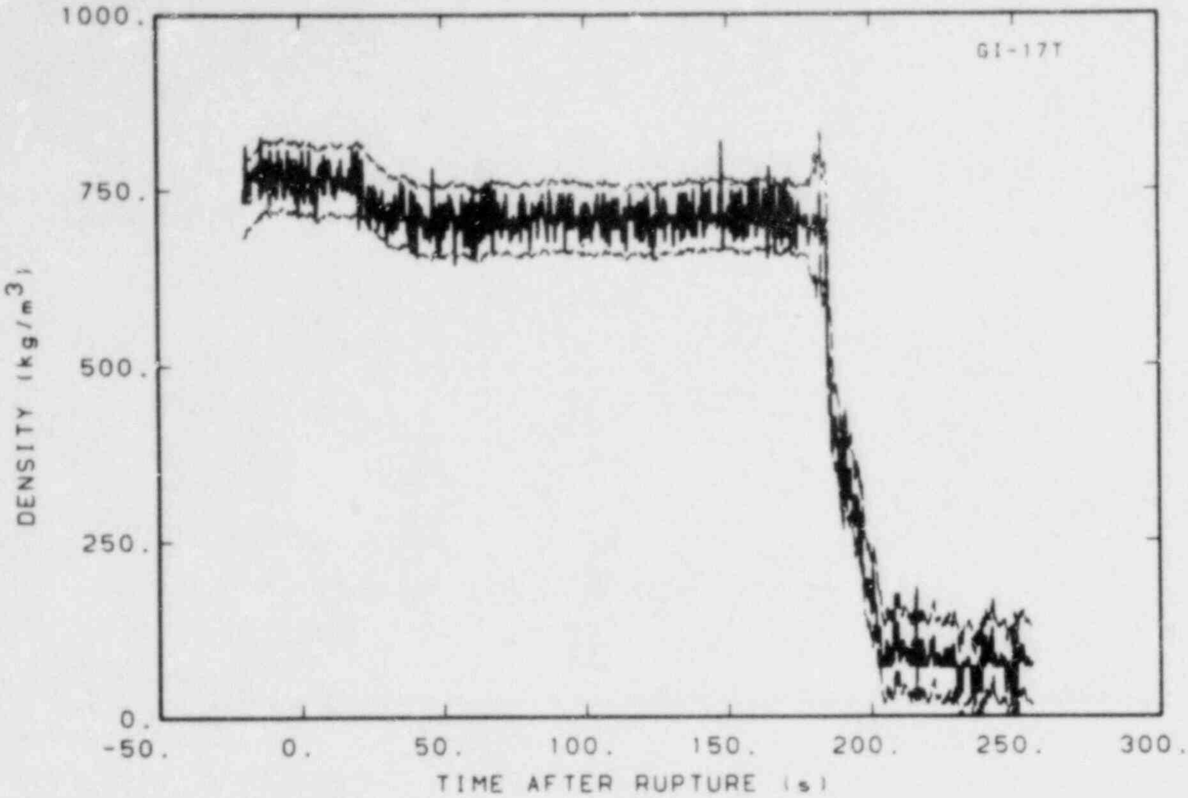

Figure C-63. Density in intact loop cold leg, Test S-SB-2 (GI-17T).

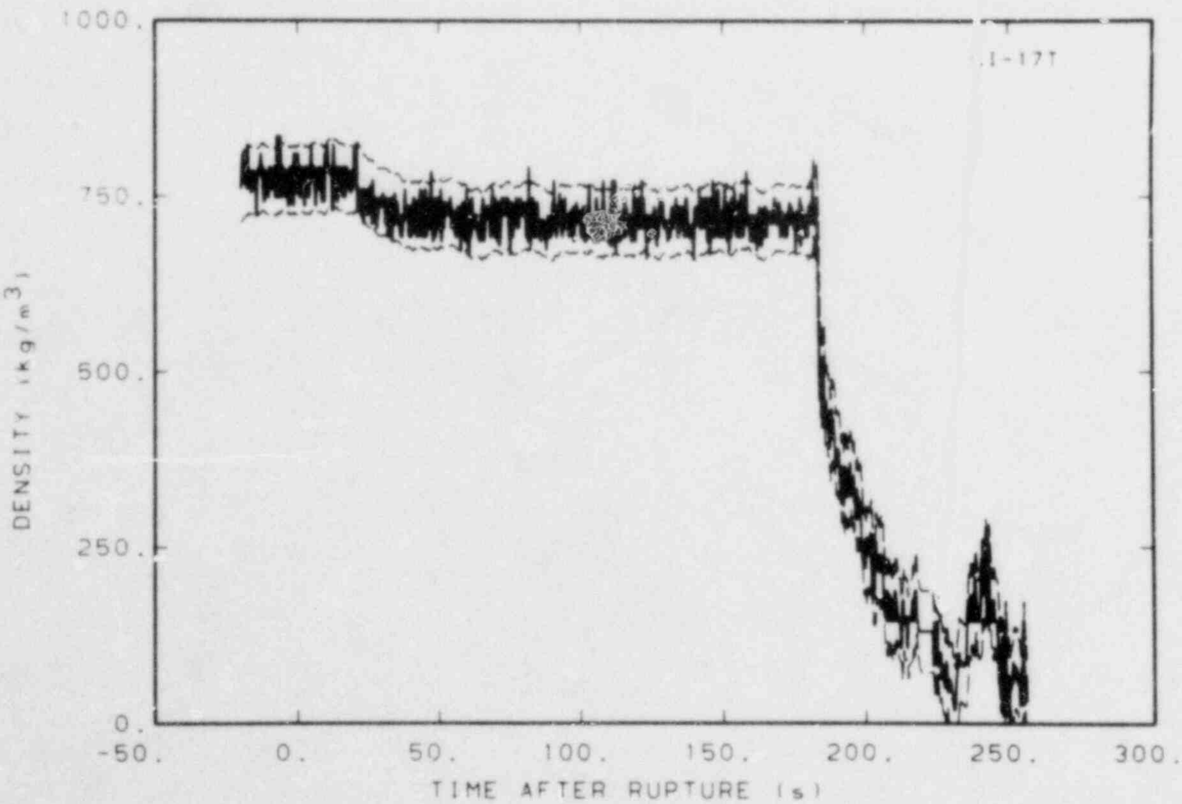

Figure C-64. Density in intact loop cold leg, Test S-SB-2A (GI-17T).

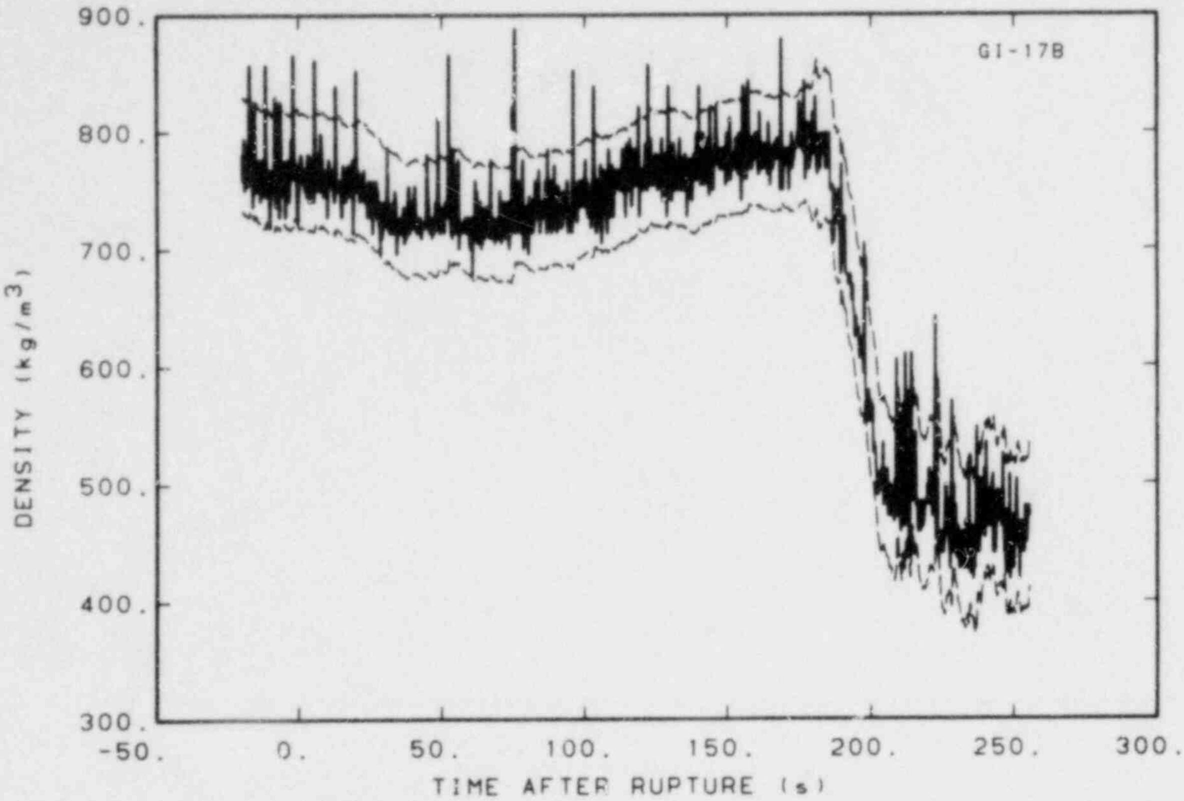

Figure C-65. Density in intact loop cold leg, Test S-SB-2 (GI-17B).

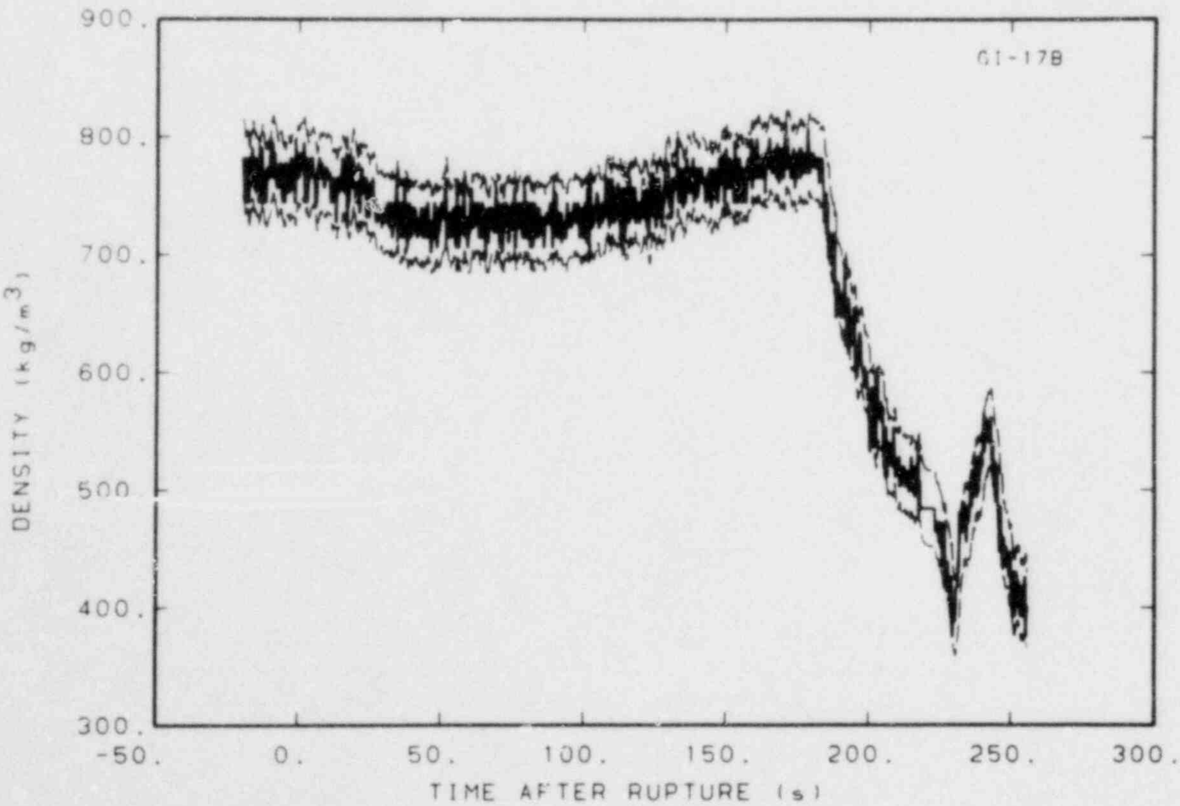

Figure C-66 Density in intact loop cold leg, Test S-SB-2A (GI-17B).

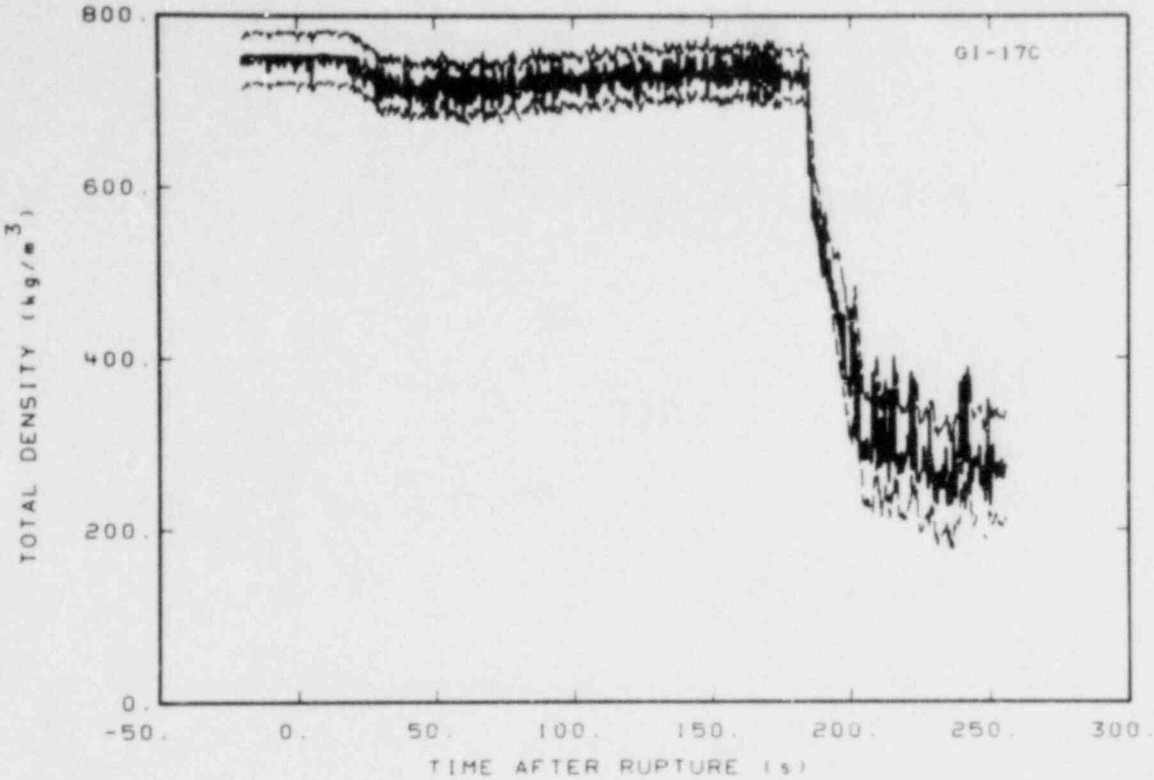

Figure C-67. Density in intact loop cold leg, Test S-SB-2 (GI-17C).

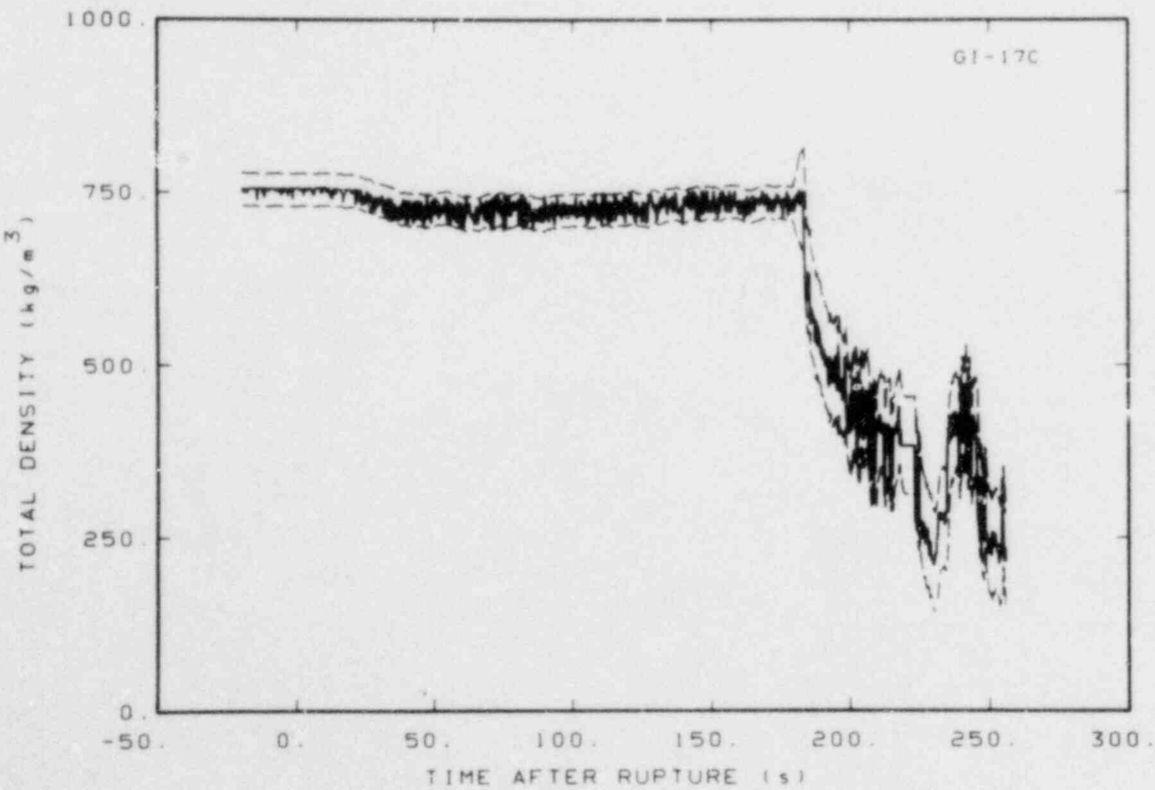

Figure C-68. Density in intact loop cold leg, Test S-SB-2A (GI-17C).

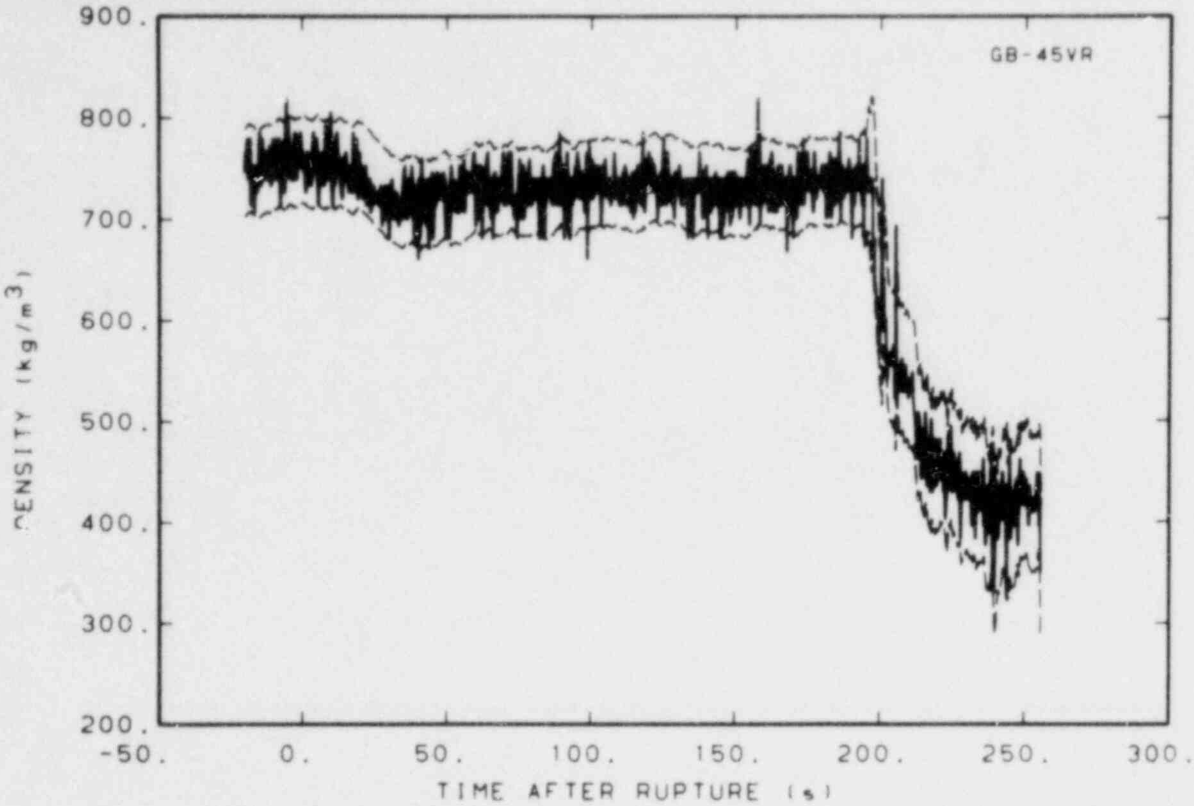

Figure C-69. Density in intact loop cold leg, Test S-SB-2 (GB-45VR).

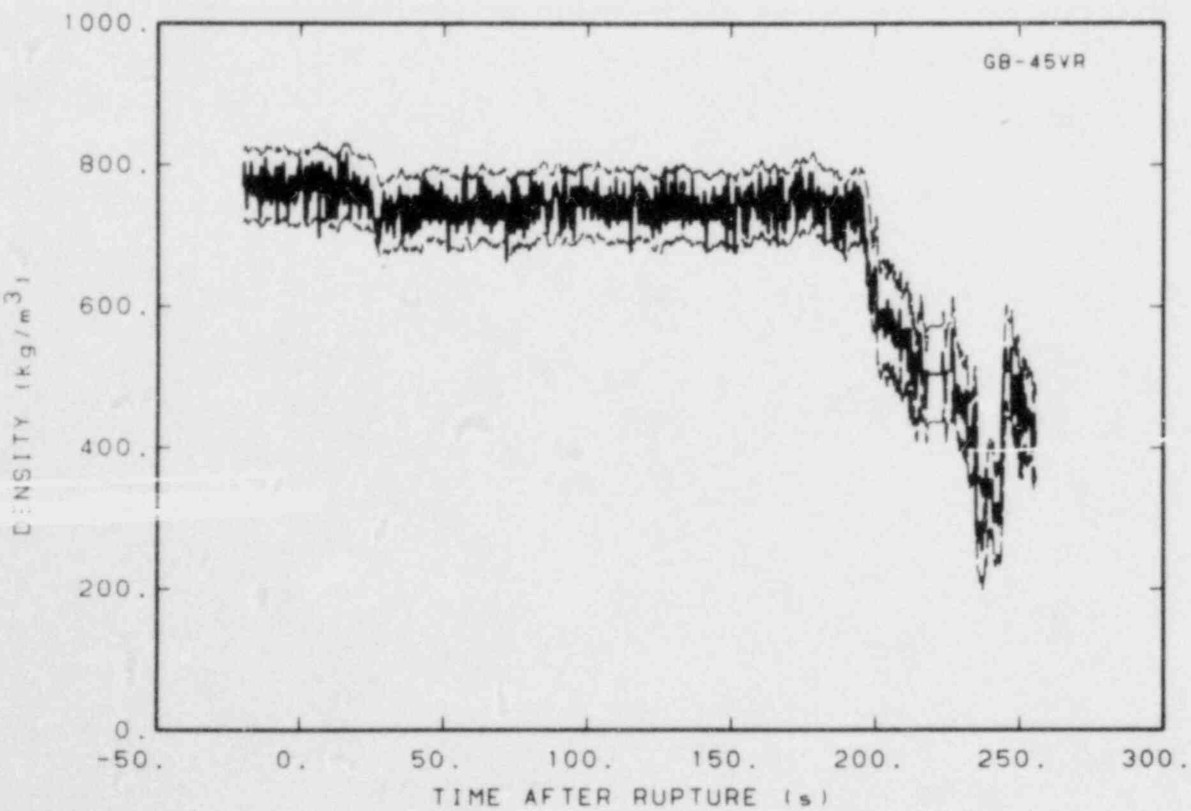

Figure C-70. Density in intact loop cold leg, Test S-SB-2A (GB-45VR).

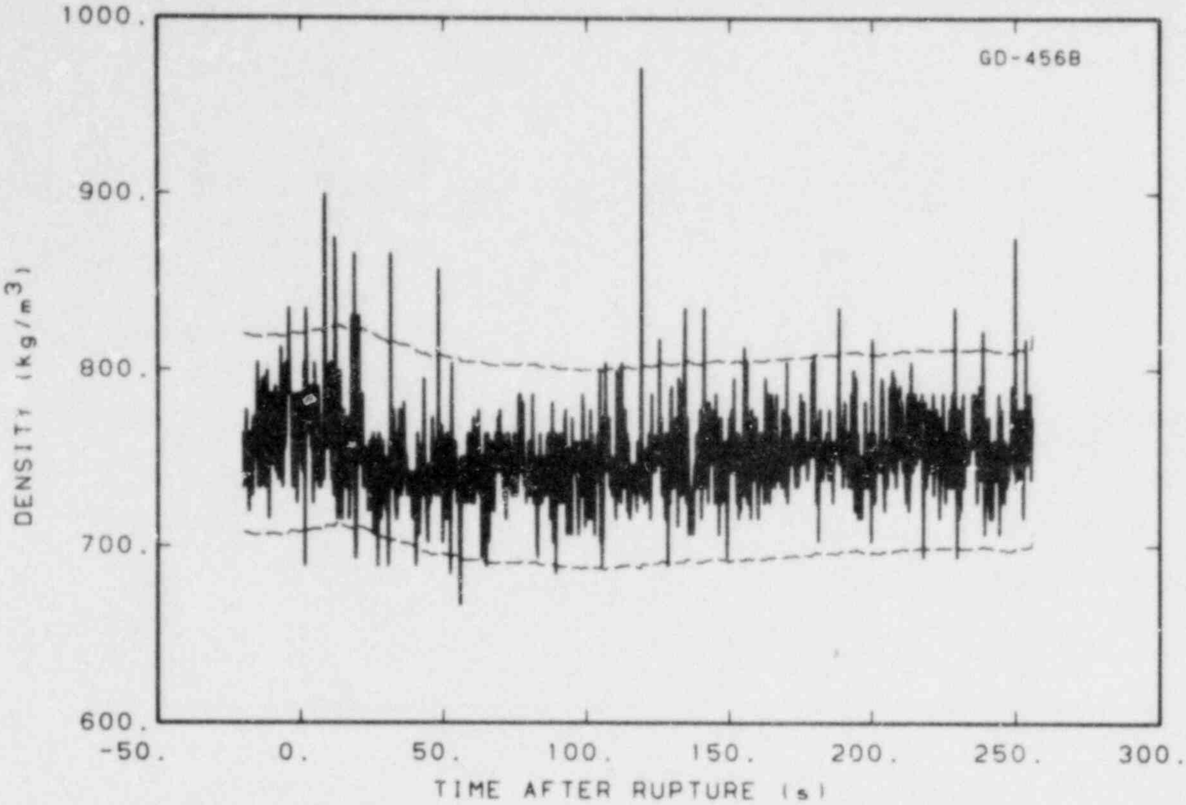

Figure C-71. Density in downcomer, Test S-SB-2 (GD-456B).

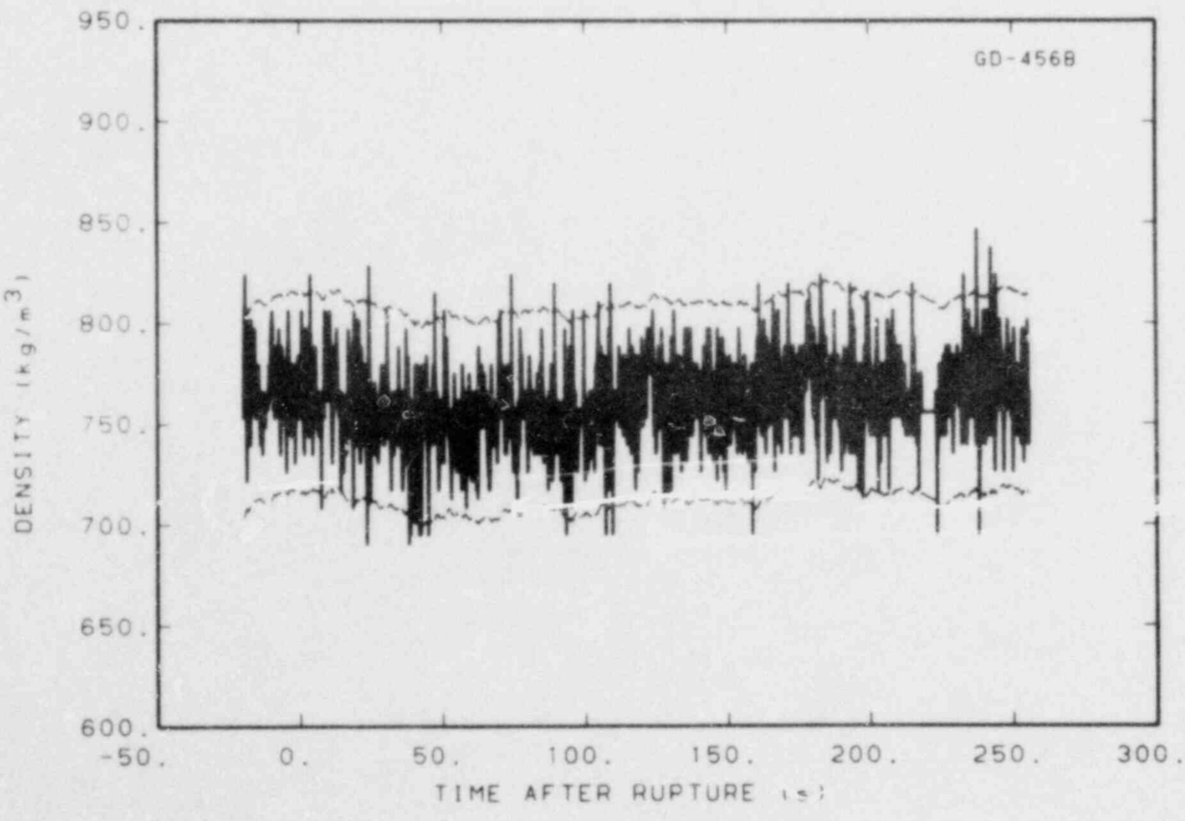

Figure C-72. D ensity in downcomer, Test S-SB-2A (GD-456B).

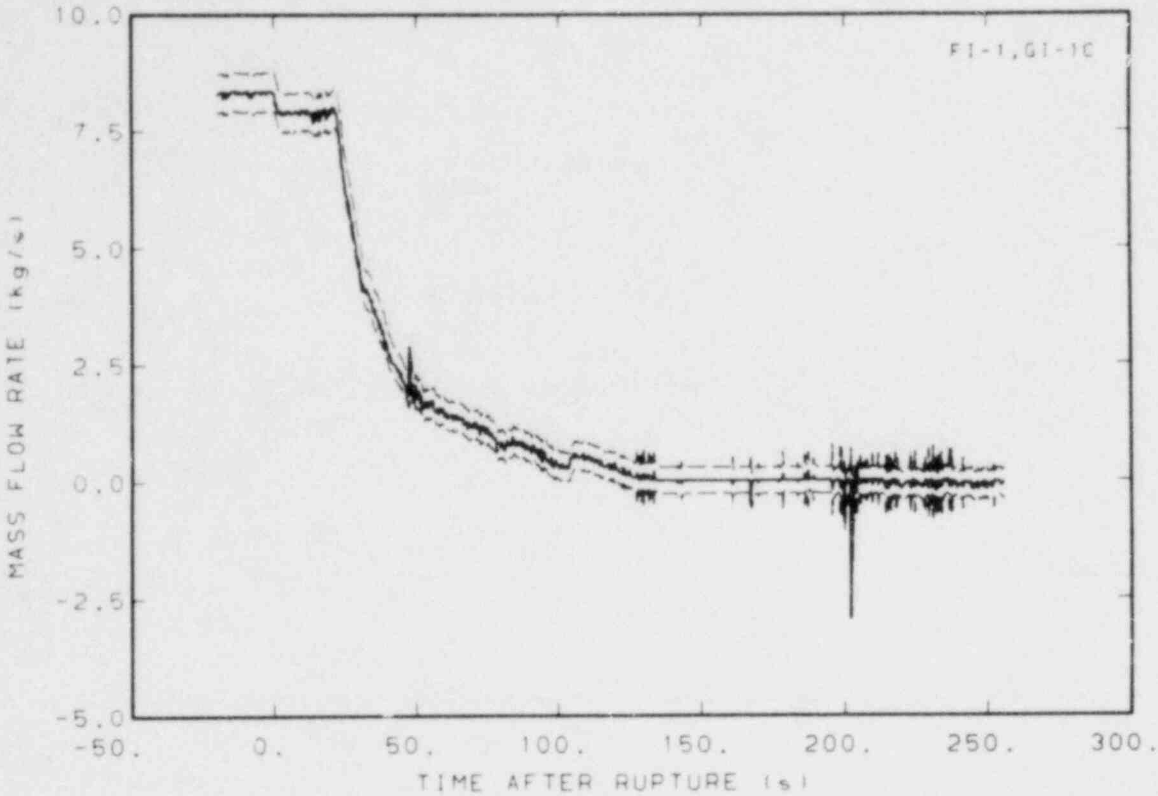

Figure C-73. Mass Flow rate in intact loop hot leg, Test S-SB-2 (FI-1 and GI-1C).

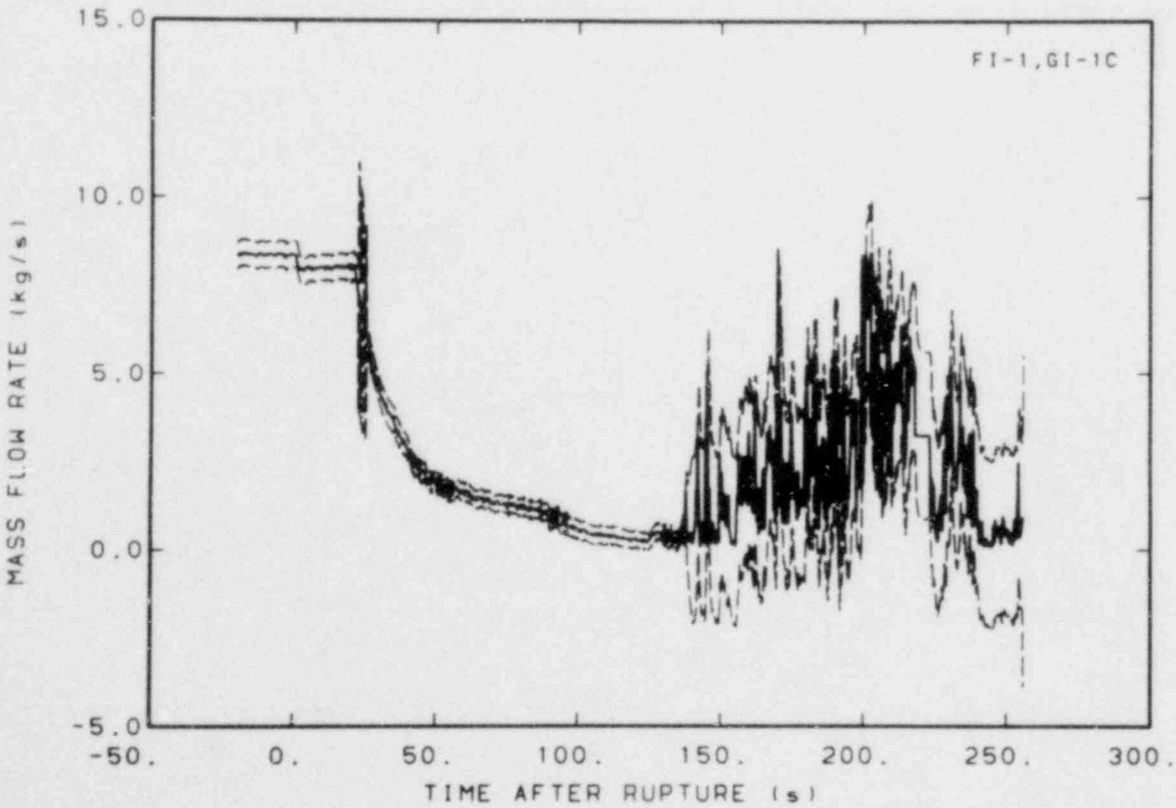

Figure C-74. Mass Flow rate in intact loop hot leg, Test S-SB-2A (FI-1 and GI-1C).

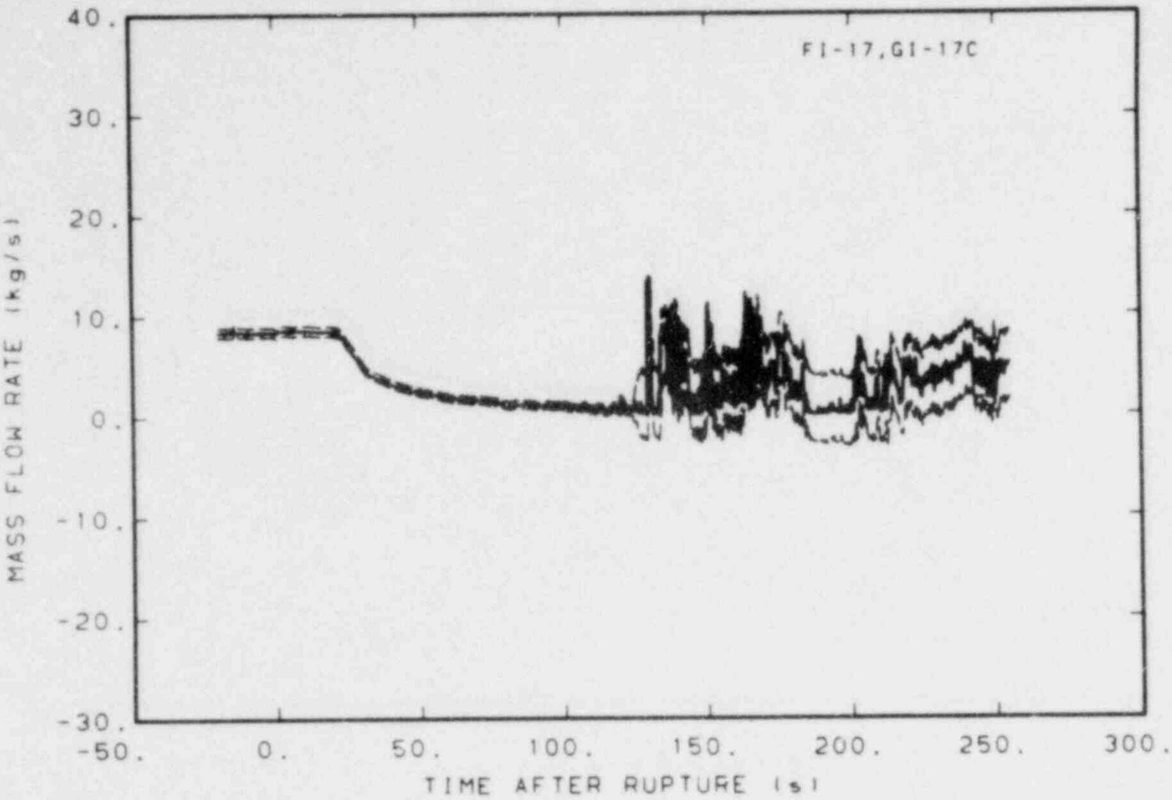

Figure C-75. Mass Flow rate in intact loop cold leg, Test S-SB-2 (FI-17 and GI-17C).

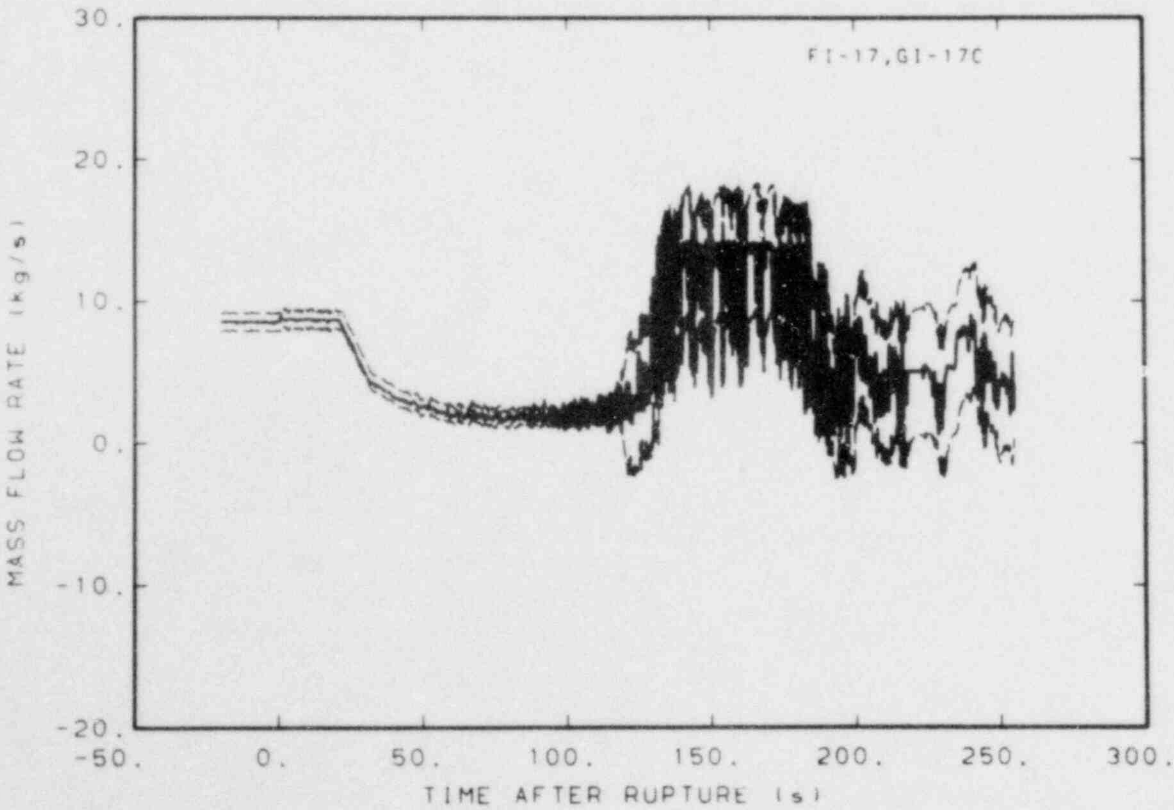

Figure C-76. Mass Flow rate in intact loop cold leg, Test S-SB-2A (FI-17 and GI-17C).

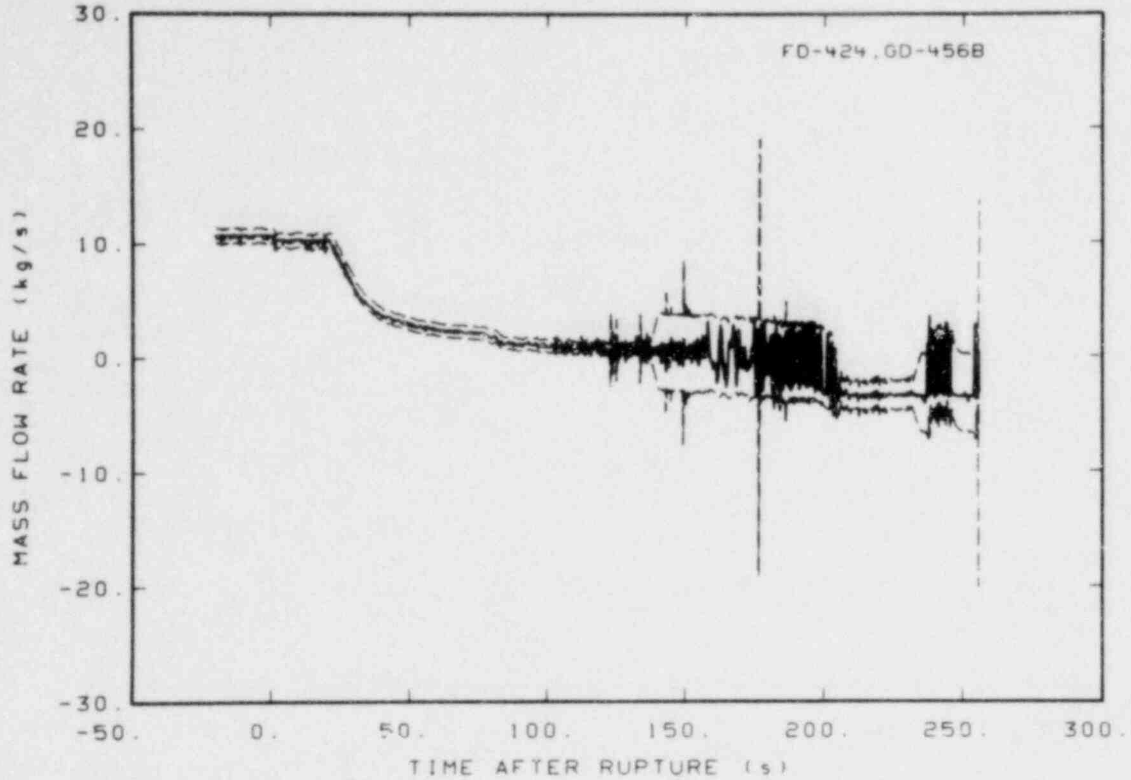

Figure C-77. Mass Flow rate in downcomer, Test S-SB-2 (FD-424 and GD-456B).

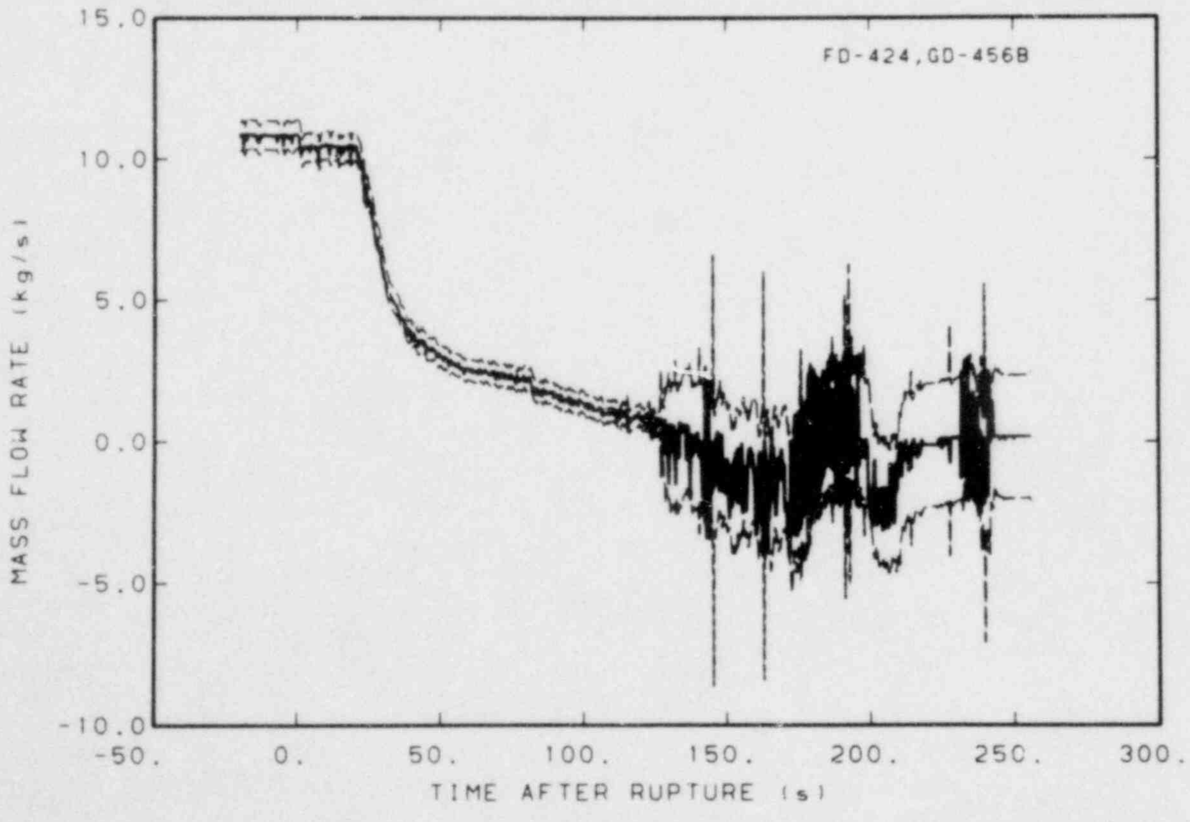

Figure C-78. Mass Flow rate in downcomer, Test S-SB-2A (FD-424 and GD-456B).

REFERENCES

C-1. G. E. P. Box and B. M. Jenkins, *Time Series Analysis—Forecasting and Control*, San Francisco: Holden-Day, 1970.

C-2. E. M. Feldman and S. A. Naff, *Error Analysis for 1-1/2-Loop Semiscale System Isothermal Test Data*, ANCR-1188, May 1975.